MAGNESITE DEPOSITS AT RUM JUNGLE,

N.T., AUSTRALIA - GENESIS AND ASSOCIATION

WITH URANIUM AND POLYMETALLIC SULFIDES

(VOLUME I)

by

YVONNE BONE, B.Sc. (HONS.)

Department of Geology and Geophysics

The University of Adelaide

This thesis is submitted as fulfilment of the requirements for the
degree of Doctor of Philosophy in Geology at the University of Adelaide.

August, 1985.

TABLE OF CONTENTS

VOLUME I

TABLE OF CONTENTS (cont'd)

TABLE OF CONTENTS (cont'd)

TABLE OF CONTENTS (cont'd)

List and location of Figures

TABLE OF CONTENTS (cont'd)

VOLUME II

Plus figures (in flap) as listed in VOLUME I

SAMPLE NUMBER CODE

The following letters were used to designate the geographical areas from whence samples were collected:-

A	Rum Jungle Complex, E.L. 1349
B	Beestons Formation, E.L. 1349
C	Celia Formation, E.L. 1349
D	Crater Formation, E.L. 1349
E	Coomalie Dolomite, E.L. 1349
G	Whites Formation, E.L. 1349
MF	Mt. Fitch Deposit
WO	Whites Deposit
WO-KF	Whites Deposit (collected : K Fuzikawa)
WO-RJ	Whites Deposit (Adelaide University collection)
IN	Intermediate Deposit
DY	Dysons Deposit
BR	Browns Deposit
WM	Mt. Minza
WC	Woodcutters Prospect
BALC	Balcanoona, South Australia
N	Kharidunga, Nepal

This thesis contains no material which has been accepted for the award of any other degree or diploma in any University, nor to the best of my knowledge and belief, does it contain any material previously published or written by another person, except where due reference is made in the text.

SUMMARY

The major aspect of this study concerns the magnesite deposits at
Rum Jungle, Northern Territory, Australia, which occur within the Lower
Proterozoic Celia Dolomite and Coomalie Dolomite. The magnesite is
spatially associated with the U and polymetallic sulfide deposits within
the Rum Jungle area, one of the U fields of the Pine Creek Geosyncline.

The processes responsible for the formation of the magnesite have
been studied with the objectives of (1) determining the genesis of the
magnesite, (2) determining the role played by magnesite in the formation
of the U and polymetallic sulfide deposits, and (3) delineating
sufficient tonnage of silica-free magnesite which could be mined by
open-cut methods.

Extensive work on the genesis of carbonates by previous workers
shows that exceptional conditions are required for the precipitation of
primary magnesite in the sedimentary environment, i.e. an alkaline,
shallow, lacustrine situation with a Mg-rich groundwater input and a
periodically high evaporation rate. Field observations of stromatolites
(Conophyton, stratiform and cryptalgal types), tepee structures and the
absence of evidence of the prior presence of evaporite minerals from
gypsum upwards support the notion of a shallow water environment.

The presence of a palaeokarst surface at the interface of the
magnesite and the overlying sequence further supports the sedimentary
environment, as do the associated fluvial clastic sediments. The trace
element geochemistry of the magnesite suggests an alkaline lacustrine
environment, i.e. low Na, K and Sr, high F, Fe and Mn, notwithstanding
diagenetic and metasomatic alteration. Ubiquitous detrital and/or
authigenic intragranular grains of tourmaline, quartz, apatite, rutile,
ilmenite, K-feldspars and clays suggest a primary chemical sediment, as

does the $\delta^{34}S$ signature of the diagenetic pyrite.

The magnesite is completely recrystallized. The fluid inclusion study indicates that the temperature of the fluids involved in this event ranged from $98^{\circ}C$ to $> 400^{\circ}C$, with a mean of $153^{\circ}C$ for 444 samples. This recrystallization resulted in two distinctly different magnesite morphologies - a bladed form and a rhomb form. These two forms have previously been mistaken as pseudomorphs after gypsum and halite. However, the fluid inclusion study shows that the bladed form usually results from the recrystallization of magnesite from a fluid with a temperature greater than $160^{\circ}C$; whereas the rhomb form results when the temperature is below $160^{\circ}C$. Observations made during a pace and compass survey of 320 magnesite outcrops in the area showed no correlation between morphology and grain size or impurity content.

Analyses by electron microprobe of the fluids in fluid inclusions in the magnesite and its associated quartz show the presence of a range of cations and anions, namely Na, Ca, Mg, Fe, K, Cl and S (probably as SO_4).

The absence of any anionic spectrum for some samples suggests the presence of CO_3 or HCO_3, which proved to be an important consideration in the formation of ore fluids and their transport, particularly for U.

The microthermometric fluid inclusion studies also indicate the presence of several fluids, the mixing of which produced a wide range of salinities, often with inverse temperature relationships. Because $CaCl_2$ appeared to be present in amounts far larger than NaCl, salinities have been presented in wt.% equivalence of $CaCl_2$.

Other diagenetic alteration included pervasive stylolitisation,
producing the following types:-

(a) sutured seam solution, particularly at the boundary between the
Coomalie Dolomite and Whites Formation (the site of most
mineralisation),

(b) non-sutured seam solution, which has given rise to nodular and
chicken-wire fabric, breccias and zoned rhombs,

(c) non-seam solution.

Stylolitisation played an important role in the formation of the
mineral deposits. Stylolitised magnesite ought to be considered a
pathfinder.

Both field observations and laboratory studies suggest that there
has been stratigraphic duplication of the two lowermost sedimentary
formations by gravity thrusting down the flanks of the diapirically
uprising Basement Complexes. This makes the names of either the
Beestons Formation and the Celia Dolomite or the Crater Formation and
the Coomalie Dolomite redundant.

As the so-called Dolomite Formations are predominantly magnesite
throughout their extent, it is suggested that they be officially renamed
either the Celia Formaton or the Coomalie Formation (and because they
also contain extensive silicified areas and intercalations of "mafic
schists" and tourmalinites). Such stratigraphic nomenclature changes do
not affect either the magnesite genesis model or the findings on U and
polymetallic sulfides, even though the mineral deposits all show a
strong stratigraphic and lithological control.

Many different mineralisation models have been proposed by workers
in the Pine Creek Geosyncline. This study shows that:-

(1) the magnesite was involved in producing a fluid suitable for

the formation and transport of U and metal complexes, e.g. uranyl carbonate complex:

(2) the magnesite was not the major source of the U or the metals:

(3) the Basement Complexes are enriched in U, and presumably constitute one of the major sources:

(4) Whites Formation is enriched in both U and metals, and presumably also a source:

(5) the mineralising fluids were predominantly low temperature, often highly saline and frequently $CO_2 \pm CH_4$ rich:

(6) shear zones, which were co-incident with the Coomalie Dolomite-Whites Formation boundary, were preferential pathways for mineralising fluids:

(7) stylolitisation processes were involved in the formation of mineralised breccias:

(8) the range of $\delta^{34}S$ values obtained indicate that the disseminated stratiform pyrite (which has reduced biogenic sulfate characteristics) was the source for the polymetallic sulfides, as indicated by the low temperature of remobilization via pervasive hydrothermal fluids:

(9) the sulfide phases present support the low temperature data obtained from the fluid inclusion studies, e.g. pyrite-marcasite -villamaninite-bravoite/siegenite:

(10) there were exceptionally high concentrations of Cu+Co+Ni+Fe to form the rare disulfides and thiospinels.

(11) the tourmalinites present support the premise of a continental type rift environment.

Magnesite from Balcanoona, South Australia, and Kharidunga, Nepal, was studied for comparison purposes. Polymetallic sulfides were discovered at the boundary of the magnesite and the overlying graphitic schist at Kharidunga. These were predominantly pyrrhotite, with veinlets of chalcopyrite.

ACKNOWLEDGEMENTS

Fig. 1: Locality Map

CHAPTER 1

INTRODUCTION

1.1 Project Initiation

This thesis study was initiated by Broken Hill Proprietary Co. Ltd. (B.H.P.) in consultation with Prof. P. Ypma of Adelaide University. B.H.P. currently imports the magnesite that is required for refractory purposes in the manufacture of their various steel products. For this reason B.H.P. was interested in locating an economically viable deposit of relatively silica-free magnesite within Australia.

At the beginning of 1979, B.H.P. was involved in the preliminary assessment of a large magnesite deposit located at Rum Jungle, Northern Territory (Fig. 1). That assessment indicated that the magnesite crops out sporadically over a large area (Fig. 2), but that the silica content, predominantly as quartz, talc or chlorite, appeared to be variable, without any apparent geological control. Therefore the preliminary aim of this study was to establish proven reserves of 10 million plus tonnes of magnesite, containing less than 5% silica, tha could be mined by open-cut methods.

1.2 Problems of Genesis of Magnesite

Magnesite ($MgCO_3$) is the stable magnesium carbonate mineral at or near the earth's surface. It belongs to the Calcite Group of the anhydrous carbonates (Dana, 1966).
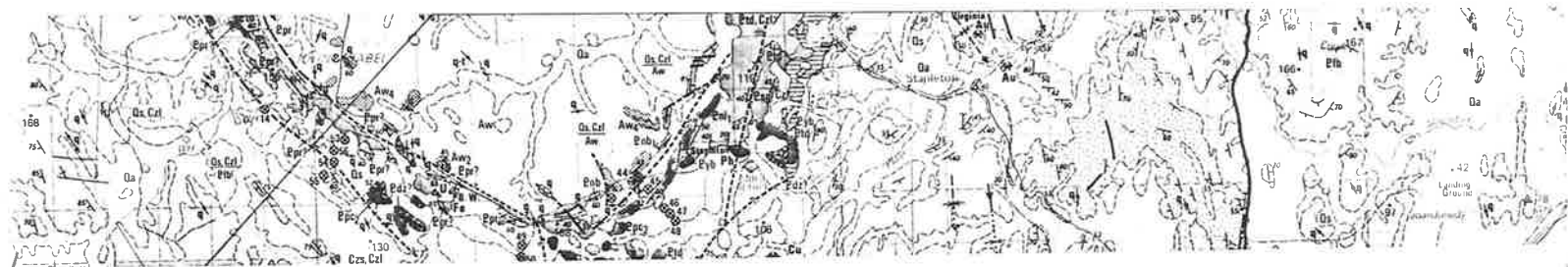
There are two major, distinctly different modes of formation of magnesite.

(a) Alteration of Mg-rich metamorphic or igneous, and occassionally alteration of Mg-rich sedimentary rocks.

This alteration process can be brought about by CO_2-metasomatism with or without Mg-metasomatism, (Frost, 1982). The alteration of the ultramafic flows at Timmins, Canada (Fyon et al., 1983) and for that matter, many Archean Greenstone Belts, is a typical example of the metasomatism of igneous rocks.

The Savage River, Tasmania (Frost, 1982) magnesite has been attributed to Mg-metasomatism of a sedimentary dolomite. It is not always possible to clearly define the origin of the precursor, as in the case of the Snarum, Norway (Josang, 1966) magnesite, where metasomatism has obliterated earlier mineralogies. The use of R.E.E. by Morteani et al., (1981) may overcome this uncertainty.

(b) Sedimentary magnesite.

Although seawater is saturated with respect to magnesite (Sayles & Fife, 1973), magnesite does not precipitate directly from normal seawater. Experimentally, it is only possible to precipitate it from seawater compositions at temperatures well above those usually pertaining to the sedimentary environment (Lippman, 1973, Sayles & Fife, 1973). However, primary magnesite is found in Recent occurrences, usually in association with other carbonates and/or evaporite minerals. These Holocene occurrences usually occur in lacustrine
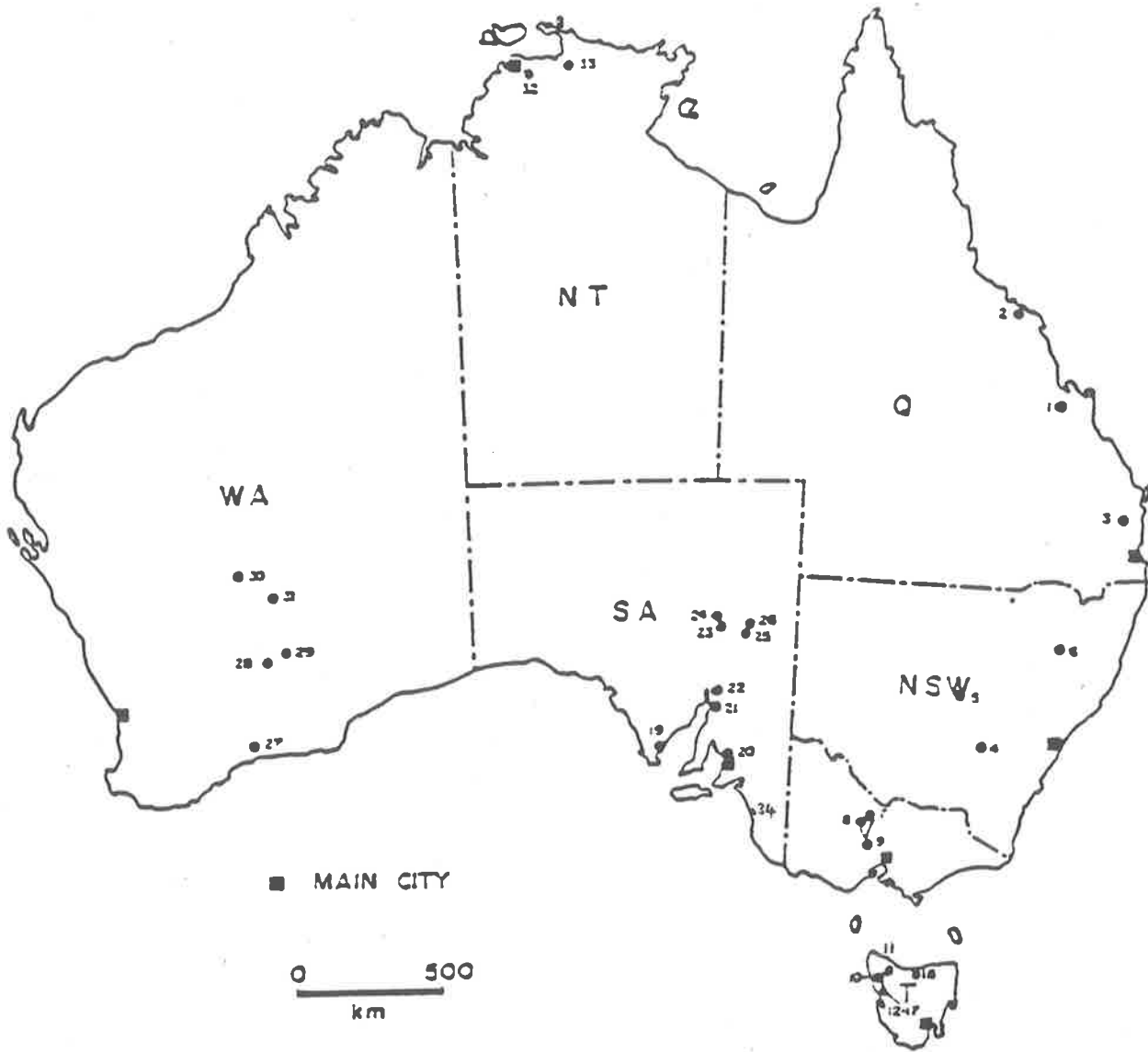
Fig. 3: Australian Magnesite Localities

10	Savage River
11	Arthur River
19	Tumby Bay
22	Mundallio
25	Balcanoona
34	The Coorong
32	Rum Jungle
33	Alligator Rivers Area

environments e.g. Lake, Bonneville, U.S.A. (Graf et al., 1961)
the Coorong, S. Aust. (von der Borch, 1965, 1976, 1979) and the
Basque Basin, British Columbia (Nesbitt, 1974, in Eugster &
Hardie, 1978).

The only documented occurrence of magnesite precipitating
in a marine environment is that of the Trucial Coast, where it
forms diagenetically within the sediment in association with
anhydrite (Kinsman, 1969b; Bush, 1973; Kendall, 1978). As
anhydrite ($CaSO_4$) forms only at elevated temperatures (+40°C),
it would seem that a temperature increase is responsible for
this occurrence.

1.3 Review of Magnesite Deposits and Occurrences

Within Australia, magnesite deposits have been recorded
within the major geosyncline and in the Yilgarn, plus an
anomalous deposit in South Australia at Tumby Bay (Fig. 3).
This study centres on the occurrence in the Pine Creek
Geosyncline at Rum Jungle, with a brief assessment of some of
the S.A. deposits.

Magnesite deposits are wide spread with the greatest
density of reported occurrences being in geosynclinal belts,
where it tends to be associated with sedimentary environments
favourable to the formation of evaporites; or in association
with ophiolite belts. Samples from many different deposits
were examined, amongst which were those at: Balcanoona S.A.
Mundalio S.A. and the Coorong, S.A. The deposit at Kharidunga,
Nepal, was studied in detail.
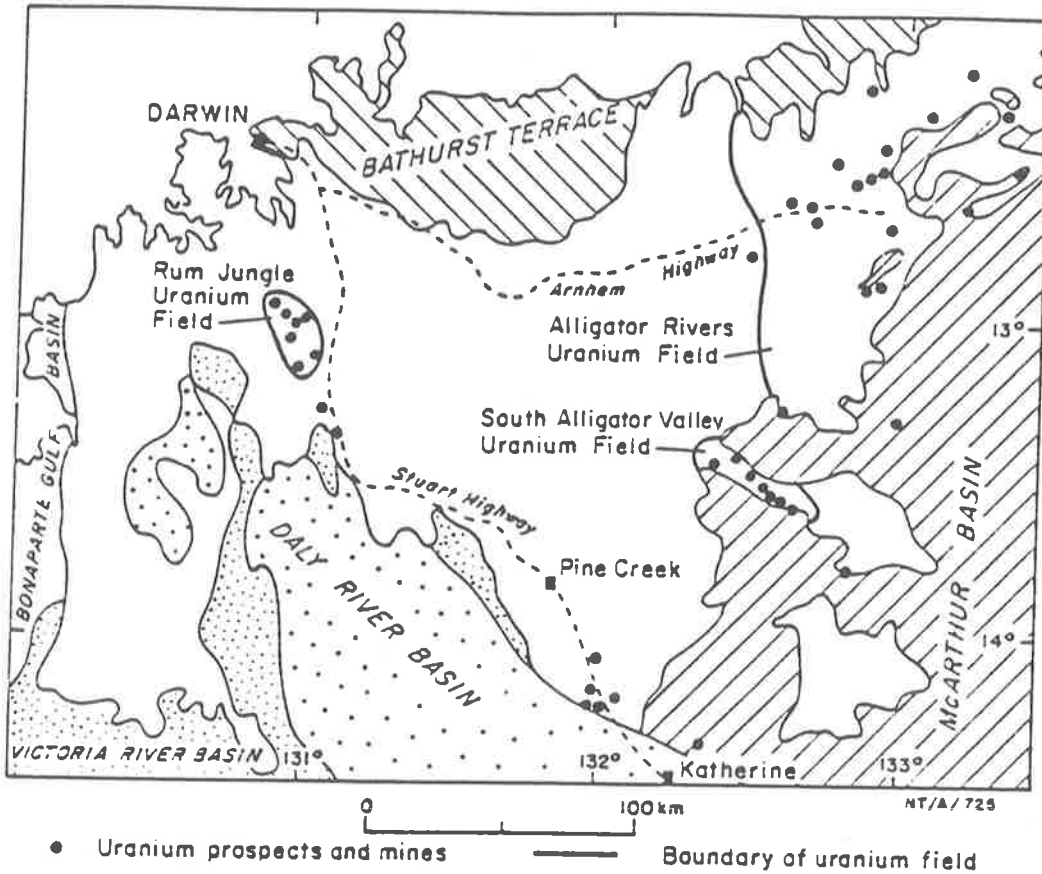
Fig. 4: Location of Rum Jungle in relation to the general structural setting of the Pine Creek Geosyncline, with locations of U mines and prospects.

(Needham et al., 1980)

B.H.P. is the major importer of magnesite for refractory use, and thus are the one company currently searching for a high-quality (i.e. silica free) product. B.H.P. holds leases at both Rum Jungle (Exploration Lease 1349) and at Balcanoona, S.A. (Fig. 3); and are awaiting further advice from their Austrian consultant, Osterreichish-Amerikanische Magnesit A.G., in particular concerning benefication.

In S.A., JOMOCO, Steetly Industries and A.C.I. Industries mine a few hundred tonnes per year from deposits occurring within the Skillogallee Dolomite at Robertstown and Myrtle Springs.

This thesis study, which was supported logistically by B.H.P., was centred upon the magnesite at Rum Jungle N.T. where it occurs within two stratigraphic units - the Celia Dolomite and the Coomalie Dolomite.

1.4 Aims of the Study

The genesis of the magnesite was the major problem addressed. This problem involves the determination of facies and diagenetic variations, and their effect on the quality of the magnesite in term of impurities. Later alteration of these impurities as a result of metamorphism and tectonism influences the production of secondary contaminants and was also considered.

Factors determining the morphology of the magnesite were also part of the study. Crick and Muir (1980) proposed that the crystal morphology represents halite and gypsum
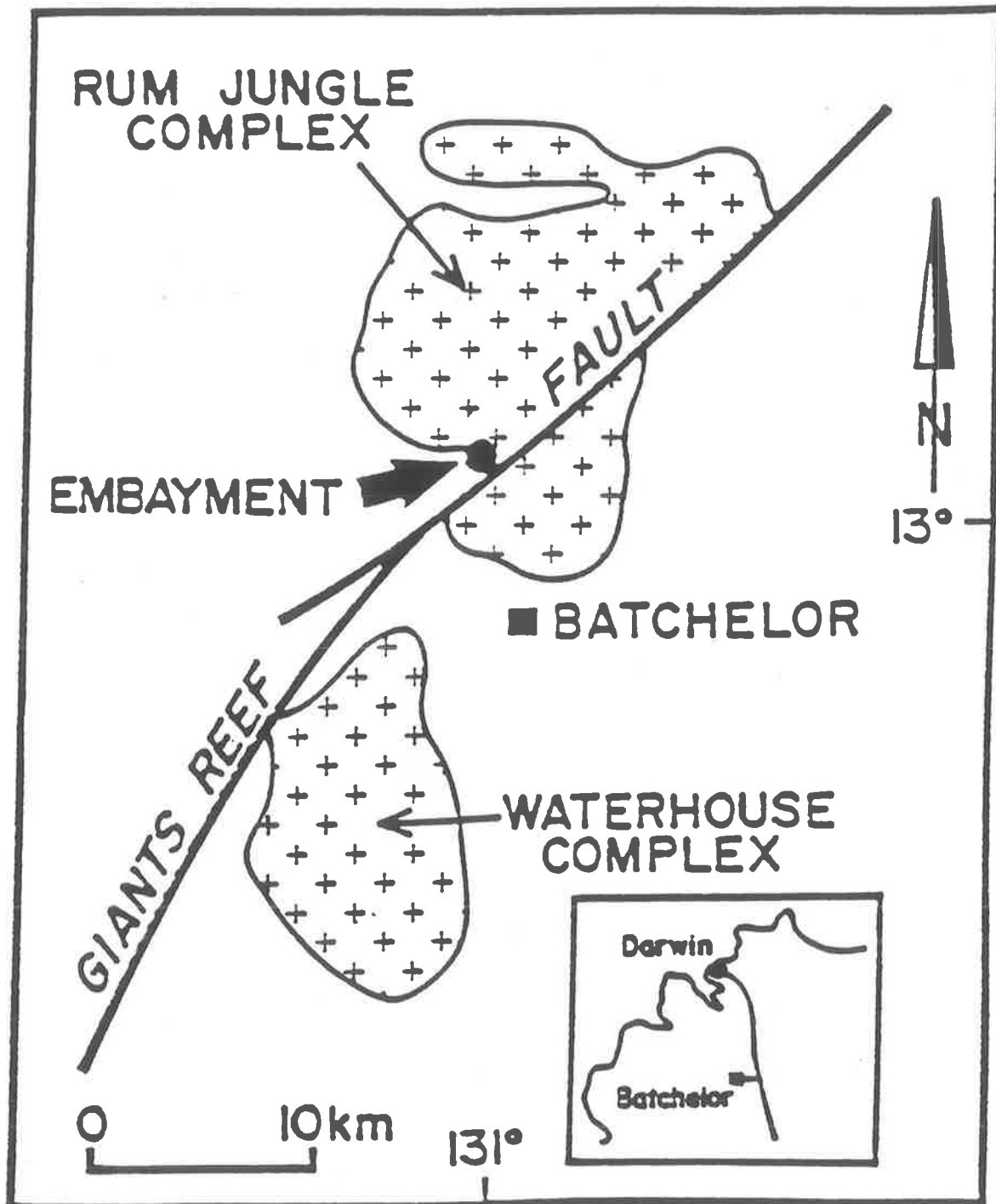
Fig. 5: Locations of Archaean age Complexes, Rum Jungle area.

(Paterson et al., 1984)

pseudomorphs. If this were so, then strong constraints would be placed on any genetic model proposed for the magnesite.

The role played by magnesite in U and/or mixed metal sulfide mineralising events was also considered.

The majority of the U deposits in the East Alligator Uranium Field and the Rum Jungle Uranium Field (Fig. 4) (Eupene, 1980; Berkman and Fraser, 1980) are closely associated with coarsely crystalline magnesite (Berkman and Fraser, 1980), the Nabarlek deposit being the exception (Fuzikawa, 1980). At Rum Jungle, some of these U deposits also contain mixed metal sulfides (Fraser, 1980). These are hosted by graphitic, chloritic, pyritic shales, either adjacent to magnesite, or as at Mt. Fitch, actually within the magnesite. So, both U and mixed metal sulfides became secondary targets.

As the Pine Creek Geosyncline has been the source of quite high grade deposits of Sn and Au, these also were added to the list of minor targets.

Many different mineralising models were proposed at the International Uranium Symposium on the Pine Creek Geosyncline held in Sydney in 1979. As a result, accurate determination of both the temperature(s) and the composition(s) of the fluids involved in the formation of the gangue minerals i.e. the magnesite and the co-existing quartz were needed. For instance, one model (Eupene, 1980) suggested that the U was "washed" into sinkholes, thus presenting a palaeokarst surface of carbonate topography as an important parameter.

10
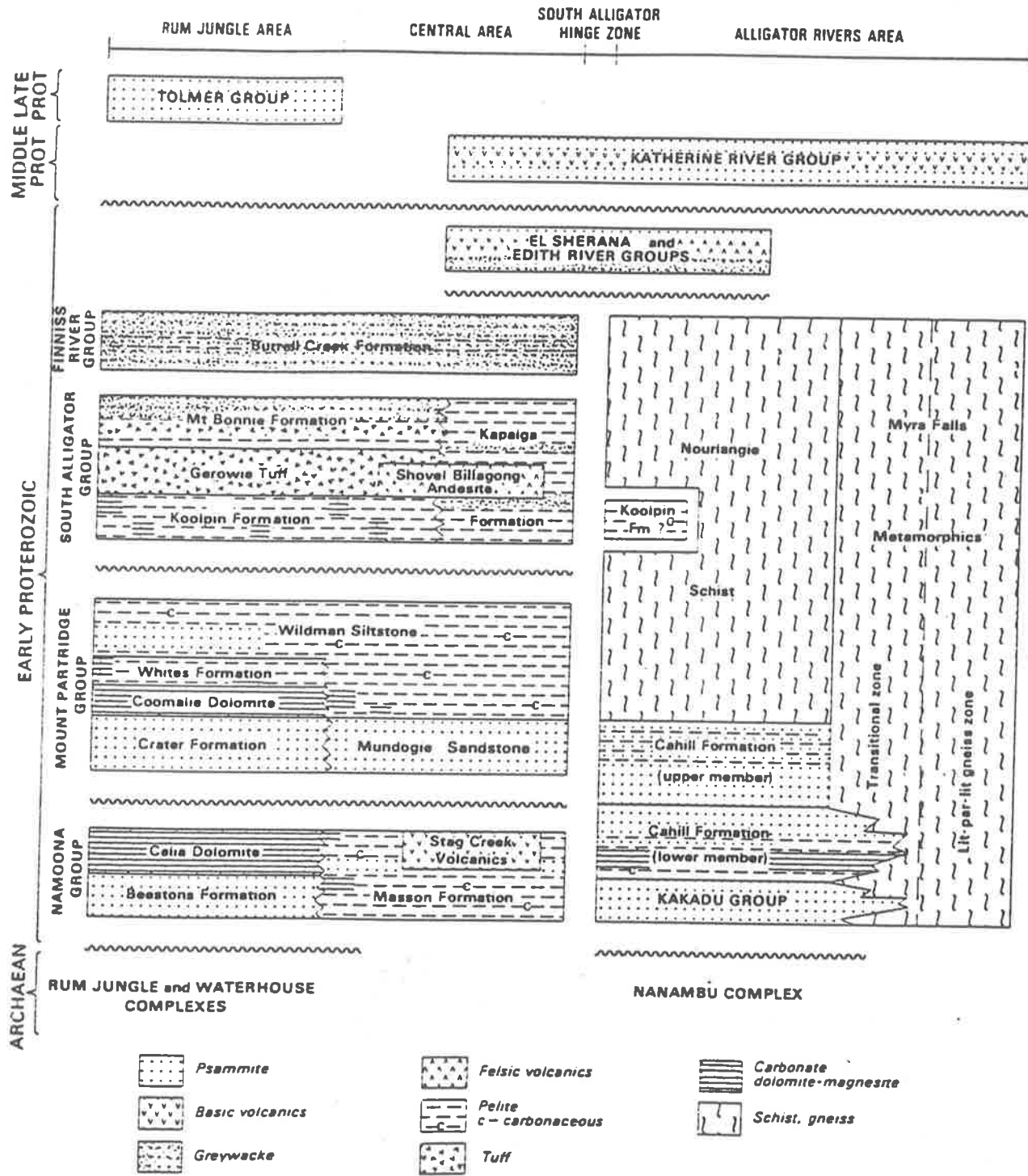
Fig. 6: Diagrammatic stratigraphy of the Pine Creek
Geosyncline

(Ewers et al., 1984)

It was hoped that by determining (1) the source of the U and the metals, (2) the source of the S within various units and the ore-bodies, (3) the temperature and possible composition of the fluids involved and (4) chronostratigraphic control, genetic models for the ore bodies could be developed - which could assist exploration, both at Rum Jungle and elsewhere.

Many other interesting questions of geological significance were briefly addressed. Such aspects include:-

1. Did gravity thrusting down the flanks of the diapirically rising domal complexes bring about a repetition of units in the onlapping sequence?

2. What is the significance of the conformable tourmaline-rich strata, which are the lateral equivalents of magnetite-quartz horizons?

3. What, is the cause and significance of the hematite quartz breccia, which frequently caps all the ore deposits at Rum Jungle?

4. What is the significance of indications of radiation damage in the overlying Mid-Proterozoic Depot Creek Sandstone (Tolmer Group).

1.5 Techniques employed

The techniques used to try to solve these problems will be dealt with in more detail in the appropriate chapters. Suffice to say that the project started with extensive field mapping followed by reconnaissance exploration i.e. drilling, geochemical and geophysical surveys. This work provided the base line, the samples and the data around which the laboratory investigations were planned and implemented. The laboratory

PLATE 1

12

a.   Basal conglomerate from the Crater Formation, E.L. 1349. The
      predominantly rounded clasts are highly siliceous, including the
      reworked Basement Complex pebbles. The matrix is highly
      ferruginised and siliceous.

b.   Magnesite outcrop, Celia Dolomite, E.L. 1349. The local term
      inology for these lichen coated, and hence dark grey coloured,
      outcrops is "elephants" The name also stems from the similarity
      between a group of these outcrops and a herd of elephants. The
      outcrops have relatively vertical sides and flat to slightly
      rounded tops.

c.   "Mafic schist" within the Celia Dolomite magnesite, Area C, E.L.
      1349. The rock is now a foliated sericite/chlorite rich rock,
      which contains up to 50% iron oxides. It is possibly an
      intercalated tuffaceous layer. The left hand one-fifth of the
      photograph shows banded quartz/tourmaline rocks - or tourmalinite.

techniques consisted of petrography, X-ray fluorescence
spectroscopy (X.R.F.), X-ray diffraction (X.R.D.), electron
microprobe analyses, thermoluminescence, S-isotope studies and
fluid inclusion studies, with the latter technique being the
major technique used.

PLATE 2

a.   Cross beds within the Crater Formation, E.L. 1349. Rock is an
     arkosic sandstone.

b.   Symmetrical ripple marks in a coarse sandstone in the Crater
     Formation, E.L. 1349.

c.   Coarse conglomerate at the base of the Crater Formation, E.L.
     1349. Many of the clasts have been derived from the Basement
     Complexes. The Crater Formation dips away from the Basement
     Complexes in a radial fashion (Fig. 2).

CHAPTER 2

GEOLOGICAL SETTING OF RUM JUNGLE

2.1 Introduction

The geographical area of Rum Jungle is situated in the
western third of the Pine Creek Geosyncline (P.C.G.S.) in the
Northern Territory, Australia, and is about 70 kms. south of
Darwin (Fig. 4). The area is referred to as the Rum Jungle
Uranium Field. The small township of Batchelor is in the
centre of this area.

The geology of the Rum Jungle area was first mapped and
described in detail by Walpole et al. (1968). Since then there
have been substantial changes in interpretation, culminating in
the many papers presented at the International Atomic Energy
Agency (I.A.E.A.) Conference "Uranium in the Pine Creek
Geosyncline" held in Sydney in 1979, which were published in
1980 in a publication of the same name (Needham et al., Stuart-
Smith et al.). In the ensuing years, work stimulated by that
conference has seen yet more re-interpretations, (Needham and
Stuart-Smith, 1983, 1984; Needham et al., 1984).

Briefly, the Pine Creek Geosyncline is Early Proterozoic
in age, consisting predominantly of metasediments that either
onlap or have been updomed by Archaean to Early Proterozoic
basement complexes. These metasediments are intruded by the
Zamu Dolerite (Bryan, 1962; Ferguson and Needham, 1978) and the
Oenpelli Dolerite (Stuart-Smith and Ferguson, 1978) followed by
Middle Proterozoic granites (Stephansson and Johnson, 1976).
The geosyncline is surrounded and/or overlain by the Middle

PLATE 3

a. Recrystallised magnesite showing bladed form. There is
    considerable variation in grain size. Outcrop 5, Area B, Celia
    Dolomite, E.L. 1349.

b. Recrystallised magnesite showing marble-like texture. Outcrop
    22, Area B, Celia Dolomite, E.L. 1349.

c. Recrystallised red and white coloured magnesite, illustrating
    that more than one recrystallisation event has occurred. The
    central white veins have a markedly different appearance to the
    peripperal white magnesite. Outcrop 21, Area A, Celia Dolomite,
    E.L. 1349.
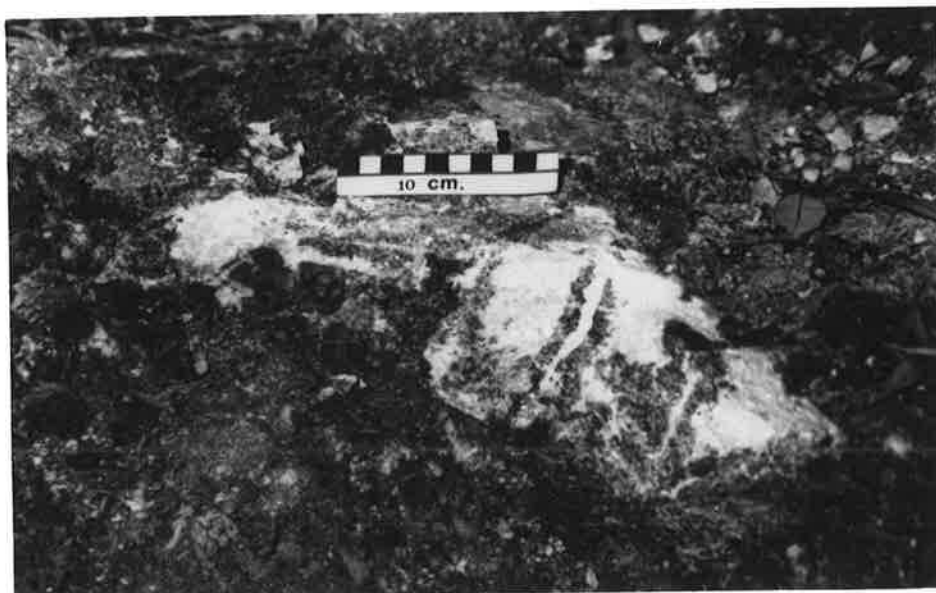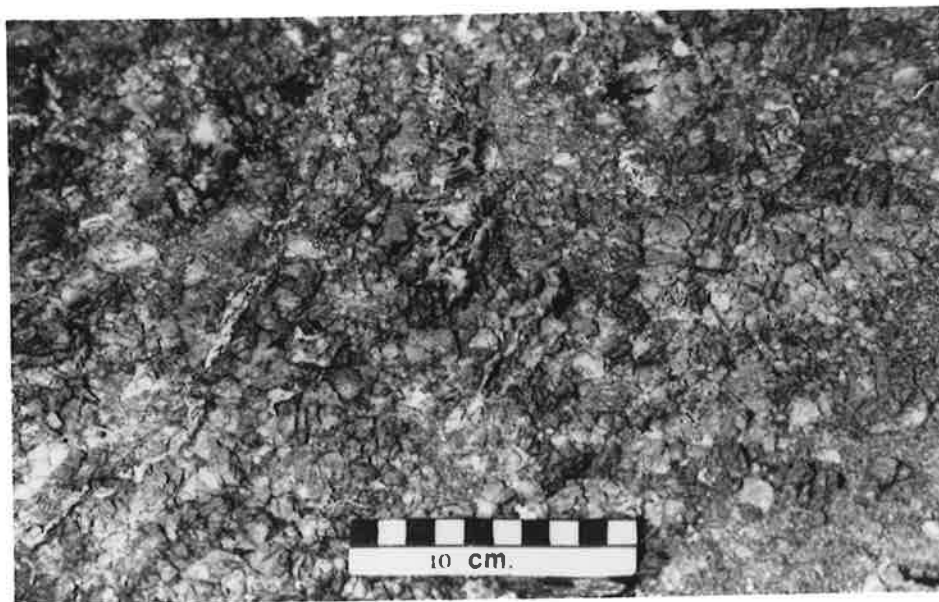
Proterozoic McArthur Basin in the east, the Palaeozoic
sediments of the Daly River Basin in the south and the Mesozoic
sediments of the Bathurst Terrace in the north. The western
margin of the Pine Creek Geosyncline is formed by the
Litchfield Complex of Archean or Early Proterozoic age, the
eastern margin is formed by the Nanambu (Fig.15).

2.2   Basement Complexes

In the Rum Jungle area, rocks of proven Archaean age occur
(Richards et al., 1977; Page et al., 1976, 1980). They are
collectively known as the Rum Jungle and Waterhouse Complexes
(Fig. 5). They consist of several granites and gneissic
granites, laced by pegmatitic dykes and veins, tourmaline -
quartz veins, plus amphibolites. Within the Complexes,
metasediments, banded iron formations, volcanics and metabasics
occur, which are thought to be older than the oldest of the
granites. Although Johnson (1974) recognised these same units
in both Complexes, the granites themselves are distinctly
different. The youngest granite (a leucocratic phase), based
on field relationships established by Needham et al. (1980)
gives an age of 2,400 Ma (Richards and Rhodes, 1967; Page et
al., 1980). Page et al's work employed combined U-Pb zircon
and Rb-Sr whole rock data which led to the same results.

The Complexes appear to be similar to Eskola's (1948)
classical mantled gneiss domes (Rhodes, 1965), often due to
some form of solid-state diapirism. Stephansson and Johnson,
(1976) suggested that this type of diapirism was due to the
later injection (may be the 1,800 Ma orogeny) of as yet unseen
granites into the roots of the Complexes, causing the doming.

a.   Coarse, crystalline quartz completely replacing an algal
        structure. The quartz bleb has a thin rim of pink talc. Outcrop
        88, Area B, Celia Dolomite, E.L. 1349.

b.   Quartz replacing algal structures within magnesite of variable
        grain size. Outcrop 8, Area A, Celia Dolomite, E.L. 1349.

c.   Fine-grained quartz replacing algal structures within magnesite.
        The cores of the algal structures are still magnesite. The outer
        skin of the quartz/algal structure is moulded after rhomb-type
        magnesite, indicating that the quartz replacement occurred after
        the magnesite had recrystallised. Outcrop 15, Area D, Celia
        Dolomite, E.L. 1349.
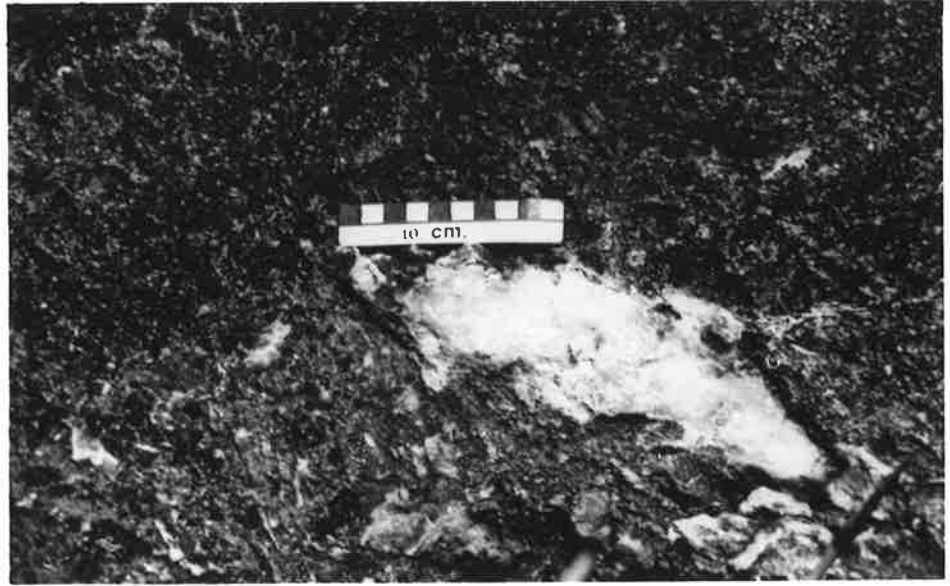
The granites do not belong to any particular type, but rather there is an approximately equal distribution of S and I type represented (Ferguson et al., 1980). The suggestion has been made that the Complexes are analogues to the Nanambu Complex in the P.C.G.S. (Walpole et al., 1968; Needham et al., 1974; Dodson et al., 1974) - an idea that has not been refuted as yet. The Complexes in both areas may well be the source of the U and Th in the respective R.J.U.F. and East Alligator Uranium Field (E.A.U.F.), as Ferguson and Weiner (1980) record anomalous U values in the former and McAndrew and Finlay (1980) have reported accessory uraninite in the latter.

2.3 Geosynclinal Sedimentation

The stratigraphic nomenclature used in this thesis will be that of Ewers et al. (1984) (Fig. 6), which differs from that of Walpole et al., (1968) and that adopted for the I.A.E.A. Symposium (1980), as this is the most recently published. However, further changes may occur again because an interpretation of the results of this study suggest the possibility of repetition of stratigraphic units due to gravity thrusting. However, for the purpose of this chapter, the stratigraphy of Ewers et al. (1984) will be used.

The Namoona Group (Beestons Formation and Celia Dolomite) and the unconformably overlying lower two units of the Mount Partridge Group (Crater Formation and Coomalie Dolomite) are shallow water assemblages of conglomerates, arkoses, arenites, minor shales, siliceous carbonates, magnesites and minor dolomites, with intercalations of possibly tuffaceous layers (Plate 1).

PLATE 5

a.   Quartz replacing algal structures in two stages: firstly,
      replacement of the rim by chert, which rapidly inverts to
      fine-grained quartz and secondly, replacement of the algal core
      by coarsely crystalline quartz. Outcrop 11, Area C, Celia
      Dolomite, E.L. 1349.

b.   Replacement of stratiform stromatolites by quartz. Host is
      magnesite. Celia Dolomite, Fossil Reserve, E.L. 1349.

c.   Stratiform stromatolites replaced by quartz in fine-grained
      magnesite. Preferential weathering of the magnesite has left the
      quartz protruding above the surface. Outcrop 6, Area D, Coomalie
      Dolomite, E.L. 1349.
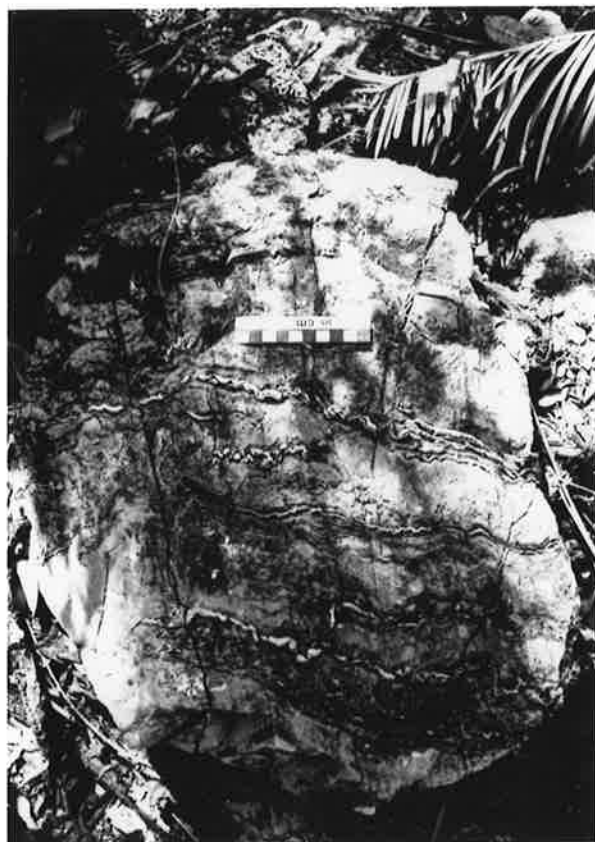
The lowermost unit, the Beestons Formation, rests unconformably on the Basement Complexes, with an excellent example of the onlapping relationship seen north-west of Batchelor (I.A.E.A. Excursion Guide, 1980). There are no major differences between the fluviatile Beestons Formation and Crater Formation, with both having the Complexes as their provenance i.e. detritus shed off the palaeogeographic highs. Both formations share an anomalously high detrital Th content. Both show evidence of their sedimentary nature, with examples of cross-bedding and ripple marks being quite common (Plate 2). Both have coarse conglomerates at the base (Plate 2), fining upwards beds, with heavy mineral banding being ubiquitous. This latter material may have been derived from the banded iron formations within the Complexes.

Fraser (1980) states that the unconformity between the Complexes and the overlying unit is commonly sheared, and that this contact shows quartz-filled tension gashes. More recently Needham and Stuart-Smith (1983) have commented that the base of the Crater Formation also "is invariably sheared", thus unintentionally lending support to the stratigraphic repetition idea previously suggested. However, they have suggested that the Beestons Formation and the Celia Dolomite are facies variants of the central geosynclinal Masson Formation and Stag Creek Volcanics of the Namoona Group, (Fig 6).

The two carbonate units, the Celia Dolomite and the Coomalie Dolomite which follow the clastic Beestons and Crater Formations show very few differences at all. They are predominantly recrystallised magnesites (Plate 3), containing visible silica, primarily in the form of chalcedony and quartz

PLATE 6

a.   A coarsely-crystalline quartz bleb (replaced algal structure)
     rimmed with a thin skin of pink talc. The host magnesite is
     variable in grain size. Outcrop 12, Area B, Celia Dolomite, E.L.
     1349.

b.   A quartz bleb (replaced algal structure) showing the rim like
     nature of the pink talc. The talc is identifiable by the many
     scratches on its soft surface. Sample C43, Celia Dolomite, E.L.
     1349.

c.   The reverse side of sample C43, showing the coarsely crystalline
     nature of the quartz and the variable thickness of the rim of
     talc.
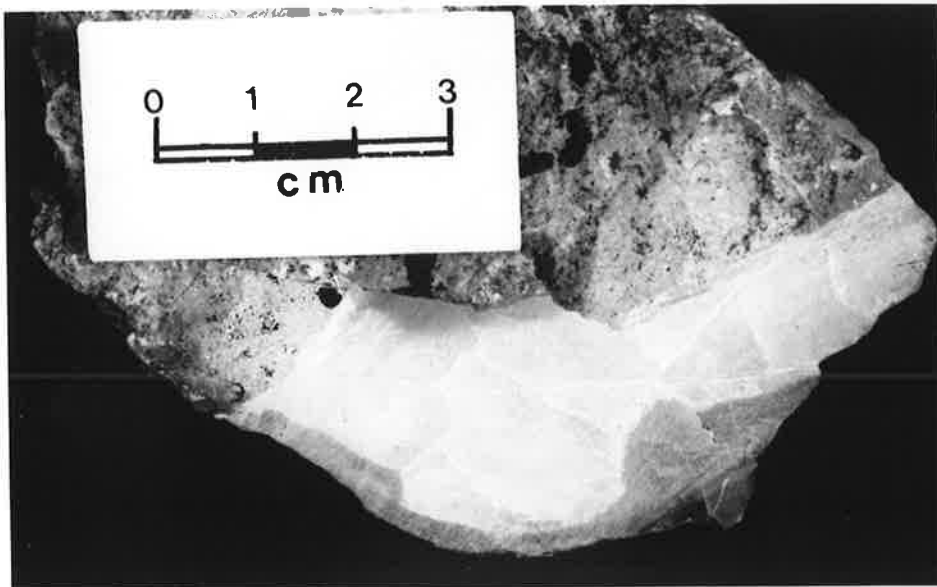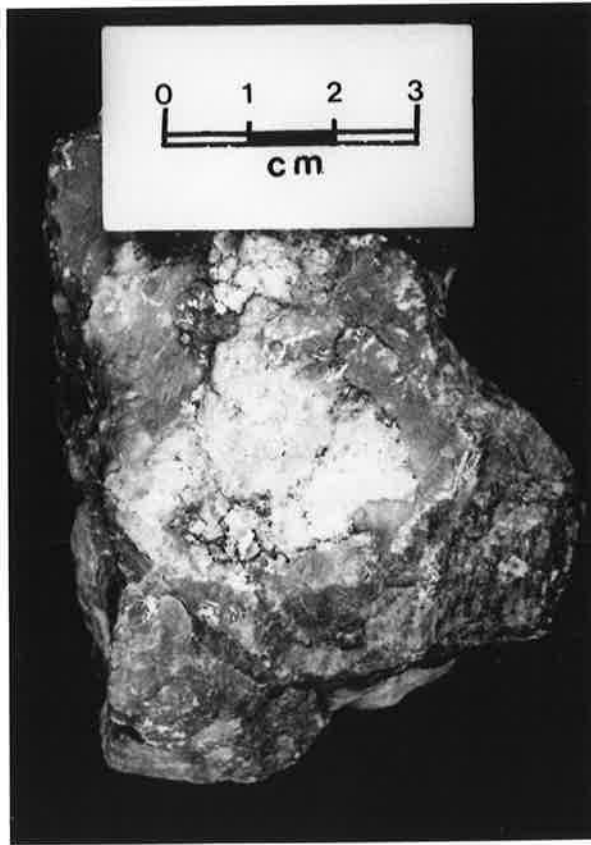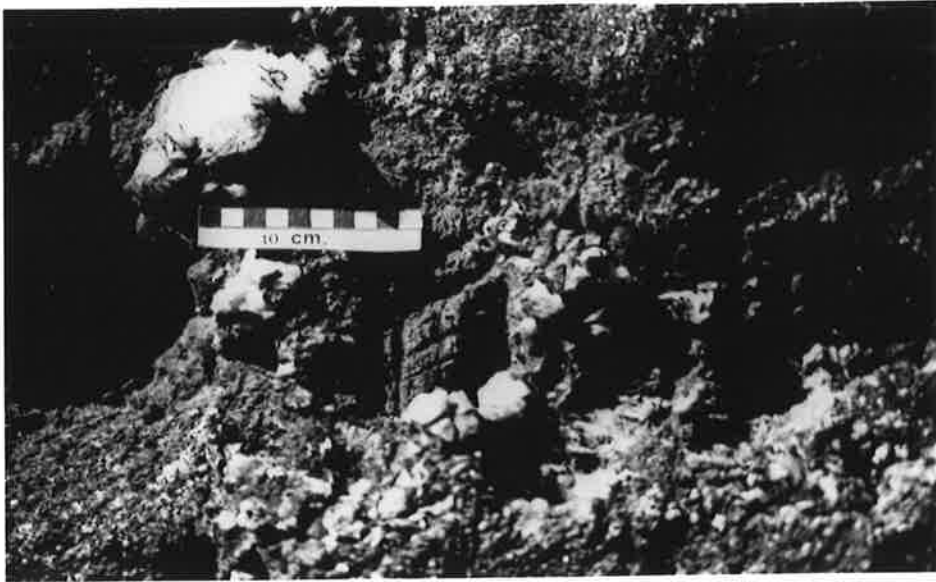
- mainly as replacement of algal structures (Plates 4, 5). Other silicates include talc, which often rims the quartzose algal structures (Plate 6) and chlorite, which is concentrated along stylolites, the latter being mainly parallel to bedding. In places, podiform silicification of entire magnesite areas has occurred (Fig. 7), often still quite clearly preserving algal structures, (Plate 7). These magnesites probably formed as primary carbonates in a series of large, alkaline lakes which were peripheral to the Complexes (Bone, 1983). In places, the units are dolomitic e.g. Mount Fitch.

The four Formations contain "mafic schists" (Roberts, 1978) and banded tourmaline-quartz beds (Plates 1, 7). These are probably tuffs and their distal equivalents. These tourmaline-quartz beds are quite distinct from the tourmaline-quartz veins which originate from the Complexes, having different mineral chemistries and formation temperatures (Chapt 4).

This new stratigraphic nomenclature makes the well known terms "Batchelor Group" and "Golden Dyke Formation" redundant.

Conformably overlying the Coomalie Dolomite is the Mount Partridge Group's Whites Formation, which is the Rum Jungle region's equivalent of the Wildman Siltstone (Central Region) and the Nourlangie Schist (Alligator Rivers Region) (Needham and Stuart-Smith, 1984). This unit was until recently known as the Masson Formation; and before that as the Golden Dyke Formation. It is host to the majority of the U and polymetallic sulfide mineralisation in the Rum Jungle area (Fig. 8). The unit is a massive, dark grey to mottled grey-

PLATE 7

a.   Complete silicification of magnesite and algal structures. The
      latter are still quite clearly discernible, and appear to be
      Conophyton type stromatolites. Fossil Reserve, Celia Dolomite,
      E.L. 1349.

b.   Banded tourmaline - quartz rock i.e. tourmalinite. All the dark
      material is tourmaline except for the light grey euhedral
      crystals in the quartz layers, which are diagenetic pyrite
      crystals. Sample B09, Beestons Formation, E.L. 1349.

c.   Massive, dark grey calcareous lutite from Whites Formation. This
      outcrop is approximately 20 m. above the top of the Coomalie
      Dolomite, E.L. 1349, Area B.
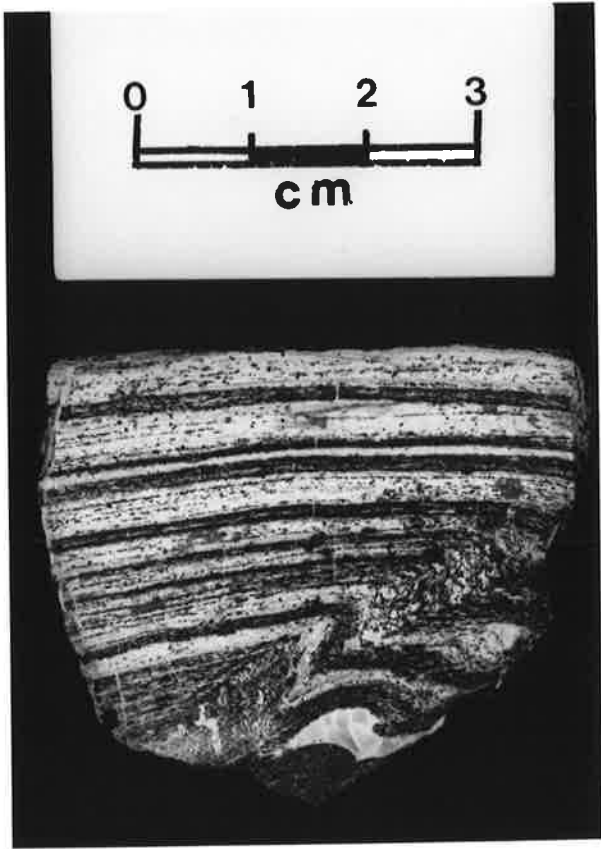
white calcareous shale/lutite (Plate 7), which contains pyrite, chlorite and sericite, intercalated with amphibolite and quartzite. The facies is indicative of a deeper water environment than that of the underlying units. No algal relicts have been observed within it. The provenance was also different, coming from the north and or west. Lithologically, the Whites Formation correlates more with the Cahill Formation in the Alligator Rivers region and the Masson Formation in the Central region than with the Formation already mentioned (it is also worth noting that the Cahill Formation is the U-host in the Alligator Rivers region (Needham and Stuart-Smith, 1976)).

Apart from the much younger (?Middle Proterozoic - more definite age unknown, Needham et al, 1980) Depot Creek Sandstone of the Tolmer Group, these are the only Formations studied and of interest to this project. The reader interested in other stratigraphic correlations is referred to Needham and Stuart-Smith 1984. The Depot Creek Sandstone probably played a role in the preservation of the mineral deposits, analagous to that envisaged for the Kombolgie Sandstone in the Alligator Rivers region (Hochman and Ypma, 1984).

2.4 Mineralisation

Uranium mineralisation is "undisputably stratabound in the main" (Needham et al, 1980) and is hosted by Whites Formation in the Rum Jungle area. This stratigraphic Formation is quite widespread, but only mineralised where outcropping granitic Archaean basement is within the immediate vicinity i.e. within 10 kms. However, these two parameters also occur without accompanying mineralisation, so that at least one other controlling factor is apparently required. It is here that the
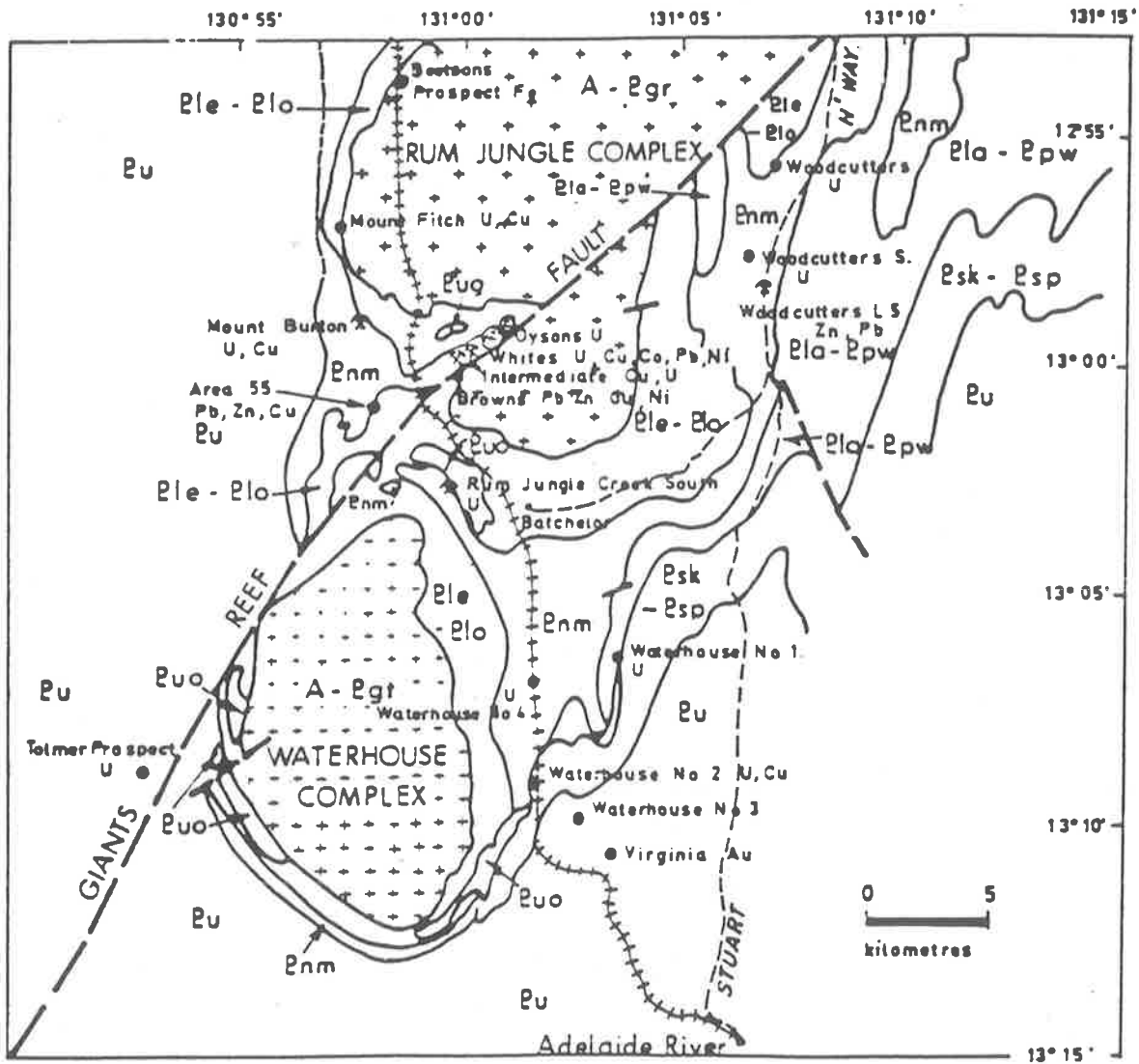
Fig. 8: U and polymetallic sulfides – mines and prospects
PuO Tolmer Group
Pu Finniss River Group
Psk-Psp South Alligator Group .
Pla-Ppw) Mount Partridge Group
Pnm-Plo)
Ple Namoona Group
A-Pgr-A-Pgt Archaean   (after Fraser, 1980)

role of magnesite assumes importance, for all the deposits are in even closer proximity to magnesite bodies than they are to any other apparent source rock (Fig. 8). This is also true for all the Alligator Rivers region deposits, except Narbarlek.

The significance of this spatial relationship can be outlined as follows: fluids passing through the magnesite contain carbonate complexes, which are suitable for the leaching of U (Chpts 3, 4, 6). The subsequently formed U carbonate complexes are transported, until appropriate changes in Eh-pH cause the precipitation of the U (Langmuir 1978).

Even this model is not comprehensive, for it can also be shown that all the deposits are associated with chloritisation, which in places is quite massive (Needham and Roarty, 1980), by Mg-rich chlorites. The apparent Mg-metasomatism could be related to the dissolution of magnesite.

Another control factor is the capping by plateau-type sandstones i.e. the Kombolgie Sandstone in the east and the Depot Creek Sandstone in the west. What role these cover rocks played, is still unresolved, but thermoluminescence studies are starting to shed some light on this issue (Hochman & Ypma, 1984).

In the Rum Jungle area there is also a number of stratiform and/or stratabound polymetallic sulfide deposits (Fig. 8). These are areas of higher concentration in an almost continuous mineralised rim-like structure around the Complexes (Fraser, 1980; Berkman and Fraser, 1980). In most cases they are co-incident with or overlap U concentrations, suggesting an interacting genesis. None of the deposits are currently being
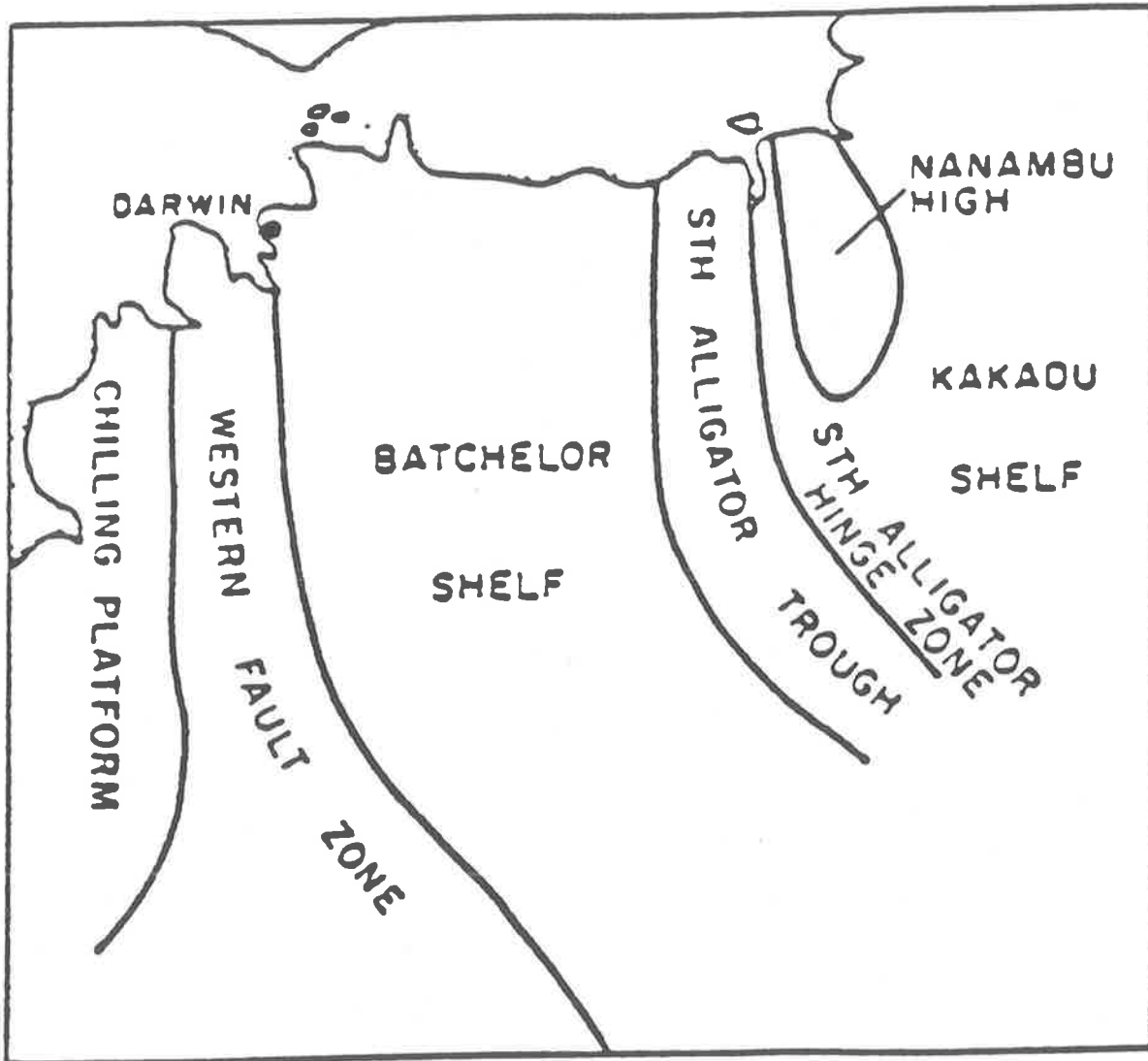
Fig. 9: Major structural elements of the Pine Creek Geosyncline.

(Stuart-Smith et al., 1980)

mined, although Geopeko expects to have the Woodcutters Deposit mine in operation in 1985. A detailed account of past mining operations, reserves etc. occurs in Fraser, (1980).

The various aspects involved with mineralisation e.g. source, formation temperature, transport mechanisms, structural control etc. will be discussed in the appropriate chapters.

2.5 Tectonic Setting

The structural elements that controlled the development of the Pine Creek Geosyncline are shown in Fig. 9. The evolution of the geosyncline involved the paralic deposition of Early Proterozoic sediments in an intracratonic basin developed by crustal sag. Maximum original thickness of this sedimentary pile may have been up to 20 kms. (Needham et al., 1980). Formation of the basin occurred between 1,870 and 2,470 Ma ago (Page et al., 1980). Stuart-Smith et al. (1980) have modelled this development into a 4-stage sequence, which although the stratigraphic nomenclature has since changed, as a sequence is still probably valid:-

"   1)   deposition of the Batchelor, Kakadu and Namoona
           Groups.

     2)   deposition of the Mount Partridge Group.

     3)   deposition of the South Alligators and Finniss River
           Groups, and dolerite intrusion; and

     4)   deformation, metamorphism, granite intrusion and
           erosion.   "

This model is illustrated in Fig. 10 and is discussed at length in their paper.
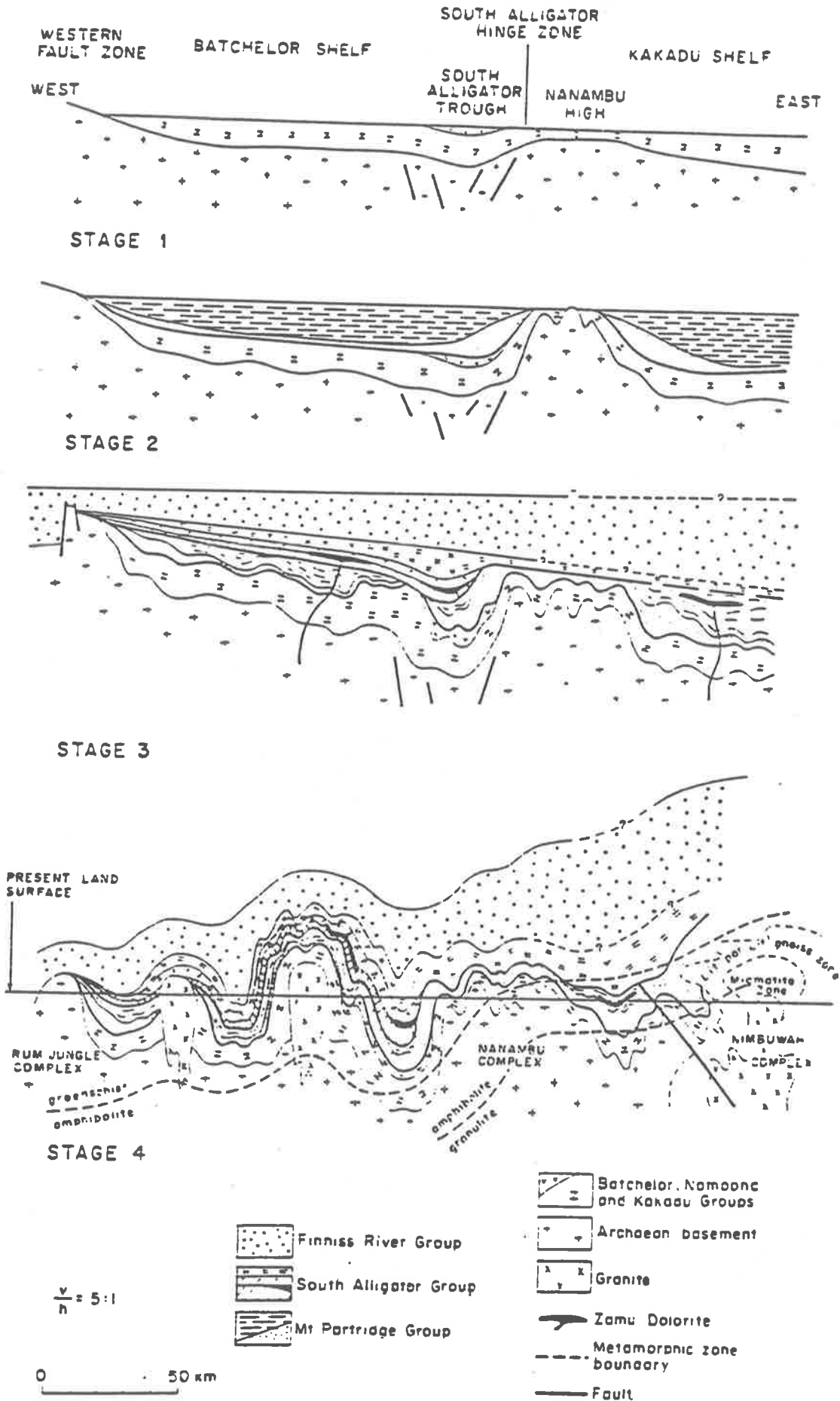
Fig. 10: Evolution of the Pine Creek Geosyncline
(Stewart-Smith et al., 1980)

An alternative tectonic model was proposed by Rossiter and Ferguson (1980). They suggested that the geosynclinal basin formed as a subsequence of rifting and movement of the Basement elements to their present position from a position approximately 500 kms SSW (Fig. 11). Locus of this wrench-shearing was along the Halls Creek Fault, and occurred approximately 1,800 - 1,700 Ma ago. This type of basin formation is usually accompanied by mafic intrusives, and the 1,700 Ma Oenpelli Dolerite (Page et al., 1980) fulfils this condition.

However, further extensive studies in the many Early to Middle Proterozoic provinces (Halls Creek, Pine Creek, Arunta, Tennant Creek, Gawler and Mt. Isa) have led to the development of a distinctive tectonic model specific to this period of time (Etheridge et al., 1984).

They list several main elements for their model:-
1. Two cycles of crustal (? lithospheric) stretching and consequent sag-type basin formation were separated by a major orogenic/magmatic event. These cycles can have four distinctly different phases (pre-rift phase; rift phase; sag phase and flysch phase), which can lead to the depositin of three sequences of differing tectonostratigraphic signature.

(a) Rift phase: quartz-rich and commonly fluviatile clastic sequence, with bimodal volcanism and intercalations. In the Rum Jungle area this is the Namoona Group according to Etheridge et al. (1984), but there is no apparent justification for not including the Crater Formation and the Coomalie Dolomite apart from the use of currently accepted stratigraphic

32
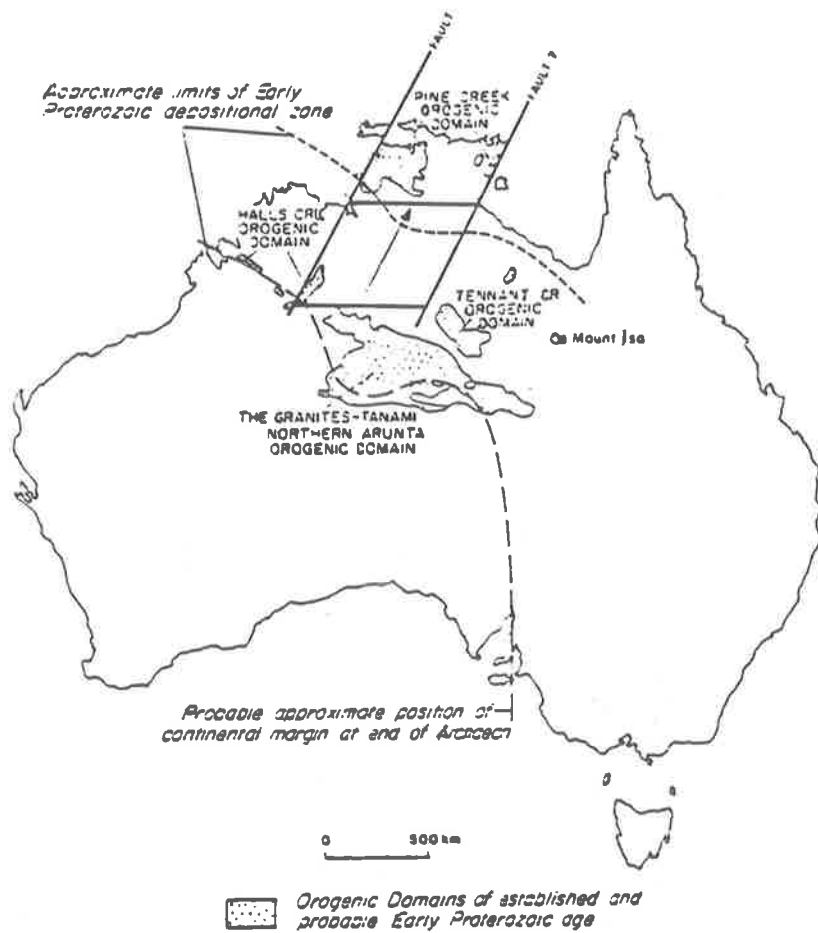
Fig. 11: Possible rifting and movement of
Basement elements.

(Rossiter and Ferguson, 1980)

correlations. These are basically the same as the two Formations (Beestons and Celia) selected; Moreover they do not fit the requirements for the next phase in time -

(b) Sag-phase: finer grained clastic sequence, usually carbonaceous, and with abundant carbonates and some Fe formations.

The sag-phase sedimentation has been equated by Etheridge et al (1984) with the Mount Partridge Group. However, the sag-phase sequence shows wide lateral extent - which is not the case for the Crater and Coomalie Formations, whereas the distribution and lithology of the Whites Formation and Wildman Siltstone fulfil these conditions.

(c) Flysch phase: turbidite or molasse facies. This phase may prelude the orogenic phase. In the Rum Jungle region this phase is represented by the South Alligator Group.

An orogenic event marks the end of this first cycle, which has been followed in other areas by a second cycle. The second cycle is not present at Rum Jungle.

However, prior to deposition of the second cycle, moderate deformation occurred in all the northern Australian provinces. An early nappe-style event was followed by a regional upright fold episode. Nisbet et al (1984) have reported early bedding-parallel thrusting in the east Pine Creek Geosyncline. Rarely is the Basement involved in the thrusting event, nor did the thrusting lead to widespread overturning or stratigraphic duplication.
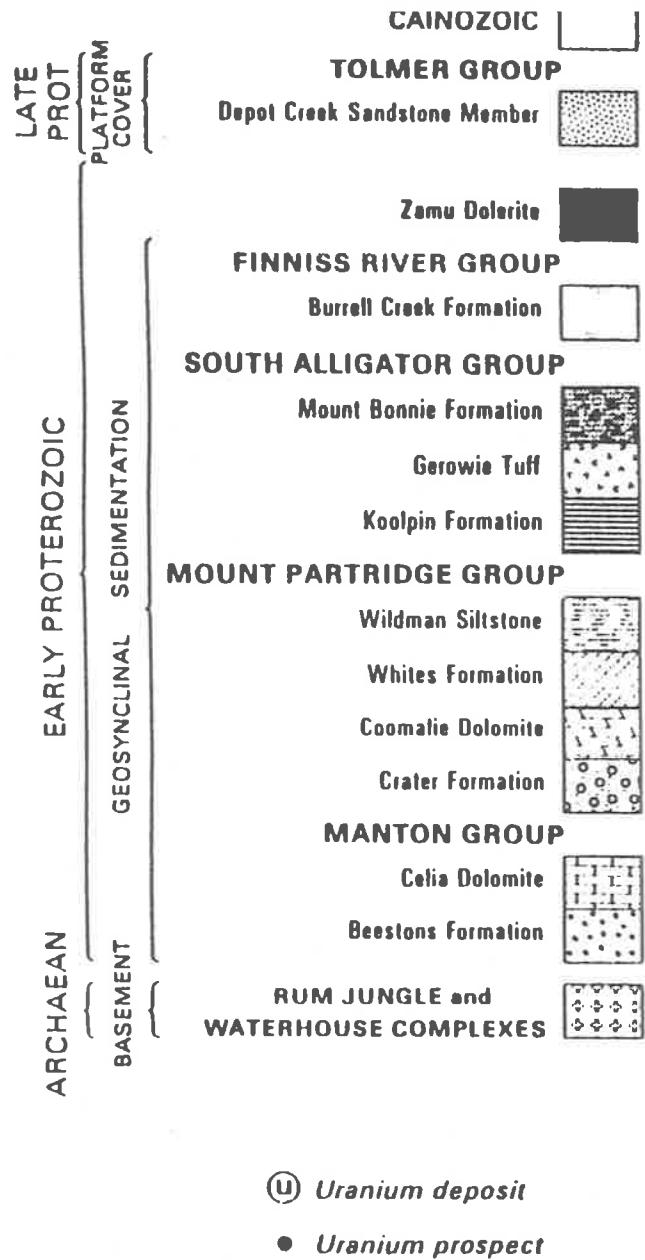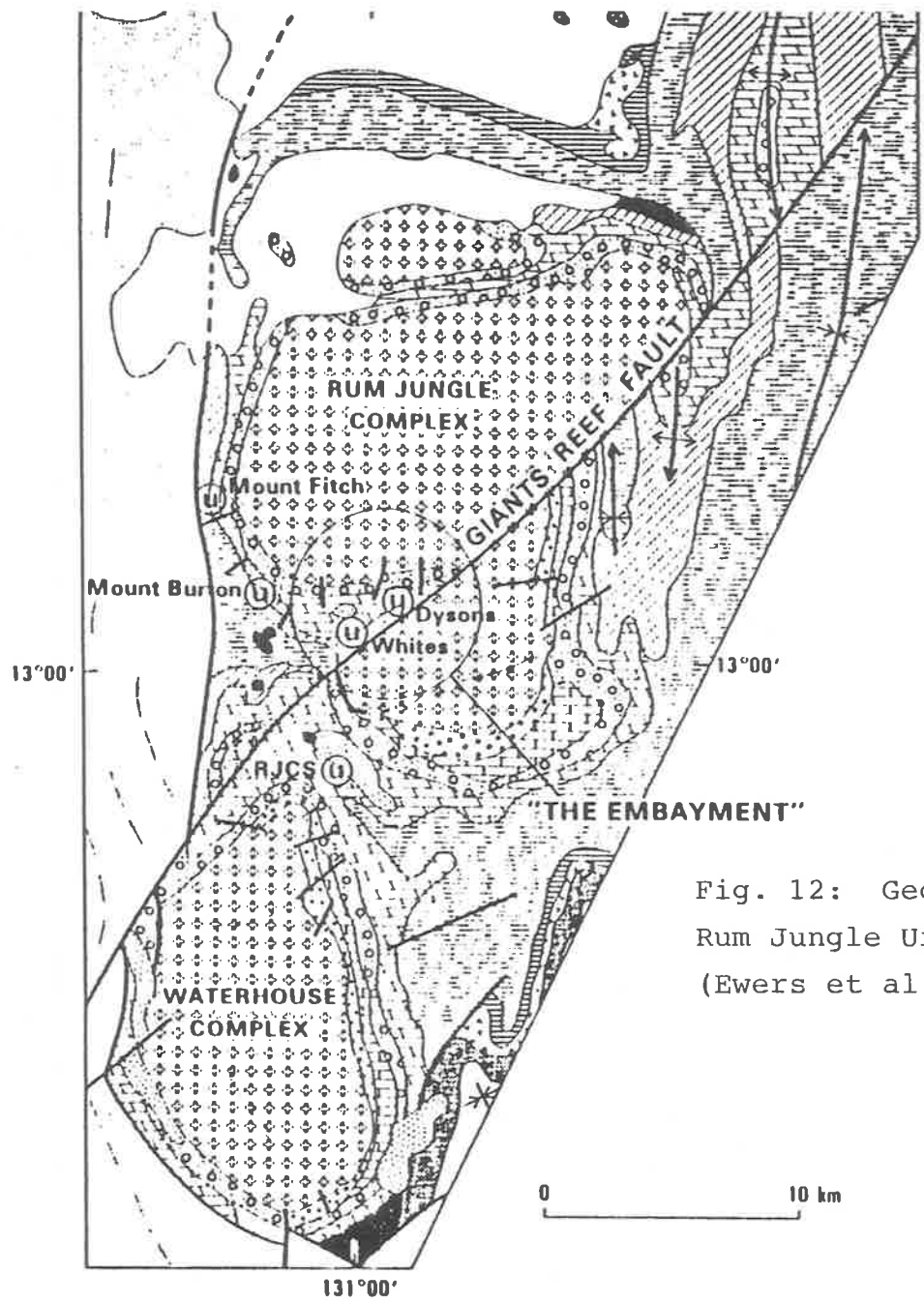
Fig. 12: Geology of the Rum Jungle Uranium Field (Ewers et al., 1984)

2. The rifting and mantle-derived magmatism were caused by small-scale convection cells within the mantle, initiated at about 2000-2200 Ma.

3. The upwelling mantle material was underplated below potential Early Proterozoic rifts and basins. Later, it was the source for extensive felsic magmatism (1750-1900 Ma).

4. The resultant sag-basin precludes the need for the formation of modern ocean floor material or island-arc development. Modern analogues are the North Sea and the Gippsland and Bass Basins.

5. Neither lateral accretion nor crustal thickening are evident in the Northern Proterozoic Basins even though orogenesis was widespread; but high heat flow was characteristic.

6. The second cycle is usually more locally developed (e.g. Mount Isa) but follows the same general pattern as the first cycle.

The Rum Jungle area is a classic example of the first cycle leading to a mid-orogenic phase of Etheridge et al's (1984) Proterozoic basin evolution model, providing the Crater Formation and the Coomalie Dolomite are relegated to the rift phase.

There have been at least four deformation events (Paterson et al., 1984) in the area, with the most spectacular being the north-east trending dextral wrench Giants Reef Fault (Fig. 5).
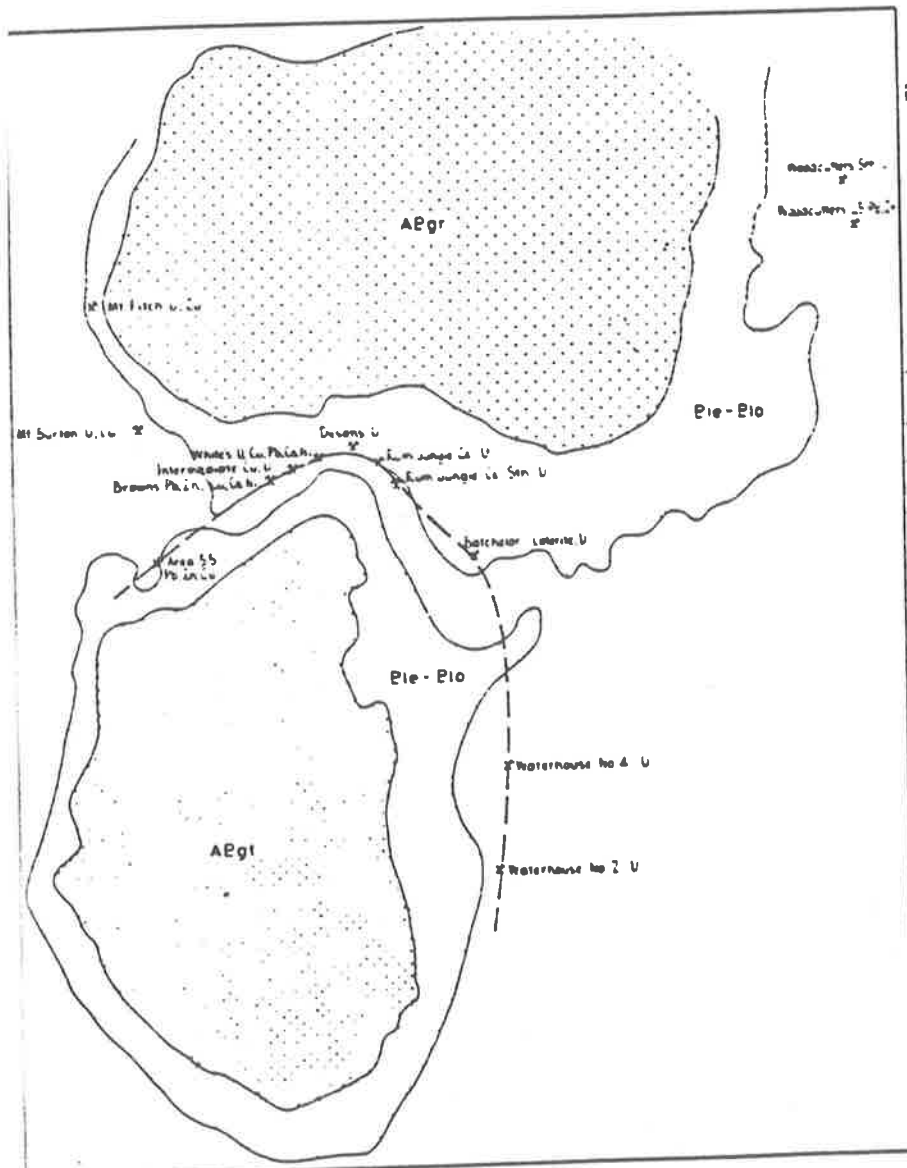
Fig. 13 :

RUM JUNGLE URANIUM FIELD
RECONSTRUCTION OF GEOLOGY
PRIOR TO
GIANTS REEF FAULTING

GEOLOGICAL REFERENCE

Namoona Group, Mt Partridge Group,
Finniss River Group

Pre-Pro Batchelor Group

APgr Rum Jungle Granite

APgt Waterhouse Granite

LEGEND

✺ Mine

✗ Prospect

--- Mineral Zoning Trend

(Fraser, 1980)

Movement along the Giants Reef Fault led to the displacement of a wedge-shaped mass of sediments, known as the Embayment (Fig. 12), and it is here that the greatest density of areas of concentration of mineralisation occurs. Shearing is commonly seen within the sediments proximal to the Giants Reef Fault, due to tension flexure folding. The Main Shear Zone (Thomas, 1956) is parallel to the Giants Reef Fault, and is associated with Browns, Dysons, Intermediate and Whites Deposits. This suggests that this structural trap, related to porosity, was partly instrumental in mineral deposition; but, there are no known concentrations of mineralisation along the Giants Reef Fault itself - which would surely have been a favourable site. Superimposing the deposits on a reconstruction of the geology of the Rum Jungle area prior to Giants Reef Faulting (Fig. 13) suggests only a stratigraphic control, with no structural element involved apart from that associated with the diapiric effects from the Complexes.

The study of Landsat imagery by Simpson et al. (1980) has shown that there are other lineament trends (Fig. 14) that may have played a role in the development of the mineral deposits e.g. two lineaments trending 100° and 110° intersect the Giants Reef Fault near Whites Deposit. This trend is the same as the main joint pattern seen in both magnesite sequences, especially on the eastern side of the Rum Jungle Complex.

2.6 Metamorphism

Regional metamorphism patterns in the provinces discussed above, and Rum Jungle in particular, do not reflect modern orogenic domain patterns. Rather, low to medium pressure metamorphic facies have developed as a result of the upright
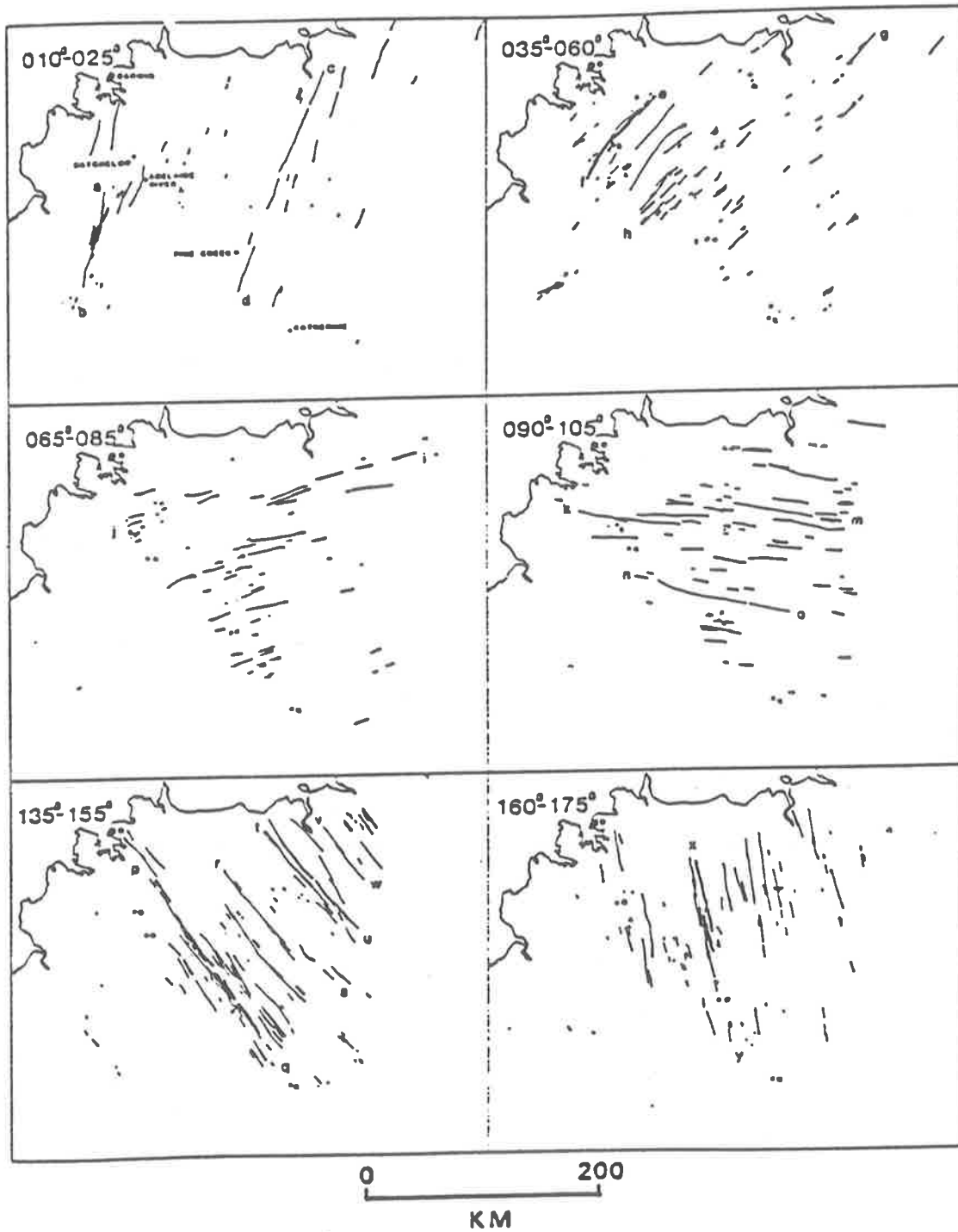
Fig. 14: Plots of specific trends and zones of all
interpreted lineaments, mapped faults, veins, linear
dykes and linear magnetic anomalies within
pre-Middle Proterozoic rocks.

(Simpson et al., 1980)

folding deformation event; with an added thermal imprint which may have been caused by the widespread and massive underplating of the crust.

Nevertheless, the Pine Creek Geosyncline can be broadly subdivided into two regional metamorphic domains. The northerly trending South Alligator Hinge Zone can be used as the dividing line (Fig. 15); with the rocks to the east (Province 1 - Ferguson, 1980) belonging to medium- and high-grade metamorphism, whilst those to the west (Province 2) are low-grade. Within Province 2, late orogenic granitoids have been responsible for localised areas of contact metamorphism.

In the Rum Jungle area, there is evidence of contact metamorphism e.g. dolerite to amphibolite. Scapolite has been reported (Stephenson and Johnson, 1976); and both in the hand specimen and petrographically the mineral could be accepted as being scapolite. However, microprobe analyses of these "scapolite" bearing rocks revealed that the mineral is a very "bleached" tourmaline.

The presence of minerals such as talc, actinolite and chlorite indicate lower greenschist facies metamorphism.
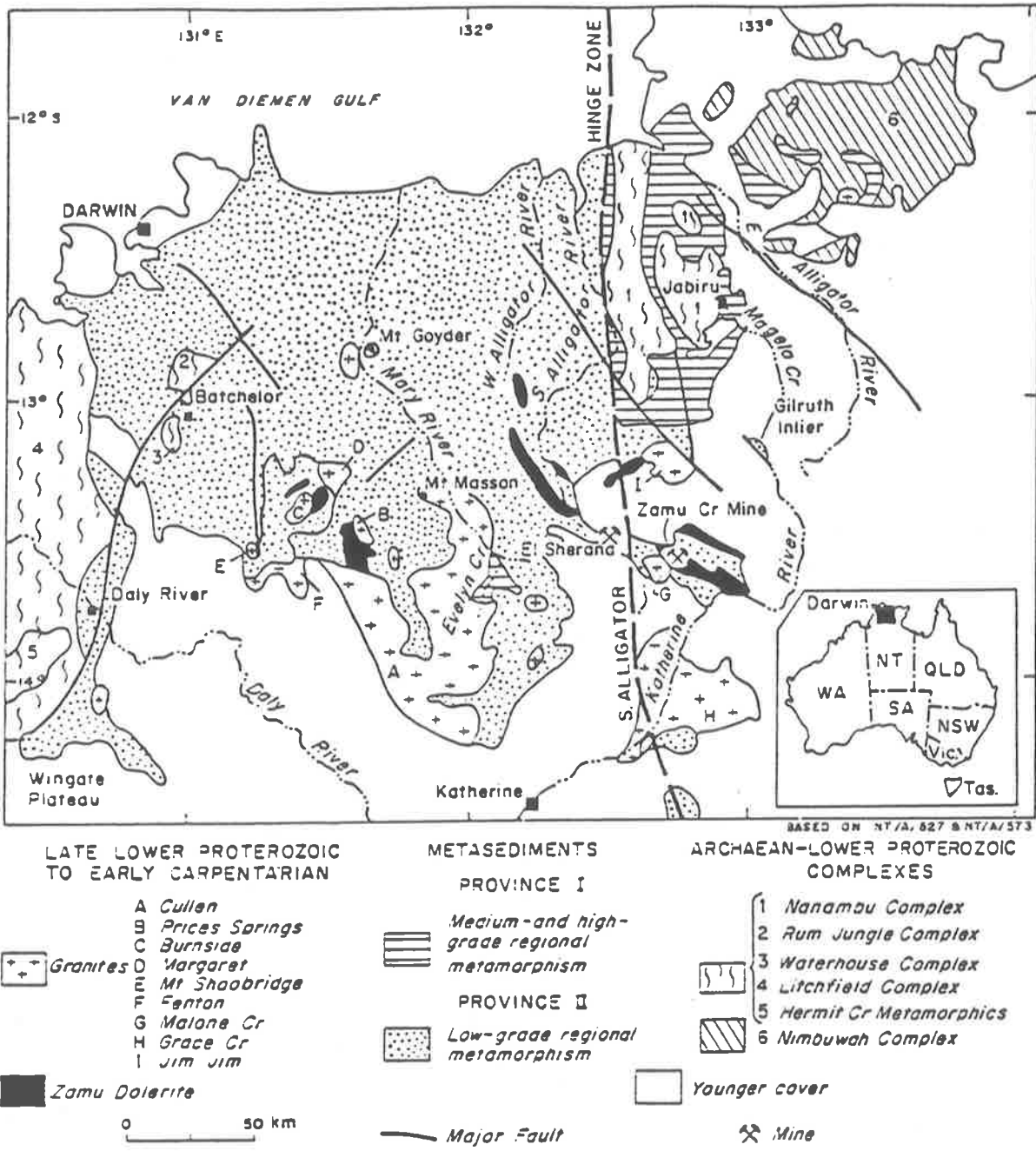
Fig. 15: Generalised geology of the Pine Creek Geosyncline showing broad metamorphic divisions

(Ferguson, 1980)

CHAPTER 3

MINERALOGY, CHEMISTRY AND GENESIS OF MAGNESITE

3.1 Economic Aspects

Magnesite has always been considered a relatively uncommon magnesium carbonate ($MgCO_3$). The mineral occurs in both modern and ancient carbonate sediments and also as as an hydrothermal and/or weathering product in comparatively small quantities.

The major use of magnesite within Australia is as a refractory, particularly within the steel industry, where it is used in the preparation of bricks for the linings of metallurgical furnaces. It is also used as a component in insulation products; and for the manufacture of other industrial minerals e.g. epsom salts, magnesia; further uses include additives in animal feedstocks and in fertilizers. None of these uses require large tonnages nor is magnesite a high cost raw material. Consequently it has never become a high order target in exploration in Australia. Nevertheless, it is advantageous, providing it is economically sound, for Australia in general and B.H.P. in particular, to be self sufficient in the raw materials needed for manufacturing purposes. Hence, it has become a low-order exploration target.

For magnesite to be suitable for use in refractory bricks the raw material needs to very pure e.g. <10% silica and preferably <5%, as the dead burning process whereby the magnesite is converted to MgO, with the release of CO_2, has the

TABLE 1

MAGNESITE QUALITY

Dead Burned Magnesite

Top Grade	Medium Grade		
93%	87%	MgO	(Min.)
3%	5%	SiO_2	(Max.)
1%	6%	$Al_2O_3 + Fe_2O_3$	(Max.)
	1.9%	CaO	(Max.)
1.6-2.5%		CaO/SiO_2	
0.05%	Low	B_2O_3	(Max.)

(Roberts, 1978)

effect of relatively doubling the content of impurities such as SiO_2. The acceptable quality/impurities are shown in Table 1. (Roberts, 1978).

At the high temperatures prevailing in the furnaces, silica reacts to form new minerals e.g. pyroxenes, thus precipitating the physical breakdown of the bricks. Similarly, refractory bricks with greater than 100 ppm B deteriorate much faster than B free ones.

The mineralogy and source of the Rum Jungle magnesite contaminants is discussed later in this chapter.

B.H.P. currently import their magnesite requirements from Greece. Thus transport costs render an intrinsically cheap raw material into a ludicrously expensive one. Hence, the generation of the target - an Australian magnesite deposit. The minimum size deposit which would be economically feasible to commission was set at 10 million plus tonnes, providing it could be mined by open-cut methods. B.H.P. holds leases on two known deposits containing reserves in excess of this figure - one at Rum Jungle, N.T., and the other at Balcanoona, S.A. The deposit at Balcanoona is situated in rough country in a declared National Park, approximately 350 kms NNE of Adelaide. A major road-building programme would be needed to develop the deposit, which would be an unlikely development due to environmental considerations.

The E.L. at Rum Jungle, on the other hand, does not have these problems. However, it does have the problem of silica contamination (& B) at levels which are above those acceptable for refractory brick manufacture without prior benefication.

a.   This magnesite sample has both the bladed and rhomb forms present. Superficially these forms resemble pseudomorphs after gypsum and halite, but in reality they are negative rhombohedra. Outcrop 127, Area C, Celia Dolomite, E.L. 1349.

b.   This sample of magnesite consists entirely of rhomb type crystals. Celia Dolomite, E.L. 1349.

c.   These large magnesite rhombs are from the Mt. Fitch Deposit. Many of the rhombs show hematite zoning, whilst some contain grains of chalcopyrite. The chalcopyrite grains do not appear to be related to this zoning.
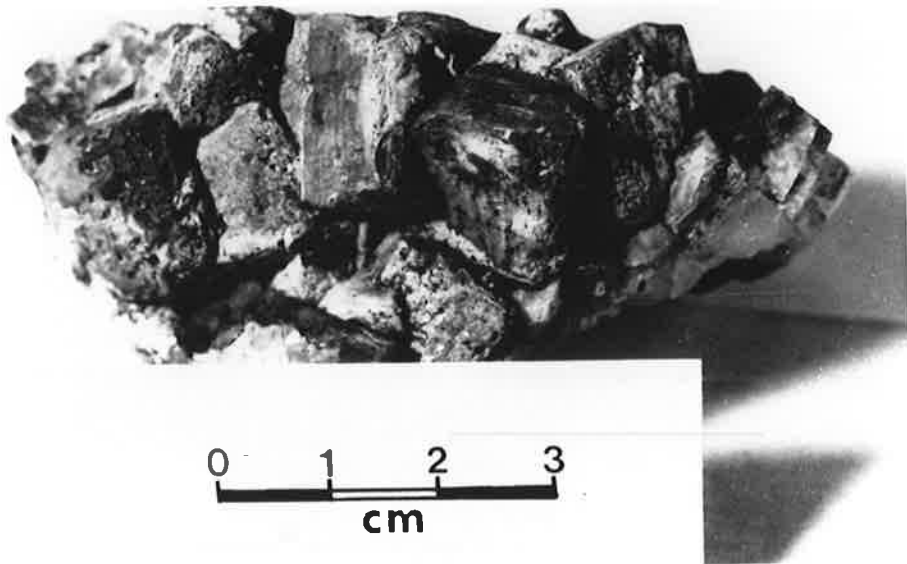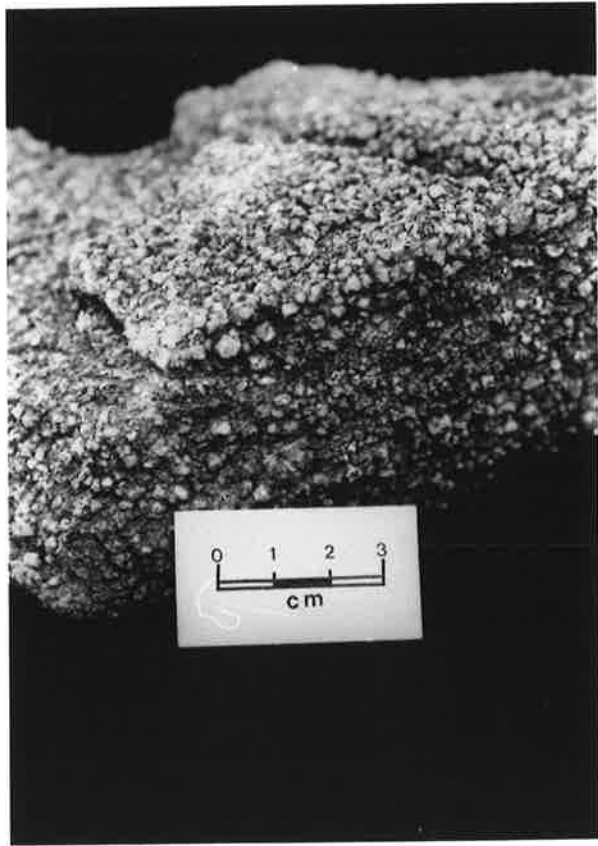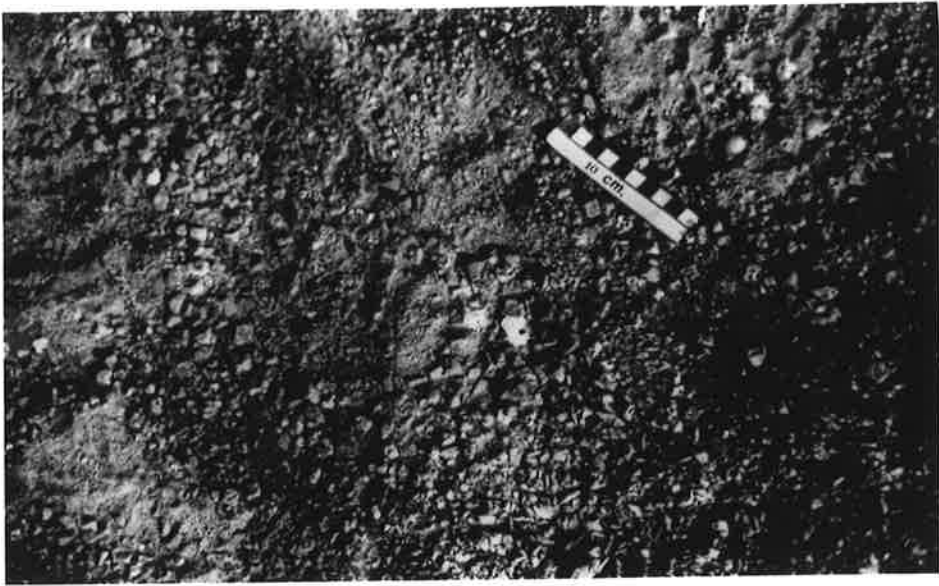
Benefication is an expensive process involving floating off such contaminants as talc and chlorite. As much of the silica is intragranular, very fine grinding would render the processing economically unviable.

Therefore the exploration target was redefined to be a deposit of 10 million plus tonnes that is (1) relatively free of silica (2) has easy access, (3) can be mined by open-cut methods, (4) is situated near existing transport facilities and (5) is not encumbered by potential environmental or Aboriginal Land preclusions.

3.2 Crystallography

Magnesite belongs to the calcite group of rhombohedral carbonates, having the trigonal space group $R\bar{3}c$ with cell dimensions of a = 4.637 Å & c = 15.023 Å . The octahedron in magnesite is closer to the ideal than that in calcite (Oh et. al., 1973). This is due to the more suitable size of the Mg^{2+} ions, which results in O-Mg-O interatomic angles of 88.25°, 91.75° and 180.0° (whereas those of calcite are 87.57°, 92.43° and 180°). This ion size difference also leads to a difference in cell volume : $MgCO_3$ = 12.36 Å^3 $CaCO_3$ = 17.47 Å^3 (Effenberger et al., 1981), with a subsequent difference in density (3.0 vs 2.7).

3.3 Crystal Morphology

Although there are 15 possible forms that calcite, and presumably magnesite could take (Hartman, 1978) there are two forms that are predominant at Rum Jungle.

TABLE 2

CORRELATION MATRIX

CELIA AREA A

	FINE	MEDIUM	COARSE	V. COARSE	BLADED	RHOMB	TALC	QUARTZ
FINE	1.0000							
MEDIUM	.4663	1.0000						
COARSE	.0989	.0468	1.0000					
V. COARSE	-.8374	-.7484	-.4366	1.0000				
BLADED	.3176	.3993	-.0434	-.3268	1.0000			
RHOMB	-.3535	-.1645	-.3415	.4184	.1080	1.0000		
TALC	.4664	.1130	.2657	-.4149	.0870	-.3643	1.0000	
QUARTZ	-.3511	.3569	-.0058	.0319	-.1160	.1965	-.1636	1.0000

TABLE 2 (CONT.)

CORRELATION MATRIX

CELIA AREA B

	FINE	MEDIUM	COARSE	V. COARSE	BLADED	RHOMB	TALC	QUARTZ
FINE	1.0000							
MEDIUM	.1466	1.0000						
COARSE	-.3061	-.1877	1.0000					
V. COARSE	-.6145	-.6877	-.1642	1.0000				
BLADED	-.2469	-.0775	.0689	-.2270	1.0000			
RHOMB	-.2738	-.4432	.1545	.3682	-.7501	1.0000		
TALC	.2752	.2598	-.1301	-.3091	.1098	-.3323	1.0000	
QUARTZ	.5213	-.2330	-.0425	-.1602	-.1221	-.0005	-.1167	1.0000

TABLE 2 (CONT.)

46c

CORRELATION MATRIX

CELIA AREA C

	FINE	MEDIUM	COARSE	V. COARSE	BLADED	RHOMB	TALC	QUARTZ
FINE	1.0000							
MEDIUM	.1707	1.0000						
COARSE	-.2254	-.3578	1.0000					
V. COARSE	-.3072	-.4033	-.0001	1.0000				
BLADED	-.0047	-.0947	-.1524	.5678	1.0000			
RHOMB	-.2684	-.2743	.6956	-.0682	-.5975	1.0000		
TALC	.1740	-.1098	.0477	.1122	.2182	-.0861	1.0000	
QUARTZ	.1642	-.1606	.0079	.1675	.1307	-.0003	.4684	1.0000

TABLE 2 (CONT.)

CORRELATION MATRIX

CELIA AREA D

	FINE	MEDIUM	COARSE	V. COARSE	BLADED	RHOMB	TALC	QUARTZ
FINE	1.0000							
MEDIUM	.0195	1.0000						
COARSE	-.0588	-.2463	1.0000					
V. COARSE	-.4379	-.3871	-.6705	1.0000				
BLADED	-.3145	-.0769	-.5542	.6617	1.0000			
RHOMB	-.0127	-.3224	.6698	-.3696	-.8692	1.0000		
TALC	.4790	-.1746	-.0148	-.1133	.1530	-.2374	1.0000	
QUARTZ	.5881	.0625	.1941	-.4800	-.3855	.1730	.0478	1.0000

TABLE 2 (CONT.)

CORRELATION MATRIX

COOMALIE AREA B

	FINE	MEDIUM	COARSE	V. COARSE	BLADED	RHOMB	TALC	QUARTZ
FINE	1.0000							
MEDIUM	.6506	1.0000						
COARSE	.6796	.6857	1.0000					
V. COARSE	-.1462	-.0939	.1734	1.0000				
BLADED	.0442	.1846	.4922	.7956	1.0000			
RHOMB	.3897	.2260	.4160	.3180	-.0415	1.0000		
TALC	.4816	.5314	.4459	-.0707	-.0374	.4142	1.0000	
QUARTZ	.6161	.4181	.3821	-.1795	.0275	.0618	.2841	1.0000

These are: -

(1)   the cleavage rhombohedron {211}; which for convenience will be designated the rhombohedral form (Plate 8) throughout this thesis and

(2)   the steep rhombohedron {110}; which will be referred to as the bladed form (Plates 9, 10).

These two forms are interpreted by Crick and Muir (1980) as pseudomorphs of cubic halite and discoidal gypsum that had formed in a sabkha environment. C.F. Blain's (pers. comm., 1981) measurements of interfacial angle measurements indicated that both forms do not correspond to halite or gypsums interfacial angles but are carbonate negative rhombohedra.

Field observation did not show any evidence that could support the idea of halite and gypsum i.e. no pseudomorphs, lack of halite hopper-type crystals, no distinct cubes, no stratigraphic continuity of "gypsum" beds, no seasonal repetition of patterns even though there is abundant evidence of the evaporite-facies sedimentary nature of the carbonate e.g. stromatolites, (Plates 11-15) and tepees (Plate 16).

Therefore, Blain's conclusion was accepted, and evidence was collected to explain the two forms of crystal morphology. The first approach was to investigate possible causes of these often-times co-existing forms. A detailed pace and compass survey of every magnesite outcrop in E.L. 1349 was carried out as part of the magnesite exploration programme, (Chpt 9). Crystal morphology was systematically recorded as one of the field parameters. It did not positively correlate with grain-size, talc content or quartz content (Table 2). It was found that both forms occur intimately associated (Appendix 2). This aspect is illustrated in Figs 16-22. However, what is not

a.   The very coarse blades of recrystallised magnesite shown can
      easily be mistaken for gypsum. Available evidence suggests that
      the primary sediment was also magnesite. Outcrop 5, Area D,
      Coomalie Dolomite, E.L. 1349.

b.   (at left) Stellate clusters of bladed form magnesite. This
      sample is particularly silica-free and pure white in colour.
      Celia Dolomite, E.L. 1349.

c.   (at right) Large bladed form magnesite crystals growing into a
      vugh. Sample is from the Mt. Fitch Deposit.

taken into account in this type of data presentation is the variability within the same outcrop. Thus, in one portion of an outcrop there may be an area of predominantly rhombohedral-form magnesite, whilst a metre away on the same outcrop there may be an area of bladed-form only magnesite (Plate 8).

Thus, one of the aims of the study was to investigate possible form-causative parameters.

Many workers have already addressed this problem in relation to carbonates, but none have specifically singled out magnesite to investigate. Calcite has been the most popular choice, undoubtedly because of its ease of precipitation in the laboratory compared to the difficulties encountered with dolomite and magnesite; the reasons for which will be discussed in the section on problems of formation.

Hartman (1978) found for calcite that the rhombohedral form occurs in low supersaturated solutions and that the bladed form occurs in high supersaturated solutions or when there are impurities present. Kirov et al (1972) found the basal plane $\{111\}$ predominates when there is an excess of Ca^{2+} ions.

Cody and Shanks (1974) attempted to simulate natural muddy environments in their experiments on the resultant morphology of evaporite minerals (e.g. gypsum) that have grown directly below the water - sediment interface. They used bentonite (sodium montmorillonite) gel as their growing medium rather than silica gel as this seems to more readily resemble natural conditions. They observed that the presence of NaCl markedly affects gypsum morphology. Cody (1976) extended this study to look at the controlling influence of the presence of a range of

PLATE 10

a.   These coarse blades of magnesite also resemble gypsum, but once
      again appearances are deceptive. Outcrop 25, Area C, Celia
      Dolomite, E.L. 1349.

b.   Quartz pseudomorphs after bladed form magnesite. The diagenetic
      quartz replacement appears to have occurred early, as the
      crystals show organic C zoning. Outcrop 5, Area D, Coomalie
      Dolomite, E.L. 1349.

c.   This outcrop of very coarse grey magnesite contains organic C,
      with the highest density being in the largest crystals. This is
      one of the best examples of the bladed form of magnesite in E.L.
      1349, and is from the same outcrop as the sample above.

trace elements, when the temperature was kept constant. He found that (1) crystal habit variability increases in the presence of Na, Li, NH_3 and K; (2) that Mn, Ni, Zn and Mg reduces habit modification and (3) that tabular gypsum crystals i.e. perpendicular to the crystallographic c axis, can only be grown under very saline conditions. Extrapolating from this finding, it can be assumed, then, that where definite tabular gypsum crystals occur, the depositional environment was very saline - such as commonly occurs in sabkhas. In a continuation of this study, Cody (1979) concludes that gypsum with a lenticular form, rather than an elongate prismatic form, is precipitated in (a) the presence of dissolved organic material or (b) if conditions are alkaline.

Where Cody (1976) kept trace element concentration constant but varied the temperature he found that quite minor temperature changes i.e. 20°C have a strong control on crystal morphology. Unfortunately, this work is all on gypsum - not magnesite, and an extrapolation cannot be made to magnesite. Nevertheless, it is clear that crystal form in the sedimentary environment is affected by a variety of factors.

A reversed approach was taken by Kitano, Okumura and Idogaki (1979). They looked at the way in which the morphology of calcium carbonate (i.e. calcite or aragonite), controls factors such as the amount of silica that is co-precipitated - and how an increase in NaCl concentration causes an increase in silica precipitation.

Once again this is not specific to the Rum Jungle magnesite form problem, but it does emphasis the fact that it is unlikely that there is a single causative parameter.
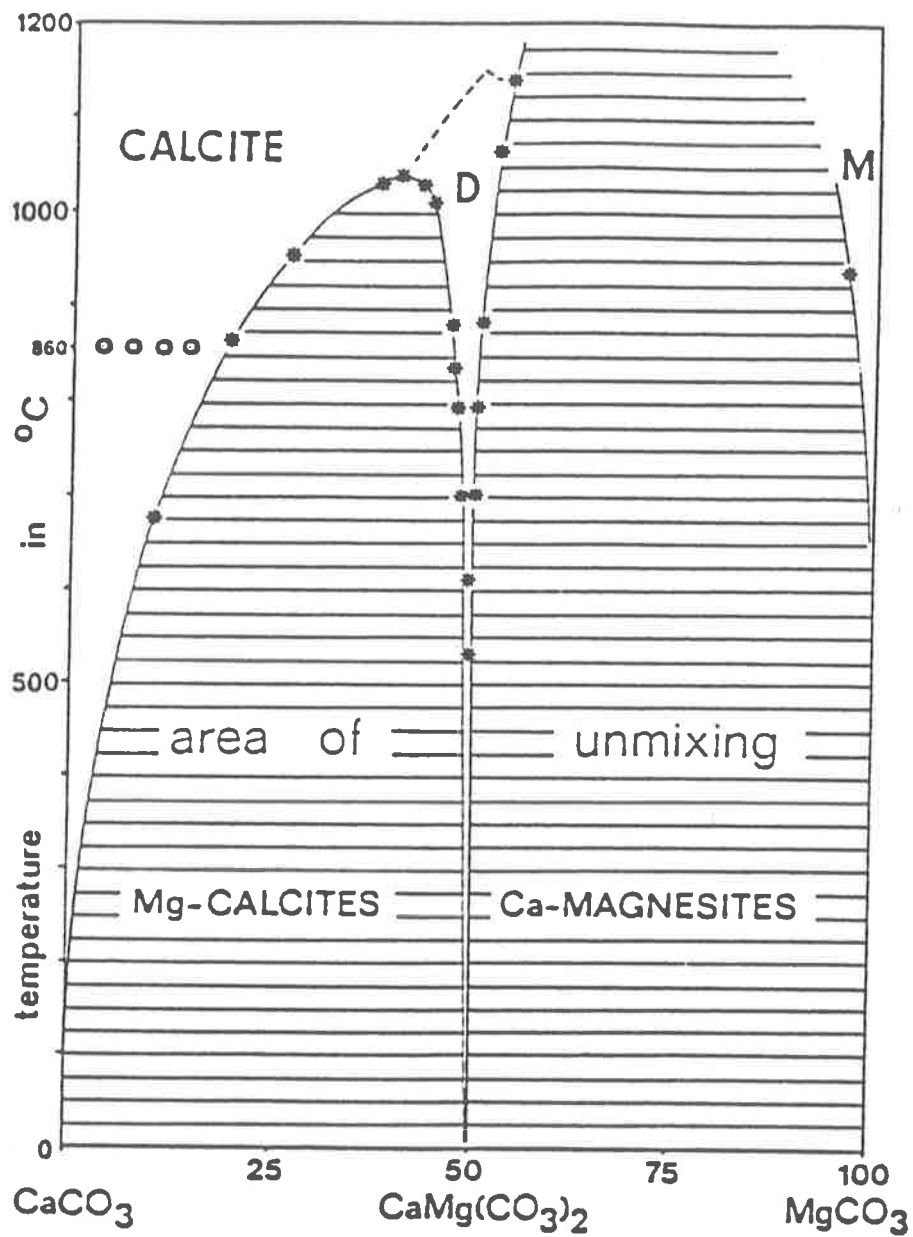
Fig. 23: Phase diagram of (water-free) $CaCO_3$ (calcite); $CaMg(CO_3)_2$ (dolomite) and $MgCO_3$ (magnesite) at temperatures between 0°C and 1200°C.

(Deelman, 1979)

A detailed fluid inclusion study of the Rum Jungle magnesites and magnesites from other localities revealed that temperature is one of the form causative parameters. Statistical analysis of the 444 Rum Jungle magnesite fluid inclusion results show that when the fluid from which the magnesite is precipitating is above 160°C the form taken is usually bladed, whereas when the fluid temperature is below 160°C, the form taken is usually rhombohedral.

This finding agrees with Ricketts (1980) experimental growth of calcite and dolomite crystals in a hydrated silica gel medium: rhombohedral crystals formed at room temperature and pressure.

This aspect of the work is dealt with in detail in Chpt. 4, and in Bone (1983).

3.4 Geochemistry of Magnesites
3.4.1 General

Magnesite is a rhombohedral carbonate of the calcite-structure type. The solid solution series calcite-dolomite-magnesite has been examined in some detail, as it is undoubtedly the most important binary phase relationship amongst all the carbonates (Figs 23, 24). Goldsmith (1983) gives an excellent detailed account of the state of the art for both the binary systems and the few ternary systems so far investigated ($CaCO_3$ and $MgCO_3$ with $FeCO_3$, $MnCO_3$, $CoCO_3$ and $NiCO_3$ e.g. Fig. 25).

However, when it comes to the incorporation of minor and trace elements into magnesite, there is some published work of
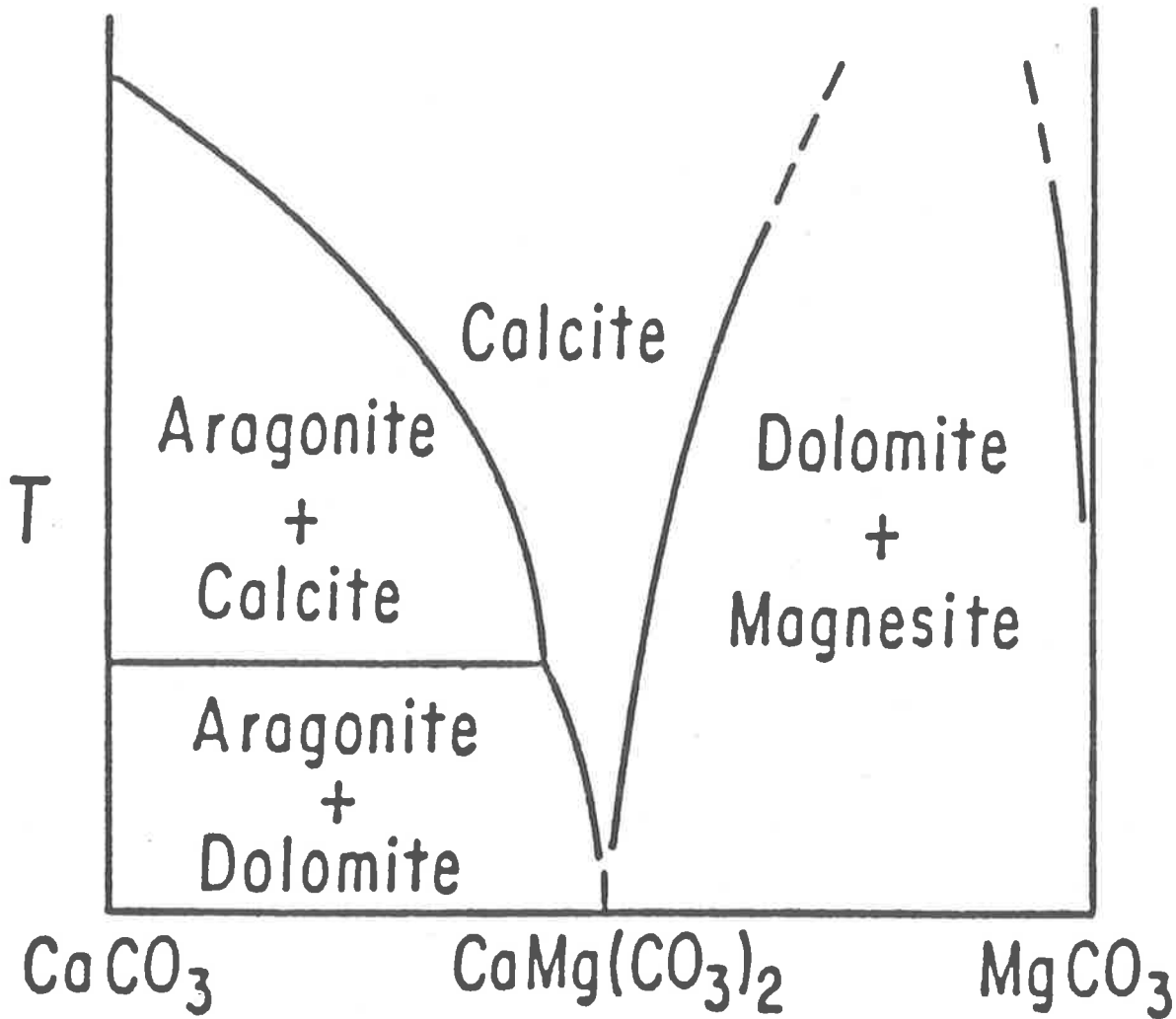
Fig. 24: Schematic diagram of the $CaCO_3$ – $CaMg(CO_3)_2$ – $MgCO_3$ system.

(Goldsmith, 1983)

an experimental nature but very little from observations on naturally occurring magnesite.

In respect to the calcite structure trace elements can be incorporated by (McIntire, 1963; Zemann, 1969):

(1)   substitution for M^{2+} in the $M^{2+}CO_3$ structure;

(2)   formation of domains

(3)   substitution at vacant lattice positions and other defects and

(4)   adsorption

Of these four mechanisms, the first is the most important and the best known, so that distribution patterns can be quantified. The other mechanisms occur in a random manner and thus cannot be treated quantitatively (Veizer, 1983).

It is likely that the same four mechanisms are applicable to minor and trace element distribution in magnesite, bearing in mind that it is ionic size and valency that are the major controls on likely substitutions in mechanism (1). For instance Sr^{2+} and Na^+ are the two elements that frequently substitute for Ca^{2+} in the calcite lattice and to a lesser extent the dolomite lattice because of their similar ionic radii (Table 3). However, these are too large to readily substitute for Mg^{2+} in the magnesite lattice. Therefore, if Sr and Na values comparable to the average for marine Ca-carbonates (Veizer, 1983) were to be found in magnesite it could be postulated that either the magnesite was secondary replacement of primary calcite or that there was enrichment in the solid state. The trace element content of the primary carbonate reflects the environment of deposition e.g. non-marine calcites are enriched in Zn, Mn, Fe, Co and Cu; but
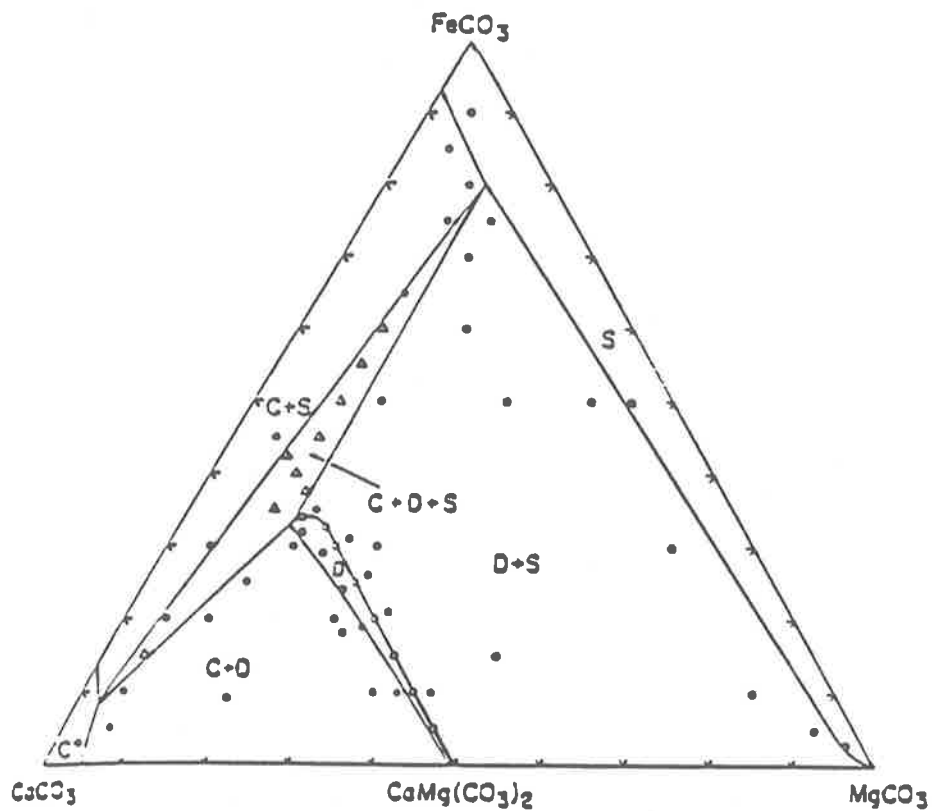
Fig. 25: Subsolidus relations in the system
$CaCO_3$ - $MgCO_3$ - $FeCO_3$ at 450°C. D = dolomite
solid solution, C = calcite solid solution,
S = siderite - magnesite solid solution. Open
circles, one-phase; filled circles, two-phase;
and triangles, three-phase assemblages.

(Goldsmith, 1983)

depleted in Mg, Sr, Na, Ba, and U. (Veizer, 1983). However, the work of Turner et al. (1981) suggests that ligand availability and pH (particularly in the freshwater environment) are also imporant parameters, when considering the potential incorporation of an element (i.e. cation) into the carbonate structure (Table 4), e.g. Co^{2+}_a increases markedly in fresh water at pH 9 whilst Ba^{2+}_a decreases. The salinity of the solution also determines the uptake of trace elements in carbonates.

One of the major problems in assessing the implications of trace element content of any sediment is post deposition changes due to diffusion of solution e.g. leaching of Sr^{2+} out of calcite can lead to much lower Sr:Ca ratios in recrystallized calcite, (Baker et al., 1982), particularly if the transporting fluid is undersaturated in the element of concern relative to the host rock. This aspect will be covered in more detail under the section on diagenesis, but it is important to bear it in mind in all geochemical considerations.

3.4.2 Geochemistry of Rum Jungle Magnesite

The major element chemistry of the Rum Jungle magnesite is shown in Appendix 3.

These can be compared with the analyses of sedimentary magnesites from South Australia and hydrothermal magnesites from various locations (resp: Frost, 1982; Dabitzias, 1980; Appendix 3). These results show little in the way of a consistently significant fingerprint for sedimentary diagenetic and metasomatic types. At best, Na values in the Vavdos

TABLE 3

The ionic radii of the elements for 6-fold co-ordination (nanometres).

Ion	Radius	Ion	Radius	Ion	Radius
Ac^{3+}	0.118	Hf^{4+}	0.078	Pt^{2+}	0.080
Ag^+	0.126	Hg^{2+}	0.110	Pt^{4+}	0.065
Ag^{2+}	0.089	Ho^{3+}	0.091	Pu^{3+}	0.108
Al^{3+}	0.051	I^-	0.216	Pu^{4+}	0.093
Am^{3+}	0.107	In^{3+}	0.081	Ra^{2+}	0.143
Am^{4+}	0.092	Ir^{4+}	0.068	Rb^+	0.147
As^{3+}	0.058	K^+	0.133	Re^{4+}	0.072
As^{5+}	0.046	La^{3+}	0.114	Re^{7+}	0.056
At^{7+}	0.062	Li^+	0.068	Rh^{3+}	0.068
Au^+	0.137	Lu^{3+}	0.085	Ru^{4+}	0.067
Au^{3+}	0.085	Mg^{2+}	0.066	S^{2-}	0.184
B^{3+}	0.023	Mn^{2+}	0.080	S^{6+}	0.030
Ba^{2+}	0.134	Mn^{3+}	0.066	Sb^{3+}	0.076
Be^{2+}	0.035	Mn^{4+}	0.060	Sb^{5+}	0.062
Bi^{3+}	0.096	Mn^{7+}	0.046	Sc^{3+}	0.081
Bi^{5+}	0.074	Mo^{4+}	0.070	Se^{2-}	0.198
Br^-	0.195	Mo^{6+}	0.062	Se^{6+}	0.042
C^{4-}	0.260	N^{3-}	0.171	Si^{4+}	0.042
C^{4+}	0.016	N^{3+}	0.016	Sm^{3+}	0.100
Ca^{2+}	0.099	N^{5+}	0.013	Sn^{2+}	0.093
Cd^{2+}	0.097	Na^+	0.097	Sn^{4+}	0.071
Ce^{3+}	0.107	Nb^{4+}	0.074	Sr^{2+}	0.112
Ce^{4+}	0.094	Nb^{5+}	0.069	Ta^{5+}	0.068
Cl^-	0.181	Nd^{3+}	0.104	Tb^{3+}	0.093
Co^{2+}	0.072	Ni^{2+}	0.069	Tb^{4+}	0.081
Co^{3+}	0.063	Np^{3+}	0.110	Tc^{7+}	0.056
Cr^{3+}	0.063	Np^{4+}	0.095	Te^{2-}	0.221
Cr^{6+}	0.052	Np^{7+}	0.071	Te^{6+}	0.056
Cs^+	0.167	O^{2-}	0.140	Th^{4+}	0.102
Cu^+	0.096	Os^{6+}	0.069	Ti^{3+}	0.076
Cu^{2+}	0.072	P^{3-}	0.212	Ti^{4+}	0.068
Dy^{3+}	0.092	P^{5+}	0.035	Tl^+	0.147
Er^{3+}	0.089	Pa^{3+}	0.113	Tl^{3+}	0.095
Eu^{3+}	0.098	Pa^{4+}	0.098	Tm^{3+}	0.087
F^-	0.136	Pa^{5+}	0.089	U^{4+}	0.097
Fe^{2+}	0.074	Pb^{2+}	0.120	U^{6+}	0.080
Fe^{3+}	0.064	Pb^{4+}	0.084	V^{2+}	0.088
Fr^+	0.180	Pd^{2+}	0.080	V^{3+}	0.074
Ga^{3+}	0.062	Pd^{4+}	0.065	V^{4+}	0.063
Gd^{3+}	0.097	Pm^{3+}	0.106	V^{5+}	0.059
Ge^{2+}	0.073	Po^{6+}	0.067	W^{4+}	0.070
Ge^{4+}	0.053	Pr^{3+}	0.106	W^{6+}	0.062
		Pr^{4+}	0.092	Y^{3+}	0.092
				Yb^{3+}	0.086
				Zn^{2+}	0.074
				Zr^{4+}	0.079

(Battey, 1981)

(ultramafic metasomatic) magnesite samples are an order of magnitude higher than those of the Rum Jungle magnesite samples; whilst the reverse is true for Fe.

There is a wide range in Si values. This is thought to be due to either the presence of SiO_2 from primary sources, detrital input or hydrogeochemically supplied (silica gel, or authigenic silicates) and/or silicates resulting from later metamorphic reactions. Considering the variability of the source of silica it is obvious that a pure magnesite is unlikely to be found in a sedimentary environment.

Silica, and its various forms, will be discussed in more detail under the general heading of diagenesis.

Rare earth element abundances are believed to be indicative of magnesite formation type, but such data were not available. Morteani et al. (1981) have devised a Yb/Ca - Yb/La variation diagram to distinguish between magmatic, hydrothermal and sedimentary carbonates.

Selected elements are treated in more detail below-

3.4.2.1 Iron and Manganese

Iron and Mn have similar hydrochemical characteristics, and will be considered jointly (Krauskopf, 1967; Hem, 1972). Figs. 2 & 4 (Garrels and Christ, 1965; Jenne, 1968) illustrate the importance of the parameters Eh and pH in controlling the transport of Fe and Mn in a fluid. Other parameters, are temperature, presence of other ions and pressure - in particular P_{CO_2}.

Calculated speciation of cations in model fresh water at pH 6

Cation	Free	OH	F	Cl	SO₄	CO₃	Log ā
Ag^+	72	*	*	28	*	*	0.15
Al^{3+}	*	90	10	-	-	*	3.14
Au^+	*	-	-	100	-	-	6.08
Au^{3+}‡	*	100	-	*	-	-	21.98
Ba^{2+}	99	*	*	*	1	*	0.01
Be^{2+}	15	57	28	*	*	*	0.82
Bi^{3+}	*	100	*	*	*	-	9.08
Cd^{2+}	96	*	*	2	2	*	0.02
Ce^{3+}	72	*	3	*	22	3	0.14
Co^{2+}	98	*	*	*	2	*	0.01
Cr^{3+}	*	98	*	*	1	-	2.41
Cs^+	100	-	-	*	-	-	0.00
Cu^+	95	-	-	5	-	-	0.02
Cu^{2+}	93	1	*	*	2	4	0.03
Dy^{3+}	65	1	6	*	21	7	0.19
Er^{3+}	63	1	7	*	19	10	0.20
Eu^{3+}	71	1	3	*	21	4	0.15
Fe^{2+}	99	*	*	*	1	*	0.01
Fe^{3+}	*	100	*	*	*	*	6.41
Ga^{3+}	*	100	*	*	-	*	7.80
Gd^{3+}	63	1	5	*	22	9	0.20
Hf^{4+}	*	100	*	*	*	-	13.28
Hg^{2+}	*	8	*	92	*	*	6.88
Ho^{3+}	65	1	7	*	19	8	0.19
In^{3+}	*	100	*	*	*	*	5.53
La^{3+}	73	*	1	*	25	1	0.14
Li^+	100	-	-	-	*	-	0.00
Lu^{3+}	59	1	8	*	15	17	0.23
Mn^{2+}	98	*	*	*	2	*	0.01
Nd^{3+}	70	1	3	*	24	3	0.15
Ni^{2+}	98	*	*	*	2	*	0.01
Pb^{2+}	86	2	*	1	4	7	0.06
Pr^{3+}	72	1	2	*	23	2	0.14
Rb^+	100	-	-	*	-	-	0.00
Sc^{3+}	*	43	41	*	*	15	2.80
Sm^{3+}	68	1	3	*	25	4	0.17
Sn^{4+}‡	*	100	-	-	-	-	24.35
Tb^{3+}	67	1	6	*	22	4	0.18
Th^{4+}	*	100	*	*	*	*	7.94
TiO^{2+}‡	*	100	-	-	-	-	7.17
Tl^+	100	*	*	*	*	-	0.00
Tl^{3+}	*	100	*	*	*	-	14.62
Tm^{3+}	66	1	8	*	20	6	0.18
U^{4+}	*	100	*	*	*	-	14.02
UO_2^{2+}‡	12	18	8	*	1	60	0.91
Y^{3+}	63	1	17	*	14	4	0.20
Yb^{3+}	58	1	7	*	17	17	0.24
Zn^{2+}	98	*	*	*	2	*	0.01
Zr^{4+}	*	100	*	*	*	-	14.33

Legend: — indicates ligand not considered
* indicates calculated abundance < 1%
‡ classified as fully hydrolysed oxidation states

Calculated speciation of cations in model sea water at pH 8.2

Cation	Free	OH	F	Cl	SO₄	CO₃	Log ā
Ag^+	*	*	*	100	*	*	5.26
Al^{3+}	*	100	*	-	-	*	9.22
Au^+	*	-	-	100	-	-	12.86
Au^{3+}‡	*	100	*	*	-	-	27.30
Ba^{2+}	86	*	*	9	5	*	0.07
Be^{2+}	*	99	1	*	*	*	2.74
Bi^{3+}	*	100	*	*	*	-	14.79
Cd^{2+}	3	*	*	97	*	*	1.57
Ce^{3+}	21	3	1	12	10	51	0.68
Co^{2+}	58	1	*	30	5	6	0.24
Cr^{3+}	*	100	*	*	*	-	5.82
Cs^+	93	-	-	7	-	-	0.03
Cu^+	*	-	-	100	-	-	5.10
Cu^{2+}	9	8	*	3	1	79	1.03
Dy^{3+}	11	8	1	5	6	68	0.94
Er^{3+}	8	12	1	4	4	70	1.08
Eu^{3+}	18	13	1	10	9	50	0.74
Fe^{2+}	69	2	*	20	4	5	0.16
Fe^{3+}	*	100	*	*	*	*	11.90
Ga^{3+}	*	100	*	*	*	*	15.33
Gd^{3+}	9	5	1	4	6	74	1.02
Hf^{4+}	*	100	*	*	*	-	22.77
Hg^{2+}	*	*	*	100	*	*	14.24
Ho^{3+}	10	8	1	5	5	70	0.99
In^{3+}	*	100	*	*	*	*	11.48
La^{3+}	30	5	1	18	16	32	0.42
Li^+	99	*	-	-	1	-	0.00
Lu^{3+}	5	21	1	1	1	71	1.32
Mn^{2+}	58	*	*	37	4	1	0.23
Nd^{3+}	22	9	1	10	12	46	0.66
Ni^{2+}	47	1	*	34	4	14	0.33
Pb^{2+}	3	9	*	47	1	41	1.51
Pr^{3+}	23	8	1	12	13	41	0.61
Rb^+	95	-	-	5	-	-	0.02
Sc^{3+}	*	100	*	*	*	*	7.41
Sm^{3+}	18	10	1	8	11	52	0.75
Sn^{4+}‡	*	100	-	-	-	-	32.05
Tb^{3+}	16	11	1	8	9	55	0.80
Th^{4+}	*	100	*	*	*	*	15.66
TiO^{2+}‡	*	100	-	-	*	-	11.14
Tl^+	53	*	*	45	2	-	0.28
Tl^{3+}	*	100	*	*	*	-	20.49
Tm^{3+}	11	21	1	5	6	55	0.94
U^{4+}	*	100	*	*	*	-	23.65
UO_2^{2+}‡	*	*	*	*	*	100	6.83
Y^{3+}	15	14	3	7	6	54	0.81
Yb^{3+}	5	9	1	2	3	81	1.30
Zn^{2+}	46	12	*	35	4	3	0.34
Zr^{4+}	*	100	*	*	*	-	23.96

Legend: — indicates ligand not considered
* indicates calculated abundance < 1%
‡ classified as fully hydrolysed oxidation states

Calculated speciation of cations in model fresh water at pH 9

Cation	Free	OH	F	Cl	SO₄	CO₃	Log ā
Ag^+	65	*	*	25	*	9	0.18
Al^{3+}	*	100	*	-	-	*	12.95
Au^+	*	-	-	100	-	-	6.07
Au^{3+}‡	*	100	-	*	-	-	30.93
Ba^{2+}	96	*	*	*	1	3	0.02
Be^{2+}	*	100	*	*	*	*	4.47
Bi^{3+}	*	100	*	*	*	-	18.01
Cd^{2+}	47	4	*	1	1	47	0.31
Ce^{3+}	*	5	*	*	*	95	2.37
Co^{2+}	20	7	*	*	*	73	0.70
Cr^{3+}	*	100	*	*	*	-	9.08
Cs^+	100	-	-	*	-	-	0.00
Cu^+	95	-	-	5	-	-	0.02
Cu^{2+}	*	3	*	*	*	96	2.62
Dy^{3+}	*	46	*	*	*	54	3.01
Er^{3+}	*	78	*	*	*	22	3.54
Eu^{3+}	*	18	*	*	*	82	2.40
Fe^{2+}	27	8	*	*	*	65	0.57
Fe^{3+}	*	100	*	*	*	*	14.99
Ga^{3+}	*	100	*	*	*	-	19.31
Gd^{3+}	*	14	*	*	*	86	2.92
Hf^{4+}	*	100	*	*	*	-	27.61
Hg^{2+}	*	100	*	*	*	*	11.79
Ho^{3+}	*	48	*	*	*	52	3.08
In^{3+}	*	100	*	*	*	*	14.57
La^{3+}	2	10	*	*	*	88	1.78
Li^+	100	*	-	-	*	-	0.00
Lu^{3+}	*	92	*	*	*	8	4.21
Mn^{2+}	62	1	*	*	1	35	0.20
Nd^{3+}	*	9	*	*	*	90	2.33
Ni^{2+}	9	2	*	*	*	90	1.07
Pb^{2+}	*	5	*	*	*	95	2.73
Pr^{3+}	1	9	*	*	*	90	2.23
Rb^+	100	-	-	*	-	-	0.00
Sc^{3+}	*	100	*	*	*	*	10.82
Sm^{3+}	*	14	*	*	*	86	2.49
Sn^{4+}‡	*	100	-	-	-	-	36.27
Tb^{3+}	*	32	*	*	*	68	2.67
Th^{4+}	*	100	*	*	*	*	19.86
TiO^{2+}‡	*	100	-	-	*	-	13.15
Tl^+	100	*	-	*	*	-	0.00
Tl^{3+}	*	100	-	-	*	-	23.57
Tm^{3+}	*	86	*	*	*	14	3.51
U^{4+}	*	100	*	*	*	-	28.77
UO_2^{2+}‡	*	*	*	*	*	100	8.61
Y^{3+}	*	14	*	*	*	85	2.57
Yb^{3+}	*	62	*	*	*	38	3.59
Zn^{2+}	6	78	*	*	*	16	1.20
Zr^{4+}	*	100	*	*	*	-	28.81

Legend: — indicates ligand not considered
* indicates calculated abundance < 1%
‡ classified as fully hydrolysed oxidation states

TABLE 4: Ligand activity/availability at differing pH conditions. (Turner et al., 1981)

It is well known that Fe^{2+} is stable in slightly acid conditions (Fig. 26). Changes in pH to neutral and higher redox potentials cause Fe^{2+} precipitation while Mn^{2+} still remains in solution (Fig. 27) achieving a separation of the two.

The co-precipitation of Fe^{2+} and Mn^{2+} in carbonates is controlled by the following factors according to Bencini & Turi (1974).

(1) concentration of Fe^{2+} and Mn^{2+}

(2) Eh, pH and total dissolved matter of the brine

(3) mineralogy of carbonate

(4) primary precipitation or metasomatic alteration.

The stability field of $MnCO_3$ is larger than that for $FeCO_3$ (Hem, 1972). However, organic complexes and bicarbonate-sulfate-organic complexes respectively could affect the stability of these carbonates with a resultant complication of the precipitation process due to the presence of oxides, hydroxides, and clay minerals. Adsorption effects often cause a correlation between the presence of clay minerals and the Fe and Mg content of carbonates (Fruth and Scherreiks, 1975).

Changes in the concentration of Fe^{2+} and Mn^{2+} will occur as a result of climatic changes, due to variations in continental discharge and a concommitant shift in such factors as pH, Eh, organic matter content and hydration reactions. Higher solubility will be enhanced if an increase in humidity also includes an increase in temperature.

The actual amount of Fe and Mn incorporated into the magnesite lattice will ultimately be controlled by the afore
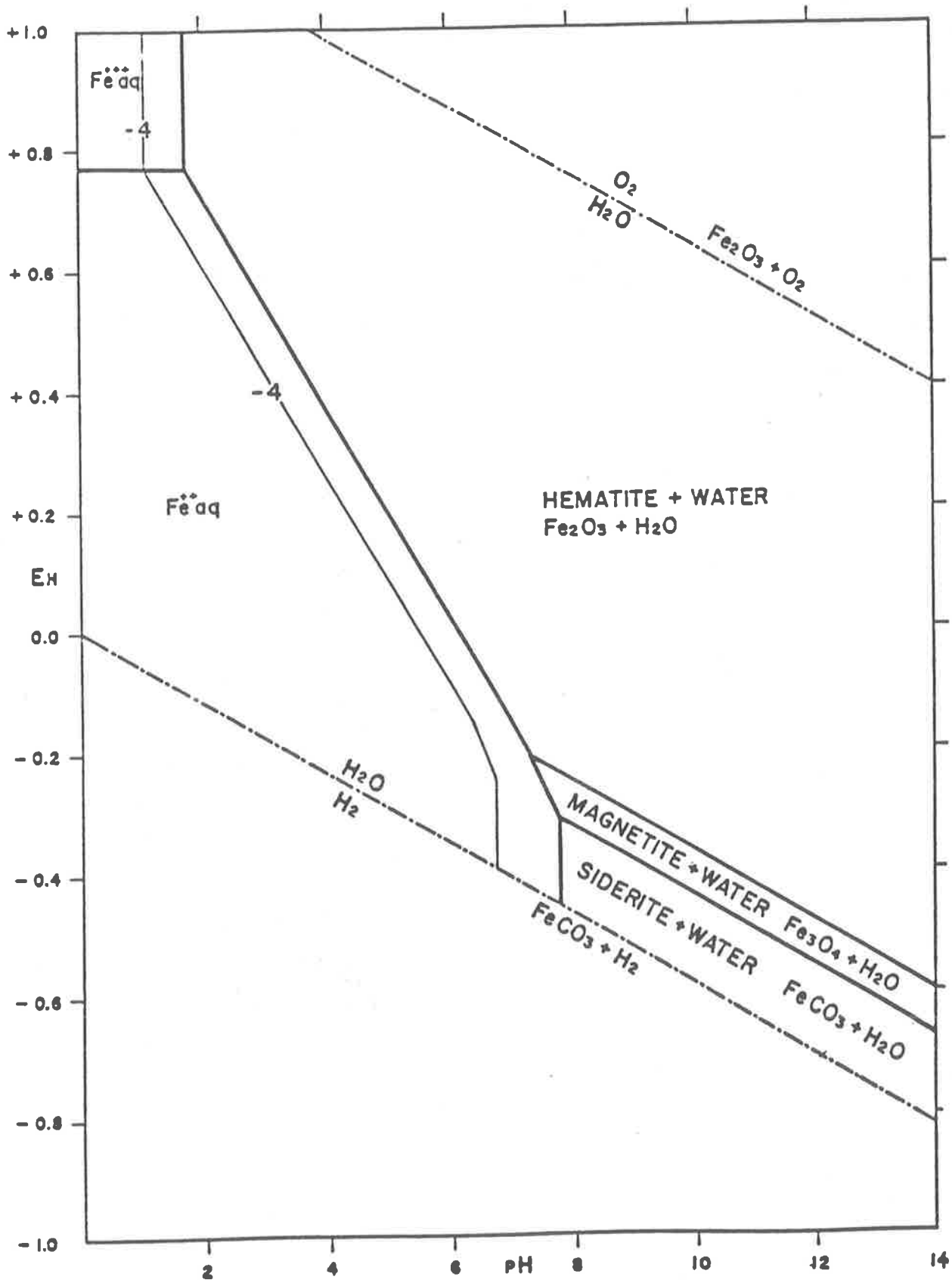
Fig. 26: Stability of Fe_2O_3, Fe_3O_4 and $FeCO_3$ at 25°C and 1 atmosphere total pressure with $P_{CO_2} = 10^{-2}$ atmospheres. Contour is for $\leq$ activity ions $= 10^{-4}$. Boundary of solids is at $\leq$ activity ions $= 10^{-6}$.

(Garrels and Christ, 1965)

mentioned chemical parameters, as the ion size is compatible for either substitution (Table 3). Care must be exercised, however, when, reconstructing palaeoenvironments based on the Fe and Mn content, as post-depositional changes can be considerable (Annovi et al., 1980). Diagenesis by diffusion processes frequently brings about an increase of Fe and Mn. The actual increases are dependent upon factors such as Eh, pH, composition and flow rate of interstitial pore waters and the degree of chemical autonomy in the system (Pingitore, 1978; 1982).

The Fe and Mn content are given in Appendix 3 for each area. There is a positive correlation between the two elements irrespective of analytical technique. This suggests that any Fe and Mn derived from clays and other accessory minerals in the magnesite rock (i.e. X.R.F. rock analyses) do not become an overriding factor when compared with magnesite lattice analyses (i.e. electron microprobe analyses). The correlation between the two is not as prominent in the analyses of dolomite, replacing magnesite.

The data suggest that the Fe and Mn content of the magnesite is indicative of substitution of Mn^{2+} ions and Fe^{2+} ions for Mg^{2+} ions.

Although a general correlation exists, there is also wide variation in actual values, particularly from one area to another. This indicates that the availability of Fe and Mn during deposition as derived from accessory minerals and diffusing waters during diagnesis controlled the incorporation of these elements rather than the Eh of the primary environment. This seems to indicate that most of the Fe and Mn

64

DIAGRAMS FOR IRON AND MANGANESE
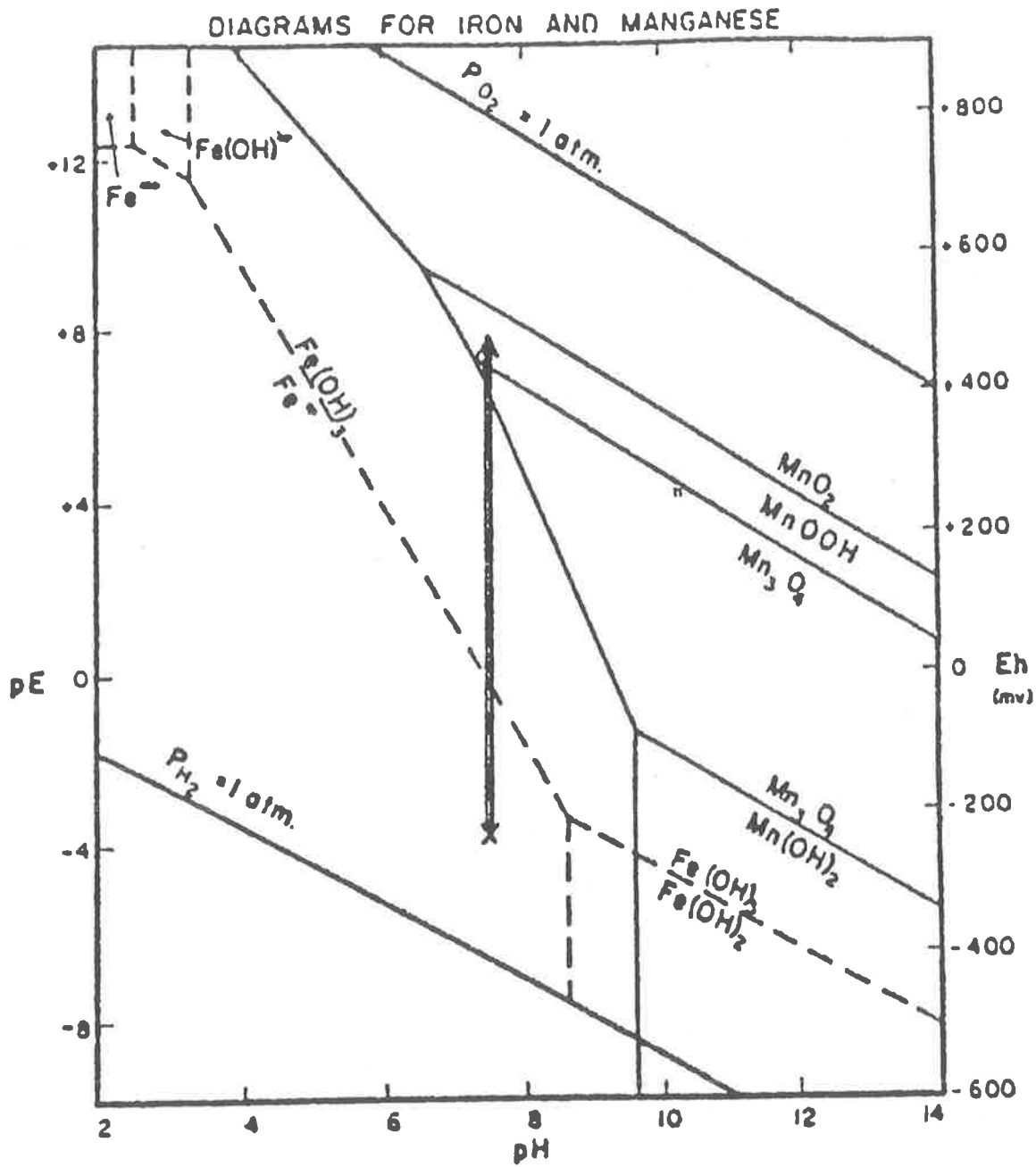
$(a_{Mn} = 10^{-4}M, a_{Fe} = 10^{-4}M, P_{CO_2} = 0, P_{Tot} = 1 atm, T = 25°C)$

Fig. 27: Eh/pH stability diagram for ferromanganese oxides.

(Jenne, 1968)

was introduced post-depositionally because a primary precipitation process is unlikely to have produced these local variations.

The higher values occur in areas of ore deposition, which were undoubtedly areas of greater physical variability e.g. shear zones etc. and hence subjected to such factors as greater flow rates of both hydrothermal and ground waters. These areas would also still be experiencing flow when the adjacent magnesite micropores had been virtually eliminated by recrystallization, so that the Fe and Mn could have been introduced to these areas over a longer period of time.

Even the lowest values of Fe and Mn are higher than those expected for seawater precipitation (Veizer, 1974). This suggests that the Fe and Mn were either derived from continental waters - which have higher concentrations than seawater (Turekian, 1972), or the entire systems has been subjected to major post-depositional changes. If the latter is the only cause, then this affect would also be evident in the concentration of other diagnostic elements e.g. Na, K etc..

3.4.2.2 Sodium

Additional information on palaeosalinity can be supplied by the Na content of carbonate rocks (Veizer, et al., 1978), providing their chemical autonomy has remained unchanged since their deposition. However, diagenetic changes can bring about major changes in concentration (Pingitore, 1982) which implies that caution must be exercised in any palaeoenvironmental reconstruction based on geochemistry. For example, Annovi

et al. (1980) have shown that very low or virtual absence of Na can be brought about by tropical type leaching of soils; and that this could have been a recent event.

The Na content of carbonate rocks is derived from three main sources (Fritz and Katz, 1972):-

(1)   incorporation as solid or liquid inclusions during crystallization of the carbonate e.g. NaCl

(2)   substitution of Na^+ for Ca^{2+} and Mg^{2+} within the crystal lattice during growth and

(3)   accessory minerals intimately associated with the carbonate

Comparison of an assessment of each of the two different analytical techniques used (X.R.F. and microprobe) enables determination of the applicable Na source category.

Preservation of inclusions, particularly fluid inclusions, as in (1), has led to the erroneous interpretation of halite as a carbonate precursor (Crick and Muir, 1980). Recrystallization of the carbonate can release the contents of these fluid inclusions to pore fluids, and hence change the composition of this fluid.

Precipitation of Na within aragonite, calcite and Mg-calcite has been investigated extensively by White (1977, 1978), but once again magnesite has been neglected. Substitution of the Na^+ ion in the carbonate lattice is dependent upon the aqueous activity ratio of Na^+/Ca^{2+}, which is analagous to saying dependent upon salinity. This implies that high Na values can be interpreted as indicating high palaeosalinity. The presence of organic substances also has

been suggested as causing an increase in Na concentration (White, 1978). Any excess Na^+ will precipitate as sodium carbonates e.g. trona (Eugster and Jones, 1979). This latter process involves/lead to an increase in pH.

However, due to the difference in ionic radii of Na^+ and Mg^{2+} (Table 3) and valency, it appears unlikely that substitution would readily occur in magnesite. The concentration threshold for Na^+ ions to become incorporated in the magnesite lattice is thus likely to be higher than that necessary for calcite. A high Na content in a magnesite would tend to suggest either (3) as the source or post-depositional increase. However, in modern carbonates a decrease of Na^+ usually occurs during diagenesis due to recrystallization in the presence of pore waters which are less saline and/or have a lower pH than those from which the sediment formed.

Notwithstanding these well recognised potential changes during diagenesis, Fritz and Katz (1972) and Veizer (1977, 1978) believe that variations in Na content still do reflect original salinity or very early diagenetic changes.

The following values are considered typical for dolomites:-

supratidal	200 - 900 ppm Na
"early" diagenetic	70 - 220 ppm Na
"late" diagenetic	<150 ppm Na
hydrothermal	<100 ppm Na

Original facies variation and later diagenetic differences would blur these boundaries somewhat. It is likely that the values in magnesite would be considerably lower in all cases.

The Na values (Appendix 3) are consistently low in all cases, except for the X.R.F. analyses from the B.M.R. This suggests that the Na content in these whole rock analyses is derived from fluid inclusion contamination, (Chpt. 6) as the Na content due to solid inclusions is also relatively low. The fluid in these fluid inclusions may have been the preserved remnants of saline pore waters that evolved as the lakes frequently dried out. Certainly analyses of these fluids (Chpt. 6) indicate that Na^+ is one of the major cations present.

The values are very similar to those obtained by Uppill (1980) for the magnesite in the Mundallio Sub-group.

3.4.2.3 Potassium

Potassium has been used as a palaeosalinity and early diagenetic indicator (Fritz and Katz, 1972; Veizer et al., 1978).

The precipitation of K within carbonates is thought to occur analogously to the Na situation. However, the greater ionic radius of the K^+ ion is probably the cause of much lower K incorporation than that of Na. This will be emphasised even more where Mg^{2+} substitution is occurring. Increasing aqueous activity of Na may also play an inhibiting role in the coprecipitation of K (White, 1977). Nevertheless, K may reflect higher salinity variations. (Veizer, et al., 1978).

Aluminosilicates e.g. sericite and illite, formed as detrital products from the breakdown of K-feldspars, will contribute to the K content of the sediment.

Electron microprobe analyses of magnesite (Appendix 3) show that there is virtually no K present. This finding lends support to the premise that the magnesite is primary (Chpt. 4). Even the whole rock analyses show low values, notwithstanding the common presence of sericite, and to a lesser extent detrital K-feldspars and illite. Unlike the Mundallio Sub-group magnesite (Uppill, 1980) there is no correlation between K and Al (or Fe), and very little variation in values.

There is a quite marked increase in K content in the (B.M.R. X.R.F.) dolomite analyses (Appendix 3) compared to the magnesite values. This is more likely to be related to the concentration of insoluble K-silicates during the process of secondary dolomitization during which the silicates were concentrated along stylolitic interfaces than to be a reflection of a primary palaeosalinity.

3.4.2.4 Strontium

The incorporation of Sr into carbonates has been studied in considerable detail (Kinsman, 1969a; Veizer and Demovic, 1974; Morrow and Mayers, 1978; Pingitore, 1982; Ohde and Kitano, 1984).

Veizer et al., (1978) contend that the Sr content of carbonate sediments reflects predominantly such properties as the mineralogy and texture, whilst Morrow and Mayers (1978) contend that hydrogeochemistry and porosity during diagenesis are the more important - a stand that Pingitore (1982) leans towards. Certainly information on all these properties can be gleaned from the Sr content of Ca-carbonates. However, it has

been shown quite conclusively that the Sr content decreases with an increase in the Mg-carbonate content (Ohde and Kitano, 1984). This is probably due to the large ionic radius of Sr (Table 3), making it physically difficult for lattice substitution to occur. This lack of suitability of Sr substitution leads to a decrease of Sr values during metamorphic annealing.

As has already been mentioned, the Sr content of the magnesite was negligible, and therefore it was not included in the electron microprobe programme, apart from three early analyses. However, the X.R.F. data by the B.M.R. (Appendix 3) does give Sr values. The Sr numbers are very low (F 30 ppm), which is in the expected range for lacustrine primary magnesites; and overall an order of magnitude lower than Uppill's (1980) Mundallio Sub-group figures. What is surprising is the order of magnitude higher concentrations in the dolomite samples. It is suggested that there has been a transfer of Sr out of magnesite into the newly forming dolomite via diffusion in pore fluids.

3.4.2.5 Summary

The geochemical studies have enabled a more positive stance to be taken on the premise that the magnesite formed as a primary carbonate under alkaline, lacustrine conditions. Differences that occur do not appear to be due to depositional facies changes but rather due to the extent of diagenesis and other post-depositional changes, processes which tend to lead to increases in Fe and Mn and a decrease in Sr.

Low Na and K values also support the premise of a non-marine environment in which a Ca poor carbonate was precipitating.

3.5 Mode of Formation of Magnesite

3.5.1 Theory

In 1970 Christ and Hostetler, after much tedious experimental work on magnesite frustratedly wrote that "no carbonate mineral has proven more difficult to investigate experimentally". Although the statement may well still stand, their work, plus the work of others in related carbonate systems that can be extrapolated to magnesite, is gradually enabling a coherent picture to emerge about the formation of magnesite. Even so, lack of agreement among the published data is dismaying e.g. Langmuir (1965) gives a calculated K_m (equilibrium constant) = $10^{-5.1}$ at 25°C, Christ and Hostetler give $10^{-8.1}$, but eventually concensus of opinion will be reached - a position that is all but reached now.

Observations of natural occurrences of Mg-carbonates indicate that magnesite, rather than the hydrous phases hydro-magnesite ($3MgCO_3 \cdot Mg(OH)_2 \cdot 3H_2O$), nesquehonite ($MgCO_3 \cdot 3H_2O$) or lansfordite ($MgCO_3 \cdot 5H_2O$) is the stable phase at surface and near surface temperatures and pressures (Uppill 1980). These observations are supported by experimental and calculated data. What is also observed is the reluctance of Mg-carbonate to form from aqueous solution, both in the laboratory and in nature, except in one or another of the hydrated forms. Indeed, the entire $MgO-SiO_2-CO_2-H_2O$ system is metastable with respect to magnesite plus solution. Nevertheless it is possible to synthesise magnesite.
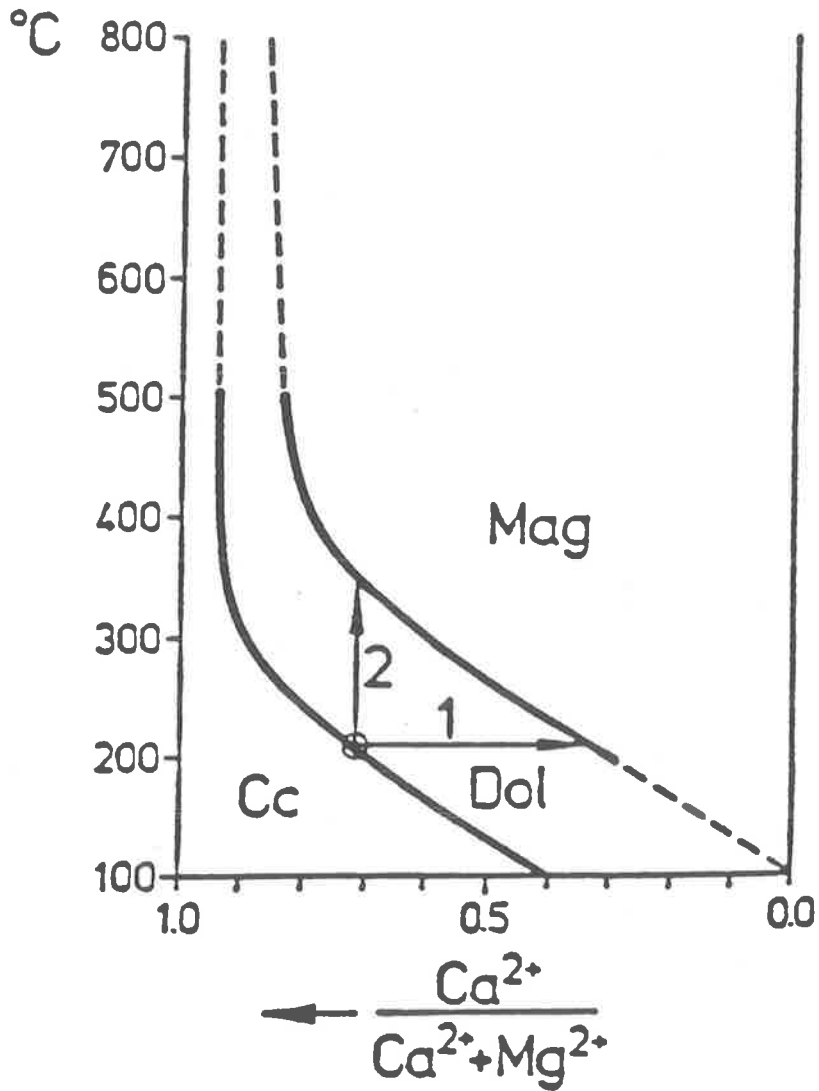
Fig. 28: T-x diagram showing the composition of the fluid phase in calcite - dolomite and dolomite - magnesite equilibria. Two alternative pathways of reaching equilibrium are shown.

(Morteani et al., 1981)

3.5.2 Experimental Data

Deelman (1979) has produced a phase diagram (Fig. 23) that shows the stability fields of calcite, dolomite and magnesite. His area of interest was more concerned with higher temperature (>500°C) phase changes than the temperatures of interest to the sedimentologist, and so the lower temperature boundaries are extrapolations. On the other hand, Johannes (1970) concerned himself with the phase changes at temperatures of 500°C down to 100°C (Fig. 28) for the calcite-dolomite boundary and from 500°C down to 200°C for the dolomite-magnesite boundary. This figure shows two alternative pathways of reaching dolomite-magnesite equilibrium:-

1. reducing the Ca/Ca + Mg ratio at a constant temperature or

2. maintaining constant composition of the solution but increasing the temperature.

This temperature increase could be achieved by various methods e.g. (a) hydrothermal fluids or (b) tectonic or sedimentary burial. The process of tectonic burial due to over thrusting is believed to have been instrumental in the formation of the quite widespread deposits of sparry magnesite in the Eastern Alps Grauwackenzone (Morteani et al., 1982).

The observed problem of kinetics of Mg-carbonate formation is apparently due to the strong attachment of the Mg^{2+} ion to its water of hydration shell - an attachment 40 times that of the Ca^{2+} ion (Morrow, 1982) - or 79 K cal/mole^{-1} more energy is required to free a Mg^{2+} ion from its sheath of H_2O molecules
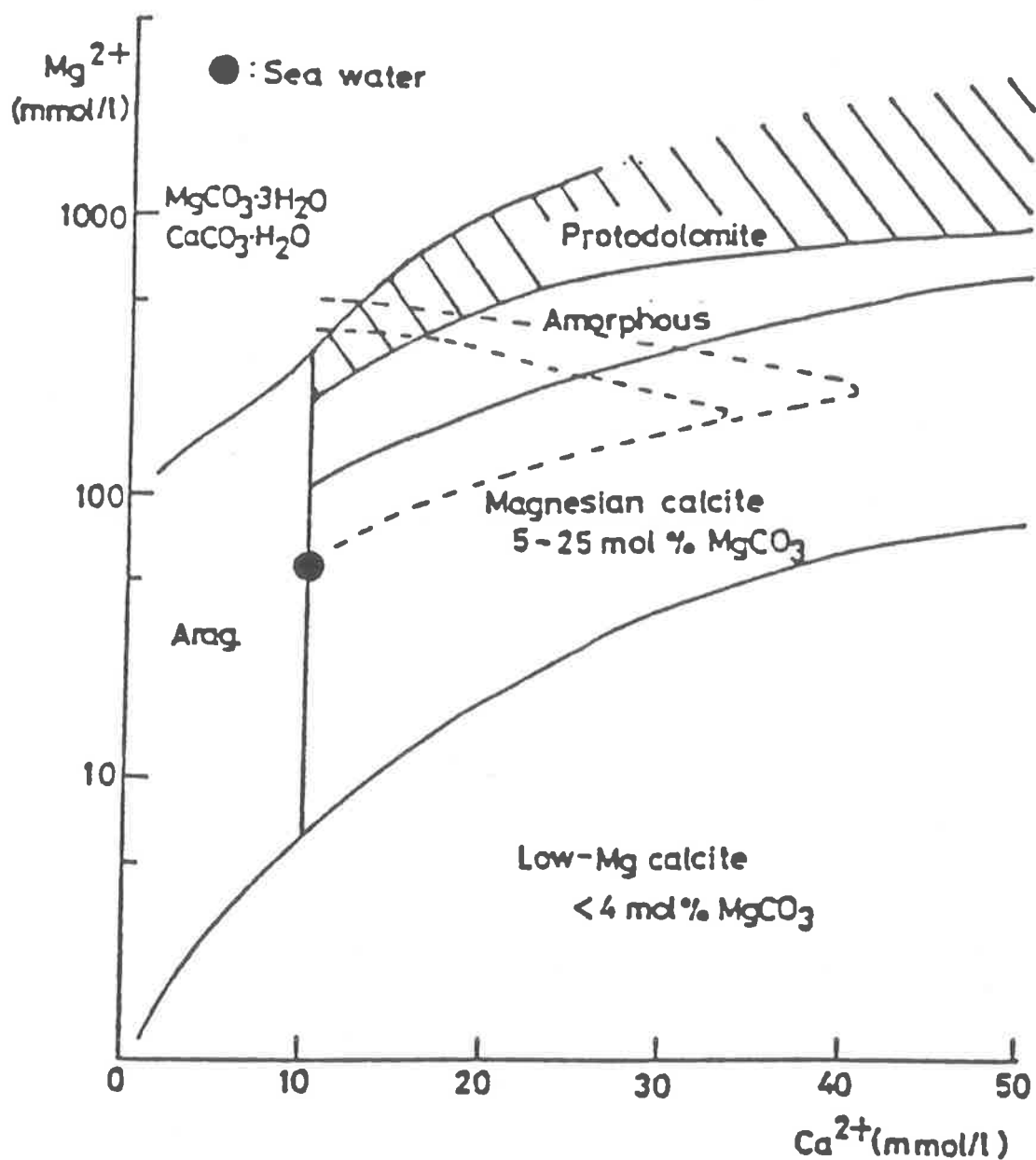
Fig. 29: Precipitation fields of carbonate minerals from $CaCl_2$ - $MgCl_2$ - (NaCl) - $NaHCO_3$ (0.18 mol/l) - H_2O solutions at 25°C. The dashed line shows the change in concentration of Ca^{2+} ions and Mg^{2+} ions as seawater evaporates.

(Ohde and Kitano, 1978)

than for a Ca^{2+} ion (Christ and Hostetler, 1970). The effect of the hydration shield of H_2O-dipoles can be reduced in the following ways:

(1) increased anionic strength

(2) decreased activity of water

Most potential ionic partners such as CO_3^{2-} ions have insufficient energy of motion (translational or vibrational) to break through this hydration sheath i.e. there is a kinetic threshold hindrance to the formation of magnesite, even though it is the thermodynamically stable phase. If the concentration of CO_3^{2-} ions is increased markedly, then there is a statistically higher probability of a CO_3^{2-} ion breaking through the Mg^{2+} ion hydration sheath. A natural environment supplying such a higher concentration is that of an alkaline lake. The alkaline lake situation can be brought about in the following way:- (Eugster and Jones 1979)

a   High evaporation rate

b   Filtered input

c   Continental facies

d   Low Ca^{2+} input

The HCO_3^{2-} is another carbonate ion instrumental in the formation of magnesite. Ohde and Kitano (1978) have shown that nesquehonite and monohydrocalcite will both precipitate from solutions with Ca^{2+} concentration <10 mmol and Mg^{2+} concentration >200 mmol (Fig. 29). Varying the $NaHCO_3$ concentration and the temperature from 25°C to 45°C causes insignificant changes in the phase boundaries. The dashed line shows the change in concentration of Ca^{2+} ions and Mg^{2+} ions in seawater during evaporation of seawater up to one fifth of its original volume. The Ca^{2+} to Mg^{2+} ratio necessary for

82
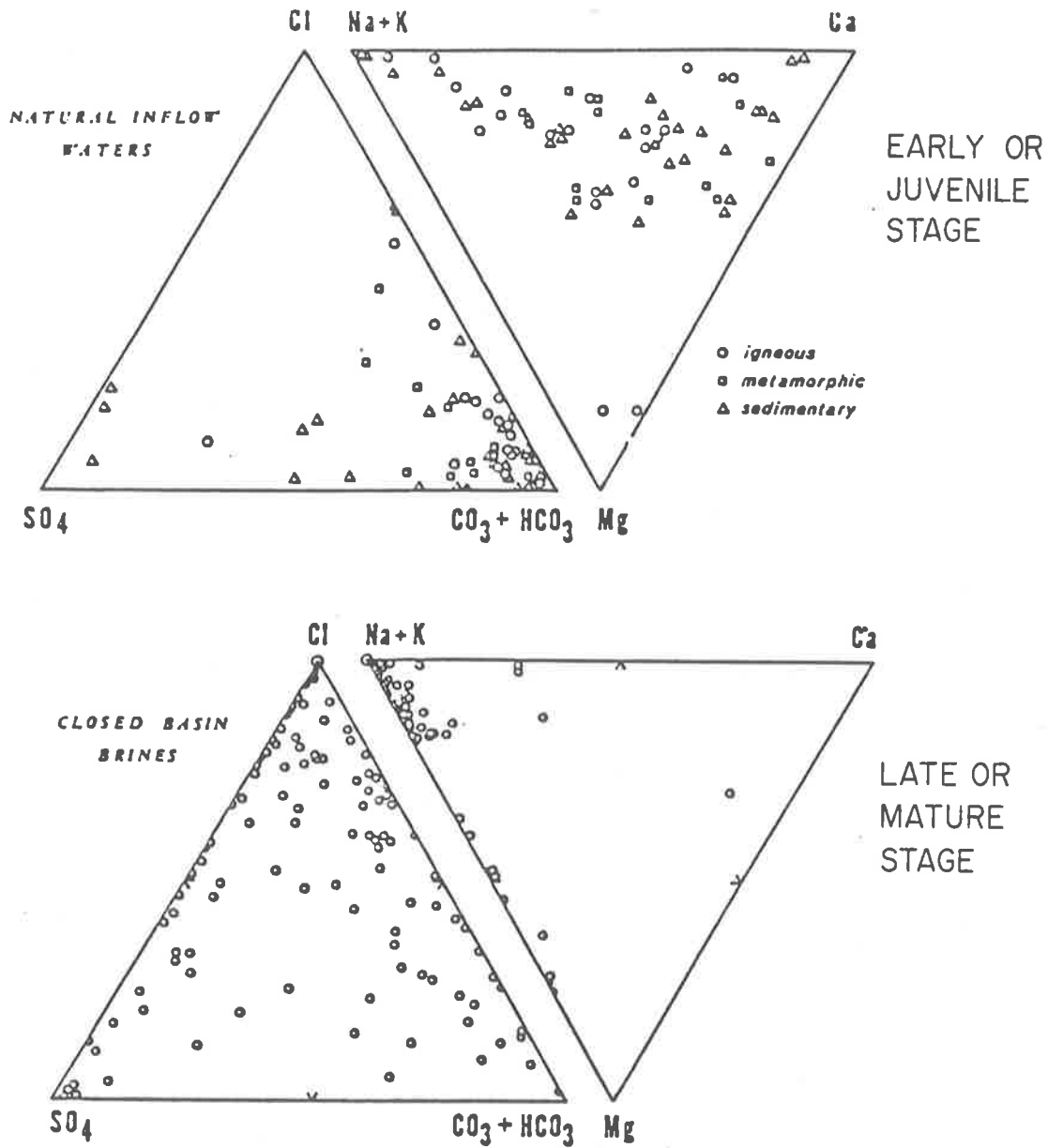
Fig. 30: Trilinear diagrams contrasting the major ion composition of inflow waters grouped by drainage basin lithology (top) with that of continental closed basin brines (bottom). It can be seen that "maturity" can lead to a marked compositional change.

(Eugster and Jones, 1979)

magnesite (or the hydrous Mg - carbonates) to precipitate cannot be achieved in normal seawater, even although seawater is ten times saturated with respect to magnesite (Christ and Hostetler, 1970) unless either Ca^{2+} ions are removed e.g. via the precipitation of gypsum and/or aragonite-calcite; or by the addition of Mg^{2+} ions to the system. Certainly, in most syn-sedimentary marine environments, the former seems to be the more likely.

It is also possible to achieve magnesite formation by increasing the salinity of the solution, be it either sea-water or continental. The salinity increase has the affect of decreasing the activity of water with, as a result, an increased precipitation due to the heightened availability of the CO_3^{2-} or HCO_3^{2-} ions. Deelman (1978, 1979) found that Na acts as a "catalytic agent" in the dehydration of the Mg^{2+} ion, particularly in the temperature range of 20°C - 50°C. At higher temperatures Li acts as an efficient "catalyst". Therefore it is not surprising that most authigenic magnesite seems to have been formed in very saline environments.

It may be well to briefly address the problems associated with the evolution of saline brines. In the six-component sea water system (Na - K - Mg - SO_4 - Cl - H_2O) there is a very complex array of possible mineral assemblages, as a consequence of the theoretically calculated 27 stable invariant points, which are connected by 69 univariant curves (Eugster, Harvie and Weare, 1980, 1982). The complexities would have been increased even further by the addition of CO_2. Although this system/model has been satisfactorily implemented by Brantley et al. (1984) for the Bocana de Virrila present day near shore
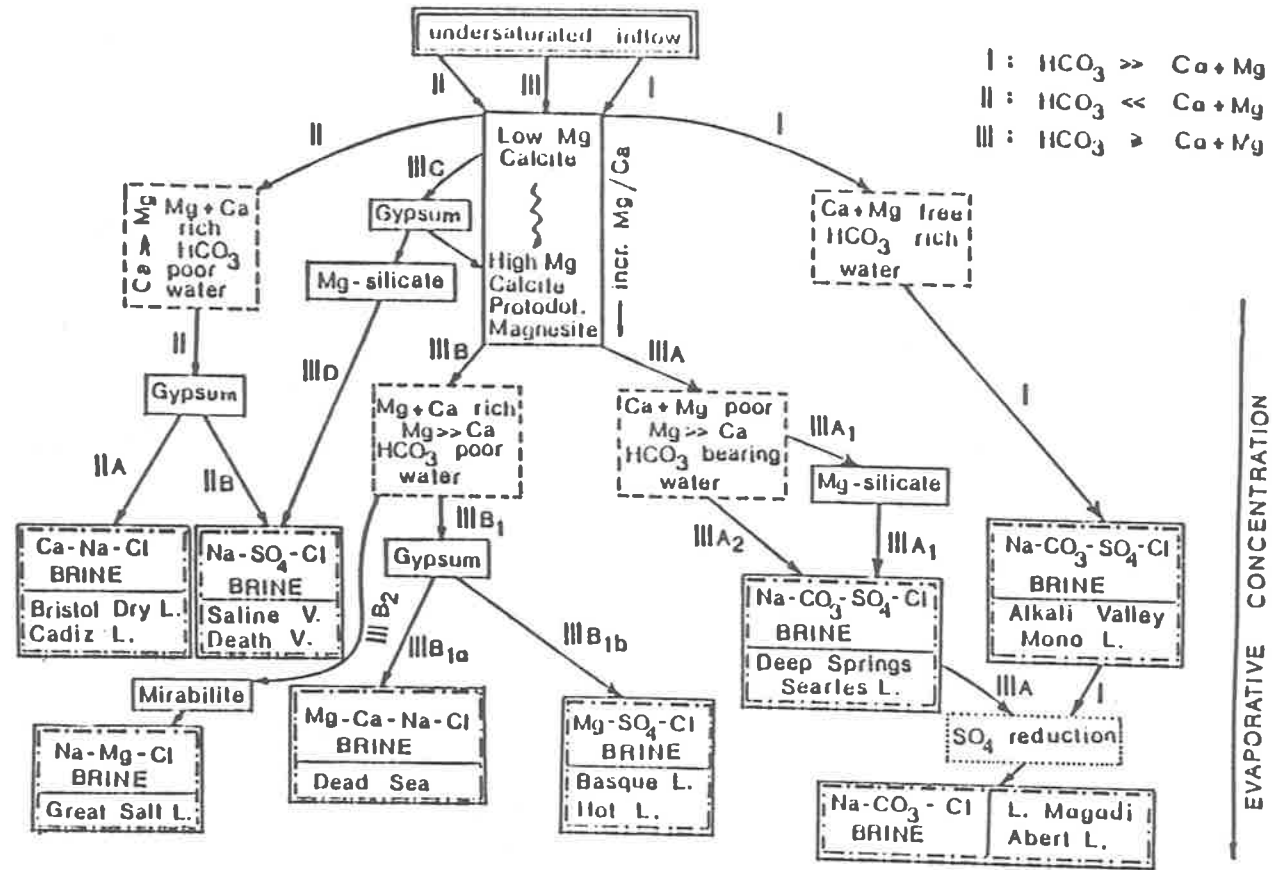
Fig. 31: Flow diagram for the geochemical evolution of closed basin brines.

(Eugster and Jones, 1979)

situation in Peru, it is more relevant to look at mechanisms of evolution of brines with the alkaline characteristics conducive to the formation of magnesite.

3.5.3 Evolution of Alkaline-Lake Type Brines.

Whereas initially formed basinal brines may have eight or more ionic species (e.g. SiO_2, Na, K, Ca, Mg, HCO_3, Cl, SO_4) present, with time, preferential removal of some causes the relative increase in abundance of the remainder (Eugster and Jones, 1979). This leads to the domination of the final brine by two, three or at most four species. The evolution patterns for ions other than Cl and HCO_3 are demonstrated in Fig. 30 (Eugster and Jones, 1970).

There are two possible alternative reasons for the presence of more than four species:-

(1) the brine is immature (and this can also apply to palaeo-brines) and/or

(2) there has been brine mixing.

Numerous processes and their complex interplay bring about the changes in these geochemically evolving brines. The various mechanisms responsible include:-

(i) mineral precipitation

Fig. 31 (Eugster and Jones, 1979) shows the affect upon the brine of the removal of solutes by the precipitation of mineral phases during the evaporative process. As can be seen, precipitation of magnesite leaves a brine of composition IIIB or IIIA. This scheme does not include SiO_2 in the inflow

water, although Eugster and Jones (1979) cite it as one of their 8 original components. If it were included it would remove the Mg - silicate problem.

As Fig. 31 shows, the cationic evolution of a brine towards Na dominance is brought about by the precipitation of Ca, Mg carbonates, gypsum and probably Mg - silicates. The solution load increases to an appropriate concentration at which precipitation occurs, due to direct evaporation from surficial water bodies or from evaporation in a subsurface condition fed by capillary draw from groundwater.

Similarly, the trend towards Cl enrichment is due to Cl, HCO_3 + CO_3 and SO_4 being the only important anions in closed basin brines. Thus, the removal of HCO_3 + CO_3 and SO_4 must of necessity lead to a marked increase in Cl enrichment. This is seen, regardless of actual concentration e.g. Great Salt Lake and the Lake Magadi basin.

So, it is not really surprising to find that the salinity of brines as indicated by fluid inclusion studies have been predominantly reported as NaCl equivalents. What is surprising is the recent number of publications referring to $CaCl_2$ equivalent brines and other combinations (Bone and Griffin, 1984). This does not imply that these brines are immature in the sense of basinal brine evolution, because metamorphic conditions favouring the new formation of Na and K silicates has to be taken into consideration.

(ii) fractionation mechanisms other than mineral precipitation.

The composition of the evolving brine could also be altered by dissolution and precipitation cycles. Although the terminal stage of the continued precipitation products will reflect the composition of the parent brine, when these products are percolated by dilute i.e. undersaturated, run-off water, a pronounced fractionation will occur due to the more soluble components dissolving first, leaving a residually enriched crust i.e. enriched in the least soluble components e.g. silica and alkaline earth carbonates. The now disproportionally enriched run-off water will either mix with the basin brine, thus altering the ratio of the solutes; or will be subjected to a further evaporative cycle - but with differing soluble efflorescent crusts forming, deeper into the basin.

Fractionation patterns will also be disrupted if there is a physical impediment to normal groundwater flow patterns e.g. intruding dyke, fracture zones. Tectonic disturbances of a short duration will also be disruptive, whereas development of a new tectonic character can bring about the cessation of the evolution of the brine. Conceivably, this could be at quite an early stage in the geochemical evolution of the brine, as suggested earlier.

Adsorption or the formation and subsequent fractional dissolution of coatings on soil particles will affect evolving brines in a similar manner. This latter process can be readily observed in South Australia to-day, where, dependent upon source, calcrete or sepiolite are forming in situ in soils (Callen, 1977; Warren, 1983).

The importance of soil hydrology is apparent when
considering the enigma of the closed basin situation at the
Coorong, South Australia (Fig. 3), where lakes within a few
hundred metres of each other are precipitating different
mineral phases e.g. magnesite, dolomite, gypsum (D. Lock, pers.
comm. 1982). These lakes can be viewed as "outcrops of the
water table," as the carbonates are clearly forming from
groundwater (von der Borch and Lock, 1979). The carbonates
form as spherules, which become spheroidal aggregates of
carbonate rhombohedra (0.3 μm) which eventually form into
individual rhombohedra. The spheroidal nature may be due to
precipitation occurring within a silica gel. Although silica
cannot be observed optically, X.R.D. analyses show
concentrations of up to 10% (D. Lock, pers. comm.). The source
area(s) and complexities of the hydrogeochemical cycle for this
area results from its gentle but continuing tectonic emergence,
which is leading to progressive restriction. It can be viewed
as a relict early rift basin unit, and thus can be correlated
with the early rift basin unit in the Adelaide Geosyncline -
the Skillogalee Formation, or more correctly - the Mundallio
Subgroup (Uppill, 1980).

(iii) loss of volatiles other than water.

Loss of volatiles can result from reduction in pressure,
increase in temperature, decrease in solubility of volatiles as
salinity increases, or organic activity.

Carbon dioxide loss can lead to the precipitation of Ca -
and Mg - carbonates, via the reaction $M(HCO_3)_2 \rightarrow MCO_3 + CO_2 + H_2O$. This reaction involves the stability of $(HCO_3)^- \rightarrow CO_2 + (OH)^-$. This mechanism explains the resultant increase in pH,

in alkaline brines. This pH increase is enhanced by the decrease in solubility of CO_2 with the increase in salinity that must eventuate as the carbonates precipitate.

Where loss of volatiles is due to the loss of H_2S by bacterial reduction, formation of sulfides can occur, in particular iron sulfides. Later oxidation of this ferrous iron significantly alters the pH, which in turn influences other solute fractionation mechanisms.

(iv) brine mixing - brine dilution.

It is well established that alkaline earth carbonates will precipitate when alkaline brines mix with dilute brines (Eugster and Maglione, 1980).

In conclusion, there are a number of pathways whereby magnesite can be precipitated directly from solution at or near the surface of the earth.

3.6. Magnesite Deposits

3.6.1 General

Recently formed magnesite of sedimentary origin is found mainly in lacustrine environments. The magnesite is frequently found in association with other carbonate minerals. Examples within Holocene sediments include Lake Magadi, Kenya (Eugster and Jones, 1979), the Basque Basin, British Columbia (Eugster and Hardie, 1978), ephemeral lakes peripheral to the Coorong, South Australia (von der Borch and Lock, 1979). Tertiary age lacustrine deposits occur at Aiani-Kozani, Greece and Bela Stena, Yugoslavia (Morteani et al., 1982).

Marine magnesites of recent formation on the other hand, are very rare. The reasons why magnesite does not normally precipitate directly from sea-water have already been discussed. It is present, however, in sabkhas along the Trucial Coast in the Persian Gulf, where it occurs in association with anhydrite (also rare - the usual sulfate being gypsum). The Trucial Coast magnesite is thought to have formed very early diagenetically within the sediment (Kinsman, 1969b; Bush, 1973).

Magnesite deposits in older sedimentary-milieus are found in all continents, with the greatest density of them being within geosynclinal belts. This is illustrated by Fig. 3, showing the major Australian occurrences. The sedimentary environment in which the magnesite is found is always the one that is favourable to the formation of evaporites, although minerals such as halite and/or gypsum are not necessarily present. This interpretation is usually based on evidence such as geochemical parameters and/or the presence of stromatolites, as the recrystallization of magnesite has usually caused alteration or destruction of primary textures which could have been diagnostic. Association with dolomite, and silica to a lesser extent is common.

Some of the deposits described in the literature occur in Manchuria (Nishihara, 1956), North Korea (Shevelev, 1978), India (Valdiya, 1968), Alligator Rivers area, Northern Territory (Gustafson and Collins, 1983), Rum Jungle, N.T. (Crick and Muir, 1980; Bone, 1983). Probably the best preserved sedimentary textures occur in the magnesite deposit of the Mundallio Subgroup, South Australia (Uppill, 1980). Another deposit at Kharidunga, Nepal, was visited by the
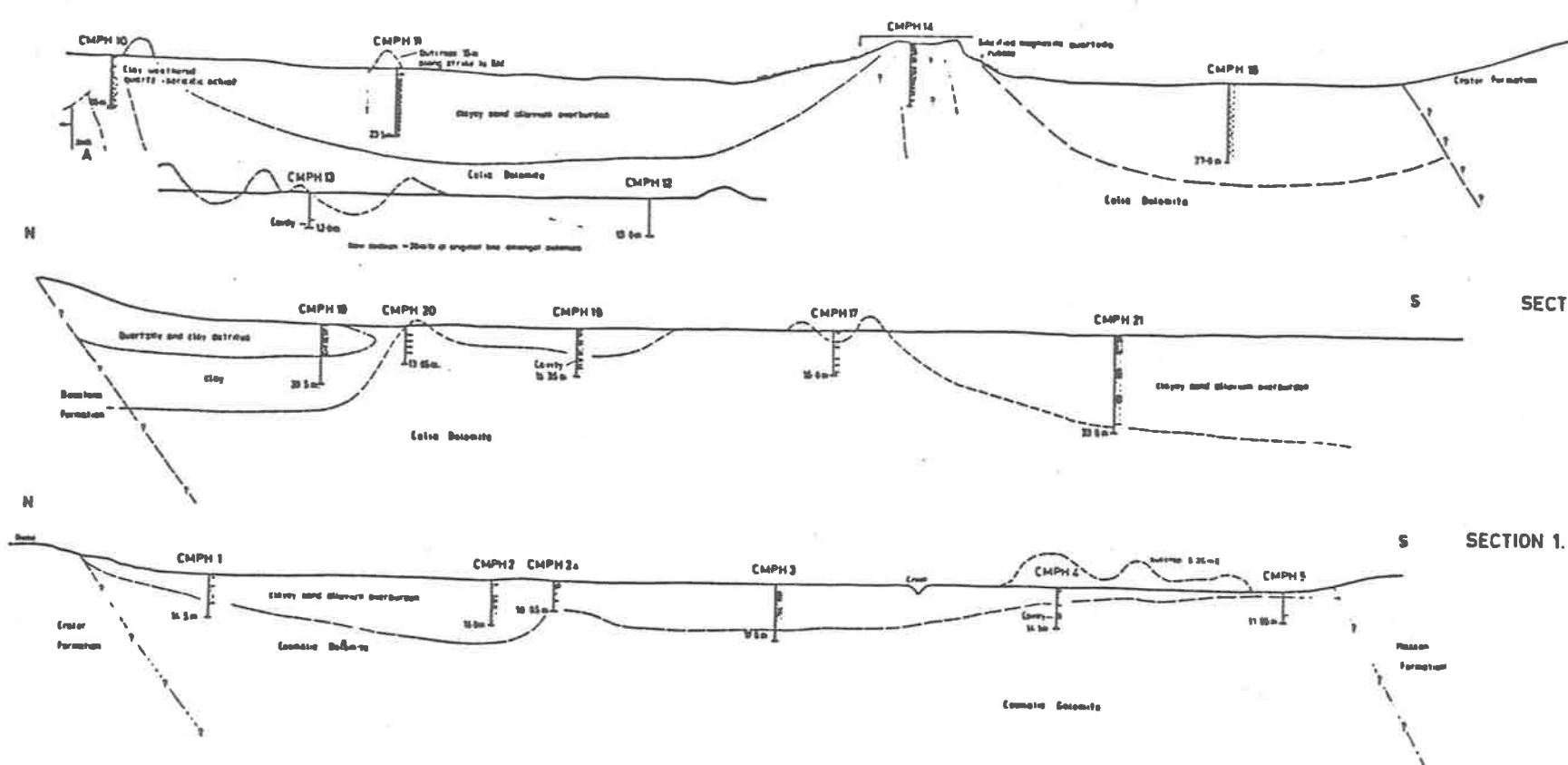
Fig. 32: Composite section profiles through drill holes, E.L. 1349, indicate karst-like topography of Celia Dolomite and Coomalie Dolomite. Scale 1:1,000 (Roberts, 1978)

author, and forms part of this thesis study, but the deposit has not yet been described in the literature.

Deposits of magnesite of definite metasomatic origin and associated with ultramafics are also well represented in the literature and can be represented by the following: - Naxos, Vavdos area Greece (Dabitzias, 1980) and Timmins (Fyon et al., 1983). Metasomatic deposits of sedimentary orign include: the Grauwackenzone, Austria and Balcanoona, South Australia (Johns, 1976). The last named is reported to result from Mg-metasomatism, but it could equally be possible that it results from the recrystallization of a primary magnesite, as is the case in the Alligator Rivers area, Rum Jungle and Kharidunga deposits.

Frost (1982) considers that the Savage River, Tasmania deposit is the result of the Mg-metasomatism of a primary dolomite, which consequently does classify it as a hydrothermal type. Apparently the deposit at Snarum, Norway is even more enigmatic, (Josang, 1966) and no definite decision has been made as to its origin. This illustrates the problem created by the recrystallisation of a magnesite of either origin, to a sparry magnesite - the most common type in all pre-Holocene magnesites.

3.6.2 Rum Jungle Magnesite Deposits
3.6.2.1 Evidence for sedimentary origin

The magnesite occurs within the Celia Dolomite and the Coomalie Dolomite (Fig. 2). The recrystallization of the magnesite has resulted in the two carbonate forms: bladed and rhombohedral which resemble the crystal-morphology of halite
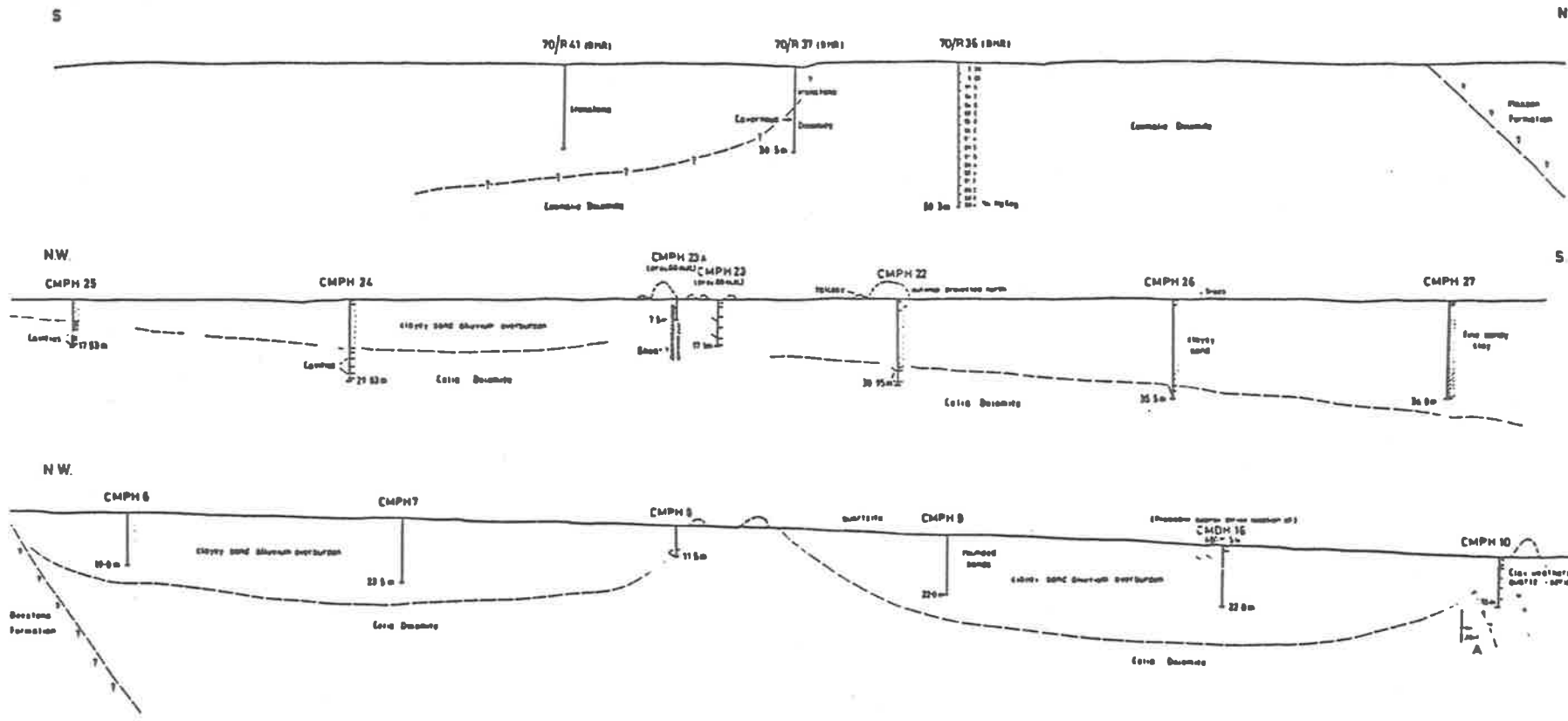
Fig. 33: Composite section profiles through drill holes, E.L. 1349, indicate karst-like topography of Celia Dolomite and Coomalie Dolomite.
Scale: 1:1,000   (Roberts, 1978)

and gypsum (Plate 8-10), but are actually the result of differences in temperature of the fluid involved in the recrystallization process as will be discussed in Chapter 6.

The most conclusive megascopical evidence for a sedimentary mode of formation is the presence of stromatolites. These are ubiquitous, and quite easily identified (Plates 11-14) in most cases, whilst others would come under the cryptalgal stromatolite category (Plate 15). The stromatolites are discussed in more detail in Chapt. 4.

Associated with the stromatolites at the Fossil Reserve locality (Fig. 7) are dome-like structures that tend to look reminiscent of tepee structures (Plates 16). Tepee structures are very common in the Coorong and Marion Lakes area (von der Borch and Lock, 1979, Botz and von der Borch, 1984) where this growth process can be observed and measured. Similar structures have also been observed in the Mundallio Sub-group magnesite (Uppill, 1980). They are formed by upwelling groundwaters. It is from this upwelling groundwater (basin brine) that the magnesite is precipitated.

Further physical evidence to support the notion of sedimentary origin for the magnesite is the presence of a palaeo-karst surface at the interface between the carbonates and overlying sequences. This karst surface has been exhumed by Recent erosion (Plates 17, 18). It is also frequently encountered in drill-holes, when there is a sudden loss of circulation as a cavern is encountered by the bit. This is illustrated in profiles of the earlier drilling programme (Figs 32, 33).
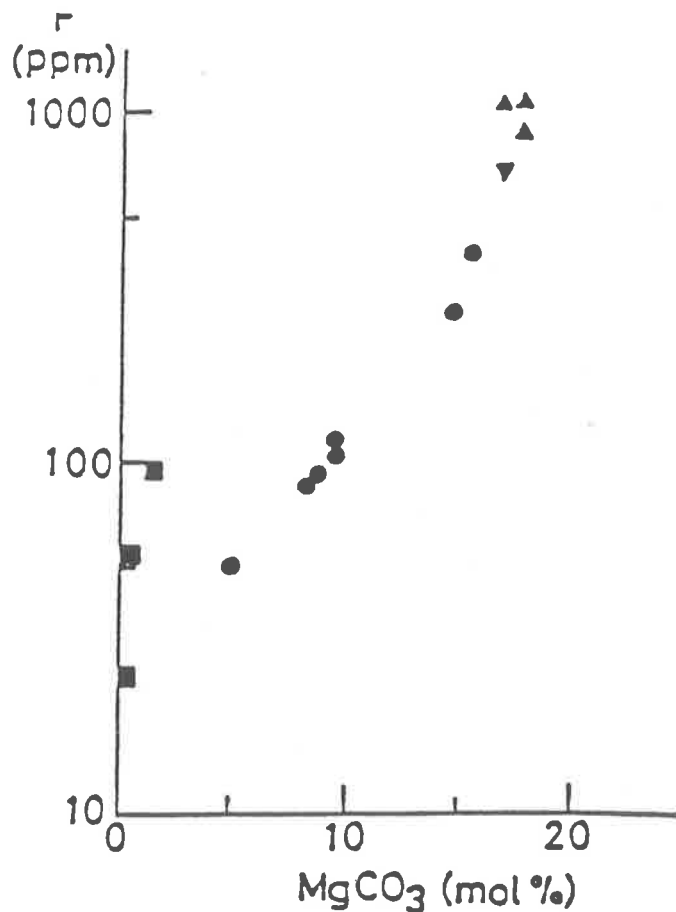
Fig. 34a: Plot of F content of marine skeletal cargbonates against $MgCO_3$ content

■ oyster, ● echinoid, ▼ starfish, ▲ calcareous alga
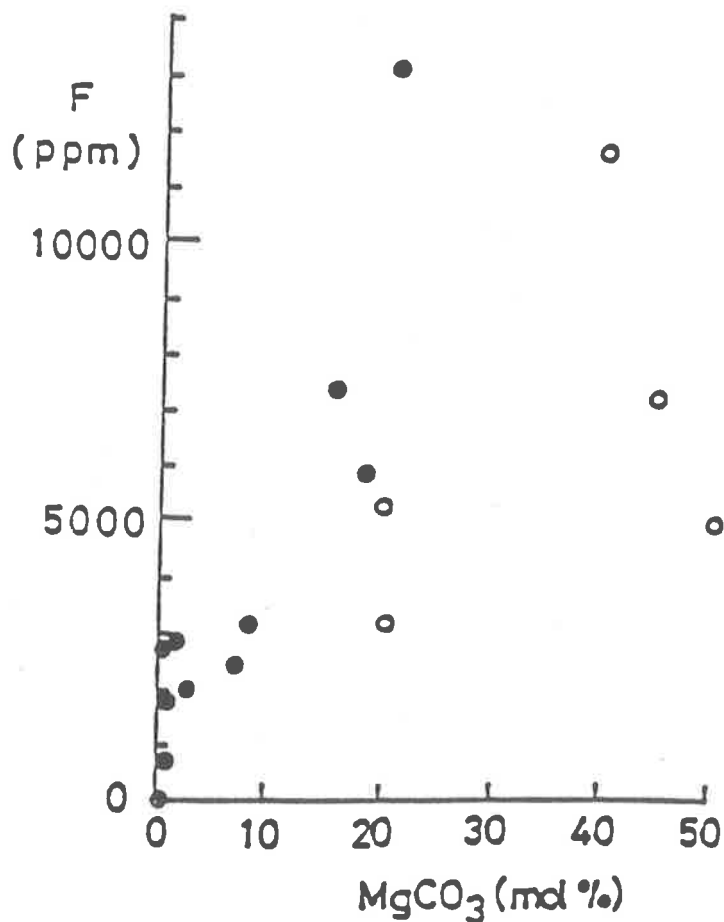
Fig. 34b: Plot of F content vs $MgCO_3$ content of Ca-Mg carbonate formed in $CaCl_2$ (25m mol/1) - $MgCl_2$ (0-1.0 mol/1) - $NaHCO_3$ (0.18) mol/1) - NaCl (.0 mol/1,02 mol/1)-NaF(F,5mg/1)-H_2O solution at 25°C.

(Ohde and Kitano, 1980)

In both the Beestons Formation and the Crater Formation there is ample evidence to conclusively support their sedimentary origin e.g. ripple marks, cross-bedding etc. (Plate 2). It is difficult to perceive a non-sedimentary origin for the inter-stratified carbonate, although this does not necessarily support the notion of magnesite as a primary carbonate.

Moreover, none of the geochemical data (Appendix 3) for the area makes it necessary to invoke a precursor to the crystalline magnesite other than magnesite itself. Indeed, the geochemical data lends support to the primary magnesite theory e.g. low Sr values. Similarly, Na values are an order of magnitude lower than the average for carbonates (Veizer, 1983).

As the F content of a carbonate sediment is controlled by the concentration of Mg^{2+} ions in the primary solution and by the Mg-carbonate content of the resulting carbonate sediment (Fig. 34, Ohde and Kitano, 1980), high F values in the recrystallized magnesite would tend to suggest that this F is associated with primary magnesite rather than calcite, unless there was an external F source at the time of recrystallization. Many of the F values (Appendix 3) are above the average for carbonates (Veizer, 1983), thus supporting the primary magnesite premise.

Solid inclusions within the magnesite grains are ubiquitous. They are usually <5μm in diameter. The rounded shape of the rutile, ilmenite grains (and of some of the quartz and tourmaline), suggest that these are detrital, as do the ragged nature of microcline grains (Plate 19). These grains were probably shed off the adjacent Complexes and blown or

washed into the lakes around the margins of the domes.
Tourmaline and apatite also occur as very small intragranular
euhedral crystals, suggesting an authigenic origin.

Although apatite is not usually formed as an authigenic
mineral in evaporite deposits (Trueman, 1971) it is commonly
found associated with Precambrian blue-green algae (Southgate,
1978). Authigenic tourmaline can also be formed in an
evaporitic environment. As will be discussed in Chapter 4 some
of the silicified magnesite areas have very high tourmaline
contents (>50%-Plate 28), but this is probably a different
genesis altogether.

There is up to 10% SiO_2 in the magnesite, and
occassionally higher proportions. This is much higher than the
average for sedimentary Ca-carbonates (5.1% SiO_2, Veizer,
1983); whilst hydrothermal magnesite has an average value of
1.2% SiO_2 (Dabitzias, 1980). The Rum Jungle figure compares
favourably with the average of 10% SiO_2 values obtained for the
lacustrine magnesites of the Coorong (von der Borch and Lock,
1979) and the Mundallio Sub-group (Uppill, 1980). Silica will
be discussed in more detail in the section on diagenesis
(Chpt. 4).

The layer silicate grains (e.g. chlorite, sericite, talc,
illite) contained in the magnesite result from low temperature
- low pressure metamorphic reactions, e.g. $3MgCO_3 + 4SiO_2 + H_2O \rightarrow$
$Mg_3Si_4O_{10}(OH)_2 + 3CO_2$. The formation of talc is considered
to be the first step in the formation of new minerals by the
thermal metamorphism of siliceous dolomites (Deer et al.,
1966), and therefore presumably, also siliceous magnesites.
The experimental investigations of Fyon et al. (1983) show that
a temperature of 400-500°C, a pressure of 2Kbars and a CO_2-

bearing fluid is necessary for the formation of a talc-magnesite-quartz assemblage. This temperature seems rather high for the Rum Jungle situation, where fluid inclusion data suggest much lower temperatures (Chpt. 6).

McNamara (1965), in contrast, gives a temperature of around 200°C and a pressure of 2 Kbars for the assemblage chlorite-magnesite-quartz, and assigns it to the lowest of his 3-fold subdivision of the greenschist facies. This temperature certainly is within the range of the fluid inclusion data.

Solid inclusion in chlorite indicate a secondary nature (Stewart, 1979) rather than an authigenic origin of the chlorite. If these inclusions e.g. quartz, have optical continuity, it indicates that they are relict grains of a precursor single grain i.e. the current host is the replacer.

The high Mg content of the Rum Jungle chlorites (Appendix 3) suggests that they formed by the metamorphism of an evaporitic type sediment (Stewart, 1979). As the chlorites also contain quite considerable amounts of Al_2O_3 (i.e. $>$ 6%), a significant quantity of clay must have been present in the original sediment. This 'clay' probably resulted from the weathering of feldspathic detritus from the Complexes source area. This idea is further supported by the presence within the magnesite of fine grains of K-feldspar, sericite and occassionally illite - with the sericite being by far the most common.

There is no petrographic evidence to suggest that this widespread chlorite results from retrograde metamorphism. This chlorite is earlier than the wall rock alteration chlorite seen

adjacent to the ore deposits. Therefore it seems reasonable to propose that the chlorite and the other metamorphic minerals e.g. talc, actinolite etc. are the result of the low-grade metamorphism of a sediment.

3.6.2.2 Evidence for lacustrine origin

Accepting that the magnesite is of sedimentary origin, the next step is to assess the possibility of formation within an alkaline lake environment, as it has been shown that a marine environment is highly unlikely.

The detrital clasts that make up the framework of the arenites of the Beestons Formation and the Crater Formation are derived from the Rum Jungle and Waterhouse Complexes. This material was shed by physical weathering processes, enhanced by the diapiric uprising of the Complexes. The permeability and porosity of the ensuing detrital sediment would have allowed the flow of groundwater. This groundwater could have a high enough Mg^{2+} content to be a potential magnesite source through involvement of any of the three processes discussed earlier, particularly in view of the geochemistry of the basement granitoids (Ferguson et al., 1980). Fritz (1982) has invoked granitoids under similar situations in Canada as being the source of alkaline groundwaters. Certainly the analyses of the fluid inclusions (Bone and Griffin, 1984 and Chpt. 6), with their range of cations and anions and their apparent CO_3 or HCO_3 component, indicate an evolving brine ideally suited to deposit magnesite. This brine appears to have been evolving along the III A pathway (Fig. 31), a premise that is supported by the lack of evidence for the presence of either halite or gypsum. The fluid inclusion data indicate the brine's
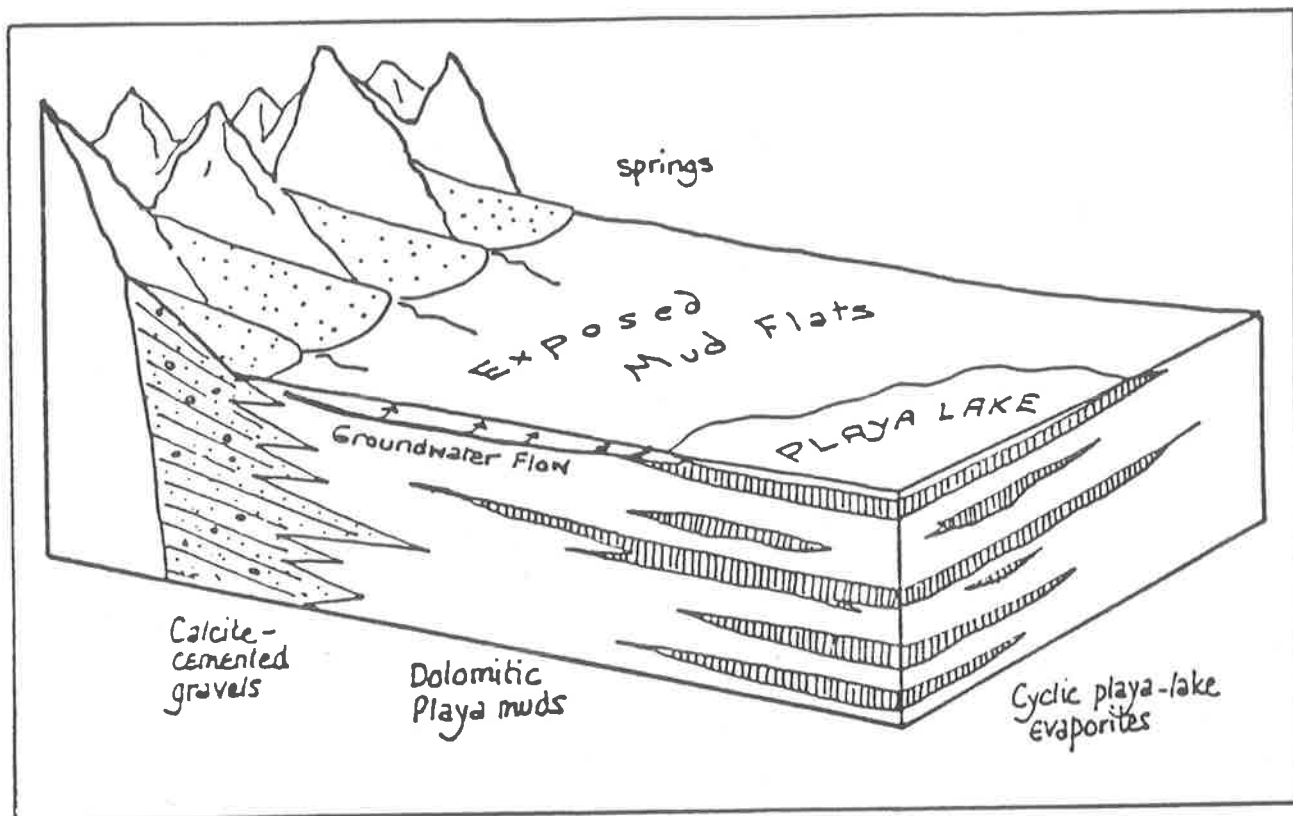
Fig. 36: Schematic block diagram showing depositional framework in the Playa Complex model. At Rum Jungle, the geochemistry of the groundwater enabled magnesitic muds to form.

(Kendall, 1979)

potential to precipitate magnesite. The precipitation mechanism is probably a complex interplay of the different processes already discussed.

It is proposed that the topographic situation was a combination of the Coorong model of Morrow (1982) and the Playa Complex model of Kendall (1979) (Figs 35, 36). In both these situations cyclic periods of flooding and exposure and dehydration of the surface of the lakes is needed to achieve magnesite precipitation. The tepee structures suggest this occurred at Rum Jungle.

Thus, the Complexes are envisaged as being rimmed by alluvial fans (proximal fluvial deposits) with the lower reaches being flooded by emerging ground water tables i.e. lakes. Unlike the Coorong situation though, the groundwater feeding these lakes was fairly homogenous, so that the only variation in precipitates is minor occurrences of dolomite. This uniformity occurs because of the radial drainage pattern that developed from the core sources.

Fractionation of the brines (as discussed in Chpt. 3.5.3) was enhanced by a physical impediment to the normal groundwater flow pattern e.g. change in slope with either waning or resurgence of diapirism. If complete cessation of diapirism occurred, then the evolution of the brine towards Na^+ and Cl^- dominance would have been prevented, and an "immature" basinal brine stage would have been fixed in time (as recorded in fluid inclusions). Dilution of this brine with infiltrating meteoric water, however, would have caused the precipitation of alkaline earth carbonates.

110

1.SEEPAGE REFLUXION OR REFLUX MODEL

$\rho = 1.05$ EVAPORITE DRAWDOWN

SL

$\rho = 1.21$

$0 - 1000$

Mg/Ca - 10-20

Salinity - 200-400‰

CO_3/Ca - <10/1

2.SABKHA MODEL (VARIANT OF REFLUX MODEL)

SL $\rho = 1.05$ LANDWARD LIMIT OF STORM TIDES

PROGRADATION $\rho = 1.21$

<10 METRES

Mg/Ca - 10-20

Salinity - 200-400‰

CO_3/Ca - <10/1

3.MIXED - WATER MODEL

SL   RECHARGE

A. SHALLOW

UNCONFINED SHALLOW COASTAL AQUIFER

2-20 METRES

Mg/Ca - 2-5

Salinity - <35‰

CO_3/Ca variable <1:1

SL   RECHARGE

IMPERMEABLE CONFINING LAYER

SOLUTION CAVERNS

100 2000 METRES

Mg/Ca - ~1:1

Salinity - <35‰

CO_3/Ca - variable <1:1

B. DEEP CONFINED AQUIFER OF DEEP CIRCULATION

4.COORONG MODEL (VARIANT OF MIXED WATER MODEL)   RECHARGE

EPHEMERAL LAKES

LAGOON

PROGRADATION

2-20 METRES

Mg/Ca - ≈2:1

Salinity - <35‰

CO_3/Ca variable up to 7:1

5.BURIAL - COMPACTION MODEL

SL.

COMPACTION SHALE MASS

PLATFORM CARBONATE

1000-2000 METRES

Mg/Ca - <1:1

Salinity - probably <35‰

CO_3/Ca - variable

Fig. 35: Dolomitisation models. The hatchured area is the site of possible carbonate formation. The Coorong Model (No. 4) is similar to the Rum Jungle situation, particularly as magnesite is currently forming in the Coorong.

(Morrow, 1982)

If, however, degassing was also on operative process, then both magnesite and sulfides could be precipitating. Although iron sulfide only exists in trace amounts in the magnesite except for the actual mineral deposit areas, it occurs as an accessory mineral in the underlying units and is quite common in the overlying Whites Formation. The S^{34} signature of this sulfide supports a sedimentary origin hypothesis (Chpt. 7 and Ewers et al., 1984).

Later diagenetic oxidation of this ferrous iron would have significantly altered the pH, which, in turn, influenced other solute fractionation mechanisms. This oxidation process can be seen to have been quite widespread at Rum Jungle e.g. Mt. Fitch, Mt. Minza.

Total annihilation of the evolution of the continental brine system could be brought about by the rapid transgression of marine waters. The conformably overlying Whites Formation is seen as a transitional phase between carbonate shelf and subtidal siltstone (Needham and Stuart-Smith, 1984), indicating a marine transgression, albeit not necessarily a rapid one. Analyses of the fluid in fluid inclusions in Whites Formation minerals to test whether this sequence contained a Na^+ and Cl^+ dominated brine was unable to be carried out due to lack of suitable material. This was most unfortunate. (Coarser grained suitable material was available from the various mineral deposits, but this was not considered to be typical).

Thus, notwithstanding the theoretical problems of formation of primary sedimentary magnesite, it is suggested that the following evidence supports a primary genesis of magnesite: stromatolites, the tepees, the associated fluvial

sediments, karstification, the geochemistry of the carbonates, the associated minerals and solid inclusions, presence of brines not dominated by Na^+ and Cl^+, and the S^{34} signature of contained diagenetic sulfides.

3.6.3. Kharidunga, Nepal

A similar suggestion is made concerning the magnesite deposit at Kharidunga, Nepal, although some of the evidence seen at Rum Jungle was not observed in the short time spent at the former location. Some of the evidence, however, was more convincing than the Rum Jungle material e.g. a road cut into the hill-side has revealed an excellent exposure of a palaeokarst surface (Plate 19).

RUM JUNGLE MAGNESITE DEPOSITS

4.1 Stratigraphy

Since the discovery of secondary U mineralization in the Rum Jungle area by J.M. White in 1949 the area has been mapped/described in some detail by numerous workers (Carter, 1953; Williams, 1963; Rhodes, 1965; Walpole et al., 1968; Berkman, 1968; Meizitis, 1969; Ingram et al., 1974; Johnson, 1974; Fraser, 1975; Crick, 1978; Needham et al., 1980; Berkman and Fraser, 1980; Fraser, 1980; Crick et al., 1981; Bone, 1983; Pagel et al., 1984; Paterson et al., 1984). The regional stratigraphy was initially described by Walpole et al. (1968). Since then there have been substantial revisions in interpretation and correlation of various formations. The most recently published stratigraphy (Ewers et al., 1984) is shown in Fig. 6, where it is compared to earlier versions. Details of the various stratigraphic units are given in Chpt. 2 on Regional Geology.

4.2 Sedimentary Environment of the Magnesite Deposits
4.2.1 Lacustrine environment
4.2.1.1 General

It has already been shown that it is more likely that the hydrochemistry necessary for the formation of magnesite can be achieved in an alkaline lake situation than in a marine environment (Chpt. 3). The lacustrine environment can lead to a number of different evaporative conditions even within the same physiographic province, as can be seen in the Coorong

a.   A very well developed tepee structure in magnesite in the Celia
       Dolomite, Fossil Reserve, E.L. 1349. The sides of the structure
       are brecciated and dragged upwards, with the fragment below the
       scale looking as though it slumped down the up tilted flank of
       the tepee.

b.   Several tepee structures along the same bedding plane. The
       central tepee structure extends into the overlying beds for more
       than 0.5 metre. A thick sequence of stratiform stromatolites
       underlie the tepees. Celia Dolomite, Fossil Reserve, E.L. 1349.

c.   A closer view of the base of the central tepee in the photo
       above. It can be seen that algae continued to adhere to the
       flanks of the heaving tepee in comparison to the planar
       orientation of the stratiform stromatolites that form the base of
       the tepee layer. All the tepee structures have their bases
       parallel to bedding.

situation to-day, where variation occurs in adjacent lakes no more than a few metres apart (Botz and von der Borch, 1984). Indeed, variation can even occur within the one lake if it is large enough to allow for local differences in evaporation rates, which leads in the Lake Chad situation to the evolution of three different brines in three different areas of the lake, two of which have a pH sufficiently high to enable magnesite precipitation (Eugster and Maglione, 1979). In contrast, the marine environment is rarely able to achieve the physio-chemical parameters necessary for magnesite precipitation, the exception being the Trucial Coast occurrence. (Chpt. 3).

4.2.1.2   Tepees

Tepee is the accepted term used to describe structures that look like cross-sections of American Indian tents. They are usually preserved in carbonate beds, where they form fractured buckles, which distort the overlying beds (Plate 16). In plan view, where these buckles intersect, an irregular polygon pattern is produced.

Tepee structures are confined to fairly limited environments. For a tepee to form there must be an extended period of exposure (von der Borch and Lock, 1979). There are two main ideas concerning the formation mechanism. Assereto and Kendall (1977) propose that crystal growth due to the accumulation of evaporative products within the sediment leads to expansion, and combined with carbonate precipitation, moisture swelling, thermal expansion being superimposed on the effects of dessication and thermal contraction, leads to disruption, which occurs in a polygonal pattern. The alternative model of von der Borch and Lock (1979) proposes

PLATE 11

a.   (at left) Conophyton type stromatolites, now silicified, within
      the Celia Dolomite, Fossil Reserve, E.L. 1349.

b.   (at right) A closer view of the previous photo, showing the
      cylindrical habit of the stromatolites.

c.   Close-up of silicified Conophyton type stromatolites. The grey
      colour is due to encrusting algae/lichen on the weathered
      magnesite, and is ubiquitous throughout the Rum Jungle area.
      Celia Dolomite, Fossil Reserve, E.L. 1349.
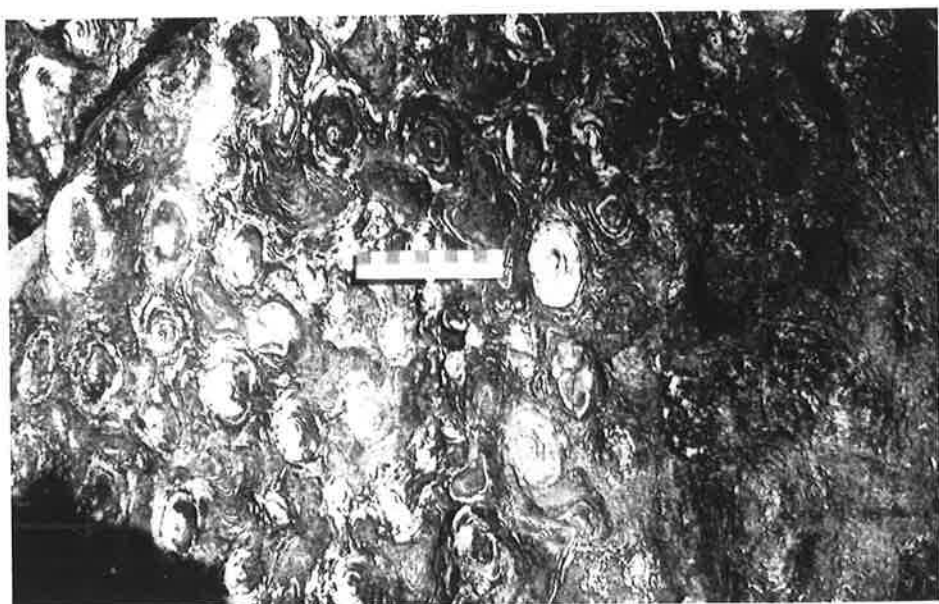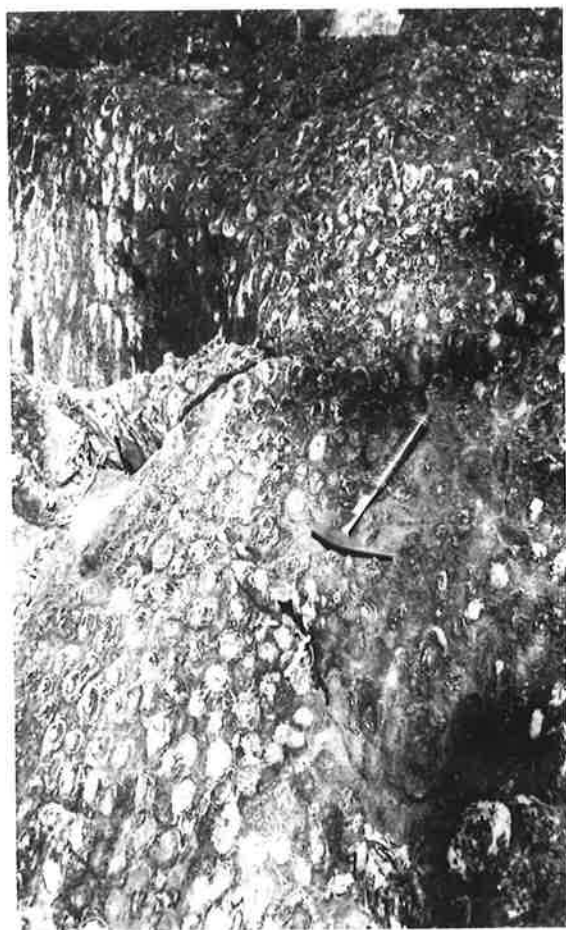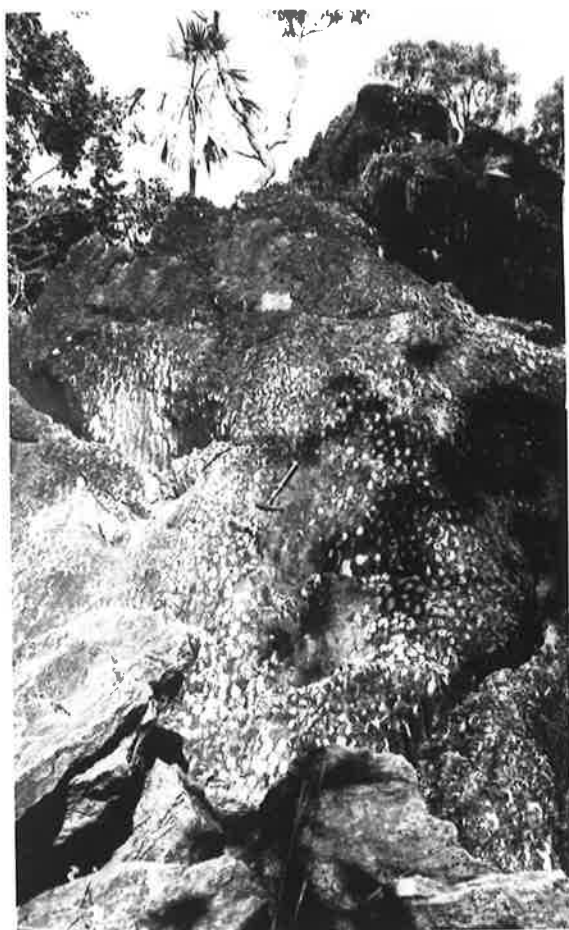
that tepee formation in ephemeral carbonates lakes results from compressional stress produced as upwelling groundwater causes extrusion of very fine grained material at polygon boundaries. There is disruption of the sediment in the centre of the polygons, leading to intraformational breccias if dessication continues. In most tepee cases reported in the literature the environment has been peritidal/supratidal, (Assereto & Kendall, 1977) or lacustrine (Warren, 1983).

Tepee structures are present in the magnesite at Rum Jungle (Plate 16 and Appendix 1). As they are parallel to bedding and associated with stromatolites, it is difficult to consider these sharply peaked domal structures as any different than normal sedimentary tepee structures. Due to the extensive post-deposition alteration of the magnesite, there is no evidence remaining of dessication. Of course, it may be that binding of the surface sediment by algal mats inhibited the formation of dessication cracks anyway. There are very few references in the carbonate literature to tepees forming in the marine environment below the supratidal line (Shinn, 1969; Assereto & Kendall, 1977).

4.2.1.3 Clay Minerals

The distribution of the very fine non-carbonate grains e.g. clays, throughout the magnesite suggests dispersal by wind as the main transporting medium. Wind blowing dust across exposed lake surfaces would achieve the wide-spread, sparse but fairly even pattern seen. Other larger particles could have been washed into the lakes during seasonal filling.

PLATE 12

120

a.   A large domal-type stromatolite, with partial silicification of
     the core. The host magnesite is fine grained. Celia Dolomite,
     Fossil Reserve, E.L. 1349.

b.   Domal stromatolites growing in close proximity to one another.
     There has been minor silica replacement of these stromatolites.
     The magnesite is much coarser than in the previous photo, but is
     from the same location.

c.   A relatively small domal-type stromatolite the rim of which has
     been completely replaced by fine grained quartz. This
     stromatolite was solitary. Outcrop 19, Area B, Celia Dolomite,
     E.L. 1349.
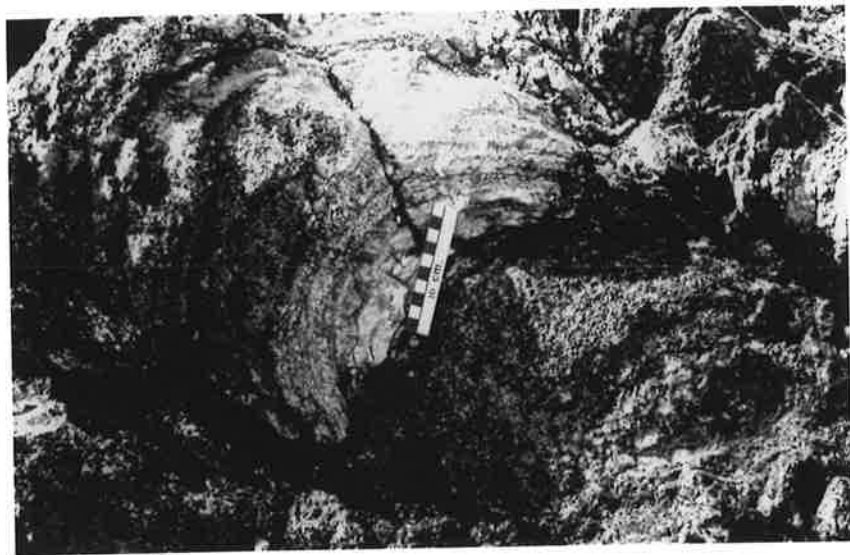
4.2.1.4 Stromatolites

The ubiquitous stromatolites occurring throughout the magnesite horizons are also supportive evidence for a shallow water environment which was not necessarily marine (Osborne, 1982). A situation where large stromatolites are actively growing in a lacustrine environment can be observed at Lake Clifton in Western Australia (Moore et al., 1984). Stromatolites are discussed in more detail in the following section.

Thus, tepees, associated accessory mineral grains and stromatolites all point to a supratidal or lacustrine environment for the site of deposition of the Rum Jungle carbonates. The fact that these carbonates were primary magnesites selects the lacustrine environment as the more likely of the two. The hydrochemistry necessary for magnesite precipitation demands that this lacustrine environment contain alkaline waters. So, it is probable tht the Celia Dolomite and the Coomalie Dolomite were deposited in an alkaline, lacustrine environment.

4.2.2 Stromatolites

Stromatolites are "laminated, lithified sedimentary growth structures that accrete away from a point or limited surface of attachment ...... commonly of microbial origin and calcareous composition" (Semikhatov et al., 1979). It has been customary to stress the laminar nature of stromatolites rather than their organic origin. More recently there has been greater emphasis placed upon the organic cause of these structures. Buick et al., (1981) go so far as to insist that "the word

PLATE 13

a.   (at left) At ground level, stratiform stromatolites grade
     upwards into more columnar forms, particularly evident in the
     vicinity of the hammer. This is followed by almost cessation of
     growth, followed by a new build-up of stratiform type.

b.   (at right) A closer view of the columnar and overlying
     stratiform stromatolites shown in the previous photo. Both forms
     are well preserved because of silicification. Outcrop 29, Area
     B, Celia Dolomite, E.L. 1349.

c.   Well laminated stratiform stromatolites, showing classic
     wrinkling and curvature. Partial silicification of the
     stromatolites enhances their morphology. Outcrop 30, Area B,
     Celia Dolomite, E.L. 1349.
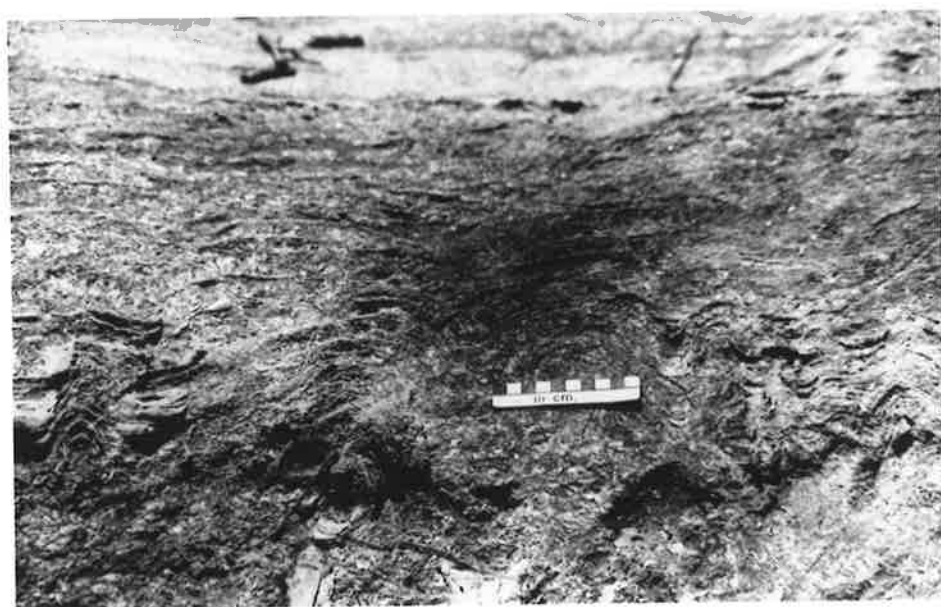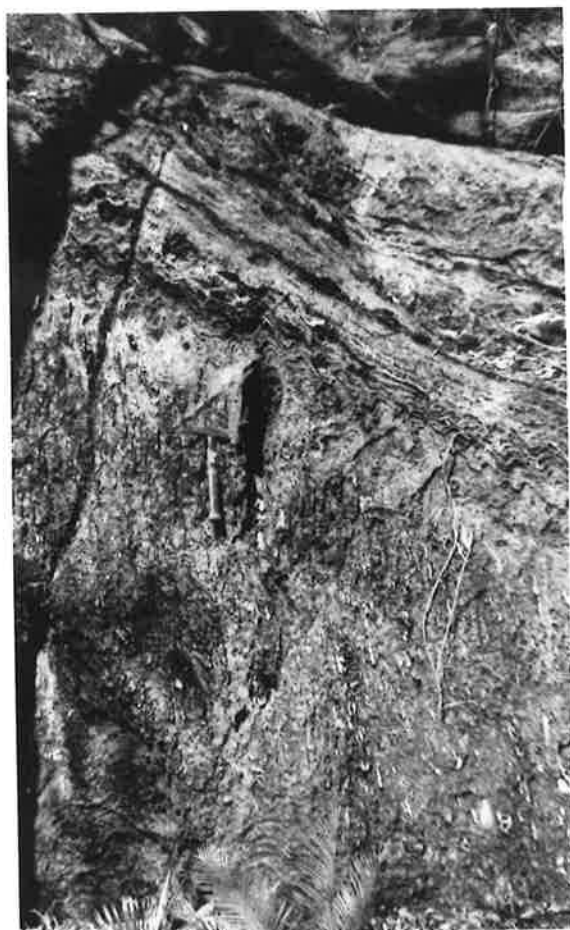
'stromatolite' should only be applied to organosedimentary structures predominantly accreted by sedimentary trapping, binding and/or in situ precipitation as a result of the growth and metabolic activities of benthic, principally prokaryotic, micro-organisms". Where it is difficult to positively prove biogenicity (e.g. in the form of filaments of blue-green algae) in so-called stromatolites older than 1600 Ma, they suggest that the term 'stromatoloid' be employed. They list 8 criteria that must be present for positive identification:-

1. The structures must occur in undoubted sedimentary or metasedimentary rocks.

2. It must be demonstrated that the structures are synsedimentary.

3. There should be a preponderance of convex-upwards structures.

4. Laminae should thicken over the crests of flexures.

5. If the structures are laminated the laminations should be waxy, wrinkled and/or have several orders of curvature.

6. Microfossils or trace fossils should be present within the structures.

7. Changes in composition of microfossil assemblages should be accompanied by morphological changes in the stromatoloid.

8. The fossils or trace fossils must be organized in a manner indicating trapping, binding or precipitation of sediments by the living organism.

Even without recourse to 6-8, mimics i.e. inorganic simulations, are usually eliminated by at least one of the previous 5, and especially by the lack of wrinkled etc. laminations.

a.   Stratiform stromatolites showing almost complete silicification,
        in a fine grained magnesite. Outcrop 11, Area A, Celia Dolomite,
        E.L. 1349.

b.   This stromatolite, preserved within fine to medium grained
        magnesite, has an inner core of very coarse, bladed magnesite.
        This inner core is surrounded by several thin layers of
        cryptocrystalline quartz. Outcrop 2, Area B, Coomalie Dolomite,
        E.L. 1349.

c.   These ovoid, blebly quartz areas within fine grained magnesite
        may be the result of partial replacement of Conophyton type
        stromatolites by silica. Outcrop 23, Area B, Celia Dolomite,
        E.L. 1349.

In reference to the structures termed stromatolites (and for convenience and continuity this term will be retained) at Rum Jungle, the first has already been demonstrated. The second will be demonstrated after a brief description of the three major types observed:-

(a) Conophyton-like (Semikhatov et al., 1979).

These are always replaced by quartz (Plate 11). They are columnar-type, and always lack lateral linkage (Grey, 1980). The occurrence of columnar stromatolites in biostromes is thought to indicate uniform substrate and a uniform depositional environment over extensive areas (Uppill, 1980). Although Playford and Cockbain (1969) have recorded stromatolites at depths of 45m, or more, it is considered more likely that Conophyton forms in a much shallower environment e.g. a similar form to Conophyton occurs in lagoonal limestones of the Belingwe Greenstone Belt, Zimbabwe (approximately 2,700 Ma) (Martin et al., 1980). This type is frequently underlain or overlain by the other two types (Plates 5, 12-14).

(b) Stratiform-type (Plates 5, 12-14).

These are usually replaced by quartz. These are always well laminated, with the laminations amply fullfilling the requirements of criterion 5. Semikhatov et al., (1979) consider that the vertical zonation i.e. from stratiform to columnar, is often associated with changes in texture or structure of the enclosing rock. This does not appear to be the case at Rum Jungle, although it may be that recrystallization has obliterated any such evidence. However, in some transgressive rhythms the stratiform type occurs both

PLATE 15

a. Cryptalgal laminates preserved as rhomb type magnesite. Celia
    Dolomite, Fossil Reserve, E.L. 1349.

b. Standing back from the above photo, the cryptalgal laminates have
    the appearance of large, domal stromatolites.

c. These cryptalgal laminates also look like domal stromatolites.
    Outcrop 20, Area B, Coomalie Dolomite, E.L. 1349.

at the top and the base of the sequence - and this certainly is seen at Rum Jungle, with the top becoming the base of the next cycle. This rhythmicity is further evidence to support the ephemeral nature of the lacustrine environment, just as iterative environmental changes are needed to produce the laminations in the stratiform type, due to diurnal or seasonal overturn.

(c)   Cryptalgalaminates (Plate 15).

This type are often found lateral to the more definitevely determined stromatolites. They are not fossils in the true organismic sense, but rather sedimentary structures formed under biological influence. There is no quartz replacement. They are usually broadly domed; occassionally stratiform.

The occurence and type of stromatolite present for all outcrops of magnesite in E.L. 1349 is listed in Appendix 1.

The second criterion is demonstrated by the fact that the co-existing stromatolites are synsedimentary, otherwise there would have been a discontinuity between stromatolites and their sedimentary host.

Criteria 3, 4 and 5 are all quite readily and convincingly observed. Criteria 6 to 8 are not met. However, as Buick et al., (1981) state that mimics are usually eliminated by failure to meet all of criteria 1 to 5, especially those concerning laminations, it seems likely that the structures seen at Rum Jungle are true stromatolites.

It is difficult to be categoric about the palaeoenvironmental implications of the presence of these 3 types of stromatolites in the Rum Jungle lakes. The Late Riphean age stromatolites on the Varanger Peninsula, N. Norway originated in fresh water and schizohaline supralittoral ponds (Siedlecka, 1982). However, work on younger (Plio-Pleistocene) lacustrine environment stromatolites from Lake Turkana, Kenya by Abell et al., (1982) shows that no single environment appears to have been favoured as they range from fluviatile to lacustrine; from turbulent to non-turbulent. Moreover, the gross morphology does not correlate with any particular characteristic of the physical environment. Similarly, no attempt has yet been made to use stromatolites for stratigraphic zoning of rocks older than 1650 ± 50 Ma.

The evidence supplied by the presence of these 3 types of stromatolites is that there were cyclic shifts in water depth in the relatively shallow water of the Rum Jungle lakes during deposition of the Celia Dolomite and the Coomalie Dolomite.

4.2.3 Evaporites

By definition, evaporites are a group of rocks that form by precipitation from concentrated brines (Kendall, 1979). They can be either primary precipitates or diagenetic precipitates. Primary precipitates are formed by sedimentary processes, and consequently structures and textures can be related to hydrodynamic and other depositional parameters. On the other hand, diagenetic precipitates are formed by post-depositional processes, and consequently their mineralogy relates to the physiochemical environment. Many workers still adhere to the previously held idea (e.g. Shearman, 1966) that

an evaporite sequence starts with gypsum, then halite etc.; but carbonates should also be considered evaporites as they can and do form as both primary and diagenetic precipitates. Those that form by the first mechanism are undoubtedly able to be modified/extensively altered by the second mechanism, thus blurring the distinction between the two genetic classes. The hydrogeochemistry of the precipitation of magnesite has been discussed already, and thus will not be repeated here.

There is no definite evidence of either halite or gypsum having formed in the Celia Dolomite or the Coomalie Dolomite at Rum Jungle. The apparent pseudomorphs have been shown to be forms of magnesite (Bone, 1983). Nevertheless, this does not mean that halite and gypsum were never formed in this environment. Indeed, it is highly probably that these more soluble minerals did form in the more distal parts of the groundwater flow i.e. lakes. However, it appears that the Rum Jungle magnesites must have originated in an environment which has been subjected to a more pluvial regime than the arid climate seen in sabkha and playa lake environments of to-day, so that any gypsum, halite and other soluble evaporite minerals formed were flushed out of the system by the inflow of seasonal fresh waters. The balance between infiltrating rainfall and groundwater inflow versus loss by evaporation and groundwater overflow must annually favour the inflow if there is an absence in the evaporite sequence from gypsum upwards. Observation of these processes occurring in the Coorong is the basis by which Muir et al., (1980) assign carbonates to a lacustrine environment in the Yalco Formation, McArthur Basin, N.T. Therefore, it can be postulated that in the Rum Jungle area during the time of magnesite formation a climatic system prevailed similar to that pertaining to the Coorong region to-

day, i.e. most of the year evaporation exceeded infiltration, but during the remainder of the year there was sufficient inflow of water to allow standing bodies of water within the lake.

The elements associated with evaporite sequences are partially fulfilled (e.g. B content, Chapt. 4). Boron is an element typical of evaporite sequences (Ortega-Gutierrex, 1984). It can be assimilated by organisms. However, there is no record of the assimilation of B by calcareous organisms such as stromatolites, whereas the 'use' by Si secreting organisms leads to considerable increases in the B content (from 70 ppm to 100-300 ppm) of the primary sediments (Truscott and Shaw, 1984). During diagenesis or greenischist facies metamorphism much of this biogenic B is released, and then becomes available to form hydrothermal tourmaline.

Tourmaline can form in the concentrated brine as an authigenic mineral. These tourmalines are usually Mg-rich, so that upon metamorphism dravite is formed. Analyses of the small (<5 μm) intragranular tourmaline grains (Plate 19) in the magnesite at Rum Jungle show them to be Mg-rich (Fig. 44). These tourmaline grains are relatively stable e.g. they are 13th in a 1-16 pressure solution solubility ranking table (Logan and Semeniuk, 1976). Not surprisingly they are concentrated along styolites.

Silica behaves as a conservative element in concentrating brines in closed basins, but it will eventually precipitate as an opaline cement (Eugster and Jones, 1979, Eugster, 1984). The development of such siliceous crusts is enhanced by the

presence of algal mats/stromatolites. It is this material that eventually becomes the bulk of the quartz-replaced stromatolites (Plates 5, 11-14).

Pyrite is not considered a common evaporite sequence mineral. Exceptional localised conditions e.g. high organic content leading to reducing environment, and a concommittant supply of S, can lead to the formation of pyrite within the top few mms. of the sediment. Discrete, small pyrite grains occur in trace amounts in some of the magnesite (Note: this pyrite is quite different to the common ore-associated pyrite).

Gypsum does not precipitate from alkaline waters (Eugster, 1984) because Ca has been exhausted by carbonate deposition before gypsum saturation is reached. However, if gypsum did form at Rum Jungle, and if hydration of this gypsum occurred (+40°C temperature) anhydrite would have formed. Anhydrite is more soluble than gypsum so it would need to be protected in order to be retained in any way. This could be achieved by the enclosure of very small lath-like crystals within authigenic quartz grains or nodules, imparting a drusy appearance to the quartz (Young, 1979). Alternatively there could be total replacement of the anhydrite by quartz, resulting in the well-documented cauliflower cherts (West, 1979). Indeed, there are features looking very much like magnesite replacement of enterolithic anhydrite (Plate 20), but closer appraisal suggests that these features result from pressure solution. (Chpt. 4.3.3)

The concentration of trace elements in the precipitating salts should increase up an evaporite sequence (Stewart,

PLATE 17

a.   (at left) Surface morphology characteristic of a karstic

landscape. Outcrop 3, Area B, Coomalie Dolomite, E.L. 1349.

b.   (at right) The same characteristic type of landscape morphology,

but at a different stratigraphic level - corroborative evidence

for the stratigraphic duplication premise suggested in 4.6.1.

Outcrop 18, Area B, Celia Dolomite, E.L. 1349.

c.   Infill of Whites Formation dololutite in a small doline in the

Coomalie Dolomite. Outcrop 8, Area C, Coomalie Dolomite, E.L.

1349.
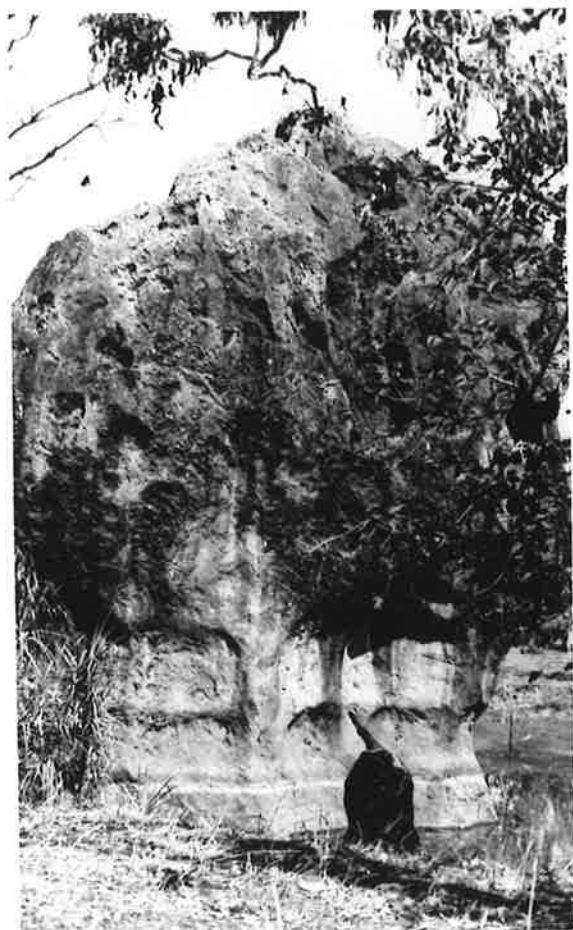
1979). There is no geochemical evidence of this occurring at Rum Jungle. Thus, this negative evidence supports the cyclic nature of the environment of deposition of the magnesites.

In conclusion, the magnesite at Rum Jungle was precipitated as a primary carbonate as the first stage in an evaporite sequence. Due to the particular climatic regime prevailing, further concentration of the lacustrine surface waters apparently did not occur.

4.2.4 Karstification

The word karst signifies a landscape with characteristic surface morphology, subsurface drainage and collapse features (e.g. cenotes/dolines) which are specificially developed on rocks, mainly carbonates, which posses a higher degree of solubility in natural waters than other rock types. It is often difficult to identify palaeokarsts, as mimicking can occur through alternative processes e.g. stylolitisation. It is also important no to misidentify a recently formed interstratal karst, formed by solutions percolating down to an exhuming unconformity or bedding plane, with a relict palaeokarst.

Wright (1982) lists the following criteria as being necessary for the recognition of palaeokarsts:-

(1) the palaeokarst should be overlain by a palaeosol or other terrestrial deposit.

(2) the palaeokarst should show truncation by overlying beds, showing that solution occurred before burial.

(3) the overlying beds should not show solution pipes etc. connecting to the present surface.

a.   (at left) Detail of preserved palaeokarst surface near the top

        of the Celia Dolomite. The material on which the hammer is

        positioned is a ferruginised palaeo-regolith, which developed on

        the underlying magnesite. Outcrop 81, Area C, Celia Dolomite,

        E.L. 1349.

b.   (at right) Another area, the Fossil Reserve, showing the

        characteristic surface morphology of a karstic landscape. This

        morphology is widespread throughout both the Celia Dolomite and

        the Coomalie Dolomite.

c.   Typical karst-type weathering; Outcrop 64, Area C, Celia

        Dolomite, E.L. 1349. Characteristic sink holes can be seen in

        many places in the Rum Jungle area (Fig. 7) where the overlying

        soil cover has collapsed into a still exhuming doline.

(4)   the overlying beds should not show any evidence of collapse into the underlying palaeokarst.

Criteria (2) and (3) are readily observed at Rum Jungle. Criterion (1) is uncertain. With criterion (4), there has been infill (as against collapse) of Whites Formation dololutites into the dolines, which is supportive evidence for karstification.

Certainly the drilling programmes indicated (Figs 32, 33)a palaeokarst, much to the annoyance of the contract drillers as they frequently lost circulation.

Plate 18 shows a well preserved palaeokarst near the top of the Celia Dolomite. There were even better examples of recently exhumed palaeokarsts in road cuttings at Kharidunga, Nepal (Plate 19).

The palaeokarst surface is an important channelway in the plumbing system involved in the deposition of both the U and the poly-metallic sulfide ore deposits at Rum Jungle. It is not fortuitous that these deposits occur at the interface between the Coomalie Dolomite and the overlying Whites Formation, for here there is a solution "freeway". Both Ferguson et al., (1980) and Eupene (1980) see the dolines as sites into which psammitic and pelitic material collapsed, with insoluble clays and carbonaceous material etc. being washed in, supplying additional material. The dolines also became favourable sites for the extraction and concentration of U by respectively adsorption on to clay surfaces under favourable hydrogeochemical conditions (Giblin, 1980) and lower pH than the surrounding carbonates.

PLATE 19

a.   Detrital quartz grains in magnesite. The central rhomb is a
      diagenetically formed dolomite crystal. Sample C34, Celia
      Dolomite, E.L. 1349. x100; plane light.

b.   The large crystal is a diagenetically formed pyrite crystal. The
      core is still pyrite, but it is progressively altering to
      limonite towards the rim (analyses given in Appendix 3). The
      small ($<5\mu m$), clear euhedral crystals are diagenetically
      formed quartz. The fluid inclusions are typical of those used in
      this study. Host is magnesite - sample E28, Coomalie Dolomite,
      E.L. 1349. x250; plane light.

c.   A palaeokarst surface revealed in a recently contructed road
      cutting at Kharidunga, Nepal. The carbonate is magnesite, whilst
      the overlying material is a carbonaceous phyllite.
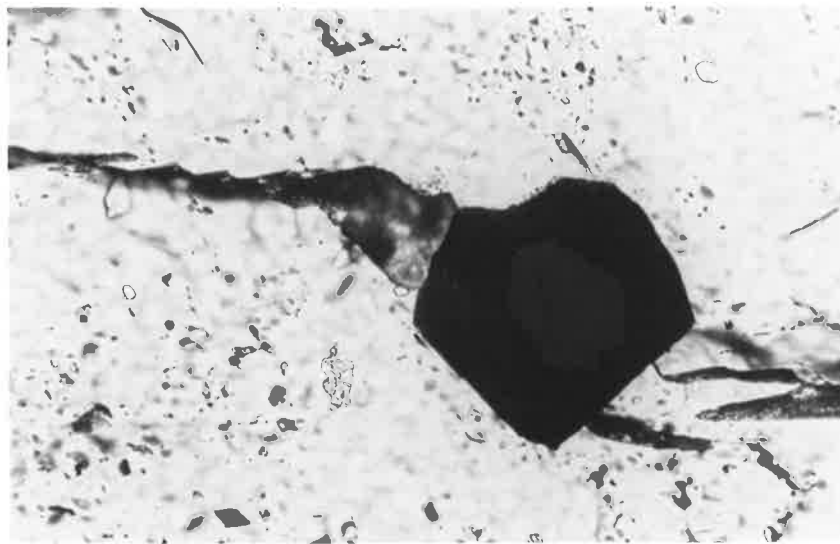
The recognition of a palaeokarst at Rum Jungle provides further support to the primary carbonate hypothesis and also supports the unconformity related genetic model for U in the P.C.G.S. (Ferguson et al., 1980; Ewers et al., 1984).

4.2.5 Palaeoclimatology

The best indicator by which palaeoclimate reconstructions can be made for the Rum Jungle magnesites is the precipitation of the magnesites themselves as primary carbonates. The sections on lacustrine environments and types of evaporite minerals discusses the reason for ascribing a pluvial regime wherein much of the year evaporation was greater than inflow. However there were short periods when the reverse applied. Using the Coorong, S.A., region as an analogue, it is likely that the environment, although arid, was more humid than that existing in areas of present day playa lake and sabkha development.

Both halite and carbonate are precipitating in lakes in Antarctica (J. Bowler, pers. comm. 1980), so the presence of these minerals is certainly not an indication for a warm climate. Indeed, Eugster (1984) states that some evaporite environments have "the driest conditions associated with arctic climates".

The period in the Proterozoic between 2.6 and 2.0 Ba was one of rapid evolution and flourishing of photosynthetic blue-green algae. Some of these have been preserved at Rum Jungle as stromatolites. The metabolic processes of these photosynthesisers gradually led to the earth's surface waters and atmosphere becoming oxidising.

TWO WATER
SYSTEM

GRAIN | MACRO-
PORE | GRAIN

REACTION ZONE   MICROPORE

DIFFUSION

FLOW

CALCITE

MICROPORE

DIFFUSION

ARAGONITE

1 μ

1000 μ

REACTION ZONE
--ENLARGED--
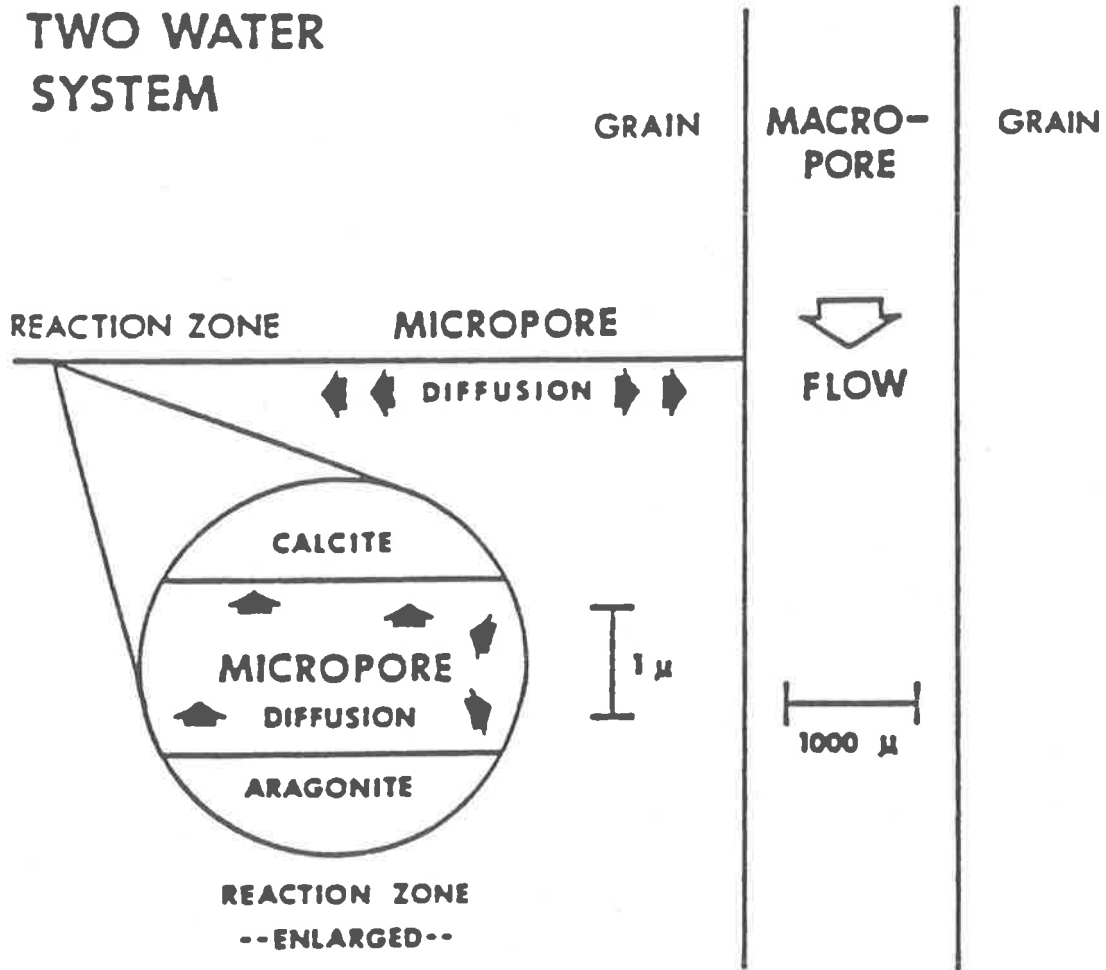
Fig. 37: Diffusion in carbonate diagenesis : pore
pathways and geometry.

(Pingitore, 1982)

Modern stromatolites occur in a wide variety of environments, including hot springs (Grey, 1980), which means that no temperature estimate can be made because of their presence.

The best palaeoclimate reconstruction that can be made is that of a mainly arid climate, with humid periods.

4.3. Diagenesis

4.3.1 General

Diagenesis can be defined as the sum of all the processes that have affected a sediment since the time it was first sealed off by being buried by overlying sediments, with a possible reduction in pore space. After this, further processes are to be termed metamorphic (Engelhardt, 1977). This definition does not incorporate a particular temperature or pressure as being the point at which diagenesis secedes to metamorphism, as did many earlier definitions. This fixed temperature/pressure boundary was often unrealistic, as this point could be reached mid-way through a process.

4.3.2 Recrystallization

Some recrystallization events may occur during the diagenetic stage. In all cases diffusion is a very important process by which the mineral-chemical change occurs. There are three parameters affecting the efficacy of diffusion in carbonate diagenesis (Pingitore, 1982).

(1) diffusion co-efficient. The cations Ca^{2+}, Sr^{2+}, Ba^{2+}, Zn^{2+}, Mg^{2+} etc. and the anion CO_3^{2-} all have similar values, but some are temperature dependent.

DIFFUSION IN DIAGENESIS
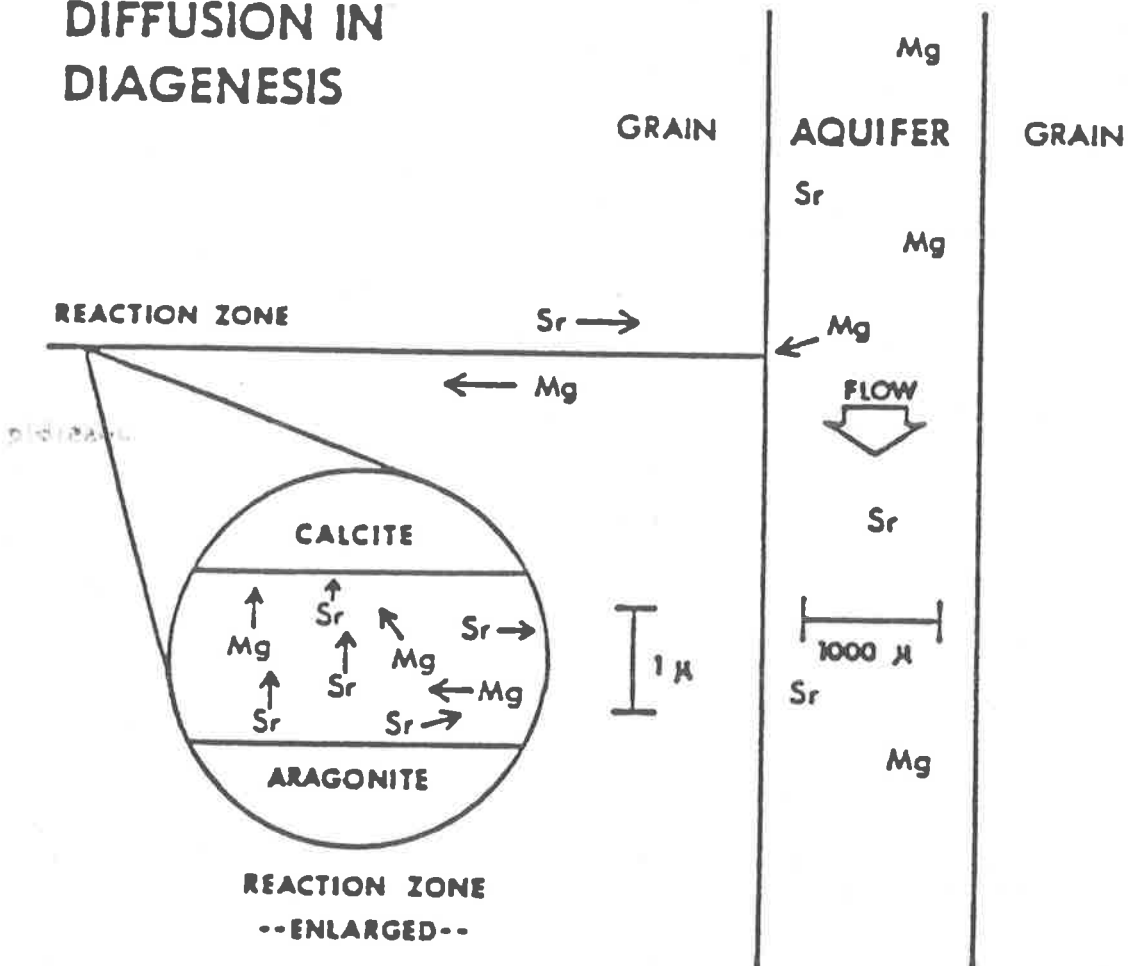
Fig. 38: "Two-way traffic", or simultaneous bidirectional diffusion typifies carbonate diagenesis. This simple model shows $CaCo_3$ and Sr^{2+} and Mg^{2+} ions. The model also applies, to CaMg $(CO_3)_2$ and $MgCO_3$ and multiple ions.

(Pingitore, 1982)

(2) pore path and geometry (Fig. 37). These refer to the distance from the aquifer to the reaction zone, and the diameter, shape and directness of the pore passage, which will be constant for different ions at a given diagenetic site. (3) concentration gradient. This is probably the most important parameter, especially for bringing about geochemical changes in the system. For instance if the concentration of Sr^{2+} is much higher in primary calcite than in the aquifer solution, Sr^{2+} will be leached out of the calcite until a new solid-fluid equilibrium has been established. The reverse is often true for Mg^{2+}, so that diagenetic recrystallization usually brings about an increased Mg concentration in carbonates. The same situation occurs in regard to Zn^{2+} and Mn^{2+} - hence carbonates are said to have a scavenging affect for these two elements (Pingitore, 1982). The interaction of these and other parameters is illustrated in Fig. 38.

A parameter not discussed by Pingitore (1982) is that of ionic radius, and its control on substitutions during recrystallization. The parameter is just as important during any recrystallization event as it is during primary precipitation, and accounts for the trace element geochemistry in the Rum Jungle magnesites - all of which have been recrystallized at least once.

4.3.3 Pressure Solution : Stylolitization

The recognition of stylolites started with Sorby (1879). Stylolites can be defined in simple terms as being due to pressure solution, or can be defined as pressure-induced recrystallization. It is one of the many processes involved in
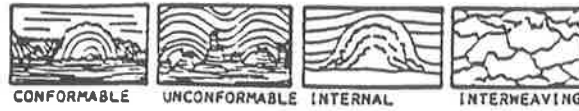
146
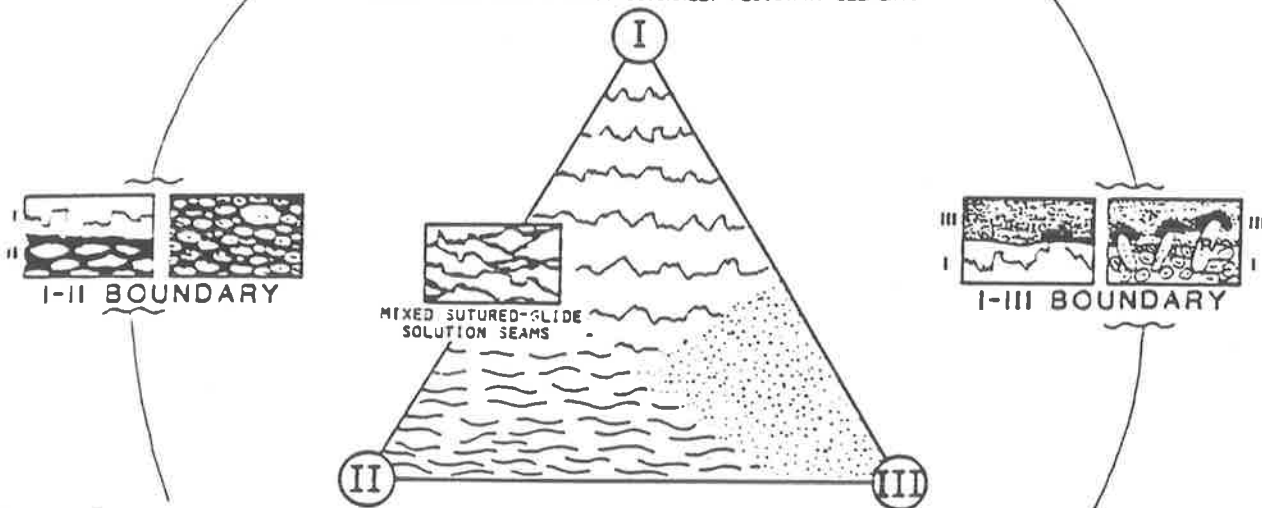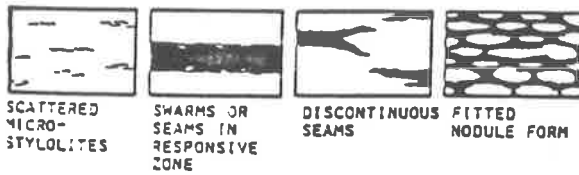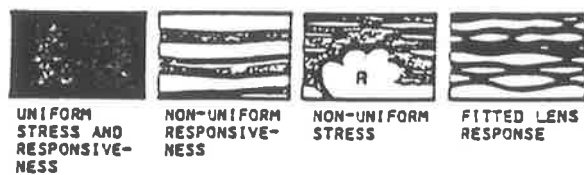
Fig. 39: Stylolite classification scheme, showing
characteristics of and controls on pressure solution
types with sketch examples. "Clean" means without
significant clay or platy silt.

(Wanless, 1979)

the lithification of a sediment, during which a diverse array of particles are converted into a thermodynamically stable assemblage (Baker et al., 1980).

There is a difference between mechanisms involved in the process of 'pressure solution' - (1) solution transfer : where water is the transfer medium, (2) grain boundary diffusion.

Grain boundary diffusion is still operative in impermeable rocks (Wanless, 1979). Buxton and Sibley (1981) suggest that pressure shadow deposition only occurs, under grain boundary diffusion transfer. Pressure shadows are rarely seen at Rum Jungle.

In the pressure solution model (Baker et al., 1980), the application of grain-to-grain stress increases the chemical potential of the strained crystals and causes dissolution of material from the point of contact. This material is then transported by either grain boundary fluid film diffusion and/or bulk pore fluid diffusion from the area of dissolution to the site of dilatency.

Therefore, dissolution and crystal growth (including recrystallization) are reactions controlled by mineral surfaces reactions i.e. directly related to surface free energy and surface area. Therefore fine grained material, under stress, should recrystallize quite rapidly, leading to a reduction in surface area. Deep-sea carbonate oozes have been found to respond to effective stress by rapid recrystallization. These oozes are subjected to the equivalent of approximately 4 km. of over-burden (200 - 250 bars and 30° - 40°C/km).

PLATE 20

a. Stylolites formed in relatively pure magnesite. The
    concommittant recrystallization of magnesite (rhomb type) has
    caused the lateral displacement of the stylolites towards
    finer-grained areas, where predominantly unidirectional flow can
    still occur. This has the affect of making the finer-grained
    magnesite superficially resemble pseudomorphic enterolithic
    anhydrite. 16.57m, Drillhole 23, Celia Dolomite, E.L. 1349.

b. Solution channelways in magnesite that have been the depositional
    site of platy minerals, thus forming stylolites. These
    relatively simple stylolites are parallel to bedding. Their
    sutured nature is due to the presence of magnesite crystals.
    Outcrop 12, Area A, Celia Dolomite, E.L. 1349.

c. These well-defined, clogged stylolites indicate that the pathway
    may only be operative over a short distance before there is the
    necessity for a new pathway to be formed. The bladed magnesite
    crystals that cause the sutured characteristic can be seen on the
    left hand side of the specimen. Sample E25, Coomalie Dolomite,
    E.L. 1349.
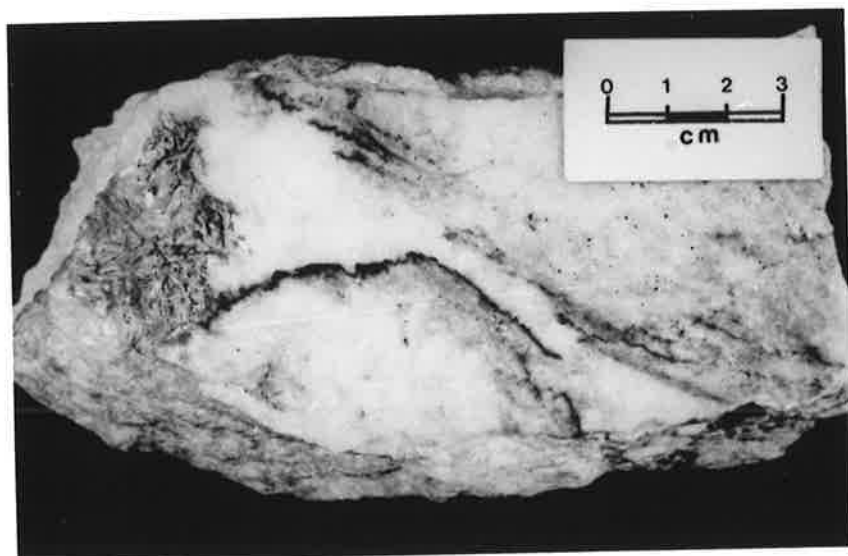
However, in coarse grained material, there is a tendency to achieve higher stress concentration at the fewer points of contact - which compensates for the smaller surface area and explains the lower recrystallization tendency of the coarser grains. It has been shown experimentally by Chai (1974), Anderson and Chai (1974) and Baker et al., (1980) that small crystals have the tendency to dissolve, which effectuates the recrystallization to larger crystals, (the Ostwald ripening process - Ostwald, 1900). Therefore, relief of strain at the grain to grain contact point appears to be the dominant driving force of pressure solution reaction rates.

Various impurities can act as retardants in the pressure solution rate e.g. interstitial material, clay minerals, organic carbon and silica. Lattice impurities such as Mg^{2+} and Ca^{2+} can also cause changes in reaction rate.

Concommittant with this recrystallization event, and/or as an alternative, there is removal of both soluble and insoluble material along permeable pathways. Frequently these pathways, because of their being the site of lower pressure, become depositional sites. Once this deposition commences, the pathway rapidly becomes obstructed, potentially permanently i.e. a stylolite has formed (Plate 20). There is then the need to utilise a new pathway, and so the process of pressure solution has to start over again (Plate 20). The result is a distortion of the primary sedimentary bedding features and may eventually lead to their complete obliteration (Plate 21).

Stylolites are usually thought of as being associated with carbonates, but they are now being more readily recognised in

a.   The on-going development of new solution channelways can
      eventually obliterate evidence of bedding features. The
      stylolites in this example have become the depositional
      environments of hematite. Although the stylolites appear to be
      more prevalent in the finer grained magnesite, they are equally
      abundant in the coarser material. Outcrop 13, Area B, Coomalie
      Dolomite, E.L. 1349.

b.   This sample is now completely silicified, but the quartz of a
      bladed nature indicates a magnesite precursor, as do the
      well-defined stylolites. Sample E13, Coomalie Dolomite, E.L.
      1349.

c.   In this example, bedding-parallel, sutured-seam stylolites
      (diagonal) show divergence resulting from alteration of the
      principal stress direction. Outcrop 59, Area B, Celia Dolomite,
      E.L. 1349.
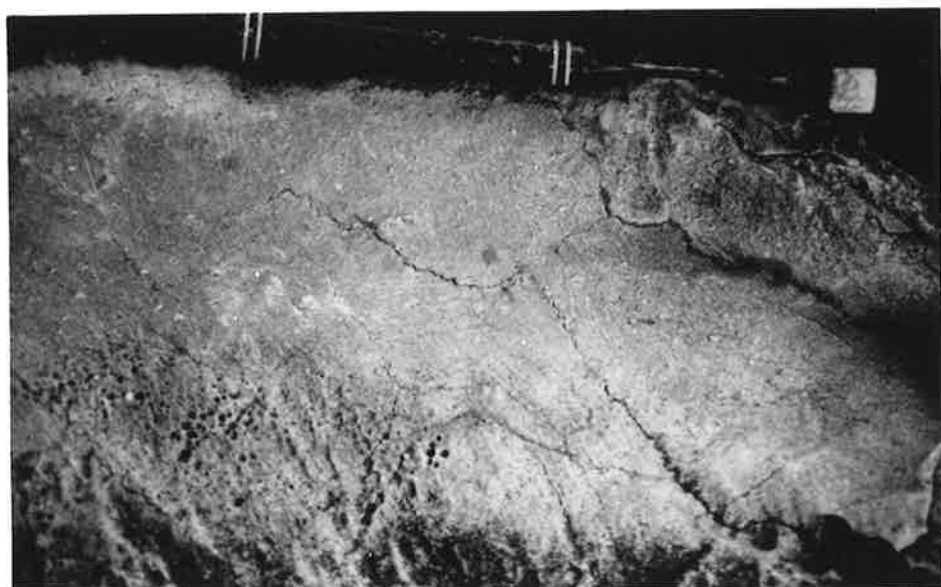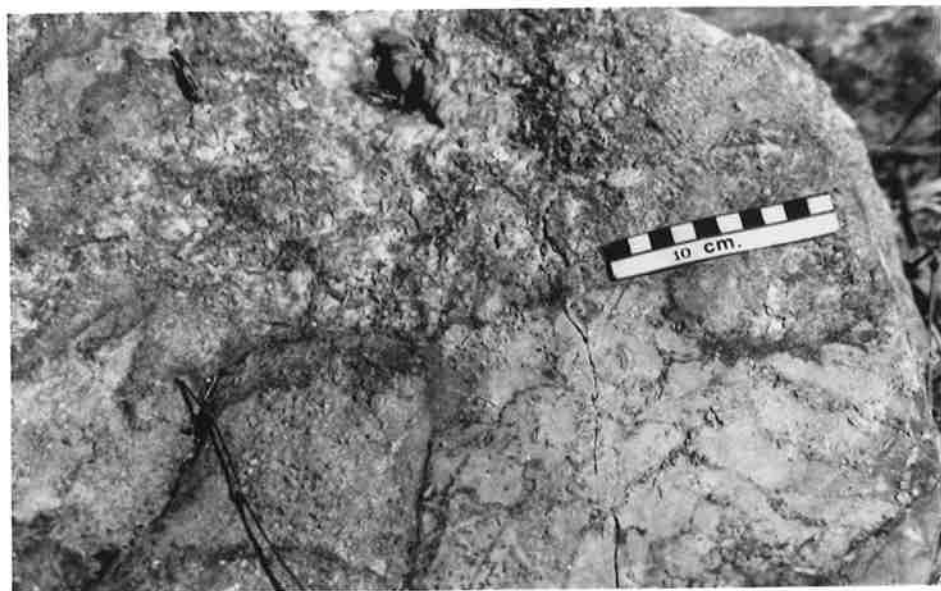
other rock types. In the Rum Jungle area, some of the stylolites seen in silicified rocks are probably inherited from the carbonate precursor e.g. Plate 21.

Wanless (1980) aptly described stylolites as "irregular, commonly discontinuous surfaces that cut limestones (and sandstones) and have a cross section resembling the trace of a stylus on a chart recorder" (Plate 21). A variety of terms have arisen to describe stylolites e.g. Fig. 39 (Wanless, 1980).

(a) sutured-seam solution. These form only when the carbonate is relatively pure and there is structural resistance to stress e.g. crystals, fossils. Where carbonates have been completely recrystallized, the geometry of the sutured-seam stylolites may be used to reconstruct the stress orientation. Overburden stress leads to horizontal stylolites i.e. parallel to bedding. Later deformation events may alter the original bedding, so that stylolites, like folds, need to be 'unfolded'.

Sutured-seam stylolites formed by tectonic stress may be sharply discordant to primary layering (Plate 22). In both cases, solution occurs along distinct surfaces, leaving the adjacent carbonate relatively unaffected. Any shortening of the carbonate unit must be parallel to the direction of maximum stress. Because of the reticulated fabric of the stylolite, any shear stress operating along the stylolite will result in an extension of the domain of brittle failure (Carannante and Gozzetta, 1972).

Sutured-seam stylolites are quite common at Rum Jungle, and are particularly spectacular where they have formed a solution surface between two units e.g. the boundary between

PLATE 22

a.   In this photo, there are two major orientations of sutured-seam
     stylolites. The first is that of the continuous stylolites
     (parallel to the scale) which are parallel to bedding and caused
     by overburden stress. The orientation of the second set
     (diagonal), which join one parallel stylolite to its adjacent
     neighbour, has been caused by a different tectonic stress
     orientation. Outcrop 88, Area B, Celia Dolomite, E.L. 1349.

b.   Sutured-seam type stylolites at the boundary of Whites Formation
     (calcilutite-upper right hand side) and Coomalie Dolomite
     (magnesite-lower left hand side). Sample W03, Whites Deposit.

c.   Sutured-seam type stylolites have become the depositional sites
     of the 'impurities' in this core sample of magnesite, once again
     leaving the magnesite looking like enterolithic anhydrite. This
     same drillhole shows this feature persisting into the ore zone.
     180m, drillhole 65, Browns Deposit.
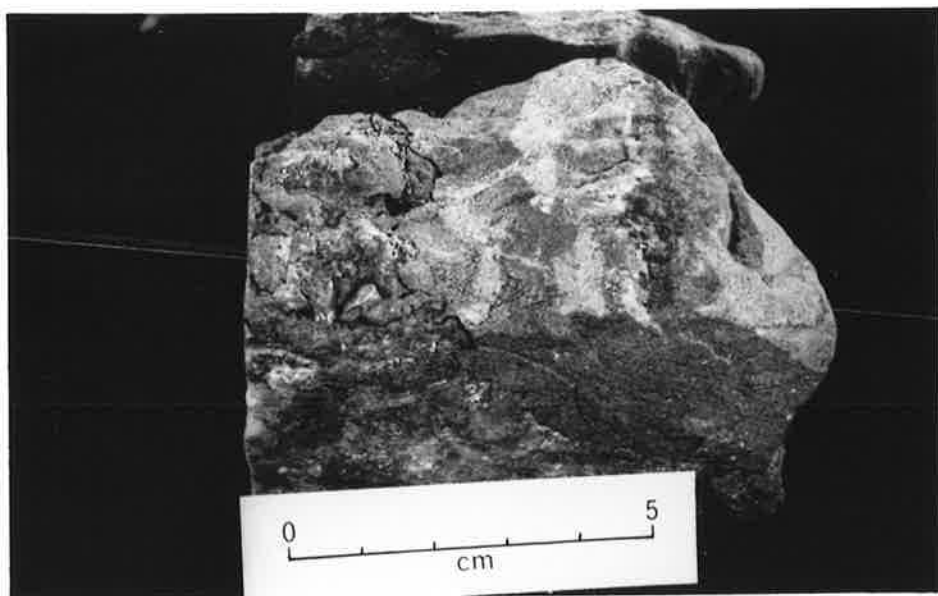
the Coomalie Dolomite and Whites Formation (Plate 22). Such lithological transitions commonly (~ 80%) have pressure solution features. Two adjacent layers respond to stress in a different manner due to variations in rock fabric, cementation etc. This effectively means that pressure solution gradients will be formed at the interface of rock types with different mechanical properties i.e. rocks reacting by brittle failure versus rocks reacting by ducile deformation.

(b) non-sutured seam solution. If there is a significant content (>10%) of fine, insoluble and platy particles, anastomosing webs of fine clay seams result, i.e. micro-stylolites, microstylolite swarms and clay seams. These small seams are formed relatively rapidly after initiation of the solution pathway. They also cease rapidly due to being quickly choked by the deposition of the fine silt and clay particles. The seam formed by these particles becomes a favourable glide plane as it is a structurally weaker zone than the adjacent surroundings. Once stress is locally relieved by lateral shear along this plane on a microscale, a new focus of maximum stress is produced some distance further on, and perhaps at a slightly different horizon. Thus a swarm of microstylolites are formed, i.e. nodules of undissolved carbonate encompassed by a fitted stylolite jacket, with considerable thinning of the intervening carbonate layers between nodules.

This reticular fabric or "nodular limestone" development is well illustrated in the Rum Jungle area. The author proposes that the so-called enterolithic anhydrite pseudomorphs are no more than nodular magnesite layers brought about by non-sutured seams solution (Plate 20). Similarly, some of the apparently brecciated sulfide ores occurring at the boundary between the Coomalie Dolomite and Whites Formation are

PLATE 23

a. (at left) Brecciated sulfide ore at Mt. Fitch shows that the clasts of chalcopyrite are encompassed by a fitted stylolite jacket, as are the clasts of magnesite. Some of the chalcopyrite clasts also show cross-cutting stylolites. Drillhole 80/06.

b. (at right) Large, hematite zoned rhombs of magnesite truncated by stylolites. The non-sutured seam stylolites are filled with pale pink talc. The remainder of the white, rhomb type magnesite is exceptionally impurity free. Drillhole 16, Celia Dolomite, E.L. 1349.

c. The development of large, discrete rhombs of magnesite brought about by the nonsutured seam solution process is shown in this sample, C56, Celia Dolomite, E.L. 1349. In the sample in the above photo, zoning has occurred during the crystal growth/stylolitic process.

suggested by this author to have formed in the same manner e.g. Browns Deposit (Plate 22); Mt. Fitch (Plate 23). The epigenetic formation of the ore deposits does not create a problem, because stylolite development can occur as (a) a single event, (b) an ongoing event or (c) multiple events (Nicholson, 1976). There are superb examples of more than one stylolite development event at Rum Jungle e.g. Plate 23, where large rhombohedra of magnesite have formed in an early event, and have then been truncated by a later event (the rhombohedra formation will be discussed shortly).

It may be that closer examination of many nodular carbonates will reveal that they have formed by this non-sutured seam solution processes, and that the diverse explanations proposed for their formation are unnecessary. The sulfate pathway genesis of any suspected "anhydrite" that has a stylolitic envelope is itself suspect. However, the author does not want to imply that all nodular carbonates are formed by this process. Indeed, there are many well substantiated alternatives e.g. chert bands after enterolithic anhydrite in the McArthur Basin carbonates (Muir et al., 1980).

Another phenomenom brought about by the non-sutured seam solution process is the growth of large, discrete carbonate rhombs (Plate 23). These rhombs are frequently zoned (Plate 23) because of a variation in clay and/or ferrous Fe content (Wanless, 1980) throughout the rhomb growth time. There is a very fine balance between preferential dissolution and precipitation during the stylolitic process, with one taking preference over the other at different times. The rhombs may eventually form such a closely intricate framework that further stylolite development is inhibited e.g. sample EO2

a.   In this sample, non-sutured seam type stylolite development has
        led to a closely intricate framework consisting almost entirely
        of zoned, magnesite rhombs and platy minerals (mainly talc).
        Sample E02, Coomalie Dolomite, E.L. 1349.

b.   'Chicken-wire' fabric. Non-sutured seam type stylolitisation has
        led to a fitted fabric development of stellate clusters of
        magnesite crystals. In turn, this stylolite jacket has become
        the site of magnesite recrystallization, thus leading to the
        'chicken-wire' appearance. Outcrop 74A, Area B, Celia Dolomite,
        E.L. 1349.

c.   Another section of the outcrop in the photo above. In this case,
        evidence of sutured-seam type stylolitisation can also be seen in
        the upper left hand side of the photo.
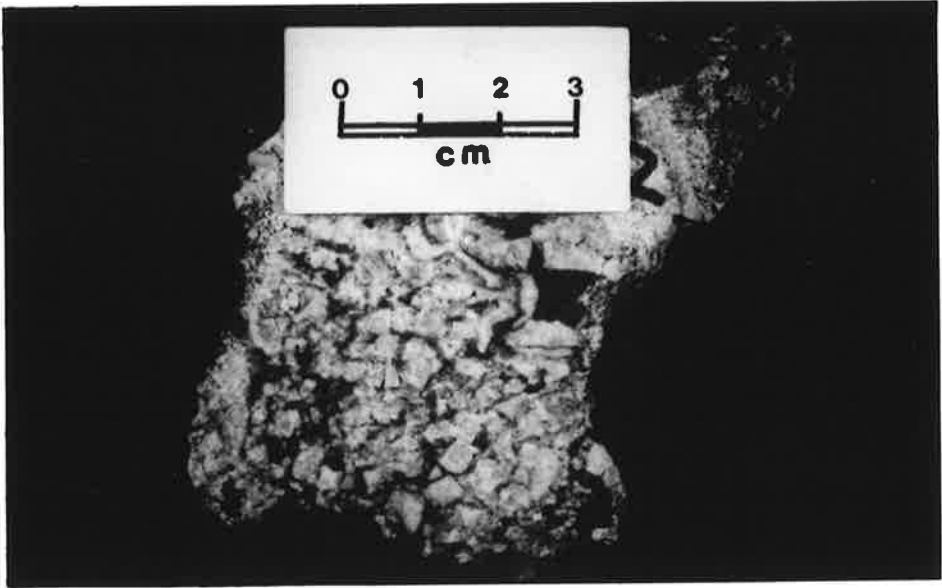
has become closely packed with segregated zoned magnesite rhombs and platy minerals (Plate 24); sample EO3 is mid-way to this stage.

Buxton and Sibley (1981) have separate categories, for fitted fabric type stylolites that are pervasive rather than planar:-

(i)   limited fitted fabric (few grains thick)

(ii) unlimited fitted fabric. This is the equivalent of Trurnit's (1968) 'network fabric', which appears to be a reasonable explanation for the "chicken-wire" fabric seen at Rum Jungle (Plates 24, 25). Once again it no longer seems necessary to invoke discrete nodules of precursor anhydrite to explain this "chicken wire" fabric, as close examination reveals very fine, wispy microstylolite envelopes.

Zenger (1983) relates chicken wire texture to "late diagenetic burial dolomitization", with stylolites acting as solution channelways, whilst the similar texture known as "zebra structure" he ascribes to healed stylolites parallel to bedding.

A further evolution of stylolitization leads to the third style -

(c) non-seam solution. This type of pressure solution is pervasive, and occurs in rocks (mainly carbonates) having no internal mineralogical discontinuities. ie minor platy mineral content and clean or pure carbonates. This stage of stylolitization usually results in considerable thinning of the unit. It may also involve considerable crystal growth, but the resultant crystals will not be zoned. Sample C56 is an example of this process (Plates 23, 25).

PLATE 25

a.   In this example, the fitted fabric nature of stylolitisation is not as obvious, although the stellate clusters of magnesite crystals are prominently displayed. Outcrop 74, Area B, Celia Dolomite, E.L. 1349.

b.   A good example of 'chicken-wire' fabric. Outcrop 74A, Area B, Celia Dolomite, E.L. 1349.

c.   Non-seam solution type stylolitisation has led to the development of unzoned crystals of magnesite, with the remainder of the magnesite being impurity free. Outcrop 12, Area B, Coomalie Dolomite, E.L. 1349.
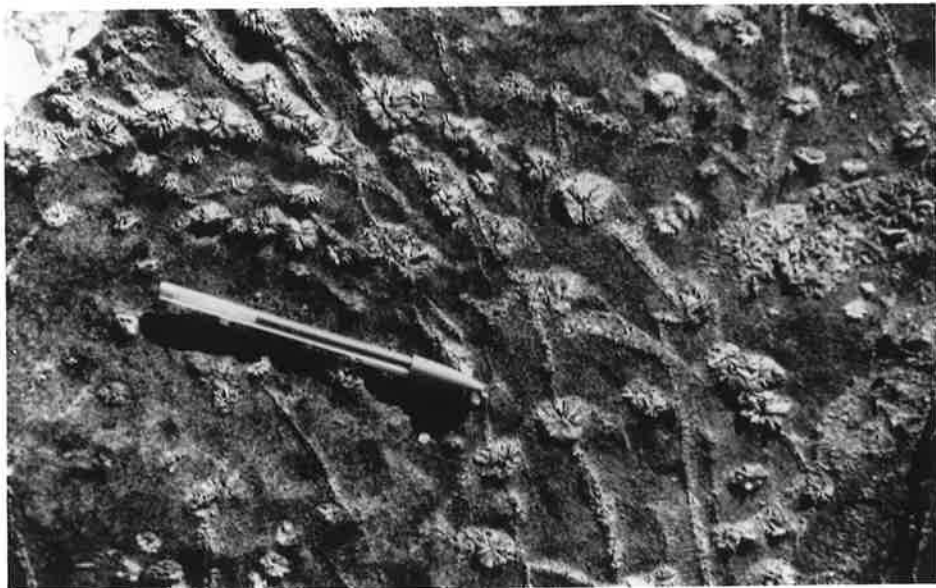
Pratt (1982) disagrees with Wanless' (1980) theories, and suggests that most examples of volume reduction, distortion and obliteration of primary features are caused by pre-lithification physical compaction. He maintains that most dolomite is precipitated post carbonate sediment lithification, but at insufficient depths for pressure solution to be affective. The "seams" of platy minerals that form as a result of this compaction may become the foci for later pressure solutions, and thus be converted to stylolites.

It is difficult to imagine a compressive pressure of sufficient magnitude to cause platy mineral segregation and alignment that did not at the same time enable fluid movement.

Wanless (1982), however, invokes the presence of his large, zoned dolomite rhombs to substantiate the veracity of his theories. This type of rhomb is not found elsewhere in the limestones. Also they are rarely intergrown, whereas if they formed after pressure solution, intergrowths would be common.

One aspect not yet mentioned (as it will be considered in depth in the next section) is the release of silica and subsequent formation of chert during this same process.

Another problem is that Wanless only discusses carbonate rhombs, whereas at Rum Jungle the two distinctly different magnesite morphologies (previously discussed) are seen to be involved in stylolite processes, although the rhomb-form is the more spectacular and more prevalent. This indicates that these processes continue to operate up to moderately high temperatures, as the majority of the bladed-form magnesite formed at temperatures greater than 160°C. Some of these

channelways, then, may have still been functioning during mineralising events. But this brings us into the domain of anchimetamorphism.

In conclusion, it can be seen that pressure solution (stylolite development) has been an enormously important process in the diagenesis and recrystallization of the Rum Jungle magnesite.

Therefore, pressure solution is surely as important when considering the responses to stress exhibited by carbonate rocks as the more generally quoted ones of compaction, deformation, neomorphism, replacement, precipitation and metasomatism; although each one has its role. Even more important is the re-acceptance that there is no substitute for the old-fashioned nose-down-on-the-rock field observation technique - that although thorough theoretical knowledge and back-up laboratory techniques are equally necessary and important, the answer is often physically visible in the rock itself.

Finally, just as there are indicator or pathfinder elements, so too, could abundantly stylolitised carbonates in mineral provinces be used as pathfinder rocks.

4.3.4 Silica

Silica occurs predominantly as quartz in the Rum Jungle magnesites. It will be discussed, that some of this quartz was originally colloidal silica, whilst the remainder was probably originally precipiated from ionic solutions as "amorphous" silica and/or authigenic quartz crystals, or was wind- and

water-derived detrital quartz grains. Silica is widespread, and variable in total concentration. In places (Fig. 7) there has been complete (i.e. 100%) silicification of the magnesite (Plate 6).

Before discussing the Rum Jungle silica genesis the forms of silica which are found in low-temperature, sedimentary environments, and the aqueous geochemistry of this silica will be discussed.

4.3.4.1 Silica derived from Ionic Solutions

These silica solutions produce monomeric silica and include anhydrous crystalline silica e.g. quartz i.e. the low pressure-temperature form of quartz - hereafter referred to simply as quartz; other products are cryptocrystalline silica e.g. chert and 'amorphous' silica e.g. opal.

The various forms can be distinguished by morphology, grain size and optical properties. However, some refractions of the diffraction pattern of quartz are produced by all of them.

4.3.4.2 Quartz

Coarse-grained (up to 1 mm and more) varieties of quartz are sometimes referred to as megaquartz, in order to distinguish these from other varieties of quartz. These occur within the magnesites at Rum Jungle as either 1. equigranular or random grain size, as intergranular mosaics, 2. as discrete, very small (<5μm), intragranular euhedral crystals

(Plate 19), 3. as large (up to 4 cms) cavity fill crystals (Plate 26), and 4. as replacement by inversion of an earlier different variety of quartz.

Apart from the euhedral crystals forms, the megaquartz also contains polygonal grains, with planar or more irregular boundaries.

4.3.4.3 Microcrystalline Granular Quartz

This granular form of crystalline quartz has very small ($<10\mu m$) polygonal grains that tend to be equant and of random crystallographic orientation. This produces a distinct spot-point extinction providing that there is good resolution at the high power needed for such small grain size. Microcrystalline granular quartz forms intragranular mosaics in the recrystallized Rum Jungle magnesites. It is also present as intergranular mosaics, and as replacement material.

4.3.4.4 Chert

This is one of many names applied to the cryptocrystalline varieties of quartz. Other names include chalcedony, agate, flint, lutecite and quartzine. The term chert is the one that appears most frequently in the carbonate literature, therefore it will be the term employed throughout this study.

Chert is characterised by its "fibrous" form, which leads to its fibrous extinction, occassionally producing undulose and/or irregular extinction (Smith, 1960). Fibre elongation is usually along one of the polar 1120 directions of quartz, i.e. along a 2-fold symmetry axis (Frondel, 1978), thus

producing length fast chert, the most common variety of cryptocrystalline quartz. Length slow chert (known as quartzine) is produced by the fibres being elongated parallel to the quartz c-axis i.e. the (0001) axis. If the fibres are orientated approximately 30° to this c-axis, the variety produced is known as lutecite. These length slow varieties used to be considered diagnostic of former evaporitic or hypersaline environments (Folk and Pittman, 1971), but Oehler (1976) has more recently shown that this is not necessarily true.

Lattice dislocations initiated during nucleation are apparently responsible for the elongation of the quartz fibres perpendicular to the c-axis [1120], thus implementing preferential growth along one of the three otherwise equivalent directions (Frondel, 1978). The rotation of the c-axis around the fibre axis leads to the development of banded chert. Opal: This is the common term for the three types of 'amorphous' i.e. non-crystalline silica, namely opal-A, opal-CT and opal-C (Jones and Segnit, 1971). Opal is commonly replaced by microcrystalline quartz during diagenesis. Von der Borch and Lock (1979) suggests that the significant quantities of opaline silica associated with the Coorong carbonates (Peterson and von der Borch, 1965) may be involved in some way in the carbonate depositional process. As it has not been reported in rocks older than the Mesozoic (Uppill, 1980), it will not be considered further.

4.3.4.5 Colloidal Silica

This form of silica is polymeric, with relatively large individual particles (> 50 Å). It can be defined as a "stable
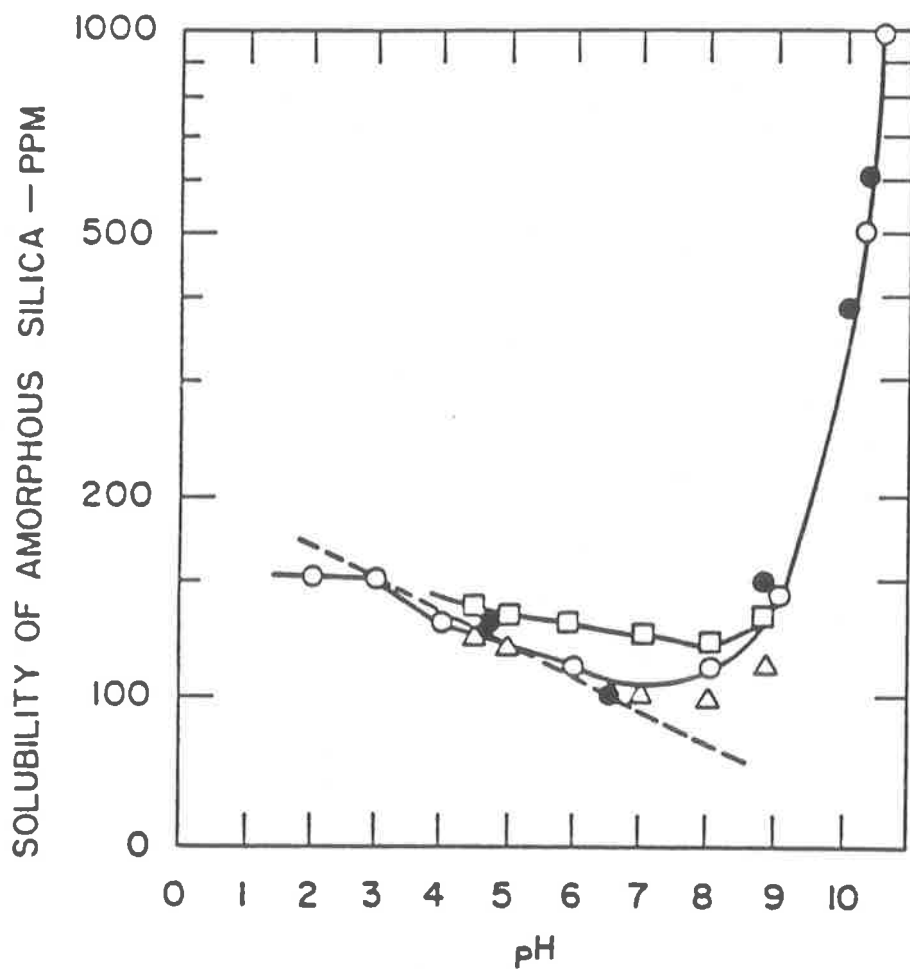
Fig. 40: Solubility of amorphous silica
vs pH at temperatures ranging from
19°C to 30°C. There is a rapid increase
in solubility once pH > 9.

(Iler, 1979)

dispersion of discrete particles of amorphous silica (Iler, 1979). Silica gel, which is a specific suspension of colloidal silica has been defined as a "coherent, rigid three dimensional net of contiguous particles of colloidal silica" (Iler, 1979) and may have been instrumental in aiding the deposition of magnesite as has been discussed in Chapter 3.

4.3.4.6 Solubility and Precipitation of Silica

The solubility of silica is dependent upon the form and crystal size of silica and the physicochemical conditions of the aqueous fluid.

The dissolution and precipitation reactions of silica involves among others, hydration (and dehydration) reactions:-

$$(SiO_2)_x + 2H_2O \underset{\text{Dehydration}}{\overset{\text{Hydration}}{\rightleftharpoons}} (SiO_2)_{x-1} + Si(OH)_4$$
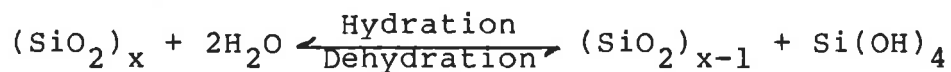
The (de)hydration dissolution process requires a catalyst that can be chemisorbed and thus increase the co-ordination number of a Si atom on the surface to greater than four, thus weakening the O-bonds with regard to the underlying Si atoms. In this reaction OH^- ions act as an appropriate catalyst (Iler, 1979). Therefore the solubility of silica is pH dependent; in particular the pH needs to be greater than 9 for significant increase in solubility to occur (Fig. 40). As discussed previously this pH is obtainable in lacustrine environments. Under these alkaline conditions, species other than $Si(OH)_4$ (or alternatively H_4SiO_4) become important e.g. $H_3SiO_4^-$ and $H_2SiO_4^{2-}$, which result in an increased solubility of 'amorphous' forms of silica (Eugster and Jones, 1979). Dissolved silica is then available to form opaline cements and
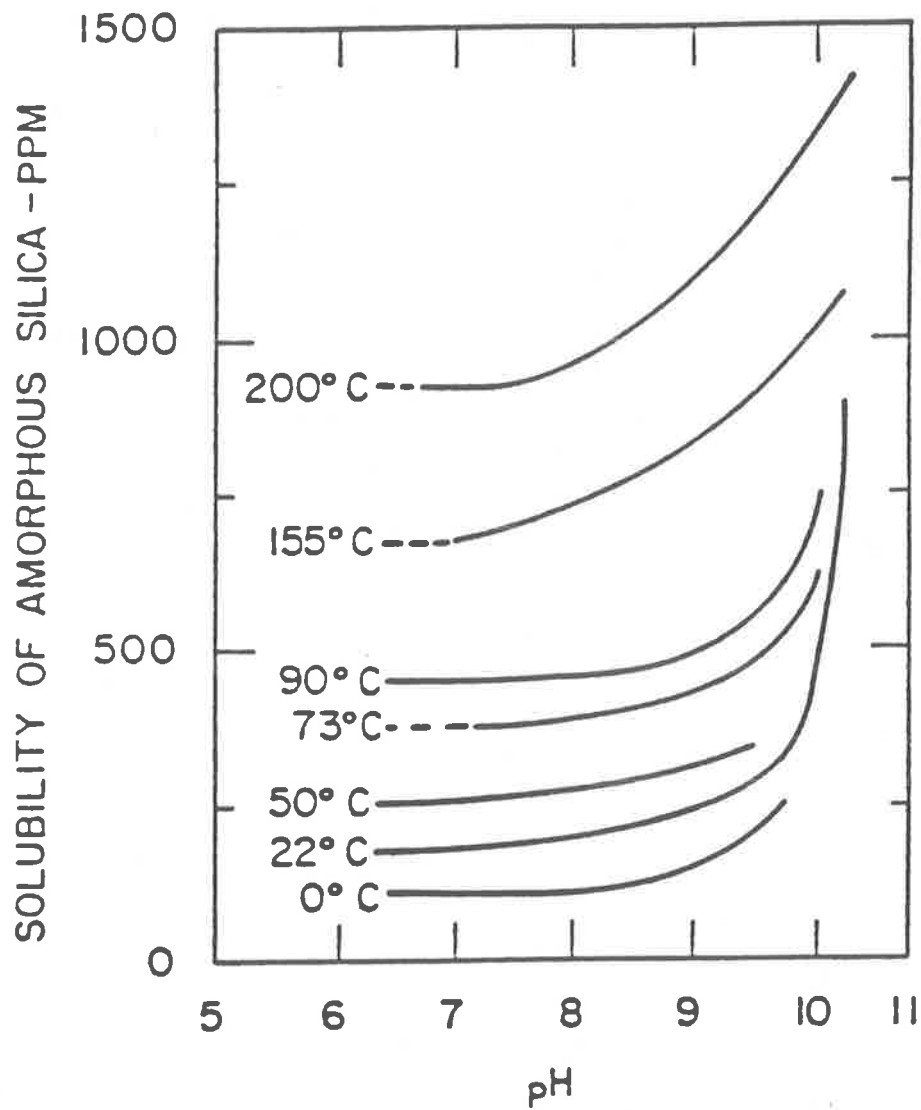
Fig. 41: Solubility of amorphous silica
vs pH at different temperatures.

(Iler, 1979)

crusts when the pH drops e.g. within algal mats and
stromatolites, as apparently none of the metabolic processes of
blue-green algae involve utilisation of Si or SiO_2 (Iler,
1979). These metabolic processes do involve the expulsion of
pH lowering by-products, as well as the lowering of the pH as a
result of decay products produced after the death of the
algae. Hence, the ubiquitous positive correlation between
stromatolites and quartz within the Rum Jungle magnesites
becomes clear. Indeed, this positive correlation is observed
worldwide throughout the geologic record. Additional sources
of silica are the detrital quartz particles that are trapped by
adherence to the mucilaginous outer-sheath of the filamentous
blue-green algae. However, it then becomes difficult to
explain why cryptalgal stromatolites in carbonates lack
silicification. It would seem that these probably grow in
detrital-free, highly alkaline environments where the silica
remains in solution. Thus, the presence of cryptalgal
stromatolites could be seen to support an alkaline lake
environment at Rum Jungle.

Temperature is another phsyicochemical parameter that
affects the solubility of silica. Fig. 41 shows the effect of
temperature on the solubility of 'amorphous' silica at
differing pH conditions. It can be seen that at the
temperatures obtained by fluid inclusions studies (Chpt. 6) on
the various types of quartz in the Rum Jungle magnesite
(average ~120°C, range 100-250°C), much of the silica would
remain in solution well below a pH of 9. This figure explains
the dual control of silica deposition. The apparent erratic
temperature pathway in sample C13, a zoned quartz crystal
(Chpt. 6) indicates that as the crystal grew two independent
variables, temperature and pH, affected silica deposition.
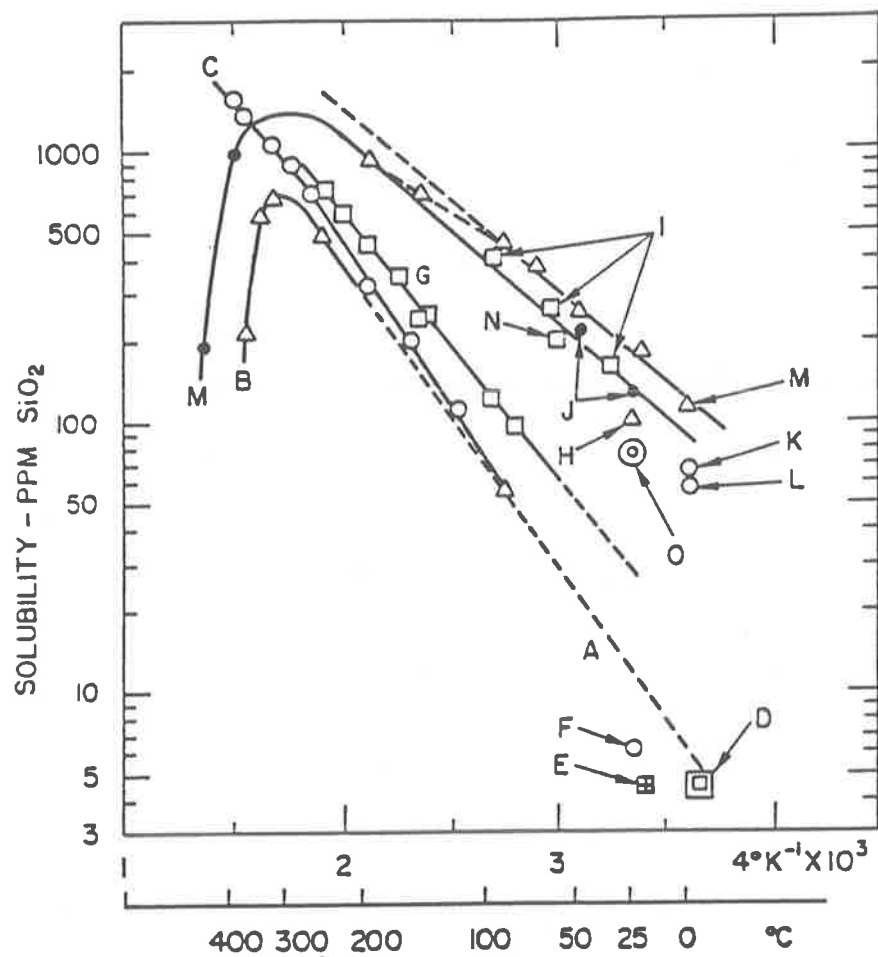
Fig. 42: Solute affect on solubility of various forms of silica at 0-500°C at autogenous pressure unless otherwise noted. A, B, E and F - quartz; C - quartz (P=1,000 bars); D - quartz (in seawater); H, I, K, L, M, and N - amorphous silica; J - amorphous silica (in 0.5 M $NaClO_4$); O - amorphous silica (in 1.0 M $NaClO_4$).

(Iler, 1979)

The presence of solutes other than complexing agents does not appear to significantly affect the solubility of silica, so that the solubility in sea water is very similar to that in fresh water (Fig. 42). Millot (1970) shows that Al^{3+} ions may theoretically decrease the solubility of silica, but that the actual concentration of Al^{3+} ions is rarely sufficient to cause a significant effect and certainly was not affective at Rum Jungle (Appendix 3). Mg^{2+} ions can cause a similiar solubility decrease but at high pH and/or high Mg concentrations Mg-silicates e.g. sepiolite, palygorskite precipitate (Callen, 1977; Eugster and Jones, 1979). However, such conditions have been observed at Rum Jungle and are thus likely to have been affective.

The solubility of silica is affected by the form of silica available for dissolution and also by grain size (Iler, 1979). Thus, quartz has a very low solubility range of 4-12 ppm at pH < 9 and temperature of 25° (Siever, 1972) whereas 'amorphous' silica has a value of 100-140 ppm (Krauskopf, 1967). As discussed, this value will vary considerably as a function of pH and temperature. Other parameters that will also cause silica concentration variability are due to (a) the availability of silica (b) dilution by meteoric waters, and (c) removal by biological processes or chemical reactions (Siever, 1972).

Besides the physicochemical parameters already discussed other precipitating mechanisms involve 1. properties of fluid flow at the precipitation site e.g. permeability and porosity, 2. presence of nucleating sites, 3. growth rates and 4. in the case of pseudomorphing silica, the nature of the
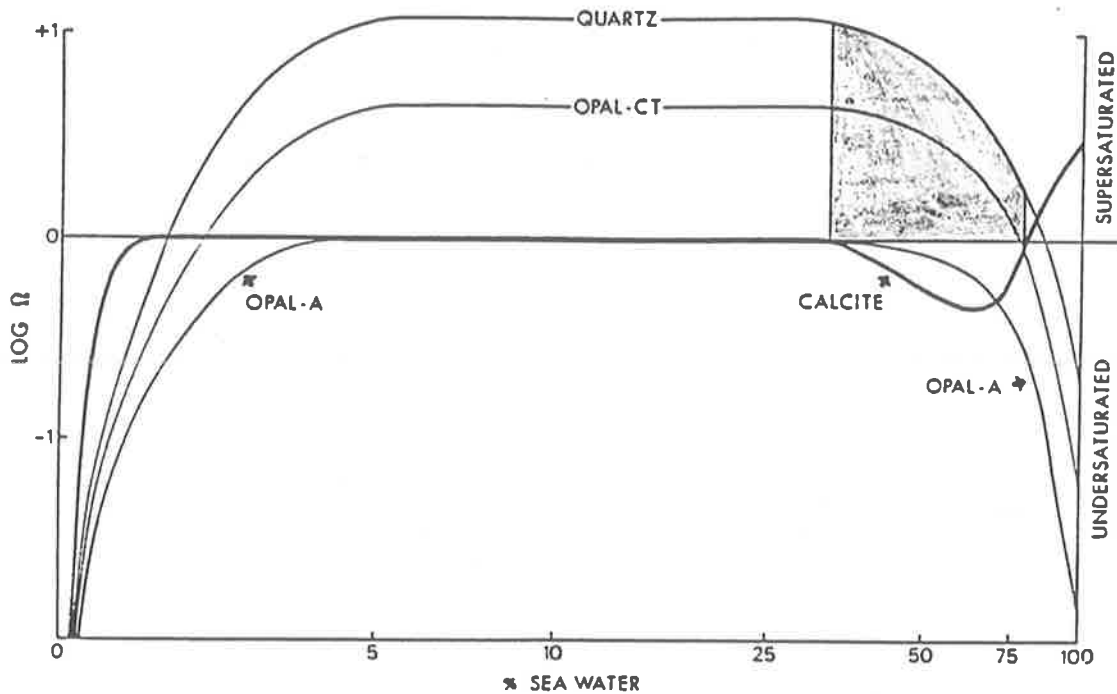
Fig. 43: Solubility relationships of silica and
carbonate in a mixed two-waters (closed with respect
to CO_2) situation. The saturation state is expressed
in terms of $\log \Omega$, where Ω = the ratio of the ion activity
product to the mineral equilibrium constant. In the above
case, mixing has produced ground water simultaneously
undersaturated with respect to calcite and supersaturated
with respect to crystalline silica. The shaded zone defines
conditions in which it is thermodynamically possible
for silica to replace carbonate.

(Knauth, 1979)

material being replaced (Millot, 1970). Stromatolites have already been discussed as a specific example of replacement.

Knauth (1979) proposes that the mixing of two solutions that are each saturated with respect to calcite (magnesite for Rum Jungle), may result in a solution that is undersaturated, if the original solutions had either different CO_2 partial pressures or different temperatures. The mixing zone could then lead to a geochemical environment where carbonates are being replaced by silica (Fig. 43). However, if the system is open to CO_2 in both solutions, the mixing zone would not necessarily be undersaturated with respect to calcite (i.e. magnesite) and silica would then precipitate in open voids etc. rather than replace carbonate.

During burial and subsequent diagenesis to a carbonate rock, replacement silica would lead to finely disseminated chert grains rather than chert nodules. This process is probably the cause of the widespread fine inter- and intra-granular mosaics of silica seen in the Rum Jungle magnesites.

There are many examples of silica replacing magnesite at Rum Jungle. However, in all samples of pseudomorphs of quartz after magnesite, it has been noted that it is the rhomb type magnesite that has been replaced (Plate 26), and not the bladed type of magnesite. This indicates that the replacement occurs predominantly at temperatures below 160°C (Bone, 1983 and Chpt. 6). This is further verified by fluid inclusion homogenization temperatures of actual quartz samples e.g. C13 (Appendix 2).

a.   Two distinctly different types of quartz are evident in this
      photo. The quartz 'bleb' is from within magnesite. The sample
      has been positioned on a mirror so that it can be seen that the
      upper and lower surfaces are both moulded after rhomb type
      magnesite. The interval vugh has then had quartz crystals grow
      into it. These quartz crystals show distinct growth zones.
      Specimen C13 (also numbered C80), Celia Dolomite, E.L. 1349.

b.   A discordant quartz-red magnesite-tourmaline vein in magnesite.
      Outcrop 41, Area B, Celia Dolomite, E.L. 1349.

c.   Close-up of a quartz-red magnesite-tourmaline vein. The
      tourmaline occurs as green, acicular needles, and has the
      composition of dravite. Outcrop 91, Area C, Celia Dolomite, E.L.
      1349.
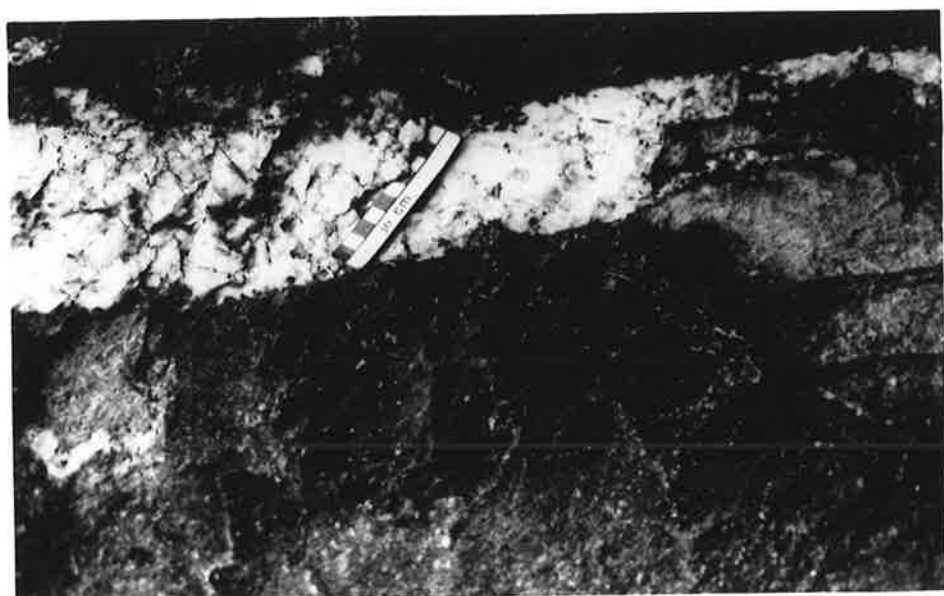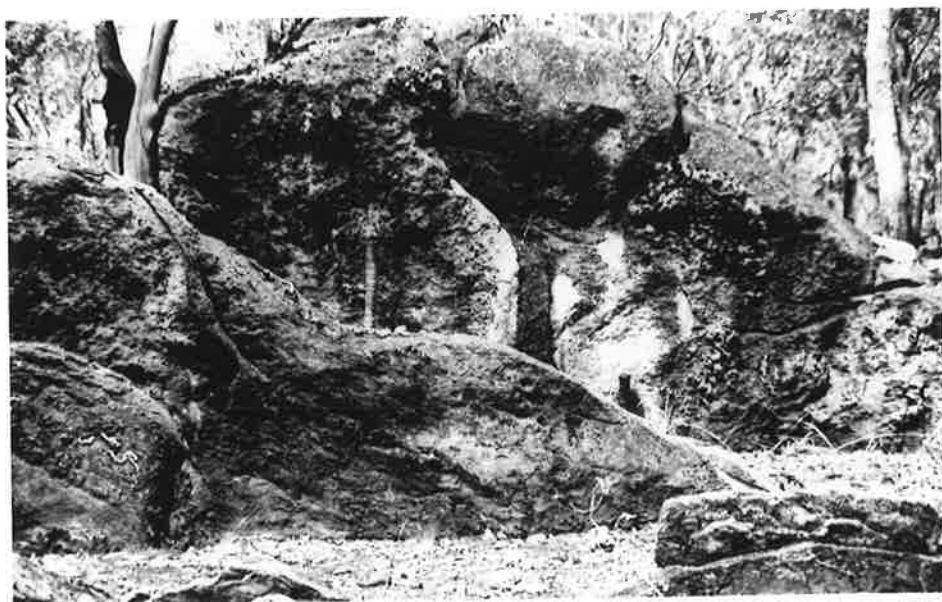
A slow growth rate and dilute solutions favour formation of the more internally ordered silica i.e. quartz (Jones and Segnit, 1971). Faster growth and more concentrated solutions will favour the growth of the more disordered forms i.e. chert and 'amorphous' silica (Meyers, 1977; Robertson, 1977).

Microprobe analyses of a wide variety of quartz samples (Appendix 3) indicate that there is no consistent concentration of elements other than Si & O. Some samples do have Al_2O_3 concentrations of up to 6.8%, but this is probably due to lattice substitution.

4.3.4.7 Formation of Colloidal Silica

Colloidal silica is precipitated by different processes (Iler, 1979):-
(a) alternate wetting and drying builds up successive coatings e.g. around hot springs, or
(b) from a dilute solution when conditions of pH and salt concentration are close to those causing precipitation by coagulation i.e. a coating forms, rather than particles adhering to each other.

Often, both soluble silica and colloidal silica precipitate together e.g. in some opal and in the walls of some geodes. However, there is usually rapid inversion of the colloidal silica to an 'amorphous' form. Kastner et al. (1977) found that the presence of carbonates enhances the rapid transformation of ocean bottom siliceous oozes to partially crystalline deposits, probably via the following pathway. :- opal-A → opal-CT → chalcedony or cryptocrystalline

quartz. However, the experimental work of Oehler (1976) suggests that the opal-CT step does not necessarily occur, and instead - proposes:

:- opal-A → chalcedony → mega-quartz.

Certainly the inversion process is well documented and accepted, and has played a major role in the formation of mega-quartz in the Rum Jungle magnesites.

Chert nodules are a common phenomenom in carbonate sequences (Uppill, 1980). Sathyanarayan and Muller (1980) clearly demonstrated that chert nodules can be secondary after dolomite, which is - in turn - pseudomorphous after calcite i.e. they have formed in the manner proposed by Knauth (1979). However, large, layer-parallel bands of chert nodules are rare at Rum Jungle. Of course, it may be that the site of the chert nodule bands was co-incident with either the stratiform stromatolites, which are now replaced by quartz, or to a much less degree with layer-parallel stylolites, many of which have quartz concentrated along them. Also, later metasomatic reactions may have involved silica in the formation of new minerals e.g. magnesite + quartz + water → talc.

Rubin and Friedman (1981), propose an entirely different chert formation model. They compare chert formation to Australian silcretes (siliceous duricrusts) and propose that the chert forms in a similar manner (Callen, 1976, 1977) i.e. associated with an erosional surface, and consider colloform or nodular chert as reworked silcrete pebbles. This model may well be applicable to the formation of the Buckshee Breccia (the former H.Q.B. - Haematite Quartz Breccia) (Fig. 12). Little is as yet resolved concerning this Formation. Even its stratigraphic level is uncertain, except that it is invariably

associated with (overlying) mineralization at Rum Jungle (Berkman, 1980; Fraser 1980; Pagel et al., 1984; Petersen et al., 1984).

In conclusion, most of the silica within the Rum Jungle magnesites results from diagenetic processes that occurred at relatively low temperatures. Inversion processes have brought about the transformation of much of the primary chert to mega-quartz. The silica was introduced into the carbonate precipitating alkaline lakes predominantly in solution, either by surface waters or within groundwaters entering these lakes (Figs 35, 36). Due to evaporation and the alkaline nature of these solutions they may frequently have been saturated with respect to silica.

A volumetrically small amount of silica was derived directly from the Complexes and the arenite formations, as detrital grains.

Silica did not precipitate as a primary sediment i.e. there are no chert bands as in B.I.F.'s. However, silicification did commence prior to lithification and compaction, and continued during these processes.

The silicification of the magnesite was pervasive and aided by the pervasive stylolitisation, so that the probability of success of delineating a silica-poor magnesite deposit for B.H.P. must be considered very low.

a.   Euhedral crystal of dravite-type tourmaline within magnesite.
       The unabraded, acicular nature of the crystal supports the
       premise of a diagenetic origin. Immediately to the right of the
       acicular crystal, there is an abraded, detrital tourmaline
       grain. Sample E28, Coomalie Dolomite, E.L. 1349.

b.   Tourmaline, chlorite and pyrite crystals concentrated along a
       stylolite within arenite. Sample D03, Crater Formation, E.L.
       1349.

c.   Tourmaline, sericite and quartz concentrated along, and
       completely clogging the lower side of a stylolite in magnesite.
       The upper half of the sample has been 'cleansed' of its
       impurities more successfully by stylolitisation than the lower
       half. Sample C17, Celia Dolomite, E.L. 1349.
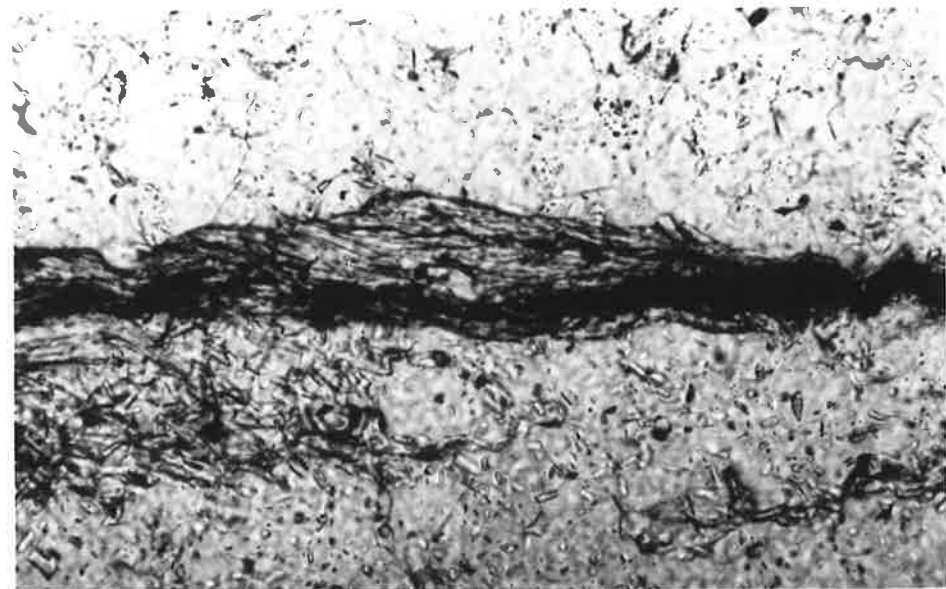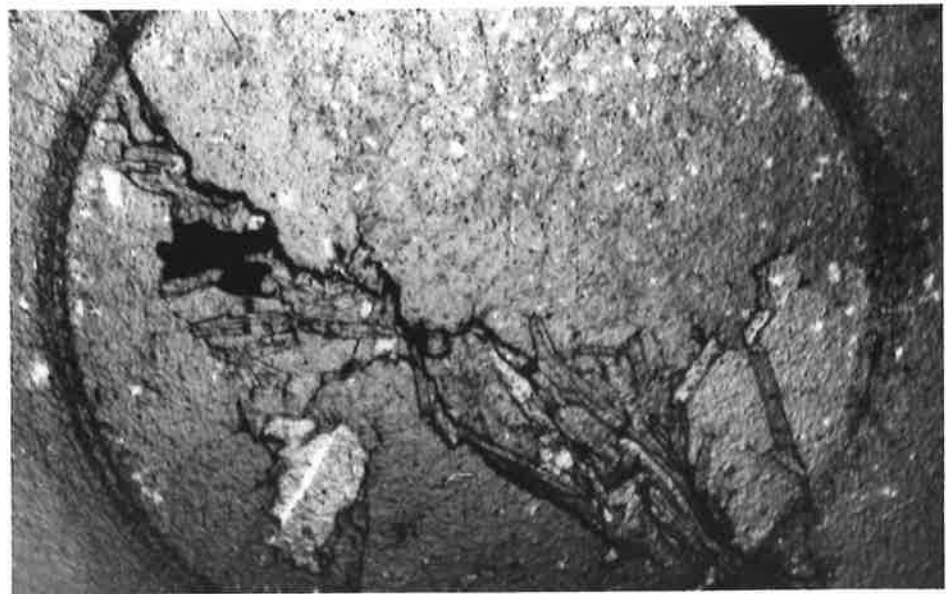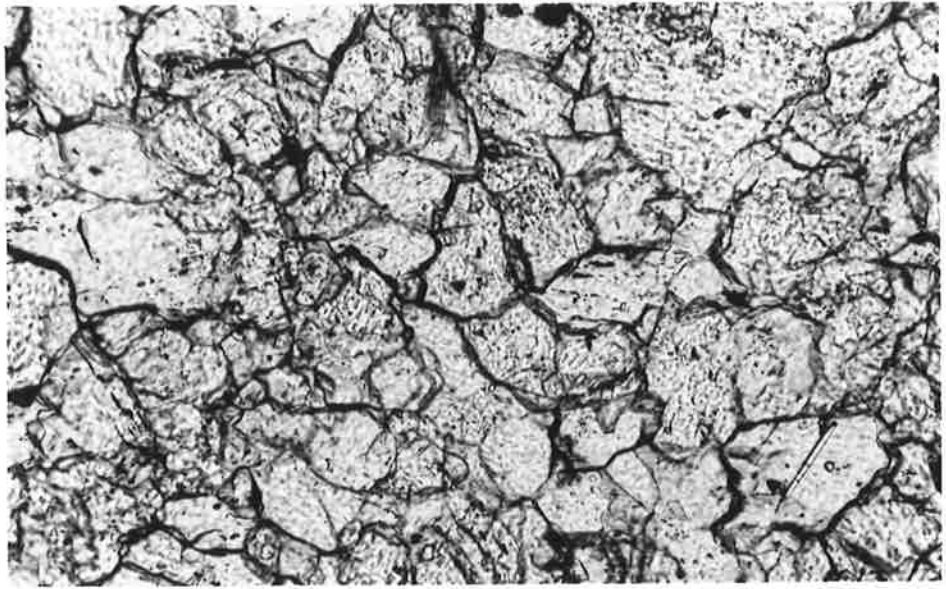
4.3.5 <u>Tourmaline</u>

Tourmaline is a complex borosilicate consisting essentially of Mg, Fe, Al, Na, Ca, B, Si and O., However, there are 12 elements that can substitute in three of the lattice sites, thus leading to wide variation in composition. Consequently, we have Mg-rich dravites and Fe-rich schorls which can be correlated with different geochemical environments (Taylor and Slack, 1984).

Tourmaline occurs in rocks representative of a wide variety of environments. Not surprisingly a range of processes can produce a concentration of tourmaline. Documented origins include: (a) granitic-plutonic; (b) detrital; (c) regional metasomatic; (d) authigenic; (e) evaporitic - sabkha and (f) submarine-hydrothermal (Slack, 1982). There is considerable overlap between (d) and (e), with (d) including diagenetic processes.

Notwithstanding the early recognition (e.g. Hitchcock, 1878) and the ubiquitous nature of tourmaline, in particular as an accessory mineral, it has received scant attention in the literature apart from reference to its presence. However, as it is gradually being recognised as a significant component (i.e. > 15% by volume) of some clastic and other metasedimentary rocks associated with stratabound mineral deposits, particularly in the Proterozoic, it is coming under closer scrutiny (Garlick, 1967; Ethier and Campbell, 1977; Gautier, 1979; Barnes, 1980a, 1980b; Nicholson, 1980; Slack, 1982; Mattson and Rossman, 1984; Shibue, 1984; Slack et al., 1984; Taylor and Slack, 1984).

Tourmaline of at least four, and possibly five different origins occurs at Rum Jungle.
(1) Late stage magmatic differentiation has led to the formation of Fe-rich schorl within the Archean complexes. This occurs as fine,

a. Banded quartz-tourmaline rock i.e. tourmalinite. White material
    is quartz, light-grey crystals are authigenic pyrite (altering to
    limonite) and darker grey is tourmaline. Minor soft sediment
    slumping can be seen in the lower section. Sample B09, Beestons
    Formation, E.L. 1349.

b. This sample has a schistose appearance, but the 'schistosity' is
    due to fine grained, aligned tourmaline crystals. White material
    is quartz, dark grey is hematite crystals growing pre-and
    synchronously with the quartz and lighter grey is tourmaline.
    There is also some sericite in this sample. Sample C48, Celia
    Dolomite, E.L. 1349.

c. This sample has quartz and tourmaline as the only minerals
    present. The tourmaline layers have been disrupted, and have the
    appearance of rip-up clasts. Sample C52, Celia Dolomite, E.L.
    1349.
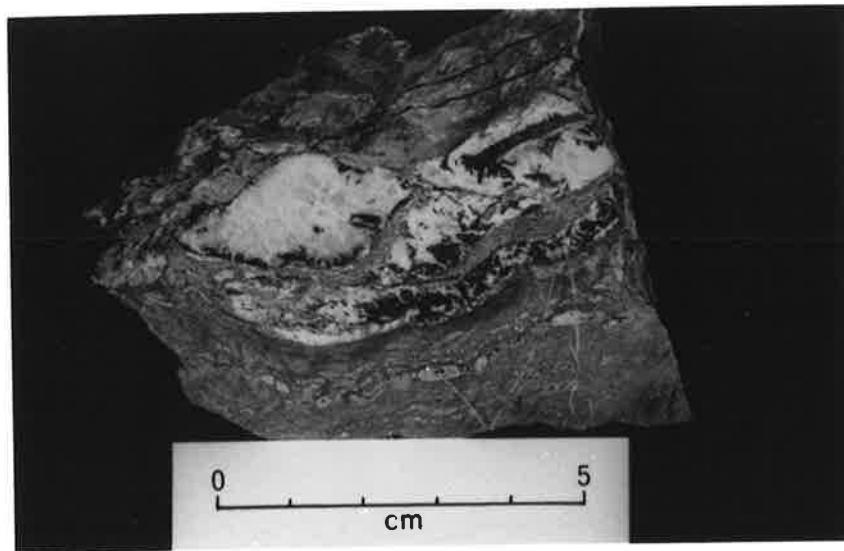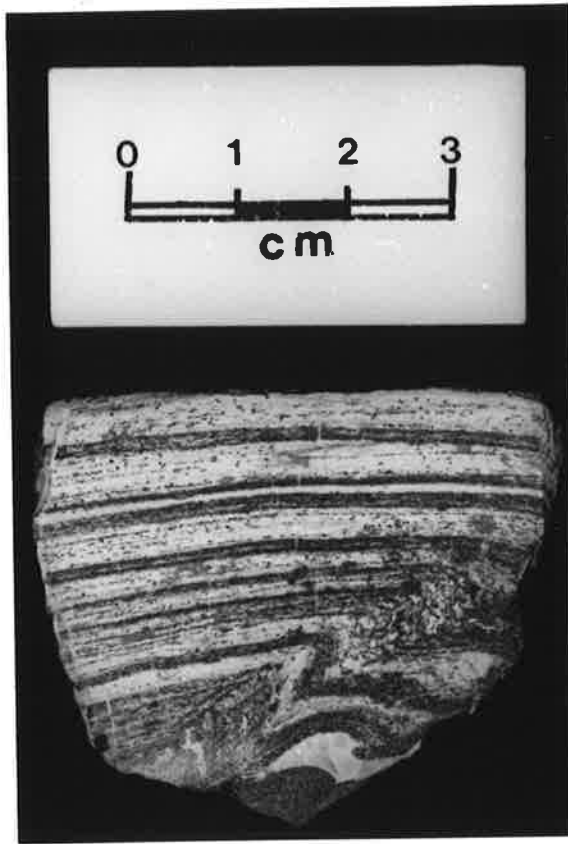
disseminated material in the granitoids and as larger crystals within the associated pegmatites.

(2) This schorl has been the source of the detrital tourmaline grains within the onlapping sediments. The detrital origin is suggested by the rounded nature. These grains may be overgrown by tourmaline occurring in crystallographic continuity. This detrital material occurs in trace amounts.

(3) Within the magnesite there are discordant veins of quartz containing green, acicular crystals of tourmaline and Fe-rich magnesite (Plate 26). Analyses of this tourmaline showed it to be dravite. So, although the origin could be considered metasomatic, the source of the B was not the same as that for the tourmaline within the pegmatites.

(4) Authigenic tourmaline grains are an order of magnitude more abundant in the sediments than the detrital variety. Although they are approximately the same size as the detrital tourmaline grains, they are readily differentiated by their perfect euhedral nature (Plate 27). No evidence is seen of abrasion, even though the extremely delicate crystals often exhibit a marked acicular habit. They also are frequently associated with other minerals with authigenic origin characteristics e.g. chlorite, quartz, albite, calcite etc. (Plate 27). The development of all these authigenic minerals probably exerted the dominant control upon pore geometry and pore surface texture during diagenesis. Certainly the tourmaline crystals were frequently the cause of the clogging up of solution channelways i.e. stylolites (Chpt. 4) during diagenesis (Plate 27).

Satisfactory microprobe analyses of these small ($< 5 \mu$m) tourmaline crystals were not possible, as there are problems with beam width when analysing tourmaline (Ethier and Campbell, 1977). However, the analyses were sufficiently accurate to indicate that these tourmalines are dravite and not schorl.

(5) The possibility of the tourmaline being of evaporitic-sabkha type
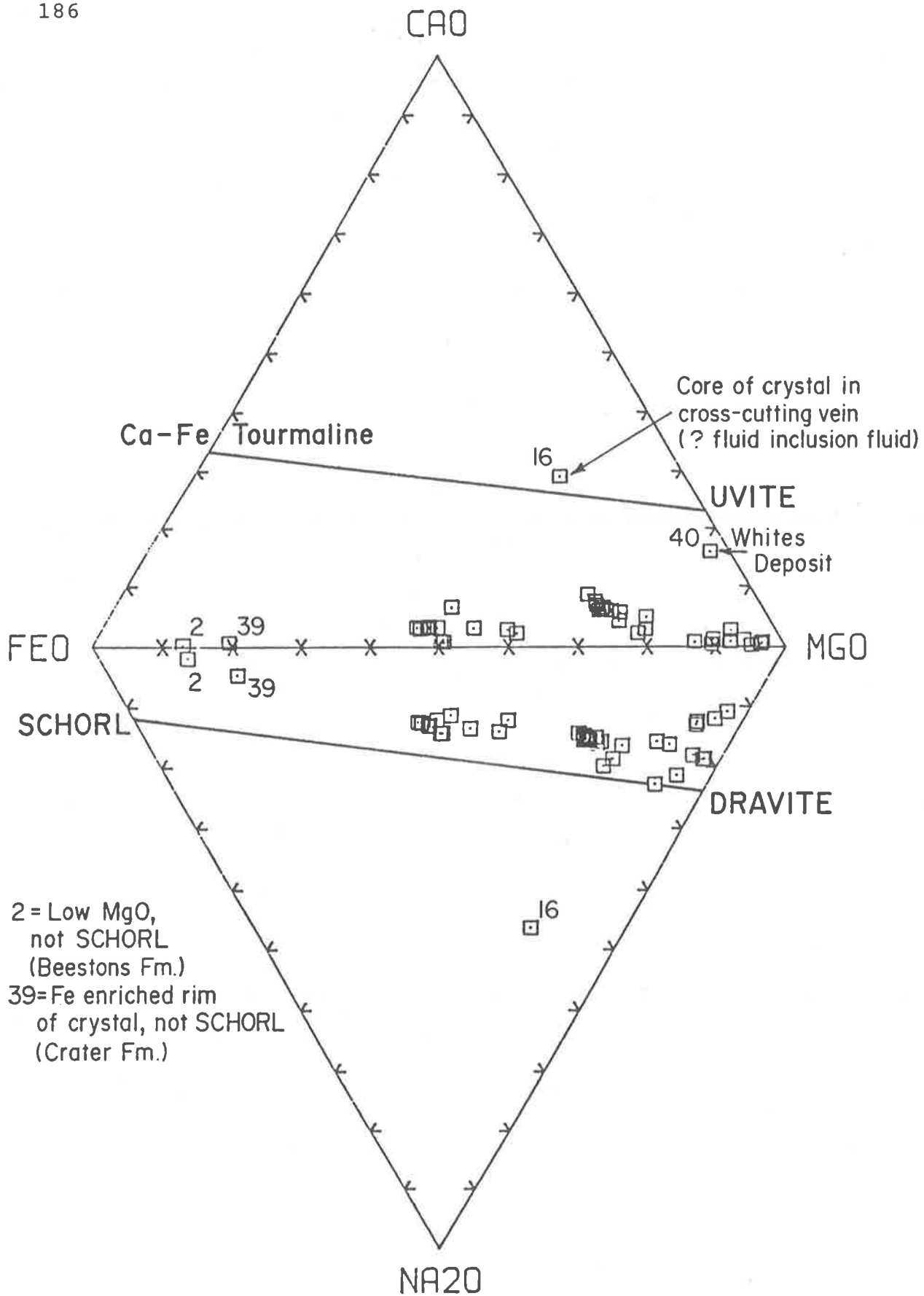
Fig. 44: Tourmaline geochemistry. The CaO-FeO-MgO and the Na$_2$O-FeO-MgO triangles in the CaO-Na$_2$O-FeO-MgO tetrahedron. Each analysis is represented by a point in each triangle.

origin seems quite likely, due to the substantial evidence available suggesting an arid, lacustrine, carbonate evaporite environment (Chpt. 4). If borates deposited in such an environment persisted (- they are highly soluble minerals) they would form dravite-type tourmaline upon diagenesis/metamorphism, and be associated with anhydrite and scapolite (Slack, 1982). However, microprobe analyses of all "scapolites" from the Rum Jungle area showed that although they looked like scapolite in the hand specimen and thin section, they were in fact "light coloured" tourmaline.

(6) Thus all the sources have been discussed except for submarine - hydrothermal.

Garlick (1967) suggests that B was transported into a lacustrine, desert environment in the same waters as the sulfides and the conglomerate clasts at Chibuluma, Zambia i.e. surface waters, whilst Gautier (1979) cites waters associated with volcanism as possible causative agents in the Tiger Ridge Field, Montana. At Sullivan, British Columbia, Ethier and Campbell (1977) consider that the B-rich sediments resulted from hydrothermal fluids emanating along fractures etc. moving into sediments adjacent to a collapse zone. They propose that the nature of the breccia and the introduction of the B are evidence of a rift associated with a thermal anomaly, and that the source of the B was either the product of a granitic magma degassing at great depth or that it was gleaned from the sedimentary pile and concentrated in the same manner as the metals.

Before accepting a submarine-hydrothermal source, there are still "tourmalinites" to be considered. In this type, tourmaline is a major component of the rock, at times constituting 50% by volume. The most common habit is as a banded quartz tourmaline rock (Plate 28), with the layers being only 1-2 mm wide or much larger. In some samples the tourmaline has the appearance of rip-up clasts within quartz (Plate 28). Occassionally the lamellae are so fine that the rock gives the impression

a.   Optical zoning in a tourmaline crystal parallel to the c axis.
        The acicular crystal shows en-echelon fracturing, indicating that
        the tourmaline formation was pre-deformation. Even so, the
        crystals have still retained their integrity, indicating that the
        deformation was not completely disruptive. Sample C53, Celia
        Dolomite, E.L. 1349. x100; crossed polars.

b.   A different field of view of the same sample as above. x100;
        crossed polars.

c.   This field of view of the same sample illustrates the irregular
        growth lamellae width, which is similar to other reported
        tourmalinites. Stress-induced quartz infills the fractures
        between the tourmaline crystal slices. x100; crossed polars.
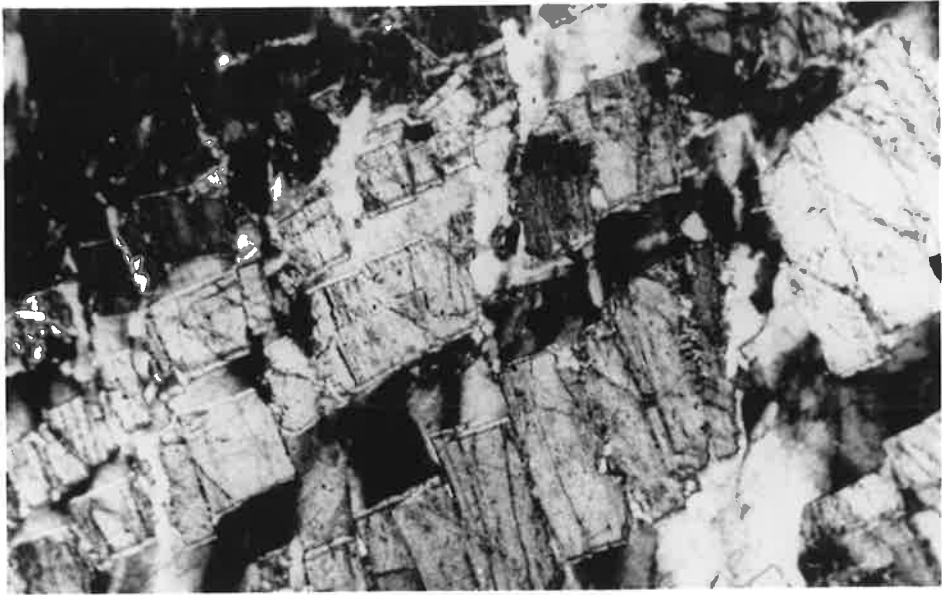
of being either a schist (Plate 28) or where there is no fabric developed, a chert.

This type of tourmaline-rich rock has now been defined as tourmalinite - a stratabound, lithologic unit containing   15% tourmaline by volume (Nicholson, 1980; Slack, 1982; Slack et al., 1984; Taylor and Slack, 1984). At Rum Jungle the tourmalinite occurs within both the arenites and the magnesite formations as either a distinct traceable unit or as lenses. Within the Beestons Formation it appears to be contiguous with a quartz/magnetite unit, which grades into a ? mafic schist (chlorite/Fe-oxides); whilst the quartz/magnetite unit is missing in the Celia and Coomalie Formations. In some cases the tourmaline is very fine grained, light green in colour and constitutes more than 50% of the rock; so that it resembles a metamorphosed amphibolite. It is suggested that some of the so-called amphibolites and mafic schists of the Rum Jungle area are actually misidentified tourmalinites.

The geochemistry of these tourmalinites (Appendix 3, Fig. 44) shows that they are dravites. The two samples (B06 (b) and D09 (p)) that plot within the schorl field are due to high Ti and a rim of oxidised Fe respectively. Sample WO-KF92B, which plots towards the uvite field, (Ca rich tourmaline) contains diagenetic dolomite. The high Na_2O and CaO in sample C52 (f) is probably due to contamination from the rupturing of a near surface fluid inclusion (Bone and Griffin, 1984).

Taylor and Slack (1984) report high average contents of Cr, (78 ppm), Cu (77 ppm), Pb (114 ppm), Sr (98 ppm) and V (195 ppm), but these values are below the detection limits obtainable in this study (Appendix 3). This study does support their findings of consistent F   Cl, low MnO_2 values and the lack of a negative correlation between Na_2O and CaO as shown by Ethier and Campbell (1977).

a.   The optical zoning (which is reflected in the chemical zoning -
        Appendix 3) parallel to the c axis is well illustrated in this
        acicular tourmaline crystal in quartz. Sample C53, Celia
        Dolomite, E.L. 1349. x100, crossed polars.

b.   Although the 'slices' of the tourmaline crystal are completely
        discrete, this photo shows that they have maintained their
        overall integrity as crystal was subjected to shearing stress.
        Same sample as above. x100; crossed polars.

c.   Acicular tourmaline and pyrite crystals of diagenetic origin in a
        quartz arenite. The δ^{34}S value obtained from pyrite from this
        sample was indicative of a bacteriogenic origin for the source of
        s. Sample D10, Crater Formation, E.L. 1349. x100; crossed polars.
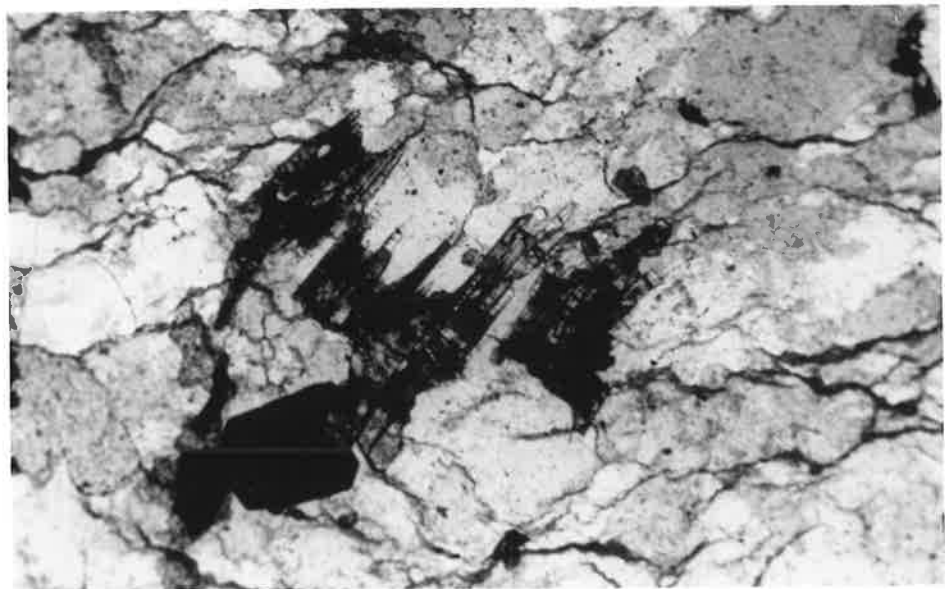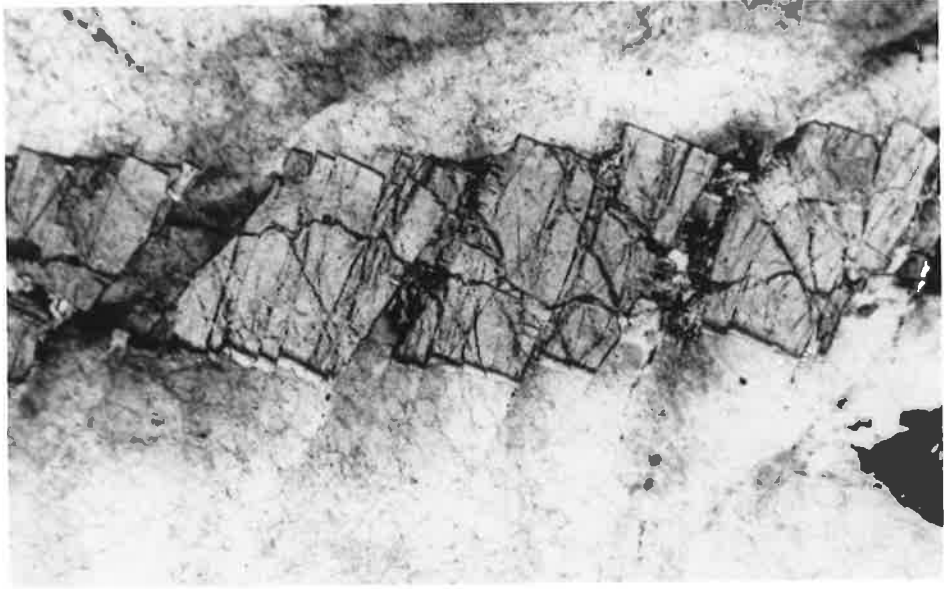
Other similarities to reported tourmalinites are the optical and chemical zoning parallel to the c axis (Plate 29, Appendix 3), with irregular growth lamellae width (Plate 29). This zoning supports the pre-regional - metamorphic origin of the tourmaline (Taylor and Slack, 1984). The en-echelon fracturing of acicular, zoned tourmaline crystals is spectacular evidence for the formation of the tourmaline prior to deformation (Plates 29 and 30).

Therefore it is envisaged that the tourmaline formed from a pre-metamorphic B-bearing fluid. The distinct layering, slump folding, rip-up clasts and the association of diagenetic pyrite suggests a diagenetic sedimentary environment. Association with chemical sediments i.e. quartz/magnetite and possible tuffs i.e. "mafic schists" suggest the formation of the tourmalinite as a chemical sediment precursor i.e. tourmaline growth was either syngenetic or early diagenetic. Such B-bearing fluids are considered to be generated primarily by hot-spring activity and mobilized by the action of CO_2 rich fluids (Buhmann and Dreybrodt, 1985), particularly in the presence of organic acids. Although most tourmalinites are still being interpreted as having been deposited in subaqueous marine environments, their formation in a shallow water, evaporitic environment (Eugster, 1980) has not received sufficient recognition, particularly in continental rift environments. All economic borate concentrations (S. Californa, Turkey) occur in rift environments and <u>not</u> in a marine sedimentary environment. The presence of a rift phase at Rum Jungle has already been discussed (Chpt. 2).

So it is proposed that the tourmalinites at Rum Jungle are of non-marine/hydrothermal origin.

The close association of tourmalinites with a variety of metallic mineral deposits suggests that they are prospective pathfinders, whilst better understanding of the formation of the tourmalinites should lead to

a.   Dolomite rhombs growing diagenetically in magnesite. Sample C63,

        Celia Dolomite, E.L. 1349. x100; plane light.

b.   A dolomite rhomb growing diagenetically in a thin stylolitic band

        of talc that lies within magnesite. Sample E19, Coomalie

        Dolomite, E.L. 1349. x100; plane light.

c.   Numerous dolomite rhombs growing diagenetically in magnesite.

        Sample C64, Celia Dolomite, E.L. 1349. x100; plane light.
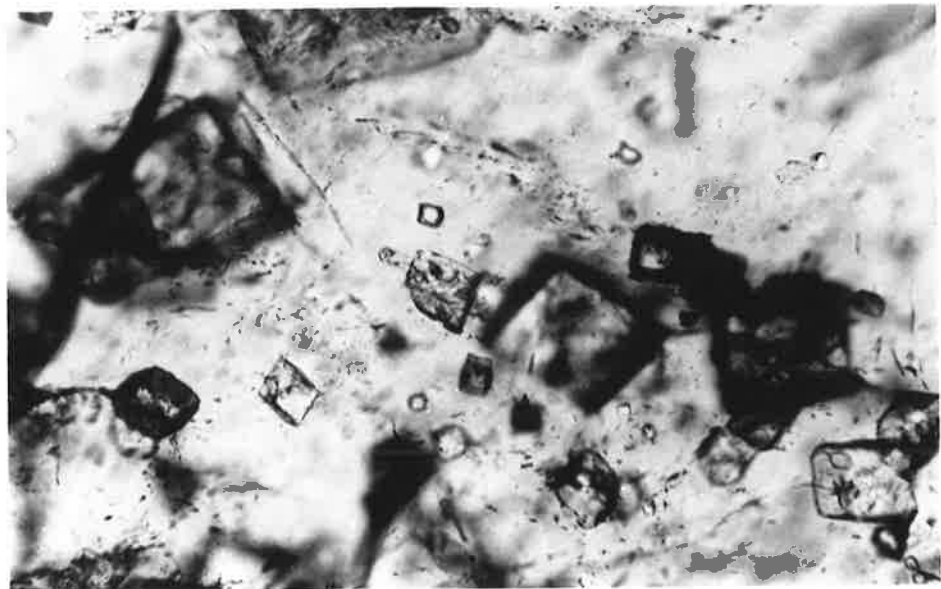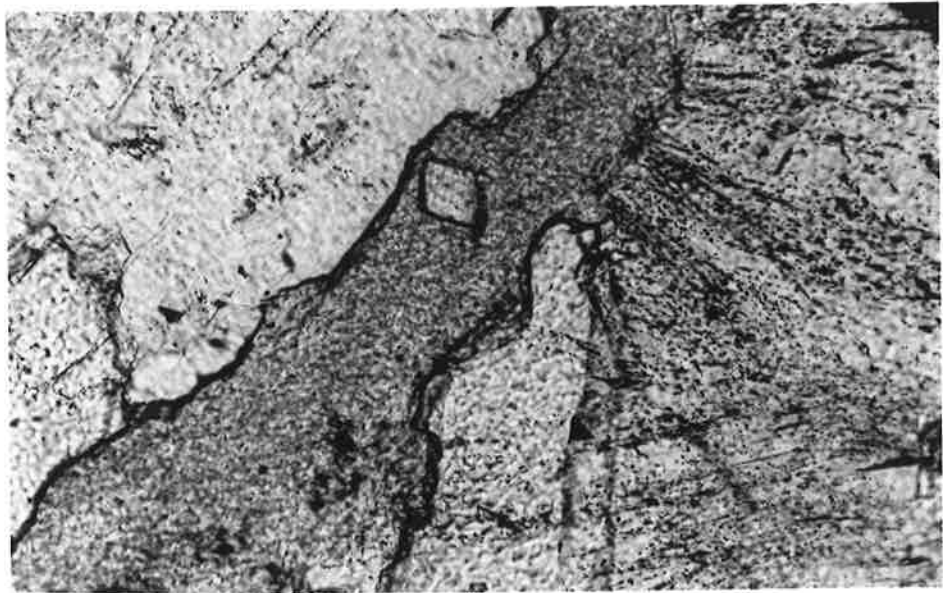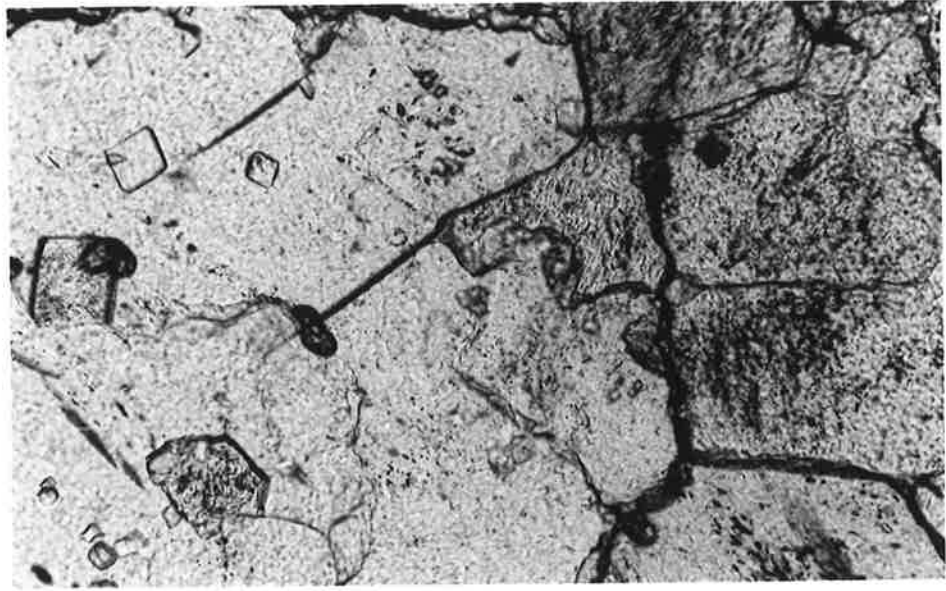
increased knowledge regarding the nature and genesis of the mineral deposits.

4.3.6 Other Diagenetic Minerals

Other diagenetic minerals present will not be dealt with in the detail applied to quartz and tourmaline. One of the difficulties with minerals that show evidence of growth post depositionally e.g. dolomite rhombs, chlorite, sericite, pyrite, etc. (Plates, 27, 30-32) lies in assigning either a burial diagenesis or a low grade metamorphism i.e. anchizone, genesis with any degree of confidence. Many so called metamorphic reactions are dependent on $P\ CO_2$ as well as temperature, and yet $P\ CO_2$ is also a function of "pressure solution", (Frisch and Helgeson, 1984) or i.e. "chemical compaction" - as defined by Fairchild (1985). So, there is a large unknown range of thermodynamic parameters into which many of these Rum Jungle area minerals fall.

Certainly experimental work has supported the argument for a metasomatic origin. The Rum Jungle chlorites and sericites, with their high Mg content (Appendix 3) compared to average hydrothermal sericites (Perry et al., 1984) indicate that the presence of magnesite was influential in their resultant chemistry, but at which side of the diagenesis - metamorphic boundary is unclear. Ewers et al., (1983) suggest that at the Nabarlek Deposit in the East Alligator Uranium Field the sericite was formed at or after 920 my ago, leading to the breakdown of the pre-existing chlorite and the formation of hematite. However, at Rum Jungle there is ample evidence to support a much earlier hematite formation e.g. zoning of hematite in diagenetic magnesite rhombs truncated by stylolites (Plate 23). Nor is the Rum Jungle chlorite any lower in Fe than would be expected for the diageneticially formed chlorite in the environment pertaining (Appendix 3).

PLATE 32

a.   Diagenetic chlorite grains concentrating along an incipient stylolite in magnesite. Sample C17, Celia Dolomite, E.L. 1349. x100; plane light.

b.   Diagenetic tourmaline and sericite concentrated along a stylolite in fine grained magnesite. Sample C17, Celia Dolomite, E.L. 1349. x100; plane light.

c.   A mosaic of diagenetic quartz grains associated with talc and sericite at the intersection of the cleavage trace in magnesite. Sample C64, Celia Dolomite, E.L. 1349. x100; crossed-polars.
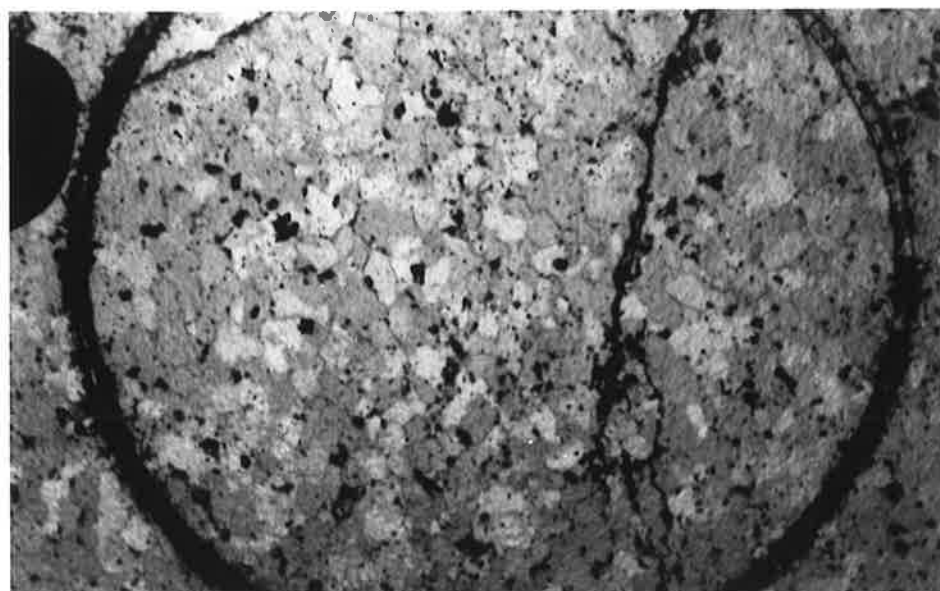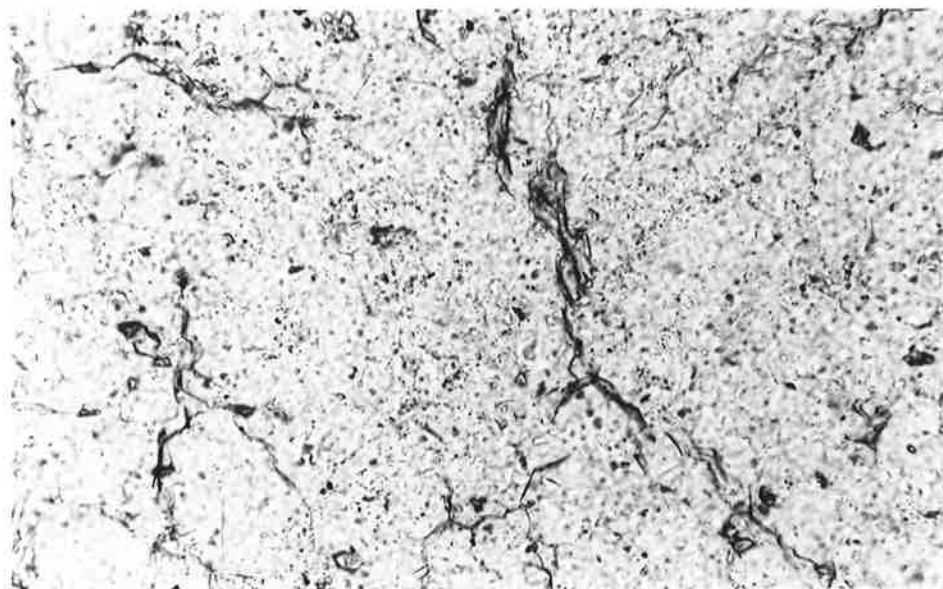
Thus it remains unclear as to whether these minerals formed diagenetically or metasomatically. It is clear that they formed under the influence of circulating fluids, the composition of which was controlled by the alkaline, lacustrine environment that evolved at the rift phase during the early development of the Pine Creek Geosyncline.

4.4 Deformation and Tectonism

The tectonic setting of the Pine Creek Geosyncline, including Rum Jungle, has been discussed in Chpt. 2.5. It is not proposed to discuss in detail the affect the four deformation events in the area, as they are adequately covered in Paterson et al. (1984). Certainly there is ample field evidence to support the deformation events e.g. inclined beds (Plate 2), faulting, joint patterns (Plate 33), folding (Plate 33).

However, there is one aspect that this study suggests that has not previously been reported, and that is the likelihood of stratigraphic duplication.

4.4.1 Stratigraphic Duplication

It has already been foreshadowed (Chpt. 2) that there is the possibility that further amendments may be appropriate in the lower section of the formal stratigraphic sequence: i.e. Beestons Formation, Celia Dolomite, Crater Formation and Coomalie Dolomite.

During the field season in 1979 the area of E.L. 1349 (Fig. 45) was mapped in considerable detail (Fig. 7). The following observations were made and compared to other areas:-

(1) The Beestons Formation and the Crater Formation are very similar. They both have:-

PLATE 33

a.   Well-developed joints in magnesite. Outcrop 91, Area C, Celia
        Dolomite, E.L. 1349.

b.   Minor parasitic folding in magnesite. Outcrop 94, Area B, Celia
        Dolomite, E.L. 1349.

c.   Minor parasitic folding in magnesite. Outcrop 74A, Area B, Celia
        Dolomite, E.L. 1349.

(a) sheared contacts at the base. Fraser (1980) has described the unconformity between the Complexes and the "overlying unit" as being commonly sheared and the contact infilled with quartz. Needham and Stuart-Smith (1983) have commented on the fact that the base of the Crater Formation "is invariably sheared". Assuming that their choice of the word "invariably" is precise, then this raises an interesting tectonic consideration, as the distribution pattern of the base of the Crater Formation is radial to the Archean Complexes, (Fig. 2).

(b) quartz pebble conglomerates at their bases (Plates 1 and 2).

(c) similar lithologies: arkoses, arenites, banded iron formations and sequences fining upwards.

(d) similar sedimentary structures: ripple marks and cross bedding (Plate 2).

(e) units which have been loosely termed "mafic schists", but which may be volcanics. (Roberts, 1978).
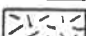
(f) ubiquitous tourmaline. The genesis of this tourmaline is somewhat enigmatic (Chpt. 4.5.5). In places it forms a banded rock with quartz (Plate 28) with up to 50% of the rock being tourmaline; in others it appears to be randomly distributed in quartzite and in yet other areas it appears as an accessory mineral in quartz veins.

(2) The Celia Dolomite and the Coomalie Dolomite are very similar. They both have:-

(a) recrystallized magnesite as their major carbonate. Magnesite formation is not common, and so it is surprising to find that exactly the same critical conditions for it to form were repeated during the Coomalie

Fig. 45
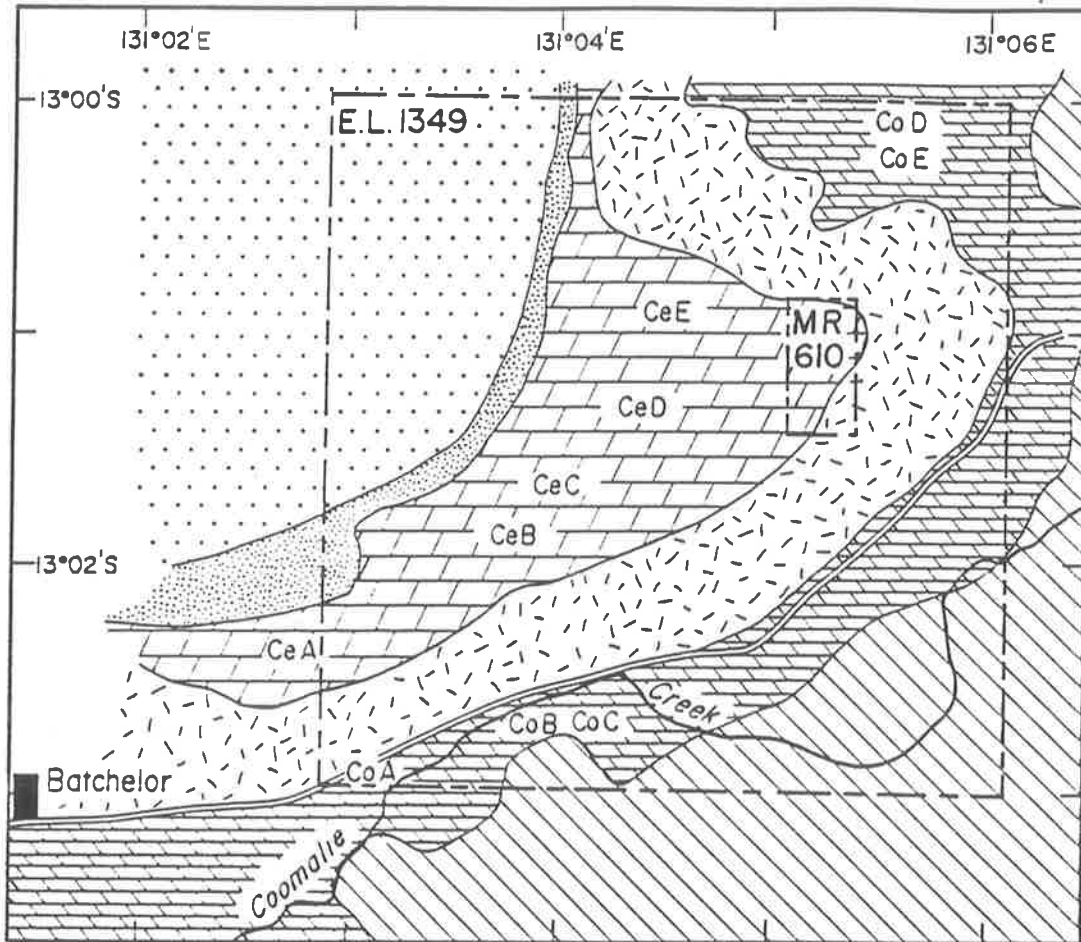
Legend:
- Whites Formation
- Coomalie dolomite (Co)
- Crater Formation
- Celia dolomite (Ce)
- Beestons Formation
- Rum Jungle Complex

PACE & COMPASS
SURVEY LOCATIONS
Rum Jungle, N.T.
SCALE: Km
0   1   2   3

Dolomite time after the deposition of the Crater Formation with its contrasting facies: a thick pile of fluvial sediments presumably representing a considerable period of time.

(b) ubiquitous stromatolites, with the same three morphologics (Plates 11-15).

(c) areas that have been completely silicified (Fig. 7).

(d) lenses of the "mafic schist" which is also seen in the Beestons Formation and in the Crater Formation.

(e) palaeokarstification.

Laboratory studies showed that the petrology and the geochemistry of magnesite samples from approximately the middle of the Celia Dolomite and the Coomalie Dolomite are virtually the same : that if the labels on the samples were lost there is no way in which they can be allocated into their correct sequence. The base of neither Dolomite is anywhere exposed. However, the tops of the two Formations show interesting differences, as well as similarities.

Firstly, the karst-like surface shows the same profile, but the infill is different to what should be expected. The Coomalie Dolomite shows material that was probably derived from the base of Whites Formation as expected. On the other hand, the Celia Dolomite cavernous areas do not contain material typical of the base of the Crater Formation. Instead, the material has been loosely described as a "quartz-sericite schist" by Roberts (1978). It is not clear whether this is a mixture of material from the base of the Crater Formation which shows signs of deformation plus material from Whites Formation (Plates 17 & 18).

Fig. 46 STRATIGRAPHIC REPETITION MODEL: RUM JUNGLE

Fluviatile clastics

Carbonates

W

E

Rum Jungle Complex
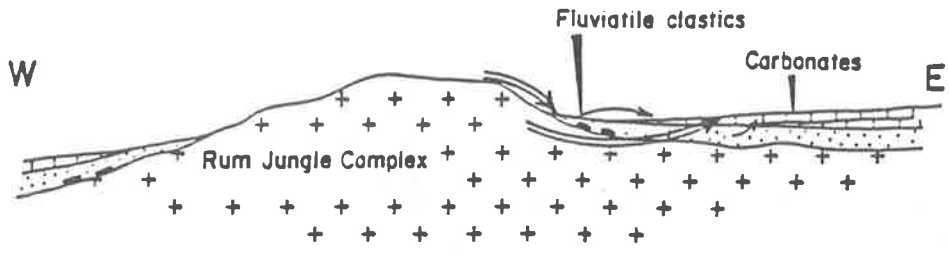
Major

Transport: Detritus or Groundwater

Minor

a) DEPOSITION STAGE

Listric fault

Celia dolomite

Beestons formation

Solid state diapirism
(not vertical)
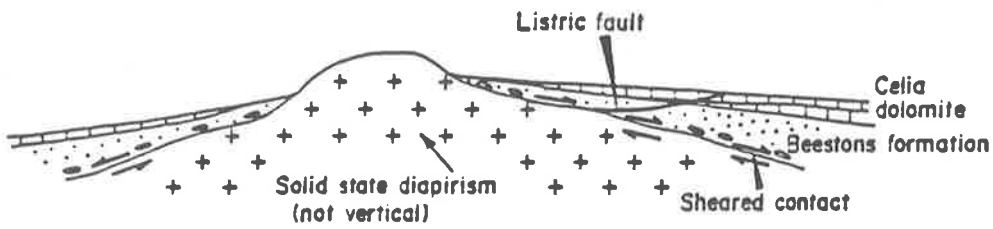
Sheared contact

b) DIAPIRISM STAGE
— Initiation of slumping

Sequence transfer
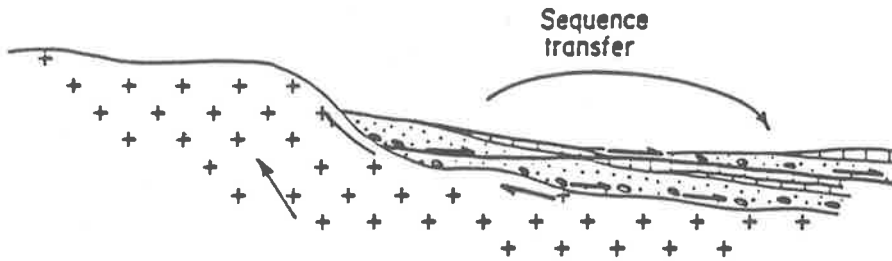
c) GRAVITY SLUMPING STAGE

New erosion surface
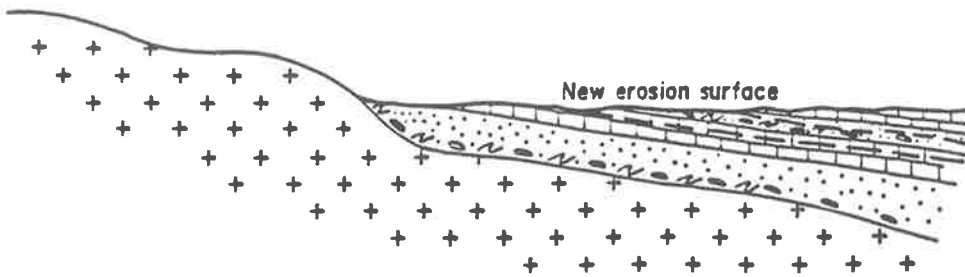
d) FINAL STAGE

Repetition of sequences

Localised T-P affects

Sheared contacts

The fluid inclusion studies also furnish some intriguing data. Once again the samples (both magnesite and quartz) from the middle of the carbonate sequences appear to be exactly the same (Chpt. 6), but once the top of the Celia Dolomite is tested marked differences appear, such as homogenization temperatures that are higher and a much greater density of fluid inclusions containing a CO_2-phase.

These differences continue into the base of the Crater Formation, but not into the middle of the Crater Formation. Indeed, it is from samples at the base of the Crater Formation that the highest homogenization temperatures were obtained.

Thus, the suggested stratigraphic repetition of Beestons Formation and Crater Formation and Celia Dolomite and Coomalie Dolomite will be explained as follows:

The most likely mechanism for achieving the duplication of the Beestons and Crater Formations would be gravity sliding down the buried flanks of the diapirically uprising domes (Fig. 46). Uneven and/or sudden uplift of the domes could have produced a disequilibrium condition causing the sliding of the sedimentary sequence, resulting in a duplication of the sequence. This mechanism is theoretically illustrated in the sand-box model of Lemon (1985). Later deformational events and weathering processes could have combined to confuse and hinder recognition of the initial tectonic events.

It is proposed that the fault between the basement and the Beestons Formation became a listric fault affecting the upper Celia Dolomite as it climbed through the stratigraphy. This increased tectonic-sedimentary loading affected the Celia Dolomite and produced localised mineral reactions of the following type-

$$3MgCO_3 + 4SiO_2 + H2O \longrightarrow Mg_3Si_4O_{10}(OH)_2 + 3CO_2$$

This involved the generation of CO_2 rich brines.

Further evidence to support this hypothesis constitute the quartz veins containing large euhedral tourmaline and magnesite near the top of the Celia Dolomite (Plate 26). This particular type of veining is not found elsewhere.

Other geochemical effects caused by this low angle thrust is the considerable quantity of "leached and bleached" tourmaline within the bottom part of the Crater Formation. This material was orginally identified as scapolite, both in the hand specimen and under the optical microscope. Electron microprobe analyses showed that it is tourmaline (Appendix 3). In fact, following this surprising result arduous searching failed to reval any "real" scapolite, even though it appears frequently in the previously cited studies (Chpt. 3.1). The tourmaline is Fe poor, and it is suggested that the Fe was removed by the hot fluids generated at the time of the gravity thrusting. It is suggested that the fault plane intersected the stratigraphy at a very small angle, and that hydrothermal geochemical readjustments only occurred in the upper part of the lower plate.

The tourmaline needles also show the result of this quite intense shearing process (Plates 29,30), yet the individual sheared portions maintain the overall integrity of the crystal, suggesting that the movement had the same sense throughout. Hence the appearance was created of an apparent stratigraphic boundary rather than a tectonic one. If the thrust had been a high angle one the tectonic nature of this boundary would have been more readily recognised.

In conclusion, the alternative interpretation of the lowermost section of the sedimentary sequence at Rum Jungle is that there are only two units below Whites Formation, not four. The hypothesis is that there was a fluvial sequence onlapping the Archaean Complexes. This was followed by the formation of a sequence of carbonates in peripherally rimming lakes. The problem of lacustrine versus marine formation of magnesite has been discussed earlier. Reactivation of the upward movement of the Complexes by magma injection into the base, probably circa 1800Ma, caused episodic diapirism of the Complexes. One such pulse brought about a detachment, and then a downflank movement of the sequence, thus creating a situation analogous to a repeated sedimentary cycle (Fig. 46).

Notwithstanding the strong evidence presented here, this thesis will continue to use the names Beestons Formation, Celia Dolomite, Crater Formation and Coomalie Dolomite in order to avoid confusion for the reader.

CHAPTER 5

FLUID INCLUSION STUDY

5.1 Principles

The composition of the fluids contained in cavities (i.e. fluid
inclusions) within host minerals has attracted the interest of
petrologists and economic geologists for many decades. Fluid inclusions
supposedly contain remnants of the fluid that once "wet the rocks"
(Pichavant et al., 1982), or at least caused recrystallization. The
composition of this fluid can provide information on the original fluid
producing the host mineral, whilst phase changes within the fluid can
help trace variations in pressure and temperature of the host. This
presumes acceptance of the assumption that the fluid composition and
density has not changed since formation of the inclusion. A variety of
methods has been used to analyse the chemical composition, and thus
simultaneously gain information on the other parameters. A major
complication is the extremely small volumes being analysed, and the
concomitant problem of contamination. New techniques have been developed
during recent years. These techniques can be classified into
non-destructive and destructive methods (Roedder, 1967 and 1972).

5.1.1 Non-destructive Methods

Most non-destructive methods used are predominantly based on the
spectroscopic and optical properties of fluid inclusions. Most
techniques provide limited, qualitative data or at best semi-quantitative
results. The specific technique itself is frequently hampered by
inadequate material for study, as in so many of the samples studied the
inclusions are either too small or host material is not sufficiently
transparent, or both, sometimes due to the large number of very small

inclusions themselves causing a clouding effect. Nevertheless, non-destructive methods do have advantages, the main ones being the possibility of repetition and/or multiple techniques being performed on the same inclusion.

Microthermometry is the non-destructive method most often employed, so that when fluid inclusions are mentioned it is usually presumed that this was the technique, unless another technique is specifically mentioned.

Certainly microthermometry offers the advantage of repetition etc. However, in some case this does not apply, as for example when:-
(a) leaking occurs due to sub-microscopic fracturing of the host mineral caused by the expansion of the fluid phase during microthermometry tests.
(b) metastable conditions are present (in some cases in this study very different results were obtained in each of 3 runs).
(c) when irreversible Eh of pH changes occur.

Another advantage of microthermometry is that very small samples can provide suitable material. Thick polished sections of the mineral or rock are the type of sample used, with the thickness dependent upon the transparency of the host material and the size of the inclusion.

The temperature obtained at the moment of occurrence of a phase change within the fluid inclusion is recorded. This is observed both during melting of the fluid from the frozen state (T_f) and during heating of the fluid until only one phase is present i.e. the fluid homogenises (T_h).

The homogenisation temperature represents the minimal temperature of entrapment of the fluid in the inclusion. It is not possible to obtain too low a temperature for a phase change due to thermal overstepping

whilst heating with the Chaixmeca stage, although it is very easy to obtain higher values due to heating too rapidly, so that equilibrium is not continously established.

There are a number of causes for variation in homogenisation temperatures:-

(a) The pressure varied during entrapment, so that different pressure corrections need to be applied for different inclusions.

(b) The fluid was boiling, so that there was heterogeneous entrapment of liquid and vapour.

(c) The inclusions trapped solid phases e.g. NaCl, that are also components of the brine.

(d) The inclusions are secondary, and are of differing ages.

(e) The inclusions have leaked either during their geological history or in the laboratory.

(f) The inclusions have necked down into two or more inclusions.

(g) The fluids(s) really did have a range of temperatures and salinities.

Where an inclusion is of a primary nature, then the Th gives the mimimum temperature of formation of the host mineral.

The interpretation of the data assumes that either the fluid inclusion has remained a closed system, i.e. constant composition - which also implies no host mineral - fluid inclusion reaction within the inclusion, and constant volume since it formed, or if this has not been so, that post-trapping changes can be recognised (Roedder and Skinner, 1968). The interpretation is frequently complicated further by the recognition that there has been more than one fluid involved, so that the range of data from the inclusions formed from the entrapment of a different fluid, or fluids can overlap with the data obtained from the first fluid. Metastable phases also demand consideration. Roedder (1963) calls attention to the lack of nucleation of ice during

supercooling. A possible explanation is the lack of nucleation centres in very pure fluids. Yet another interpretation problem is the certainty with which fluid inclusions can be assigned as either primary or secondary. Several workers (Hollister and Burruss, 1976; Konnerup and Madsen, 1977; Swanenberg, 1980) have worked on this and associated problems, but Roedder's work, summarised in his 1980 paper is the most comprehensive. His statement "I must admit to some uneasiness concerning the possibilities of ambiguity in the interpretation of some of these data" is a warning that should not be ignored. It is only when the fluid inclusion data interpretations compare positively with data from other independent methods that assertive statements should be made, such as changing "possibly" to "probably".

5.1.2 Other Non-destructive Methods

These are predominantly spectroscopic methods. Although the information supplied is more definitive than that from microthermometry, there are disadvantages, such as the need for specialised equipment and expertise. The various methods have been described by Roedder (1972). Laser excited Raman spectroscopy is proving to be the most useful, although until recently it was limited to determining the presence and concentration of polar components. The technique has now been extended to include the determination of the electrolytes (including hydrates) dissolved in the aqueous phase of the fluid inclusions, (Dubessy et al., 1982) e.g. $NaCl.2H_2O$; $CaCl_2.6H_2O$; $MgCl_2.12H_2O$; $FeCl_3.6H_2O$; $MgCl_2.6H_2O$. It can be used successfully on very small inclusions (Dhamelincourt et. al., 1979; Rosasco and Roedder, 1979; Guihaumou et al, 1984).

Fig. 47:

Calibration for Chaix Meca thermal stage   25/11/82

OBSERVATION —×— (for a 10x lens)
                  —⊙—⊙— (for a 25x lens)
UNCERTAINTY ═══

MEASURED TEMPERATURE

(Light intensity = 2.5 amps)
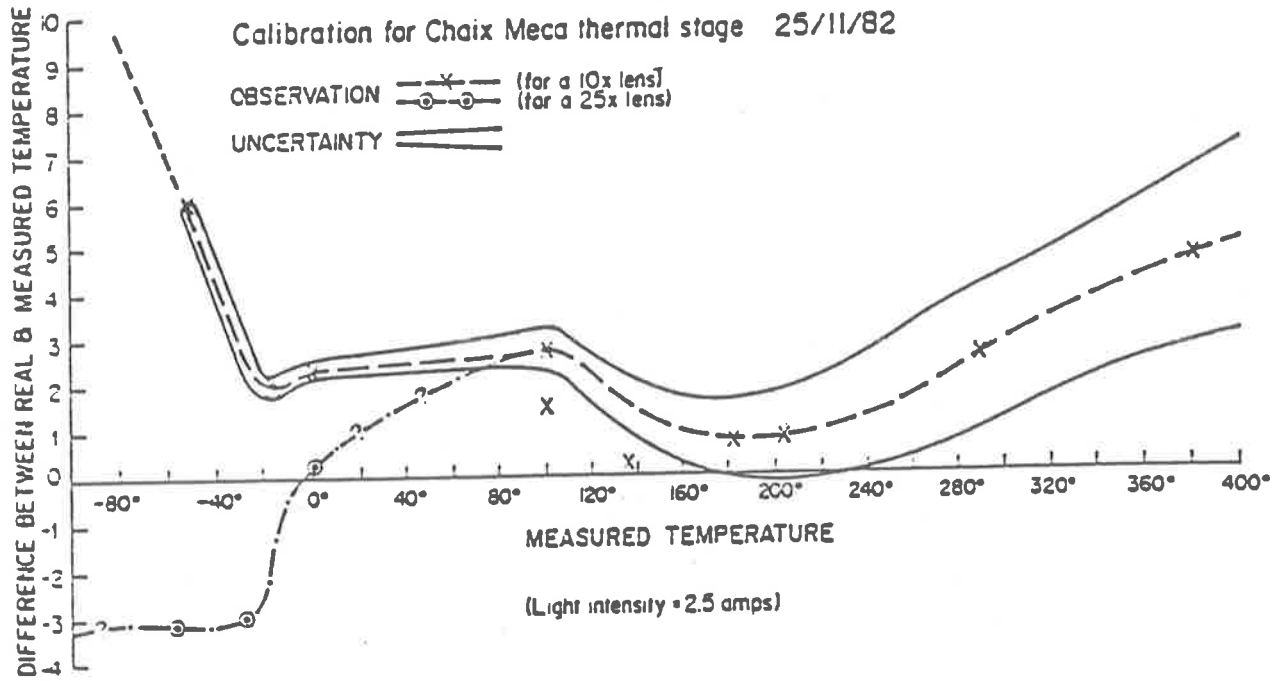
5.2 Methods

5.2.1 Equipment and Calibration

This study was performed on equipment built by the Societe Chaix Meca in Nancy, France, and acquired by the University of Adelaide in 1975. A detailed description of the equipment can be found in Leroy (1971) and its use in Poty et al. (1976). The equipment was fitted to a Leitz Ortholux SMPol Lux microscope. Calibration of the stage was carried out several times during the study by E. Bleys, (technical officer, University of Adelaide). The last calibration curve determined is shown in Fig. 47. Previous curves showed only minor variations from this curve. The discrepancies in the range $30^{o}C$ to $400^{o}C$ do not significantly affect the results or their interpretation. However the discrepancies are quite significant at low temperatures, especially in the vicinity of the eutectic for CO_2, where a correction of $+4^{o}C$ is needed.

5.2.2 Fluid Inclusion Sections

Ermakov (1965) recommends sections of 0.2 to 0.1 mm thickness for semi-transparent minerals, whereas Roedder (1972) suggests that thicknesses outside of the range of 0.5 to 5 mm would seldom be necessary. Leroy (1971) and Schwartzkopff et al. (1974) recommend 0.1 to 0.25mm. If the inclusions are large, i.e. the longest dimension > 0.1mm, then naturally thicker sections will be necessary. As most of the inclusions in this study had their longest dimension < 0.01 mm in length, doubly polished sections were preferable to minimise the effects of scattered reflections off surface boundaries and scattering of light. These are particularly troublesome problems with carbonates. Sections approximately 0.2mm thick were used.

5.2.3 Carbonate Specific Problems

There are many problems working with carbonates (read : magnesites) in fluid inclusion studies. Because of the perfect rhombohedral cleavage of magnesite, samples frequently shatter along the cleavage plane prior to reaching the homogenisation temperature of the fluid inclusion. This is a different phenomenon to that of decrepitation, where the internal pressure of the fluid inclusion exceeds the strength of the host mineral, and so rupturing of the walls of the fluid inclusion occurs. The temperature at which decrepitation occurs can provide useful information analogous to the homogenisation temperature, and is widely used by the Russian workers in the fluid inclusion field. It is also a useful technique for samples that only contain very small fluid inclusions that are too small to observe phase changes optically, or in the case of opaque minerals. The method has been largely superseded in the West by the availability of more sophisticated heating stages, attached to petrological microscopes.

A second problem is that of double refraction, whereby two images, one slightly off-set, of the same object are seen. When there are also many focal planes within the thin section under scrutiny, each with its own display of fluid inclusions, it is usually difficult to obtain a clear image and becomes very difficult to determine phase changes with confidence. If the thickness of the thin section is reduced in order to reduce the number of focal planes, then there is the risk of leakage to the surface, or of the grinding process causing "annealing" of the magnesite (Baker et al., 1980) and thus of changes occuring within the fluid inclusion.

The third major problem with the carbonates is the retention of primary fluid inclusions within magnesite. It is quite possible that some of the fluid inclusions in the magnesite are primary, but

considering the ease with which magnesite is physically altered, even in the early stages of diagenesis, it is more realistic to work from the premise that all the fluid inclusions are secondary. As the magnesite shows extensive recrystallisation and ubiquitous stylolitisation, it is quite evident that the changes that have occurred would lead to the destruction of many, if not all, of the primary fluid inclusions. Using Roedder's allocation parameters (Roedder, 1979) the data obtained from primary fluid inclusions was compared to that obtained from secondary fluid inclusions e.g. trains of fluid inclusions transecting grain boundaries . It was found that there was no significant difference in the two groupings. Similarly with fluid inclusions in quartz, where the primary, pseudo-primary or secondary nature allocation can be more confidently made, it was found that variation both within the quartz and between quartz and magnesite was insignificant. Therefore, the premise is that the fluid inclusions are probably secondary, but have formed almost synchronously with or immediately following the formation of the primary fluid inclusions.

Another problem that has been addressed is the calculation of the temperature correction needed due to pressure. Once again the inherent physical properties of magnesite prevented satisfactory resolution of this problem. Fortunately, at the obtained homogenisation temperatures, corrections would be minimal, notwithstanding the fact that slightly different corrections for different salinities and CO_2 content would apply. Therefore, all data are presented as uncorrected (for pressure) homogenisation temperatures.

5.2.4 Selection of Samples

Samples were selected to provide information on a number of quite different facets of the overall study. They were collected from the whole of the Rum Jungle Suite over a large geographic area (Figs 2, 7).

Further samples were collected from Balcanoona, S.A. and Kharidunga, Nepal in order to carry out comparison studies. Samples were selected from the present erosion surface, mine dumps and drill core.

The samples contained both single crystals and/or polycrystalline aggregates. A selection was made of coarse-, medium- and fine-grained material to eliminate bias resulting from the inclusion of only the easier to work on coarse-grained material. Similarly a range of fluid inclusions were chosen, i.e. in diameter, but it must be admitted that preference was given to the larger ones. Unfortunately, in many samples no choice was available as only small, i.e. $\leqslant 5$ um, fluid inclusions occurred. It appears from the results that these precautions were not necessary; that neither type of grain nor size of either grain or fluid inclusion are temperature related parameters.

Once samples were selected, the magnesite samples were grouped into three categories:
(1) Showing both rhombohedral and bladed forms intimately associated;
(2) Showing distinct and discrete rhombohedral form only (Plate 8);
(3) Showing distinct and discrete bladed form only (Plates 9, 10);

5.2.5 Description of Fluid Inclusion Types

Many of the inclusions are prismatic negative-crystal shaped, others clearly related to cleavage in the magnesite are rhomb-shaped, whilst a minority are the entirely irregular in shape group. The type related to cleavage are seen in some of the quartz samples, seeming to indicate an inherited pattern from a magnesite precursor, and the other two types are common in all the quartz samples.

Within each type, there is a range of fluid inclusions with the following phases; (1) liquid only; (2) liquid + vapour (most common); (3)

a.   Fluid inclusions in magnesite showing three phases - CO_2
      liquid, CO_2 vapour and a H_2O-rich liquid. Invariably
      CO_2-containing fluid inclusions show a negative crystal shape.
      Sample CO9, Celia Dolomite, E.L. 1349. (largest fluid inclusion
      is approx. 8 μm in length).

b.   These three phase H_2O-rich fluid inclusions in magnesite were
      amongst the largest observed in this study. They contained
      numerous daughter minerals adhering to the walls of the fluid
      inclusion. The sample decrepitated prior to the daughter
      minerals dissolving. Sample MF8, Mt. Fitch. (largest fluid
      inclusion is approx. 25 μm in length).

c.   These fluid inclusions are also from sample MF8. On the left is
      a large (approx. 20 μm in width) cleavage related fluid
      inclusion, which may have leaked. In the centre is a large
      two-phase negative crystal type fluid inclusion (with other small
      fluid inclusions above and below this focal plane appearing to be
      within this fluid inclusion). On the right are trails of
      liquid-phase only negative crystal type fluid inclusions.
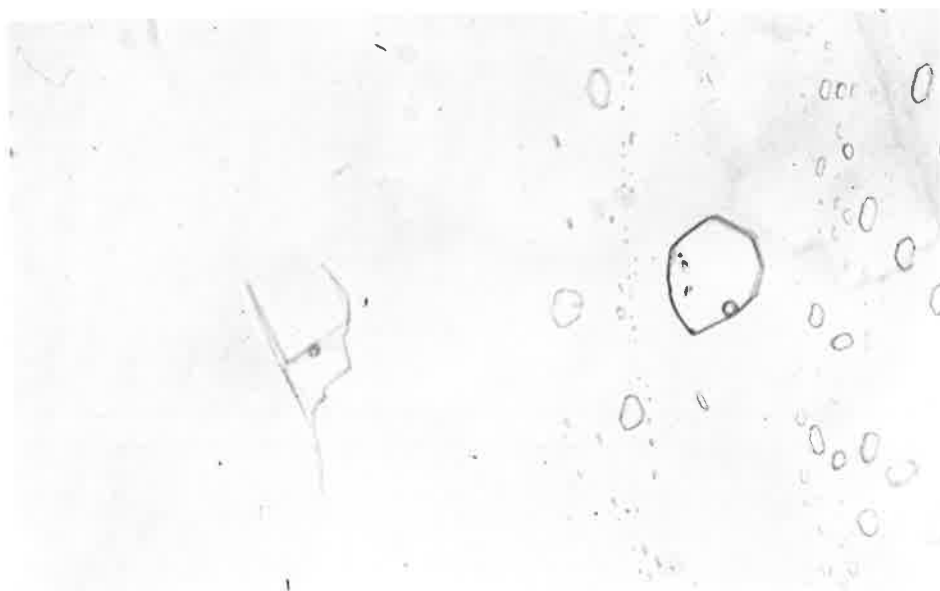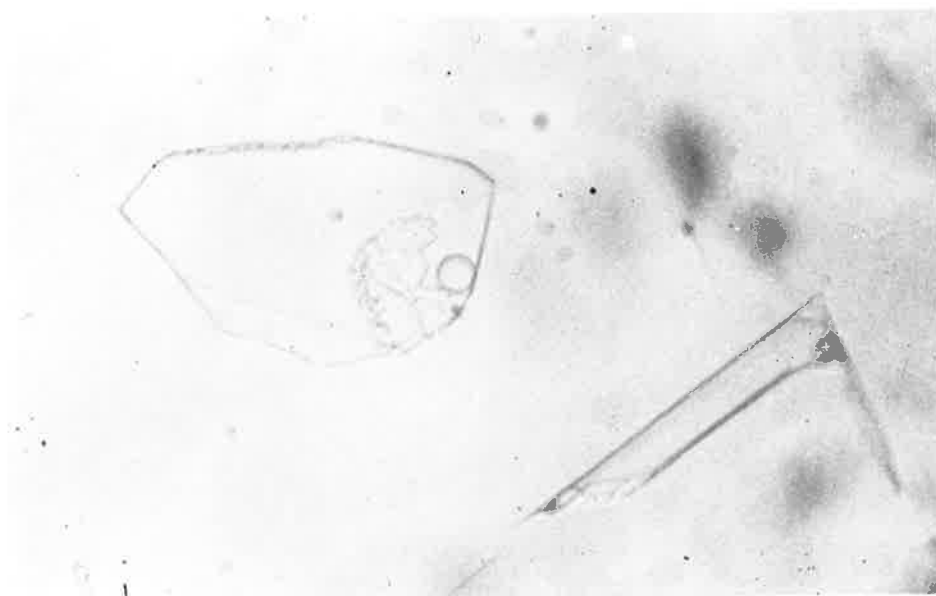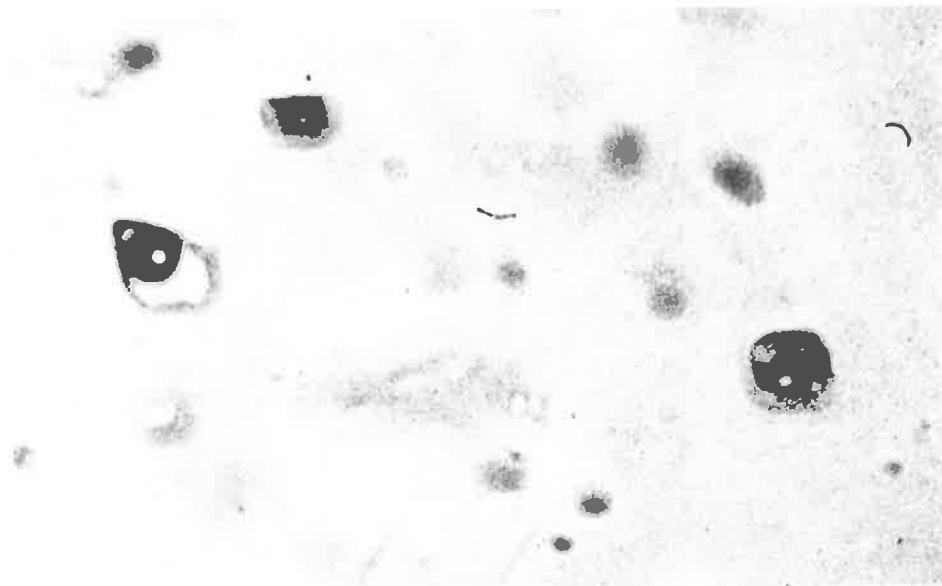
liquid + vapour + daughter minerals(s); (4) two immiscible liquids; (5) two immiscible liquids + vapour. No pattern emerged in relation to the phases present either in distribution or in obtained temperatures; except that fluid inclusions containing an optically visible CO_2 phase almost always show a prismatic negative-crystal shape.

Apart from the Mt. Fitch rhomb type fluid inclusions, the majority of the fluid inclusions are small i.e. <10 um in length. The Mt. Fitch material contains fluid inclusions up to 25 um in length (Plates 34, 35).

Freezing runs were attempted first. If a result was obtained, then a second run was made on the same fluid inclusion. This was then followed by a heating run on that same fluid inclusion; and followed by a second run where possible. This allowed confidence in the data; that could then be used in constructing and interpreting T_h vs T_f plots. However, in many cases, either T_f or T_h was unobtainable. Nevertheless, the one temperature obtained was recorded and utilised in the construction of histograms. All details of fluid inclusion work and results are presented in Appendix 2.

5.3 Theory

5.3.1 Petrographic Microscopy

The petrographic microscope is both the most used and the most useful of the non-destructive tools. With the aid of the usual accessories, information can be gained on the following:-

(a) inclusion morphology.

(b) daughter minerals.

(c) identification of phases i.e. solid, liquid, vapour.

(d) phase ratios.

(e) viscosity of liquid phases.

PLATE 35

a.   Three-phase, cleavage related fluid inclusion in magnesite. The daughter mineral is a bright orange hexagon and is probably hematite. Sample MF8, Mt. Fitch. (Width of fluid inclusion approx. 30 μm).

b.   This type of fluid inclusion was considered to be secondary in formation, as most of them are related to the magnesite cleavage. Sample BR4, Browns Deposit. x320.

c.   Many fluid inclusions formed hydrates as they were warmed after freezing. This photo shows the formation of a hydrate at -40°C. A liquid and vapour phase are also present. Same sample as above sample. (Length of fluid inclusion approx. 10 μm).
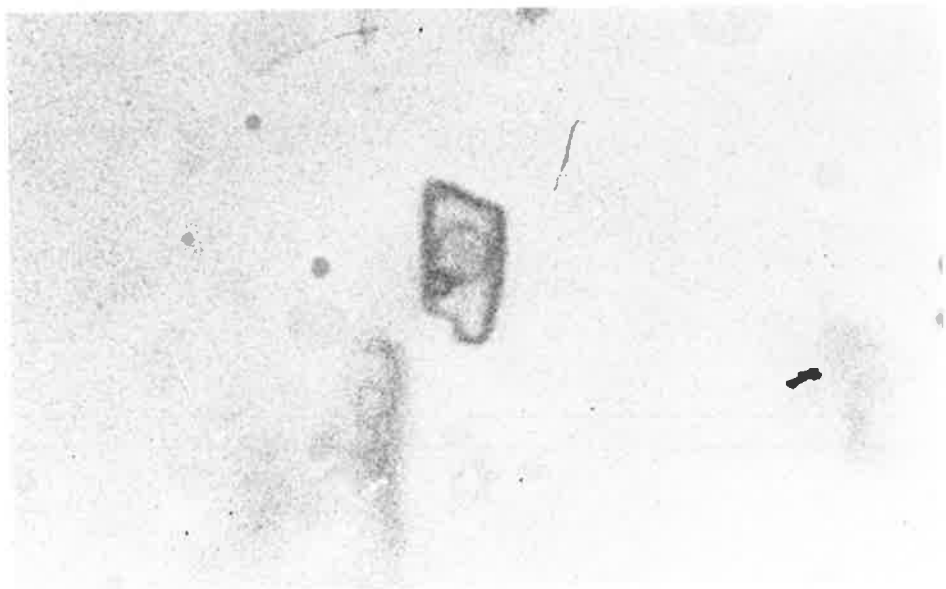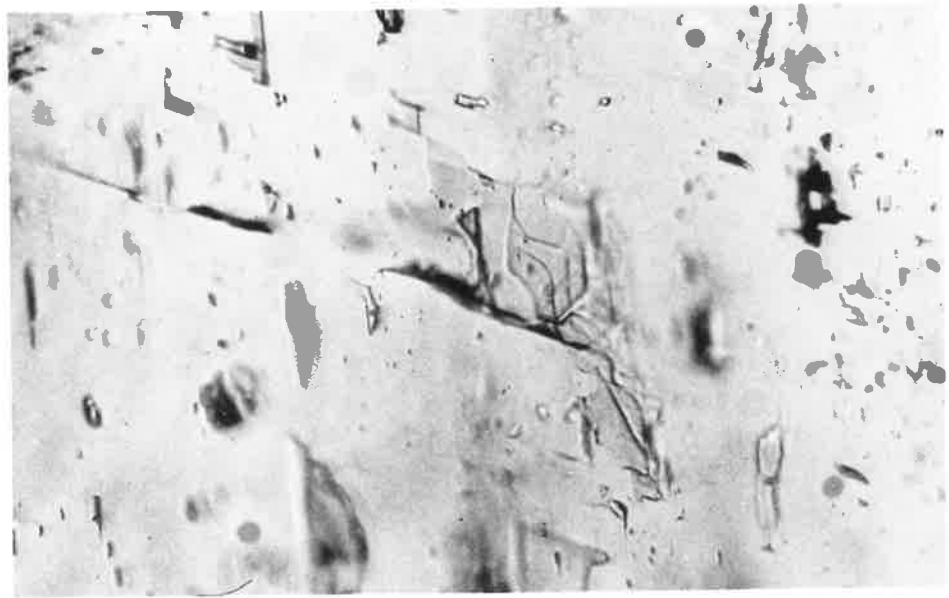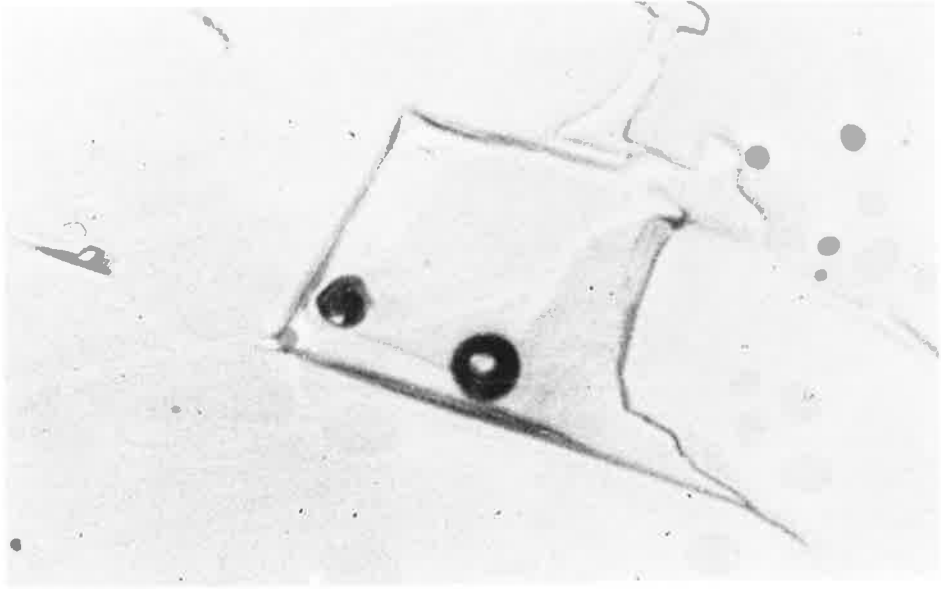
(f) vapour bubble movement in a thermal gradient.

(g) colour of liquid and solid phases.

(h) wetting characteristics - to assist in identification of liquefied gases.

(i) index of refraction.

(j) phase changes due to absorption of light (characteristic for CO_2).

(k) birefringence.

(l) magnetic properties - of daughter minerals.

5.3.2   Microthermometry

Microthermometry is the technique employed to measure phase transition temperatures in fluid inclusions. These are then compared to experimentally determined phase transitions in known systems.

The cooling and/or heating is carried out by the use of a special stage(s) fitted on to the petrographic microscope. The phase changes that occur furnish information on the composition of the fluid inclusion, bearing in mind that the interpretation will not be unambiguous.

Many different techniques have evolved over the past 20 years, descriptions of which can be found in papers by Roedder (1962); Ypma (1963); Bazarov (1966); Hayakawa et al. (1969); Kelly and Goddard (1969); Khetasurov (1971); Leroy (1971); Kharmalov (1973); Kalyuzhnyi (1973); Smith (1973); Gallup et al: (1975); Hollister and Crawford, 1981; Bussink et al., 1984 etc.

Microthermometry induces phase changes in the fluid inclusions, which can be used to identify the components of the fluid, to infer their relative abundance and to supply information on either the pressure or the density.

PLATE 36

a.   This group of photos shows evidence of metastable behaviour. The
     mineral is magnesite. This photo was taken at $20^{o}C$ prior to
     any treatment. The fluid inclusion on the left contains liquid
     only.

b.   After freezing, the fluid inclusion on the left produced a vapour
     phase upon melting. Photo taken at $0^{o}C$.

c.   Upon re-freezing, the fluid inclusion on the left has frozen,
     whilst that on the right remains liquid. Sample BR4, Browns
     Deposit. (left hand fluid inclusion is 10 μm in length).
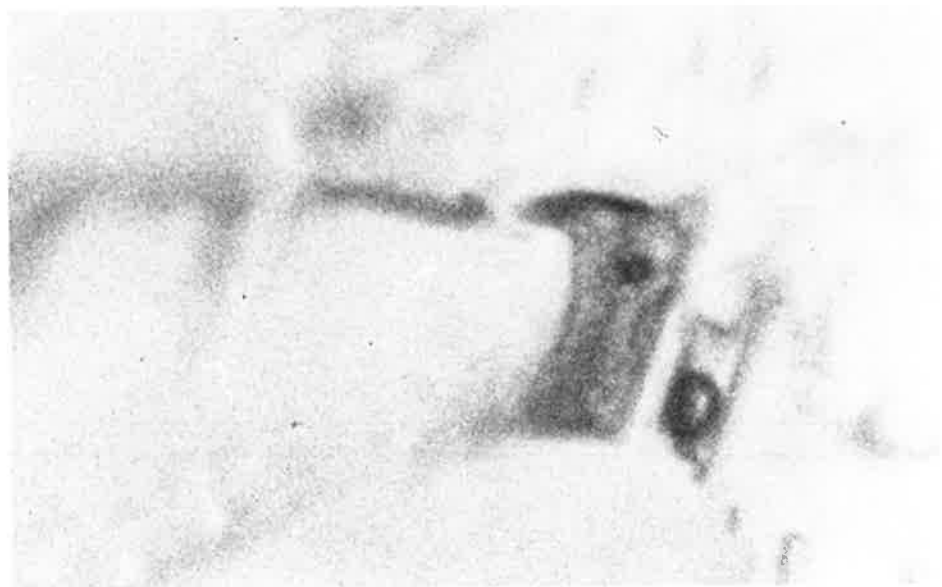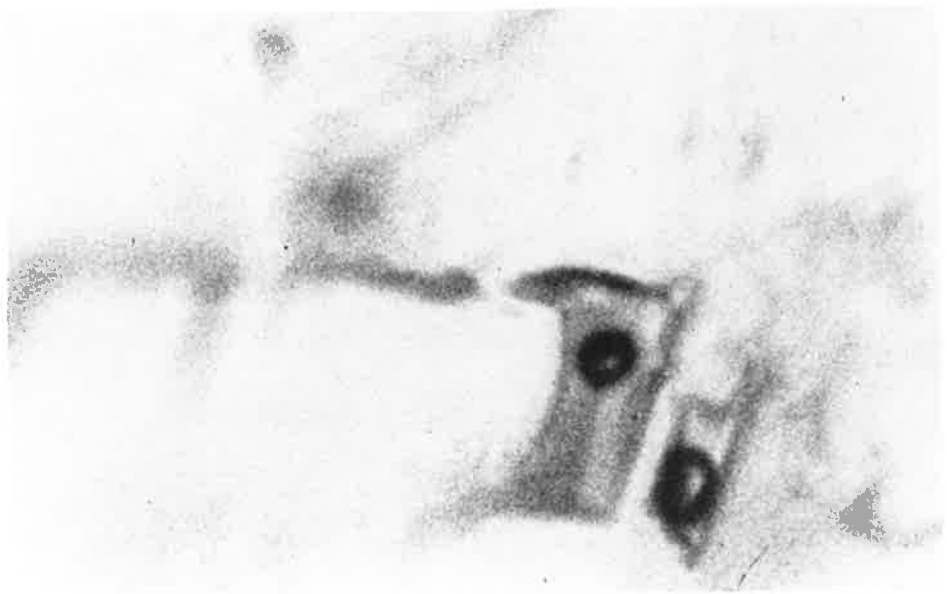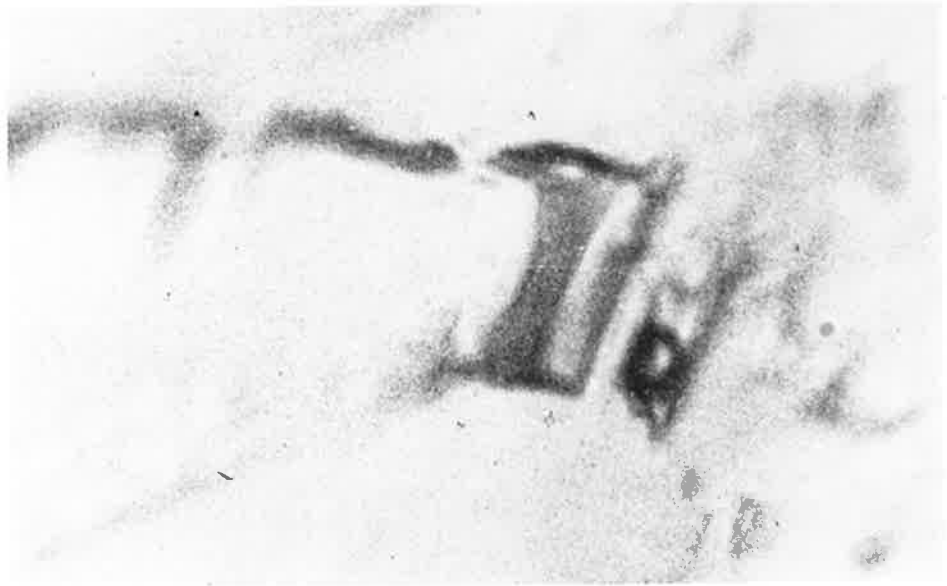
5.3.2.1   Cooling

Cooling of fluid inclusions is carried out until part or all of the contents freeze. A marked undercooling is generally necessary to bring about freezing of liquids, liquefaction of gases or vapour bubble nucleation in liquids. Phase transition temperatures are then recorded as the inclusion is heated. These transitions are often difficult to observe, being little more than a slight increase in granularity or a slight increase in tonal colour.

(a)   First Melt (Eutectic = T_e)

Observation of the first melting temperature of the fluid inclusion gives the eutectic melting temperature (hereafter referred to as T_e) and is due to the solution for one or more components in the system. Fig. 48 shows the system $NaCl-H_2O$ which has a T_e of -21.1^oC. The depression of the eutectic below -21.1^oC indicates the presence of other soluble salts such as $CaCl_2$ and $MgCl_2$ which have eutectics of -49.8^oC and -33.6^oC respectively, or multi-component solutions such as $NaCl+CaCl_2+KCl$ (T_e of -10.6^oC). Such mixtures can depress the eutectic lower than the temperatures of the individual components e.g. $56\%NaCl+22.75\%MgCl_2$ has an eutectic of -35^oC (Crawford, 1981) which could also be interpreted as solely due to $CaCl_2$.

The fluid may also contain an immiscible phases such as CO_2 (freezing point of -56.6^oC) or CH_4 (freezing point of -182.5^oC) (Weast, 1974; Kreulen; 1980; Bussink et al., 1984). Fortunately, immiscible phases are frequently observed optically during microscopy at room temperature, but this is not sufficient to identify the nature of the immiscible phases. In H_2O - salt systems at moderate to high temperatures and low pressure and also in H_2O - carbonic species systems at low to moderate temperatures it is likely that fluid
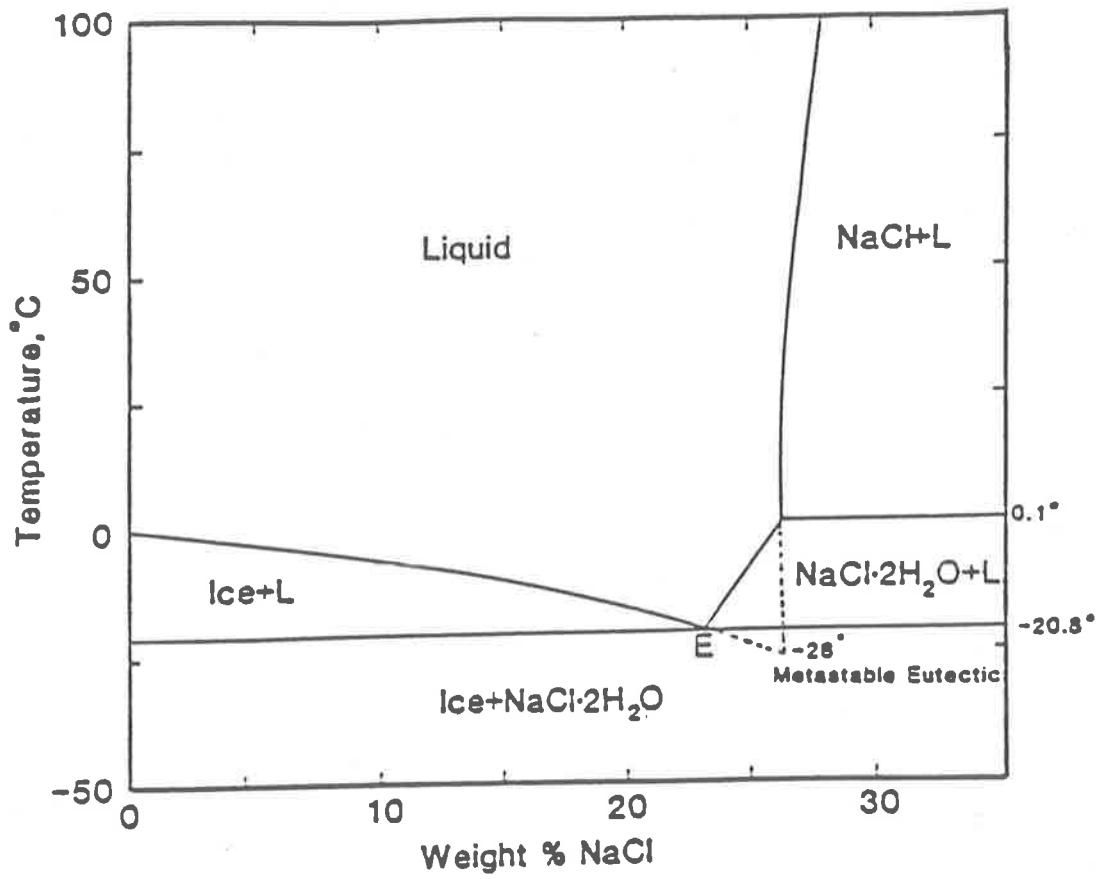
Fig. 48: NaCl-H$_2$O system, temperature -
composition diagram at 1 bar. All phases
coexist with vapour.

(Crawford, 1981)

immiscibility will exist. Fluid immiscibilty is the equivalent of a stable mechanical mixture solution which is not the same as a homogeneous chemical (mixture) solution, or as it is more usually referred to as - a homogeneous solution. So, care is needed when talking about "unmixing". Although unmixing usually results from fluid immiscibilty when temperature and/or pressure is lowered, there are other causative parameters to be considered, e.g. boiling, or mixing of fluids of different origin.

(b) Last Melt (T_f)

This is the temperature at which all the fluid in the fluid inclusion has melted. It is this temperature that is usually reported in the literature, and also from which salinities are calculated. The salinity is reported as a wt. equivalent of the either known or most likely solute component within the fluid e.g. NaCl or $CaCl_2$.

Normally fluid salinities can be estimated by one of three alternative methods, which are mutually exclusive.

(a) The equivalent salinities of fluid inclusions containing halite as a daughter mineral can be obtained from the temperature of dissolution of the halite, upon heating, using the halite solubility data of Keevil (1942) and Potter et al. (1977).

(b) Freezing point depression temperatures i.e. T_f furnishes the appropriate salinity for those fluid inclusions that do not contain either daughter minerals or clathrates, using the data of Potter (1978).

(c) Where a clathrate (or hydrate) forms on heating from the frozen state, then the melting temperature of this clathrate can give a rough estimate providing that CH_4 is not also a component or there is any other component present that forms a clathrate with H_2O.

As can be seen in Fig. 48, in NaCl brines with salinities greater
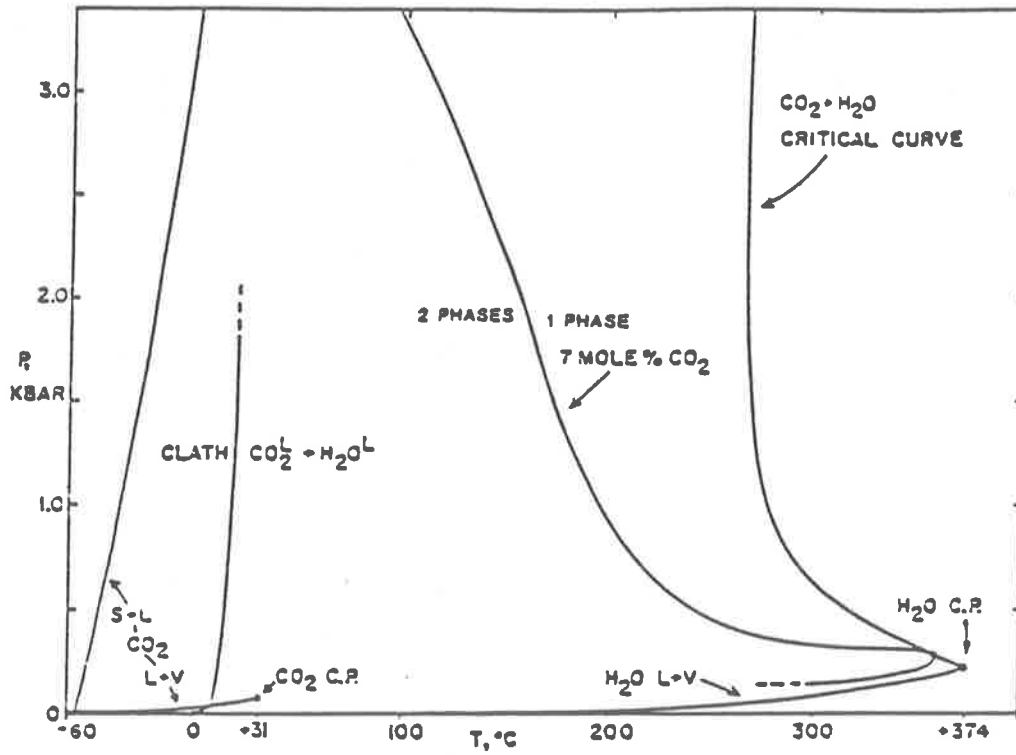
Fig. 49: Phase equilibria in the CO_2-H_2O system.
The high pressure clathrate stability curve
(clathrate + CO_2 - rich liquid + H_2O - rich
liquid) is unknown above 1.8 Kbar.

(Burruss, 1981)

than 26.3 wt.%, NaCl.2H$_2$O melts incongruently to NaCl and liquid. This requires that a distinction can be made between ice and NaCl.2H$_2$O. The latter melts as a fine grained aggregate, whereas ice crystals tend to recrystallise to a few large chunks during heating (Crawford, 1981). Fortunately there is a fairly marked contrast in the refractive indices of ice and the hydrates. Other metastability problems are discussed by Roedder (1967, 1971, 1976).

(c) Condensation of Volatiles

Another problem of freezing temperature interpretation arises when the fluids contain components that can form clathrate hydrates (commonly called simply "clathrates"). Clathrates consist of a group of solids in which water is structured around a molecule which at atmospheric temperature and pressure is in the gas phase. Within these compounds there can be a number of different small molecules, usually gases, which are bounded by polyhedral ice-like lattices of water molecules (Burruss, 1981). The clathrates formed from CO_2 and $CH4_2$ are the ones of most interest in fluid inclusion studies. Fig. 49 shows the CO_2 - H_2O clathrate equilibria in the pure system. The phase equilibria will be dependent upon clathrate solid solution, and other components soluble in water. A solid solution of CO_2 and CH_4 will melt at temperatures below those of the pure components, when the pressure is kept constant. The melting temperature is also determined by the salinity of the aqueous solution, e.g. a one molar NaCl solution melts approximately 2°C lower than that in equilibrium with pure water at a given pressure (Larson, 1956; Bozzo et al., 1973). Thus Burruss (1981) points out that the addition of both CH_4 and NaCl, or a similar solute, could affect the equilibria in the erstwhile pure CO_2 - H_2O system to the same degree, as interpreted by the observation of the melting of the appropriate clathrate. Burruss (1981) gives the example of "if CH_4 approximately 30% in the CO2 - rich gas phase, the clathrate in the NaCl free system

232
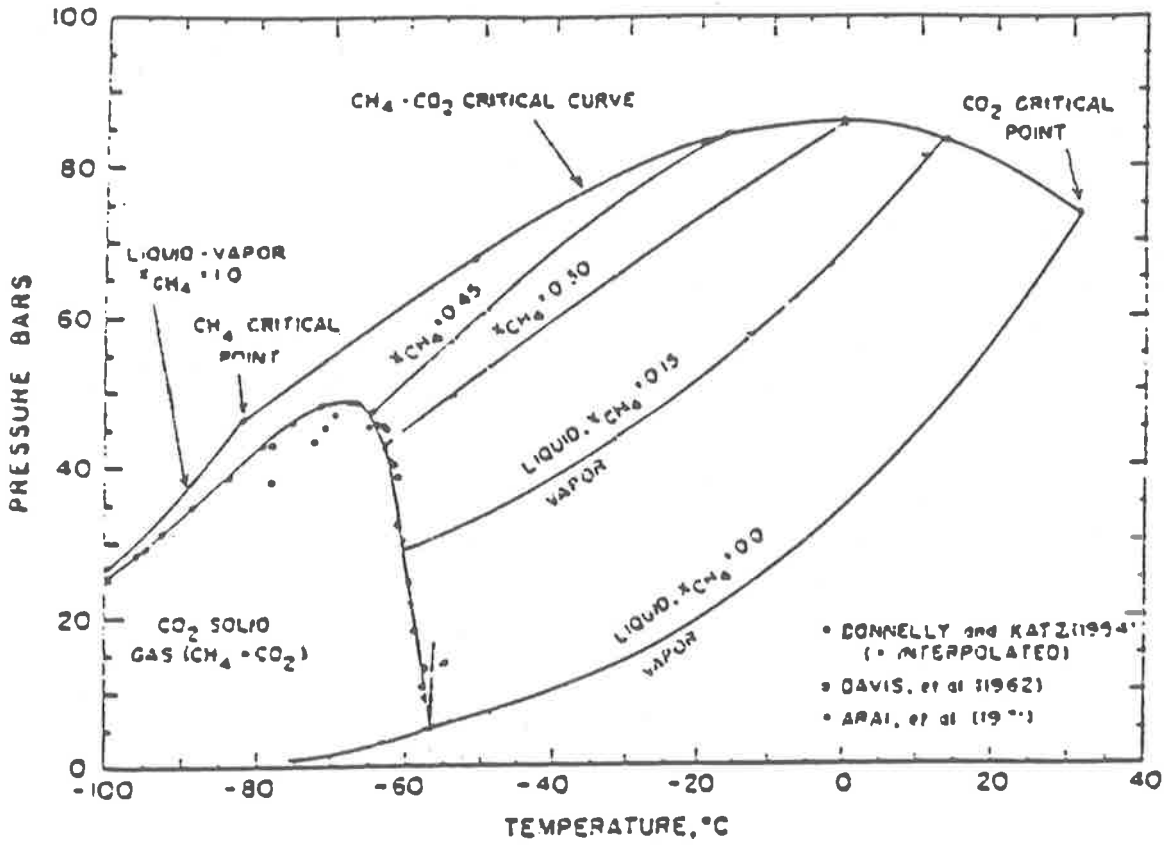
Fig. 50: Experimentally observed P,T phase equilibria for the system CO_2-CH_4.

(Burruss, 1981)

melts at approximately +12°C, equivalent to the invariant point (d).
(Fig. 3.12). However, in the presence of an aqueous phase with 6% wt.
NaCl, the invariant point would shift to approximately +10°C, the same
as that for the pure CO_2 clathrate in equilibrium with pure H2O". So
what can be stated categorically is that if a shift occurs in the melting
temperature of the clathrate from the invariant point of +10°C, then
the fluid must contain an additional component, or in other words,
reproducible deviations from known binary system transitions indicate the
presence of one or more additional components. Pure methane clathrate is
stable up to +24°C (Roedder, 1963). The presence of CO_2 and CH_4
phases in a fluid is not an unusual situation and can be brought about by
a number of geological processes. Luckscheiter and Morteani (1980)
report that CH_4 can be formed by thermochemical reactions. They also
suggest that the solubility of a salt in a brine is reduced as the
fluid's CO_2 content increases, whilst Pichavant et al. (1982) discuss
the extremely low mutual solubility of CO_2 and NaCl. Possible sources
of CO_2 are -

(a) decarbonation reactions within carbonates.

(b) oxidation of organic matter during metamorphism or radiolysis.

(c) deep seated origin e.g. degassing of the mantle.

(d) reactions such as - $CO_2 + 4H_2 = 2H_2O + CH_4$. High pressure
drives the reaction towards CH_4, low temperature towards CO_2.

The formation of the clathrate also affects the salinity of the
residual liquid phase, thus giving a misleading T_f. As the liquid
phase usually melts before the clathrate, the salinity figure will need
to be corrected to accomodate for the amount of H_2O tied to the
clathrate molecule (Hollister and Burruss, 1976; Weisbrod et al., 1976;
Swanenberg, 1980). Collins (1979) discusses the aspects of the system
$H_2O - CO_2 - NaCl$, which can be further extended to include $CaCl_2$.
CO_2 has the ability to form mixed clathrates with other gases, which
may be present in optically indectable amounts. The mixed clathrates may

a.   The fluid inclusion in the centre of the field of view shows the
       behaviour expected of a liquid-vapour type, whilst that 10 m to
       the right, to all appearances the same type, did not alter during
       the freezing runs. Photo taken at $-85^{O}C$. A small fluid
       inclusion in the upper left is ice only at this temperature.
       Sample WM1, Mt. Minza. (main fluid inclusion is approx. 12 m in
       length).

b.   Photo taken at $-125^{O}C$.

c.   After allowing to warm, those fluid inclusions that had frozen
       have melted. The dark daughter mineral is a bright orange
       hexagon-probably hematite. Photo taken at $-5^{O}C$.
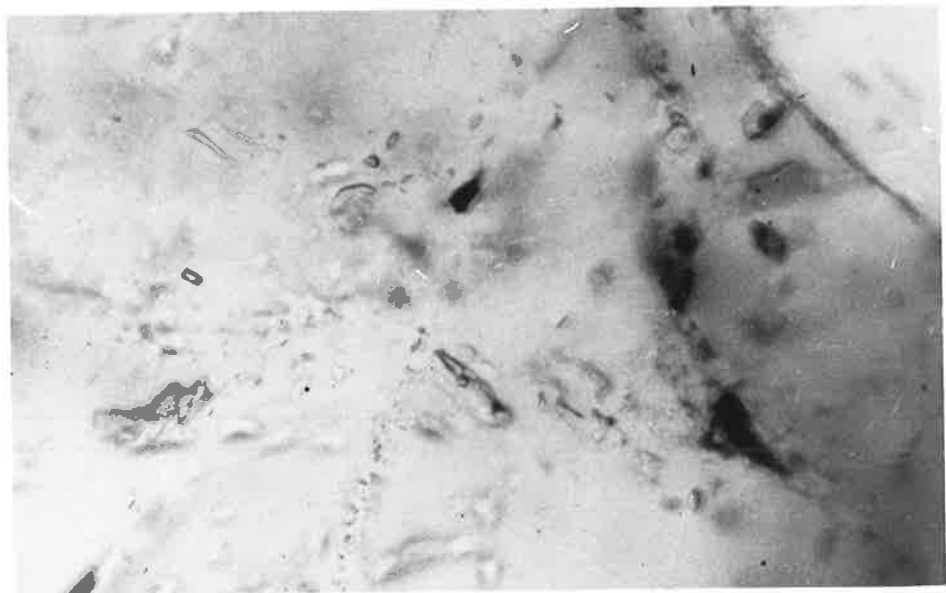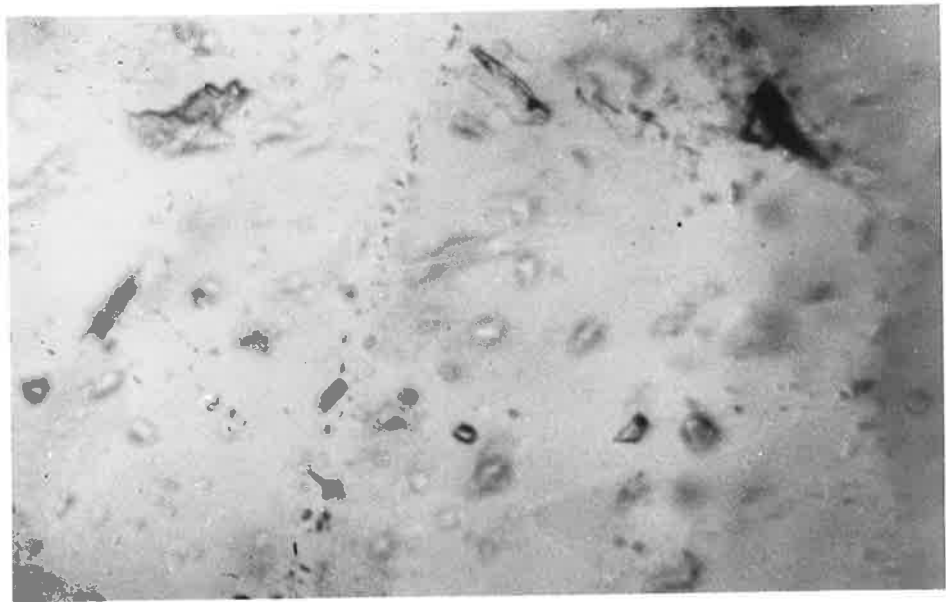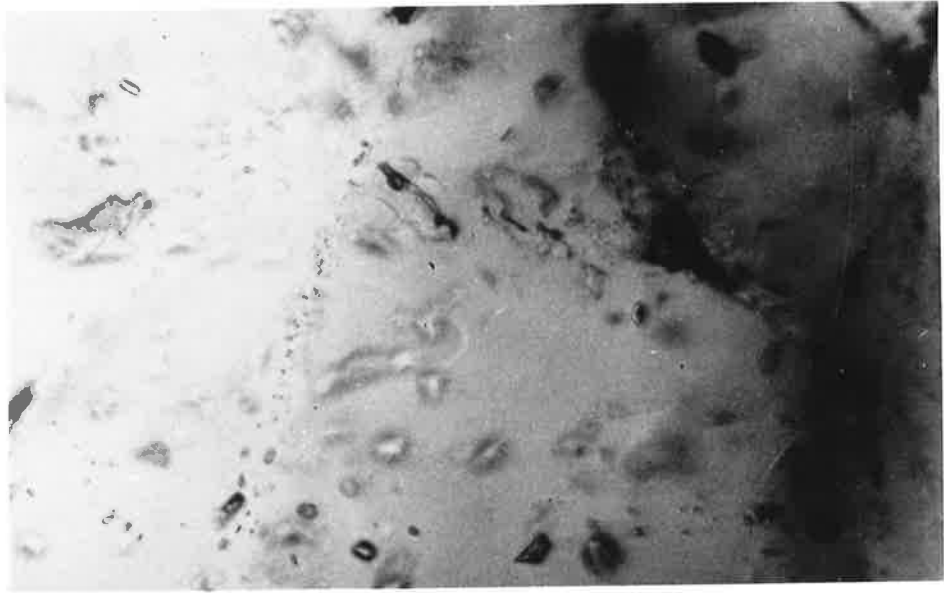
then only be suspected / detected by the melting temperature of the clathrate. Nevertheless, even these small volumes can invalidate the use of phase transition temperatures of the presumed pure clathrate e.g. $CO_2.5.75H_2O$ to calculate the NaCl equivalent salinity, because the shift will be masked by the opposite shift caused by the addition of any other salt to the hydrous phase.

5.3.2.2   Heating

The homogenisation temperature (hereafter referred to as T_h) is the temperature at which one of the fluid phases disappears and the inclusion becomes homogeneous with regard to the fluid phases, when heated. In the case of brines which have nucleated a daughter mineral(s), this may occur either before or after dissolution of the soluble salt.

When the inclusion contains two distinct fluid phases, there are three possible behaviours:-

(a) disappearance of one liquid phase due to its decrease in volume.

(b) disappearance of vapour phase due to its decrease in volume.

(c) sudden disappearance of the phase boundary (meniscus) due to the occurence of critical phenomena.

Where T_h is into the vapour phase in some fluid inclusions in the sample and is into the liquid phase in other fluid inclusions of the same type within the same sample, and this occurs at approximately the same temperature, then it is indicated that the original trapped fluid was on a L-V curve, i.e. boiling point curve.

The observed T_h often needs to be corrected for pressure effects (Klevstov and Lemmlein, 1959; Samoylvich and Ketchikow, 1968). Pressure corrections need to be applied in all instances where T_h occurs in one phase only (Potter, 1977). In this study no pressure corrections were

applied as at the obtained temperatures corrections would be minimal because of the high density of the fluids, notwithstanding the fact that slightly different corrections for different salinities and different CO_2 content would apply.

Critical phenomena, i.e. homogenisation at the critical point, is of limited use as a pressure calibration point because of the uncertainty of chemical composition, especially considering the prevalence of multi-component systems. Besides the use already mentioned, the critical temperature is helful in the identification of densities for pure CO_2. Or to put it another way, critical phenomena (homogenisation) close to $31.1^{\circ}C$ indicates that CO_2 is the dominant component of a CO_2 - rich phase. A range of temperatures indicates a range of CO_2 densities (Collins, 1981). Where there is a CH_4 component as suggested by a depression of the CO_2 eutectic, then critical phenomena can be significant in estimating the CH_4 concentration (Fig. 50, Hollister and Burruss, 1976).

Other phenomena observed whilst heating have already been discussed e.g. dissolution of volatiles, whilst that of decrepitation i.e.the fracturing of the fluid inclusion due to increased internal pressure and the dissolution of solids will be discussed under the heading of daughter minerals.

5.3.2.3   Daughter Minerals

Another salinity fingerprint can be obtained by the observation of the behaviour of daughter minerals. Daughter minerals are products of saturation due to pressure and temperature changes. Other enclosed solids, such as ice, clathrates etc., are products of phase changes of one or more fluids. The presence of a daughter mineral per definition implies that its components were present as dissolved constituents in the

a.   (at left) A group of fluid inclusions, of apparently similar

        type (i.e. liquid-vapour phase type) photographed at -30°C

        whilst cooling. Mineral is magnesite.

b.   (at right) Photographed at -50°C, whilst cooling.

c.   (at left) Photographed at -85°C, whilst cooling.

d.   (at right) Photographed at -43°C, whilst warming. The ice in

        many fluid inclusions has already passed T_F, indicating highly

        saline, mixed - chloride brines. Sample WC1, Woodcutters

        Prospect. (largest fluid inclusion approx. 15 μm in length).
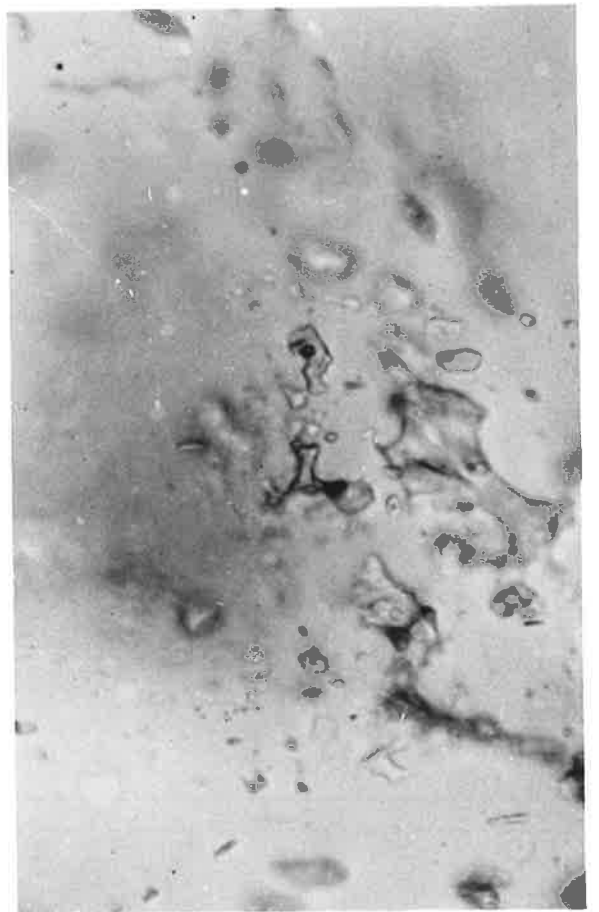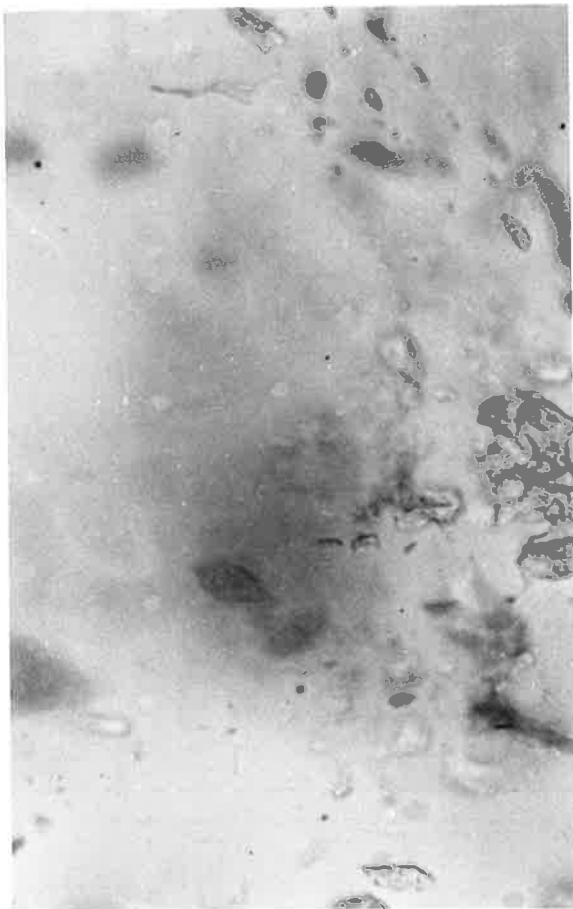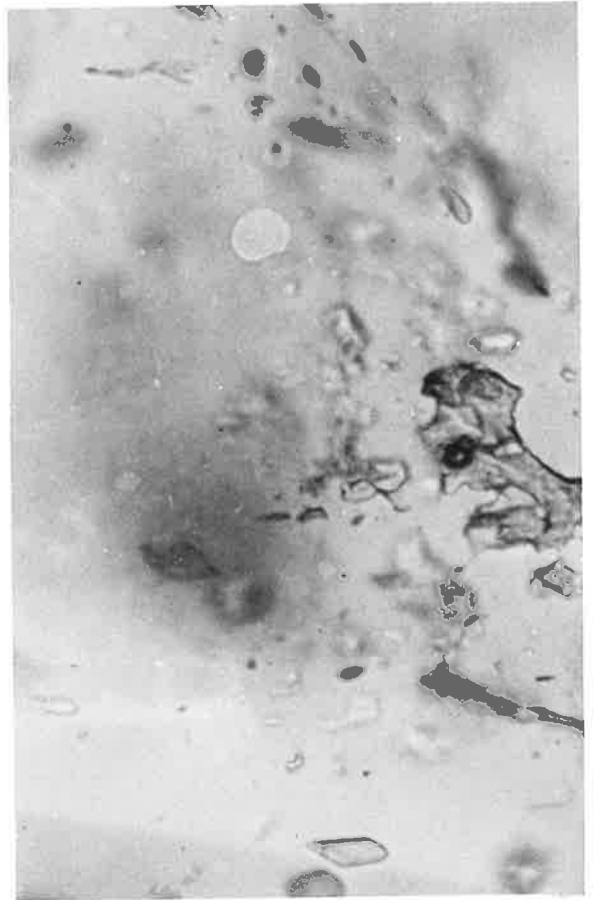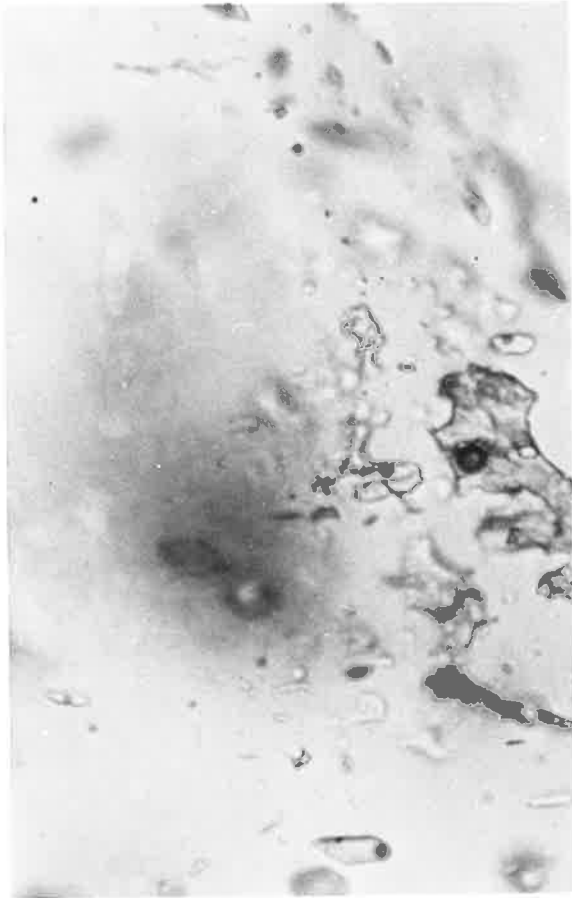
fluid inclusion at the time of entrapment (Metzser, 1977).

The simplest interpretation involves the temperature and rate of dissolution of the daughter mineral upon heating. The problem becomes more complex within multi - component systems, e.g. when a NaCl crystal is the sole daughter mineral present the salinity determined from its dissolution temperature can be grossly misleading if no heed is paid to T_e and T_f because a brine containing up to 30 wt. % $CaCl_2$ and less than 5 wt. % NaCl will nucleate only a NaCl daughter mineral. Without referring to the T_e the presence of the $CaCl_2$ would not be suspected. T_f in the presence of a daughter mineral gives only the minimum salinity (Larsen et al., 1973; Bodnar and Bethke, 1981; Leroy, 1979).

In a saturated boiling solution, the lowest melting temperature of a daughter mineral (T_s) is usually in the same range as the average homogenisation temperature (Pichavant et al. 1982). This finding disagrees with Chivas and Wilkins (1977) and Eastoe (1978) who quote daughter minerals as giving evidence of fluid unmixing for undersaturated fluids.

The solubility of NaCl in water vapour is so low compared to its solubility in water that inclusions homogenising into a vapour phase should show dissolution of a NaCl daughter mineral before T_h is reached. Chivas and Wilkins (1977) found that within cases where higher values for T_s were obtained, this discrepancy disappears with time until eventually the two temperatures co-incide (the section needs to be held at temperature for up to three hours).

The dissolution of the daughter mineral does not always occur prior to decrepitation (hereafter referred to as T_{de}) of the inclusion. When there is a range of homogenisation temperatures within the same field of

view, rupturing of the lower T_h fluid inclusions sometimes occurs prior to reaching T_h of the higher temperature fluid inclusions., thus precluding repeat runs on all the inclusions. As NaCl decreases the vapour pressure of the H_2O, one may expect higher T_{de} for brine rich inclusions. Decrepitation occurs annoyingly often in fluid inclusions in host minerals that exhibit good cleavage e.g. carbonates (not only for those containing daughter minerals). However, where repetition was possible, the reproducibility of the results was satisfactory.

The literature contains ubiquitous references to unidentified daughter minerals. Unfortunately this work does not break this pattern.

Because of their very small size and also because of optical distortion due to change in medium i.e. fluid inclusion brine, daughter mineral and host mineral both below and above the fluid inclusion, it is difficult if not impossible to make definitive identifications using only the petrographic microscope. Certainly it is a useful tool to allow possible suggestions (Eadington and Wilkins, 1980) but usually one cannot even decide whether the daughter mineral is isotropic or anisotropic; cubic or hexagonal in outline! So, one is confronted with the problem of not even being able to differentiate between the two most commonly expected groups - the chlorides and the carbonates.

The dissolution temperature of true daughter minerals is one method of differentiating between these two groups, e.g. sylivite dissolves at temperatures up to $100^0 - 110^0C$ whereas halite has a much smaller temperature coefficient of solubility and can persist until quite high temperatures, but still ambiguities arise due to differing pressures, temperatures and densities at the time of entrapment, and also due to the actual brine components.

It sometimes happens that T_h occurs before dissolution of the

Fig. 51 Daughter mineral dissolution T-°C   RUM JUNGLE

BALC (m)   [?]   [?] DECREP.
                                              AT 330°C

150°   409
[145]   →
[340]   [237]   [253]
DIO (Q)

BR4 (m)   [152]

                        [197]
E28A (m)   [184] [200][198]   [186]

[97]   E40(Q)

        E24(m)   [155]

NOTE: C43(Q) DISS AT 60.0, 82.7, 86.8 & 88.6, 77.0
                       (119) (102) (117)   (116) (115)

[171][182][175] C80(Q)

132.9
[143]   C64(m)   [198]   [118] BOTH IN   [140]
                               [140] ← SAME F.I. →

  C32(m)   [260] [210][214]   [?]   [152]
160   200   250   300   350

(T$_H$ of fluid inclusion indicated thus — [118])
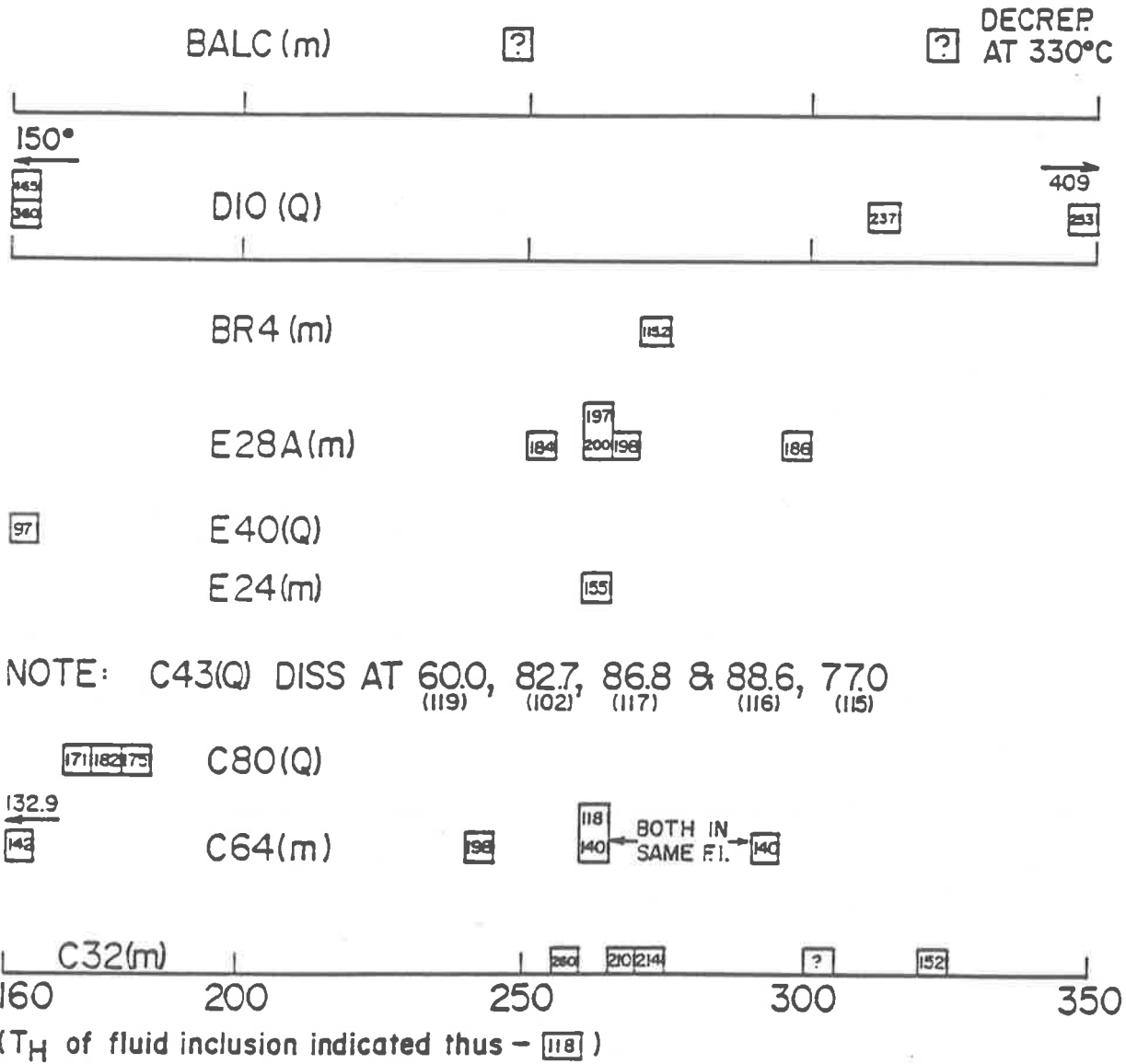
daughter mineral. Indeed, in this study, this was the rule rather than the exception (Fig. 51), suggesting that the brines consist of highly saline and dense solutions. "Under these circumstances, the liquid - vapour - homogenisation occurs along a univariant line (solid - liquid - vapour) in the phase diagram and disappearance of the solid occurs in the divariant liquid - solid field at a point determined by the composition and specific volume of the fluid" (Crawford, 1980). Thus, it is seen in samples D10 (quartz), BR4 (magnesite), E28A (magnesite), E40 (magnesite), C64 (magnesite) and C32 (magnesite) where this is the case (Fig. 51) the actual fluid inclusion data indicates highly saline brines in all cases, even where there is evidence of a low salinity brine in the same system i.e. same sample e.g. BR4.

Not all true daughter minerals will dissolve upon heating : irreversible changes may have taken place since entrapment. These may be related to the ability of H^+ ions to diffuse through the crystal lattice. Another possibility for the lack of dissolution of daughter minerals is that a volume change of the section of inclusion containing the daughter mineral has occurred due to necking down (Fig. 52). Some supposedly daughter minerals may well be due to the entrapment of solid particles that were already in the fluid.

A number of the fluid inclusions containing true daughter minerals contain hematite as the daughter mineral or as one of those present (Plate 35). As the size of the hematite daughter mineral is positively correlated with the size of the fluid inclusion, it is suggested that chemical changes have occurred within the fluid inclusion post entrapment that this is not a case of fortuitous entrapment of a pre-existing solid particle. Formation of hematite would be brought about by an increase in oxygen fugacity within the fluid inclusion.

Dubessy et al. (1980) report evidence for the presence of free H^+ and also in some cases free O^{2-} amongst the volatile components in
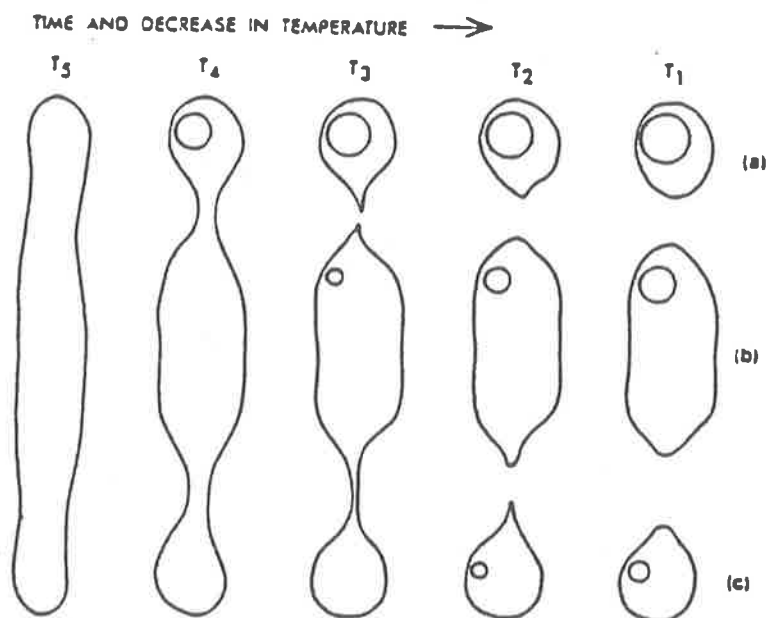
Fig. 52: Necking down of fluid inclusions - a common phenomenom in carbonates. The original fluid inclusion, trapped at temperature T_5, breaks up during slow cooling to form three separate fluid inclusions (a), (b) and (c). During microthermometric tests, (a) would homogenise above T_5, (b) above T_3 and (c) between T_2 and T_3.

(Roedder, 1981)

fluid inclusions in quartz at both the Oklo Deposit (Gabon) and the Rabbit Lake Deposit (Canada), formed by the radiolysis of H_2O and/or organic material. If, as they suggest, this H_2 has been present since the Precambrian, then it would seem that the diffusion rate is extraordinarily slow. If this process is responsible for the post entrapment formation of the hematite daughter minerals seen at Rum Jungle, then one would expect that there would not be as many present in the magnesite as in the quartz, due to differing diffusion rates due to different lattice structures. This is not the case. They appear with apparent lack of host mineral control e.g. Crater Formation quartz and Mt. Fitch magnesite.

The daughter minerals in individual samples will be discussed in the treatment of individual areas.

5.3.3 Destructive Methods

As the aim is to obtain quantitative and qualitative information on all the phases present, most of the destructive methods involve the extraction of the contents of the inclusions. The pursuit of this aim is fraught with difficulties. It is rare that the host minerals contains fluid inclusions of one type only, so that any bulk crushing and leaching method will provide a liquid that represents a mix of all the fluid inclusions from that particular sample; without the ability to ascertain the ratio of the mix. Consequently, analyses of bulk extraction fluids gives at best qualitative data, and not necessarily comprehensive at that. The experimental work of Savel'yeva and Naumov (1979) showed that discrepancies arising in analyses result from the breaking of the inclusion during grinding, and they consequently recommend the decrepitation method. The use of the fluid from one inclusion only in order to eliminate some of these problems is precluded by the fact that the average fluid inclusion has a mass of approximately 10^{-11}gms. Another

inherent danger is the ease of contamination, and its greatly magnified affect on such small volumes.

If however the method is employed, then there are a number of analytical options available, such as standard chemical techniques (Roedder, 1967; Eadington, 1979), gas chromatography (Ypma, 1979; Cuney et al., 1976; Behar and Pineau, 1979; Kreulen and Schuiling, 1982; Bussink et al., 1984), inductively coupled plasma atomic emission spectroscopy (Thompson et al., 1980; Rankin et al., 1982; Alderton et al., 1982) or neutron activation analysis (Touray, 1976; Grappin et al., 1979; Luckscheiter and Parckh, 1979). Rankin et al. (1982) used I.C.P. to obtain multi-element data on fluids by collecting the fluid ejected from the fluid inclusion when it decrepitated upon heating. Their work was particularly centred upon uranium : carbon ratios in fluid inclusion brines in granites, but could well have potential as an uranium exploration tool, by placing the emphasise on other ratios e.g. U:Th. There is very likely a difference in the ratios of decrepitate derived sample and the actual fluid inclusion brine due to probable biased losses due to volatilisation.

It is hoped that the focused microbeam technique currently being employed and assessed will prove consistently successful. Tsui and Holland (1979) and Bennett and Grant (1980) report success on large inclusions using the laser microprobe, whilst Deboule and Eloy (1982) have improved the technique and are using it for the chemical analysis of fluid inclusions in ores. Eadington (1974) and Ypma and Fuzikawa (1980) employed electron microprobe and S.E.M. techniques successfully, especially on daughter minerals, whilst Nambu et al.'s (1980) work on using the ion microprobe on frozen samples looks exciting. In this study an attempt was made to deliberately cause sample damage using the focused beam of the electron microprobe, and as the fluid inclusion shattered, to instantly record qualitative data using the EDAX Energy Dispersive

System. One of the problems with this technique is the inability to obtain meaningful numbers for any of the elements that are a stoichiometric component of the host mineral, but fortunately, quartz and magnesite from the same rock usually contain the same fluid inclusion types, so that both minerals can be used and compared.

The most comprehensive paper on the use of fluid inclusions in mineralised areas is Roedder's (1977) "Fluid Inclusions as Tools in Mineral Exploration".

The results from the fluid inclusion study will be discussed in the following chapter.
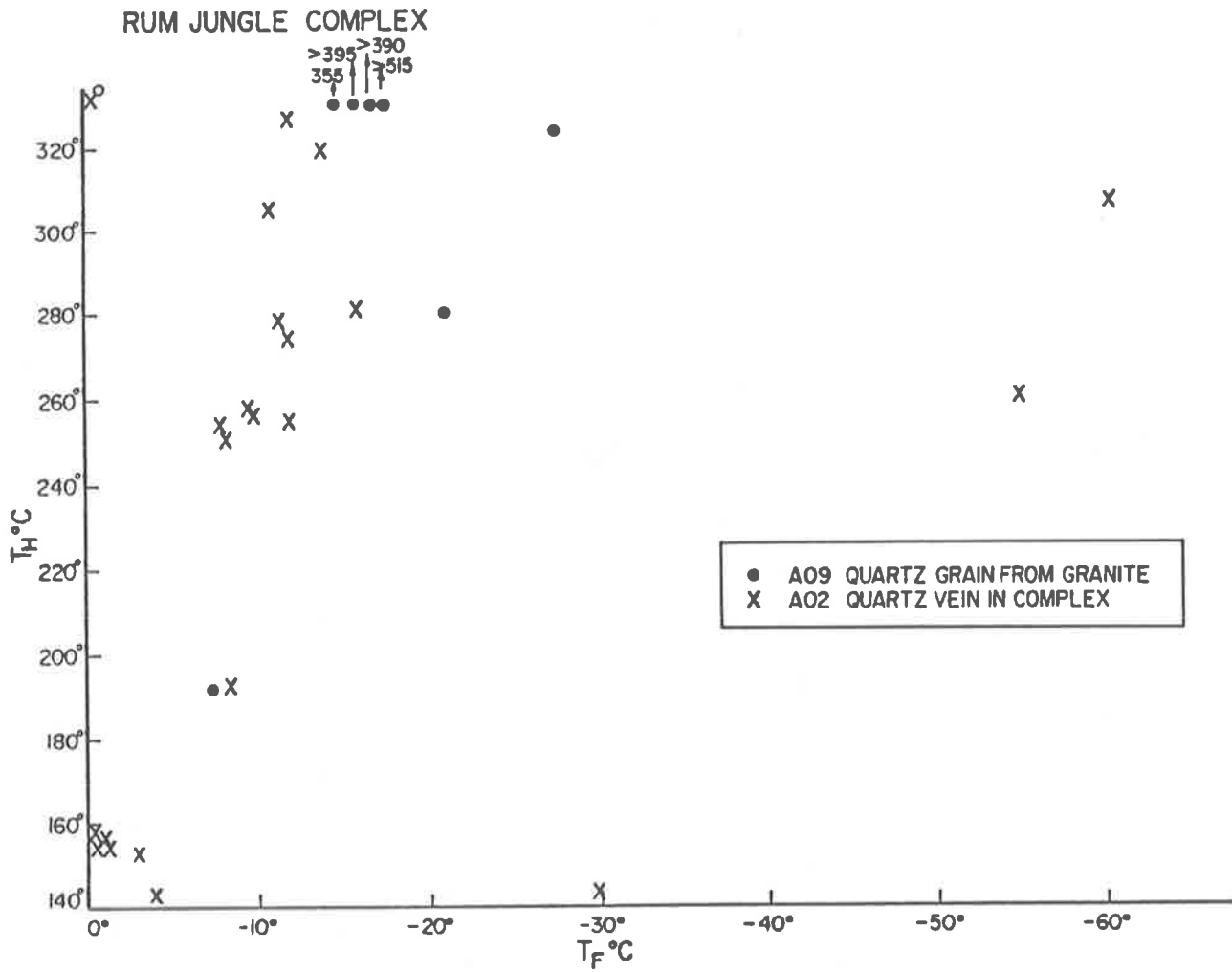
Fig. 54: Homogenisation temperature vs Final melting temperature.

CHAPTER 6

FLUID INCLUSION STUDIES - INDIVIDUAL AREAS

6.1 Introduction

The following individual areas were sampled and studied E.L.1349, Mt.
Fitch Deposit, Dyson's Deposit, White's Deposit, Intermediate Deposit,
Brown's Deposit, Mt. Minza Prospect and Woodcutters Prospect.
(Fig. 1). Within E.L. 1349, material from the Rum Jungle Complex,
Beestons Formation, Celia Dolomite, Crater Formation and Coomalie Dolomite
was studied; whereas for all the other areas the Coomalie Dolomite was
the selected target, including quartz associated with the Coomalie
Dolomite's magnesite or the Formation immediately overlying the Coomalie
Dolomite. The other two areas that were selected for reasons of
comparison were Balcanoona, S.A. (Fig. 3) and Kharidunga, Nepal (Fig.
53). All fluid inclusions studied and data obtained are shown in Appendix
1.

6.2 E.L. 1349

Fig. 7 shows the location and stratigraphy of E.L. 1349 and the
sample locations.

6.2.1 Rum Jungle Complex

Only two quartz samples were chosen for study from this area, as the
data is peripheral to the major problems being investigated.

Sample A09 was chosen as being representative of the granitoids.
Sample A02 was from one of the typical quartz-tourmaline veins that cut
the Complex, particularly the eastern margin.
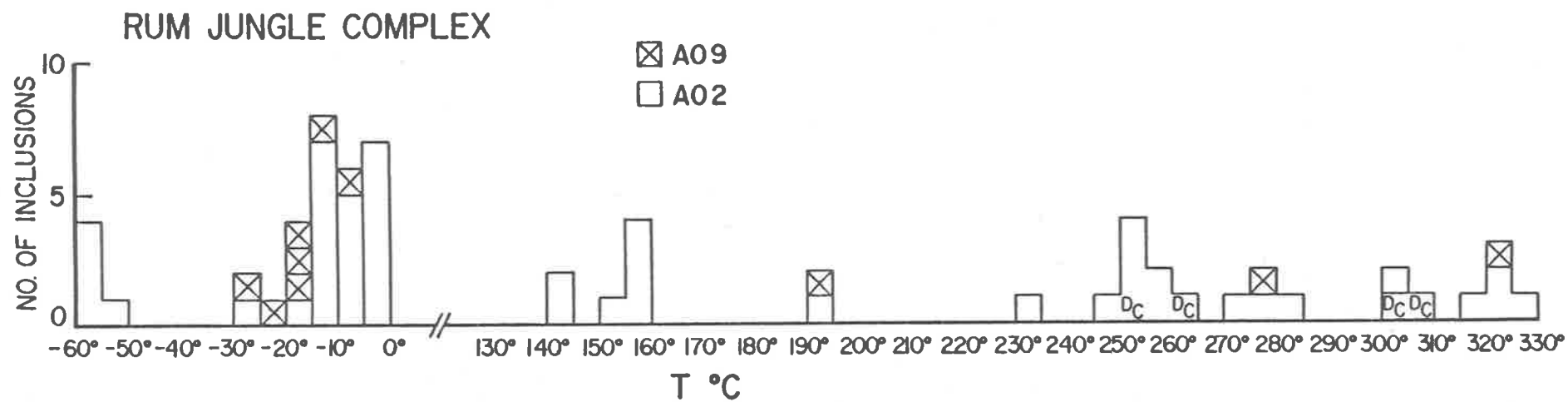
Fig. 55: Histograms of final melting and homogenisation temperatures.

Fig. 54 is a plot of the homogenisation temperatures against melting temperatures from fluid inclusions, whilst Fig. 55 shows all the temperatures obtained. Several types of brine are present; a low temperature - very low salinity brine; a medium - to - high temperature - more saline brine probably containing $CaCl_2$ and possibly a low - to - medium - low salinity brine. All brines have a CO_2 component, but it is not always visible.

Many of the fluid inclusions contain one or more daughter minerals, including some of the fluid inclusions that contained a CO_2 phase. One fluid inclusion had a hematite daughter mineral, whilst in many inclusions in sample AO2 the fluid turned an orange colour upon heating, suggesting that they contained a $FeCl_2$ component in the brine.

In both samples there are many fluid inclusions with a liquid phase only present.

6.2.2 Beestons Formation

Sample BO9, a banded quartz-tourmaline rock (Plate 28), was selected to see whether it was closely related to sample AO2, the quartz tourmaline vein rock from within the Rum Jungle Complex. It would appear that the quartz in sample BO9 crystallized from a different brine than that in sample AO2 although they do have some similarities e.g. CO_2 phases, and hematite daughter minerals. Many fluid inclusions contained a liquid phase only, but upon melting (after freezing) they developed a vapour phase which showed rapid Brownian movement at room temperature. There is an inverse relationship between salinity and temperature (Fig. 56). Seven of the 9 melting temperature figures indicate a highly saline brine, with likely $CaCl_2$ and $MgCl_2$ components (Fig. 57).

254

BEESTONS FORMATION
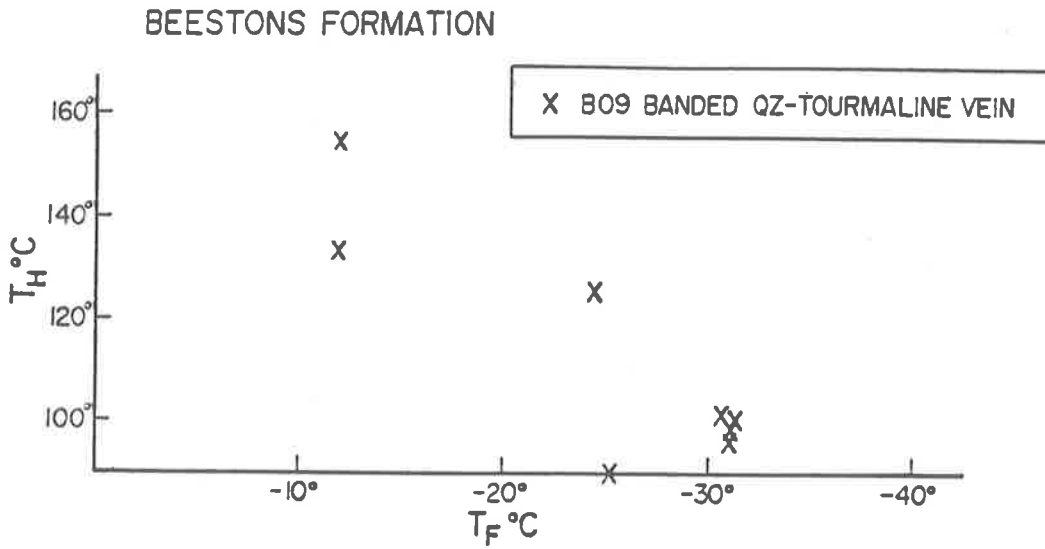
Fig. 56: Homogenisation temperature vs Final melting temperature.
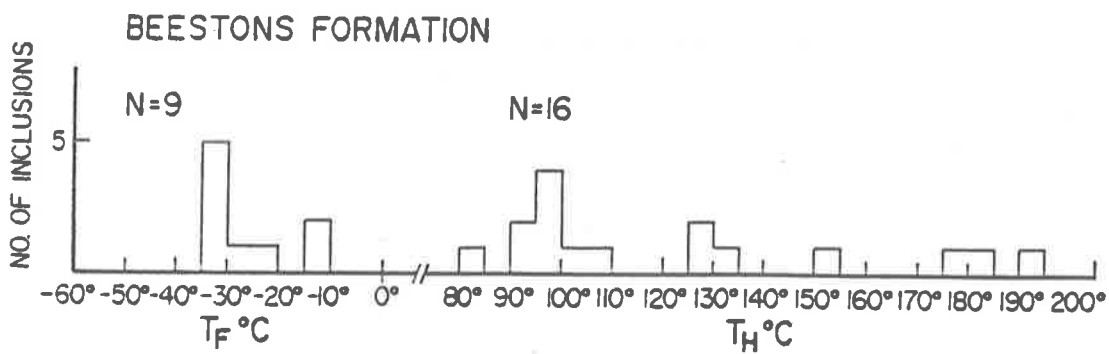
Fig. 57: Histograms of final melting and homogenisation temperatures.

6.2.3 Celia Dolomite

18 samples were selected from within the Celia Dolomite. 9 of these were magnesite; the other 9 were quartz.

6.2.3.1 Magnesite samples (Fig. 28):

C09 :- this sample shows bladed form morphology. It has arc like trails of small fluid inclusions cutting across the cleavage. There is a definite relationship between salinity and temperature (Fig. 59). There were many negative crystal type fluid inclusions with CO_2 phases (Plate 34, Fig. 60).

C27 :- this sample has large rhombs within a finer rhomb-type matrix. The fluid inclusions in the section studied in detail looked like primary fluid inclusions (Appendix 2), whereas in other sections where the fluid inclusions were clearly related to cleavage, and thus of a secondary nature, homogenisation temperatures were overall much lower. None of the fluid inclusions froze, indicating that the brine was probably highly saline (Fig. 61).

C28 :- this sample has both forms intimately associated. Some of the fluid inclusions contain daughter minerals, none of which dissolved upon heating. None of the fluid inclusions froze, indicating that the brine was probably highly saline (Fig. 61).

C32 :- this sample contains both forms. Of the 16 fluid inclusions studied, freezing was only achieved in three (Fig. 61). This observation plus the low final melting points of these three, suggests highly saline $CaCl_2$-rich brines. Many of the fluid inclusions contain one or more daughter minerals, only some of which dissolved prior to decrepitation (Fig. 51). The shape and anisotropy of these daughter minerals suggested that they were carbonates.

Some of the fluid inclusions behaved quite differently with each temperature cycle. C32A (Appendix 2) is an example of such behaviour:-
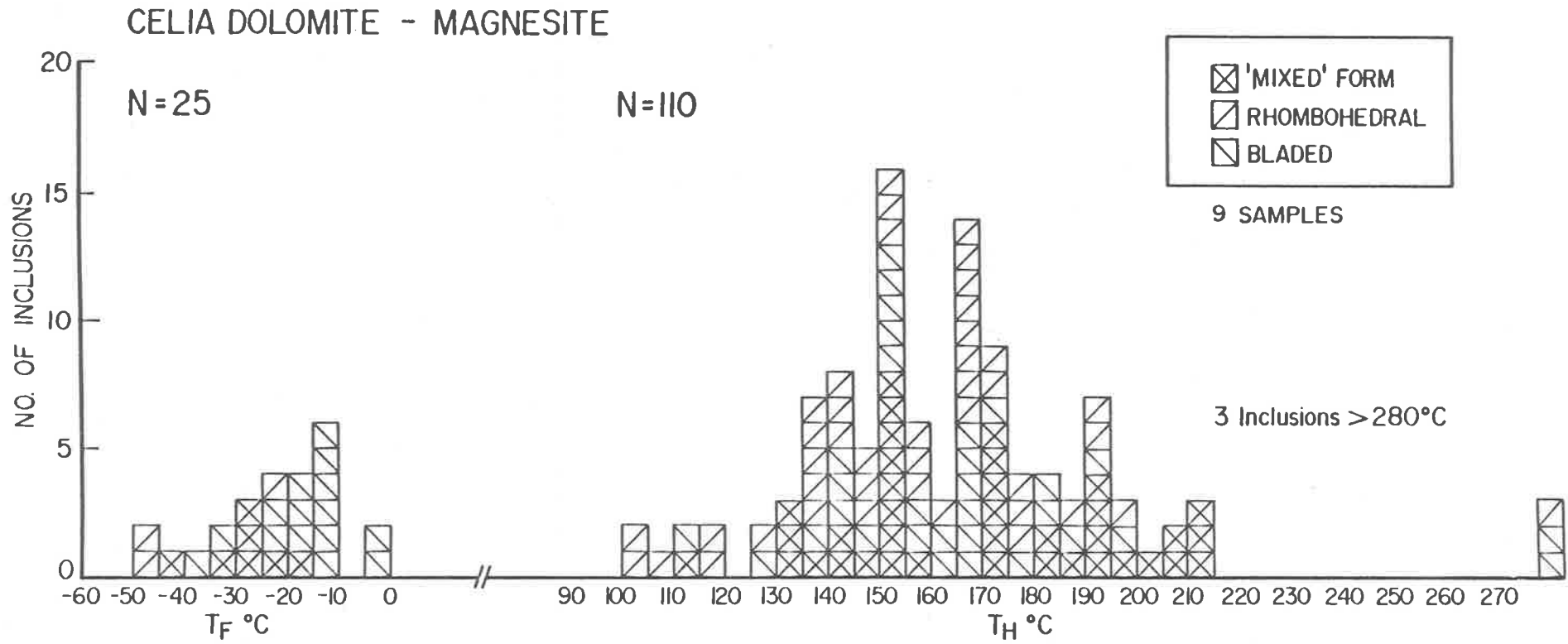
Fig. 58: Histograms of final melting and homogenisation temperatures.

(1) Freezing

1st Run: The fluid in the fluid inclusion froze at approximately $-100^{O}C$. T_e was not obtained. T_f occurred at $-44^{O}C$. A hydrate formed as the temperature increased, which melted at approximately $+15^{O}C$.

2nd Run: Freezing did not occur, even though the temperature was kept at $-140^{O}C$ for 10 minutes.

3rd Run: Freezing occurred at $-119^{O}C$. T_f occurred at $-41.7^{O}C$. There was Brownian movement of the bubble at $0^{O}C$. A hydrate that formed at approximately $-15^{O}C$ did not melt by $+50^{O}C$.

(2) Heating

1st Run: The aforementioned hydrate of run three dissolved at $+86.5^{O}C$. T_h occurred at $153.7^{O}C$. The temperature was allowed to stabilise at room temperature ($26^{O}C$) for a period of 1 hour, but the hydrate did not reappear.

2nd Run: T_h occurred at $153.3^{O}C$.

Nothwithstanding the fact that there was non-reproducibility of all of the phase changes (i.e. some meta-stable phases were obviously present), this data strongly supports the premise that at least one of the brines being investigated is a $CaCl_2$-rich brine i.e. T_f of $-44^{O}C$ and $-41.7^{O}C$ (T_f in the pure $CaCl_2$ system is $-49.8^{O}C$), and the melting point temperatures of the hydrates formed ($+15^{O}C$ and $+86.5^{O}C$) are suggestive of hydrates in the $CaCl_2$ system (Fig. 62).

C56 :- this sample shows the bladed morphology. Of the 6 fluid inclusions examined, 5 showed homogenisation of the fluid phase at a temperature above that of the average for the total study i.e. $152.94^{O}C$. Some of the fluid inclusions contain hematite daughter minerals, but no other species of daughter minerals was found. None of the fluid inclusions froze (Fig. 61).

C58 :- this sample shows the rhombohedral morphology. Some of the fluid inclusions contain hematite daughter minerals. Of the 6 fluid inclusions examined, 5 homogenised at a temperature below that of the average for the

258
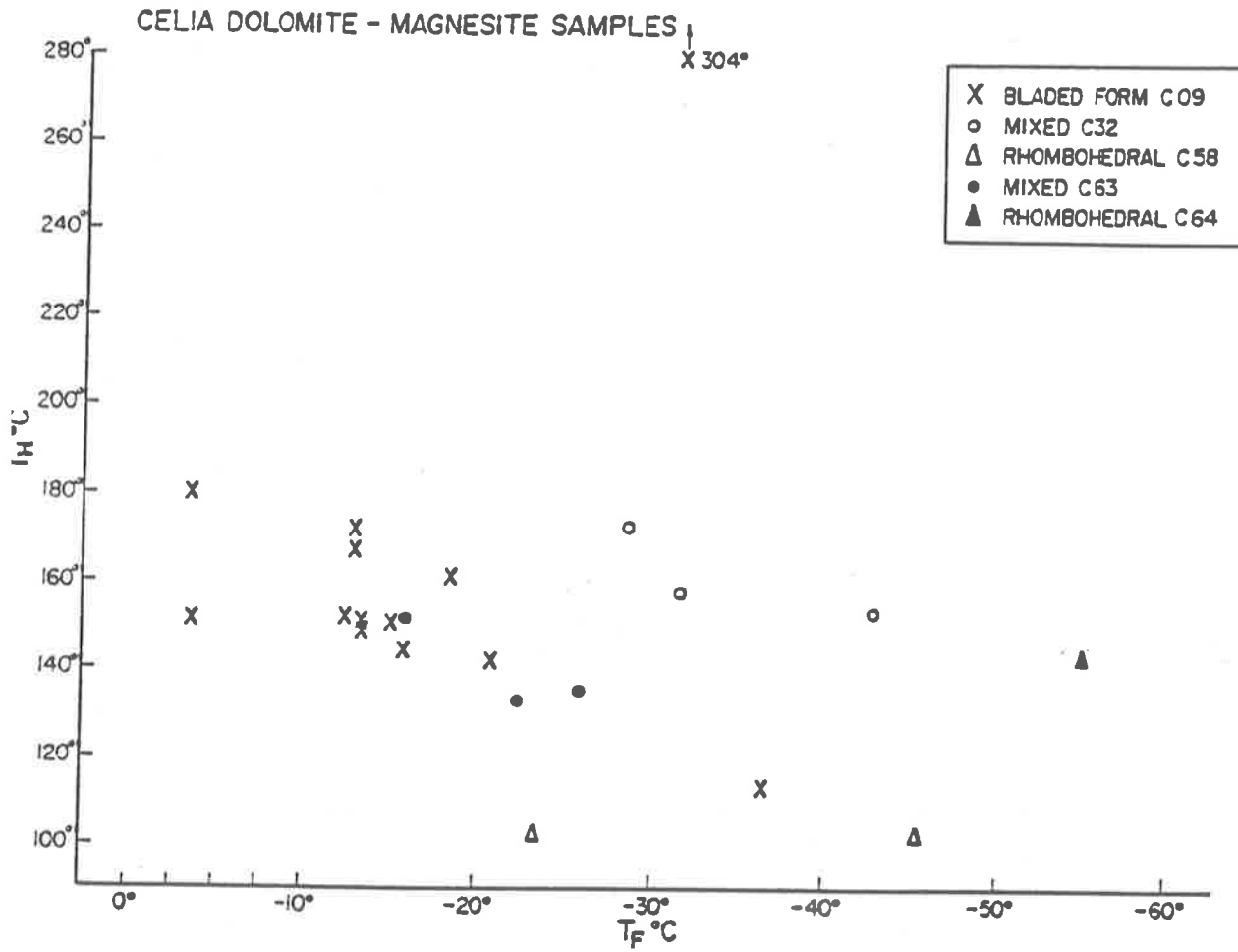
Fig. 59: Homogenisation temperature vs Final melting temperature.

total study i.e. 152.94^{o}C. The fluid inclusion that homogenised at 242°C was one which contained a CO_2 phase, so that this temperature should not be considered as a typical homogenisation temperature, because of the possibility of inhomogeneous entrapment (Fig. 61).

C64 :- this sample shows the rhombohedral morphology. At least half of the fluid inclusions contained one or more daughter minerals. Many of these daughter minerals only dissolved at temperatures above the fluid inclusion homogenisation temperature (e.g. 240°C). In one of the fluid inclusions, a solid formed at -60°C which melted at approximately -40°C. This fluid inclusion had a T_e of approximately -70°C, suggesting that both CO_2 and CH_4 were present, even though the CO_2 could not be observed optically at room temperature. In 8 of the fluid inclusions studied the vapour phase did not reappear after the first heating run, suggesting the existence of meta-stable conditions. Similarly, many of the daughter minerals that had dissolved during the first heating run failed to reappear upon cooling (Fig. 61).

C71 :- this sample shows markedly red zoned rhombs. There are trails of fluid inclusions parallel to and associated with the hematite zoning, so although these trails look like they are located on cleavage planes, which is normally a criterion for secondary fluid inclusions, they may well be primary ones i.e. the hematite zoning is likely to be related to the growth of the crystal and not a later phenomenon. The homogenisation temperatures of these fluid inclusions is marginally higher than the homogenisation temperatures of fluid inclusions in white coloured magnesite with rhombohedral morphology. It is also worth noting that none of the bladed magnesite contains this distinctive hematite. Where there is association of hematite with samples of magnesite that has the bladed magnesite present the actual bladed crystals are white or grey in colour (and no hematite can be observed even in thin section) and the red hematite is within the finer grained matrix, which is usually the rhomb type. The grey colouration is due to carbonaceous material.

Fig. 60
CO_2 Homogenisation Temperature

N3 (m)   ☐☐ L to V

KHARIDUNGA, NEPAL   N1 (m)

RUM JUNGLE COMPLEX   A09 (Q)

A02 (Q)

D12 (Q)

D11 (Q)

D10 (Q)

CRATER
FORMATION   D03 (Q)

C37 (Q))

C54 (Q))

CELIA DOLOMITE

C22 (Q))

C52 (Q)

C09 (m)
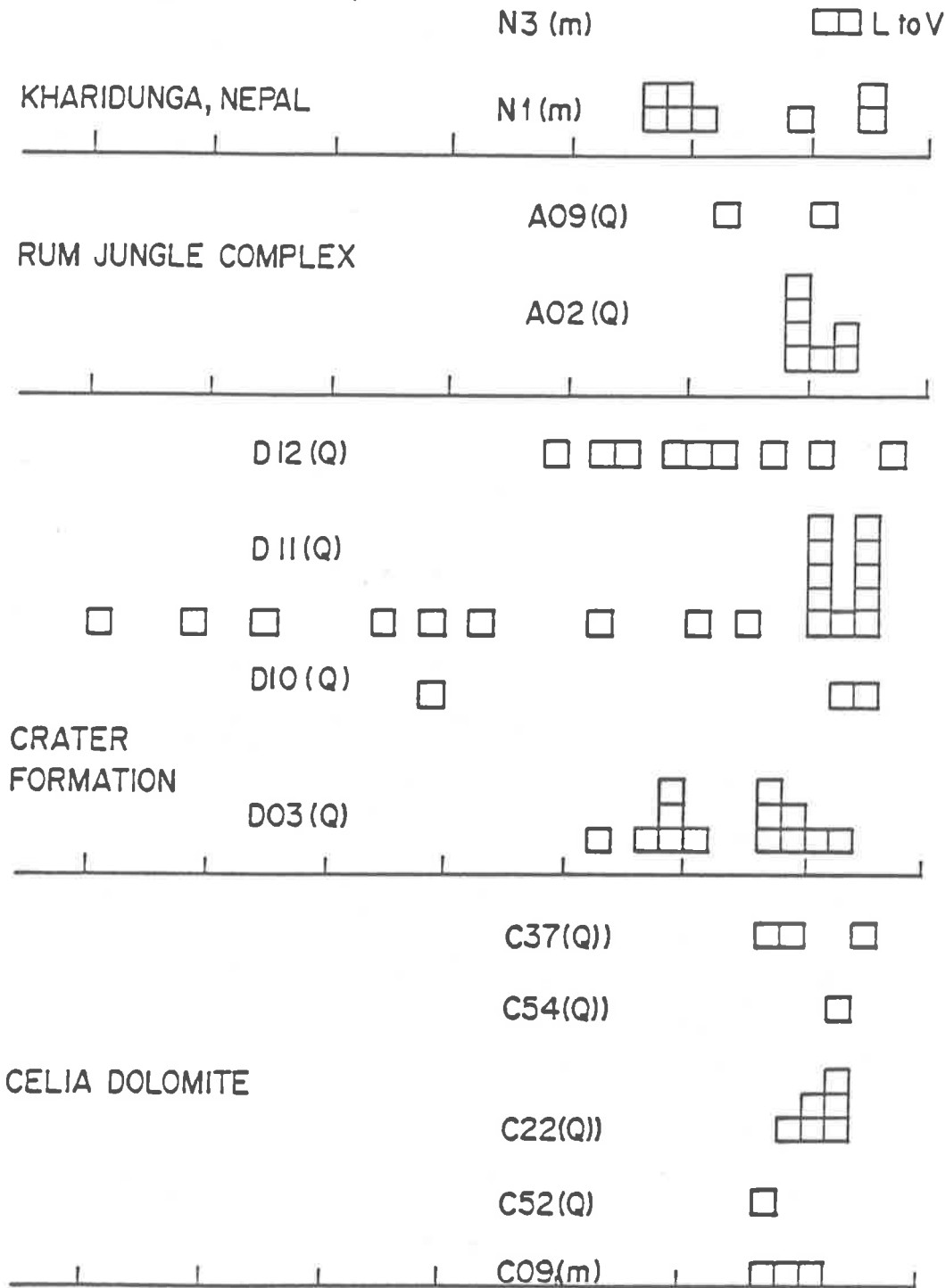
In this sample all 14 fluid inclusions studied had a higher homogenisation temperature than the average for the study. The fluid did not freeze in any of the fluid inclusions - indicating highly saline fluids (Fig. 61).

6.2.3.2 Quartz samples (Fig. 63):

The quartz samples show many results similar to those shown by the magnesite samples (Fig. 58):-

C11 :- this sample consists quartz crystals up to 1 cm in length growing into vughs from a highly ferruginous quartz-rich matrix. In this and in many of the other quartz samples it is the low T_e that alerts one to the presence of brine components other than NaCl, as T_f is often lower than $-20.8^{\circ}C$. Five of the 15 fluid inclusions studied did not freeze. Two fluid inclusions formed hydrates, one of which was seen to melt at $-12.6^{\circ}C$. A definite inverse relationship between salinity and temperature can be seen (Fig. 58).

C13 :- this sample (Plate 26) consists of quartz crystals of up to 3 cms in length growing into a vugh. Both sides of the vugh must have previously been occupied by magnesite (Plate 26) as the quartz crystals replace the rhombohedral form. In thin section the quartz adjacent to the vugh boundaries shows relict rhombohedral cleavage traces. These traces have a high density of very small (< $5\mu m$) fluid inclusions along them. Consequently, where the planes of fluid inclusions cross one another there is a concentration of clusters of fluid inclusions.

Two separate sections were cut to investigate this sample. The first was taken from near the perimeter of the vugh. Many of the fluid inclusions in this section contained cubic daughter minerals, most of which dissolved around $175^{\circ}C$ (Fig. 51).

The other section concerned a zoned quartz crystal, and was selected
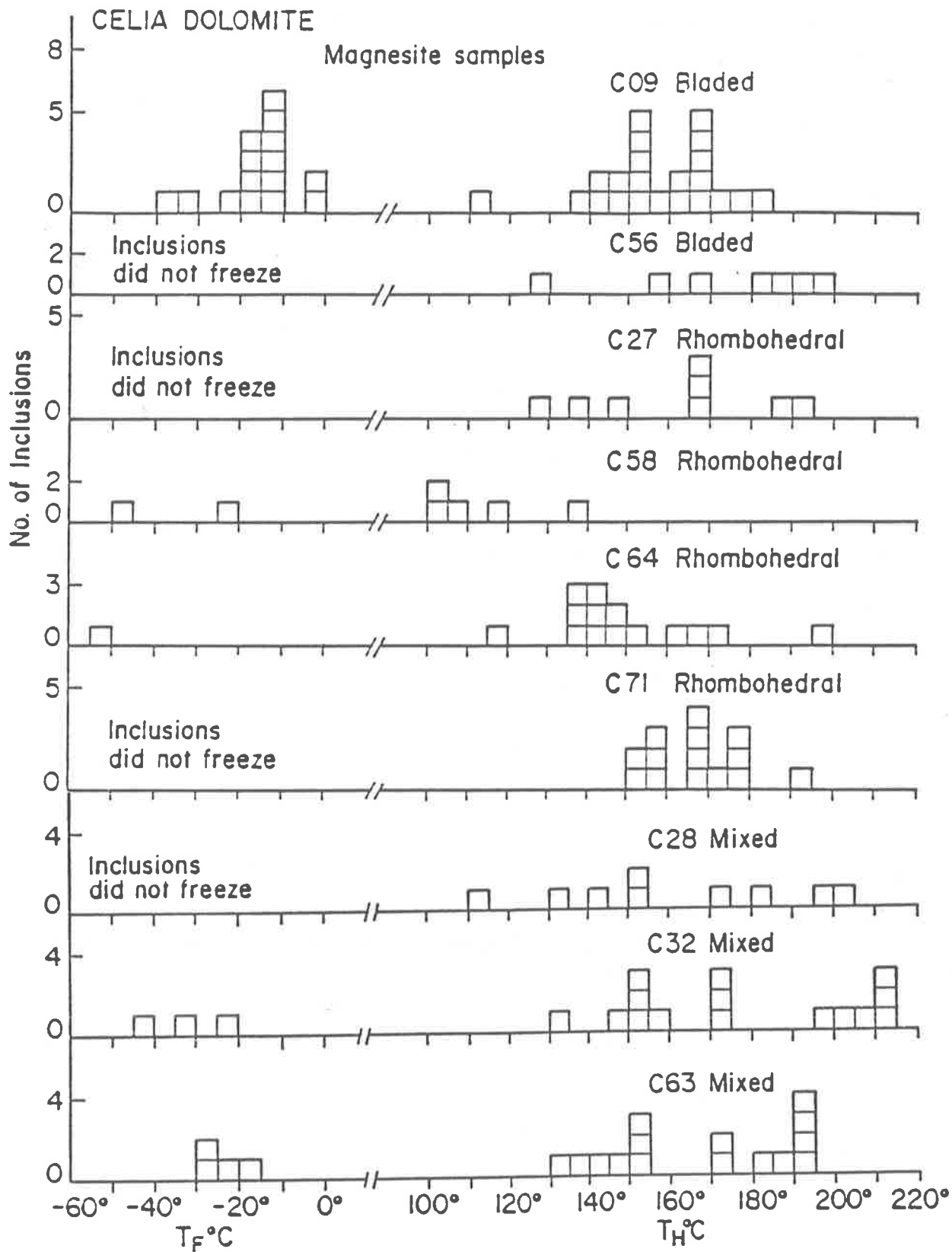
Fig. 61: Histograms of final melting and homogenisation temperatures.

to determine temperatures and salinities of the brine during the growth of the crystal (Chpt. 4). Five distinctive zones were selected and a total of 63 fluid inclusions within these zones were studied. In general, it can be stated that no systematic change appeared to have occurred during the growth of the crystal (Figs. 59, 64). However, within each growth zone where both T_h and T_f figures were obtained the inverse relationship between salinity and temperature can be observed (Fig. 59). Unlike the other section, few daughter minerals were observed in this section, apart from one fluid inclusion in the third zone from the rim of the crystal. This fluid inclusion had at least 6 daughter minerals present, none of which dissolved by 270°C. T_h was not observed for this fluid inclusion as the bubble kept "hiding" behind these daughter minerals!

C22 :- this sample is similar to the previous two except that it concerns microcrystalline quartz and not individual quartz crystals. The quartz has completely filled a void that previously contained carbonate. Pseudomorphs of stellate clusters (of carbonate) can be seen very faintly in thin section, suggesting that the precursor mineral was bladed magnesite. In some fields of view the fluid inclusions contain up to 90% liquid CO_2 and vapour volumetrically, which shows rapid Brownian movement at room temperature. There is a narrow range of CO_2 homogenisation temperatures in this sample (Fig. 60). It is an interesting and useful sample inasmuch as three of the CO_2 containing three phase fluid inclusions actually reached total homogenisation temperature, but with differing behaviour (Fig. 60) i.e. one fluid inclusion homogenised into the vapour phase at 359.6^{o}C whilst the other two homogenised into the liquid phase (rapidly) at 288.8^{o}C. This temperature is higher than that of a pure H_2O-CO_2 mixture which suggests the presence of dissolved salts in the fluid. The "popping" of the bubble at +7.0^{o}C and +6.5^{o}C after freezing of the brine suggests a low concentration of CO_2 having been dissolved in the brine or the melting of a CO_2-clathrate.

Fig. 62:

SYSTEM CaCl₂·H₂O
(Data from Seidell–Linke, 1965)
(Fuzikawa, 1979)
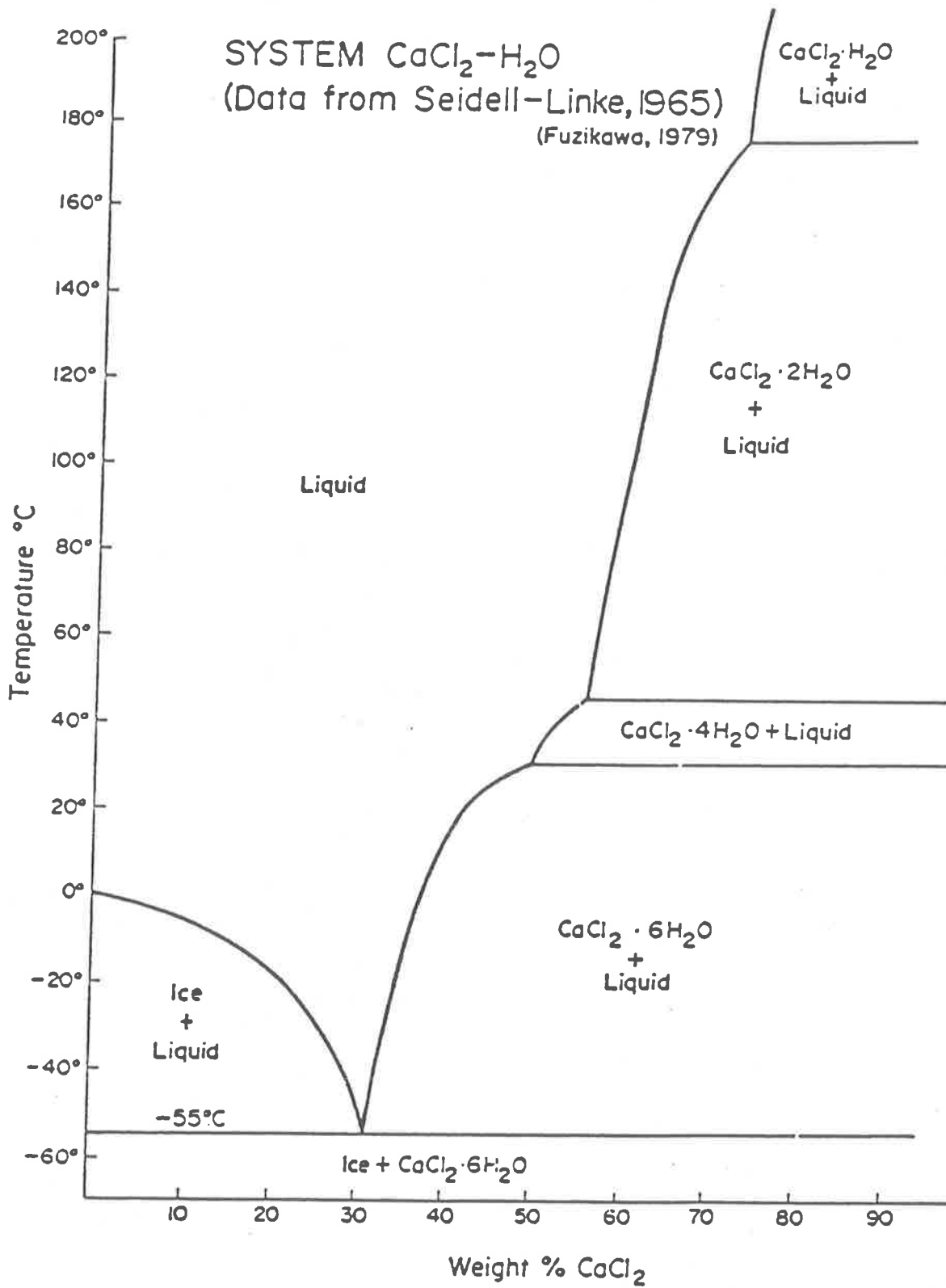
C33 :- this sample is practically the same as C22, except that the individual grains of quartz are much larger and more translucent. In this section the quartz shows relict rhombohedral cleavage. Six of the fluid inclusions studied formed hydrates during the freezing runs. These dissolved over a large range of temperatures i.e. $-3.3^{\circ}C$ to $-19.3^{\circ}C$. The consistently low T_f indicates the probable presence of $CaCl_2$ in the brines.

C37 :- this sample came from an apparent cross-cutting quartz vein which had green, acicular tourmaline crystals and rhombohedra of red magnesite associated with it (Plate 26). The quartz grains have very seriate boundaries - so much so that they are suggestive of stylolites. The tourmaline is later than the quartz and the magnesite.

The data obtained from this sample suggest that it is closely related to either the banded quartz-tourmaline material within the Beestons Formation or to quartz-tourmaline veins within the Rum Jungle Complex i.e. the data is intermediate between these two sets of data.

C43 :- this sample consists of dark crystalline quartz with a pink talc rim of 2 to 15 mms width (Plate 6). The sample was enclosed by magnesite. The boundary between the quartz and the talc is relatively sharp. There are very small crystals of tourmaline in both minerals. These are equant in habit in the talc and acicular in the quartz. Stylolites occur within both minerals, with the tourmaline concentrated along these in the talc, whereas the distribution of tourmaline appears to be random within the quartz grains. There is intragranular chlorite and talc in the quartz, particularly near the talc rim.

Four fields of view were selected, starting with a quartz grain within the talc, to material approximately 1.5 cms away from the talc. No significant difference in the results was discerned (Fig. 58). No CO_2 rich phases were identified optically. The consistently low T_e indicates the presence of additional components above to those of the Ca-Mg-Na-Cl system; possibly K, Fe and/or Li-Cl mixed chlorides. There

CELIA DOLOMITE – QUARTZ SAMPLES
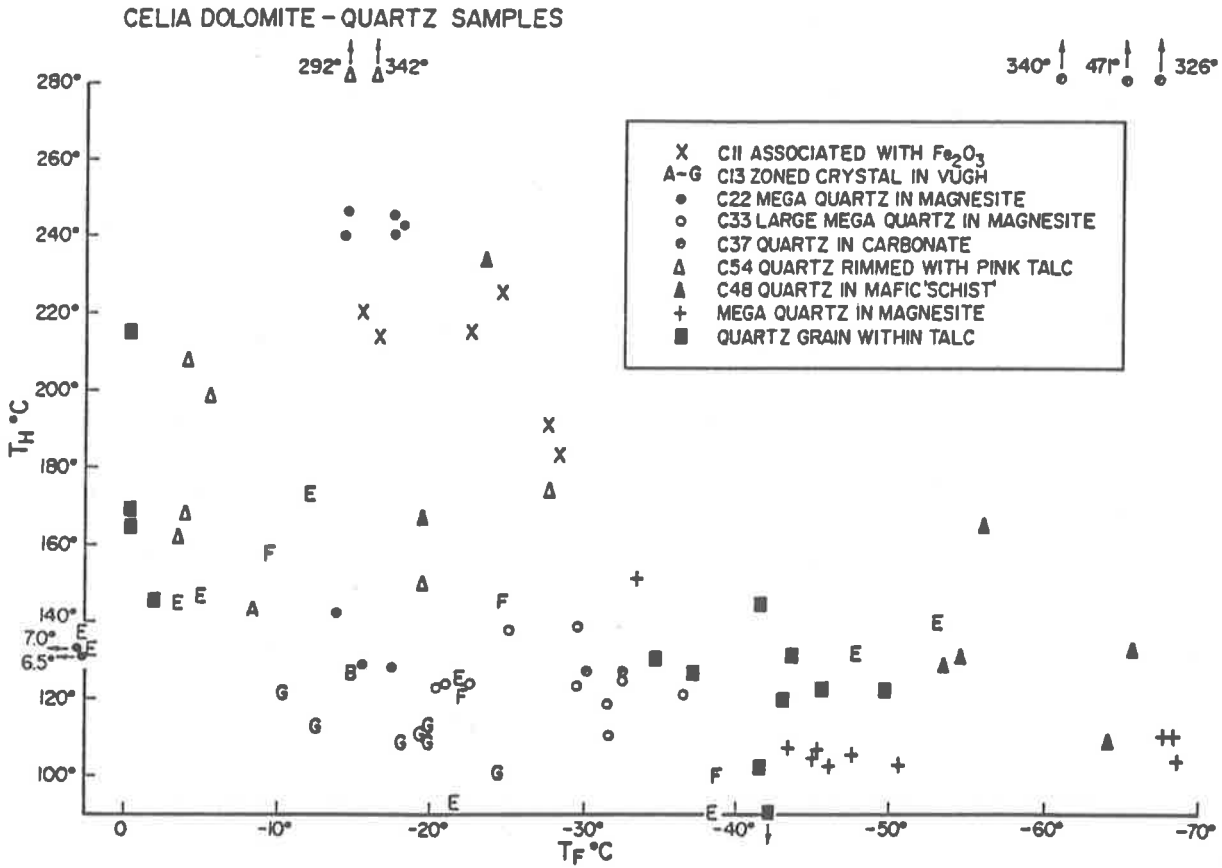
Fig. 63: Homogenisation temperature vs Final
melting temperature.

were few daughter minerals observed, but those present were remarkable for their low dissolution temperatures (Fig. 51), which could indicate K or Mg salts.

C48 :- this sample consists of layers of dark crystalline quartz, showing a pull-apart effect, within the so-called mafic schist (Plate 28). The quartz layers are parallel to the foliation of the platy minerals within the schist. Hematite has formed later, and has been concentrated along and within the quartz layers, growing from the rim inwards (Plate 28). There is also evidence of sericitisation, which suggests a similar process to that suggested by Ewers and Ferguson (1983) for Nabarlek i.e. the breakdown of chlorite to sericite producing hematite.

All the fluid inclusions in which CO_2 phases were visible under the microscope were too small to test with the freezing stage.

C52 :- this sample is a quartz-tourmaline rock in which the tourmaline content is approximately 65%. It shows a semblance of banding but with some disruption i.e. rip-up clasts. This is seen markedly in thin section, where the quartz grains show an angular fine grained mosaic and undulose extinction with zones of partial grain growth (Plate 28). The tourmaline also shows deformational effects due to moderate deformation i.e. sheared and boudinaged grains (Plate 28). There has been new quartz growth between the pull-apart segments. Unfortunately this deformation has destroyed any usable fluid inclusions, so that only minimal data was obtained.

C54 :- this sample is practically the same as C43, except that it has a composite texture. The quartz shows pseudo-cleavage, along which there are trails of very fine fluid inclusions. The quartz shows undulose extinction and seriate boundaries. There were many clusters of very small fluid inclusions that contained CO_2 phases but only one of these was large enough to use.

Overall there was no significant difference in the brines present

(a) CELIA DOLOMITE –QUARTZ SAMPLES

N=106

N=160

NO. OF SAMPLES

7 SAMPLES > 270°C

$T_F °C$

$T_H °C$

(b) CELIA DOLOMITE   SAMPLE C13   Zoned quartz crystal
A core ⟶ G rim

N=26

N=60

NO. OF SAMPLES

$T_F °C$

$T_H °C$
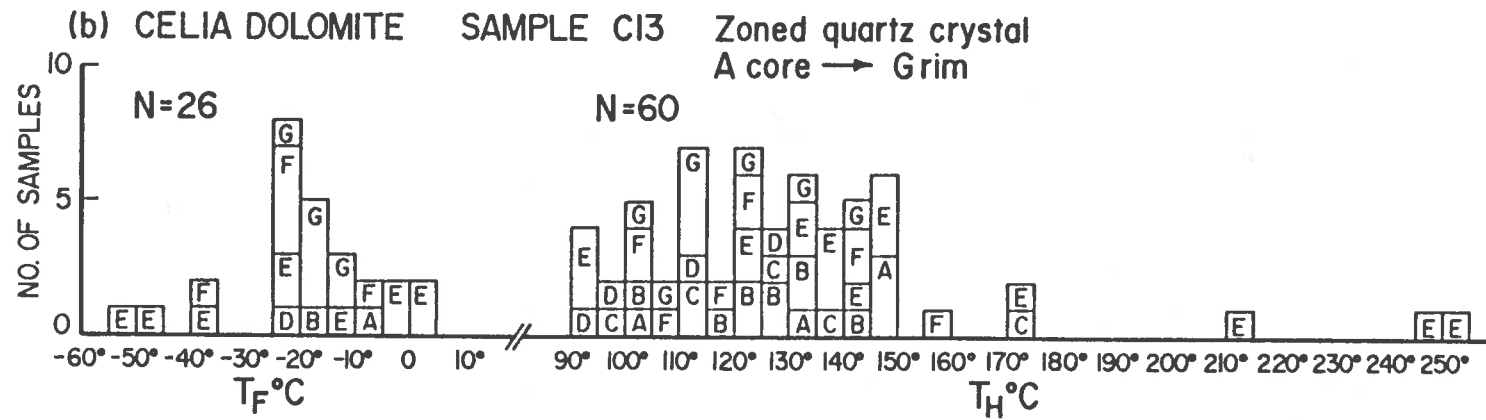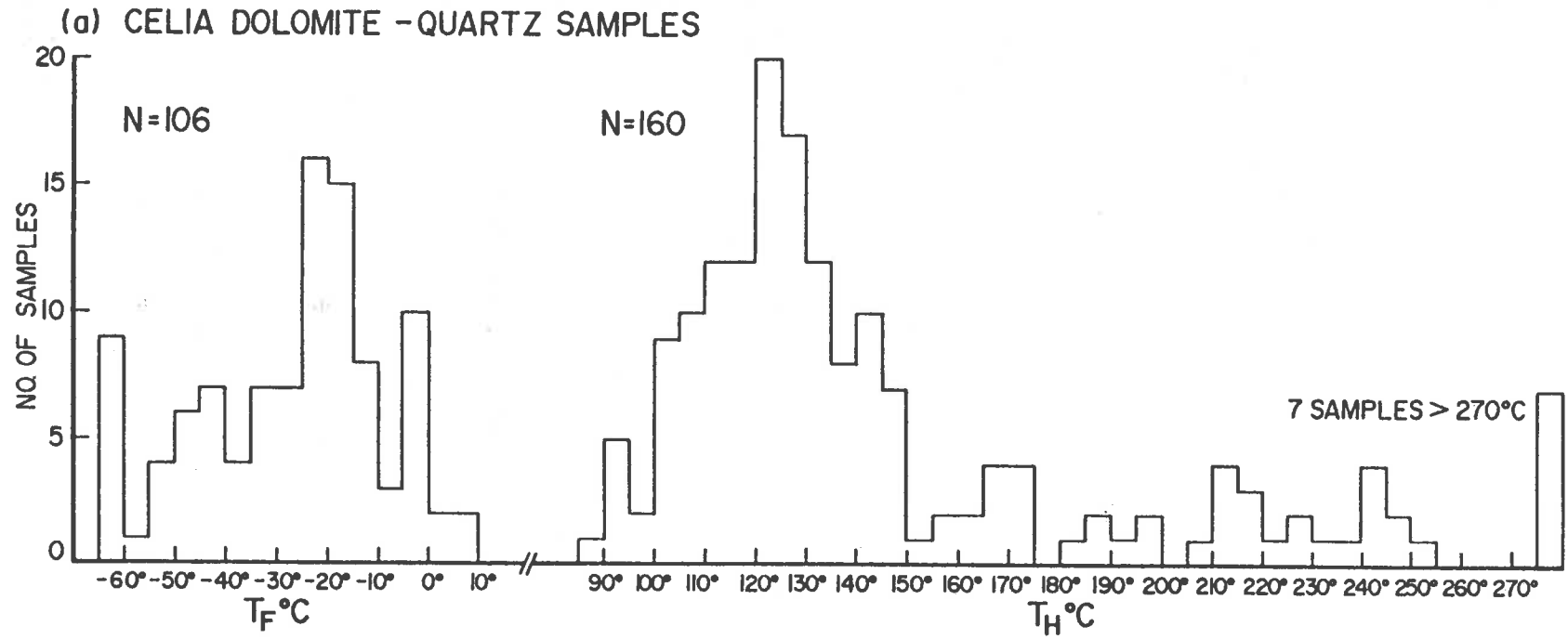
Fig. 64 (a) & (b): Histograms of final melting and homogenisation temperatures.

during the recrystallisation of the magnesite and those involved in the formation of the various types of quartz, regardless of its host rock.

Although it has been suggested that the cleavage in the quartz is a relict from a carbonate precursor, this is not necessarily the case: e.g. the sudden stress caused by tectonic shock (Florke et al., 1981) - or temperature. A sudden temperature increase of about $100^{o}C$ seems to be a minimum prerequisite (Behr et al., 1984) for this effect to occur. Above $300^{o}C$ there is less likelihood of deformationally induced cleavage formation (Florke et al., 1981). As this portion of the Celia Dolomite shows the best development of this quartz cleavage, the deformational origin may be the more valid one.

6.2.4 Crater Formation

Five samples were selected from the Crater Formation for correlation purposes with the Celia Dolomite (Figs. 65, 66).
D03 :- this arenite has a high component of detrital grains from the Rum Jungle Complex granitoids e.g. quartz, microcline, amphibole ($\geqslant$ 10%). The matrix is highly sericitised. The arenite also shows areas rich in later quartz (i.e. diagenetic quartz), tourmaline and limonite after pyrite. This diagenetic quartz is the best sample for estimations of pressure conditions at the time of the entrapment of the fluids because the following parameters were available:- (a) T_h CO_2; (b) CO_2 density; (c) T_{tot} (which is a good estimate of the actual filling temperature); and (d) degree of filling.

Using Swanenberg's (1980) MRK-derived isochores for the system H_2O-CO_2 (Fig. 67) pressure estimates range from 1.4 to 1.8 Kbars (8 values), with a mean of 1.60 Kbars. Although Swanenberg's isochores are calculated for the pure H_2O-CO_2 system, the approximation of P and T are the best available at this stage.
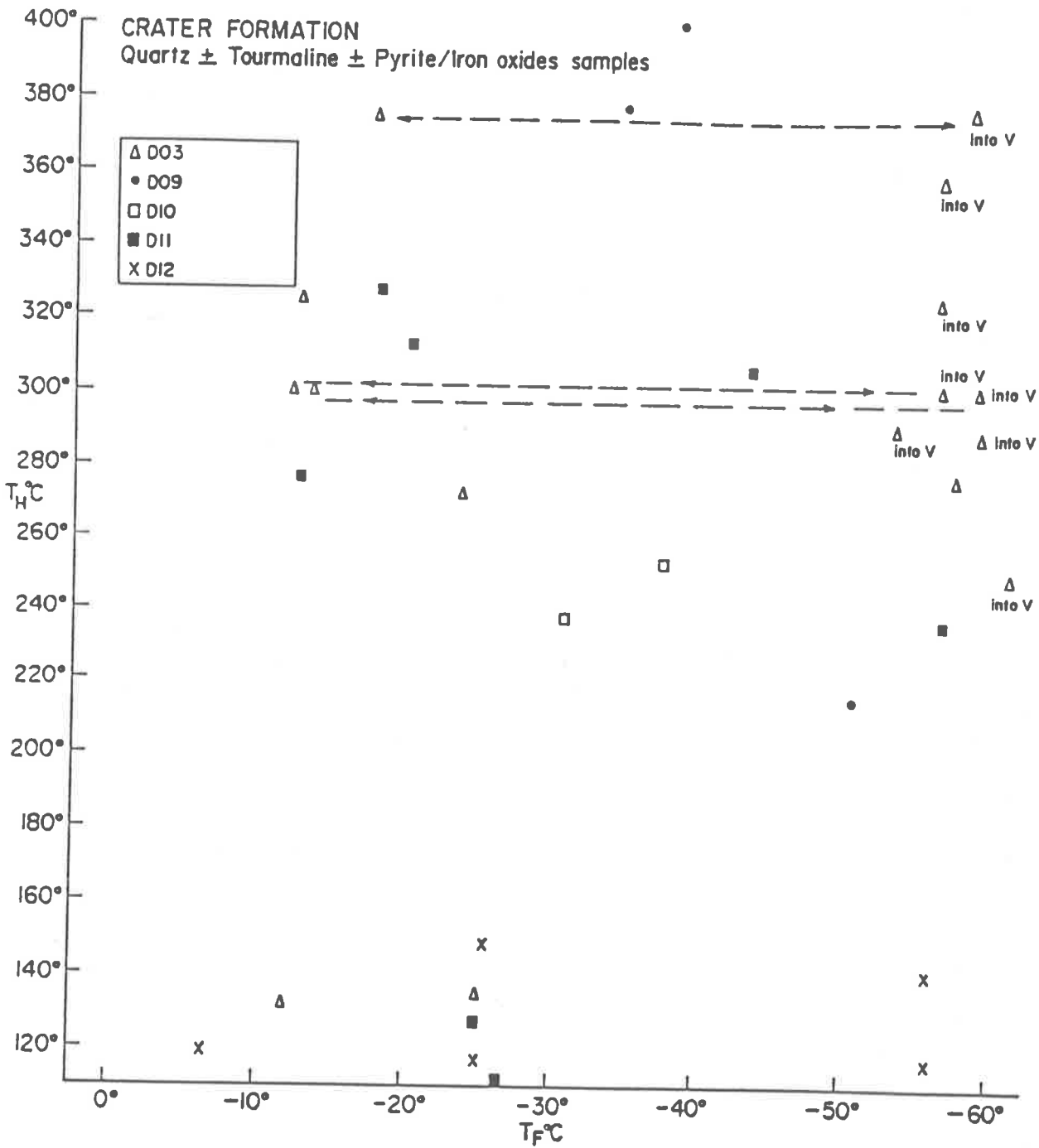
Fig. 65: Homogenisation temperature vs Final melting temperature.

A common T_f for the CO2 content of the inclusions is in the range -55°C to -60°C. With some of these fluid inclusions it was actually possible to also record the T_f of the liquid phase (range of -17.8°C to -12.0°C). In two of these fluid inclusions two distinct "bubbles" formed at -13.2°C. This phenomenom and its explanation has been previously reported by Collins (1979). There was only one fluid inclusion that showed the formation of a hydrate - at -21.7°C, which melted at -18.0° C. Consequently these T_f figures of the liquid phase of these CO_2 rich fluid inclusions cannot be directly converted to a salinity figure, as it is now well established that the presence of a hydrate will increase the salinity of the remaining liquid phase by up to 50% (Collins, 1979). Where no clathrate was seen, it is likely that it was "missed" simply because the fluid inclusions that had to be used were so small, but nevertheless they were probably there! Therefore, caution is very necessary before attempting to calculate salinity numbers from any data derived from fluid inclusions in which CO_2 is either a visible or suspected phase.

D09 :- the minerals toumaline (75%) and quartz (15%) in this iron rich rock were formed in situ, and have since been marginally modified by deformation. Although in none of the fluid inclusiobs could a CO_2 phase be positively identified optically, they nevertheless have the appearance of typical CO_2 containing fluid inclusions. The majority were <5μm in length, with the vapour phase volume well above average. Many of them gave an homogenisation temperature well above the average, with two of these homogenising into the vapour phase at temperatures corresponding to those of similar type fluid inclusions that homogenised into the liquid phase. The wide range of T_{tot} suggests inhomogeneous entrapment, which can be explained by the mixing of two fluids. The mixing could have been effectuated by tectonic jolting resulting from gravity thrusting. These fluid inclusions giving the wide range of T_{tot} only occur in the vicinity of the area in which it is proposed that the gravity thrusting occurred i.e. the eastern margins of the Complexes. As there is little
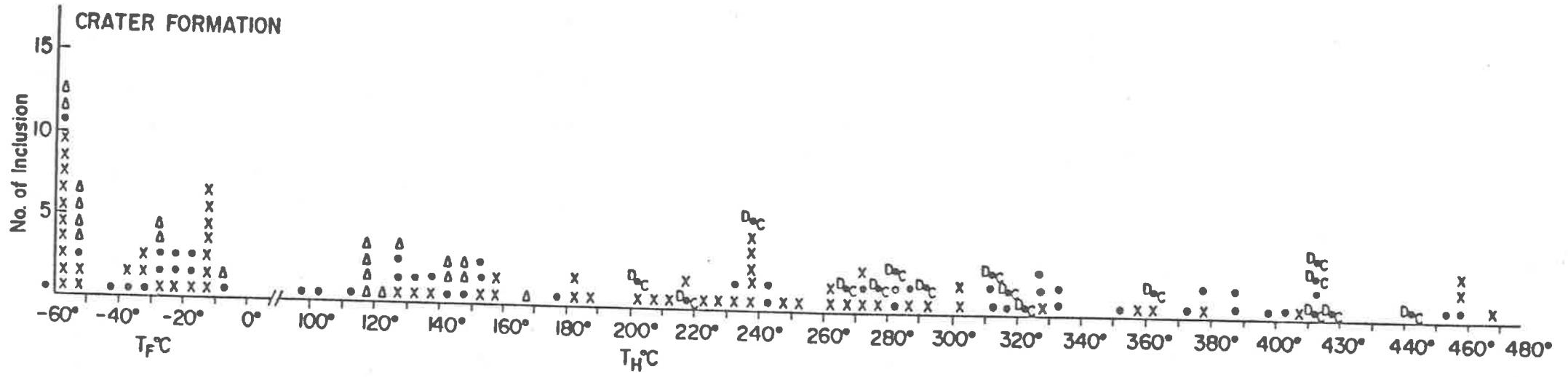
Fig. 66: Histograms of final melting and homogenisation temperatures.
See Fig. 65 for legend.

doubt that this quartz is not detrital, these temperatures are very significant when reconstructing the evolution of the mineralogy present, and the events that subsequently modified or completely changed it.
D10 :- this quartz rich rock has had a more complex history than a cursory glance would suggest. The quartz has undergone recrystallisation, and yet is still very fine grained on the whole, with the grains showing complexly seriate boundaries and undulose extinction. Both the tourmaline and the pyrite pseudomorphs (now limonite with pyrite cores) formed after the quartz, but as the tourmaline shows imbrications due to shearing, it was formed pre-deformation (Plate 30).

The pyrite was used for S isotope determinations, which indicate a non-magmatic source for the S (Chpt. 7). This suggests that the tourmaline and the pyrite are diagenetic.

There was quite a variation in the three fields of view selected for detailed microthermometric determinations.

In the first, the fluid inclusions occur in trails of secondaries, with few being large enough to use. The second showed trails of fluid inclusions that did not transect grain boundaries. Many of these fluid inclusions look like the CO_2 type although this could not be confirmed. However, in the third field of view, much larger fluid inclusions (i.e. 5-8 μm) did show a separate CO_2 phase when cooled.

Daughter minerals were not common, but those present showed a bi-modal dissolution temperature distribution (Appendix 2).
D11 :- this sample is similar to D09, but with a lower tourmaline content. The quartz is more granular in the hand specimen, whilst the tourmaline is preferentially enriched in Fe.

The majority of the fluid inclusions have a CO_2 phase present plus
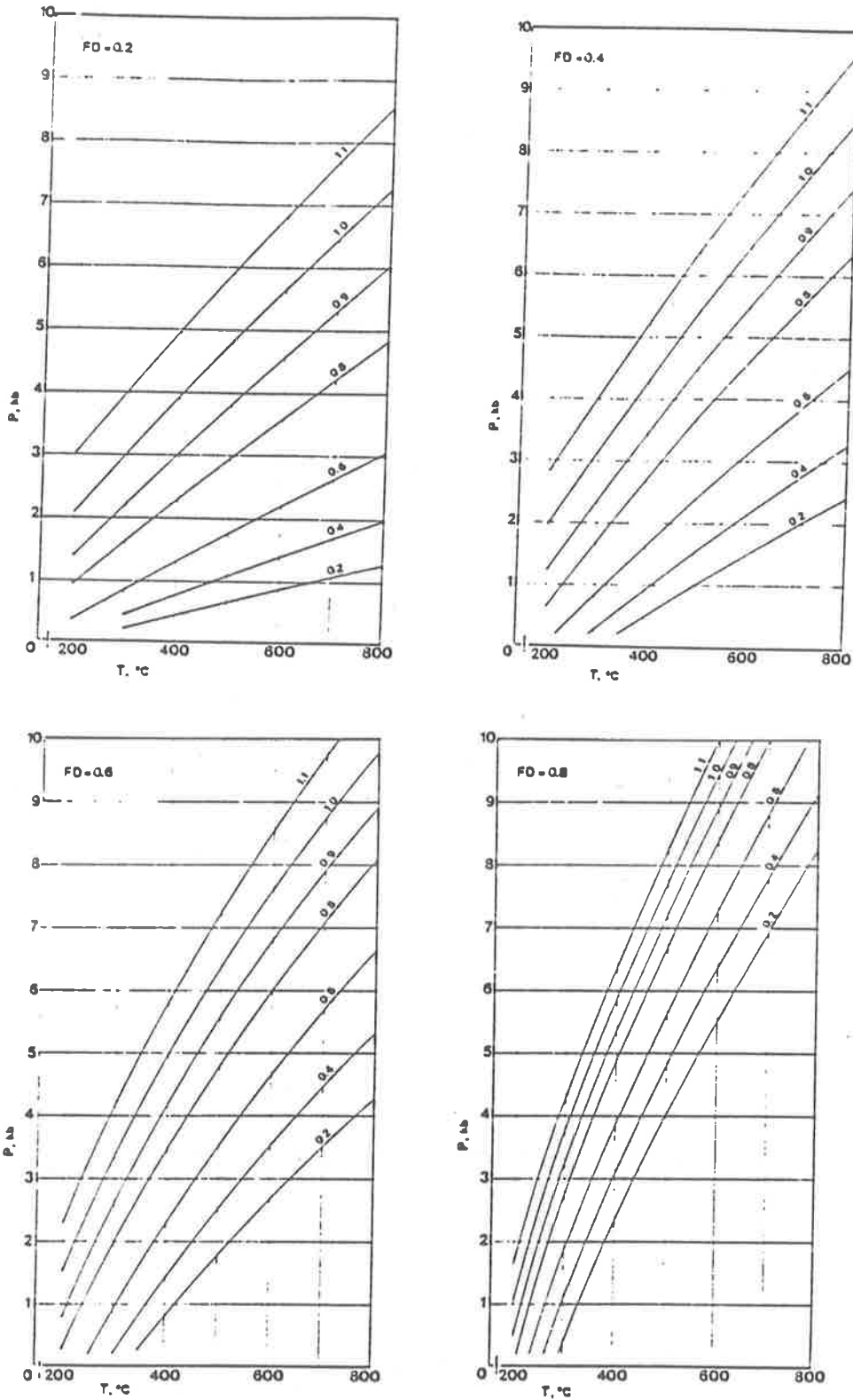
Fig. 67: MRK-derived isochores for the system H_2O-CO_2. FD=degree of filling (V_{H2O}/V_{TOTAL}) at approximately 20°C. Numbers along isochores are densities of CO_2 in the bubble at approximately 20°C.

(Swanenberg, 1980)

one or more daughter minerals in the same fluid inclusion (up to five daughter minerals were seen). In only two cases did a daughter mineral dissolve prior to decrepitation (Fig. 51). There were some excellent diagnostic fluid inclusions, e.g. two adjacent fluid inclusions showed CO_2 homogenisation at approximately $30^{\circ}C$ (Fig. 60) and then gave total homogenisation temperatures at $398.7^{\circ}C$ into the vapour phase for one fluid inclusion and $400.2^{\circ}C$ into the liquid phase for the other. This implies that CO_2 densities can be determined which allows the calculation of pressures (1.5 Kbars).

There is a very wide range of CO_2 homogenisation temperatures - from $-0.6^{\circ}C$ to $32.6^{\circ}C$ (Fig. 60), indicative of a range of densities. This is suggestive of trapping of an inhomogeneous fluid, which could be the result of boiling.

D12 :- this sample appears to have orginally been a banded quartz-tourmaline rock, similar to those seen in the Beestons Formation and in the Celia Dolomite, which has undergone major chemical alteration since. The bi-modal grain size quartz grains show seriate boundaries and undulose extinction. There are relict limonite pseudomorphs after pyrite sparsely distributed throughout the quartz bands.

Unusual metastable daughter mineral behaviour is shown in some of the fluid inclusions in this sample e.g. some fluid inclusions show a large cubic shaped daughter mineral at room temperature. When the fluid inclusion is frozen and allowed to warm to room temperature this daughter mineral dissolves at $-39^{\circ}C$, and does not always re-precipitate. However, when it does (at $+14.9^{\circ}C$) it dissolves at approximately $100^{\circ}C$. This behaviour is suggestive of metastability of $CaCl_2$ hydrates and transformation of hexahydrates to quadrihydrates (Fig. 62). Some of the solid inclusions are true daughter minerals, and their shape, colour and insolubility suggests such minerals as hematite, pyroaurite and dawsonite. This latter mineral can form by the decomposition of silicates
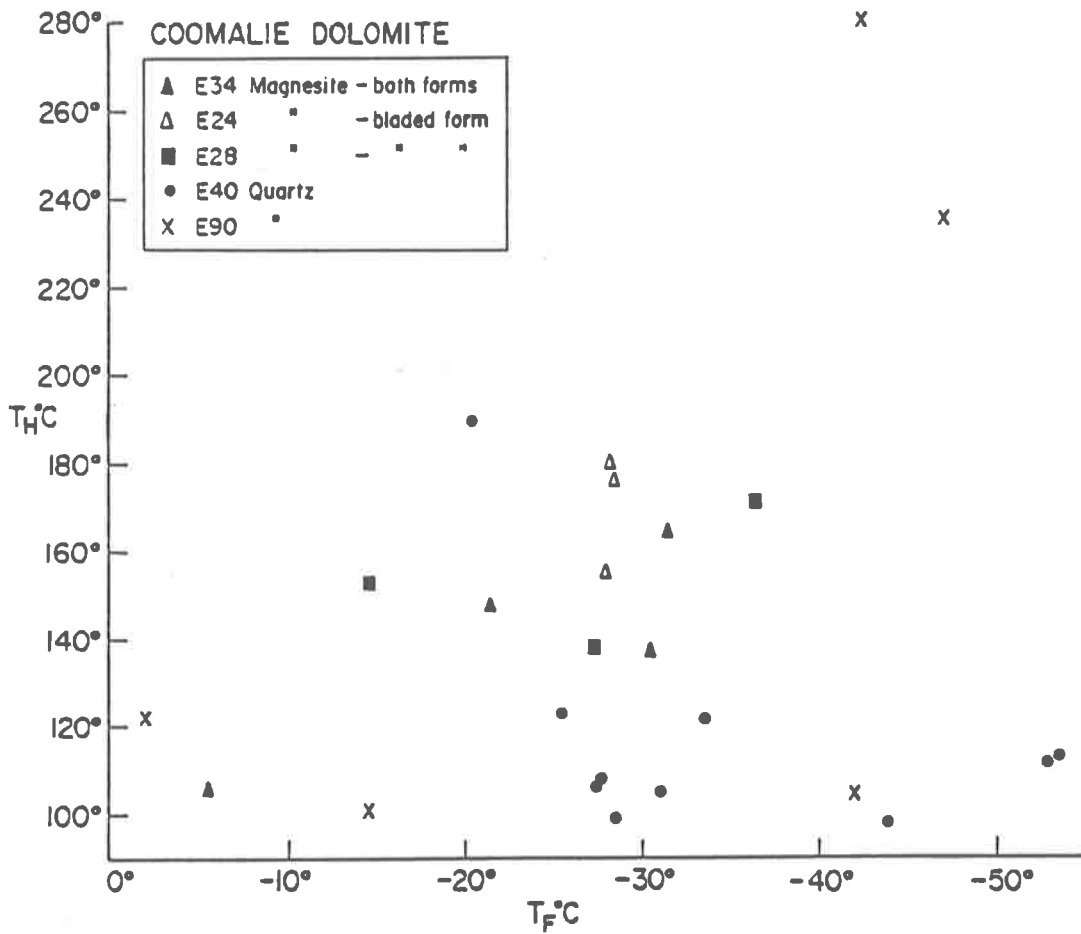
Fig. 68: Homogenisation temperature vs Final melting temperature.

containing Na and Al (Dana, 1966), such as feldspars derived from the Complexes.

Almost all of the fluid inclusions contain CO_2, in addition to one or more daughter minerals. A range of CO_2 homogenisation temperatures was obtained (Fig. 60).

One of the main problems in assessing this data from the Crater Formation is - why is there such a disproportionate number of fluid inclusions where $T_h = T_{tot}$, giving the necessity for large pressure corrections compared to all the other sequences (and areas)? This discrepancy could be related to the fact that these high temperature fluid inclusions are all from the vicinity of the base of the Crater Formation where it overlies the Celia Dolomite. The only other samples that show somewhat similar behaviour are those from the top of the Celia Dolomite in this same area! One possible explanation could be that this sample area was the locus of gravity thrusting of the arenite-magnesite sequence (Fig. 46). This thrusting event could have coincided with the mixing of two pre-existing fluids e.g. low temperature saline fluid and hydrothermally influenced higher temperature less saline fluid. Although the influence of the tectonic event could be widespread, it would be only in the vicinity of the actual thrust plane that most mixing took place. Similarly there would be more opportunity for the entrapment of CO_2 rich fluids of differing density within the immediate zone of the tectonic activity.

6.2.5 Coomalie Dolomite

This formation does not show any significant difference to the Celia Dolomite, except that the particular behaviour of fluid inclusions within samples collected from the vicinity of the top of the Celia Dolomite is not seen in any of the fluid inclusions in Coomalie Dolomite samples
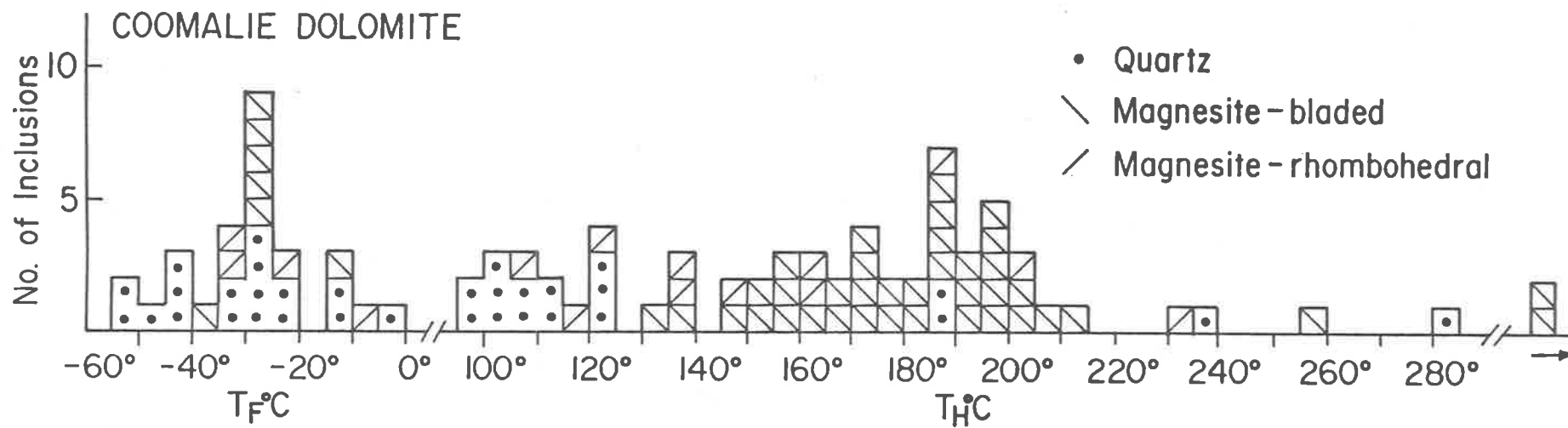
Fig. 69: Histograms of final melting and homogenisation temperatures.

(Figs. 68, 69).

Seven samples were selected from within the Coomalie Dolomite : 5 of magnesite and two of quartz. These were; -

E18 :- this sample of fairly uniform grey coloured magnesite showed the rhombohedral type morphology. The fine grained magnesite contains many flakes of wispy grey-black carbonaceous material. None of the fluid inclusions froze, suggesting a very saline brine (Fig. 70).

E24 :- this samples of white, coarse bladed type magnesite had very few usable fluid inclusions (Fig. 70).

E25 :- this sample of white and grey magnesite is of the bladed type (Plate 25). It contains microscopic grains of pseudomorphs of limonite after pyrite, some with pyrite cores. Some of the bladed magnesite occurs as stellate clusters. The brine would not freeze in any of the fluid inclusions, which suggests that it is highly saline (Fig. 70).

E28 :- this sample consists of very coarse (up to 2 cms in length) grey and white bladed magnesite. Some of these "blades" contain solid inclusions of dolomite and pyrite (Plate 19). Most of the fluid inclusions are related to cleavage, and are therefore probably secondary. Very few of them froze when cooled, suggesting that they contain a highly saline brine (Fig. 70). This hypothesis is enhanced by the formation of a hydrate in one of the fluid inclusions that did freeze. Although no CO_2 - phase was seen at room temperature, two of the fluid inclusions had the appearance of the CO_2 type. Many of them contained daughter minerals, which dissolved over quite a range (227-290°C) of temperatures. (Fig. 51).

E34 :- this sample consists of white, crystalline magnesite matrix with randomly dispersed grey, medium grained blebs of rhombohedral type magnesite throughout. It contains ubiquitous solid inclusions of apatite and dolomite (Plate 19), but few fluid inclusions. Those that are present are not associated with any cleavage (Fig. 70).

E40 :- this sample was dominantly a very coarse: white magnesite with both

280
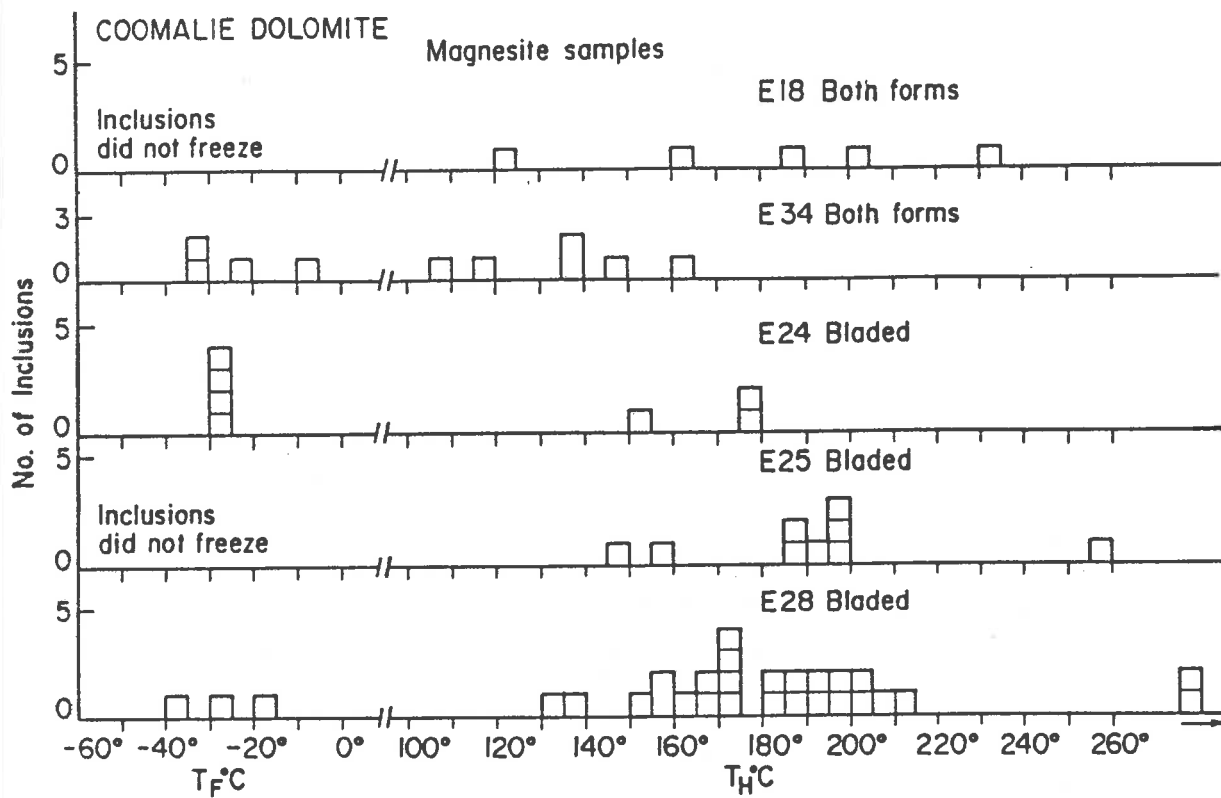
Fig. 70: Histograms of final melting and homogenisation temperatures.
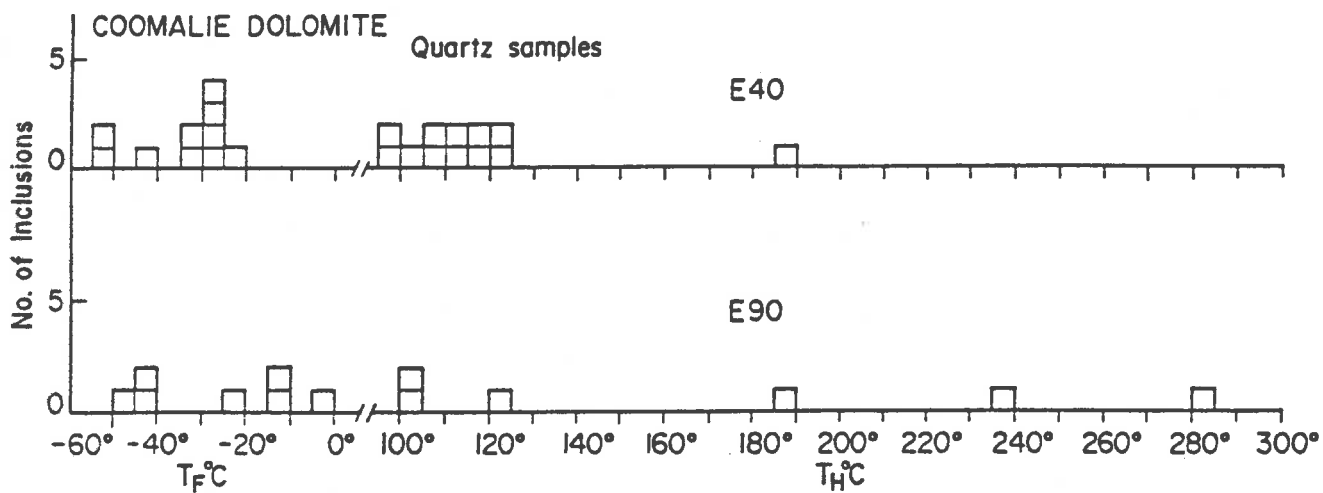
Fig. 71: Histograms of final melting and homogenisation temperatures.

morphologies present. It was from knot of quartz within the magnesite that the fluid inclusions were selected for study. Very low first melting temperatures were observed in this sample (-69°C - Fig. 71).

E90 :- this sample consisted of a large knot of quartz from within bladed type magnesite. It contains parallel traces of very small fluid inclusions, giving a pseudocleavage like appearance. The fluid inclusions are particularly concentrated where two traces cross. Many of the fluid inclusions have bubbles showing Brownian movement and daughter minerals at room temperature, but they are too small to use.

6.3 Mt. Fitch

Six samples were selected from the open cut at Mt. Fitch : three of magnesite and three of quartz. (Figs. 72, 73).

MF2 :- this sample consists of both forms of magnesite. Many of the rhombs showed hematite zoning, especially the larger ones. There is a high chlorite component within the sample, plus minor pyrite and accessory chalcopyrite. The sample has a remarkable low T_e value (-73.0^{o}C - Appendix 2 - Fig. 74).

MF3 :- this sample consists of fairly pure massive quartz with a thin veneer of later small quartz crystals on one face. There was a narrow range of homogenisation temperatures (101°C-149.1^{o}C), from fluid inclusions that showed a diversity of behaviour during freezing runs (Appendix 2 - Fig. 75).

MF4 :- this massive crystalline quartz sample contains wisps of carbonaceous shale. The fluid inclusions gave very similar results to those of MF3 (Fig. 75), except that in every case the vapour phase disappeared completely on freezing - then suddenly "popping" (i.e. not growing in size from a pin-point, but re-appearing suddenly at total volume) at temperatures from -20.9^{o}C up to -1.3^{o}C. As these fluid inclusions did not contain atypically small vapour phases, this is

282a

Fig. 72: Homogenisation temperature vs Final melting temperature.

Fig. 73: Histograms of final melting and homogenisation temperatures. See Fig. 72 for legend.

282c

Fig. 74: Histograms of final melting and homogenisation temperatures.
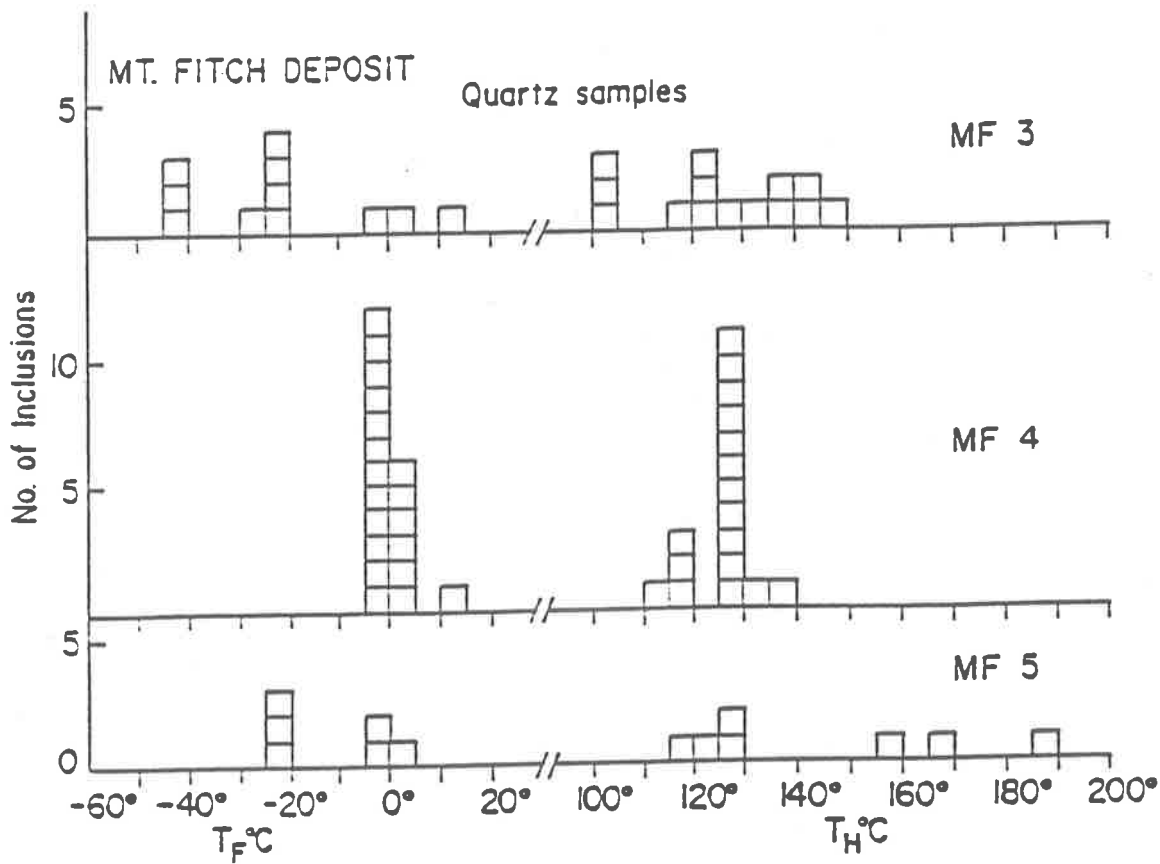
Fig. 75: Histograms of final melting and homogenisation temperatures.

unlikely to be entirely due to metastability of a H_2O - rich fluid inclusion, as it does reappear prior to T_f. To further confuse the issue, some fluid inclusions that contained a liquid phase only at room temperature formed and retained a vapour phase during and after freezing runs. A simplistic interpretation of this behaviour is unlikely to correctly account for all the atypical phase changes observed.

MF5 :- This sample is similar to MF4, but with a greater carbonaceous shale content (approximately 25%). (Appendix 2 - Fig. 75).

MF7 :- This sample consists of white to translucent coarse crystalline rhombohedral type magnesite, with magnesite crystals growing into vughs within the sample. It contains minor amounts of chlorite. All the fluid inclusions in the sample appear to be related to cleavage. On the other hand, they may be related to the growth zones of the rhomb-type crystals, as these are physically similar. There are many trails of rhomb-shaped liquid-phase only fluid inclusions. On cooling, many of these separate into liquid and vapour phases, which persist on heating up to T_h. This behaviour strongly supports the presence of CO_2 which dissolves in water on cooling. Freezing of the fluid occurs at approximately - 70°C.

Another fluid inclusion in the same field of view showed behaviour typical of a H_2O-rich fluid inclusion (Hollister et al., 1981) i.e. the bubble contracted when the liquid froze etc.

There seems little doubt that there were at least two different brines involved at the time of the recrystallisation of this magnesite (Fig. 74).

MF8 :- this sample of magnesite consists of similar but coarser material to that in MF7. There was hematite zoning present, and also intragranular chalcopyrite and pyrite. A large rhomb-shaped crystal (2cms across diagonally) was used to cut a thin section for study. This crystal contained intragranular chalcopyrite. Although the temperature was held at -120°C for 15 minutes, the liquid in none of the fluid inclusions

Fig. 76: Homogenisation temperature vs Final melting temperature.
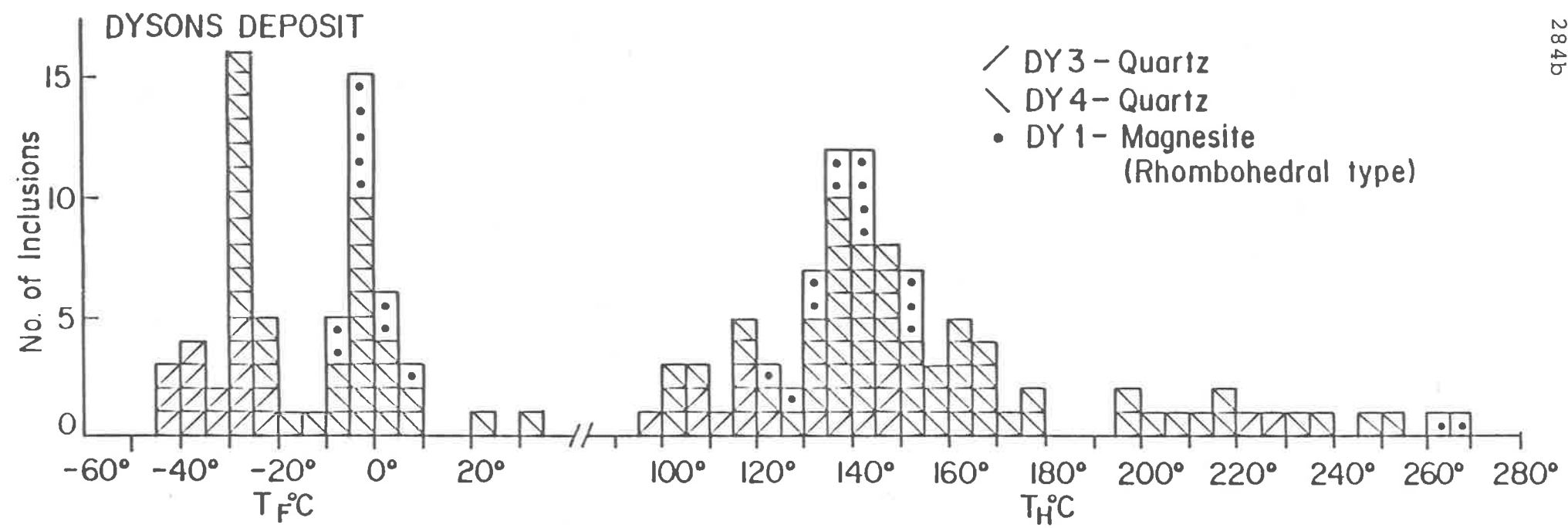
Fig. 77: Histograms of final melting and homogenisation temperatures.

froze. This lack of freezing not only included fluid inclusions with many daughter minerals (Plate 34), which one would expect to be highly saline anyhow, but also those in the long trails of negative-crystal type, which contained a liquid phase only (Plate 34). T_h occured over a restricted range of 98.2°C to 138.5°C (Fig. 74).

Many of the fluid inclusions contain several daughter minerals; always including a bright orange hexagonal crystal (Plate 35) which is probably hematite. This observation applies to inclusions with a vapour phase and not to monophase liquid filled inclusions. The size of this hematite daughter mineral is always related to the size of the fluid inclusion. This feature is discussed further in the section on Daughter Minerals. It was not possible to identify other daughter minerals present with any degree of confidence. In some cases, they (6 or more) appear to have precipitated on the wall of the fluid inclusion (Plate 34). The fluid inclusion always decrepitated prior to the dissolution of any of these daughter minerals.

As this crystal contains chalcopyrite, the brine in the fluid inclusion could have been associated with the transport and deposition of the sulfide. This does not, however, necessarily mean that this was the primary mineralising event.

Samples MF2, MF3, and MF5 show the inverse relationship between salinity and temperature (Fig. 72).

6.4 Dysons Deposit

Three samples were selected from those collected from the old mine dumps at Dysons Deposit.
DY1 :- this sample consists of rhombohedral type, translucent to opaque magnesite, with minor hematite. The fluid inclusions in this sample gave

Fig. 78:   Homogenisation temperature vs Final
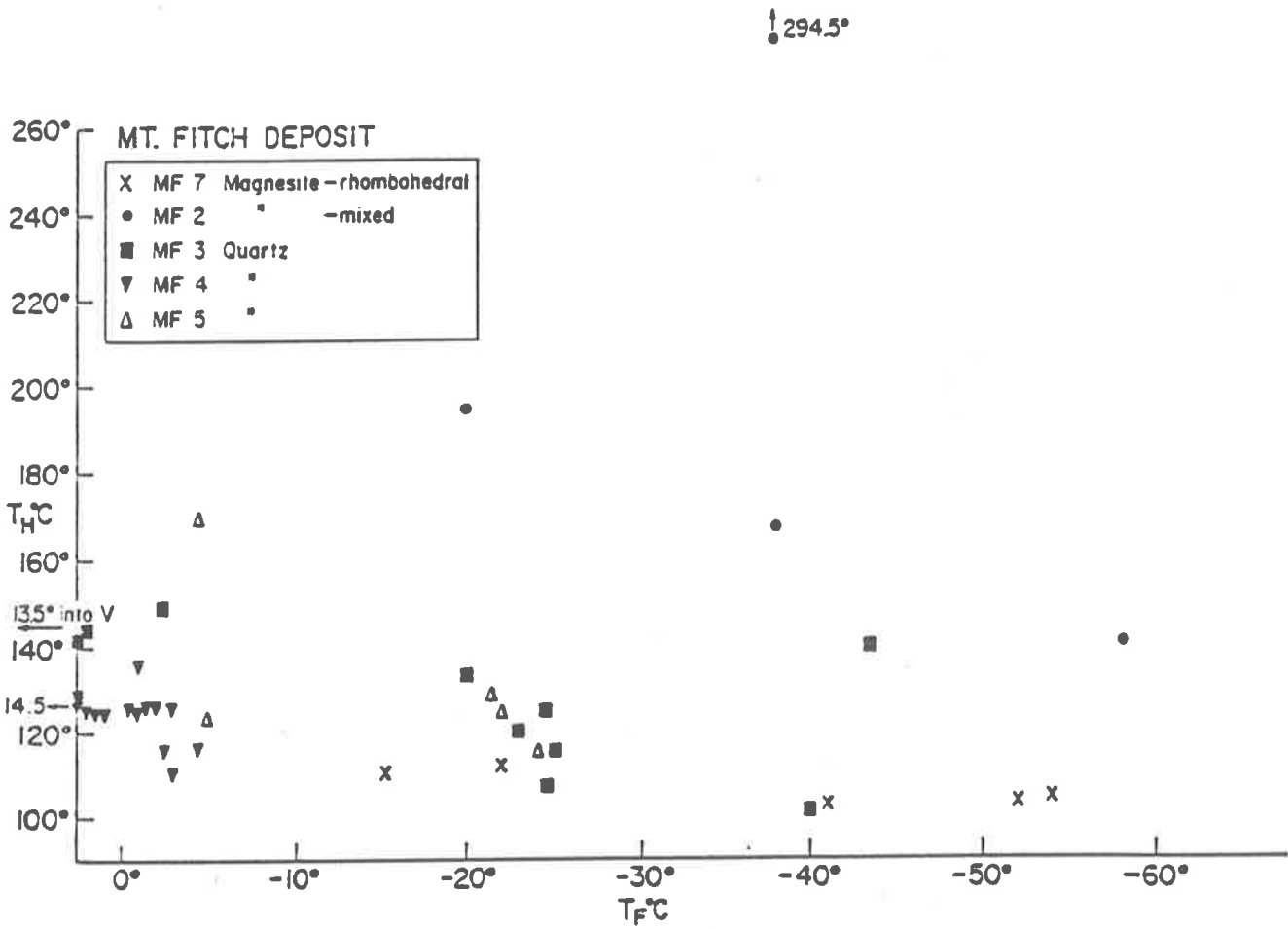melting temperature.
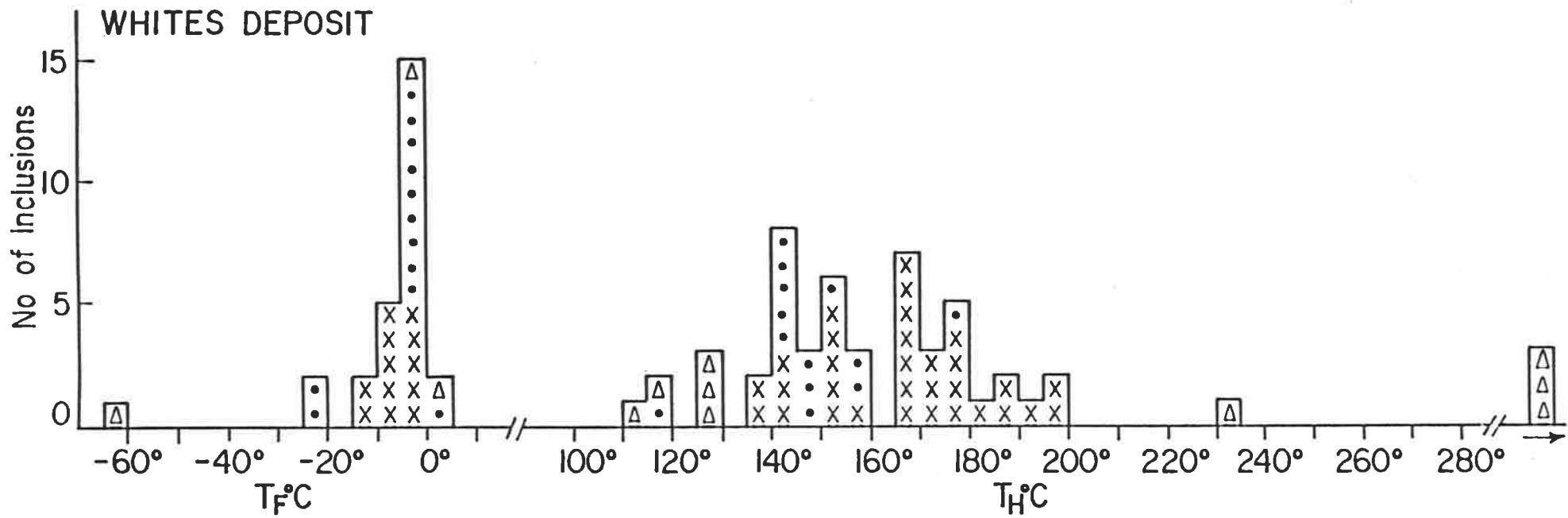
Fig. 79: Histograms of final melting and homogenisation temperatures.
See Fig. 78 for legend.
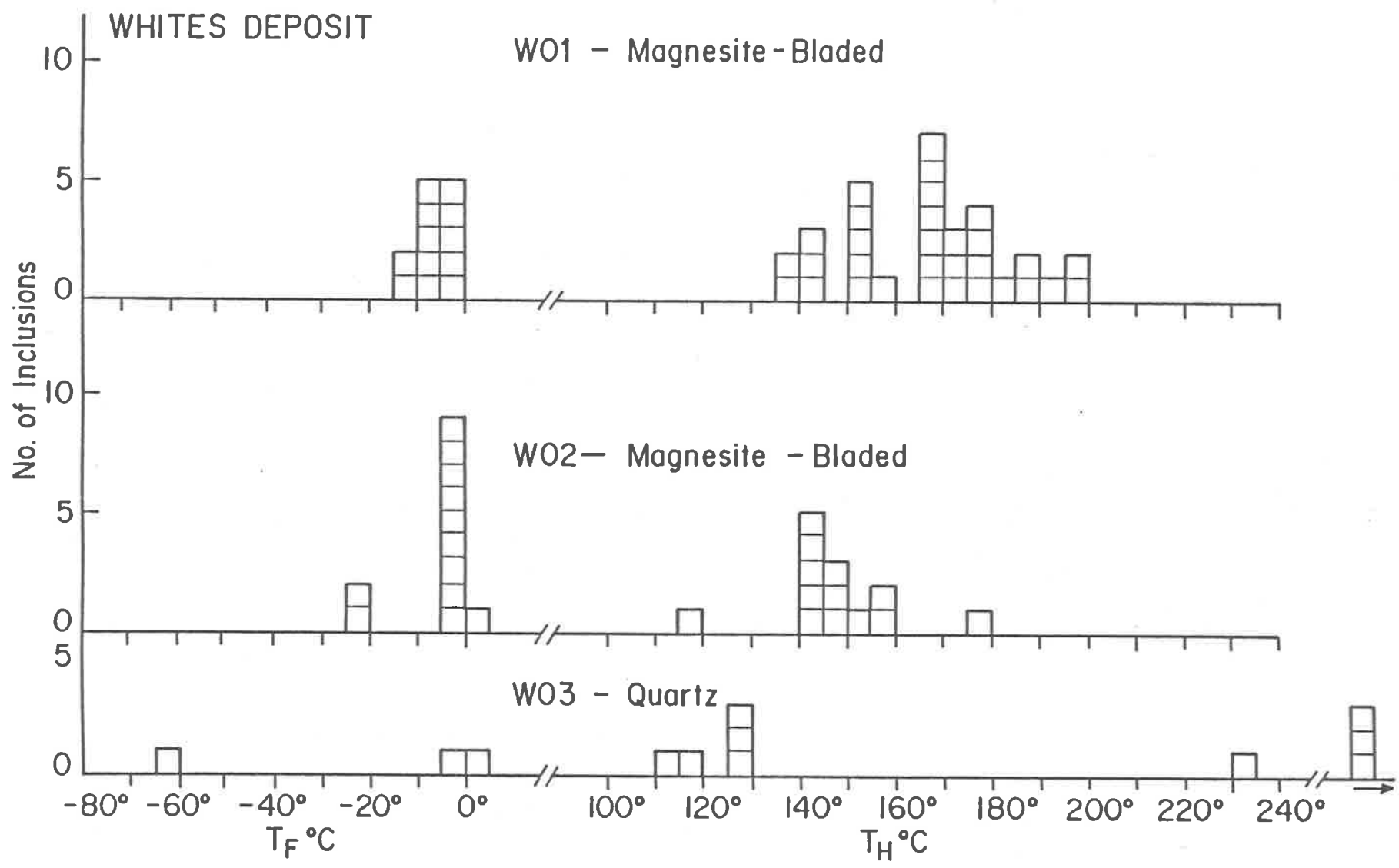
Fig. 80: Histograms of final melting and homogenisation temperatures.

consistently high T_f figures (Fig. 76). The T_e values could only be determined for two fluid inclusions (-37°C and approximately -36°C). These values indicate a mixed chloride brine. Therefore it may be that T_f is actually T_m of an unrecognised hydrate, bearing in mind the size of the fluid inclusions.

DY3 :- this sample consists of crystalline quartz with minor amounts of shale and pyrite. All but one of the fluid inclusions were less than 10 ms, so that it was very difficult to be sure of the presence of ice. However, as five of the fluid inclusions had a T_e below that of $NaCl+MgCl_2+CaCl_2$ it is necessary to invoke additional components (Fig. 76).

DY4 :- this sample consists of carbonaceous shale with ubiquitous pyrite crystals and anastomosing quartz veinlets and discrete quartz grains. It also contains minor chlorite and tourmaline.

There were three distinctly different types of behaviour exhibited by the fluid inclusions when they were subjected to cooling:-
(a) Vapour phase suddenly dissappears at approximately -37°C, and reappears suddenly i.e. "pops" on heating at temperatures up to +30C. in about 70% of the case (b) vapour phase shrinks considerably upon freezing in about 20% of the case (c) no freezing occurs in about 10% of the cases.

Possible explanations have been presented previously.

All three samples show an inverse relationship between salinity and temperature (Fig. 77).

6.5 White Deposit

Three samples were selected from those collected at the old mine dumps at Whites Deposit (Figs 78, 79).

W01 :- this sample consists of bladed type white magnesite, with some
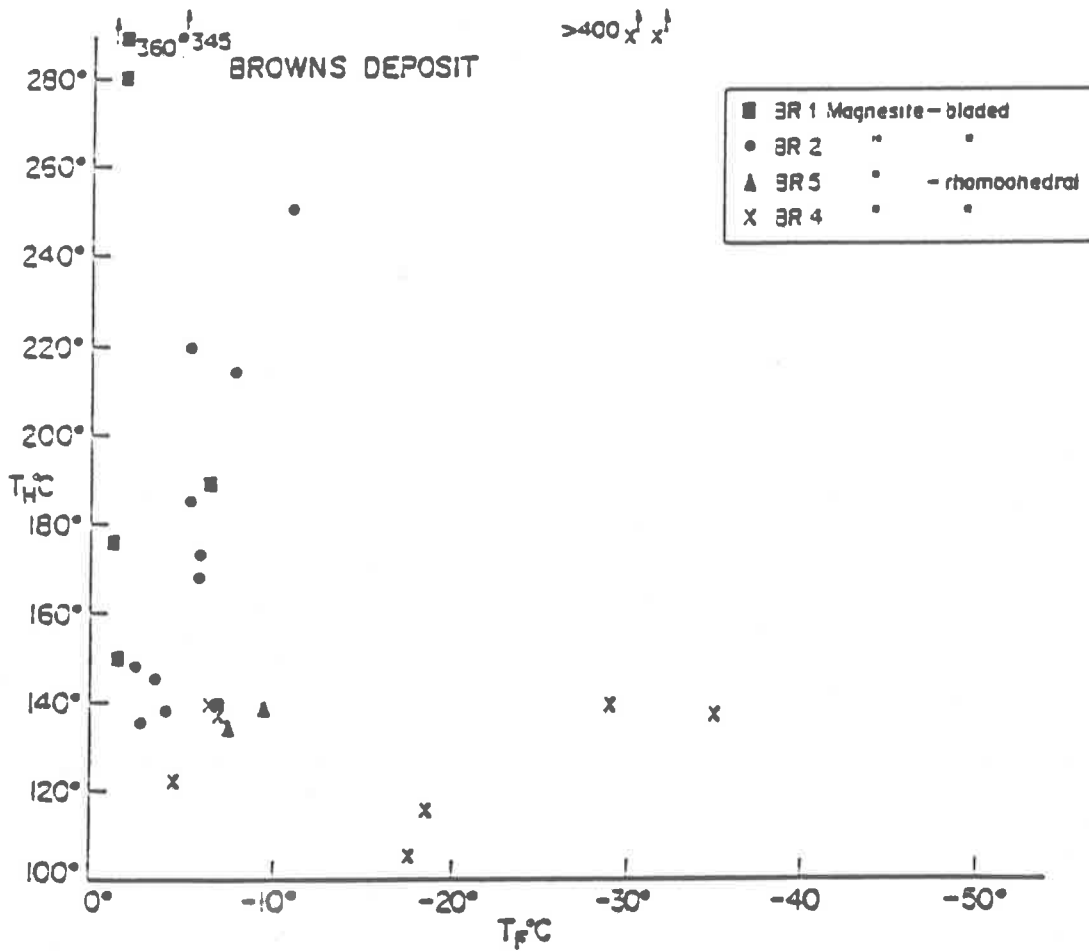
Fig. 81: Homogenisation temperature vs Final
melting temperature.
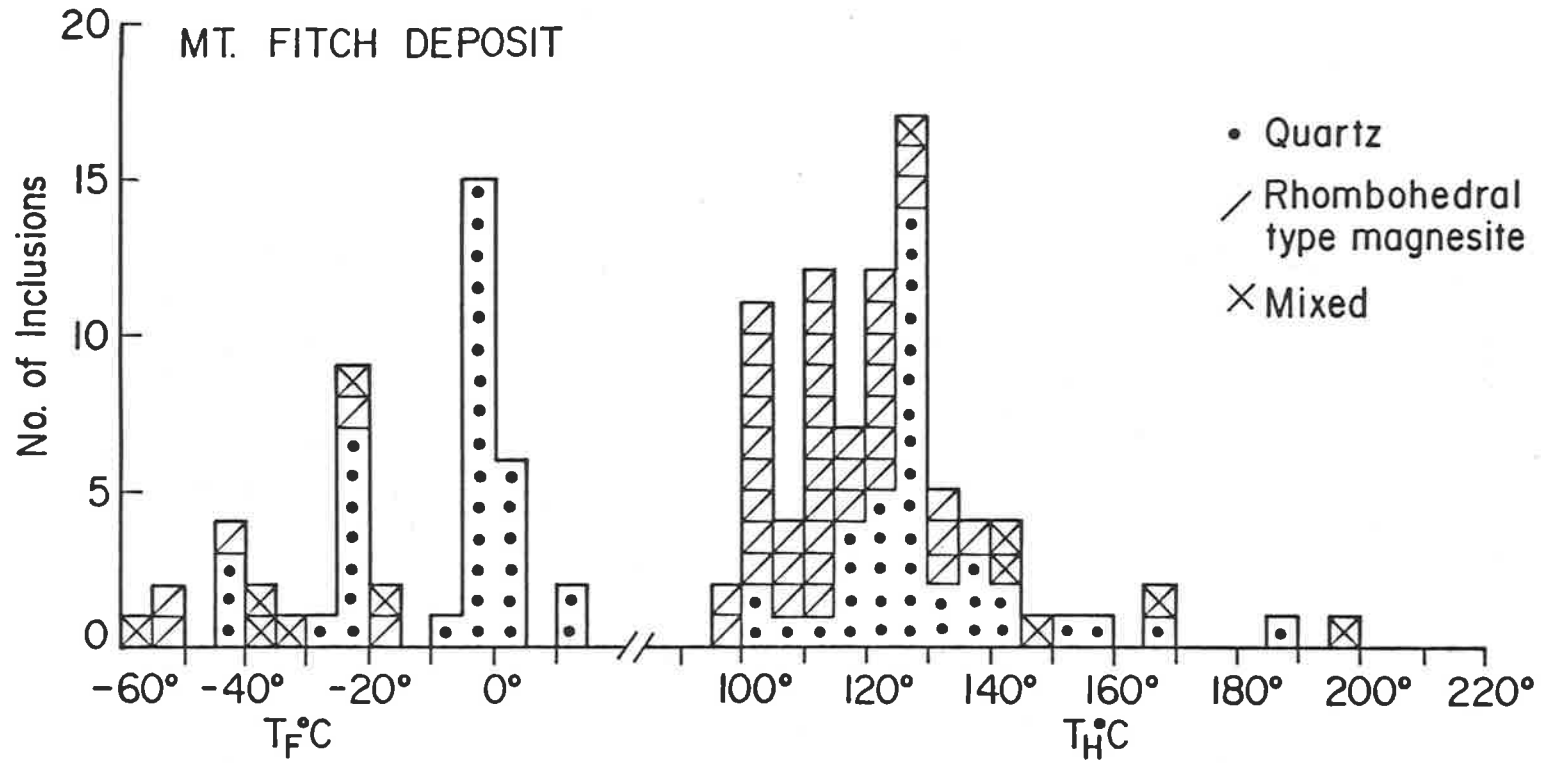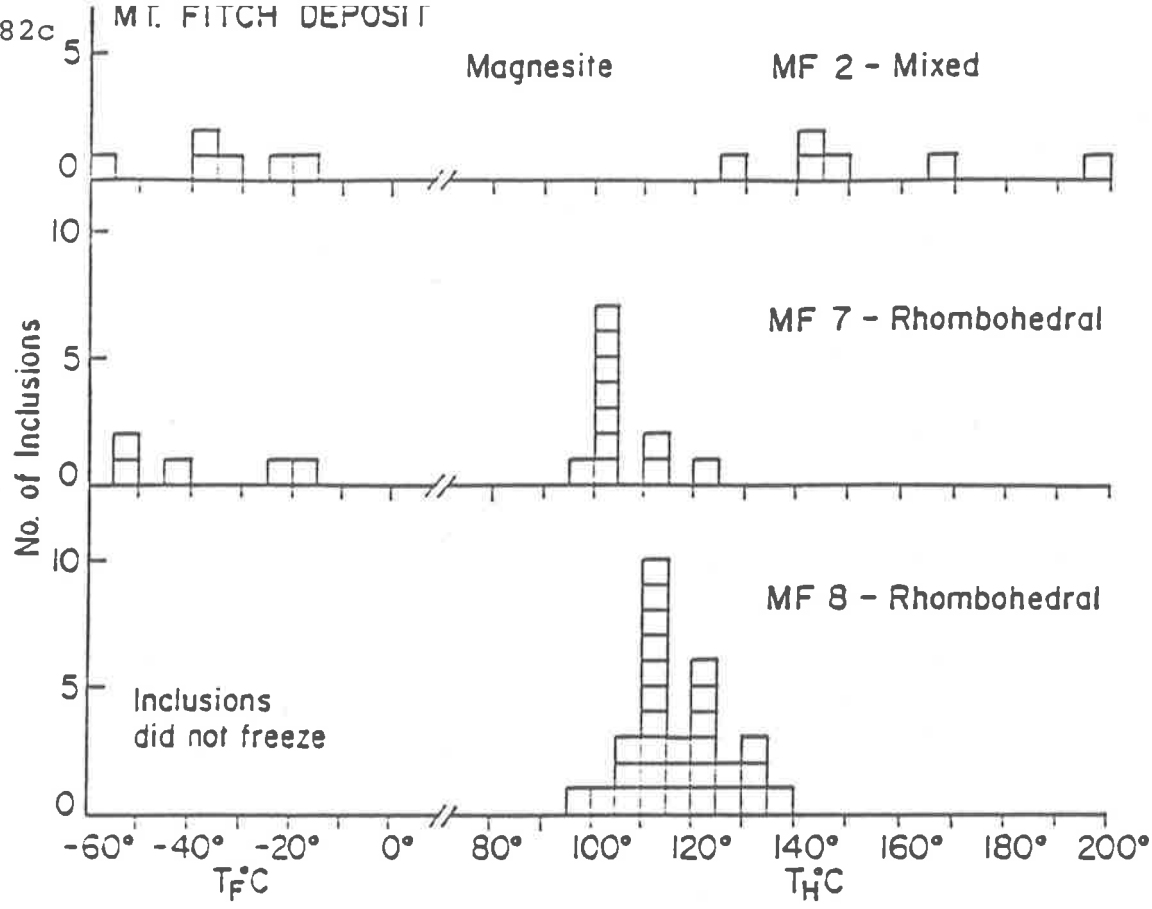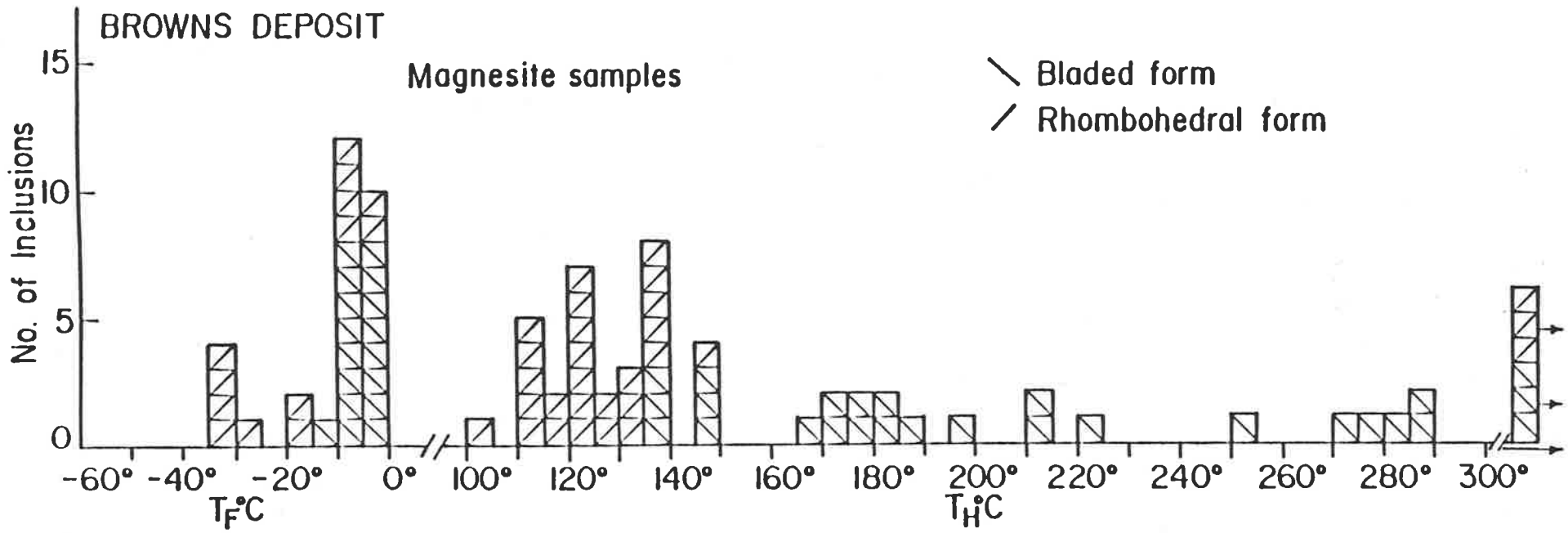
Fig. 82: Histograms of final melting and homogenisation temperatures.
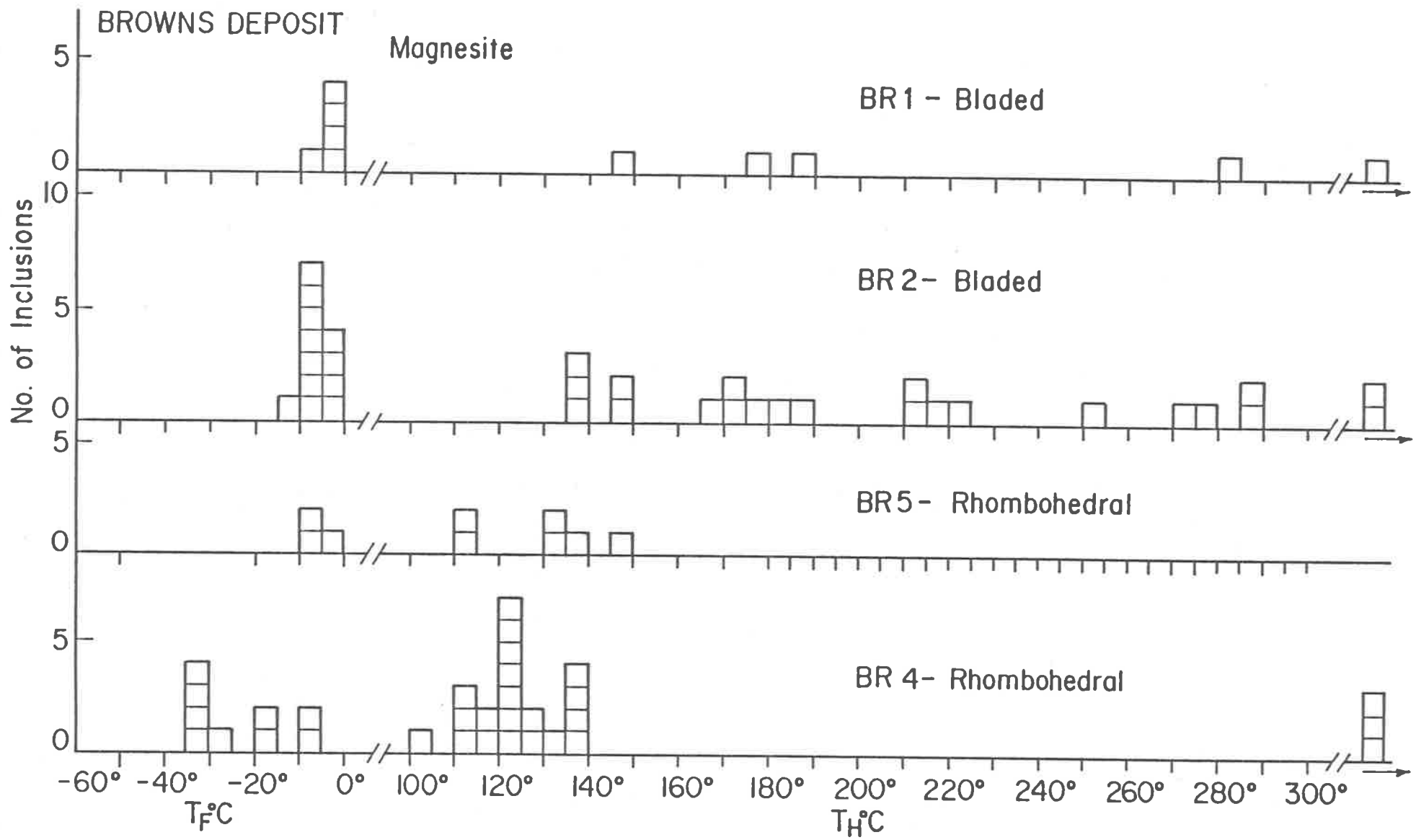
Fig. 83: Histograms of final melting and homogenisation temperatures.

malachite staining. There was a narrow range of temperatures for both T_h, T_f and T_e in this sample i.e. 137.2°C to 197.3°C, -10.6°C to -3.0°C and -45°C respectively (Fig. 80). None of the fluid inclusions contained daughter minerals (Fig. 80)

WO2 :- this sample consists of magnesite showing both morphologies, plus discrete quartz blebs. The boundary between quartz and magnesite has the appearance of a stylolite, and has carbonaceous and chloritic material concentrated along it. The fluid inclusions exhibit similar behaviour to those in the previous sample (Fig. 80).

WO3 :- this sample consists of magnesite and quartz similar to that in WU2, plus a part of a larger clast of breccia (Plate 22). The boundary between quartz and magnesite is extremely convoluted. The breccia consists of clasts of carbonaceous shale (? Whites Formation) and shaly psammite, which have both been cross cut by narrow veins (less than 2mms) of magnesite. These veins also cut the magnesite and the quartz (Plate 22).

The fluid inclusions selected for study occur in the quartz. They consist of intragranular arcuate trails. Although the presence of a CO_2 phase could not be confirmed there is certainly a suggestion of its presence e.g. low T_f high T_h and dark appearance of the bubble (Fig. 80).

6.6 Browns Deposit

The four samples studied from the Browns Deposit were selected from drill core, which was kindly supplied by C.R.A. Exploration, Darwin, (Figs 81, 82).

BR1 :- this sample consists of coarse, bladed type magnesite, with some hematite. Most of the fluid inclusions appear to be related to cleavage. Many of the smaller fluid inclusions contain daughter minerals, with some having a daughter mineral but no vapour phase.

PLATE 39

a. Bladed form magnesite at Balcanoona, South Australia. The similarity to the bladed form magnesite at Rum Jungle is remarkable.

b. Magnesite outcrops at Rum Jungle masquerading as a herd of 'elephants.' Area B, Celia Dolomite, E.L. 1349.

c. Exhumed karst is Area A, Coomalie Dolomite, E.L. 1349.
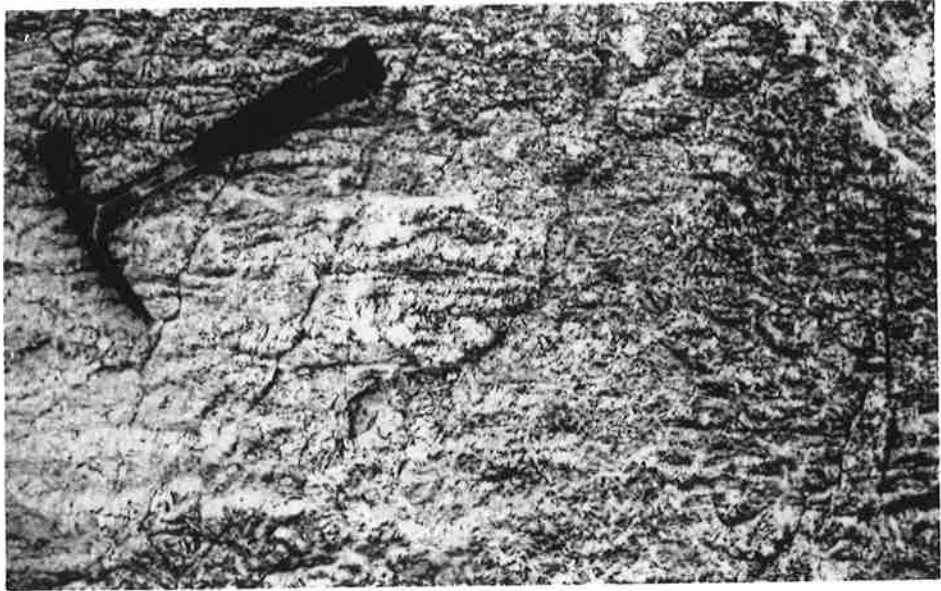
Two distinctly different types of behaviour are seen when cooling this sample (Appendix 2, Fig. 83). In one case, the bubble disappears at approximately $-45^{o}C$, which indicates a high pressure CO_2 rich fluid. In another case the vapour phase expands until it almost completely fills the fluid inclusion, which suggests a CO_2-rich fluid inclusion - even though this was not seen as a three-phase fluid inclusion at room temperature.

BR2 :- this sample is similar to BR1. Although not seen, the dark appearance of the vapour phase certainly suggests that there may be CO_2 present. The range of homogenisation temperatures (Fig. 83) also suggests that the higher limit of the range may be approaching T_{tot} - which implies that although there is some CO_2 present, the internal pressure is not sufficient to exert an overpressure (resulting in decrepitation).

BR4 :- this sample consists of predominantly carbonaceous shale (? Whites Formation) with interspersed rhombohedral type magnesite grains and disseminated pyrite, with the latter occurring as both microscopic-fine grains and as quite large anhedral grains. The magnesite contains intragranular solid inclusions of quartz, apatite and tourmaline.

Five fields of view were selected for study, as this sample contained a variety of usable fluid inclusions (Plates 35, 36 - Appendix 2). The data (Fig. 83) supports the premise of mixing of a presumably higher temperature CO_2-rich fluid and a lower temperature highly saline fluid, as the minimum number of phases involved in the system.

BR5 :- this sample is from a breccia zone, and consists of clasts of carbonaceous shale (? Whites Formation), some of which are mineralised, together with clasts of pyrite up to 1.5cms in length in a matrix of coarse, white, rhombohedral type magnesite. There are minor small euhedral grains of pyrite within the magnesite. The magnesite has recrystallised in two different stages.

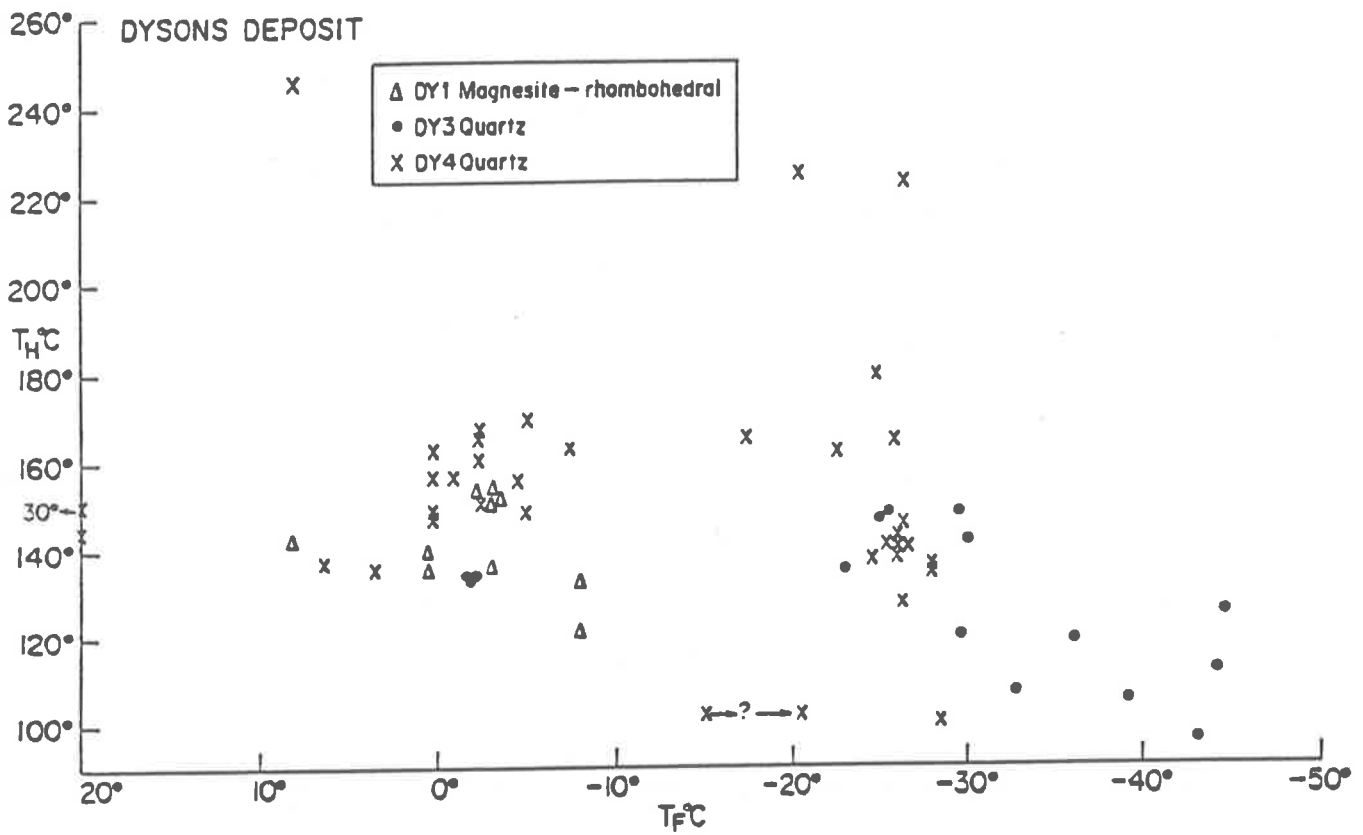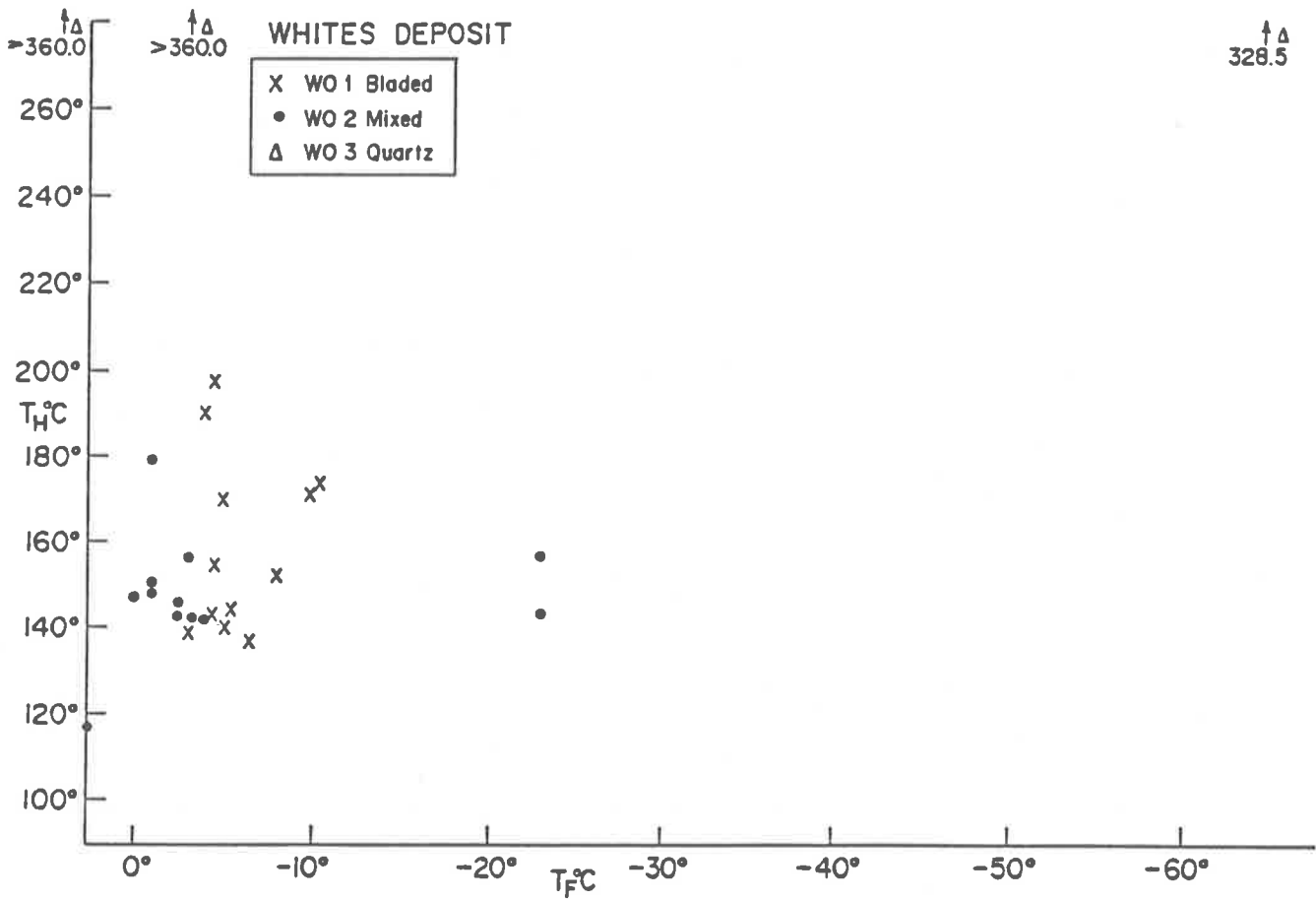All the fluid inclusions appear to be related to cleavage. Many of

Fig. 84: Homogenisation temperature vs Final melting temperature.
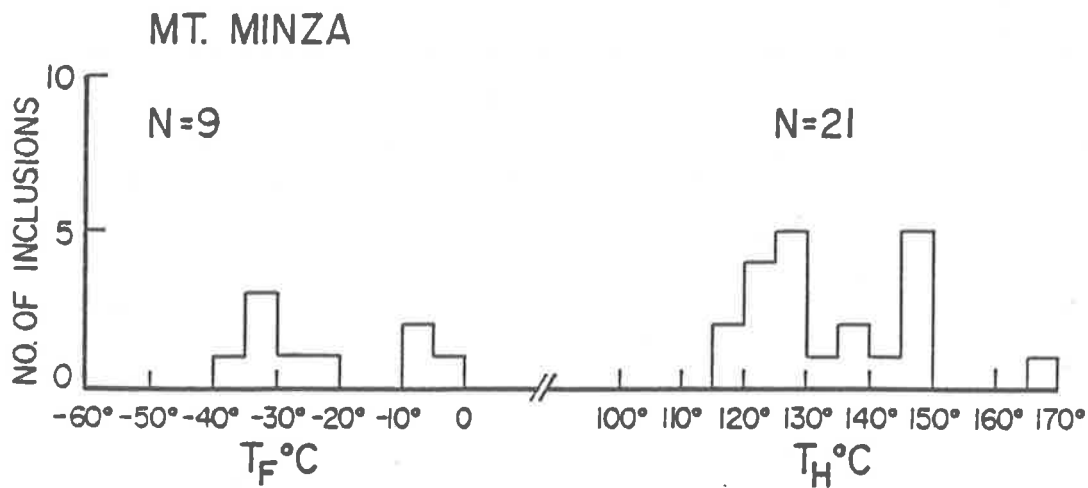
Fig. 85: Histograms of final melting and homogenisation temperatures.

the fluid inclusions are filled with a brown liquid phase, distinctly
different from the more common colourless liquid. The clear liquid filled
inclusions have a much smaller vapour phase and appear to be more
pervasive. The brown liquid filled inclusions appear to be related to
fractures rather than to cleavage. It has been suggested that this
unusual colouration may be due to the transparent nature of the carbonate,
so that total reflection from the cleavage faces is occurring. However
this phenomenom was not observed in any other carbonates except those
associated with sulphide mineralisation.

6.7 Mt. Minza

There was only one sample available from this area (C.R.A.
Exploration drillcore). This sample consists of coarse, rhombohedral type
magnesite, which in part was very rich in hematite, both intra- and
inter-granular to the magnesite.

The cooling runs on 21 fluid inclusions failed to freeze the liquid
of 12 of the fluid inclusions, indicating a high degree of metastability.
No fluid inclusion indicated optically that a CO_2 phase was present.
One fluid inclusion showed an ice T_m of $-35.5^{\circ}C$, then formed a hydrate
(? $CaCl2.6H2O$) which melted between $-3.8^{\circ}C$ and $-2.9^{\circ}C$, which behaviour
indicates a salinity of approximately 35wt % $CaCl2$. This has been
expressed as wt % $CaCl2$ due to the low T_e of $-50^{\circ}C$. Another fluid
inclusion that had a T_f of $-7.7^{\circ}C$ contained two daughter minerals
(Plate 37), one of which was red, not unlike the Mt. Fitch material.
However, this was the only fluid inclusion containing daughter minerals.
No explanation can be offered for the fluid inclusion that had an
exceptionally high T_f of $-2.5^{\circ}C$ especially as this fluid inclusion's
T_h was not any different from those of the area. When looked at on a
regional scale, it does slot into the low salinity brine. The remaining
five fluid inclusions melted in the range of $-21.3^{\circ}C$ to $-32.9^{\circ}C$, but
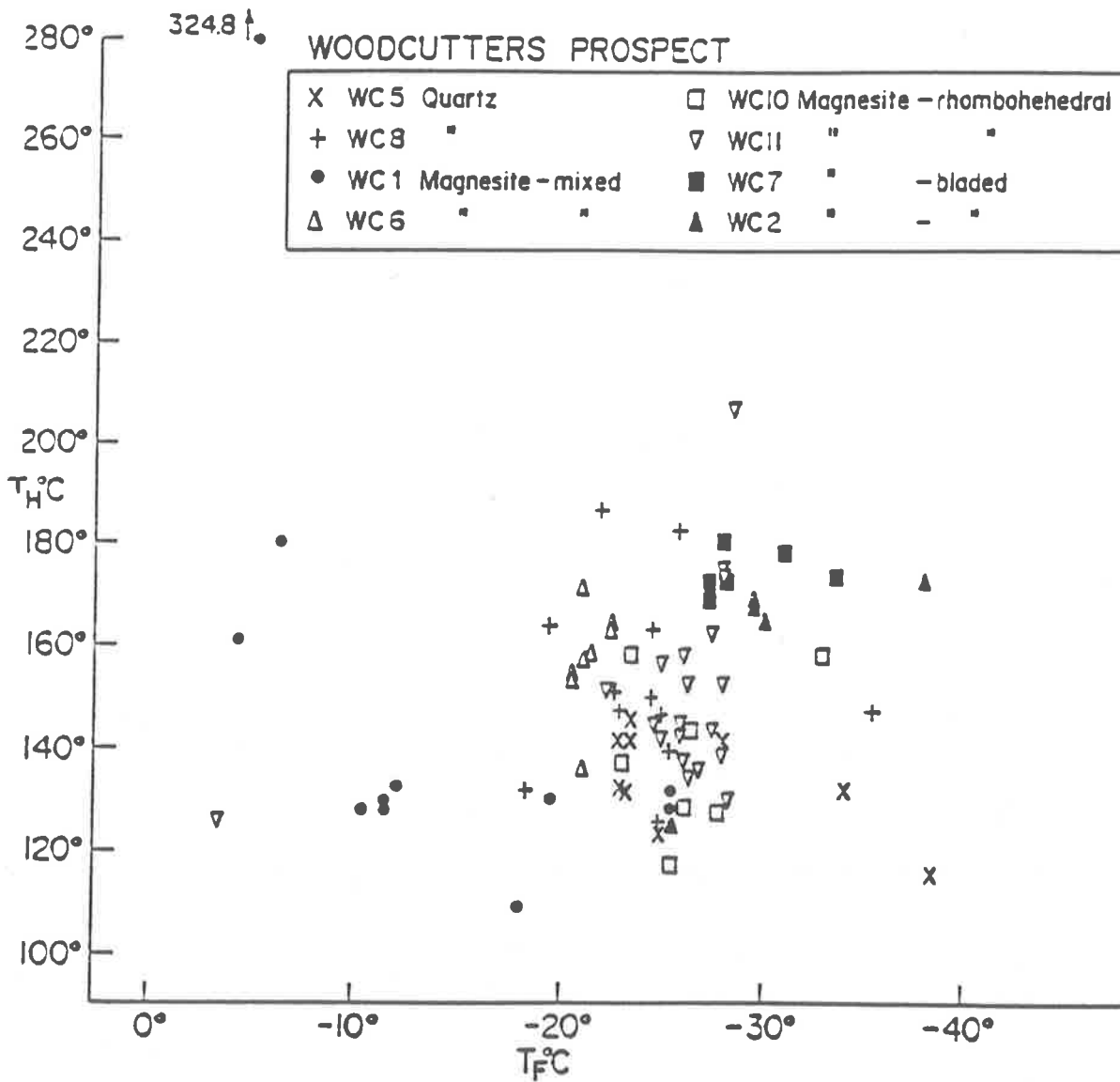
Fig. 86: Homogenisation temperatures vs Final melting temperature.

all of them had a T_e of approximately $-50^{\circ}C$, indicating a $CaCl_2$-rich brine of 24 wt % $CaCl_2$ ± 2% (Figs 84, 85).

6.8 <u>Woodcutters Prospect</u>

Geopeko kindly supplied core material from one of their drill holes in this area, and it was from this material that sections were cut for study (Figs 86, 87).

WC1 (42.73m) :- this sample consists of exceptionally well-zoned magnesite rhombs within a matrix of bladed type magnesite. The rhombs had dark grey carbonaceous cores, with white rims. Carbonaceous material was concentrated along the stylolites which in places truncated the rhombs, similar to that shown in Plate 23. Small carbonaceous shale fragments contain ubiquitous chlorite grains and some euhedral pyrite grains.

The fluid inclusions in the magnesite give the impression of containing CO_2 in some cases, although this could not be confirmed optically at room temperature. Assessment of the data suggests the presence of a low temperature brine - of approximately 5-23 wt.% $CaCl_2$ equivalent (Fig. 88). Plate 38 shows the metastable phase behaviour frequently seen.

WC2 (143.00m) :- this sample consists of material similar to WC1 except that the magnesite is all of the bladed type (Fig. 88). The fluid inclusions are mainly related to cleavage.

WC5 (28.80m) :- this sample consists of grey and white magnesite, without any zoning. The grain size is much finer than the previous two samples. Stylolites are well preserved. Quartz blebs have white cores and grey rims, with a transitional boundary, suggesting that the impregnation of the quartz by the carbonaceous material occurred after the formation of the quartz. The fluid inclusions studied occurred in this quartz.
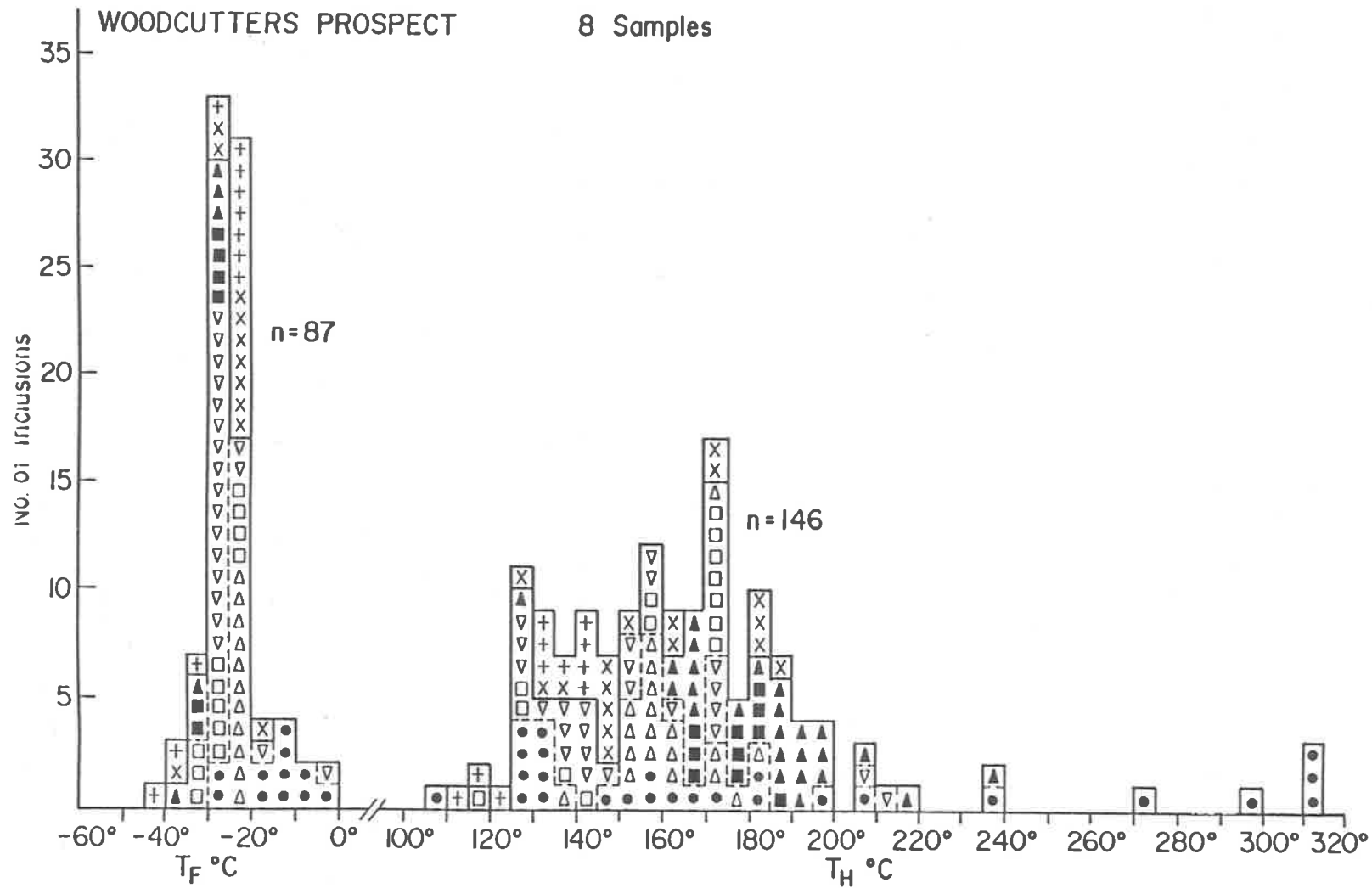
Fig. 87: Histograms of final melting and homogenisation temperatures.
See Fig. 86 for legend.
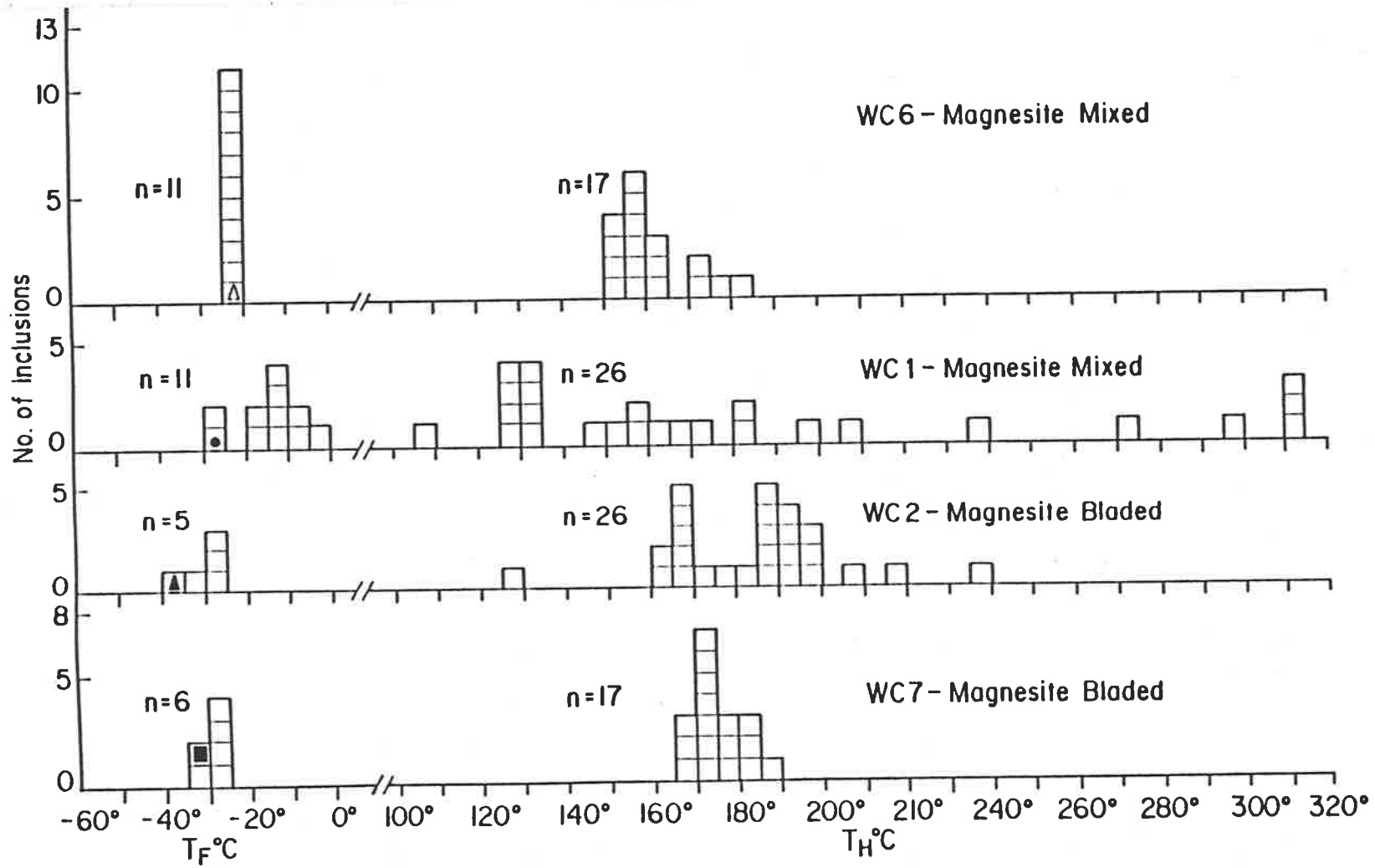
Fig. 88: Histograms of final melting and homogenisation temperatures.
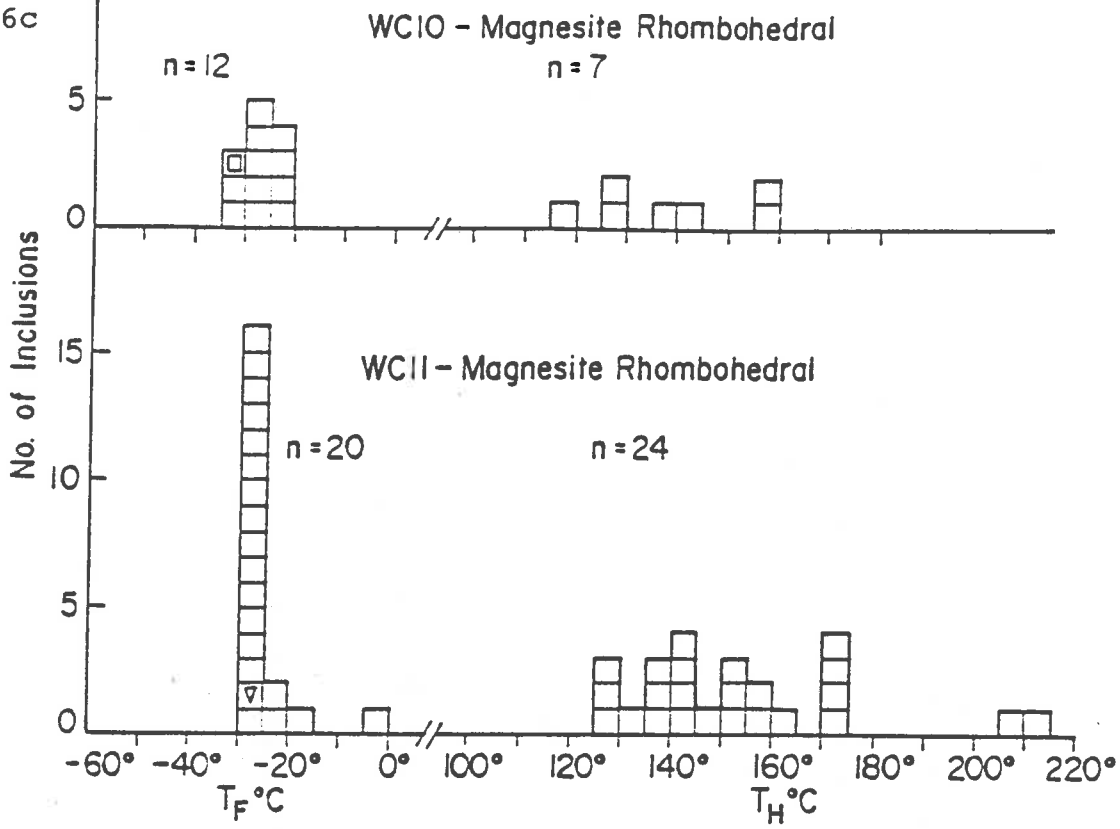
Fig. 89: Histograms of final melting and homogenisation temperatures.
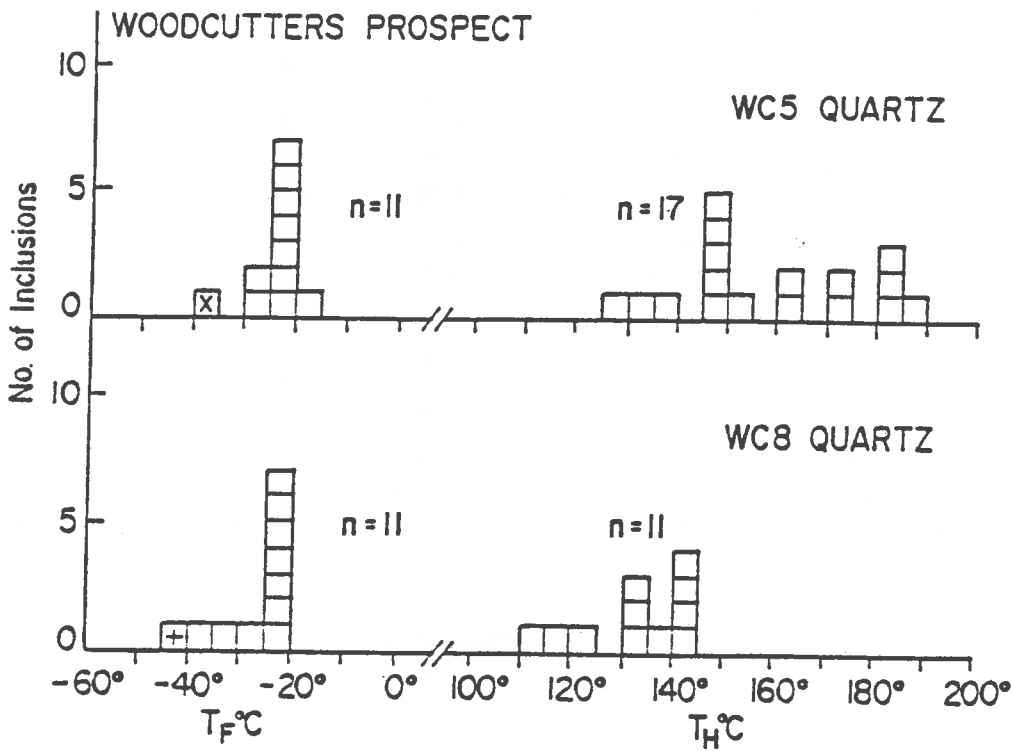
Fig. 90: Histograms of final melting and homogenisation temperatures.

Three of the fluid inclusions have a T_e of less than -57^oC (Fig. 90).

WC6 (97.25m) :- this sample consists of two quite different types of magnesite - one being the same as that in WC2, the other consisting of large (up to 2 cms in length) crystals of talc rich magnesite (Fig. 88).

WC7 (68.70m) :- this sample consists of blades of white magnesite and amorphous blebs of pink talc in a carbonaceous matrix. The fluid inclusion data suggests a low temperature saline brine (Fig. 88).

WC8 (15.22m) :- this sample consists of opaque, fine grained quartz with some talc blebs. Many of the fluid inclusions formed a $CaCl_2$ hydrate during the cooling runs, so that a true salinity figure cannot be obtained from T_f (Fig. 90). It is unfortunate that theoretical data for the system $NaCl + CaCl_2 + MgCl_2$ is unavailable, as analyses of these brines show that all three cations are present.

WC10 (90.80m) :- this exceptionally pure sample of white rhombohedral type magnesite was one of the few from this area to appear to have daughter minerals present in the fluid inclusions (Fig. 89). These were of uncertain affinity, having the appearance of a thin wavy line (dawsonite?).

WC11 (60.30m) :- this sample consists of white and grey rhombohedral type magnesite. The results from the 24 fluid inclusions studied were very consistent and uncomplicated, and indiate a low temperature, saline (24 wt. % $CaCl_2$) brine (Fig. 89).

The Woodcutters Prospect area does not appear to have been significantly affected by the maximum temperature stage of the higher temperature CO_2 rich fluids i.e. it does not appear that its rocks have been modified by either tectonic or magmatic influence. Why this should be so will be discussed in more detail later.

6.9 Balcanoona, South Australia

The magnesite from this location was chosen for comparison studies
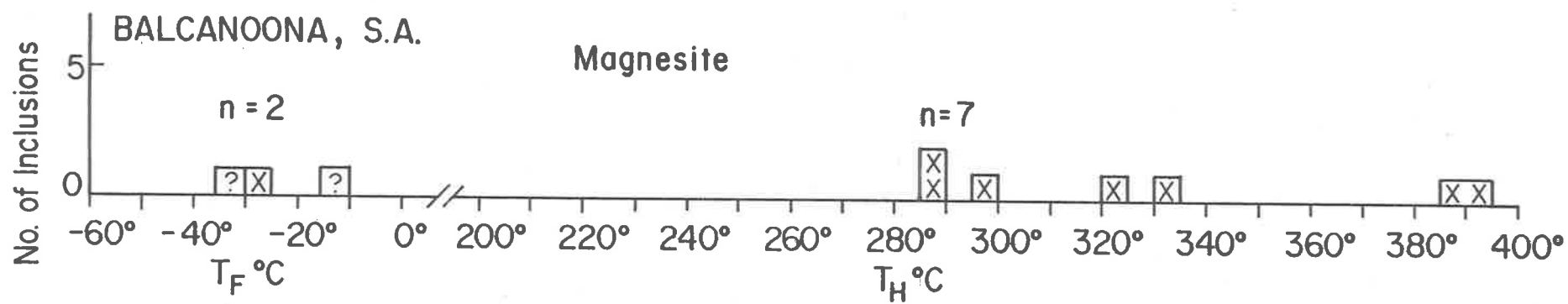
Fig. 91: Histograms of final melting and homogenisation temperatures.

because of similar appearance to the magnesite at Rum Jungle (Plate 39). The deposit and its genesis is discussed by Johns (1976). It weathers to give the familiar "elephants" of Rum Jungle. Indeed, it is difficult if not impossible to allocate the correct location to unlabelled specimens. The one apparent difference is the lack of rhombohedral type magnesite at Balcanoona.

Only one sample was selected for study, and from this ten fluid inclusions from two fields of view were studied. The fluid involved in the recrystallisation of this magnesite was a medium-temperature - saline brine (Fig. 91). No evidence of the presence of CO_2 was observed.

6.10 Kharidunga, Nepal

Although the magnesite deposit currently being worked at Kharidunga (Plate 40) was visited to test another aspect of this study, the immediate impact upon arrival at the site was that here again were the familiar "elephants" (Plate 40). Closer inspection confirmed that this material also was visually exactly the same as that at Rum Jungle and Balcanoona (Plate 40, 41). Vigorous searching during a day spent on site failed to locate any true rhombohedral type magnesite, but in all other aspects the similarity was amazing. Four samples were selected for comparison studies (Figs 92, 93).

N1 :- this sample contains blades of white-rimmed grey magnesite, associated with mica, (phengite). Thirty fluid inclusions in three fields of view were tested. The results (Fig. 94) show that there have been two different brines involved; a medium temperature CO_2 rich brine and a medium temperature $CaCl_2$ rich saline brine.

N2 :- this sample consists of white bladed type magnesite, with flakes of mica and microscopic interstitial talc. Although there are no CO_2 type fluid inclusions visible, some of the very small fluid inclusions could well contain a small volume of CO_2 as suggested by the dark rims of the
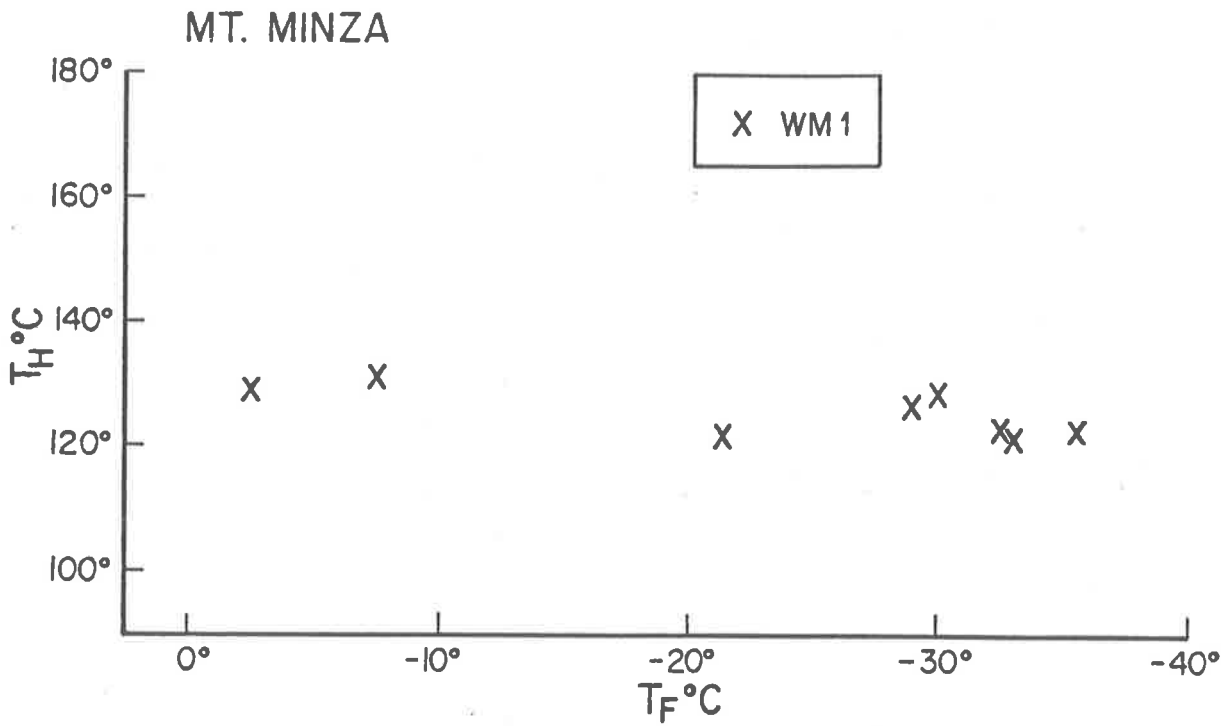
Fig. 92: Homogenisation temperature vs Final melting
temperature.
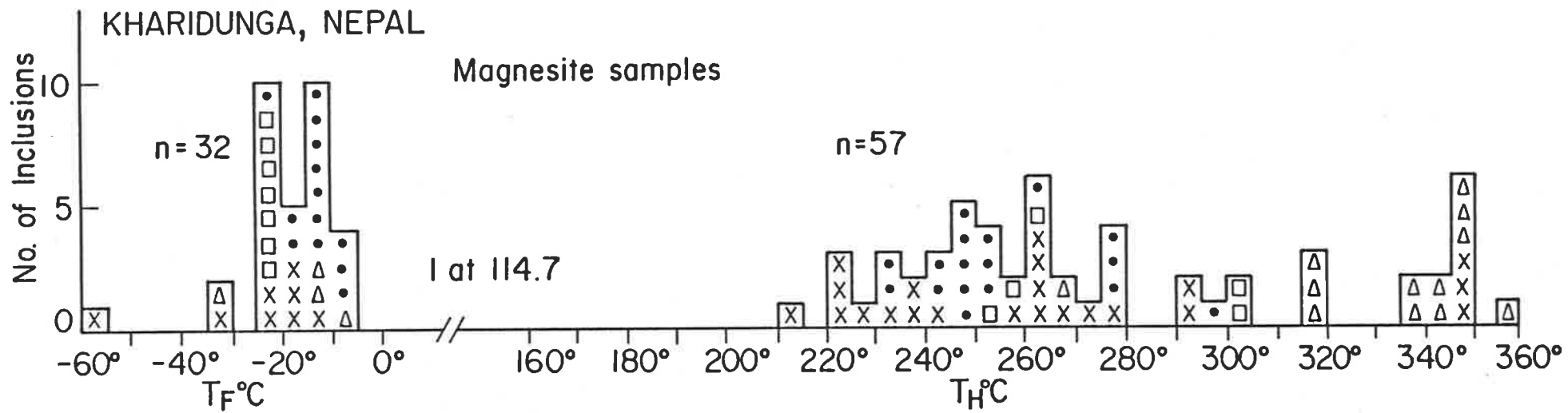
Fig. 93: Histograms of final melting and homogenisation temperatures.
See Fig. 92 for legend.
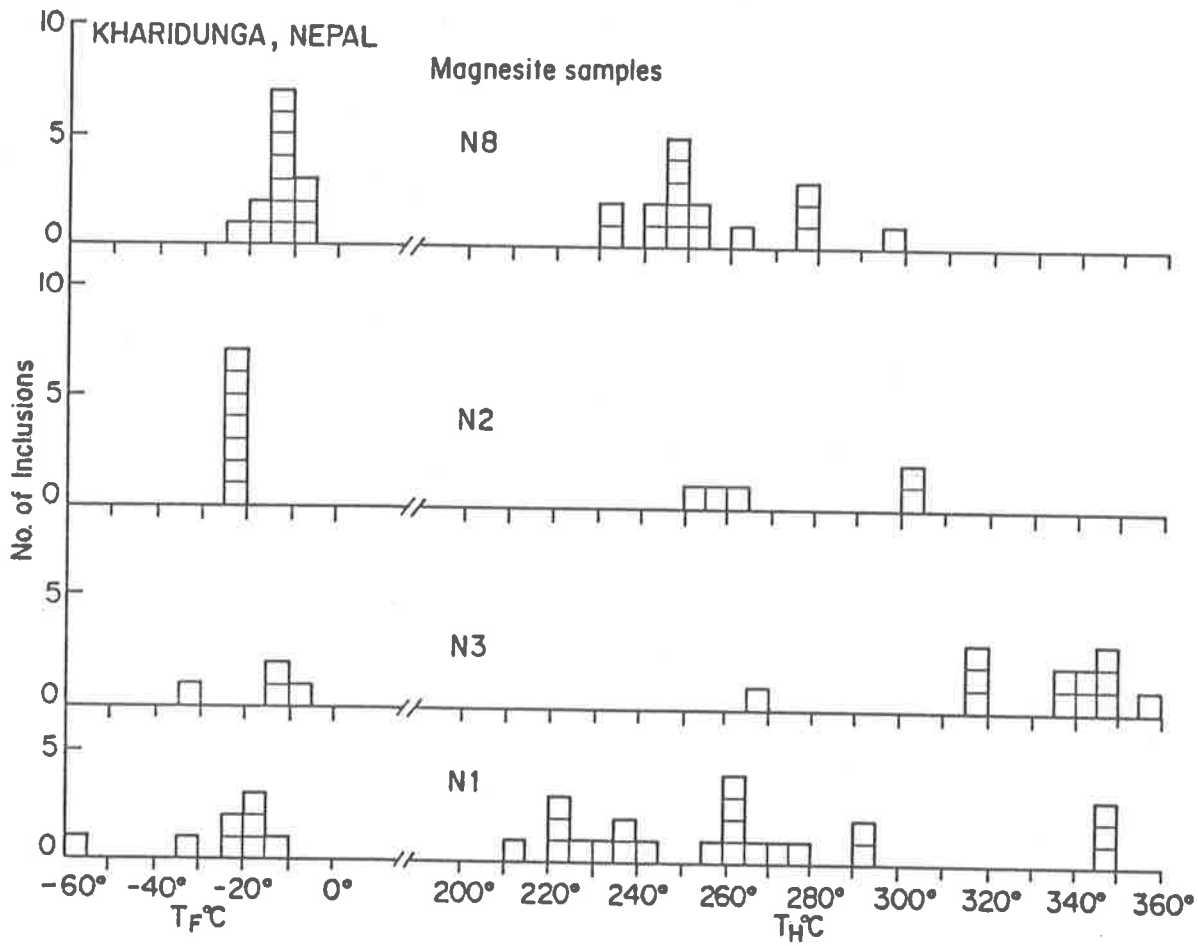
Fig. 94: Histograms of final melting and homogenisation temperatures.

vapour phase. This was not confirmed by T_e, and although two fluid inclusions formed a solid phase during the freezing runs which melted at 0.0^oC and $+ 5.0^oC$, these could have been hydrates rather than clathrates. For the other fluid inclusions a saline brine (approximately 22 wt. % $CaCl_2$) of medium temperature is suggested (Fig. 94).

N3 :- this sample (Plate 41) is similar to N2. Many of the larger fluid inclusions are three phase CO_2 type. There are also many trains of fluid inclusions that transect grain boundaries; others with daughter minerals do not have a CO_2 phase - but all three types show the same morphology. The CO_2 contents studied homogenised into the vapour phase (i.e. $T_h CO_2$ - Figs 60, 94).

N8 :- this sample is different to the others inasmuch as it was collected stratigraphically above the magnesite horizon, and is associated with massive sulfides. It superficially resembles rhombohedral siderite (Plate 41), but probe analyses confirm that it is magnesite. The sulfide veins (predominantly pyrrhotite with minor chalcopyrite) cut across grain boundaries, and also preferentially follow cleavage traces (Plate 41).

The brine associated with this sample does not appear to have been as saline as in the other samples from lower in the sequence (Fig. 94). One anomalous fluid inclusion (small gas phase) gave, and reproduced, a T_h of 114.7^oC, but unfortunately no T_f could be obtained. Approximately half of the fluid inclusions viewed homogenise into the vapour phase at around 250^oC. Others which had not homogenised at this temperature would have homogenised into the liquid phase if the sections had not decrepitated at 299^oC. No fluid inclusions with convincing CO_2 phases present were observed.

The brines involved in the recrystallisation of the magnesite at Kharidunga appear to have been similar to those at Rum Jungle, except that they did not decrease in temperature to the same extent, and consequently become neither as saline nor able to form rhombohedral type magnesite.

PLATE 40

a.   General view of magnesite mining operations at Kharidunga, Nepal.

b.   The magnesite is mined by open-cut methods but with little

       mechanisation.   In the middle foreground is the remnants of an

       'elephant'.

c.   Outcrop of bladed-type magnesite at Kharidunga, Nepal.   The

       similarity to the bladed form at both Rum Jungle and Balcanoona

       is obvious.
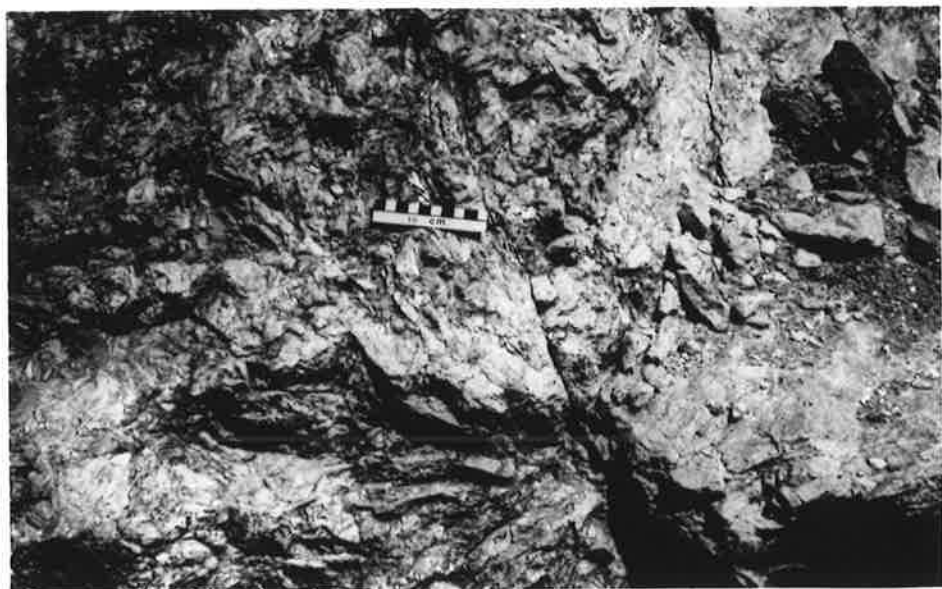
6.11 Fluid Analysis

6.11.1. Qualitative analysis of the fluid in the fluid inclusions.

The data obtained by microthermometric techniques has led to the theoretical calculation of the composition of the fluids contained within fluid inclusions. This was at first, calculated in terms of NaCl equivalent brines, by reference to existing chemical data. Later, when the significance of the depressed first melting temperature was appreciated, and it was recognised that the presence of other components was necessary for this temperature to fall below that of the eutectic for the $NaCl - H_2O$ system, it became expedient to calculate the composition in terms of $CaCl_2$ - rich brines (or mixtures of the two).

It is possible to check the validity of these calculated compositions by various other techniques which have already been discussed in Chapter 5 and in Bone and Griffen, (1984). The main problems with these techniques are that either: (1) the highly specialised equipment is limited in its availability to most workers, or (2) for the more readily available techniques such as fluid extraction, there is no control over or knowledge of which type of fluid inclusion is being analysed - let alone information on individual fluid inclusions.

Therefore a somewhat different approach of using the electron microprobe to that employed by Eadington (1974) was attempted, with pleasing results. Most workers now have access to an electron microprobe. The technique developed during this study is relatively simple, and only requires an electron microprobe with an energy dispersive X-ray analysis system (EDS) attachment.

A standard doubly-polished fluid inclusion section is coated and mounted in the normal way. Using optical microscopy, a near-surface fluid

a.   A magnesite outcrop at Kharidunga, Nepal. It shows stellate
       clusters of bladed form magnesite crystals within finer grained
       magnesite, which is remarkably similar to many of the outcrops at
       Rum Jungle.

b.   White, bladed type magnesite. Sample N3, Kharidunga, Nepal.

c.   Cleavage rhombohedra of magnesite with transecting veins of
       pyrrhotite and minor chalcopyrite. Sample N8, Kharidunga, Nepal.

10 cm

10 cm
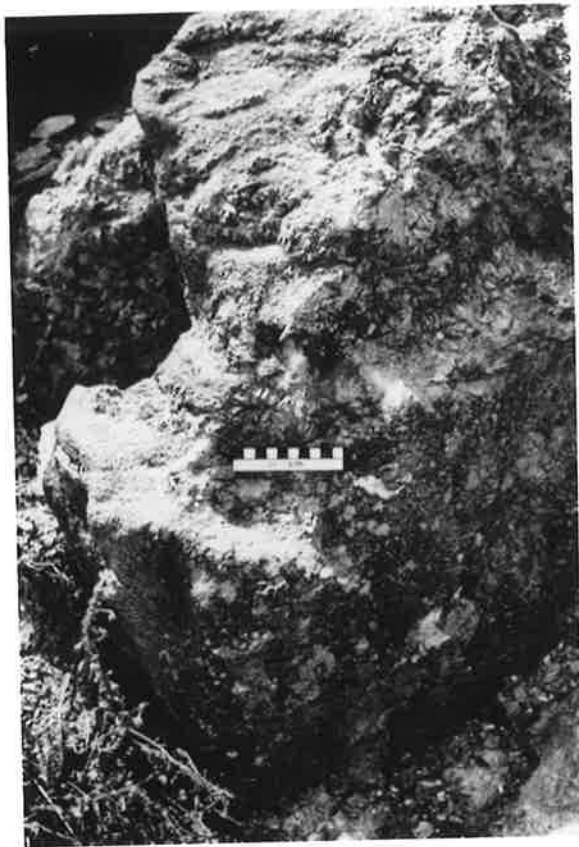
inclusion is located under the electron beam and the beam current increased, generally to around 150-200 nanoamps. The use of a finely focussed beam results in localised heating of the specimen, and may lead to decrepitation of the fluid inclusion. Approximately only one in twenty fluid inclusions in the material examined did decrepitate. However, when a fluid inclusion did decrepitate, the evacuated chamber environment resulted in surface deposits of the solute occurring together with daughter mineral salt crystals in the vicinity of the fluid inclusion site. This process may be observed through the optical microscope or on the display CRT of the electron microprobe.

It is important to record the qualitative analysis of the host mineral immediately surrounding the fluid inclusion prior to its decrepitation. This analysis is done routinely whilst waiting hopefully for the fluid inclusion to decrepitate.

The surface deposits from decrepitated fluid inclusions can be qualitatively analysed by collecting the X-ray spectrum from the host phase and then comparing this with the X-ray spectrum from the surface deposits. Subtraction, by either use of the analog signal through electronic hardware routines in the EDS system, of the host spectrum from each of the spectra from the surface deposits gives a qualitative analysis of the material and thus nonvolatile part of the fluid composition. The subtraction of the host mineral spectrum is an essential step as in most, if not all cases, the electron beam penetrates through the surface deposits to the underlying host mineral, so that the final spectrum is a composite of the composition of both the host mineral and that of the fluid that was previously entrapped within the fluid inclusion. Results may be either recorded photographically (Plates 42, 43) or relative peak heights may be recorded from each spectrum using conventional software.

Although the technique is laborious and gives qualitative rather than

PLATE 42

a.   Spectrum from the fluid within a fluid inclusion in quartz. Mg
     is the only element present besides the background Si. Sample
     C43, Celia Dolomite, E.L. 1349.

b.   The same sample as above. The fluid in this fluid inclusion has
     Na, Mg, S, Cl, K and Ca present, as well as the host Si.

c.   Spectrum from the fluid within a fluid inclusion in magnesite.
     Besides the background host Mg, Ca and Fe (to the right of the Ca
     peak) are the only elements present apart from minor quantities
     of S and Cl. Sample E28, Coomalie Dolomite, E.L. 1349.
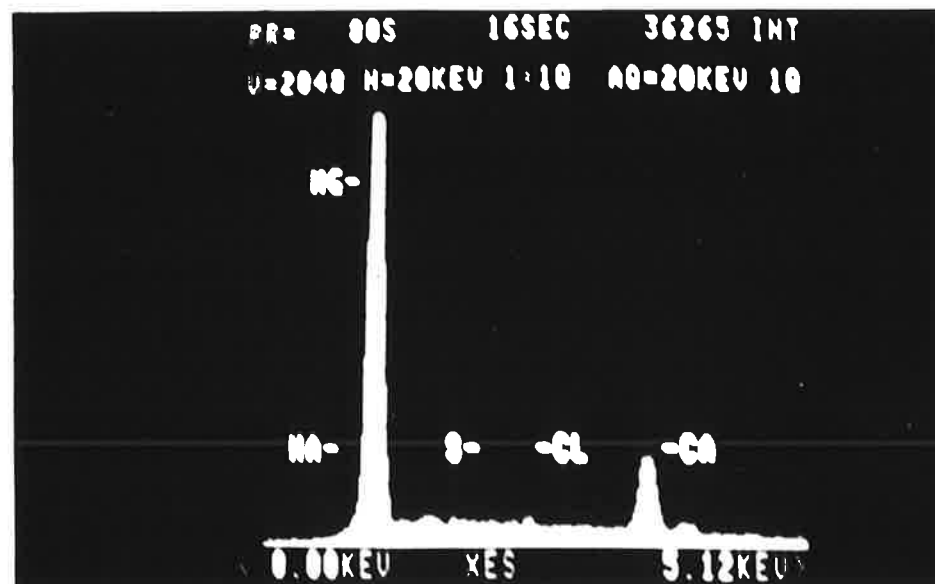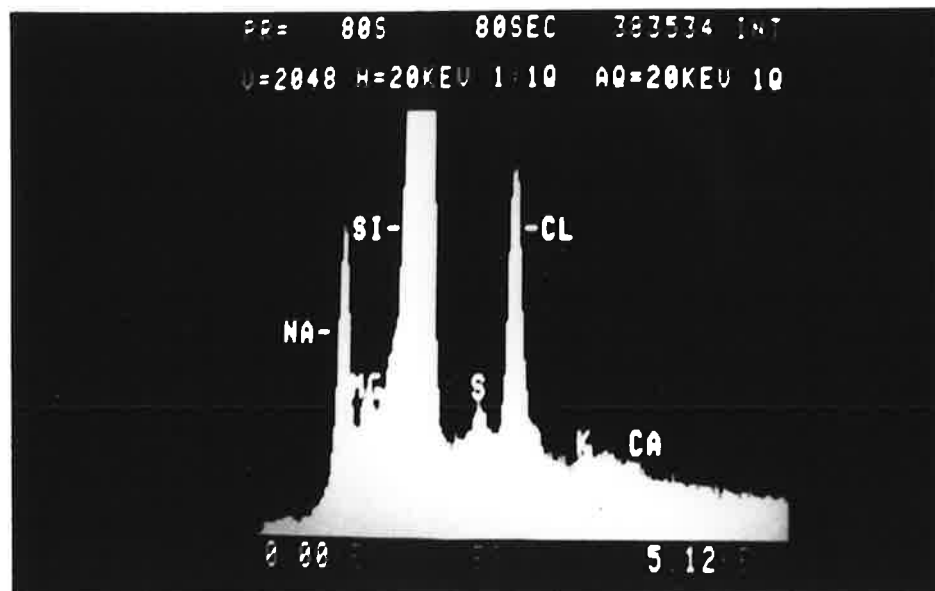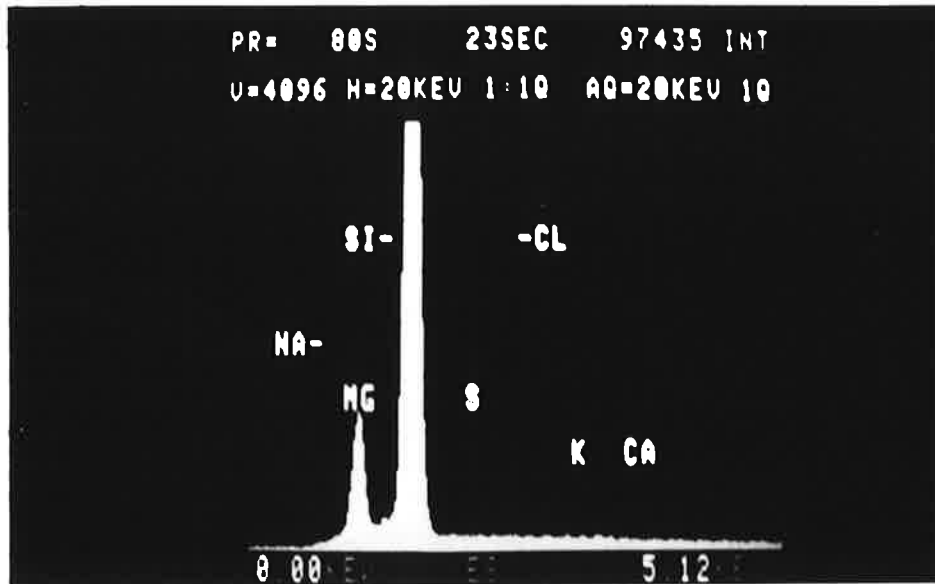
quantitative results, it provides very specific information that is otherwise normally unattainable. One tremendous advantage of this technique over other destructive techniques is that it allows the analysis of individual, typed fluid inclusions.

Indeed, although it was not done in this study, there is no technical reason why this method cannot be employed on the same fluid inclusions from which microthrmometric results have been obtained, although it is usually suggested that such fluid inclusions being very close to the surface are not the ones chosen for microthermometry.

Obviously, accurate ratios cannot be obtained, but "rough" ratios of those elements above $Z = 8$ can be calculated. The qualitative results of both cation and anion elements allows propositions concerning the various compounds/complexes e.g. chlorides, carbonates, bisulfides etc. dissolved in the fluid to be made. This is of paramount importance where genetic modelling of ore deposits is concerned.

6.11.2. Results and Discussion of Results

A study of two samples from E.L. 1349 was undertaken, using the JEOL 733 Superprobe and KEVEX EDS system in the Electron Optical Centre, University of Adelaide. This study was encouragingly successful.

The samples chosen were a quartz specimen from the Celia Dolomite (C43, Plate 6) and a magnesite specimen from the Coomalie Dolomite (E28). The samples have already been discussed, and the complete microthermometric data and geochemical analyses are given in Appendices 2, 3. They were selected partly because of the purity of the host mineral (as against those containing many intra- and intergranular accessory minerals) and partly because they contained fluid inclusions that were representative of the entire study. None of the fluid inclusions

PLATE 43

a.   (at left) Spectrum from the fluid within a fluid inclusion in
        magnesite. Na, Ca and Cl are present besides the background host
        Mg. Sample E28, Coomalie Dolomite, E.L. 1349.

b.   (at right) The same sample. Na, S, Cl and Ca are present
        besides the background host Mg. See text for further
        explanations of these spectra.

c.   Grains of pyrite extracted from a quartz arenite to use in the S
        isotope study and to analyse. Sample D10, Crater Formation, E.L.
        1349.

contained daughter minerals.

Counting times were extended for up to two minutes to ensure that all elements present were identified. This then allowed selection of a time suitable to show these elements advantageously.

The results are photographically presented in Plates 42, 43. In this study photographs of the scans before decrepitation were not taken, however it is recommended that this step be incorporated as a routine step in the technique. As so few of those fluid inclusions selected eventually decrepitate, this routine of taking background scans of all fluid inclusions could prove to be time consuming. The photographs selected for presentation in Plates 42, 43 are those of spectra of decrepitated fluid inclusions that (1) showed nothing unusual beforehand and (2) which also gave a spectra that occurred frequently.

Plate 42, Fig. 1. C43 : Si is the only element present in the background host mineral. After a 23 second counting time of the decepitation product Mg is the only other element present in the spectrum. As there is no anion element present, it is likely that the fluid contains a Mg-carbonate species. It certainly appears that neither a chloride nor a sulfate (nor bisulfide) is present.

Plate 42, Fig. 2. C43 : In contrast, this fluid shows many cations and anions, as well as the background Si, Na, Mg, S, Cl, K, and Ca are all present, which presents the problem of not knowing which element combines with which. There are numerous possibilities; plus the fact that due to the evidence from Fig. 1 of the possibility of carbonate-type species, then carbonates must also always be considered as a possibility. Therefore, the best approach to the problem is to look at the known anions, take that one which is present in the greatest proportion - in this case, Cl - and match it with an appropriate "quantity" of cations -
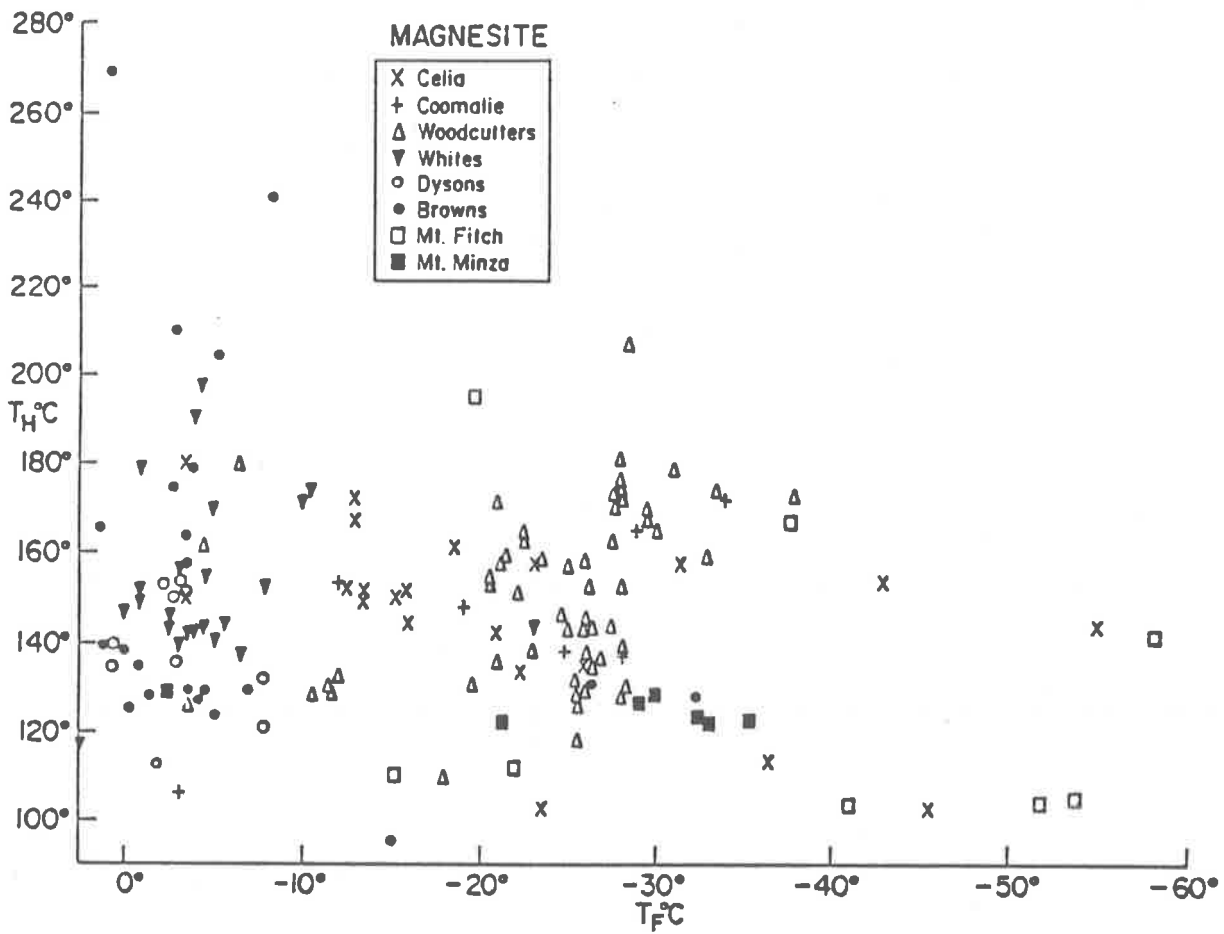
Fig. 95: Homogenisation temperature vs Final melting temperature.

in this case - Na, which is the most abundant cation. If there is still an excess of Cl ions after having used all Na-ions, there must be at least two different chloride species present in the fluid, maybe more, as there is Mg, Ca and K available, plus a hint of an Fe peak. If there is also an S-species present, this could be present as a sulfate e.g. $CaSO_4$ or bisulfide, depending on Eh, pH etc.. So, the minimum number of dissolved species present is four, of which at least two are chlorides, and at least one is an S-species.

Plate 42, Fig. 3. E28 : Mg and very minor Si are the only elements present in the background host mineral. The situation is similar to that in Fig. 1., except that there is a minimal amount of Cl and S present, but nowhere near enough to accomodate the Ca and Fe (peak to the right of Ca) present, especially as it is likely that some of the Mg peak comes from the fluid. Therefore there is the probability of carbonate species.

It must be emphasised that using this technique Mg as a component of the brine cannot be differentiated from the background Mg of the magnesite host in this sample - but by using more than one mineral host a composite picture can be built up.

Plate 43, Fig. 1. E28 : The Na present in this fluid is far in excess of the available Cl ions, so, there must be some other anion present in the fluid in order to utilise the Na, plus the Ca that is present and possibly also some Mg. Once again it is probably a carbonate species.

Plate 43, Fig. 2. E28 : Here there is a marked contrast with the fluid inclusions discussed in the previous four figures. In this fluid there appears to be an excess of Cl ions, as well as a minor amount of S - far more than needed to combine with all the Na and Ca indicated. There are two possible explanations immediately obvious. The first (and most likely) is that the fluid Mg component is masked by the background i.e.
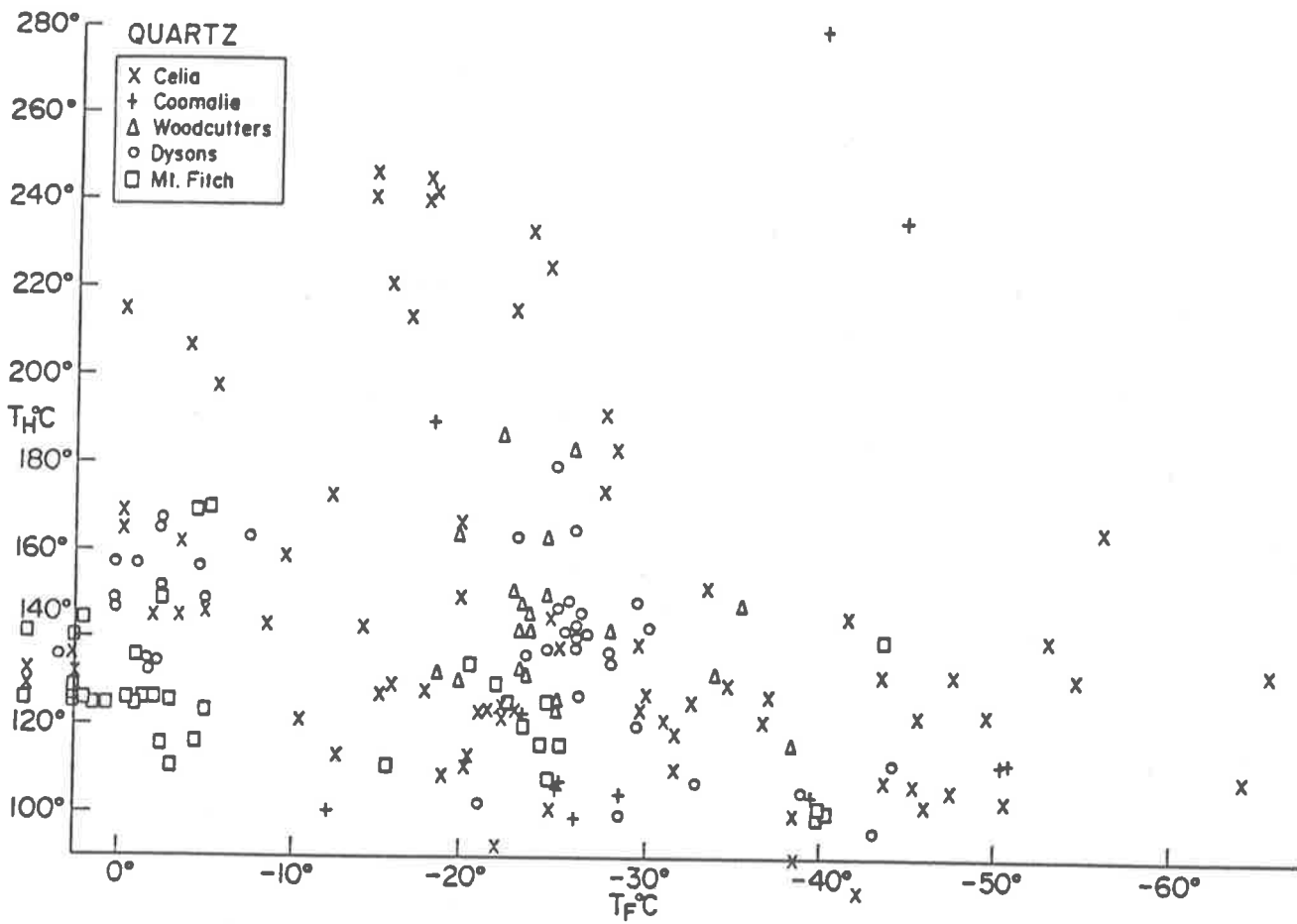
Fig. 96: Homogenisation temperature vs Final melting temperature.

host mineral, peak. The other explanation (pers. comm. P. Ypma) involves the hygroscopic nature of Ca^{2+} i.e. that the Ca within the fluid has not all volatilised and become available for scanning; that a higher temperature than that obtained in this technique is needed in order to record a more "accurate approximate" analysis.

6.12 Conclusions

6.12.1 Brine Salinities

It has been customary to report salinities of brines in terms of weight % equivalent NaCl, and more recently also in weight % equivalent $CaCl_2$. The choice of presentation has been determined by the temperature at which melting from the frozen state first begins. Using this technique, the brines in this study would probably have been simply reported as $CaCl_2$ - rich brines, with actual salinities determined by referring the obtained T_f's to pre-determined graphs (Fig. 62). Undoubtedly $CaCl_2$ - rich brines are present, as indeed are $NaCl_2$ - rich brines, and CO_2 - rich brines and probably others as well. However, the results of the electron microprobe technique of analysing the fluids in fluid inclusions has shown that (a) Mg-rich fluids are present as well in some fluid inclusions and (b) that it is likely that carbonate or bicarbonate complexes are also present.

In view of this, numbers for all salinities types have not been proposed. Rather, all of the data obtained, without exception, has been meticuously presented, along with the appropriate reference graphs.

Certainly, there is not doubt that on the basin of salinity variations more than one fluid has been involved in both the magnesite and the quartz genesis (Figs 95, 96). It also appears likely that the same fluids were trapped by both minerals. It is somewhat unsatisfactory not to be able to

314

Fig. 97
HOMOGENISATION TEMPERATURES
OF ALL MAGNESITE SAMPLES

n=444   152.94°C
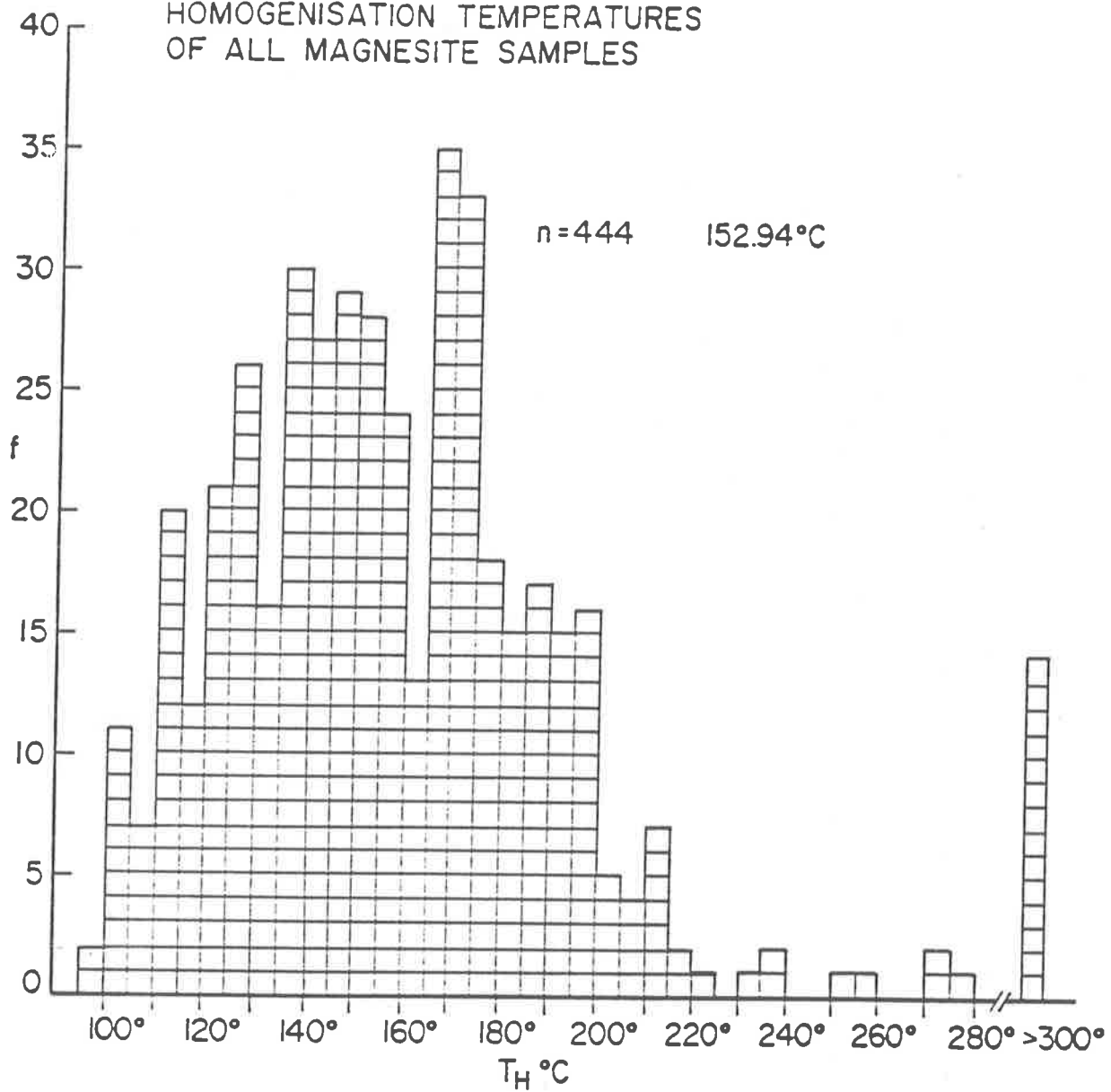
Fig. 98
HOMOGENISATION TEMPERATURES OF
MAGNESITE SAMPLES WITH BOTH FORMS PRESENT

n=107   158.08°C
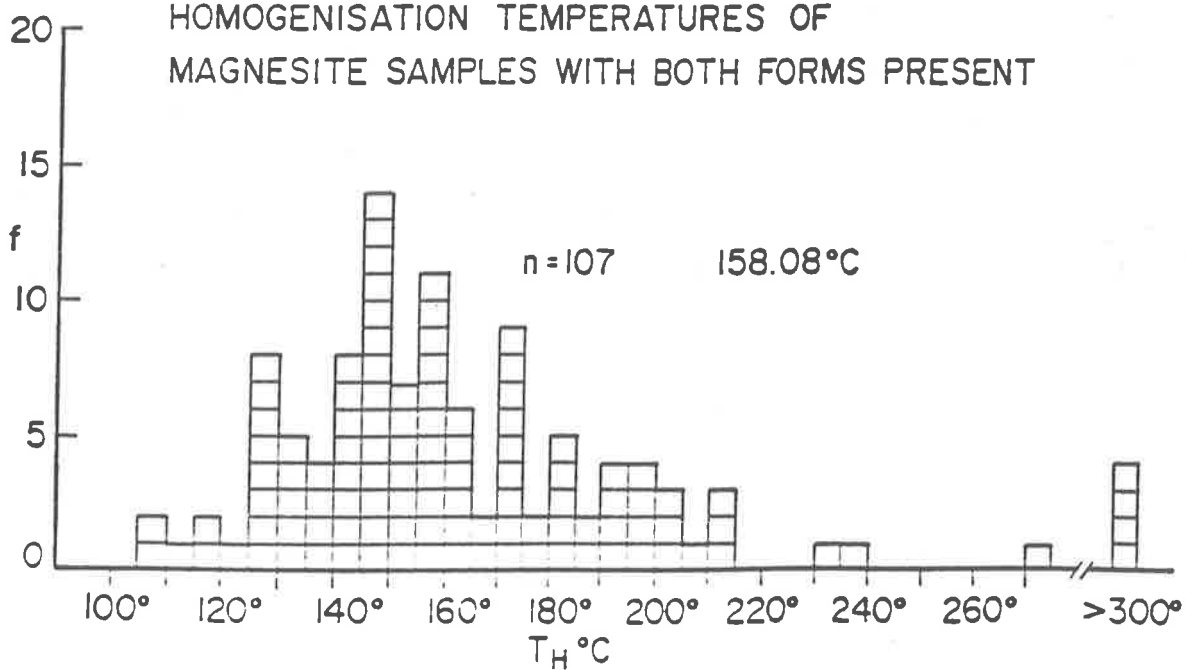
be more specific in terms of fluid chemistry but it would now be a retrograde step to suggest that only one brine was involved of such and such a salinity.

6.12.2 Temperature control on magnesite form

Fig. 97 is a histogram of all the homogenisation temperatures of the fluid inclusions studied in the magnesite samples. This is a fairly normal looking curve at first glance, with a mean value of 152.94^{O}C. However, closer perusal shows that there is a sharp break at 160°C, suggesting that there are two poulations present, whose upper and lower distributions quite closely overlap.

Therefore the values obtained from magnesite samples that show both the rhombohedral form (Plate 8) and the bladed form (Plates 9, 10) in the same sample were replotted. The resultant histogram (Fig. 98) shows only a slight difference to the first, with a mean of 158.08^{O}C. However, when histograms are plotted of the values obtained from magnesite samples with only the rhombohedral form present and from magnesite samples with only the bladed form present a significant difference becomes obvious (Figs 99, 100): the former gives a mean of 131.11^{O}C, the latter 173.39^{O}C.

It would appear, then, that the temperature of the fluid involved in the magnesite recrystallisation event was a form controlling parameter. This is not to say that there were not other interacting parameters involved in the resultant magnesite form.

Statistical analysis of these two histograms, using the Kolmogorov Smirnoff Test, confirms that there is a significant difference in the two populations (Fig. 101).

Fig. 99
HOMOGENISATION TEMPERATURES OF
RHOMBOHEDRAL FORM MAGNESITE SAMPLES

n = 176   131.11°C

T_H °C
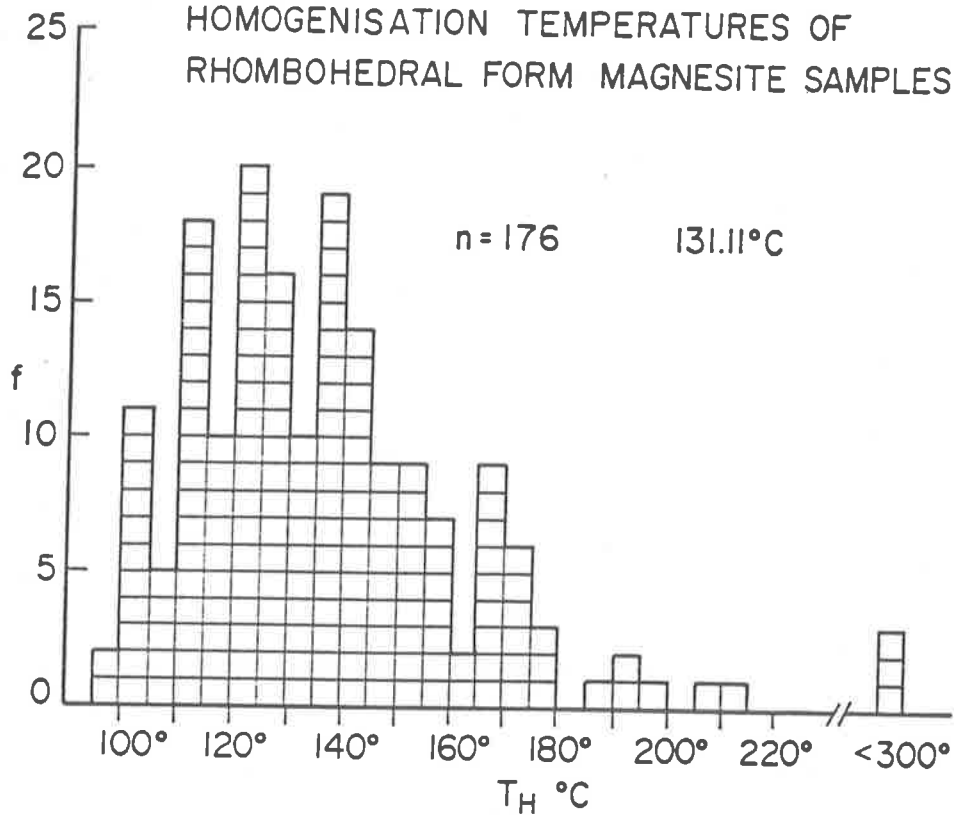
Fig. 100
HOMOGENISATION TEMPERATURES OF
BLADED FORM MAGNESITE SAMPLES

n = 161   173.39 °C

T_H °C
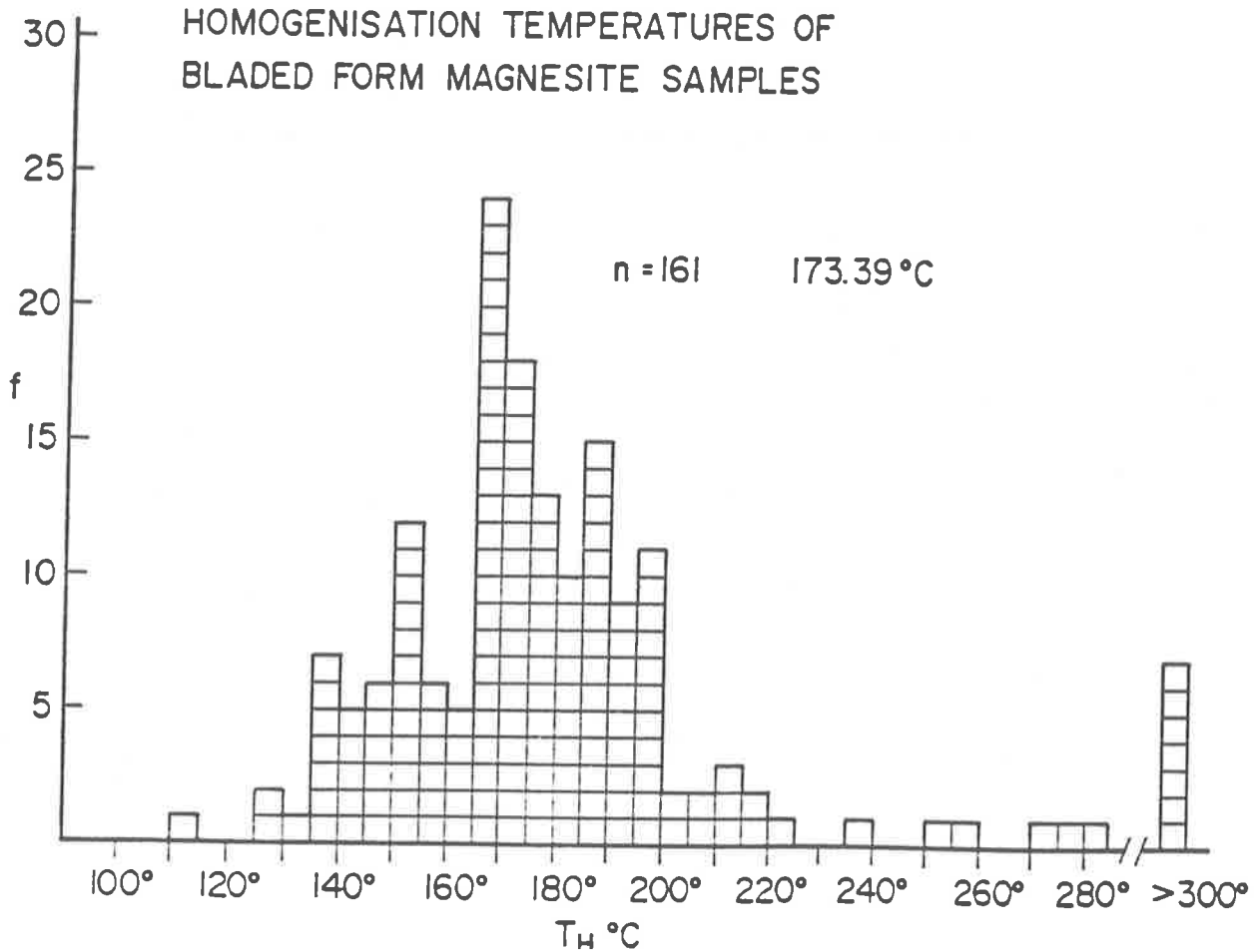
Indeed, there are undoubtedly many, such as trace element concentration etc.

So, if the temperature of the fluid was greater than 160°C at the time of the recrystallisation of the magnesite, the form taken was most likely to be "bladed", if it were below 160°C, the form taken usually "rhombohedral".

6.12.3. Brine Generation and Mineralisation

The special role of magnesite follows from the consideration that during the weathering of Ca-carbonates, no Ca-carbonate silicates form in significant amount in the sediments, so that Ca^{2+} is removed from the system as gypsum, at the expense of S that has been released by the oxidation of sedimentary sulfides e.g. pyrite (Garrels and Lerman, 1984). Thus, a Ca-rich system acts in an inhibiting manner as regards metal sulfide formation unless there is a concommittant massive production of H_2S by anaerobic bacteriogenic reduction of this sulfate. This problem does not arise if the carbonate is magnesite, as Mg-silicates readily form during weathering leaving fluids of favourable pH and ligand availability suitable for the leaching and transport of metal (carbonate and bicarbonate) complexes and S species.

The intercalated stratiform tourmalinites indicate hot spring activity at the time of rifting, which would have contributed hydrothermal fluids into the system.

The composite picture that has built up, is that fluids of varying composition have been trapped during the recrystallisation stage of the magnesite and quartz. Possibly this is the result of the mixing of the two fluids according to the model presented in Fig. 46. Tectonic disturbances could have initiated mixing of these fluids, thus enabling a

318

Fig. 101:
KOLMOGOROV SMIRNOFF TEST
Magnesite forms: Fluid inclusion homogenisation temperatures
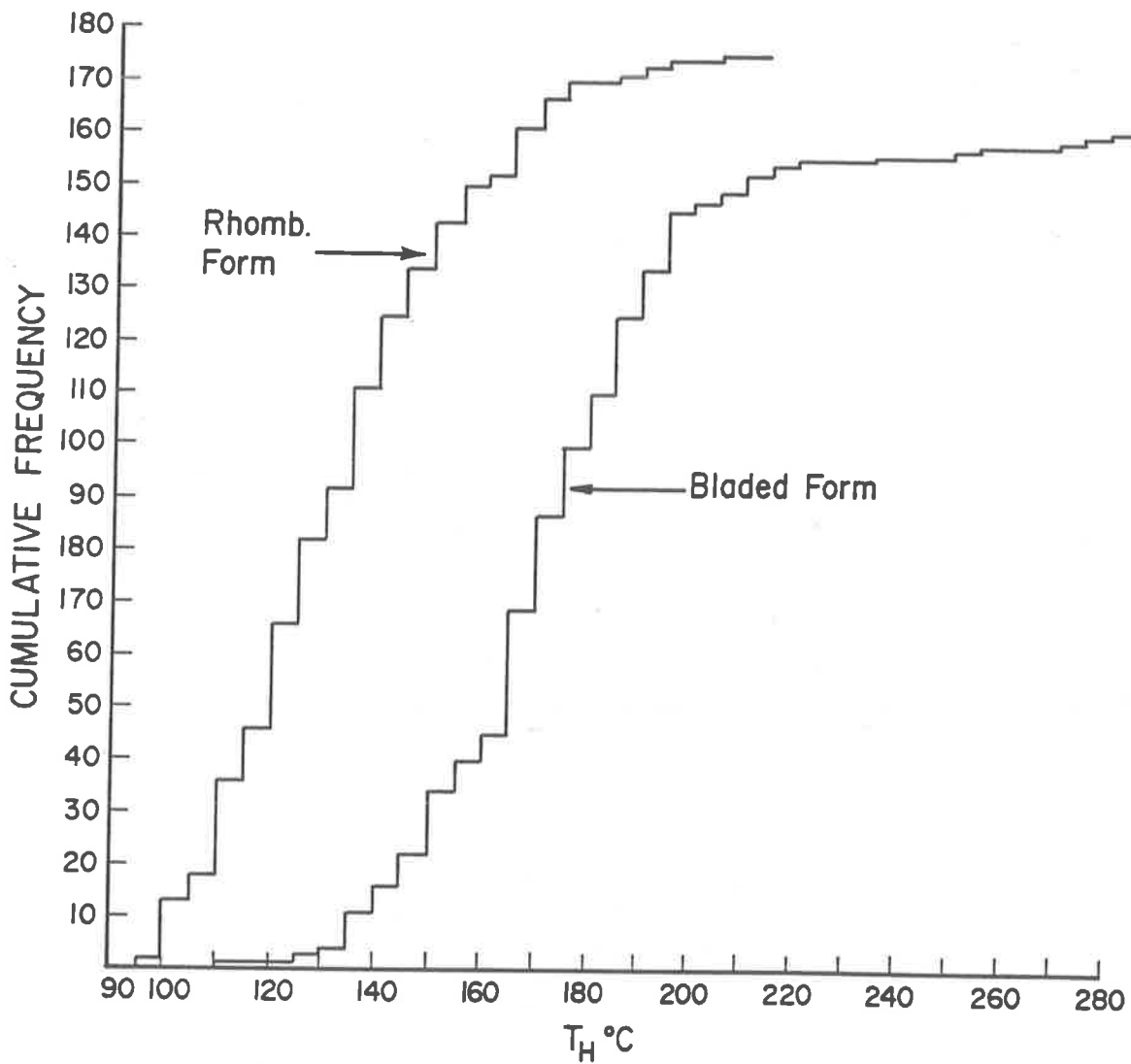
variety of reactions to occur. This tectonic event also probably produced the brecciation (e.g. Giants Reef Fault Zone) and shear zones which are particularly concentrated in The Embayment area - as are the mineralised deposits. The brecciated zones would have been preferential pathways for migratory mineralising fluids. They would also have provided large surface areas on to which the ore minerals and their gangue components could crystallise, at the appropriate change of conditions.

Certainly, one of the important points highlighted by the qualitative analysis of the fluids in the fluid inclusions is the possible presence of both carbonate complexes and saline brines in the fluids. This adds support to the transport mechanisms of the U - mineralisation models in the Pine Creek Geosyncline of Ypma and Fuzikawa (1980) and also of Ferguson et al. (1980).

There seems to be little doubt now that saline brines are insufficient in themselves to transport U and/or base metals at concentrations high enough to result eventually in massive ore bodies. For example, Giordano and Barnes (1981) found that at conditions of temperature of $200^{\circ}C$, $\lesssim m_s$ of 10^{-1} to 10^{-3} mole/l, $\log {}^a O_2$ of -41 to -46 and a pH of 6.2 - 7.2, the maximum galena solubility is only 10^{-2} ppm. These concentrations are 3 to 4 orders of magnitude too low to produce ore deposits, in view of fluid transport restrictions, although there is dissension as to the actual concentration needed e.g. for the Mississippi Valley Type deposits, Giordano and Barnes (1981) and Giordano (1985) quote a minimum concentration of 10 ppm Pb, whereas Sverjensky (1981) suggests 1 ppm is sufficient. Increased leaching of source rocks can be achieved by increasing the temperature and/or the ionic strength of the brine, but the trends shown by Long and Angino (1983) were neither simple nor linear. What they did show was that changing the salt components of the brine changes the amount and type of mobilisation e.g. Ca^{2+} effectively

leaches Pb and Zn, whilst K^+ was found to be effective in mobilising Cu.

But the point is, even this lower figure of 1 ppm Pb can not be achieved without invoking additional complexes e.g. the ligands SO_4^{2-}, CO_3^{2-}, HCO_3^-, NH_3^-, Br^- and $S_2O_3^{2-}$ etc.. Sergeyeva et al. (1972) demonstrated that oxidised U may be transported in neutral to acidic solutions at 200^0C as the complex UO_2CO_3 , whilst in basic solutions other uranyl-carbonate complexes would be functioning. Even so, these fluids are barely capable of achieving a 10ppm level. Rather, the proposed addition of organometallic complexes e.g. salicylate ($C_7H_5O_3$) would eliminate this particular problem (Giordano and Barnes, 1981; Giordano, 1985). For this area there is ubiquitous evidence in the Celia Dolomite and the Coomalie Dolomite of the availability of organic material in the form of stromatolites, capable of forming an organic complex.

However, high temperature, highly saline brines are insufficient metal and U leachers unless coupled with acidity or alkalinity (Eugster, 1985). Eugster (1985) has defined a new sedimentary type (Green River Type) and re-defined the Creede Type, both of which are applicable to the Rum Jungle situation:-
(a) Green River Type: these are formed from fluids that have ambient to slightly elevated temperatures and are alkaline (OH^- or carbonate rich), with the H.Y.C. Deposit at McArthur River given as an example.
(b) Creede Type: hot ($100-200^0C$), alkaline brines, already carrying metals or leaching them from their hosts interact with carbonate or siliciclastic host rocks to deposit sulfides.

The important parameter in both cases is the initial alkaline nature of the fluid. The addition to the fluid of the oxidised products of the decomposition of organic matter e.g. blue-green algae, enhances the

aggressive capability of the fluid to acquire base metals.

Once deposition of sulfides et al. occurs, the fluid becomes acid, leading to the further development of thinning and brecciation in the carbonate-rich lenses at Rum Jungle. It also explains the discordant, sparry carbonate veins that are quite common in The Embayment area. It is also responsible for the sericitisation alteration (which is a different sericite event to that referred to in the section on diagenesis - Chpt. 4) seen in the silicates within and adjacent to the ore-bodies (Paterson et al., 1984).

A U-deposition model that may be applicable to the Rum Jungle situation is detailed by Leroy (1978). This genetic model looks at the possibility of uraninite deposition from a CO_2^- rich transporting fluid which also carries uranyl-carbonate complexes. When this fluid encounters a "corridor" (e.g. palaeokarst or shear zone) the pressure drops and boiling of the fluid occurs. This destroys the uranyl-carbonate complex:-

$$UO_2(CO_3)_2{}^{-2} + 2H^+ \rightarrow 2HCO_3{}^- + UO_2{}^{-2}$$
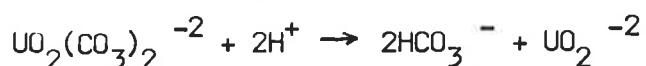
When $UO_2{}^{-2}$ is reduced, to attain equilibium with pyrite, pitchblende is formed. CO_2 is lost during the boiling stage, so that later fluids are CO_2 poor. At Rum Jungle, in this model, the unconformity is important as the "corridor", especially as it is a buried palaeokarst.

This is a simple 1-stage model, and is probably but one event in a multiplicity of events.

Looking at the close spatial association of U ores and hematite, Spirakis (1981) noted that some hydrothermal fluids deposit primary

hematite, indicating that they were oxidising with respect to Fe. Rich et al. (1977) believe that some hydrothermal fluids are also oxidising with respect to U - a situation which may have existed at Mt. Fitch, and that in high temperature fluids the U is transported in the hexavalent state and then precipitated by reduction to the tetravalent state just as it is in low temperature solutions. Sergeyeva et al. (1972) demonstrated that oxidised U may be transported in neutral to acidic solutions at $200^{\circ}C$ as the complex $UO_2CO_3{}^{O}$. In alkaline solutions other uranyl-carbonate complexes apply.

So, the paragenetic sequence that applies as there is a progressive change from oxidising to reducing conditions is:- $Fe_2O_3 \longrightarrow$

$$Fe_3O_4 \longrightarrow UO_2 \longrightarrow FeS_2$$

This reducing environment could be brought about by the oxidation of primary pyrite by surface-derived waters. This process could explain the primary and secondary pyrite seen.

Simplified, this model becomes

$$4UO_2CO_3{}^{O} + H_2S + 4H_2O \longrightarrow 4UO_2 + SO_4{}^{-2} + 4H_2CO_3{}^{O} + 2H^+$$

As the temperature decreases, there will be a S component derived from sedimentary sulfide and possibly an additional bacteriogenic S source, leading to:-

$$nUO_2CO_3{}^{O} + (n+1)H_2S \longrightarrow nS^{-2} + nUO_2 + 2H^+ + nH_2CO_3{}^{O}$$
$$\text{(partly oxidised)}$$
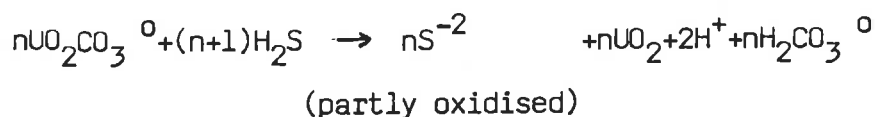
This reaction is a means of providing the partly oxidised S necessary for the precipitation of pyrite (and other sufides), which concommittantly

forces the first equation to the right i.e. precipitation of more UO_2. This could explain why the minerals i.e. magnesite and quartz which are host to the UO_2 at Rum Jungle give fluid inclusion homogenisation temperatures 200°C i.e. this is the last stage in the cooling of a solution that was originally at a higher temperature.

There are other areas similar to the situation that exists in The Embayment area that are unmineralised and so one might question the validity of the model. However, it is well to remember that "we do not have to assume that the fluids necessarily remained of constant character throughout" (Taylor and Rowntree, 1980).

Thus speculation regarding the source of the fluids in regard to the saline brines continues. As already suggested one possible source is the evaporite - type carbonates themselves. If this were so, then there would have been synchronous mixing, as these are undoubtedly the source of the carbonate complexes fluids. The fluid inclusion temperatures do not support the idea. An alternative is the hydrothermal source - possibly associated with the volcanics and/or sills from the rift environment. Certainly the S isotope study shows a magmatic S component as well as a sedimentary S source (Chpt. 7). Yet other sources to be considered are the overlying sequences, and in particular the Tolmer Sandstone. Thermoluminescence studies (author's work - unpubl.) show that at some stage there was U either in or moving through the Tolmer Sandstone. It is difficult to envisage the fluids moving upwards through the aquatard of Whites Formation, into the Tolmer Sandstone, and then circulating back down into the area of the Whites Formation - Coomalie Dolomite boundary. There would need to be some heat source of post Tolmer Sandstone age to initiate the setting up of a convection cell e.g. an intruding dyke; or a zone of high porosity transgressing through to the Tolmer Sandstone e.g. a fault zone. The former is not seen, the latter could be present in the form of the Giant Reef Fault, or the Mount Fitch Fault etc. The second

suggestion does not explain a mechanism of descending fluids, so although possible, it seems unlikely that the Tolmer Sandstone was the source of the U and/or base metals.

Rather, it is more likely that the major source (but not necessarily only source) of the U was the granitoid complexes and the clastic sediments derived from these, whilst that of the base metals was the mafic volcanics/sills (especially in view of the high Co-Ni values in the sulfides - Chpt. 8).

In conclusion it can be stated that several fluids were involved in transporting these heavy metals: - complex brines, carbonate complexes and also possibly organometallic complexes, whilst at the same time acknowledging Eugster's (1985) warning that "the least understood aspect of sediment hosted ore deposits is the origin of the metal-carrying fluids".

PLATE 44

a.   Relict pyrite grains in chloritic dolulutite. The pyrite cores
      are weathering to pyrite towards the rim (analyses - Appendix
      3). Sample GO4, Whites Formation, E.L. 1349. x100.

b.   Pyrrhotite (right hand side) in magnesite. A small chalcopyrite
      veinlet can be seen in the lower left hand side of the
      magnesite. Sample N8, Kharidunga, Nepal. x100.

c.   The boundary between the underlying magnesite and overlying
      graphitic metapelites at Kharidunga, Nepal. There was no
      evidence of the karst development seen elsewhere at this
      particular position.

CHAPTER 7
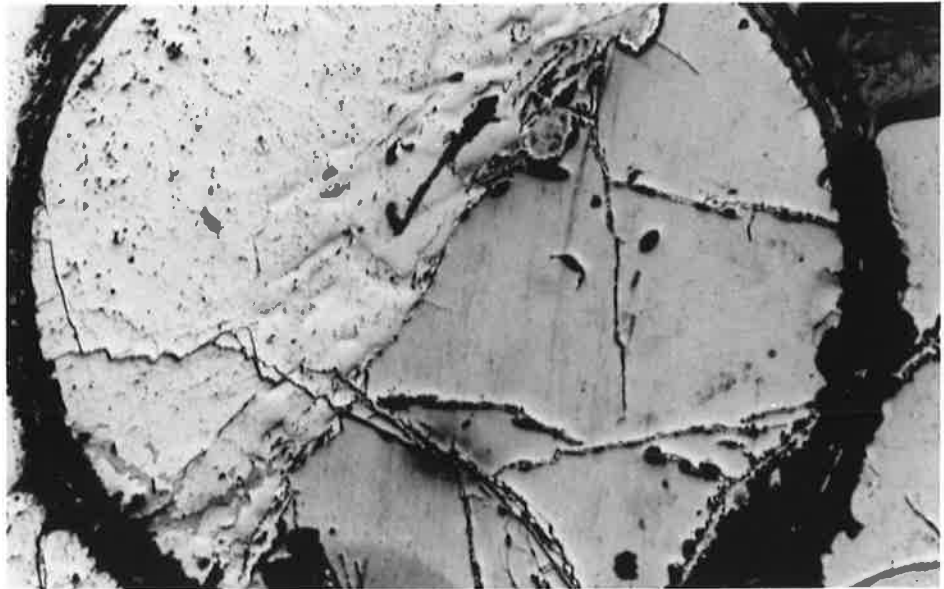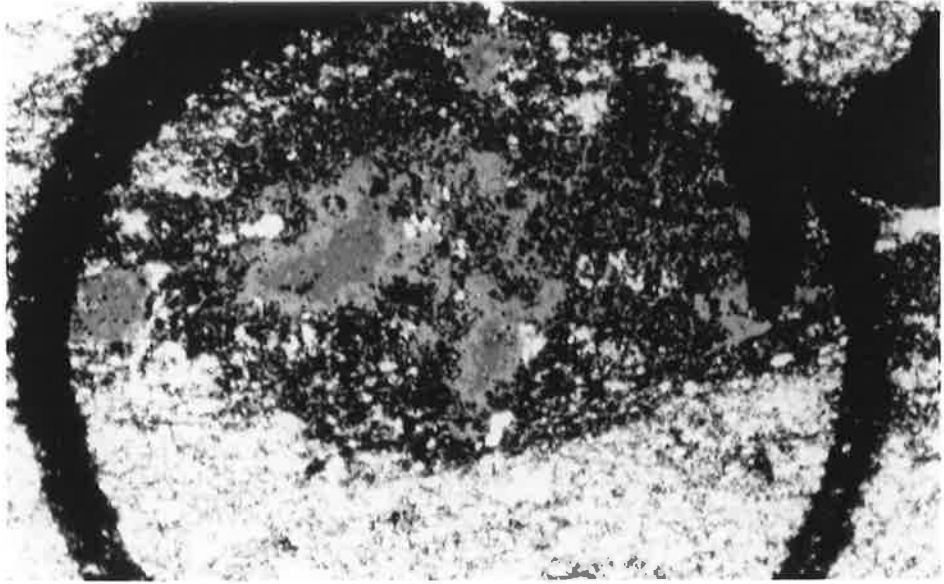
SULFUR ISOTOPE STUDY

7.1 Introduction

A S isotope study was undertaken on a variety of sulfide minerals from different areas and different stratigraphic horizons in the Rum Jungle Area.

These were:-

(1) pyrite from the Crater Formation (Plates 30, 43); E.L. 1349 (Fig. 72).

(2) pyrite and galena from Browns Deposit and chalcopyrite from Mount Fitch (Fig. 1 - Plate 46); both from shear zones straddling the Coomalie Dolomite-Whites Formation boundary.

(3) pyrite, chalcopyrite and galena from the Embayment deposits (Whites, Dysons and Intermediate - Fig. 8, Plate 45). These samples were from the Whites Formation, but still within or immediately adjacent to shear zones.

(4) pyrite (from E.L. 1349) from unsheared Whites Formation (Plates 44, 45). The samples contained either primary and/or secondary pyrite.

Previous S isotope studies in the area have been reported by Donnelly and Roberts (1976), who concentrated their effort on the Browns and Woodcutters Deposits.

Pyrrhotite (Plate 44) from graphitic meta-pelites (Plate 44) overlying the Kharidunga, Nepal, magnesite was also studied.

The aims of the study were to:-

(1) characterise the sulfur in terms of isotopic composition

a.   Euhedral crystal of marcasite intimately associated with pyrite,
      within sphalerite and chalcopyrite. The marcasite appears to be
      altering to pyrite. Sample WO-Cpl, Whites Deposit. x200, crossed
      polars.

b.   Textural evidence for at least two generations of pyrite
      formation within the polymetallic sulfide deposits. The euhedral
      core of this pyrite crystal is relatively undeformed, in contrast
      to the pyrite overgrowth material rimming it. Sample WO-Cpl,
      Whites Deposit. x250.

c.   Pyrite grains within dololutite. It can be seen that the pyrite
      is weathering to limonite. Sample G108, Whites Formation, E.L.
      1349.
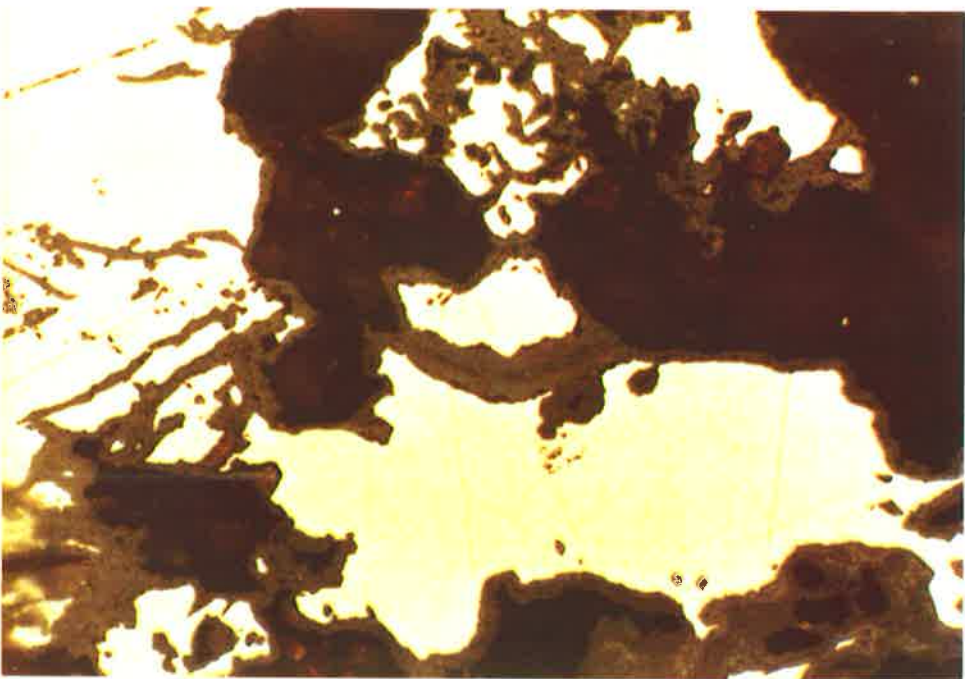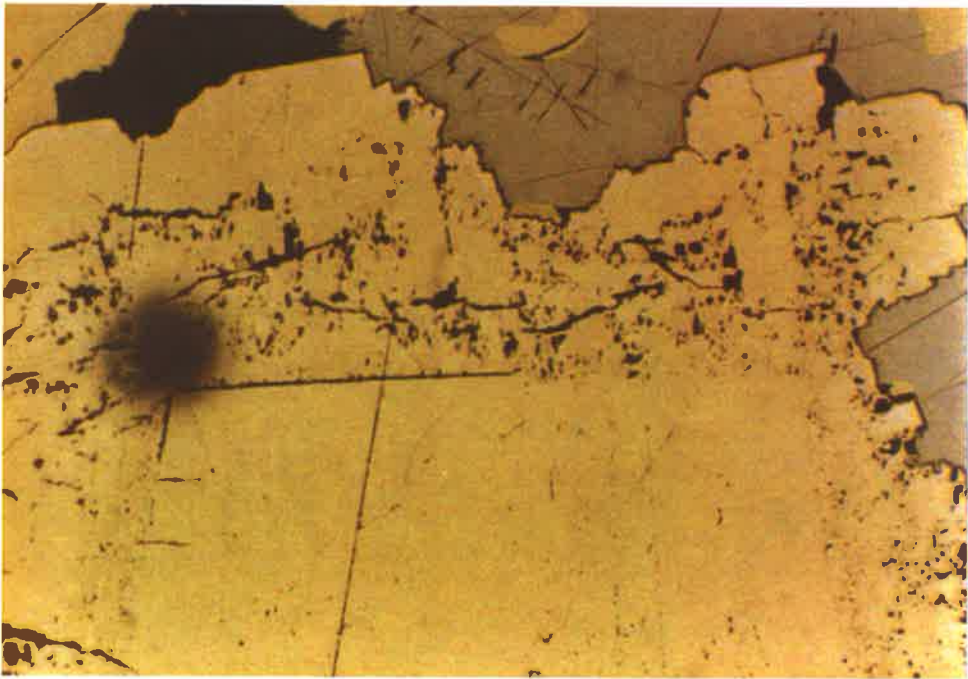
(2) determine whether a vertical homogeneity existed for the apparent diagenetic sulfides from the Crater Formation up in to Whites Formation.

(3) determine whether there was a lateral S isotope variation within Whites Formation.

(4) compare these results with previous studies: in particular that done on the Woodcutters Deposit by Donnelly and Roberts (1976).

(5) check formation temperatures obtained from the Fluid Inclusion study by the use of co-existing sulfides.

(6) compare these Rum Jungle areas with the Kharidunga deposit and thus compare resultant genetic models.

7.2 Sample Selection, Preparation and Analytical Technique.

It was difficult to obtain sufficient sample material from which to select fresh and uncontaminated samples. For example, there appeared to be only one sample from the Crater Formation that contained diagenetic pyrite grains in sufficient quantity, purity, and size. Even so, this sample had to be crushed and panned (on a Frantz Isodynamic Magnetic Separator), in order to obtain a relatively pure sulphide sample. Many field samples appeared to be too contaminated or altered.

All mineral concentrates were checked for purity under the microscope. Similar preparation applied to the material from Whites Formation, E.L. 1349 which was taken from drill holes in the C-horizon soil geochemical rotary drilling programme. Those cuttings that had the greater quantities of visible sulfides were selected.

For the other areas, samples were obtained by collecting from old mine dumps, from company drill core and from material collected previously by Professor E. Rudd and Dr. K. Fuzikawa of the University of Adelaide. From these samples those were selected which contained sulfides coarse enough to be extracted with a dental drill. This was performed on a polished

PLATE 46

a.   Major sulfide present is chalcopyrite. Euhedral crystals of high

relief are pyrite; the greyish - pink low relief crystals are

villamaninite. Drillhole sample MF 80/06, Mt. Fitch. x200.

b.   Chalcopyrite with small pyrite and villamaninite crystals plus a

larger two-stage pyrite crystal. This latter pyrite crystal is

the reverse of that shown in Plate 45b i.e. this one shows a

pure, undeformed rim. Drillhole sample MF 80/06, Mt. Fitch. x200.

c.   Chalcopyrite with euhedral pyrite and villamaninite crystals

intimately associated. Drillhole sample MF 80/06, Mt. Fitch.

x250.
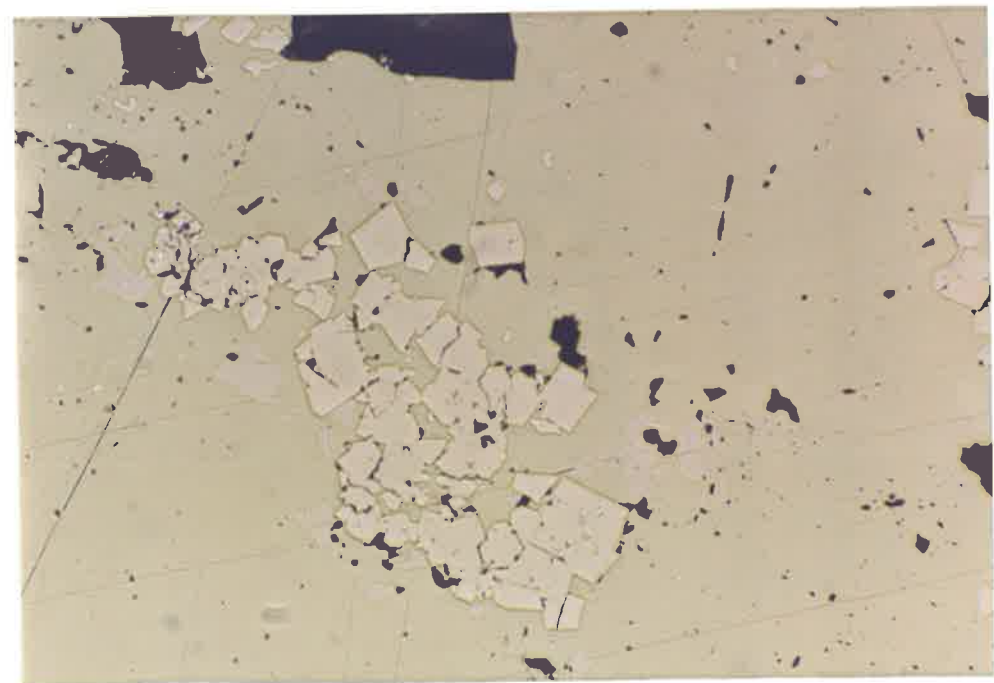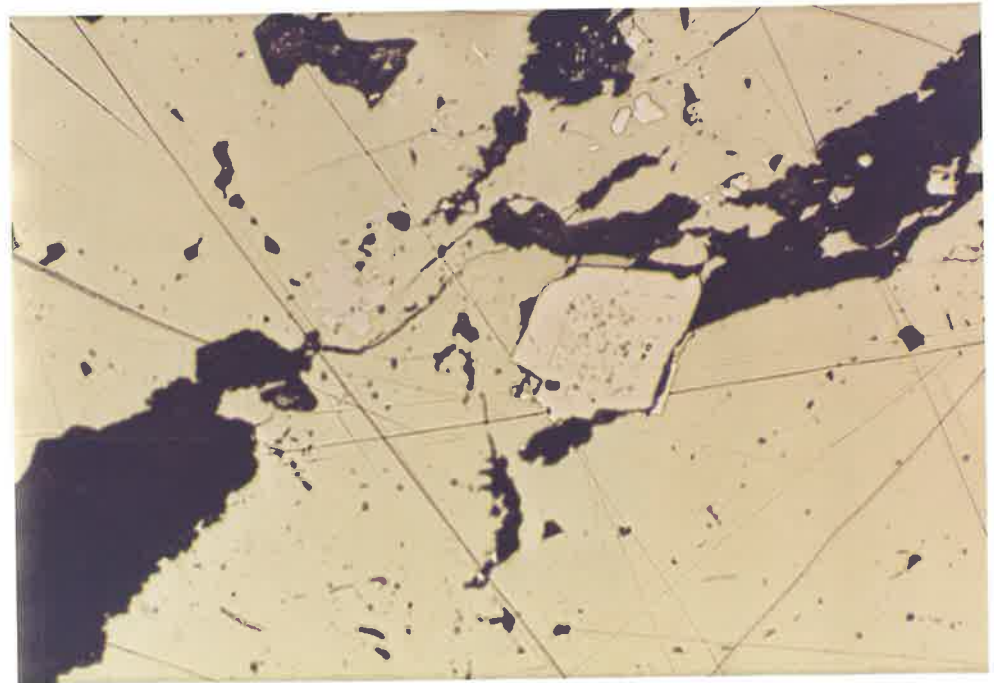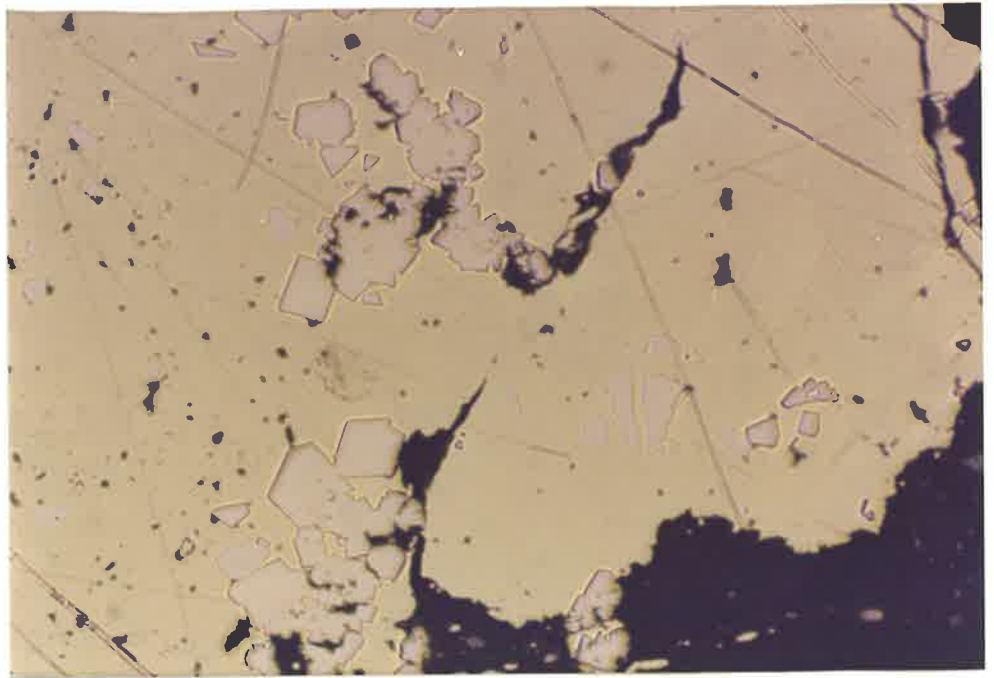
surface under a low power microscope, so that impurities could be avoided.

The mineral concentrates and hand picked samples were then used to obtain a sample of SO_2 from which the S isotope ratios could subsequently be measured on a Micromass 602E mass spectrometer. The SO_2 samples were obtained by burning for 20 minutes a weighed amount of sulfide mixed with excess cupric oxide. The gas released was purified by removing non-condensables, whilst the gas was frozen in a liquid nitrogen trap. After volatilization H_2O and CO_2 were removed by passing the gas through a dry ice/acetone mixture trap and a n-pentane/liquid nitrogen slurry trap respectively.

7.3 Theoretical Considerations

Stable isotope geochemistry of sulfur involves measuring the ratio of ^{32}S to ^{34}S. The results are then compared to the ratio from the accepted international standard - namely the troilite (FeS) from the Canyon Diablo meteorite ($^{34}S/^{32}S = 0.0450045$). Variations from this standard ratio are usually expressed by ^{34}S per mil, which is defined:-

$$^{34}S(\text{\textperthousand}) = \frac{^{34}S/^{32}S \text{ sample} - {}^{34}S/^{32}S \text{ standard}}{^{34}S/^{32}S \text{ standard}} \times 100$$

During the laboratory proceedings the Canyon Diablo meteorite troilite was measured to check the reliability of the system, and once accurate results were obtained, the unknown samples was run. Also run were internal standards e.g. Kanmantoo chalcopyrite, Broken Hill galena etc., and replicates of the unknowns to check reproducibility of results. Only those results which met these criteria have been tabulated, and considered in formulating hypotheses or models.

Until just over twenty years ago, sulfur isotope values were mainly

concerned with the deviation of $\delta^{34}S$ values from "magmatic" values. The near zero $\delta^{34}S$ values obtained from sulfides within porphyry Cu deposits had been interpreted as indicating that magmatic S in such systems was also of that order. This extrapolation greatly oversimplifies magmatic systems. Indeed, a complete understanding is needed of the processes whereby volatiles are evolved and expelled from individual magma sources before a solution to the problem of the isotopic composition of magmatic S can be attempted (Eastoe, 1983). Similarly, deviations of the order of $\pm$ 10‰ were interpreted as being cuased by biogenically derived S (Ohmoto and Rye, 1979), although Rye and Ohmoto had earlier (1974) warned that a range or statistical distribution of $\delta^{34}S$ values alone is not sufficient basis to warrant such a conclusion. Nevertheless, the reduction of sulfate by anaerobic bacteria is the most likely and certainly the most effective pathway whereby isotopic fractionation at low temperature occurs, with the creation of biogenic S isotope ratios (Ohmoto, 1972). There is a lack of agreement on $\delta^{34}S$ values for seawater (which is presumed to be approximately the same as that of the sedimentary sulfates from which the values are obtained – Garrels and Lerman, 1984) and/or sulfate for Middle Proterozoic and older rocks. Seccombe and Clark (1981) have postulated a figure of + 10‰ for Archaean seawater sulfate which disagrees with the figure of 0‰ for sulfate in the Archaen hydrosphere, given by Perly et al. (1971). Thode and Monster (1964) propose a figure of +15‰ for Proterozoic seawater sulfate. There is little doubt that at any particular time the S isotope composition of seawater sulfate was relatively homogeneous (Claypool et al., 1980), although it is well established and documented that there was considerable variation throughout time (Ohmoto and Rye, 1979). This leaves us with a probable figure of +10 to +15‰ for seawater sulfate at the time cf deposition of the Rum Jungle sediments. The other two problems are best considered jointly, as they are interdependent. Many workers have shown quite conclusively that sulfate was present in Archaean seawater and that sulfate reducing bacteria were already active during this time e.g. Ripley

and Nicol, (1981). However values of +0.5 to +3.5‰ for bedded sulfides
in the organic rich Cahill Formation (ca 2,200-1,800 Ma) have been used by
Donnelly and Ferguson (1980) to "indicate that despite the presence of
significant sulfate, sulfate reducers may not have evolved by this time".
However, this postulation of "significant sulfate" is derived from Crick
and Muir's (1980) erroneous identification of magnesite as having been
formed by replacement of primary halite and gypsum (Bone, 1983). In fact,
no sedimentary sulfate was identified during the course of the study.

A wide range of $\delta^{34}S$ values for 10 Early Proterozoic volcanogenic
sulfide deposits (ca 2,500-1,800 Ma) from - 3.0% to + 7.8‰ suggests the
presence of an oxidised S source to Seccombe (1977), if the sulfate ratio
is derived from a bacteriogenic reduction of seawater sulfate. Other
parameters that may affect the derivation of $\delta^{34}S$ from the expected
sulfate-sulfide equilibrium values (Campbell et al., 1978) include:
(1) the rate at which the sulfate is reduced to H_2S, regardless of
whether it be by biogenic or chemical pathways, and
(2) the rate at which sulfate in the sulfide forming system is
replenished. This replenishment rate is drastically affected when the
environment is not an open marine one. For example, Nielsen (1979) has
found that approximately 6 cms below the sediment water interface there is
no longer an equibilrium situation between H_2S and sulfate. This depth
is well above the maximum depth at which diagenetic pyrite can still
form. Consider this along with Nielsen's (1979) findings of (1)
predominantly close to zero values for fresh water basins and (2) values
of +10‰ to +15‰ for many intercontinental saline basins (e.g. Dead Sea,
Caspian Sea, the Great Salt Lake), and one can understand Chambers (1982)
warning to workers to restrict their interpretation of ancient sulfides to
"open or closed with respect to sulfate".

Further factors controlling S isotope ratios are pH, oxygen fugacity
(fO_2), temperature and total S isotopic composition ($\delta^{34}S_{\xi S}$) of

TABLE 5

SULFUR ISOTOPE DATA

Sample No.	Location /	Formation	Mineral	34S%.
D10	E.L.1349,	Crater Fm.	PYR	+6.5
"	"	"	"	+7.9
M.F.2	MtFitch,	Coomalie Dolomite /Whites Fm	Chalcopyrite	+1.9
MF 80/06	"	"	"	+2.2
"	"	"	"	+2.8
BR 4	Browns Deposit,	"	Pyrite	+3.3
"	"	"	"	+5.1
"	"	"	"	+4.3
BR 5	"	"	"	-2.2
KF82	"	"	Galena	-2.8
RJ7	Whites Deposit	Whites Fm/ Shear Zone	Pyrite	-4.2
RJ10	"	"	Chalcopyrite	-2.7
"	"	"	"	-3.0
RJ13	"	"	Pyrite	-4.1
RJ14	"	"	Galena	-7.3
RJ30	"	"	Chalcopyrite	-2.9
WO-Pyl	"	"	Pyrite	-3.1
"	"	"	"	-4.0
"	"	"	"	-3.6
WO1	"	"	Galena	-5.8
"	"	"	"	-3.4
"	"	"	Pyrite	-3.3
WO2	"	"	"	-0.6
WO1-cpl	"	"	Chalcopyrite	-1.4
KF92	"	"	Pyrite	-2.6
RJ20	Dysons Deposit	"	"	-2.5
RJ26	"	"	"	-4.7
"	"	"	"	-1.3
DY-4	"	"	"	-3.35
DY-7	"	"	"	+2.5
DY-8	"	"	"	-2.9
KF-91	Intermediate Deposit	"	"	-2.3
950W-650S	E.L. 1349	Whites Fm	"	+11.05
950W-740S	"	"	"	+9.9
" "	"	"	"	+9.36
950W-820S	"	"	"	+12.47
1050W-690S	"	"	"	+8.5
1050W-770S	"	"	"	+10.03
1800E-700S	"	"	"	+19.4
N7	Kharidunga	?	Pyrrhotite	+13.9
"	Nepal	"	"	+13.5
N9	"	"	"	+13.2
"	"	"	"	+13.6

the fluid. The sulfide forming at any one time does not necessarily represent the $\delta^{34}S$ value of the bulk of the ore fluid, but rather is controlled by the distribution of S species within the fluid and the fractionation occurring within them (Schuiling et al., 1983). Temperature will markedly affect equilibrium isotope fractionation within these species. There is a kinetic hindrance to equilibrium establishment at temperatures below $200^{\circ}C$ due to decreasing rate of chemical and isotopic exchange reactions. Thus ongoing precipitation of a sulfide can give a species with a range of $\delta^{34}S$ values. Similarly the concentration of S in the fluid will affect the $\delta^{34}S$ value e.g. where $T = 250^{\circ}C$ and $^{34}S_{\Sigma S} = 0\%$, pyrite precipitating from a solution containing ΣS of 0.1m, can show a range of $\delta^{34}S$ values from -26.5% to + 4% whereas if the ΣS is 0.001m, the range reduces to -18% to 0% (Ohmoto, 1972). Yet another fractionation affect can be brought about by the ongoing precipitation of certain sulfides e.g. galena has a lower reduced partition ratio function compared to other sulfides (Ohmoto, 1972). This leads to a continuously increasing $\delta^{34}S_{\Sigma S}$ value in the remaining fluid. Even further variations can be achieved by replacement processes involving earlier formed sulfide mineralisation by reactions with a hydrothermal fluid.

Thus it becomes mandatory that S-istope studies be intergrated with detailed geological, mineralogical and other detailed geochemical studies such as fluid inclusions before attempting to interpret the results and propose feasible models.

7.4 Sulfur Isotope Data and their Interpretation

Sample and $\delta^{34}S$ data obtained are shown in Table 5. The $\delta^{34}S$ numbers are further shown in Fig. 102.

The distribution of values in Fig. 102 shows that there is variation

Fig. 102 RUM JUNGLE AREA

S Isotopes values
All samples

Chalcopyrite
Pyrite
Galena

No. of samples

$\delta^{34}S(‰)$
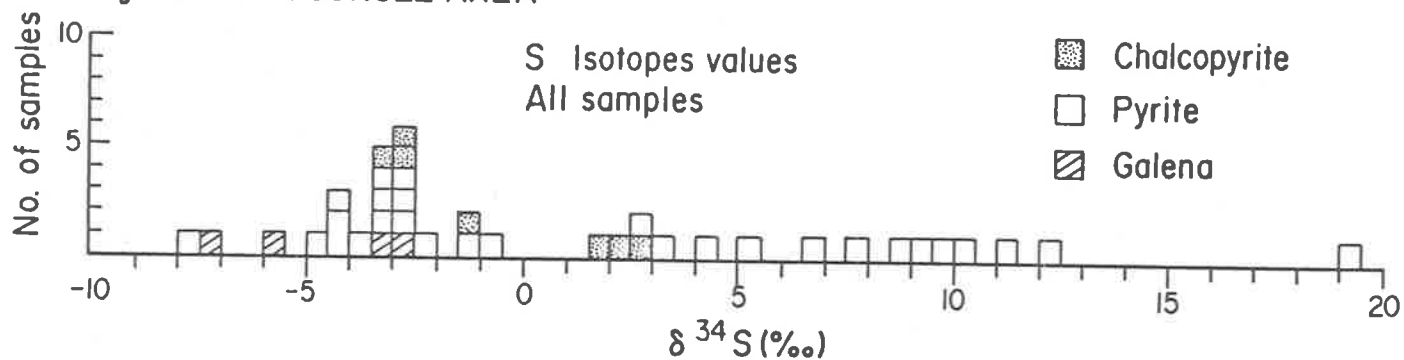
RUM JUNGLE AREA

ISOTOPIC ZONATION OF S ISOTOPE VALUES IN TIME AND SPACE

Geographic Distribution (Horizontal – not to scale)
Stratigraphic Sequence (Vertical – not to scale)

EL-1349   WHITES FM   YOUNGEST
WEST (of Rum Jungle Complex)   NOT SHEARED   EAST (of Rum Jungle Complex)

THE EMBAYMENT   WHITES FM. – SHEAR ZONE
(WHITES, INTERMEDIATE & DYSONS)

ASSOCIATION OF COOMALIE DOLOMITE & WHITES FM.
(BROWNS & MT FITCH)   – SHEAR ZONE

EL-1349   CRATER FM.   OLDEST

$\delta^{34}S(‰)$
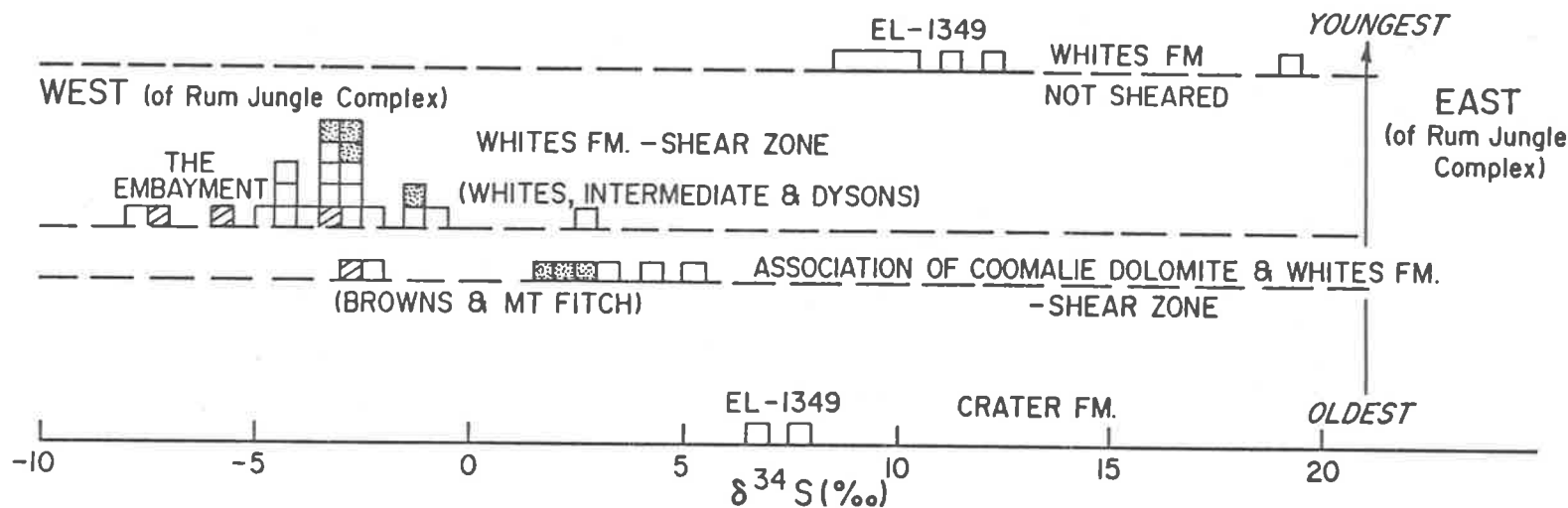
in both time and space. The diagenetic pyrite (Chpt. 4) in the Crater Formation has a mean value of +7.2‰ (two values only). In view of the parameters previously considered, the process of sulfur generation was most likely that of bacterial reduction from a sulfate source in an open system. There is ubiquitous evidence of stromatolites in the Rum Jungle area so that it is not unreasonable to assume that bacterial reducers were also prevalent.

A similar process is envisaged for the diagenetic pyrite in the stratigraphically higher Whites Formation within E.L. 1349. Here the average value (for 7 samples) is somewhat higher - namely +11.52‰ , including an anomalously enriched value of +19.4‰ . When this is excluded the average value drops to +10.21‰ (maximum deviation of +1.71‰ . The situation within The Embayment (Fig. 12) is quite different. Here, the sulphide samples are from vein type material, in a zone that is best described as a shear zone cutting across the Coomalie Dolomite - Whites Formation boundary, except for sample DY7, which has the appearance of stratabound pyrite, i.e. disseminated euhedral crystals in carbonaceous shale.

The values for The Embayment group (excluding Browns Deposit, which has a somewhat different geological setting) range from -7.3‰ to + 2.5‰ . The average value for the 22 samples is -3.22‰ , which consists of averages of -2.98‰ for the 16 pyrite samples, -5.5‰ for the three galena samples and -2.50‰ for the 4 chalcopyrite samples.

This range is barely within the limits for magmatic source S. Nevertheless, two possible magmatic sources were available: (1) basic intrusives (amphibolites) which could have supplied S in a primary fluid or which could have been leached by migratory fluids, or (2) the proposed reactivation at depth of the granitoid complexes, which may have given rise to hydrothermal fluids moving through shear zones.

These shear zones, by their very nature, were favourable mineralisation depositional sites.

However, the addition of the values obtained for the Mt. Fitch and Browns Deposits extends the range of values from -7.3‰ to +5.1‰ . This range is considered to be outside the standard deviation limits of mantle S (Ewers et al., 1984). Thus it seems more likely that the sulfides were precipitating from pervasive hydrothermal fluids which were undergoing δ $^{34}S_{CS}$ value changes due to various fractionation mechanisms operating.

The O and C stable isotope values obtained by Donnelly and Roberts (1976) support the premise of an algae-rich lacustrine carbonate, as the ^{18}O values are significantly below the range reported for marine carbonates and the ^{13}C values indicate an organically derived CO_2 contribution to the formation of the carbonate (Ewers et al., 1984). Therefore, it is likely that the enriched sedimentary pyrite values resulted from the deposition of this pyrite in organic-rich sediments from H_2S which was produced by sulfate reducing bacteria. Later interactions between these sulfides and hydrothermal fluids led to the production of the ore-forming fluids from which the range of metal sulfides over a considerable period of time precipitated in favourable environments, eventuating in the range of values presented.

To obtain temperature from S-isotope studies co-existing species need to be in equilibrium (Rye and Ohmoto, 1974). Textural evidence of the samples containing co-existing species showed that this was not the case. The only sample where a possible equilibrium between pyrite and galena occurred was WO-1, but the temperature calculated appeared to be totally unrealistic : > 800°C, and presumably was due to disequilibrium.

The four pyrrhotite samples from Kharidunga gave results within a very narrow range : namely +13.2‰ to +13.9‰ . These numbers would seem

a.   Massive pyrrhotite with minor magnesite. Sample N9, Kharidunga,

        Nepal.

b.   Classic boxwork gossan similar to that which led the author to

        the discovery of the sulfides at Kharidunga, Nepal. The sulfides

        occur in an analogous position to those occurring at Rum Jungle.

        Sample N12.

c.   Massive pyrrhotite with minor chalcopyrite and cleavage

        rhombohedra of magnesite. Sample N10, Kharidunga, Nepal.

to indicate a sulfate derived source for the S. Unfortunately precise age

for this material is not available, but it is probably Precambrian (pers.

comm., G.S. Thapa, Dept. of Mines and Geology, Kathmandu).

7.5 Conclusions

To re-iterate the conslusions relative to the aims as set out

earlier:-

(1) (a) Disseminated stratiform sulfides have sulfate-reduced

characteristics.

(b) Crosscutting vein sulfides have "magmatic" characteristics.

However, there is no need to invoke a magmatic source, as low temperature

remobilization via pervasive hydrothermal fluids could have achieved the

same characteristics.

(2) There was similarity in values obtained for diagenitic pyrite

stratigraphically up section. The variation between the time of the

Crater Formation and Whites Formation is due to a later event, and has no

chronostratigraphic significance.

(3) By utilising Donnelly and Roberts (1976) data as well as that of this

study, variation in δ^{34}S values in Whites Formation is due to

fractionation processes.

(4) This work supports that done by Donnelly and Roberts (1976) on the

Browns Deposit and Woodcutters Prospect, as per the conclusions.

(5) No temperature data was obtained.

(6) The figures obtained from the pyrrhotite from the carbonaceous shale

(which lithologically and stratigraphically is analagous to Whites

Formation) at Kharidunga are similar to those from Whites Formations, E.L.

1349. Therefore, the S- source at Kharidunga could also have been from

the reduction of sulfate in an open system.

TABLE 6

Co:Ni values and ratios

Sample		Co(ppm)	Ni(ppm)	ratio	mineral
D10	(b)	.05	.06	.8	pyrite
"	(c)	.07	.02	3.5	"
"	(d)	.07	.04	1.8	"
E28	(a)	.06	.02	3.0	"
"	(b)	.07	.03	2.3	"
G04		.27	.43	.6	"
G108	(a)	.08	.35	.2	"
"	(b)	.08	.33	.2	"
"	(c)	.08	.24	.3	"
"	(d)	.08	.15	.5	"
G950W/					
650S	(a)	.05	.02	2.5	"
"	(c)	.03	.07	.4	"
"	(f)	.08	.03	2.7	"
G950W/					
740S	(a)	1.48	.04	37.3	"
"	(b)	.05	.02	2.5	"
"	(c)	.06	.02	3.0	"
G950W/					
820S	(a)	.07	.03	2.3	"
"	(b)	.06	.22	.3	"
S1050W/					
690S	(a)	.05	.06	.8	"
"	(b)	.05	.13	.4	"
"	(c)	.03	.06	.5	"
G1050W/					
740S	(a)	.05	.06	.8	pyrite
"	(b)	.04	.08	.5	"
"	(c)	.05	.03	1.7	"
"	(d)	.12	.17	.7	"
WO-PY1		.06	.10	.6	"
WO-PY3	(a)	.09	.10	.9	"
"	(b)	.05	.07	.8	"
WO-Cp1	(a)	.09	.02	4.5	"
"	(b)	.09	.02	4.5	"
"	(c)	.07	.02	3.5	"
"	(e)	.02	.03	.7	"
"	(f)	.10	.04	2.5	"
WO-RJ13	(a)	.07	.01	7.0	"
WO-KF					
92W	(b)	.05	.45	.1	"
IN-KF					
91	(b)	.05	.01	5.0	"
DY4	(b)	.06	.12	.5	"
DY7	(a)	.07	.02	3.5	"
"	(b)	.07	.02	3.5	"
"	(c)	.06	.03	2.0	"
"	(f)	.06	.03	2.0	"
DY8	(a)	.04	.04	1.0	"
"	(b)	.04	.05	.8	"

CHAPTER 8

PYRITE AND RELATED SULFIDES

8.1 PYRITE

Pyrite (FeS_2) is one of the most common sulfide minerals. As with tourmaline, it occurs in a variety of environments. Unlike tourmaline, pyrite has been studied extensively for decades (Fleischer, 1955; Berner, 1970a; Sinclair, 1967; Ohtagaki et al. 1974, Vaughan and Craig, 1978; Maynard, 1983). This is undoubtedly due to the early recognition of its close affinity with metallic mineral deposits.

Synsedimentary pyrite, which is of particular interest to this study, can be formed contemporaneously with the early diagenesis of the enclosing sediment by the bacteriogenic reduction of inorganic sulfate to H_2S, which in turn reacts with sedimentary Fe to produce Fe-sulfides (Rickard, 1973). At Rum Jungle, authigenic (diagenetic) pyrite occurs as discrete crystals disseminated (a) sparsely throughout the Beestons (Plate 28) and Crater Formations (Plate 30) and the magnesite sequences (Plate 19) and (b) ubiquitously in Whites Formation (Plate 44, 45). The S isotope data indicates that this pyrite formed from S that shows bacteriogenic - origin characteristics (Chpt. 7). It appears likely that this pyrite is primary.

In contrast, the pyrite that occurs within the polymetallic deposits within the area shows great complexity in textures (Plate 45, 46), geochemistry (Appendix 3) and sequence of mineralisation. The S isotope data indicates that the sulfides (including pyrite) could have formed from S from the remobilization of the primary pyrite (Chpt. 7). However, an additional source of metals to form the polymetallic sulfides is required apart from that of the sedimentary environment (Rickard, 1973), which could also be sourced in the alkaline, lacustrine waters. It is suggested

TABLE 6 (cont.)

Co:Ni values and ratios

Sample		Co(ppm)	Ni(ppm)	ratio	mineral
BR4	(a)	.06	.07	.9	pyrite
"	(b)	.09	.05	1.8	"
"	(c)	.19	.02	9.5	"
BR5		.08	.03	2.7	"
MF80/06	(a)	.67	.79	.8	pyrite
WO-Cpl	(a)	.07	.03	2.3	marcasite
"	(b)	.08	.02	4.0	"
"	(c)	.08	.02	4.0	"
"	(d)	.03	.07	.4	"
BR4		.05	.03	1.7	"
BALC	(a)	.11	.17	.6	pyrite
"	(b)	.09	.04	2.2	"
"	(c)	.07	.05	1.4	"
N1		.03	.02	1.5	"
N7	(b)	.06	.01	6.0	pyrrhotite
N8	(a)	.04	.01	4.0	"
"	(b)	.06	.01	6.0	"

that the hydrothermal fluids, evidence for which is supplied by the presence of the extensive stratiform tourmalinites (Chpt. 4), were that source. Certainly there is textural evidence for at least two, and possibly three generations of pyrite formation (Plates 45, 46).

Roberts (1982) has used the trace element content of pyrite to differentiate between pyrite formed from base-metal bearing fluids and diagenetic pyrite. He found that the former had relatively high Ag, Cu, Pb and Mo contents, whilst the latter contained higher Mn, Ti and Ni. Similarly at Rum Jungle Cu and Pb (and V) were higher in the base metal environment, but Ni was lower in the diagenetic pyrite, whilst there was no appreciable difference in Ag (Appendix 3). Nevertheless, the trace element contents do support the hydrothermal origin for the pyrite for the polymetallic sulfide deposits. Further evidence was sought from the Co and Ni contents.

The Co : Ni ratio in pyrite was hoped to be a definitive indicator of (a) environment of formation, (b) source of metals and (c) degree of metamorphism (Fleischer, 1955; Hawley and Nichol, 1961; Loftus-Hill and Solomon, 1967; Davidson, 1969 and Mookherjee and Philip, 1979). Although the initial expectations have not been entirely fulfilled, it must be accepted that convincing data can only be generated from simple one source situations - that when complexities can be demonstrated there will naturally be departure from expected ratios and values. Indeed, recent reassessment of the Co:Ni ratios is leading to its tentative acceptance of this method (Bralia et al., 1979; Roberts, 1982; Campbell and Ethier, 1984).

The Co:Ni ratios and values obtained from pyrite, marcasite and pyrrhotite from Rum Jungle (and Balcanoona and Kharidunga for comparative purposes) are given in Table 6. Samples D10(b) to G1050W/740S(d) are considered to be diagenetic pyrite. Samples WO-Pyl to WOCpl (d) are

352

Fig. 103 Co:Ni VALUES IN PYRITE SAMPLES
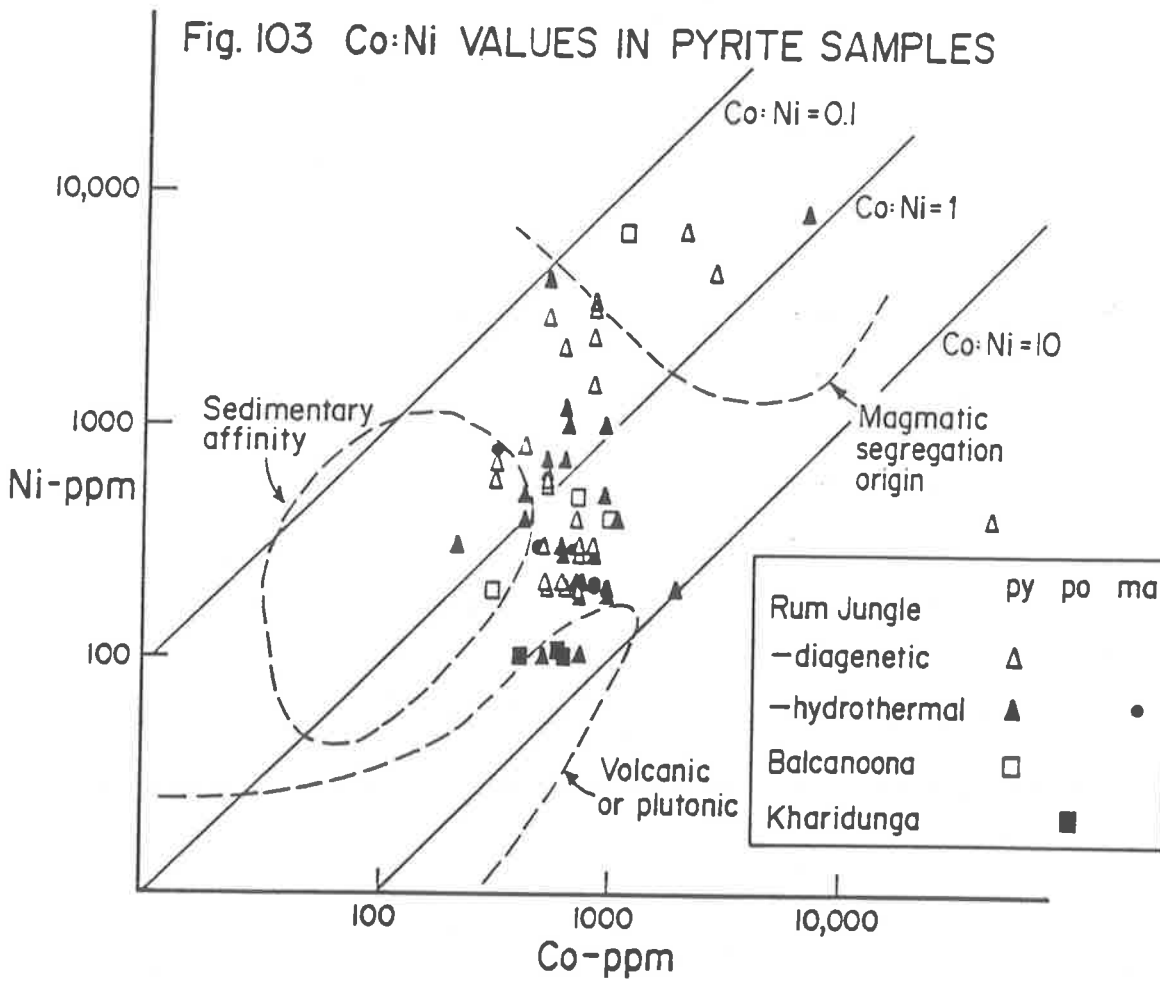
(Dashed fields from Campbell & Ethier, 1984)

likely to have resulted from hydrothermal fluid influence. Fig. 103 shows that this data does not fit into the fields prescribed by Campbell and Ethier (1984). Rather, overlapping fields (sedimentary and hydrothermal) can be constructed. Nor do the ratios fit those given by Bralia et al., (1979). In fact, comparison with Fig. 5 in Bralia et al. (1979) shows that the areas investigated in this study are anomalously enriched in both Co and Ni. It is suggested that this is due to the marked capacity of HCO_3^- to form Co and Ni (and other trace metals) complexes (Fouillac and Criaud, 1984). The spatial association of magnesite was a contributing factor in the formation of HCO_3^- and CO_3^{2-} rich hydrothermal fluids. Consequently it is unrealistic to expect the pyrite at Rum Jungle to reflect "normal diagenetic" Co and Ni values and ratios.

Other trace elements of interest contained within the pyrite were U, Au, V, Cr, Se, As, Sn and Bi (Appendix 3), with the first two being of major interest. Table 7 shows the correlation matrix for these elements. The element Cr within the hydrothermal pyrite is particularly interesting. It occurs in 22% of the 32 analysed samples. When it is present, it has a correlation of 1.00 with both U and V but only 0.03 with Au, whereas Au itself occurs in 25% of the samples and has a correlation of 0.38 with U and 0.50 with V. It appears, then, that the most useful pathfinder elements for U and/or Au in pyrite are U and Au! - (plus V and Cr). With the increasing interest being shown in the development of an economically viable bacteriogenic process incorporating the breakdown of pyrite to release Au, the values obtained in this study may be of interest in the future. However, it must be emphasised that the reported Au values (Appendix 3) are to be taken cautiously because the Au X-ray spectrum is enhanced by interference lines (B. Griffin, 1984, pers. comm.). The conclusion is that only pyrite samples with Au values above the detection limit do contain Au.

Further analytical work showed that no particular geochemical halo

TABLE 7

CORRELATION MATRIX - TRACE ELEMENTS IN PYRITE

	V	U	Cr	Se	As	Sn	Bi	Au
*	22/16	17/15	7/9	8/11	12/10	4/4	12/8	8/7
V								
U	12/8							
Cr	7/6	7/5						
Se	4/7	3/5	3/5					
As	7/6	6/4	2/3	4/5				
Sn	2/1	1/3	2/-	2/3	3/2			
Bi	7/2	6/6	2/2	3/3	9/4	2/1		
Au	4/3	3/3	1/2	2/3	4/2	2/1	4/4	

* Numbers of samples with element present above detection limit.

First number: hydrothermal pyrite samples (total = 32)

Second number: diagenetic pyrite samples (total = 29)

(analyses in Appendix 3)

pattern results from the oxidation of the pyrite to Fe-oxides (Appendix 3).

Further suggestions concerning the genesis of the pyrite are discussed in Chpt. 10.

8.2 Marcasite

Minor amounts of marcasite occur at Rum Jungle intimately associated with the pyrite (Plate 46). Vaughan and Craig (1978) suggest that although the two sulfides can be considered polymorphs, there may actually be compositional differences. This difference was not found at Rum Jungle (Appendix 3), so that the marcasite has e.g. Pb values an order of magnitude higher than the maximum quoted by Vaughan and Craig (1978).

It seems more likely that the marcasite formed as the preferred Fe-disulfide as the pH dropped (Maynard, 1983).

8.3 Pyrrhotite

It is well documented that pyrrhotite plus S can form from the breakdown of pyrite during metamorphism (Kullerud and Yoder, 1959) if a sufficiently high temperature is reached ($> 380^{\circ}C$; Sundblad, 1981). Other workers (e.g. Vokes, 1969; Sangster and Scott, 1976) have proposed that pyrrhotite can be deposited as a primary or diagenetic constituent of sulfide ore bodies.

No pyrrhotite was found at Rum Jungle during this study, although it has been reported by earlier workers (e.g. Fraser, 1980).

Pyrrhotite was the dominant sulfide overlying the Kharidunga magnesite (Plates 44, 47). Certainly the metamorphic grade indicated (?phengite) and the temperatures obtained from fluid inclusions suggest that the
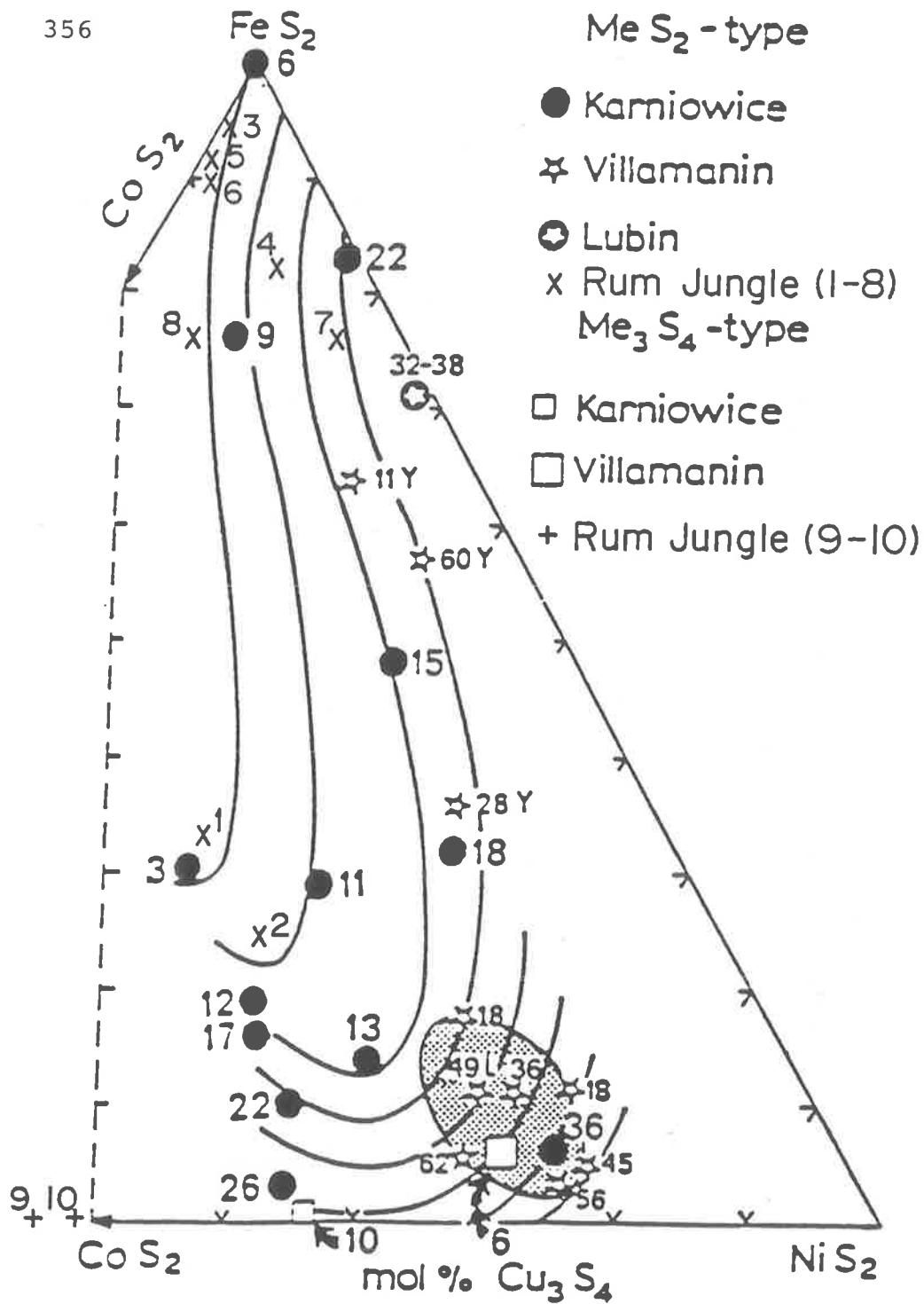
Fig. 104: Compositions of the Cu-Ni-Fe-Co disulfides. Numbers and contours indicate CuS_2 content calculated on the bases of Cu+Ni+Fe+Co=1 and Ni+Fe+Co=1. Sources: Rum Jungle - this study; remainder from Fig. 1, Zakrzewski, 1984.

metamorphogenic breakdown of pyrite could have been responsible for the formation of this pyrrhotite. However, insufficient information is available from which to draw firm conclusions. Certainly the similarity in the trace element content (Appendix 3) of both the pyrite and pyrrhotite, plus the δ^{34}S values of the pyrrhotite suggest a similar origin for both i.e. diagenetic; nor do the values exceed those given as maxima by Vaughan and Craig (1978).

8.4 The Villamaninite - Bravoite Series and the Thiospinels

A considerable range of polymetallic sulfides occur in the Rum Jungle area, many of which have been studied in depth by various workers e.g. Needham, 1981.

The particular group that will be briefly covered in this section have been selected because this study is apparently the first report of their occurrence in Australia. The group consists of the Cu-Co-Ni-Fe disulfides of the villamaninite - bravoite series. They are intimately associated with siegenite, one of the Cu-Co-Ni-Fe thiospinels.

During examination of polished sections, very small grains of a mineral tentatively identified at this stage as cobaltion pyrite were observed (Plate 46). The small idiomorphic crystals (cubic or cubo-octahedral), which morphologically resemble the nearby rows of secondary pyrite crystals, are lower in hardness and reflectivity than the pyrite and have a pinkish yellow/grey colour (Plate 46).

Electron microprobe analyses of 10 of these grains from 4 samples (Appendix 3) show that their composition varies from villamaninite to cuprian bravoite (Ypma et al., 1968; La Iglesia, 1974; Moh, 1980; Zakrzewski, 1984) to siegenite (Vokes, 1967; Vaughan and Craig, 1978).
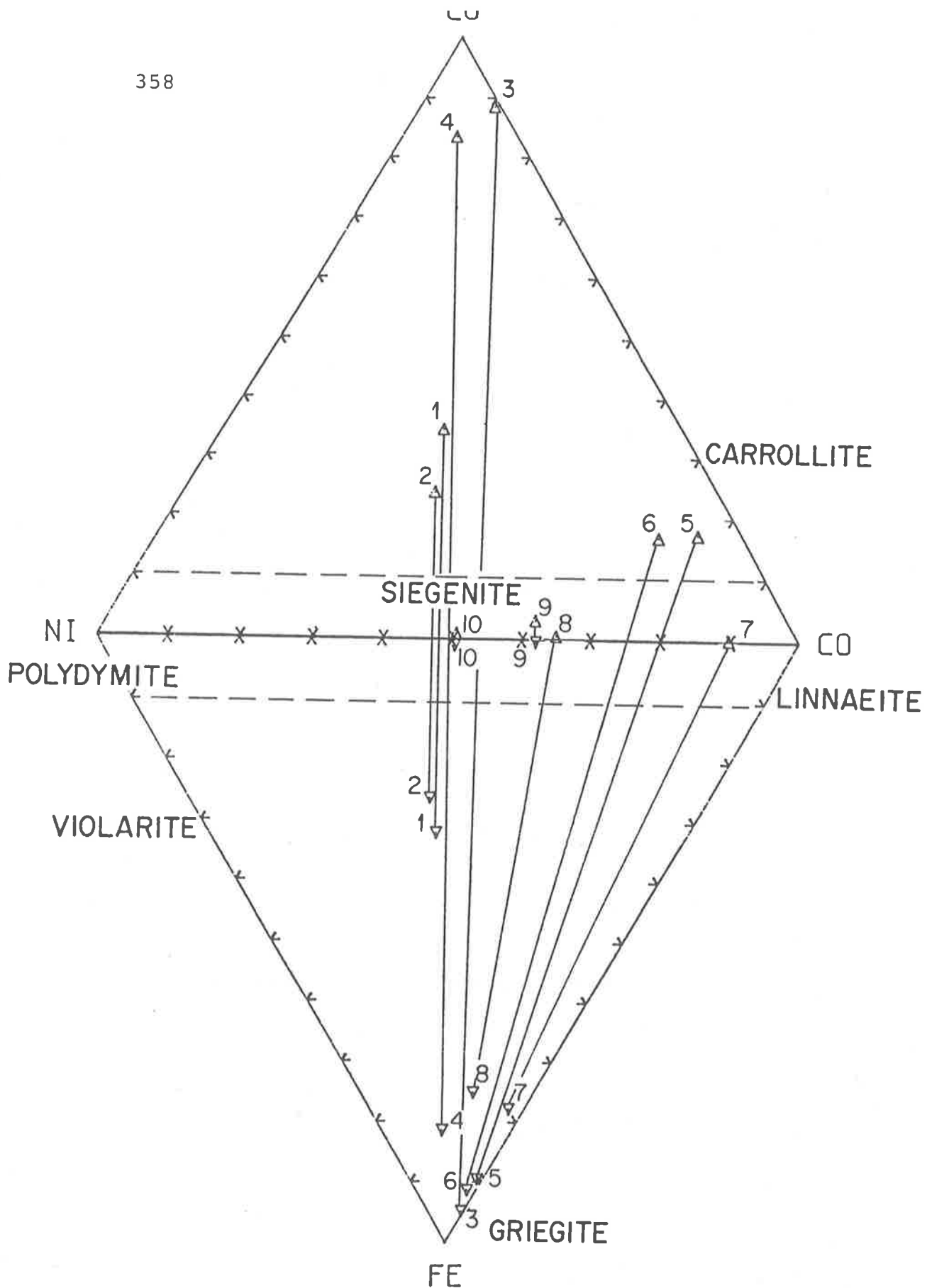
Fig. 105: The Cu-Co-Ni and the Co-Ni-Fe triangles in the Cu-Co-Ni-Fe tetrahedron. Each Rum Jungle sample analysis is represented by a point in each of the triangles, joined by a tie line.

Villamaninite is the only known ternary compound in the Cu-Ni-S disulfide system (Moh and Kullerud, 1982). Villamaninite is an extremely rare mineral and has only been described from a few localities (Zakrzewski, 1984). This rarity is due to the preferential formation of stable sulfides such as chalcopyrite and pentlandite when Fe is also available in the system, as Ni + Cu sulfides are metastable in the presence of Fe except under unusual geochemical conditions e.g. the temperature <200°C, so that the aforementioned equilibrium assemblages cannot be established due to slow reaction rates (Moh and Kullerud, 1982). Even at this low temperature their villamaninite analyses showed evidence of considerable solid solution, although the 1:2 cation to anion ratio was invariant. Although the Rum Jungle samples plot in the same field as the villamaninite - bravoite samples in Zakrzewski's (1984) study (Fig. 104), there is deviation from the 1:2 ratio. There are a number of alternative explanations for this deviation:-

(a) the S depletion correlates with those analyses that show low totals. If S is the aberrant element, then addition of the appropriate amount of S to give a total of 100% also restores the 1:2 ratio. This is applicable to the villamaninite grains rather than to the bravoite grains (Appendix 3)

(b) the compositions are partly dependent upon the limitations of the technique. As many of the grains are very small ($\leqslant$10μm) there is the possibility of contamination (i.e. inclusion of) from the host material. This is probably the cause of the high Pb value in WO-RJ7 (Appendix 3), as this grain is enclosed by galena.

(c) Some of the grains are S-enriched thiospinels. Certainly the two samples from Whites Deposit are siegenite (Appendix 3). Zakrzewski (1984) suggests that the cuprian siegenite at Kariowice, Poland formed from villamaninite i.e. they are intimately associated. Similarly, Ypma et al. (1968) noted bornite, marcasite and regular bravoite as alteration products of villamaninite at the type locality, Villamanin, Spain, with the eventual complete alteration to linneite (i.e. the thiospinel series) + chalcopyrite + bornite. Fraser (1980) recorded the occurrence of
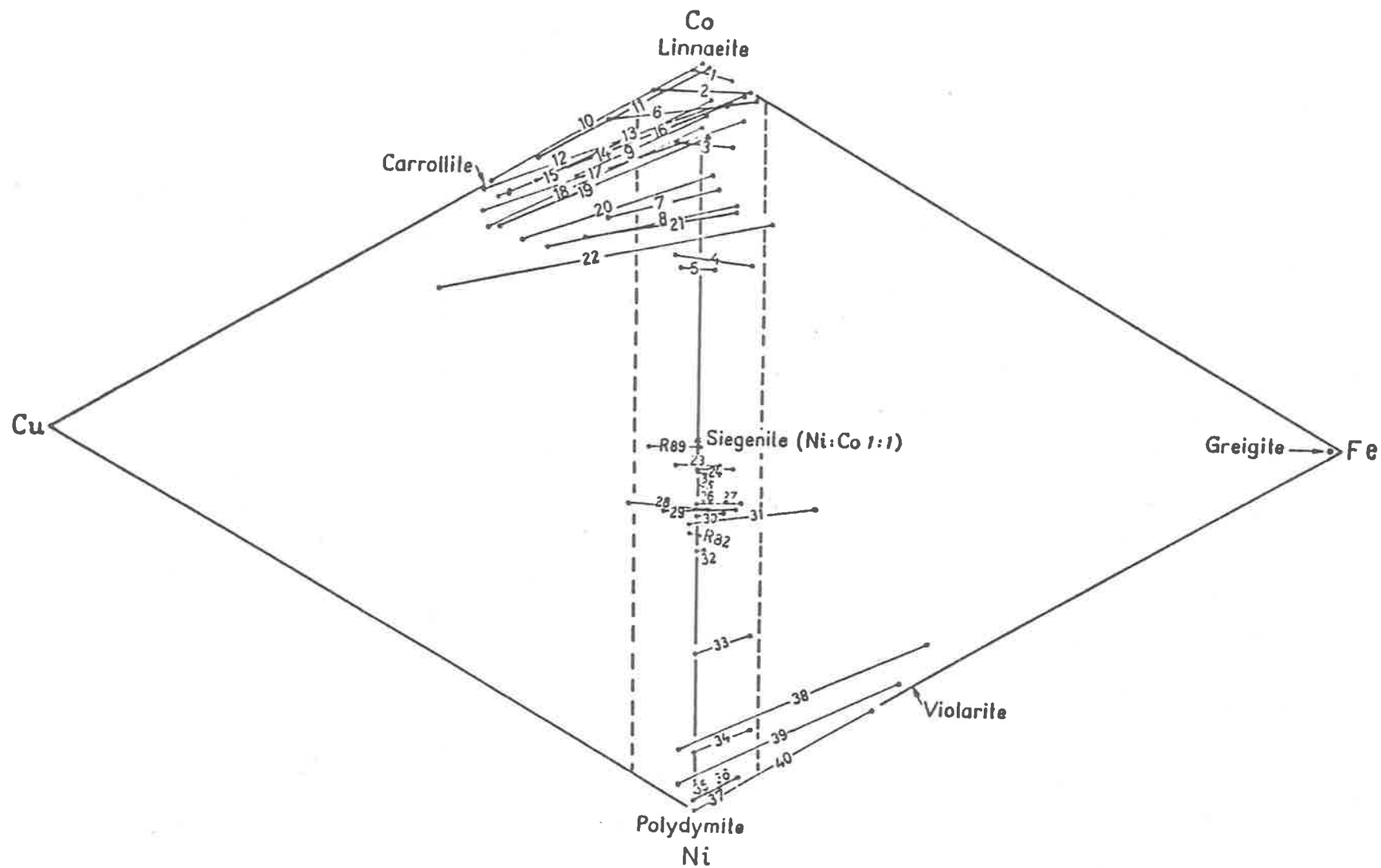
Fig. 106: The Cu-Co-Ni and the Co-Ni-Fe triangles in the Cu-Co-Ni-Fe tetrahedron. Each analysis is represented by a point in each triangle, joined by a tie-line.

(Vokes, 1967)

linneite, bravoite,? carrolite and ? cobaltnickelpyrite at Whites Deposit.

When all the samples are plotted on the Cu-Co-Ni-Fe thiospinel diagram (Fig. 105), the two Whites Deposit samples plot in the siegenite field. However, when the remainder are compared to Voke's plot (1967 - Fig. 106) it can be seen that they do not plot in the field(s) of any known thiospinels. It is suggested that this is because they are S-depleted disulfides.

Currently, material coarse enough to extract for X.R.D. work is unavailable. If and when it does become available, further work will be undertaken on this exciting find in order to further the understanding of the genesis of the polymetallic sulfides at Rum Jungle.

Meanwhile, it is proposed that the Mt. Fitch samples belong to the villamaninite - bravoite series.

TABLE 8

CALCULATED MINERALOGICAL COMPOSITION OF CORE SAMPLES

Sample No.	(CaMg)CO₃	MgCO₃	Talc	Clay	Qtz.	Total Impurities	Tot.CO₃	Total
CMPH 2a	2.40	93.65		.60	.80	1.4	96.0	97.4
3	1.08	83.26		.56	11.80	12.4	84.3	96.7
4a	.35	91.56		.30	3.95	4.3	92.4	96.7
4b	.75	82.34	7.2	1.71	2.75	11.7	83.1	94.8
5	1.15	93.40		.97	4.05	5.0	94.5	99.5
9	2.96	88.62		2.54	1.31	3.9	91.6	95.5
12	1.74	91.00		.58	5.00	5.6	92.71	98.3
16a	1.31	91.64		.24	3.74	4.0	92.9	96.9
16b	2.83	90.08	0.6	.24	3.18	4.0	92.9	96.9
16c	1.87	92.94		.15	2.64	2.8	94.8	97.6
16d	1.97	87.42	3.7	.26	3.34	7.3	89.4	96.7
16e	2.24	91.39	1.	.32	3.25	4.6	93.6	98.2
17a	.32	88.55	1.2	.51	5.13	6.8	88.6	95.4
17b	2.07	90.95		.26	3.98	4.2	90.9	95.1
18a	2.43	88.28		.90	4.70	5.6	90.7	96.3
18b	1.41	86.41	1.88	.74	5.59	8.2	87.8	96.0
20	1.34	89.15		.98	5.00	6.0	90.5	96.5
21	.55	84.08	.62	1.57	9.59	11.8	84.6	96.4
22a	1.15	26.19	15.2	1.41	1.11	17.7	77.3	95.0
22b	1.12	80.04	14.1	1.28	-ve	15.4	81.2	96.6
22c	.98	87.92	6.3	.85	-ve	7.2	88.9	96.1
23a	1.28	78.97	5.8	1.94	7.56	15.3	80.2	95.5
23b	.95	72.72	20.4	2.26	-ve	22.5	73.7	96.2
24a	1.44	85.79		.51	7.11	7.6	87.2	94.8
24b	1.38	84.83	5.0	1.00	4.35	10.4	86.2	96.6
24c	2.33	88.01		.74	5.70	6.5	90.3	96.8
24d	.92	78.77	11.82	.30	4.61	16.8	79.7	96.5
25a	14.48	64.83	1.56	2.82	10.78	15.2	79.81	94.5
25b	38.22	49.91		.31	13.50	13.8	88.13	101.9
26a	1.38	84.45	6.65	1.31	2.36	10.3	85.83	96.1
26b	1.87	79.50	15.34	.81	.31	16.5	81.37	97.9

(Roberts, 1978)

CHAPTER 9

EXPLORATION : E.L. 1349

9.1 Introduction

The targets selected by B.H.P. for exploration within E.L. 1349 (Figs. 7, 45) have been outlined previously. Nevertheless, they will be briefly repeated here, along with an outline of the exploration programme and its results. The intricacies of exploration philosophy and procedures will not be discussed.

(a) Magnesite

The major exploration target within E.L. 1349 was a relatively silica free magnesite deposit of 10^+ million tonnes, that could be mined by open cut methods.

(b) Uranium and polymetallic sulfides

These were considered secondary exploration targets within E.L. 1349, as they were already known to occur in the area.

(c) Gold

Gold is known to occur extensively within the Pine Creek Geosyncline, although it has not been found in economically viable concentrations within the Rum Jungle area. Therefore it was assigned the lowest order priority in the ensuing exploration program.

9.2 Magnesite

9.2.1 Ground Selection

Previous drilling for U and polymetallic sulfides by other mining companies and the B.M.R. had shown that there were thick sequences of
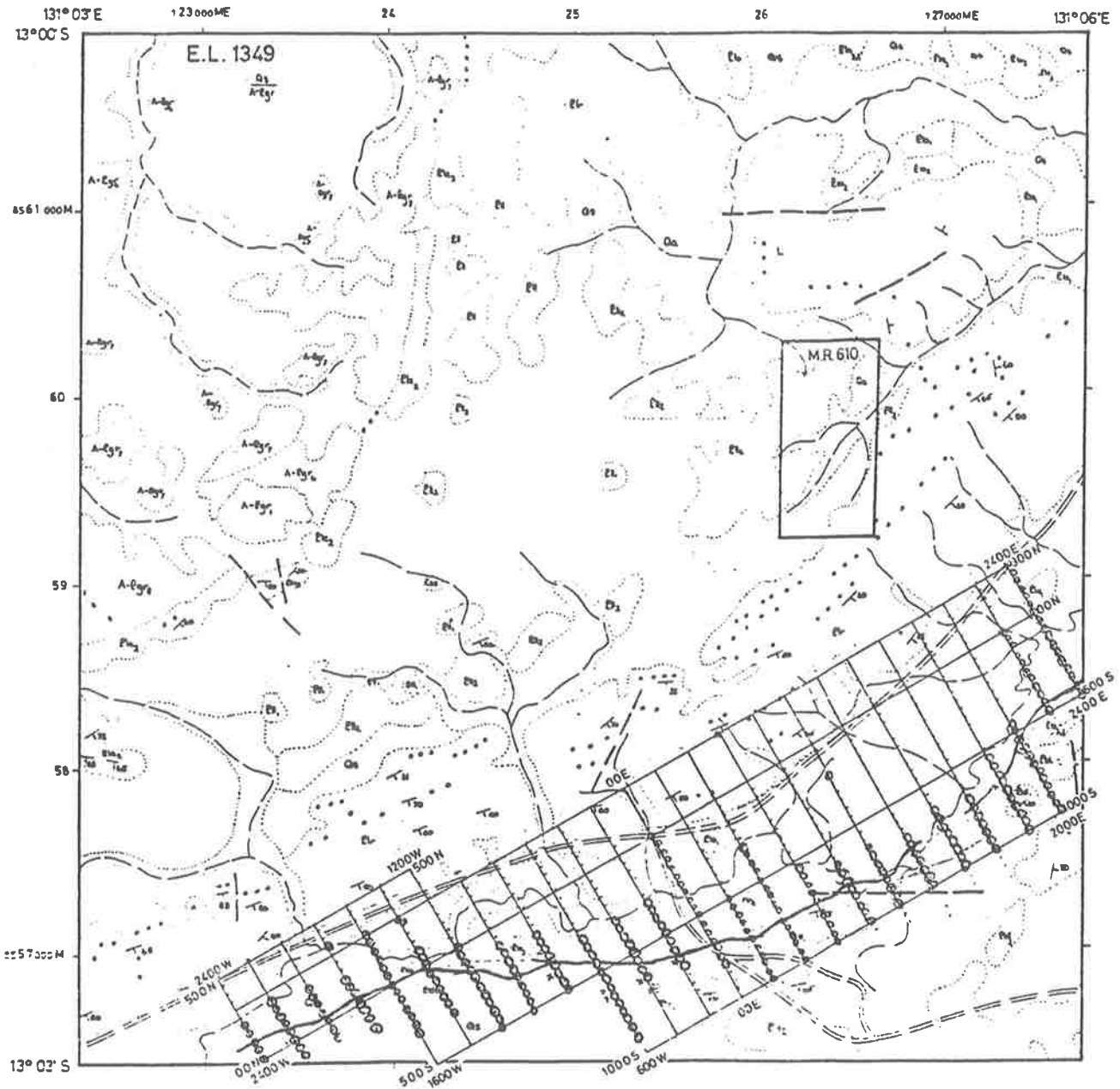
Fig. 107: Grid and holes drilled, E.L. 1349 geochemical drilling programme. See Fig. 108 for legend. Heavy line through grid is actual Coomalie Dolomite - Whites Formation contact established by drilling. Scale - 1:25,000.

magnesite, not dolomite as previously accepted, rimming the basement complexes. The B.M.R. carried out limited reconnaissance drilling of the magnesite in 1969 (Roberts, 1978), which showed that the carbonate areas 2 kms NNE to E of Batchelor indicated the best potential for the target sought by B.H.P. Consequently, this area was taken up as E.L. 1349.

9.2.2 Reconnaissance Programme

In 1978, Roberts undertook a reconnaissance program of mapping, sampling and shallow percussion drilling (with diamond cored "tail") to provide preliminary data upon which to base a more detailed follow-up program. Recalculating the analyses of the core samples from these 16 drill holes to mineralogical compositions (Table 8) showed that the carbonate in both the Celia Dolomite and the Coomalie Dolomite was predominantly magnesite (generally <2% dolomite). This preliminary program also showed that the magnesite was extensive, had a buried karst topography and that it seemed to be unpredictably contaminated by silica. Unless this latter finding could be altered to an acceptable predictability, the project would founder, as a raw product with a maximum of 5% silica was required (Chpt. 1).

It was at this stage that the writer became involved in the project and carried out the remainder of the evolving exploration program over the following two years. The logistics and results only will be emphasised in this Chapter, as the theoretical considerations and magnesite genesis models have been discussed in the previous chapters.

9.2.3 Pace and Compass Survey

The details concerning the acquisition of data (Appendix 1) for this survey are presented in Appendix 4.1, being a compilation of reports forwarded to B.H.P. during the exploration programme.

Fig. 108a
E.L. 1349 RUM JUNGLE, N.T.
GEOCHEMICAL SOIL SURVEY
Cu Histogram

FREQUENCY

ppm

(plus 1 at 1300)
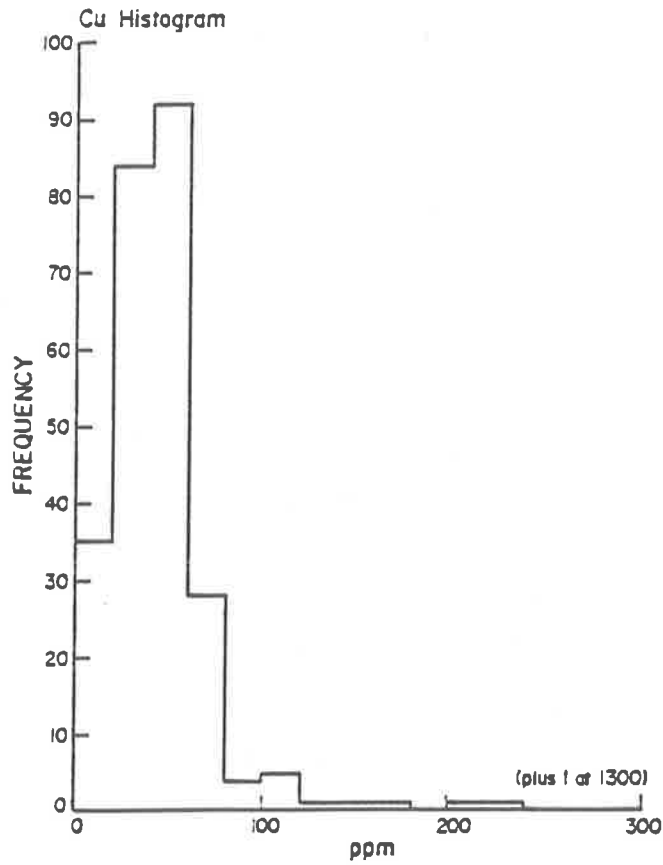
Fig. 108 b
E.L. 1349 RUM JUNGLE, N.T.
GEOCHEMICAL SOIL SURVEY
CUMULATIVE FREQUENCY DIAGRAM

Cu

ppm

.0 -49 Percentile	≤ 40ppm
50-74 "	41-50 "
75-89 "	51-70 "
90-94 "	71-85 "
95-974 "	86-115 "
975-100 "	> 115 "

CUMULATIVE FREQUENCY - %

Fig. 109a
E.L. 1349   RUM JUNGLE, N.T.
GEOCHEMICAL SOIL SURVEY

Pb Histogram
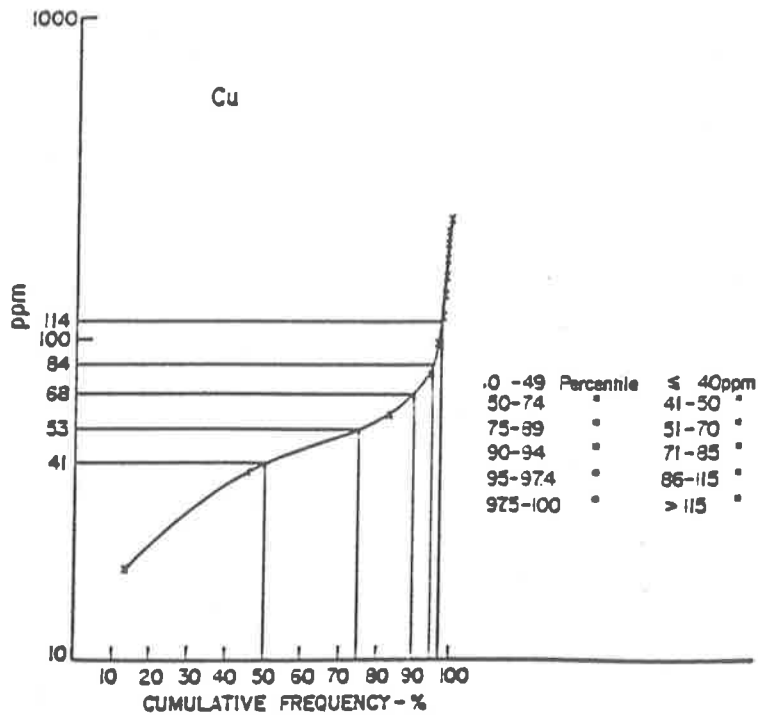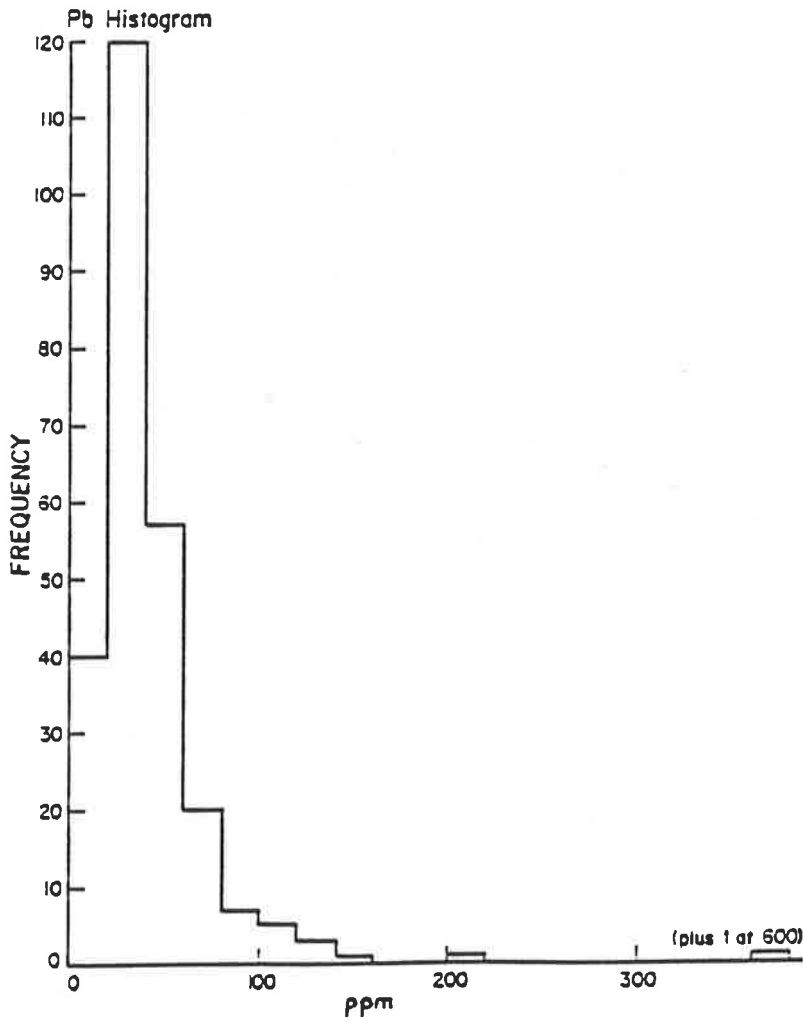
Fig. 109b
E.L. 1349 RUM JUNGLE, N.T.
GEOCHEMICAL SOIL SURVEY
CUMULATIVE FREQUENCY DIAGRAM

0 – 49 Percentile	≤ 30 ppm
50 – 74 "	31 – 50 "
75 – 89 "	51 – 70 "
90 – 94 "	71 – 95 "
95 – 97.4 "	96 – 125 "
97.5 – 100 "	> 125 "
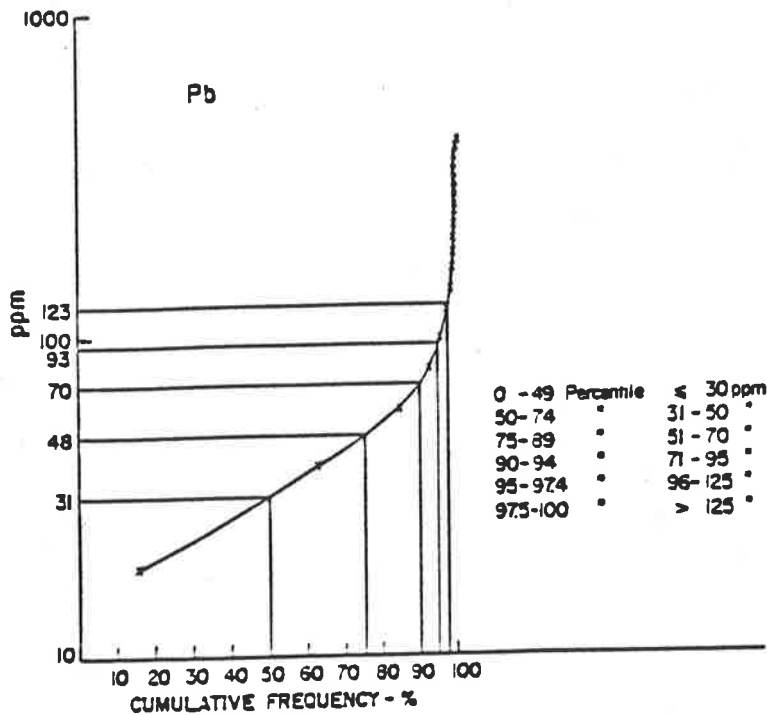
Fig. 110a
E.L. 1349 RUM JUNGLE, N.T.
GEOCHEMICAL SOIL SURVEY

Zn Histogram
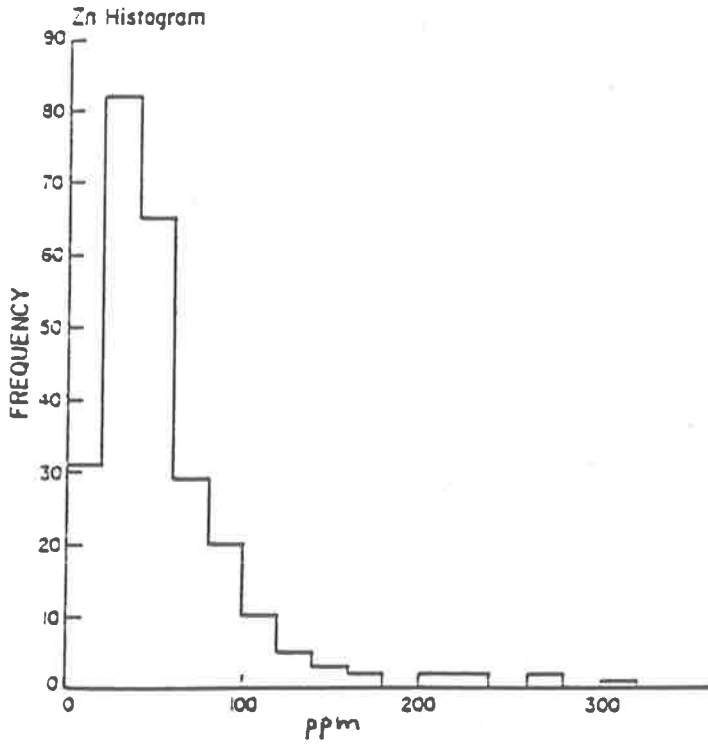
Fig. 110b
E.L. 1349 RUM JUNGLE, N.T.
GEOCHEMICAL SOIL SURVEY
CUMULATIVE FREQUENCY DIAGRAM

0 – 49	Percentile	≤ 40 ppm	
50 – 74	"	41 – 65	"
75 – 89	"	66 – 100	"
90 – 94	"	101 – 155	"
95 – 97.4	"	156 – 210	"
97.5 – 100	"	> 210	"
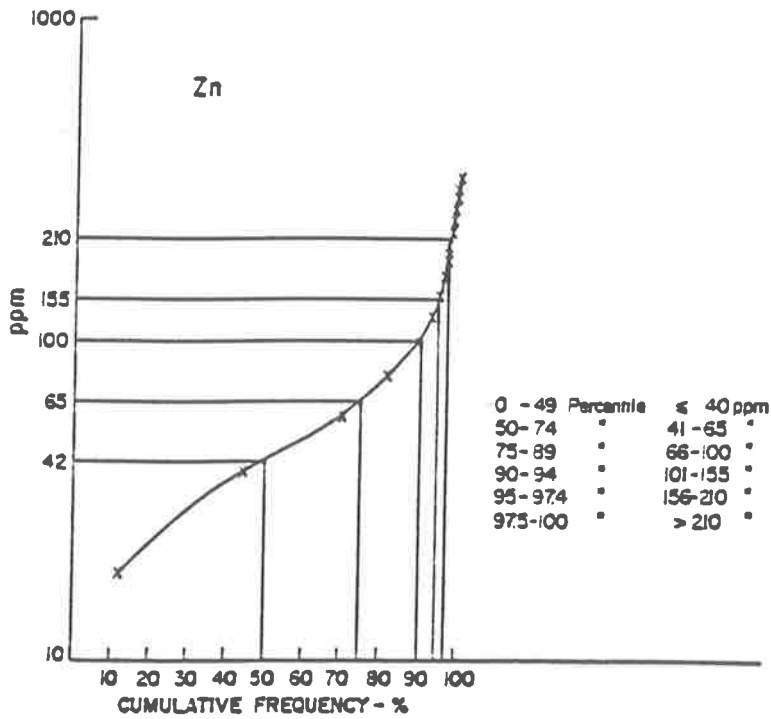
The data was presented in both plan form (Figs. 16-22) and as a comprehensive data bank (Appendix 1). Selected sections of this data bank were also analysed for correlations between parameters (Table 2). There was no consistent correlation between any of the observed parameters, which was disheartening as far as the magnesite mining project was concerned.

9.2.4. Drilling

The area chosen for a follow-up drilling program was rimmed by outcropping magnesite (Plate 39) between areas CeB and CeC (Fig. 45). It was considered that if relatively shallow subcropping magnesite was present, this would be the most feasible site for an open cut mine.

Once again it was found that:-

(a) the carbonate was predominantly magnesite,

(b) there was no pattern to the impurity content and

(c) there was a palaeokarst surface present, which would hinder open-cut development.

At this stage the magnesite field exploration program was halted. Samples were sent to Osterreichish - Amerikanische Magnesit A.G., Austria for beneficiation tests to assess the feasibility of removing the silica. Whilst awaiting these results E.L. 1349 became the subject of a Land Claim by local Aborigines. This claim was eventually allowed, with B.H.P. having the right of appeal. Understandably this has considerably reduced the company's interest in the project, so that it is currently shelved.

Fig. IIIa
E.L. 1349 RUM JUNGLE, N.T.
GEOCHEMICAL SOIL SURVEY

Ni Histogram

(plus 1 at 1100)
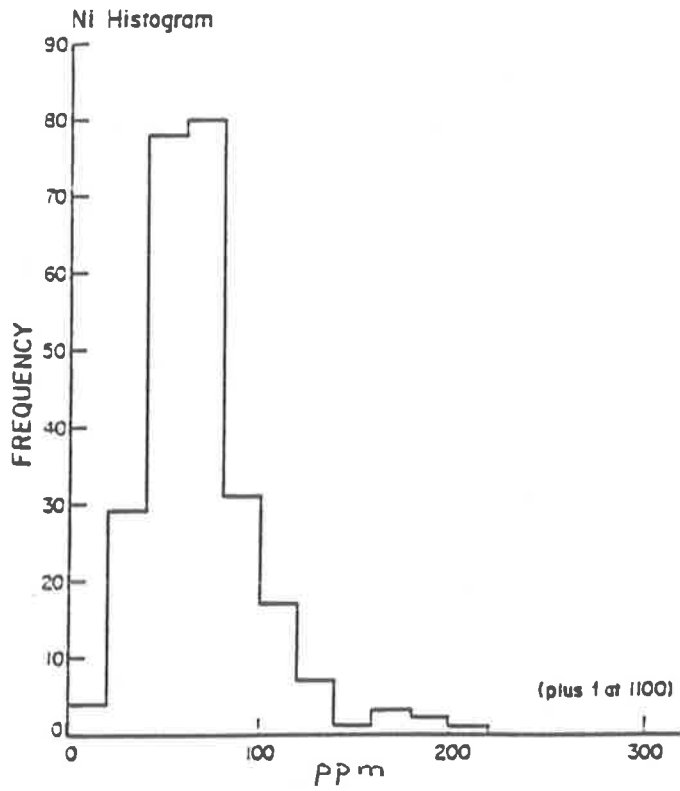
Fig. III b
E.L. 1349 RUM JUNGLE, N.T.
GEOCHEMICAL SOIL SURVEY
CUMULATIVE FREQUENCY DIAGRAM

	Percentile		
0 – 49	Percentile	≤ 60 ppm	
50 – 74	"	61 – 80	"
75 – 89	"	81 – 105	"
90 – 94	"	106 – 120	"
95 – 97.4	"	121 – 160	"
97.5 – 100	"	> 160	"

Fig. 112a
E.L 1349 RUM JUNGLE, N.T.
GEOCHEMICAL SOIL SURVEY

Co Histogram
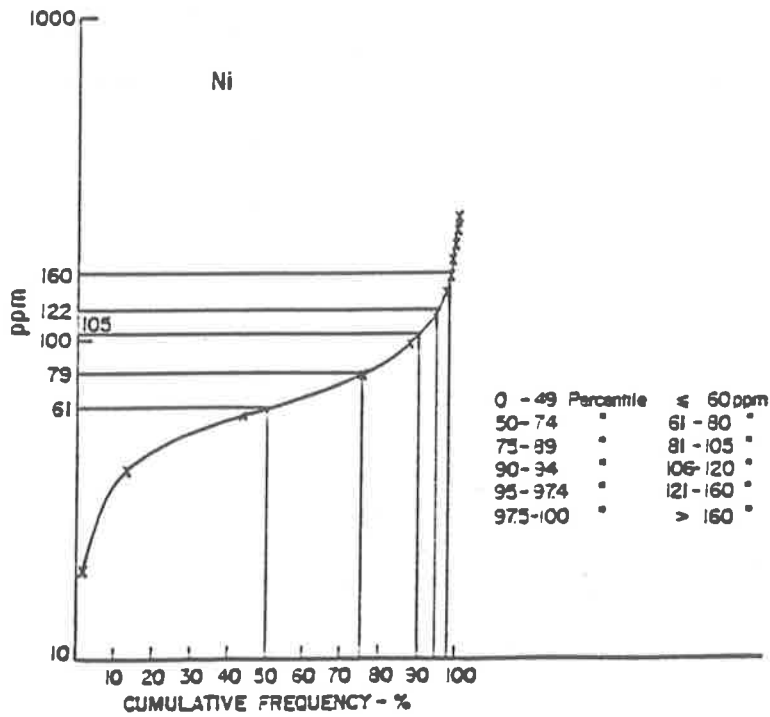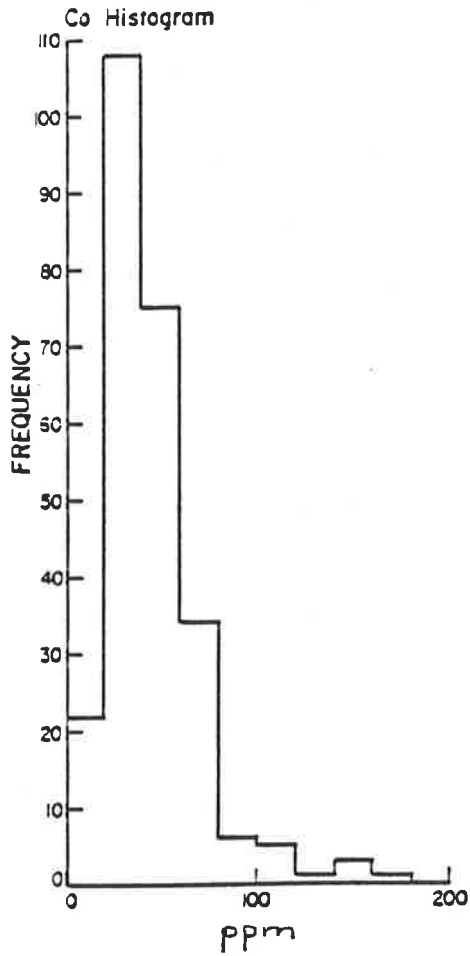
Fig. 112b
E.L 1349 RUM JUNGLE, N.T.
GEOCHEMICAL SOIL SURVEY
CUMULATIVE FREQUENCY DIAGRAM

	Percentile		
0 – 49	Percentile	≤ 40 ppm	
50 – 74	"	41 – 55	"
75 – 89	"	56 – 70	"
90 – 94	"	71 – 90	"
95 – 97.4	"	91 – 115	"
97.5 – 100	"	> 115	"

CUMULATIVE FREQUENCY - %
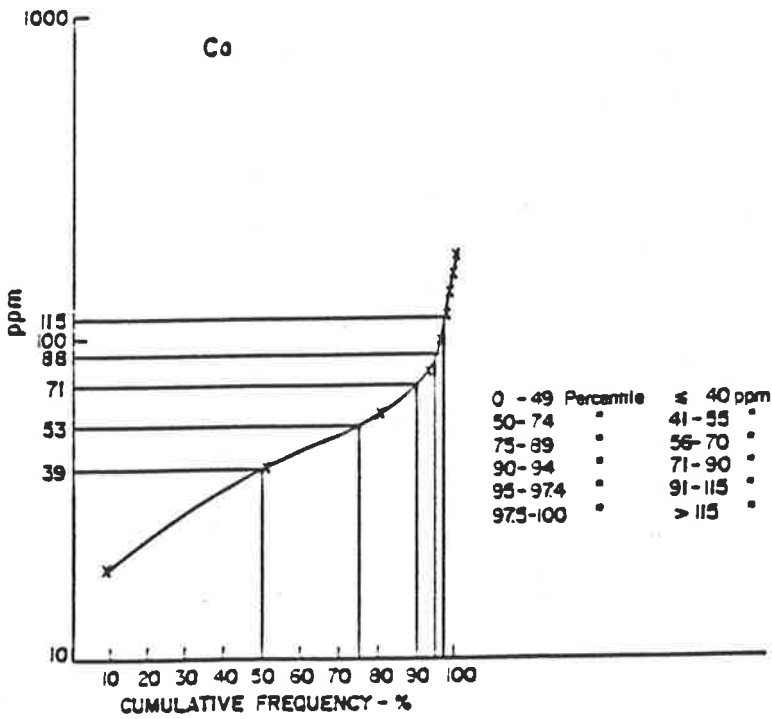
Fig. 113a
E.L. 1349 RUM JUNGLE, N.T.
GEOCHEMICAL SOIL SURVEY

Mo Histogram
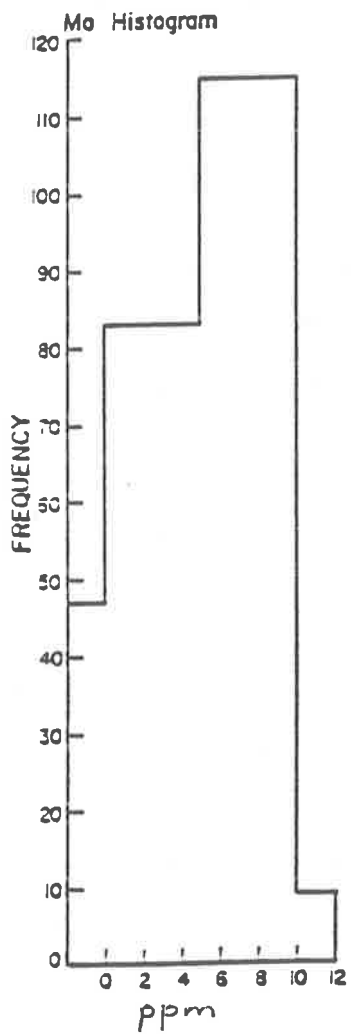
9.3 Polymetallic sulfides and U

9.3.1 Introduction

These two targets were treated in tandem. Elsewhere in the Pine Creek
Geosyncline U is consistently associated with unconformities. In the Rum
Jungle area both targets are specifically located at or adjacent to the
boundary between the Coomalie Dolomite and Whites Formation. Detailed
mapping showed that the southern third of E.L. 1349 (Fig. 107) contains
this contact over a distance of approximately 5 kms.

9.3.2 Reconnaissance Geochemical Drilling

Report Appendix 4.2. outlines the reconnaissance geochemical (soil
survey) drilling programme whilst Report Appendix 4.3. details the
down-hole radiometric logging results. The results from these programmes
are shown in Figs. 108-114. Follow-up target locations (for polymetallic
sulfides) were selected from these results. However, prior to making a
decision regarding further drilling for U, it was decided to investigate
further the suggestions proposed (Appendix 4.3.), as these areas were in
the vicinity of a Rn anomaly reported by the B.M.R. (Mutton, 1980).
Consequently, during May 1980 magnetic and - radiometric surveys were
carried out along fill-in and extended grid lines (Fig. 115). This work
was immediately followed by an α- radiometric survey, in collaboration
with the B.M.R., using the alphaMETER technique - a relatively new
detection tool. The results of these surveys are shown in Fig. 116. From
these results, further drill sites were selected.

The final exploration stage drilling programme was carried out in
September - October, 1980. The results for both targets were
disappointing (maximum values Cu 530 ppm; Pb 80 ppm; Zn 860 ppm), and it

Fig. 114a
E.L. 1349 RUM JUNGLE, N.T.
RADIOMETRIC SURVEY – TOTAL COUNTS

Histogram
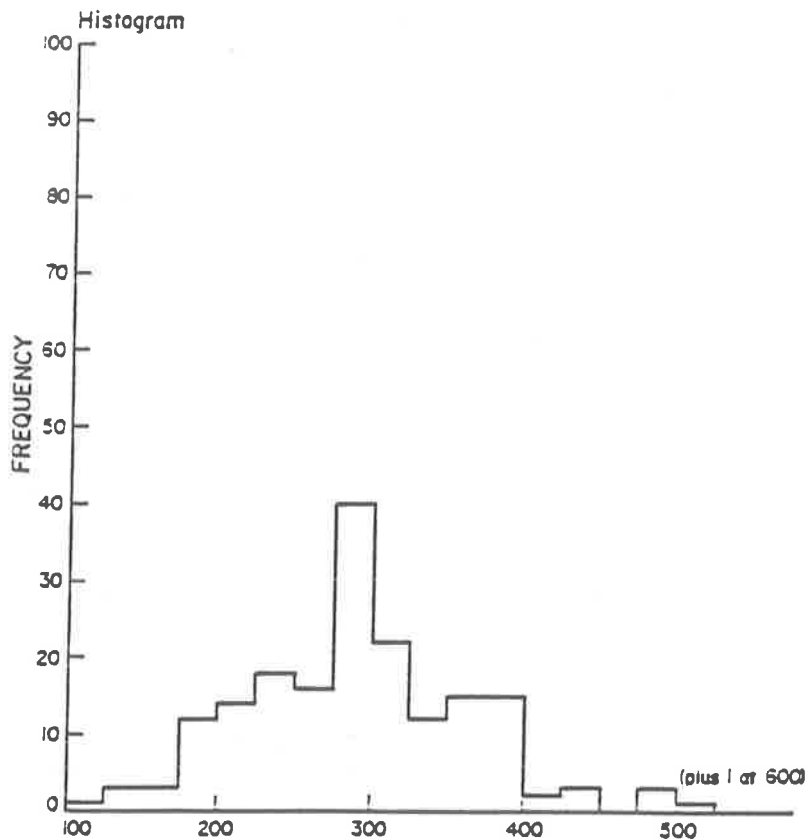
Fig. 114b
E.L. 1349 RUM JUNGLE, N.T.
RADIOMETRIC SURVEY – TOTAL COUNTS
CUMULATIVE FREQUENCY DIAGRAM

0 –49	Percentile	< 280
50 –74	"	280–339
75 –89	"	340–379
90 –94	"	380–399
95 –97.4	"	400–444
97.5–100	"	> 445
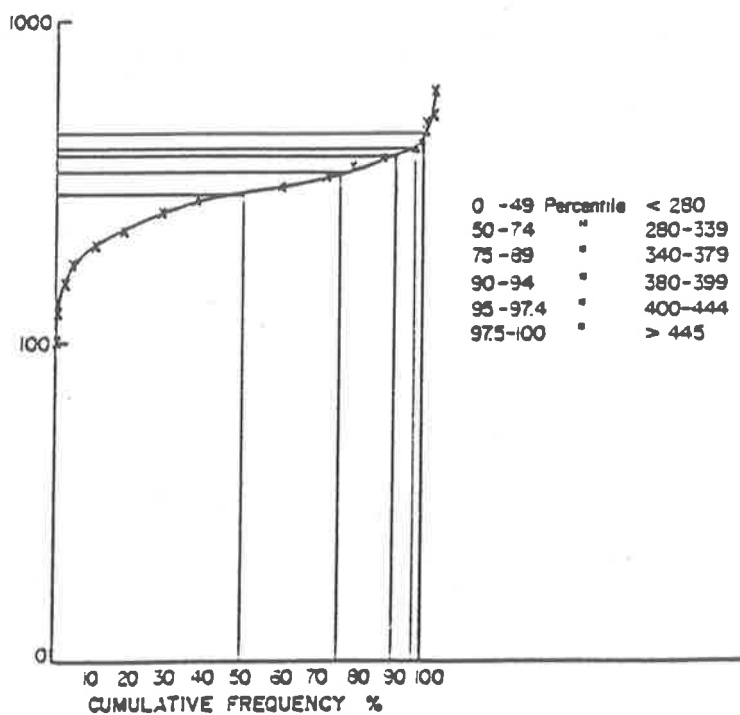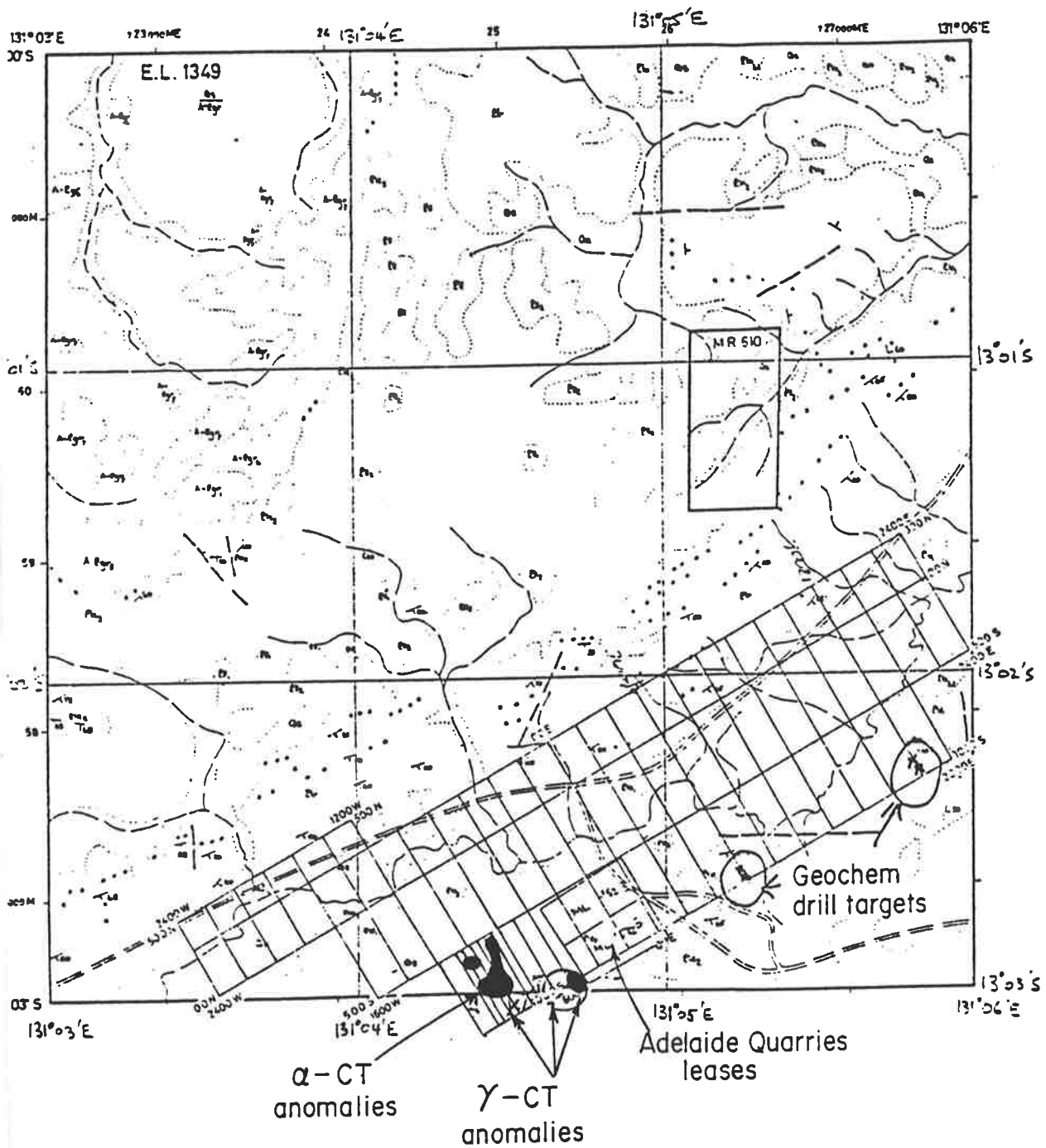
Fig. 115: Geochemical drilling programme, E.L. 1349 –
anomalous areas. See Fig. 108 for legend. Scale – 1:25,000.
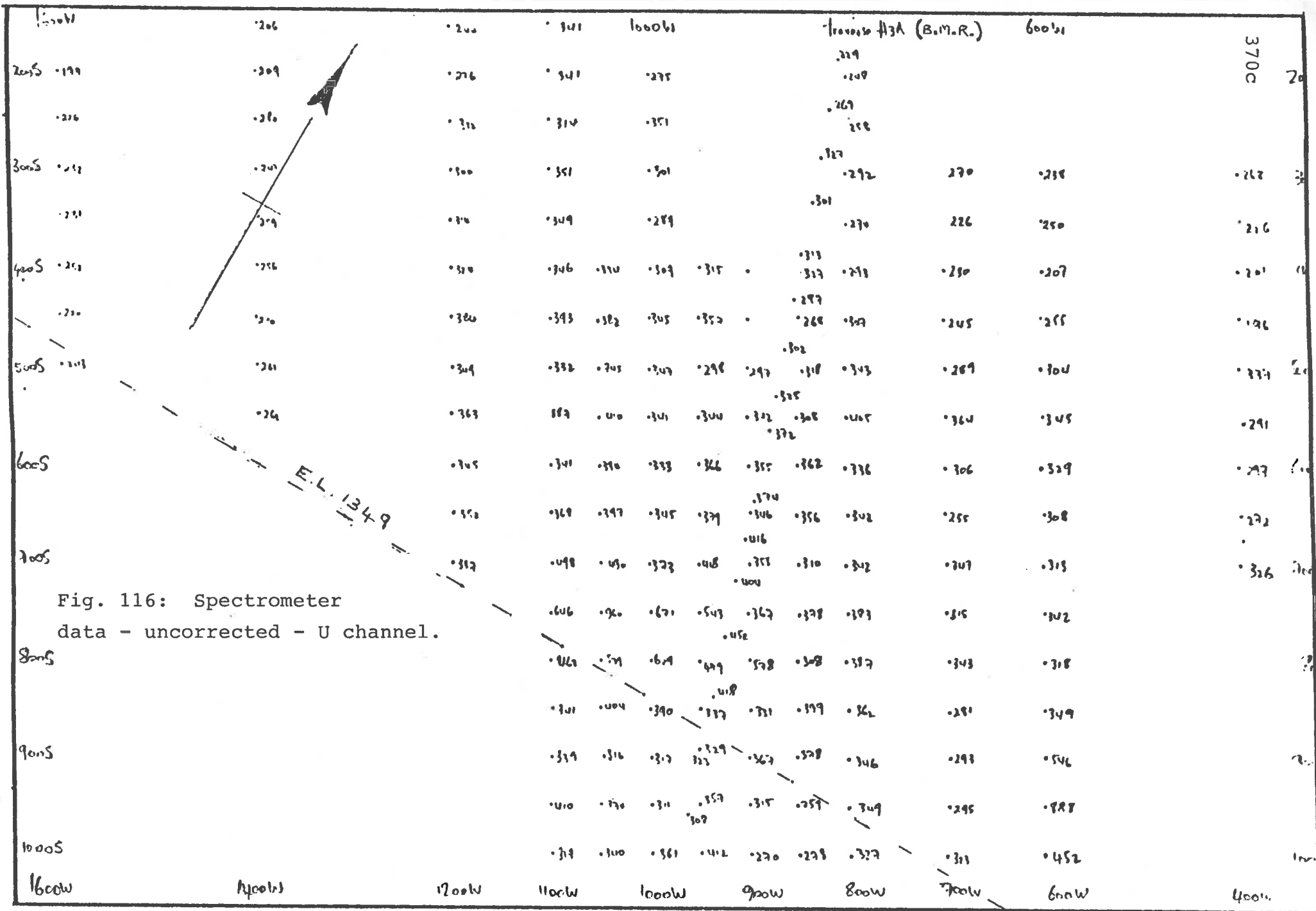
Fig. 116: Spectrometer
data - uncorrected - U channel.

was recommended that no further work be carried out on these aspects of the overall programme.

9.4 <u>Gold</u>

Au values from selected samples from this drilling programme and from potentially auriferous conglomerates within the arenites were of little interest (<0.1ppm; Ag 2ppm). Au values within pyrite from throughout the area are spasmodically well above the detection limit of the electron microprobe (Chpt. 8; Appendix 3). However, the pyrite does not occur in sufficient concentration to warrant investigating the metallurgical processes whereby the Au could be extracted economically, given the current economic situation.

CHAPTER 10

CONCLUSIONS

The magnesite deposits at Rum Jungle were formed as primary sediments in an alkaline, shallow lacustrine environment. Mg-rich groundwater input and a periodically high evaporation rate enabled the maintenance of the critical hydrogeochemical conditions required for the deposition of magnesite. The presence of stromatolites, tepee structures and the absence of evidence of the prior presence of evaporite minerals from gypsum in the evaporative column support the notion of a shallow water environment.

The presence of a paleokarst surface at the interface of the magnesite and the overlying calcilutite sequence further supports the sedimentary environment, as do the associated fluvial clastic sediments.

The trace element geochemistry of the magnesite suggests an alkaline lacustrine environment, i.e. low Na, K and Sr, high F, Fe and Mn, notwithstanding diagenetic and metasomatic alteration. Ubiquitous detrital and/or authigenic intra - and intergranular grains of tourmaline, quartz, apatite, rutile, ilmenite, K-feldspars, chlorite and clays suggest a dominantly chemical sediment, as does the $\delta^{34}S$ signature of the diagenetic pyrite.

The magnesite has been completely recrystallized at least once. Homogenisation temperatures of the fluid inclusions indicate that the temperatures of the fluids involved in the major pervasive recrystallization event ranged from $98^{\circ}C$ to $> 400^{\circ}C$, with a mean of $153^{\circ}C$ for 444 samples. This recrystallization resulted in two distinctly different magnesite morphologies - a bladed form and a rhomb form. These two forms have previously been mistaken as pseudomorphs after

gypsum and halite respectively. However, the fluid inclusion study shows that the bladed form usually results from the recrystallization of magnesite from a fluid with a temperature greater than $160^{\circ}C$; whereas the rhomb form results when the temperature is below $160^{\circ}C$. Field observation showed no correlation between morphology and grain size or visual impurity content.

Analyses by electron microprobe of the fluids in fluid inclusions in the magnesite and its associated quartz show the presence of a range of cations and anions, namely Na, Ca, Mg, Fe, K, Cl and S (probably as SO_4). The absence of any anionic spectrum for some samples suggests the presence of $CO_3{}^{2-}$ or $HCO_3{}^{-}$.

The microthermometric fluid inclusion studies also indicate the presence of several fluids, the mixing of which produced a wide range of salinities, often with inverse temperature relationships. Although salinities have been presented as wt.% equivalence of $CaCl_2$, NaCl and $MgCl_2$ are undoubtedly present as well.

Other diagenetic alteration included pervasive stylolitisation, producing the following types:-
(a) sutured seam solution, particularly at the boundary between the Coomalie Dolomite and Whites Formation (the site of most polymetallic sulfide mineralisation).
(b) non-sutured seam solution, which has given rise to nodular and chicken-wire fabric, breccias and zoned rhombs.
(c) non-seam solution.

Stylolitisation played an important role in the formation of the mineral deposits, both in the formation of the breccia-type mineralisation and in providing solution pathways. It is suggested that stylolitised magnesite be considered a pathfinder.

In view of the pervasive nature of the contamination of the magnesite by diagenetic minerals, it is unlikely that a relatively silica-free magnesite deposit of 10 million plus tonnes is present in the area.

As the Celia Dolomite and the Coomalie Dolomite are predominantly magnesite throughout their extent, it is suggested that they be officially renamed Formations. This would allow for the fact that they also contain extensive silicified areas and intercalations of "mafic schists" and stratiform tourmalinites.

Both field observations and laboratory studies suggest that there has been stratigraphic duplication of the two lowermost sedimentary formations by gravity thrusting down the flanks of the diapirically uprising Basement Compexes. This makes the names of either the Beestons Formation and the Celia Dolomite or the Crater Formation and the Coomalie Dolomite redundant.

Such stratigraphic nomenclature changes do not affect either the magnesite genesis model or the findings on U and polymetallic sulfides, even though the mineral deposits all show a strong stratigraphic and lithological control. However, as the latter two names are those which appear in the literature in relation to mineralization, it would probably be less confusing if the names Crater Formation and Coomalie Formation were to be adopted.

Although the genesis of the magnesite was the focus of this study, associated U and polymetallic sulfide deposits were also considered.

The Basement Complexes are enriched in U, and presumably constitute one of the major sources. Whites Formation is enriched in both U and metals, and presumably a source of both. Thus the magnesite, although it contained anomalous U and metal values, was not the only source. It is very likely that the carbonates were involved in producing a fluid

suitable for the formation and transport of U and metal complexes, e.g. uranyl carbonate and bicarbonate complexes. The intercalated stratiform tourmalinites indicate hot spring activity at the time of rifting, which would have contributed hydrothermal fluids into the system. It is most likely that these early stage hydrothermal fluids leached U and metals from the rocks through which they passed. The mixing of meteoric and hydrothermal fluid types accounts for the range of temperatures recorded in the fluid inclusion study and for the inverse relationship sometimes seen between temperature and salinity. Overall, the mineralising fluids were predominantly low temperature, often highly saline and frequently $CO_2 \pm CH_4$ rich. The low temperature of the fluids, at the appropriate geochemical conditions, particularly pH, enabled the formation of specific sulfides such as marcasite, and villamaninite.

The distribution of the mineralising fluids was enhanced by the gravity sliding event, with localised increase of temperature and CO_2 formation. Shear zones, which may also be related to this event, and which are co-incident with the Coomalie Dolomite - Whites Formation boundary, were preferential pathways for these mineralising fluids.

The range of $\delta^{34}S$ values obtained indicate that the disseminated stratiform pyrite (which has reduced biogenic sulfate characteristics) was the major S source for the polymetallic sulfides. The hydrothermal fluids also contained high concentrations of Co and Ni, and due to the exceptional geochemical conditions pertaining, villamaninite - bravoite and siegenite were formed. This is the first reported Australian occurrence of the extremely rare disulfide, villamaninite.

The magnesite deposits at Balcanoona, South Australia and Kharidunga, Nepal that were studied for comparison purposes were found to be similar in most respects. Both were subject to higher metamorphic grades, and both recorded higher fluid inclusion homogenisation temperatures. Not

surprisingly, neither deposit contained rhomb type magnesite.

It is suggested that these deposits also were formed in a similar manner to the Rum Jungle magnesite deposits.

Previously unreported polymetallic sulfides were discovered at the boundary of the magnesite and the overlying graphitic schist at Kharidunga. These were predominantly pyrrhotite, with veinlets of chalcopyrite.

REFERENCES

ABELL, P.I., AWRAMIK, S.M., OSBORNE, R.H. and TOMELLIN, S., 1982:
   Plio-pleistocene lacustrine stromatolites from Lake Turkana, Kenya :
   Morphology, stratigraphy and stable isotopes. Sediment. Geol., 32, pp.
   1-26.

ALDERTON, D.H.M., THOMPSON, M., RANKIN, A.H. and CHRYSSOULIS, S.L., 1982:
   Development of the ICP linked decrepitation technique for the analysis
   of fluid inclusions in quartz. Chem. Geol., 37, pp. 203-213.

ANDERSON, T.F. and CHAI, B.H.T., 1974: Oxygen isotope exchange between
   calcite and water under hydrothermal conditions. in Hofmann, A.W.,
   Giletti, B.J., Yoder, H.S. and Yund, R.A. (eds) Chemical Transport and
   Kinetics. Carnegie Inst. Washington Publ., 634, pp. 219-227.

ANNOVI, A., FONTANA, D., GELMINI, R., GORGONI, C., and SIGHINOLIFI, G.,
   1980: Geochemistry of carbonate rocks and ferruginous horizons in the
   Verrucano in Southern Tuscany - Palaeoenvironmental and
   palaeogeographic implications. Palaeogeog., Palaeoclim., Palaeoecol.,
   30, pp. 1-16.

ASSERETO, R.L.,. and KENDALL, C.G. ST. C., 1977: Nature, origin and
   classification of peritidal tepee structures and related breccias.
   Sedimentology, 24, pp. 153-210.

BAKER, P.A., KASTNER, M., BYERLEE, J.D. and LOCKNER, D.A., 1980:
   Pressure solution and hydrothermal recrystallization of carbonate
   sediments - an experimental study. Marine Geol., 38, pp. 185-203.

BAKER, P.A., GIESKES, J.M. and ELDERFIELD, H., 1982: Diagenesis of
   carbonates in deep-sea sediments - evidence from Sr/Ca ratios and

interstitial dissolved Sr^{2+} data. J. Sed. Pet., 52, No. 1. pp. 71-82.

BARNES, R.G., 1980a: A metallogenic study of the Purnamoota-Yalcowinna 1:50,000 sheet, northern Broken Hill block: New South Wales Geological Survey Report, GS 1980/116, 198p.

BARNES, R.G., 1980b: Types of mineralization in the Broken Hill block and their relationship to stratigraphy. in Stevens, B.P.J. (ed.) A guide to the stratigrapny and mineralization of the Broken Hill block, New South Wales. New South Wales Geol. Survey Records, 20, pt. 1, pp. 33-70.

BATTEY, M.H., 1981: Mineralogy for students. Longman Inc., New York, 355p.

BAZAROV, L. Sh., 1966: A device for freezing inclusions in minerals. (Abstr.). Fluid Inclusion Research - Proceed. of COFFI, 2, p. 28.

BEHAR, F. and PINEAU, F., 1979: Analyse de CO_2, H_2O, hydrocarbures des inclusions fluides par chromatographic en phase gazeuze : application aux fentes alpines et aux roches metamorphique. Bull. Mineral., 102, pp. 611-621.

BEHR, H.J., HORN, E.E. and PORADA, H., 1983: Fluid inclusions and genetic aspects of the Damara Orogen. in Martin, H. and Eder, F.W. (eds.). Intracontinental Fold Belts. Springer-Verlag, Berlin, pp. 611-649.

BENCINI, A. and TURI, A., 1974: Mn distribution in the Mesozoic carbonate rocks from Lima Valley, northern Appennines. J. sedim. Petrol., 44, pp. 123-135.

BENNETT, J.N. and GRANT, J.N., 1980: Analysis of fluid inclusions using a pulsed laser microprobe. Mineral. Mag., _43_, pp. 945-947.

BERKMAN, D.A., 1968: The geology of the Rum Jungle Uranium deposits. Aust. Inst. Min. Metall. Symp., Uranium in Australia, pp. 12-31.

BERKMAN, D.A. and FRASER, W.J. 1980: The Mount Fitch copper and uranium deposits, Rum Jungle Uranium Field, N.T., Australia. _in_ Ferguson, J. and Goleby, A.B. (eds.). Uranium in the Pine Creek Geosyncline. IAEA Proceed. Series, Vienna, pp. 343-350.

BERNER, R.A., 1970: Sedimentary pyrite formation. Am. J. Sci., _268_, pp. 1-23.

BODNAR, R.J. and BETHKE, P.M., 1980: Systematics of "stretching" of fluid inclusions as a result of overheating. EOS, _61_, p. 393.

BONE, Y., 1983: Interpretation of magnesites at Rum Jungle, N.T., using fluid inclusions, J. Geol., Soc. Aust., _30_, pp. 375-381.

BONE, Y., and GRIFFIN, B.J., 1984: Qualitative analysis of the fluid in fluid inclusions, using the electron microprobe, Geol. Soc. Aus. 7th Conv. Extend. Abstr. pp. 67-69.

BOTZ, R.W. and von DER BORCH, C.C., 1984: Stable isotope study of carbonate sediments from the Coorong area, South Australia. Sedimentology. _31_, pp. 837-849.

BOZZO, A.T., CHEN, H-S., KASS, J.R. and BARDUHN, A.J., 1973: The properties of the hydrates of chloride and carbon dioxide. 4th Internat. Sym. on Fresh Water from the Sea, _3_, pp. 437-451.

BRALIA, A., SABATINI, G. and TROJA, F., 1979: A revaluation of the Co/Ni ratio in pyrite as a geochemical tool in ore genesis problems. Mineral. Deposita (Berl.) 14, pp. 353-374.

BRANTLEY, S.L., CRERAR, D.A., MOLLER, N.E. and WEARE, J.H., 1984: Geochemistry of a modern marine evaporite: Bocana de Virrila, Peru. J. Sed. Pet., 54, No. 2, pp. 447-462.

BRYAN, R., 1962: Lower Proterozoic basic intrusive rocks of the Katherine-Darwin area, Northern Territory. BMR Geol. Geophs. Aust. Rec., 1962/7.

BUSSINK, R.W., KREULEN, R. and DE JONG, A.F.M., 1984: Gas analyses, fluid inclusions and stable isotopes of the Panasqueira W-Sn deposits, Portugal. Bull. Mineral., 107, pp. 707-713.

BUHMANN, D. and DREYBRODT, W., 1985: Geochemistry of B in concretions and host rocks of Emsian age in the Rheinische Schieforgebirge, Federal Republic of Germany. Chem. Geol., 48, pp. 189-212.

BUICK, R., DUNLOP, J.S.R. and GROVES, D.I., 1981: Stromatolite recognition in ancient rocks : an appraisal of irregularly laminated structures in an Early Archaean chert-barite unit from North Pole, W.A. Alcheringa, 5, pp. 161-182.

BURRUSS, R.C., 1981: Analysis of fluid inclusions : phase equilibria at constant volume. Am. J. Sci., 281, pp. 1104-1126.

BUSH, P., 1973: Some aspects of the diagenetic history of the sabkha in Abu Dhabi, Persian Gulf. in Purser, B.H. (ed.). The Persian Gulf - Holocene Carbonate Sedimentation and Diagenesis in a Shallow Epicontinental Sea. Springer-Verlag, New York, pp. 395-407.

BUXTON, T.M. and SIBLEY, D.F., 1981: Pressure solution features in a shallow buried limestone. J. Sed. Pet., 51, No. 1, pp. 19-26.

CALLEN, R.A., 1977: Late Cainozoic environments of part of north eastern South Australia. J. Geol. Soc. Aust., 24, No. 3, pp. 151-169.

CAMPBELL, F.A., ETHIER, V.G., KROUSE, H.R. and BOTH, R.A., 1978: Isotopic composition of S in the Sullivan Orebody, British Columbia. Econ. Geol., 73, pp. 246-268.

CAMPBELL, F.A. and ETHIER, V.G., 1984: Nickel and cobalt in pyrrhotite and pyrite from the Faro and Sullivan orebodies. Canad. Mineral., 22, pp. 503-506.

CARANNANTE, G. and GOZZETTA, G., 1972: Stiloliti e sliccoliti come meccanismo di deformazione delle masse rocciose. Bollo. Soc. Natur. in Napoli, 81, pp. 157-170.

CARTER, E.K., 1953: The geology of the Embayment area, Rum Jungle, Northern Territory. BMR, Record 130/53.

CHAI, B.H.T., 1974: Mass transfer of calcite during hydrothermal recrystallization. in Hofmann, A.W., Giletti, B.J., Yoder, H.S. and Yund, R.A. (eds.). Chemical Transport and Kinetics, Carnegie Inst. Washington Publ., 634, pp. 205-218.

CHAMBERS, L.A., 1982: Sulfur isotope study of a modern intertidal environment, and the interpretation of ancient sulfides. Geochim. Cosmochim. Acta, 46, pp. 721-728.

CHIVAS, A.R. and WILKINS, R.W.T., 1977: Fluid inclusion studies in relation to hydrothermal alteration and mineralization at the Koloula

Porphyry Cu prospect, Guadalcanal. Econ. Geol., _72_, pp. 153-169.

CHRIST, C.L. and HOSTETLER, P.B., 1970: Studies in the system $MgO-SiO_2-CO2$ H_2O (II) : The activity-product constant of magnesite. Am. Jour. Sci., _268_, pp. 439-453.

CLAYPOOL, G.E., HOLSTER, W.T., KAPLAN, I.R., SAKAI, H. and ZAK, I., 1980: The age curves of sulphur and oxygen isotopes in marine sulphate and their mutual interpretation. Chem. Geol., _28_, pp. 199-260.

CODY, R.D. and SHANKS, H.R., 1974: A comparison of calcium sulfate dihydrate grown in clay gels and in sodium silicate gels. J. Cryst. Growth, _23_, pp. 275-281.

CODY, R.D. and SHANKS, H.R., 1976: Growth and early diagenetic changes in artificial gypsum crystals grown within bentonite muds and gels. Geol. Soc. Am. Bull., _87_, pp. 1163-1168.

CODY, R.D., 1979: Lenticular gypsum : occurrence in nature, and experimental determinations of effects of soluble green plant material on its formation. J. Sed. Pet., _49_, pp. 1015-1028.

COLLINS, P.L.F., 1979: Gas hydrates in CO_2 - bearing fluid inclusions and the use of freezing data for estimation of salinity. Econ. Geol., _74_, pp. 1435-1444.

COLLINS, P.L.F., 1981: The geology and genesis of the Cleveland Tin Deposit, Western Tasmania : Fluid inclusion and stable isotope studies. Econ. Geol., _76_, pp. 365-392.

CRAWFORD, M.L., 1981: Phase equilibria in aqueous fluid inclusions. _in_ Hollister, L.S. and Crawford, M.L., (eds.). Short Course in Fluid

388

Inclusions : Applications to petrology, Min. Assoc. Canada, 6, pp. 75-100.

CRICK, I.H., 1978: Interim report on the Batchelor 1:100,000 sheet, N.T., BMR, Record 1978/11.

CRICK, I.H., and MUIR, M.D., 1980: Evaporites and uranium mineralisation in the Pine Creek Geosyncline. in Ferguson, J. and Coleby, A.B. (eds.). Uranium in the Pine Creek Geosyncline, IAEA Proceed. Series, Vienna, pp. 531-542.

CRICK, I.H., JOHNSON, K., JORRITSMA, P.J., BULTITUDE, J.M. and d'ADDARIO, G.W., 1981: Geology of Rum Jungle, Northern Territory, Australia. Australia 1:100,000 Geological Special Mapsheet. BMR, Aust.

CUNEY, M., PAGEL, M. and TOURET, J., 1976: L'analyse des gaz des inclusions fluides par chromatographie en phase gazeuse. Soc. Franc. Mineral. Crist. Bull., 99, pp. 169-177.

DABITZIAS, S.G., 1980: Petrology and genesis of the Vavdos cryptocrytalline magnesite deposits, Chalkidiki Peninsula, Northern Greece. Econ. Geol., 75, pp. 1138-1151.

DANA, E.S., 1966: A textbook of Mineralogy. in Ford, W.E., (ed.). John Wiley and Sons, New York, 851p.

DAVIDSON, C.F., 1962: On the Co:Ni ratio in ore deposits. Mining Mag., 106, pp. 78-85.

DEBOULE, E. and ELOY, J.F., 1982: Improvements of Laser probe mass spectrometry for the chemical analysis of fluid inclusions in ores. Chem. Geol., 37, pp. 191-202.

DEELMAN, J.C., 1978a: Experimental ooids and grapestones : carbonate aggregates and their origin. J. sedim. Petrol., _48_, pp. 503-512.

DEELMAN, J.C., 1979: "Protodolomite" re-examined. N. Jl. Miner. Mh., _79_, pp. 337-356.

DEER, W.A., HOWIE, R.A. and ZUSSMAN, J., 1966: Rock forming Minerals. 5. Non-Silicates. Longmans, London.

DHAMELINCOURT, P., BERRY, J.M., DUBESSY, J.C. and POTY, B., 1979: Analyze d'inclusions fluides a la microsonde mole a effet Raman. Bull. Mineral., _102_, pp. 600-610.

DODSON, R.G., NEEDHAM, R.S., WILKES, P.G., PAGE, R.W., SMART, P.G. and WATCHMAN, A.L., 1974: Uranium mineralisation in the Rum Jungle - Alligator Rivers province, N.T., Australia. _in_ Formation of Uranium Ore Deposits Proceed. Symp., Athens, IAEA, Vienna, pp. 551-568.

DUBESSY, J., PAGEL, M., POTY, B., KOSZTOLANYI, C. and BENY, J.M., 1980: Evidence, by Raman spectroscopy, of free hydrogen and free oxygen in fluid inclusions from two uranium deposits. (Abstr.), IMA 80, Orleans, p. 129.

DUBESSY, J., AUDEOUD, D., WILKINS, R., and KOSZTOLANYI, C., 1982: The use of the Raman microprobe MOLE in the determination of the electrolytes dissolved in the aqueous phase of fluid inclusions. Chem. Geol., _37_, pp. 137-150.

EADINGTON, P.T., 1974: Microprobe analysis of the non-volatile constituents in fluid inclusions. Neues. Jb. Miner. Mh., _11_, pp. 518-525.

EADINGTON, P.T., 1979: Composition of fluid inclusions - non destructive methods of analysis and the destructive determination of liquid compositions. Fluid Inclusions Conf., Melb.

EADINGTON, P.T., and WILKINS, R.W.T., 1980: The origin, interpretation and chemical analysis of fluid inclusions in minerals. Inst. of Earth Resources, CSIRO, Tech. Comm. 69.

EASTOE, C.J., 1978: A fluid inclusion study of the Panguna porphyry copper deposit, Bougainville, Papua New Guinea. Econ. Geol. 73, pp. 721-748.

EASTOE, C.J., 1983: Sulfur isotope data and the nature of the hydrothermal systems at the Panguna and Frieda Porphyry Copper Deposits, Papua New Guinea. Econ. Geol., 78, pp. 201-213.

EFFENBERGER, H., MEREITER, K. and ZEMANN, J., 1981: Crystal structure refinements of magnesite, calcite, rhodochrosite, siderite, smithsonite and dolomite, with discussion of some aspects of the stereochemistry of calcite-type carbonates. Z. Kristallogr., 156, pp. 233-243.

ENGELHARDT, W.V., 1977: The Origin of Sediments and Sedimentary Rocks. Halsted Press, New York, 359p.

ERMAKOV, N.P., 1965: Studies of mineral-forming solutions. in Ingerson, D.E. (ed.). Research on the Nature of Mineral-forming Solutions. Inter. Series Mono. in Earth Sciences, Pergamon Press, 22, Pt. 1., pp. 1-348.

ESKOLA, P.E., 1948: The problem of mantled gneiss domes. Q. Jl. geol. Soc. Lond., 104, pp. 461-476.

ETHERIDGE, M.A., WYBORN, L.A., RUTLAND, R.W.R., PAGE, R.W., BLAKE, D.H. and DRUMMOND, B.J., 1984: The BMR model - A discussion paper. Workshop on Early to Middle Proterozoic of Northern Australia, Record 1984/31.

ETHIER, V.G. and CAMPBELL, F.A., 1977: Tourmaline concentrations in Proterozoic sediments of the southern Cordillera of Canada and their economic significance. Can. J. Earth Sci., 14, pp. 2348.

EUGSTER, H.P. and HARDIE, L.A., 1978: Saline Lakes. in Lerman, A. (ed.). Lakes - Chemistry, Geology, Physics. Springer Verlag, New York, pp. 237-293.

EUGSTER, H.P. and JONES, B.F., 1979: Behaviour of major solutes during closed-basin brine evolution. Am. J. Sci., 279, pp. 609-631.

EUGSTER, H.P. and MAGLIONE, G., 1979: Brines and evaporites of the Lake Chad basin, Africa. Geochim. Cosmochim. Acta, 43, pp. 973-981.

EUGSTER, H.P., HARVIE C.E. and WEARE, J.H., 1980: Mineral equilibria in a 6-component seawater system, $Na-K-Mg-Ca-SO_4-Cl-H_2O$ at $25^{o}C$. Geochim. Cosmochim. Acta, 44, pp. 1335-1347.

EUGSTER, H.P., 1984: Geochemistry and sedimentology of marine and nonmarine evaporites. Eclogae geol. Helv. 77, No. 2, pp. 237-248.

EUGSTER, H., 1985: Oil shales, evaporites and ore deposits. Geochim. Cosmochim. Acta., 49, No. 3, pp. 619-636.

EUPENE, G.S., 1980: Stratigraphic, structural, and temporal control of mineralization in the Alligator Rivers U Province, N.T. Aus. Proc. 5th Quadrennial 1A60D Symp.

EWERS, G.R., FERGUSON, J. and DONNELLY, T.H., 1983: The
 Nabarlek uranium deposit - Petrology, geochemistry, and some
 constraints on geochemistry. Econ. Geol., 78, pp. 823-837.

EWERS, G.R., FERGUSON, J., NEEDHAM, R.S. and DONNELLY, T.H., 1984: Pine
 Creek Geosyncline, N.T. in Ferguson, J. (ed.). Proterozoic Unconformity
 and Stratabound Uranium Deposits. IAEA, Vienna, pp. 135-206.

FAIRCHILD, I.J. 1985: Petrography and carbonate chemistry of some
 Dalradian dolomitic metasediments: preservation of diagenetic
 textures. J. Geol. Soc. London, 142, pp. 167-185.

FERGUSON, J., and NEEDHAM, R.S., 1978: The Zamu Dolerite: A Lower
 Proterozoic preorogenic continental tholeiite suite from the Northern
 Territory, Australia, J. Geol. Soc. Aust. 25, pp. 309-322.

FERGUSON, J. and WINER, P., 1980: Pine Creek Geosyncline : Statistical
 treatment of whole rock chemical data. in Ferguson, J. and Goleby,
 A.B., Uranium in the Pine Creek Geosyncline, IAEA Proceed. Series,
 Vienna, pp. 191-208.

FERGUSON, J., CHAPPELL, B.W. and GOLEBY, A.B., 1980: Granitoids in the
 Pine Creek Geosyncline. in Ferguson, J., and Goleby, A.B. (eds.).
 Uranium in the Pine Creek Geosyncline, IAEA Proceed. Series, Vienna,
 pp. 73-90.

FERGUSON, J., 1980: Metamorphism in the Pine Creek Geosyncline and its
 bearing on stratigraphic correlations. in Ferguson, J. and Goleby,
 A.B.. Uranium in the Pine Creek Geosyncline. IAEA Proceed. Series,
 Vienna, pp. 91-100.

FLEISCHER, M., 1955: Minor elements in some sulphide minerals. Econ.
 Geol., 50th Anniv. Vol., pp. 970-1024.

FLORKE, O.W., MIELKE, H.G., WEICHERT, S. and KULKE, H., 1981: Quartz and rhombohedral cleavage from Madagascar. Am. Mineral., 66, pp. 596-601.

FOLK, R.L. and PITTMAN, J.S., 1971: Length slow chalcedony : a new testament for vanished evaporites. J. sedim. Petrol., 41, pp. 1045-1058.

FOUILLAC, C. and CRIAUD, A., 1984: Carbonate and bicarbonate trace metal complexes : Critical reevaluation of stability constants. Geochem. J., 18, pp. 297-303.

FRASER, W.J., 1975: The embayment line of mineralisation, Rum Jungle. in Knight, C.L. (ed.). Economic Geology of Australia and Papua New Guinea. Australas. Inst. Min. Metall., Monograph Series No. 5, I. Metals, pp. 271-277.

FRASER, W.J., 1980: Geology and exploration of the Rum Jungle Uranium Field. in Ferguson, J. and Goleby, A.B. (Eds.). Uranium in the Pine Creek Geosyncline, IAEA Proceed. Series, Vienna, pp. 287-298.

FRISCH, C.J. and HELGESON, H.C., 1984: Metasomatic phase relations in dolomites of the Adamello Alps. Am. J. Sci., 284, No. 2, pp. 121-185.

FRITZ, P., BARKER, J.F., GALE, J.E., WITHERSPOON, P.A., ANDREWS, J.N., KAY, R.L., LEE, D.J., COWART, J.B., OSMOND, J.K. and PAYNE, B.R., 1980: Geochemical and isotopic investigations at the Stripa test site (Sweden). Symp. on Underground Disposal of Radioactive Wastes. IAEA, Vienna, 243/6, 2, pp. 341-365.

FRITZ, P. and FRAPE, S.K., 1982: Saline groundwaters in the Canadian Shield - a first overview. Chem. Geol. 36, pp. 179-190.

394

FRONDEL, C., 1978: Characters of quartz fibres. Am. Mineral., 63, pp. 17-27.

FROST, M.T., 1982: The magnesite deposit at Main Creek, Savage River, Tasmania. Econ. Geol., 77, pp. 1901-1911.

FRUTH, I. and SCHERREIKS, R., 1975: Facies and geochemical correlations in the Upper Hauptdolomit (Norian) of the eastern Lechtaler Alps. Sediment. Geol., 13, pp. 27-45.

FUZIKAWA, K., 1982: Fluid inclusions and oxygen isotope studies of the Nabarlek uranium deposit. Ph.D. Thesis (Unpubl.) Univers. of Adelaide.

FYON, J.A., CROCKET, J.H. and SCHWARCZ, H.P., 1983: Magnesite abundance as a guide to gold mineralization associated with ultramafic flows, Timmins area. J. Geochem. Expl., 18, pp. 245-266.

GALUP, A.L., GREENWOOD, B. and WILSON, J.F.,1975: A microscope cold stage. (Abstr.). Fluid Inclusion Research - Proceed. of COFFI, 8, pp. 59.

GARLICK, G.D., 1967: Special features and sedimentary facies of stratiform sulphide deposits in arenites. in James, C.H., (ed.). Sedimentary Ores Ancient and Modern (rev.). Inter-Univ. Geol. Cong., 15th, Leicester 1967, Proc. : Leicester, Univ., Department Geol. Spec. Pub. 1, pp. 107-169.

GARRELS, R.M. and CHRIST, C.L., 1965: Solutions, Minerals and Equilibria. Freeman - Cooper, San Francisco.

GARRELS, R.M. and LERMAN, A., 1984: Coupling of the sedimentary sulfur and carbon cycles - an improved model Am. J. Sci., 284, pp. 989-1007.

GAUTIER, D.L., 1979: Preliminary report of authigenic tourmaline crystals in a productive gas reservoir of the Tiger Ridge Field, North Central Montana. J. Sed. Pet. 49, pp. 911-916.

GIBLIN, A.M., 1980: The role of clay adsorption in genesis of uranium ores. in Ferguson, J. and Goleby, A.B. (eds.). Uranium in the Pine Creek Geosyncline. IAEA, Vienna, pp. 521-530.

GIORDANO, T.H. and BARNES, H.L., 1981: Lead transport in Mississippi Valley type ore solutions. Econ. Geol., 76, pp. 2200-2211.

GIORDANO, T.H., 1985: A preliminary evaluation of organic ligands and metal-organic complexing in Mississippi Valley-Type ore solutions. Econ. Geol., 80, pp. 96-106.

GRAF, D.L., EARDLEY, A.J. and SHIMP, N.F., 1961: A preliminary report on magnesium carbonate formation in glacial Lake Bonneville. J. Geol. 69, pp. 219-223.

GRAPPIN, C., SALIOT, P., SABOURAUD, C. and TOURAY, J.C., 1979: Les variations des rapports Cl/Br, Na/Br et K/Br dans les inclusions fluides des quartz de la cicatrice evaporitique de Bramans - Termignon (Vanoise, Alpes francaises). Chem. Geol., 25, pp. 41-52.

GREY, K., 1981: Small conical stromatolites from the Archaean near Kanowna, W.A. Geol. Surv. W.A., Annual Report for 1980.

GREY, K., 1982: Aspects of Proterozoic stromatolite biostratigraphy in W.A. Precambrian Research, 18, pp. 347-365.

GUILHAUMOU, N., DHAMELINCOURT, P., TOURAY, J.C. and BARBILLAT, J., 1978: Analyse a la microsonde a effet Raman d'inclusions gazeuses du systeme

N_2 - CO_2. C.R. Acad. Sci. Franc., 287, ser. D., pp. 1317-1319.

GUILHAUMOU, N., VELDE, B. and BENY, C., 1984: Raman microprobe analysis of gaseous inclusions in diagenetically recrystallised calcites. Bull. Mineral., 107, 193-202.

GUSTAFSON, L.B. and CURTIS, L.W., 1983: Post - Kombolgie metasomatism at Jabiluka, Northern Territory, Australia, and its significance in the formation of high-grade uranium mineralization in Lower Proterozoic rocks. Econ. Geol., 78, No. 1, pp. 25-56.

HARTMAN, P., 1978: On the validity of the Donnay-Harker Low. Canad. Mineral., 16, pp. 387-391.

HARVIE, C.E., EUGSTER, H.P. and WEARE, J.H., 1982: Mineral equilibria in the 6 - component seawater system, Na-K-Mg-SO_4-Cl-H_2O at 25^OC. II Composition of the saturated solutions. Geochim. Cosmochim. Acta., 46, pp. 1603-1618.

HAWLEY, J.E. and NICHOL, J., 1961: Trace elements in pyrite, pyrrhotite and chalcopyrite of different ores. Econ. Geol., 56, pp. 467-487.

HAYAKAWA, N., NAMBU, M. and AOSHIMA, T., 1969: Trial manufacture of a heating stage for use under high pressure. (Abstr.). Fluid Inclusion Research - Proceed. of COFFI, 2, p. 45.

HEM, J.D., 1972: Chemical factors that influence the availability of iron and manganese in aqueous systems. Bull. Geol. Soc. Am., 83, pp. 443-450.

HITCHCOCK, C.H., 1878: The geology of New Hampshire, Pt. 5, Economic Geology. Concord., New Hampshire Geol. Survey, 103p.

HOCHMAN, M.B.M., 1978: Geochemical Investigations in the Mt. Bundey Area, N.T. B.Sc. (Hons.) Thesis, University of Adelaide. (Unpubl.).

HOCHMAN, M.B.M. and YPMA, P.J.M., 1984: Thermoluminescence as a tool in exploration. J. Chem. Expl., 22, pp. 315-331.

HOCHMAN, M.B.M. and YPMA, P.J.M., 1984: Thermoluminescence applied to uranium exploration and genesis of the Westmoreland uranium deposits - implications for the Northern Territory. Aus. I.M.M. Conf., Darwin, N.T., pp. 215-224.

HOLLISTER, L.S. and BURRUS, R.C., 1976: Phase equilibria in fluid inclusions from the Khtada Lake metamorphic complex. Geochim. Cosmochim. Acta, 40, pp. 163-175.

HOLLISTER, L.S., CRAWFORD, M.L., ROEDDER, E., BURRUSS, R.C., SPOONER, E.T.C. and TOURET, J., 1981: Practical aspects of microthermometry. in Hollister, L.S. and Crawford, M.L. (eds.). Short Course in Fluid Inclusions : Application to Petrology. Min. Assoc. Candad, 6, pp. 278-304.

HOLLISTER, L.S. and CRAWFORD, M.L., 1981: (eds.). Short Course in Fluid Inclusions : Application to Petrology. Min. Assoc. Candad, 6, 304 p.

ILER, R.K., 1979: The Chemistry of Silica. John Wiley and Sons, Inc., 835 p.

INGRAM, J.A., 1974: Uranium Deposits. Min. Resour. Rep., BMR Geol. Geophy. Aust., 6.

JOHANES, W., 1970: Zur entstehung von magnesitvorkommenz. N. Jb. Miner. Abh., 113, pp. 274-325.

JOHNS, K.H., 1976: Magnesite in South Australia; in Knight, C.L. (ed.). Economic Geology of Australia and Papua New Guinea, 4. Industrial minerals and rocks. Australas. Min. Metall., Monogr., 8, pp. 219-220.

JOHNSON, K., 1974: Progress Report : Geological review and revision of the Rum Jungle area, Northern Territory, B.M.R., Record 1974/41.

JONES, J.B. and SEGNIT, E.R., 1971: The nature of opal I. Nomenclature and constituent phases. J. Geol. Soc. Aust., 18, pp. 57-68.

JONES, J.B. and SEGNIT, E.R., 1972: Genesis of cristobalite and tridymite at low temperatures. J. Geol. Soc. Aust., 18, pp. 419-422.

JOSANG, O., 1966: Geologiske og petrografiske undersokelsel i Modumfeltet. Norges Geol. Undersokelse 235.

KALYUZHNYI, V.A., 1973: New instruments for studies of inclusions of mineral-forming fluids and principles of their use. (Abstr.), Fluid Inclusion Research - Proceed. of COFFI, 7, pp. 90-91.

KASTNER, M., KEENE, J.B. and GIESKES, J.M., 1977: Diagenesis of siliceous oozes - I. Chemical controls on the rate of opal-A to opal-CT transformation - an experimental study. Geochim. Cosmochim. Acta, 41, pp. 1041-1059.

KEEVIL, N.B., 1942: Vapour pressures of aqueous solutions at high temperatures. J. Am. Chem. Soc., 64, pp. 841-850.

KELLY, W.C. and GODDARD, E.N., 1969: Telluride ores of Boulder County, Colorado. (Abstr.). Fluid Inclusion Research - Proceedings of COFFI, 3, p. 30.

KENDALL, A.C., 1978: Continental and supratidal (sabkha) evaporites : Facies models 11. Geoscience Can., 5, No. 2, pp. 66-78.

KENDALL, A.C., 1978: Subaqueous evaporites : Facies models 12. Geosci. Can., 5, No. 3, pp. 124-139.

KENDALL, A.C., 1979: Facies Models 13. Continental and supratidal (sabkha) evaporites. Geosci. Canada, Reprint Series.

KHARMALOV, Ye. S., 1973: Construction of an apparatus for fine control of the speed of freezing of preparations in a cryostage by the use of liquid nitrogen. (Abstr.). Fluid Inclusion Research - Proceed. of COFFI, 7, p. 99.

KHETAGUROV, G.V., 1971: Technique of studying gas liquid inclusions in a microthermochamber. (Abstr.). Fluid Inclusion Research - Proceedings of COFFI, 4, p. 38.

KINSMAN, D.J.J., 1969a: Interpretaton of Sr^{2+} concentrations in carbonate minerals and rocks. J. sedim. Petrol., 39, pp. 486-508.

KINSMAN, D.J.J., 1969b: Modes of formation, sedimentary associations and diagnostic features of shallow - water and supratidal evaporites. Bull. Am. Ass. Petrol. Geol., 53, pp. 830-840.

KIROV, G.K., VESSELINOV, I. and CHERNEVA, Z., 1972: Conditions of formation of calcite crystals of tabular and acute rhombohedral habits. Krist. Tech., 7, pp. 497-509.

KITANO, Y., OKUMURA, M. and IDOGAKI, M., 1979: Behaviour of dissolved silica in parent solution at the formation of calcium carbonate. Geochem. J., 13, pp. 253-260.

KLEVTSOV, P.V. and LEMMLEIN, G.G., 1960: Pressure correction for the homogenization temperatures of aqueous NaCl solutions. Acad. Sci. U.S.S.R. Earth Sci. Sec., 128, pp. 995-997.

KNAUTH, L.P., 1979: A model for the origin of chert in limestone. Geol., 7, pp. 274-277.

KÖNNERUP-MADSEN, J., 1977: Composition and microthermometry of fluid inclusions in the Kleivatn granite, South Norway. Amer. J. Sci., 277, pp. 673-696.

KRAUSKOPF, K.B., 1967: Introduction to geochemistry. McGraw-Hill, New York, 721 pp.

KREULEN, R., 1980: CO_2 - rich fluids during regional metamorphism on Naxos (Greece) : Carbon isotopes and fluid inclusions. Am. J. Sci., 280, pp. 745-771.

KREULEN, R., and SCHUILING, R.D., 1982: N_2 - CH_4 - CO_2 fluids during formation of the Dome de l'Agout, France. Geochim. Cosmochim. Acta, 46, pp. 193-203.

KULLERUD, G. and YODER, H.S., 1959: Pyrite stability relations in the Fe-S system. Econ. Geol., 54, pp. 533-572.

LA IGLESIA, A., CABALLERO, M.A. and MENENDEZ DEL VALLE, F., 1974: Estudio mineralogico de la Villimaninita (Cu, Ni, Co, Fe) $(SeS)_2$. Bol. Geol. Minero., 85, pp. 50-55.

LANGMUIR, D., 1965: Stability of carbonates in the $MgO-CO_2-H_2O$: J. Geol., 73, pp. 730-754.

LARSON, L.T., MILLER, J.D., NADEAU, J.E. and ROEDDER, E., 1973: Two sources of error in low temperature inclusion homogenization temperature, and corrections on published temperatures, for the East Tennessee and Laisvall deposits. Econ. Geol., 68, pp. 113-116.

LARSON, S.L., 1956: Phase studies of the two-component carbon-dioxide water system involving the carbon dioxide hydrate. Univ. Microfilms No. 15, 235, Ann. Arbor., Michigan, Diss. Abstr., 16, 248 p.

LEMON, N.M., 1985: Physical modelling of sedimentation adjacent to diapirs and comparison with the Oratunga breccia body in the Central Flinders Ranges, South Australia. A.A.P.G. (in press).

LEROY, J., 1971: Les episienites non mineralisees dans le massif de granite a deux micas de Saint-Sylvestre (Limousin - France). Equilibres entre mineraux et solutions. These, Univ. Nancy, I, (unpubl.).

LEROY, J., 1979: Contribution to the evaluation of internal pressure in fluid inclusions when they decripitate. Bull. Mineral., 102, pp. 584-593.

LIPPMAN, F., 1973: Sedimentary Carbonate Minerals. Minerals, Rocks and Inorganic Materials 6, Springer - Verlag, Berlin, 228 pp.

LOFTUS-HILLS, G. and SOLOMON, M., 1967: Co, Ni and Se in sulphides as indicators of ore genesis. Mineral. Deposita (Berl.), 2, pp. 228-242.

LOGAN, B.W. and SEMENIUK, V., 1976: Dynamic metamorphism : processes and products in Devonian carbonate rocks, Canning Basin, W.A. Geol. Soc. Vic., Spec. Pub. 6.

402

LONG, D.T. and ANGINO, E.E., 1982: The mobilization of selected trace
metals from shales by aqueous solutions : effects of temperature and
ionic strength. Econ. Geol., <u>77</u>, No. 3, pp. 646-652.

LUCKSCHEITER, B. and PAREKH, P.P., 1979: A new method for the
determination of dissolved elements in fluid inclusions. N. Jb.
Mineral. Mh., <u>1979</u>, pp. 135-144.

LUCKSCHEITER, B. and MORTEANI, G., 1980: Microthermometrical and chemical
studies of fluid inclusions in minerals from Apline veins from the
Penninic rocks of the central and western Tauern Window. Lithos, <u>13</u>,
pp. 61-77.

MARTIN, A., NISBET, E.G. and BICKLE, M.J., 1980: Archaean stromatolites
of the Belingwe Greenstone Belt, Zimbabwe (Rhodesia) Precambrian
Research, <u>13</u>, pp. 337-362.

MATTSON, S.M. and ROSSMAN, G.R., 1984: Ferric iron in tourmaline. Phys.
Chem. Minerals, <u>11</u>, pp. 225-234.

MAYNARD, J.B., 1983: Geochemistry of Ore Deposits. Springer - Verlag,
New York, 303p.

McANDREW, J. and FINLAY, C.J., 1980: The nature and significance of the
occurrence of uranium in the Nanambu Complex of the Pine Creek
Geosyncline. <u>in</u> Ferguson, J. and Goleby, A.B. (eds.). Uranium in the
Pine Creek Geosyncline, IAEA Proceed. Series, Vienna, pp. 357-362.

McINTIRE, W.L., 1963: Trace element partition coefficients - a review
of theory and application to geology. Geochim. Cosmochim. Acta, <u>27</u>,
pp. 1209-1264.

McNAMARA, M., 1965: The lower greenschist facies in the Scottish Highlands. Geol. For. Stockh. Forh., 87, pp. 347-389.

MEITZITIS, Y., 1969: Compilation of part of the Embayment area, Rum Jungle district. BMR, Record 1969/25.

METZGER, F.W., KELLY, W.C., NESBITT, B.E. and ESSENE, E.J., 1977: Scanning electron microscopy of daughter minerals in fluid inclusions. Econ. Geo., 72, No. 2, pp. 141-152.

MEYERS, W.J., 1977: Chertification in the Mississippian Lake Valley Formation, Sacramento Mountains, New Mexico. Sedimentology, 24, pp. 74-105.

MILLOT, G., 1970: Geology of Clays. Weathering, Sedimentology, Geochemistry. Springer - Verlag, New York, 429p.

MOH, G.H. and KULLERUD, G., 1980: The Cu-Ni-S system and low temperature assemblages. in Ramdorhr, P. (ed.). Ore genesis, Springer - Verl., Heidelberg, pp. 678-688.

MOH, G.H. AND KULLERUD, G., 1980: Ore syntheses, phase equilibria studies and applications. N. Jb. Miner. Abh., 139, No. 2, pp. 113-154.

MOOKHERJEE, A. and PHILIP, R., 1979: Distribution of Cu, Co and Ni in ores and host-rocks, Ingladhal, Karnataka, India. Miner. Deposita, 14, pp. 33-55.

MOORE, L., KNOTT, B. and STANLEY, N., 1984: The stromatolites of Lake Clifton, Western Australia. Search, 14, No. 11-12, pp. 309-314.

MORROW, D.W. and MAYERS, I.R., 1978: Simulation of limestone diagenesis
- a model based on strontium depletion. Can. J. Earth Sci., 15, pp.
376-396.

MORROW, D.W., 1982: Diagenesis 1. Dolomite - Part 1: The chemistry of
dolomitization and dolomite precipitation. Geoscience Canada. 9, No.
1, pp. 5-13.

MORROW, D.W., 1982: Diagenesis 2. Dolomite - Part 2: Dolomitization
models and ancient dolostones. Geosci. Canada, 9, No. 2, pp. 95-107.

MORTEANI, G., SCHEY, F. and MOLLER, P., 1981: The formation of the
magnesite deposits in the Northern Grauwackenzone and the Innsbrucker
Quartzphyllit (Austria) as deduced from the R.E.E. fractionation.
Erzmetall., 34, No. 10, pp. 559-562.

MORTEANI, G., MOLLER, P., and SCHEY, F. 1982: The rare earth element
contents and origin of the sparry magnesite mineralizations of
Tux-Lanersbach, Entachen Alm, Spiessnagel, and Hochfilzen, Austria, and
the lacustrine magnesite deposits of Aiani-Kozani, Greece, and
Bela-Stena, Yugoslavia. Econ. Geol., 77, No. 3, pp. 617-631.

MUIR, M., LOCK, D. and von DER BORCH, C., 1980: The Coorong model for
penecontemporaneous dolomite formation in the Middle Proterozoic
McArthur Gp. N.T. Aus. SEPM Special Publ., No. 28, pp. 51-67.

MUTTON, A.J., 1980: Description of a radon anomaly detected east of
Batchelor, N.T., BMR Prof. Opinion : Geophy/M/79.014, 16p.

NAMBU, M., 1980: The analysis of fluid inclusions in microgram range
with an ion microanalyzer. 26th Int. Geol. Congress (abstr.) 1, pp. 67.

NEEDHAM, R.S. and STUART-SMITH, P.G., 1976: The Cahill Formation - host to uranium deposits in the Alligator Rivers Uranium Field, Australia. BMR J., 1, pp. 321-334.

NEEDHAM, R.S., 1981: A regional analysis of the Pine Creek Geosyncline metalliferous province, Northern Territory. M.Sc. Thesis (unpubl.). James Cook Univ. of North Queensland.

NEEDHAM, R.S. and ROARTY, M.J., 1980: An overview of metallic mineralization in the Pine Creek Geosyncline. in Ferguson, J. and A.B. Goleby (eds.). Uranium in the Pine Creek Geosyncline, IAEA Proceed. Series, Vienna, pp. 157-174.

NEEDHAM, R.S., CRICK, I.H. and STUART-SMITH, P.G., 1980: Regional geology of the Pine Creek Geosyncline. in Ferguson, J., and Goleby, A.B. (eds.). Uranium in the Pine Creek Geosyncline. IAEA Proceed. Series, Vienna, pp. 1-22.

NEEDHAM, R.S. and STUART-SMITH, P.G., 1984(3): Changes in stratigraphic nomenclature and correlation in Early Proterozoic rocks of the Darwin - Katherine area, N.T. BMR Journal - 'Note'.

NEEDHAM, R.S. and STUART-SMITH, P.G., 1984(3): The relationship between mineralisation and depositional environment in Early Proterozoic metasediments of the Pine Creek Geosyncline. Aus. IMM Conference, Darwin, pp. 201-211.

NICHOLSON, P.M., 1980: The geology and economic significance of the Golden Dyke Dome, Northern Territory. in Ferguson, J. and Goleby, A.B., (eds). Uranium in the Pine Creek Geosyncline. IAEA, Vienna, pp. 319-334.

NICHOLSON, R., 1976: A stylolitic marble from the Caledonian metasedimentary sequence of southern Troms. Norsk Geologisk Tidsskrift, 56, pp. 321-324.

NIELSON, H., 1979: Sulfur Isotopes. in Jager. E. and Hunziker, J.C. (eds.). Lectures in Isotope Geology. Springer-Verlag.

NISBET, B.W., ETHERIDGE, M.A., HOBBS, B.E. and WALL, V.J., 1981: Early bedding - parallel thrusting in the East Pine Creek Geosyncline. Int. Conf. on Deform. Processes in Tectonics, (Abst.), p. 7.

NISHIHARA, O., 1956: Origin of the bedded magnesite deposits of Manchuria. Econ. Geol., 51, pp. 698-711.

OEHLER, J.H., 1976: Hydrothermal crystallization of silica gel. Bull. geol. Soc. Am., 87, pp. 1143-1152.

OH, K.D., MORIKAWA, H., IWAI, S. and AOKI, H., 1973: The crystal structure of magnesite Am. Min., 58, pp. 1029-1033.

OHDE, S. and KITANO, Y., 1978: Synthesis of protodolomite from aqueous solution at normal temperature and pressure. Geochem. J., 12, pp. 115-119.

OHDE, S. and KITANO, Y., 1980: Incorportation of fluoride into Ca-Mg carbonate. Geochem. J., 14, pp. 321-324.

OHMOTO, H., 1972: Systematics of sulphur and carbon isotopes in hydrothermal ore deposits. Econ. Geol., 67, pp. 551-578.

OHMOTO, H. and RYE, R.O., 1979: Isotopes of Sulphur and Carbon. in Barnes, H.L., (ed.). Geochemistry of Hydrothermal Ore Deposits. Wiley,

New York, pp. 509-567.

OHTAGAKI, T., TAKAHASHI, H. and OBARA, K., 1974: Geology of the Hanawa mine, Akita Prefecture. in Ishihara, S. (ed.). Geology of Kuroko Deposits. Soc. of Mining Geologists of Japan, Tokyo, pp. 157-168.

ORTEGA-GUTIERREZ, F., 1984: Evidence of Precambrian evaporites in the Oaxacan granulite complex of Southern Mexico. Precambrian Research, 23, pp. 377-393.

OSBORNE, R.H., LINK, M.H. and LICARI, G.R., 1978: Modern lacustrine stromatolites, Walker Lake, Nevada (abstract). AAPG Bull., 62, p. 551.

OSTWALD, W., 1900: Uber die vermeintliche Isomerie des roten und gelben Quecksilberoxyds und die Oberflachenspannung fester Korper. Z. Phys. Chem. Stoechiom. Verwandschaftsl., 34, pp. 495-503.

PAGE, R.W., 1976: Geochronology of Archaean and Lower Proterozoic rocks in the Rum Jungle - Alligator Rivers area, Northern Territory, Australia, 25th Int. Geol. Congr., Abstracts Section 1A, Sydney.

PAGE, R.W., COMPSTON, W. and NEEDHAM, R.S., 1980: Geochronology and evolution of the late-Archaean basement and Proterozoic rocks in the Alligator Rivers Uranium Field, Northern Territory, Australia. in Ferguson, J. and Goleby, A.B., (eds.). Uranium in the Pine Creek Geosyncline, IAEA Proceed. Series, Vienna, pp. 39-68.

PAGEL, H.O., BORSHOFF, J. and COLES, R., 1984: Veinlike uranium deposits in the Rum Jungle area - geological setting and relevant exploration features. Aus. I.M.M. Conference, Darwin, pp. 225-234.

PARRY, W.T., BALLANTYNE, J.M. and JACOBS, D.C., 1984: Geochemistry of

hydrothermal sericite from Roosevelt Hot Springs and the Tintic and Santa Rita Porphyry Copper Systems. Econ. Geol., _79_, pp. 72-86.

PATERSON, J., VON PECHMANN, E., and BORSHOFF, J., 1984: Nature of uranium mineralization and associated wall rock alteration in the White's East area of the Embayment, Rum Jungle, Northern Territory. Aus. I.M.M. Conference, Darwin, pp. 235-248.

PERRY, E.C., MONSTER, J. and REIMER, T., 1971: Sulfur isotopes in the Swaziland System : barites and the evolution of the Earth's atmosphere Science, _171_, pp. 1015-1016.

PETERSON, M.N.A. and von DER BORCH, C.C., 1965: Chert : Modern inorganic deposition in a carbonate - precipitating locality. Science, _149_, pp. 1501-1503.

PICHAVANT, M., RAMBOZ, C. and WEISBROD, A., 1982: Fluid immiscibility in natural processes : Use and misuse of fluid inclusion data I Phase equilibria analysis - A theoretical and geometrical approach. Chem. Geol., _37_, pp. 1-48.

PINGITORE, N.E. 1978: The behaviour of Zn^{2+} and Mn^{2+} during carbonate diagenesis : theory and applications. J. sedim. Petrol., _48_, pp. 799-814.

PINGITORE, N.E. 1982: The role of diffusion during carbonate diagenesis. J. Geol. Pet., _52_, No. 1, pp. 0027-0039.

PLAYFORD, P.E. and COCKBAIN, A.E., 1969: Algal stromatolites : deep water forms in the Devonian of Western Australia. Science, _165_, pp. 1008-1010.

POTTER, R.W., 1977: Pressure corrections for fluid-inclusion homogenization temperatures based on the volumetric properties of the system NaCl - H_2O. Jour. Research U.S. Geol. Surv. 5, No. 5, pp. 603-607.

POTTER, R.W., CLYNNE, M.A. and BROWN, D.L., 1978: Freezing point depression of aquaeous sodium chloride solutions. Econ. Geol., 73, pp. 284-285.

POTY, B., LEROY, J. and JACHIMOWICZ, L., 1976: Un nouvel appareil pour la mesure des temperatures sous le microscope : l'installation de microthermometrie Chaixmeca. Bul. Soc. Fr. Min. Cristall., 99, No. 2-3, pp. 182-186.

PRATT, B.R., 1982: Limestone response to stress pressure solution and dolomitization - discussion and examples of compaction in carbonate sediments. Jour. Sed. Pet., 52, No. 1, pp. 323-334.

RANKIN, A.H., ALDERTON, D.H.M., THOMPSON, M. and GOULTER, J.E. 1982: Determination of U:C ratios in fluid inclusion decrepitates by inductively coupled plasma emission spectroscopy. Mineral. Mag., 46, pp. 179-86.

RHODES, J.M., 1965: The geological relationships of the Rum Jungle Complex, Northern Territory. BMR Rept. Geol. Geophys. Aust., 89, 10.

RICHARDS, J.R. and RHODES, J.M., 1967: Geochronology of the Rum Jungle Complex. Aust. J. Sci. (Abstracts) Melb. Congress.

RICHARDS, J.R., RUXTON, B.R. and RHODES, J.M., 1977: Isotopic dating of the leucocratic granite, Rum Jungle, Australia. Proc. Australas. Inst. Min. Metall., 264, pp. 33-43.

RICKARD, D.T., 1973: Limiting conditions for synsedimentary sulfide ore formation. Econ. Geol., 68, No. 5, pp. 605-617.

RICKETTS, B.D., 1980: Experimental investigation of carbonate precipitation in hydrated silica gels. J. Sed., Pet., 50, pp. 963-970.

RIPLEY, E.M. and NICOL, D.L., 1981: Sulfur isotopic studies of Archean slate and graywacke from northern Minnesota : evidence for the existence of sulfate reducing bacteria. Geochim. Cosmochim. Acta., 45, pp. 839-846.

ROBERTS, C., 1978: E.L. 1349 Rum Jungle, N.T. : Magnesite exploration. Progress Report, Unpubl., B.H.P.

ROBERTS, F.I., 1982: Trace element chemistry of pyrite : a useful guide to the occurrence of sulfide base metal mineralization. J. Geochem. Expl., 17, pp. 49-62.

ROBERTSON, A.H.F., 1977: The origin and diagenesis of cherts from Cyprus. Sedimentology, 22, pp. 11-30.

ROEDDER, E., 1963: Studies of fluid inclusion II Freezing data and their interpretation. Econ. Geol., 58, No. 2, pp. 166.

ROEDDER, E., 1967: Fluid inclusions as samples of ore fluids. in Barnes, H.L. (eds.). Geochemistry of Hydrothermal Ore Deposits. Penn. State Univ., pp. 515-566.

ROEDDER, E. and SKINNER, B.J., 1968: Experimental evidence that fluid inclusions do not leak. Econ. Geol., 63, No. 7, pp. 715-729.

ROEDDER, E., 1971: Fluid inclusion studies on the porphyry type ore

deposits at Bingham, Utah, Butte, Montana, and Climax, Colorado. Econ. Geol., 66, pp. 98-120.

ROEDDER, E., 1972: Composition of fluid inclusions. Data of Geochemistry, U.S.G.S., Professional Paper 440-JJ, Sixth Ed., 164 p.

ROEDDER, E., 1976: Fluid inclusion evidence on the genesis of ores in sedimentary and volcanic rocks. in Wolf, K.H. (ed.). Handbook of Strata-Bound and Stratiform Ore Deposits, 2, Geochemical Studies, Elsevier, Amsterdam, pp. 67-110.

ROEDDER, E., 1979b: Fluid inclusions as samples of ore fluids. in, Barnes, H.L., (ed.). Geochemistry of Hydrothermal Ore Deposits. Wiley, New York, pp. 684-737.

ROEDDER, E., 1981: Origin of fluid inclusions and changes that occur after trapping. in, Hollister, L.S. and Crawford, M.L. (eds.). Short Course in Fluid Inclusions: Application to Petrology. Min. Assoc. Canada, 6, pp. 101-137.

ROSASCO, G.J. and ROEDDER, E., 1979: Application of a new Raman microprobe spectrometer to nondestructive analysis of sulphate and other ions in individual phases in fluid inclusions in materials. Geochim. Cosmochim. Acta, 43, pp. 1907-1915.

ROSSITER, A.G. and FERGUSON, J., 1980: A Proterozoic tectonic model for northern Australia and its economic implications. in Ferguson, J. and Goleby, A.B. (eds.). Uranium in the Pine Creek Geosyncline, IAEA Proceed. Series, Vienna, pp. 209-232.

RUBIN, D.M. and FRIEDMAN, G.M., 1981: Origin of chert grains and a halite-silcrete bed in the Cambrian and Ordovician Whitehall Fm of

412

Eastern New York State. J. sedim. Petrol., 51, No. 1, pp. 69-72.

RYE, R.O. and OHMOTO, H., 1974: S and C isotopes and ore genesis : A review.

SAMOYLOVICH, L.A. and KHETCHIKOV, L.N., 1968: Pressure corrections to the homogenization temperatures of aqueous salt solutions. Geochem. Intern., 5, pp. 1184-1189.

SANGSTER, D.F. and SCOTT, S.D., 1976: Precambrian strata-bound, massive Cu-Zn-Pb sulfide ores of North America. in Wolf, K.H. (ed.). Handbook of Strata-Bound and Stratiform Ore Deposits. Elsevier, New York, 6, pp. 129-222.

SATHYANARAYAN, S. and MULLER, G., 1980: Origin of nodular chert in the carbonate rocks of the Kàladgi Gp (Younger Precambrian) Karnataka, India Sed. Geol., 25, pp. 209-221.

SAVEL'YEVA, N.I. and NAUMOV, G.B., 1979: Methods of analyzing salt composition for fluid inclusions in minerals. Geochem. Internat., 16, No. 3, pp. 65-70.

SAYLES, F.L. and FYFE, W.S., 1973: The crystallization of magnesite from aqueous solution. Geochim. cosmochim. Acta, 37, pp. 87-99.

SCHUILING, R.D., ANDRIESSEN, P.A.M., KREULEN, R., POORTER, R.P.E., DE SMETH, J.B., VERGOUWEN, L., VRIEND, S.P. and ZUURDEEG, B.W., 1983: Introduction to Geochemistry. Vening Meinesz Lab., Utrecht, 291 p.

SCHWARTZKOPFF, J., SANDRIN, L., BARABAS, A., and LEROY, J., 1974: Preparation of doubly polished thick sections for fluid inclusion studies at the Centre de Recherches Petrographiques e Geochimiques,

Nancy. Unpubl. Chaixmeca booklet, pp. 28-31.

SECCOMBE, P.K., 1977: Sulfur isotopes and trace metal composition of stratiform sulfides as an ore guide in the Canadian Shield. J. Geochem. Explor., _8_, pp. 117-137.

SECCOMBE, P.K. and CLARK, P.G.S., 1981: Sulfur isotope and element variations in the South Bay Mine, Northwestern Ontario. Econ. Geol., _76_, pp. 621-636.

SEMIKHATOV, M.A., GEBELEIN, C.D., CLOUD, P., AWRAMIK, S.M. and BENMORE, W.C., 1979: Stromatolite morphogenesis - progress and problems. Can. J. Earth Sci., _16_, pp. 992-1015.

SERGEYEVA, E.I., NIKITIN, A.A., KHODAKOVSKIY, I.L. and NAUMOV, G.B., 1972: Experimental investigation of equilibria in the system $UO_3-CO_2-H_2O$ in 25-200°C temperature intervals. Geochem. Internat., _9_, pp. 900-910.

SHEARMAN, D.J., 1966: origin of marine evaporites by diagenesis. Inst. Min. Met., Trans. Sec. B. _75_, pp. 208-215.

SHEVELEV, A.I., 1978: Lithological association of magnesite deposits in dolomite complexes. Litholog. Mineralog. Resources, _13_, pp. 379-383.

SHIBUE, Y., 1984: Chemical compositions of tourmaline in the vein-type tungsten deposits of the Kaneuchi Mine, Japan. Mineral. Deposita.

SHINN, E.A., 1969: Submarine lithification of Holocene carbonate sediments in the Persian Gulf. Sedimentology, _12_, pp. 109-144.

SIEDLECKA, A., 1982: Supralittoral ponded algal stromatolites of the

414

Late Precambrian Annijokka Member of the Batsfjord Fm. Varanger Pen., North Norway. Precambrian Research, 18, pp. 319-345.

SIEVER, R., 1972: The low temperature geochemistry of silicon. in Wedepol, K.H. and Turekian, K. (eds.). Handbook of Geochemistry Vol II - 14, Springer, Berlin.

SIMPSON, C.J., HUNTINGTON, J.F., LEISHMAN, J. and GREEN, A.A., 1980: A study of the Pine Creek Geosyncline using integrated Landsat and aeromagnetic data. in Ferguson, J. and Goleby, A.B. (eds.). Uranium in the Pine Creek Geosyncline, IAEA Proceed. Series, Vienna, pp. 141-156.

SINCLAIR, A.J., 1967: Trend surface analysis of minor elements in sulfides of the Slocan Mining camp, British Columbia, Canada. Econ. Geol., 62, pp. 1095-1101.

SLACK, J.F., 1982: tourmaline in Appalachian - Caledonian massive sulphide deposits and its exploration significance. IMM Trans., 91, pp. B81-89.

SLACK, J.F., HERRIMAN, N., BARNES, R.G. and PLIMER, I.R., 1984: Stratiform tourmalinites in metamorphic terranes and their geologic significance. Geology, 12, pp. 713-716.

SMITH, F.W., 1973: A simple microscope freezing stage. Miner. Mag., 39, pp. 366-367.

SORBY, H.C., 1879: On the structure and origin of limestones. Quart. J. Geol. Soc. London, 35, pp. 56-95.

SOUTHGATE, P.N., 1978: Middle Cambrian hypersaline environments along the eastern margin of the Georgina Basin. in Cook, P.J. and Shergold,

J.D. (eds.). 1st International Field Workshop and Seminar on Proterozoic - Cambrian phosphorites : Project 156.

STEPHANNSON, O. and JOHNSON, K., 1976: Granite diapirism in the Rum Jungle area, Northern Australia, Precambrian Research, 3, pp. 159-185.

STEWART, A.J., 1979: A barred-basin marine evaporite in the Upper-Proterozoic of the Amadeus Basin, Central Australia. Sed., 26, pp. 33-62.

STUART-SMITH, P.G., and FERGUSON, J., 1978: The Oenpelli Dolerite - a Precambrian continental tholeiitic suite from the Northern Territory, Australia, BMR J. Aust. Geol. Geophys. 3, pp. 125-133.

STUART-SMITH, P.G., WILLS, K., CRICK, I.H. and NEEDHAM, R.S., 1980: Evolution of the Pine Creek Geosyncline. in Ferguson, J. and Goleby, A.B., (eds.). Uranium in the Pine Creek Geosyncline, IAEA Proceed. Series, Vienna, pp. 23-38.

SUNDBLAD, K., 1981: Chemical evidence for and implications of a primary FeS phase in the Ankarvattnet Zn-Cu-Pb massive sulphide deposits, Central Swedish Caledonides. Mineral. Deposita, 16, pp. 129-146.

SVERJENSKY, D.A., 1981: The origin of a Mississippi Valley-type deposit in the Viburnum Trend, southeast Missouri. Econ. Geol., 76, pp. 1848-1872.

SWANENBERG, H.E.C., 1980: Fluid inclusions in high-grade metamorphic rocks from S.W. Norway. Geologica Ultraiectina, Univ. Utrecht, no. 25, 147pp.

TAYLOR, B.E. and SLACK, J.F., 1984: Tourmalines from Appalachian -

Caledonian massive sulfide deposits : Textural, chemical and isotopic relationships. Econ. Geol., _79_, pp. 1703-1726.

TAYLOR, G.H. and ROWNTREE, J.C., 1980: The symposium - Restrospect and discussion. _in_ Ferguson, J. and Goleby, A.B., (eds.). Uranium in the Pine Creek Geosyncline, IAEA, Vienna, pp. 751-758.

THODE, H.G. and MONSTER, J., 1964: Sulfur isotope geochemistry of petroleum, evaporites and the ancient sea. _in_ Young, A. and Galley, J.E. (eds.). Fluids in Subsurface Environments : Am. Assoc. Pet. Geol. Mem. _4_, pp. 367-377.

THOMAS, W.N., 1956: A report on the geological investigations of the Rum Jungle Uranium Field, Northern Territory. Territory Enterprises Pty. Ltd. Report (Unpubl.).

THOMPSON, M., RANKIN, A.H., WALTON, S.J., HALLS, C. and FOO, B.N., 1980: The analysis of fluid inclusion decripitate by inductively-coupled plasma atomic emission spectroscopy : an exploratory study. Chem. Geol., _30_, pp. 121-133.

TOURAY, J-C., 1976: Activation analysis for liquid inclusion studies : a brief review. Bull. Mineral., _99_, pp. 162-164.

TRUEMAN, N.A., 1971: A petrological study of some sedimentary phosphorite deposits. Bull. AMDEL, No. 11.

TRURNIT, P., 1968: Analysis of pressure solution contacts and classification of pressure solution phenomena. _in_ Muller, G. and Friedman, G.M. (eds.). Recent Developments in Carbonate Sedimentology in Central Europe. Springer-Verlag, Berlin, pp. 75-84.

TRUSCOTT, M.G. and SHAW, D.M., 1984: Boron in chert and Precambrian siliceous iron formations. Geochim. Cosmochim. Acta, 48, pp. 2213-2320.

TSUI, T.F. and HOLLAND, H.D., 1979: The analysis of fluid inclusions by laser microprobe. Econ. Geol., 74, No. 7, pp. 1647-1653.

TUREKIAN, K.K., 1972: Chemistry of the Earth. Holt, Rinehart and Winston, New York, 131 pp.

TURNER, D.R., WHITFIELD, M. and DICKSON, A.G., 1981: The equilibrium speciation of dissolved components in freshwater and seawater at 25°C and 1 atm. pressure. Geochim. Cosmochim. Acta, 45, pp. 855-881.

UPPILL, R.K., 1980: Sedimentology of the Late Precambrian Mundallio Subgroup : a clastic carbonate (dolomite, magnesite) sequence in the Mt. Lofty and Flinders Ranges, S.A. Ph.D. thesis. University of Adelaide. (unpubl.).

VALDIYA, K.S., 1968: Origin of the magnesite deposits of Southern Pithoragarh Kumaun Himalaya, India. Econ. Geol., 63, pp. 924-934.

VAUGHAN, D.J. and CRAIG, J.R., 1978: Mineral Chemistry of Metal Sulfides. Cambridge Univ. Press, London, 493p.

VEIZER, J., and DEMOVIC, R., 1974: Strontium as a tool in facies analysis. J. sedim. petrol., 44, pp. 95-115.

VEIZER, J., 1974: Chemical diagenesis of belemnite shells and possible consequences for palaeotemperature determinations. N. Jb. Geol. Palaeont. Abh., 147, pp. 91-111.

VEIZER, J., LEMIEUX, J., JONES, B., GIBLING, M.R. and SAVELLE, J., 1977:

418

Sodium : Palaeosalinity indicator in ancient carbonate rocks. Geol.,
5, No. 3. pp. 177-179.

VEIZER, J., LEMIEUX, J., JONES, B., and GIBLING, M.R., 1978:
Palaeosalinity and dolomitization of a Lower Palaeozoic carbonate
sequence, Somerset and Prince of Wales Islands, Arctic Canada. Can. J.
Earth Sci., 15, pp. 1448-1461.

VEIZER, J., 1978: Simulation of limestone diagenesis - a model based on
Sr depletion : discussion. Can. J. Earth Sci., 15 pp. 1683-1685.

VEIZER, J., 1983: Trace elements and isotopes in sedimentary carbonates.
in Reeder, R.J., (eds.). Carbonates : Mineralogy and Chemistry.
Mineralog. Soc. Am., Reviews in Mineralogy, 11, p. 265.

VOKES, F., 1967: Linnaeite from the Precambrian Raipas Group of
Finnmark, Norway. Mineral. Deposita, 2, pp. 11-25.

VOKES, F., 1969: A review of the metamorphism of sulphide deposits.
Earth Sci. Rev., 5, pp. 99-143.

von der BORCH, C.C., 1965: The distibution and preliminary geochemistry
of modern carbonate sediments of the Coorong area, South Australia,
Geochim. Cosmochim. Acta, 29, pp. 781-799.

von der BORCH, C.C., 1976: Stratigraphy and formation of Holocene
dolomitic carbonates of the Coorong area. J. sedim. Petrol., 46, pp.
952-966.

von der BORCH, C.C. and LOCK, D., 1979: Geological significance of
Coorong dolomite. Sed., 26, pp. 813-824.

WALPOLE, B.P., CROHN, P.W., DUNN, P.R. and RANDAL, M.A., 1968: Geology of the Katherine Darwin region, Northern Territory, Bureau Mineral Resources, Bull. 82.

WANLESS, H.R., 1979: Limestone response to stress : pressure solution and dolomitization. J. sedim. Petrol., 49, pp. 437-462.

WANLESS, H.R., 1982: Limestone response to stress : Pressure solution and dolomitization - reply. J. sedim. Petrol., 52, pp. 328-332.

WARREN, J.K., 1983: On pedogenic calcrete as it occurs in the vadose zone of Quaternary calcareous dunes in coastal South Australia. J. sedim. Petrol., 53, 3, pp. 787-796.

WEISBROD, A., POTY, B. and TOURET, J., 1976: Les inclusions fluides en geochimie - petrologie : tendences actuelles. Bull. Soc. Fr. Miner. Cristall., 99, pp. 140-152.

WEST, I.M., 1979: Review of evaporite diagenesis in the Purbeck Formation of S. England. Sym. Sedimentation jurassique W europeen A.S.F. Pub. speciale No. 1.

WHITE, A.F., 1977: Sodium and potassium coprecipitation in aragonite. Geochim. Cosmochim. Acta, 41, pp. 613-625.

WHITE, A.F., 1978: Sodium coprecipitation in calcite and dolomite. Chem. Geol., 23, pp. 65-72.

WILLIAMS, P.F., 1963: Geology of the Rum Jungle district (NT) with particular reference to the orebodies. Territory Enterprises Pty. Ltd., Report (unpubl.).

WRIGHT, P., 1980: Contrasting depositional themes of Lower Carboniferous peritidal carbonates. IAS 3rd Eur. Mtg., Copenhagen. 1982, Abstr.

WRIGHT, V.P., 1982: The recognition and interpretation of paleokarsts : two examples from the Lower Carboniferous of South Wales. J. sedim. Petrol., 52, No, 1. pp. 83-94.

YOUNG, H.R., 1979: Evidence of former evaporites in the Cambro-Ordovician Durness Group, Northwest Scotland. Sed. Geol., 22, pp. 287-303.

YPMA, P., EVERS, H.J. and WOENSDREGT, C.F., 1968: Mineralogy and geology of the Providencia mine (Leon, Spain), type - locality of villimaninite. Neues Jahrb. Mineral Monatsh., pp. 174-191.

YPMA, P., 1979: Notes on phase changes of the system H_2O-CO_2-CH_4-H_2 in Fluid Inclusions. in Workshop Manual on Fluid Inclusions. La Trobe Univ., Melbourne.

YPMA, P., 1979: Water - Soluble Salts - CO_2 systems. in Workshop Manual on Fluid Inclusions. La Trobe Univ., Melbourne.

YPMA, P., and FUZIKAWA, K., 1980: Fluid inclusion and oxygen isotope studies of the Nabarlek and Jabiluka deposits, Northern Territory, Australia. in Ferguson, J. and Goleby, A.B. Uranium in the Pine Creek Geosyncline. IAEA, Vienna, pp. 375-396.

ZAKRZEWSKI, M.A., 1984: Minerals of the bravoite-villimaninite series and cuprian siegenite from Karniowice, Poland. Canad. Mineral., 22, pp. 499-502.

ZEMANN, J., 1969: Crystal Chemistry. in Wedepohl, K.H., (ed.). Handbook
of Geochemistry, 1., Springer, Berlin, pp. 12-36.

ZENGER, D.H., 1983: Burial dolomitization in the Lost Burro Formation
(Devonian), east-central California, and the significance of late
diagenetic dolomitization. Geol., 11, pp. 519-522.